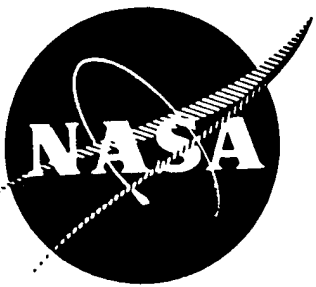


NASA CR- 134975
SCI Special Report 75154



FILAMENT-REINFORCED
METAL COMPOSITE PRESSURE VESSEL
EVALUATION AND PERFORMANCE DEMONSTRATION
FINAL REPORT

DISTRIBUTION STATEMENT A
Approved for public release;
Distribution Unlimited

by

R. E. Landes

STRUCTURAL COMPOSITES INDUSTRIES, INC.
Azusa, California

Prepared for

NATIONAL AERONAUTICS AND SPACE ADMINISTRATION

NASA Lewis Research Center
Contract NAS 3-16770
James R. Faddoul, Project Manager

19960503 042

DISCLAIMER NOTICE



**THIS DOCUMENT IS BEST
QUALITY AVAILABLE. THE
COPY FURNISHED TO DTIC
CONTAINED A SIGNIFICANT
NUMBER OF PAGES WHICH DO
NOT REPRODUCE LEGIBLY.**



STRUCTURAL COMPOSITES INDUSTRIES INC.

6344 NORTH IRWINDALE AVENUE AZUSA, CALIFORNIA 91702 (213) 334-8221

76-2003- 852

10 September 1976

Picatinny Arsenal
Dover, NJ 07801

Attention: Distribution

Subject: Final Report, NASA CR-134975
titled "Filament Reinforced Metal
Composite Pressure Vessel Evaluation
and Performance Demonstration"

Gentlemen:

Enclosed please find your copy(s) of the Subject report prepared for the
NASA Lewis Research Center under Contract NAS 3-16770.

Sincerely,

R. E. Landes, Program Manager

REL:dn

1. Report No. NASA CR-134975	2. Government Accession No.	3. Recipient's Catalog No.	
4. Title and Subtitle FILAMENT-REINFORCED METAL COMPOSITE PRESSURE VESSEL EVALUATION AND PERFORMANCE DEMONSTRATION		5. Report Date May 1976	
7. Author(s) R. E. Landes		6. Performing Organization Code	
9. Performing Organization Name and Address Structural Composites Industries, Inc. 6344 North Irwindale Avenue Azusa, California 91702		8. Performing Organization Report No. SCI Special Report 75154	
12. Sponsoring Agency Name and Address National Aeronautics and Space Administration Lewis Research Center 21000 Brookpark Road, Cleveland, Ohio 44135		10. Work Unit No.	
15. Supplementary Notes Project Manager, James R. Faddoul Materials and Structures Division NASA Lewis Research Center, Cleveland, Ohio 44135		11. Contract or Grant No. NAS 3-16770	
16. Abstract Advantages of filament overwrapped metal composite pressure vessels for future flight vehicles and the technology readiness of the vessels for the application were verified in this full scale hardware demonstration program. Two different Kevlar-49 filament-reinforced metal sphere designs were developed, and six vessels of each type were fabricated and subjected to performance tests consisting of fatigue cycling, sustained loading, and hydrostatic burst. The 61 cm (24 inch) diameter Kevlar-49/cryoformed 301 stainless steel pressure vessels demonstrated the required pressure cycle capability, burst factor of safety, and a maximum pressure times volume divided by weight (pV/W) performance of 210 J/g (834 000 in-lb/lbm) at burst; this represented a 25-30% weight saving over the lightest weight comparable, 6Al-4V Ti, homogeneous pressure vessel. In addition to these capabilities of the Kevlar/stainless steel spherical vessels, both the Kevlar/stainless steel design and the 97 cm (38 inch) diameter Kevlar-49/2219-T62 aluminum sphere design demonstrated the anticipated safety characteristics of composite vessels consisting of non-fragmentation and controlled failure mode features when pressure cycled to failure at operating pressure; when failure occurred during pressure cycling, the mode was localized leakage and not catastrophic. Kevlar/stainless steel vessels utilized a unique conical boss design, and Kevlar/aluminum vessels incorporated a tie-rod to carry port loads; both styles of polar fittings performed as designed during operational testing of the vessels.		13. Type of Report and Period Covered Contractor Report July 1972 through October 1975	
17. Key Words (Suggested by Author(s)) Pressure Vessel 2219-T62 Aluminum Kevlar Fiber Composite Cryoformed 301 Stainless Steel		18. Distribution Statement Unclassified Unlimited	
19. Security Classif. (of this report) Unclassified	20. Security Classif. (of this page) Unclassified	21. No. of Pages 384	22. Price*

* For sale by the National Technical Information Service, Springfield, Virginia 22151

HII

**COMPOSITE TANKAGE APPLICATION
(KEVLAR- 49 FILAMENT REINFORCED CRYOFORMED 301 STAINLESS STEEL CONSTRUCTION)**

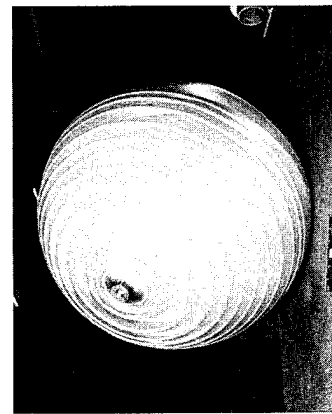
PARTIALLY COMPLETE KEVLAR-49
FILAMENT OVERWRAPPED 301 GRES LINER



INITIAL KEVLAR-49 FILAMENT
WINDINGS APPLIED TO 301 GRES LINER

LIGHT-WEIGHT KEVLAR/301 GRES
PRESSURE VESSEL AFTER CRYOSIZING
(Vessel Performance Factor, $P_B V/W > 830,000$ Inch)

25 IN. DIAMETER CRYOFORMED
301 STAINLESS STEEL LINER ASSEMBLIES



HII

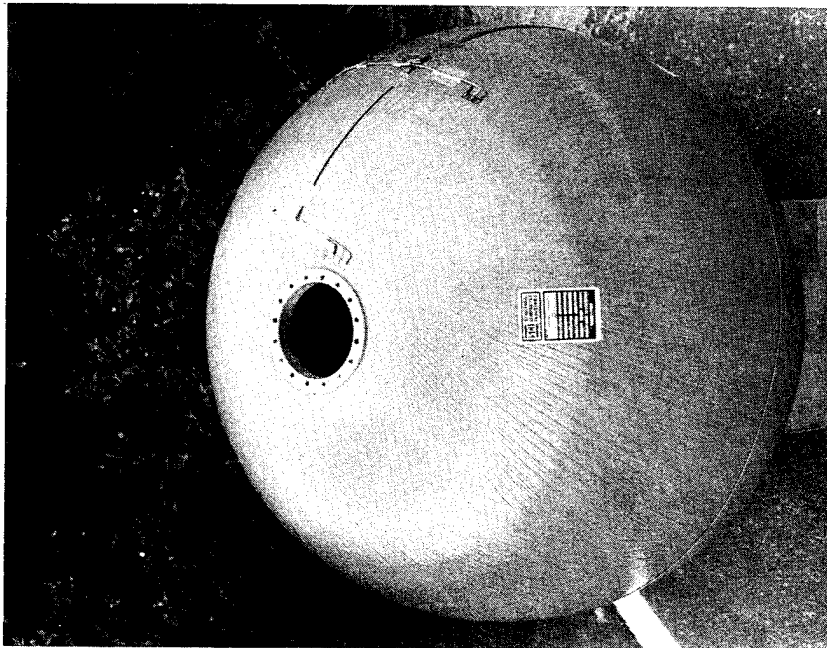
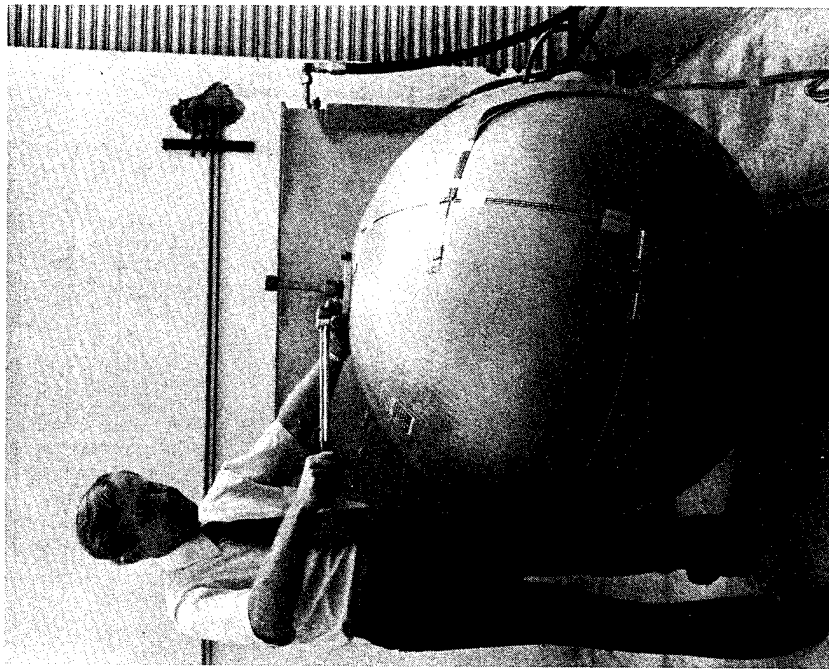
FOREWORD

This report describes the work performed by Structural Composites Industries, Inc. (SCI) under Contract NAS 3-16770. The contract was initiated in July 1972, then technically redirected in July 1973 to reflect new NASA objectives. The work was administered by Mr. James R. Faddoul of the NASA Lewis Research Center.

SCI personnel who conducted the investigation include R. E. Landes, Program Manager and E. E. Morris, Engineering Manager. Pressure vessel filament-winding was accomplished by R. J. Robinson and instrumentation and testing was conducted under the direction of K. A. Hansen.

ARDE, Inc. participated in the program as a subcontractor, supplying design details for the overwrapped 301 stainless steel vessels and fabrication of the required cryoformed metal liner assemblies. ARDE personnel who contributed to the investigation include A. Cozewith and D. Gleich.

Guidance in fracture mechanics design considerations for the metal liners was provided throughout the program by Mr. W. D. Bixler of The Boeing Company, and metallurgical analyses of tested vessels were conducted by the NASA Lewis Research Center under the direction of Mr. James R. Faddoul.



**KEVLAR -49 FILAMENT REINFORCED
2219-T62 ALUMINUM PRESSURE VESSEL**

TABLE OF CONTENTS

	<u>Page</u>
SUMMARY	1
I. INTRODUCTION	3
A. BACKGROUND	3
1. Load-Sharing Concept	3
2. Establishment of Designs	5
3. Fracture Mechanics of Metal Liner	5
4. Failure Modes	7
B. PROGRAM PLAN	8
1. Program Objective	8
2. Scope of Work	8
II. DESIGN, FABRICATION, AND TEST OF KEVLAR-49 OVERWRAPPED 2219 ALUMINUM PRESSURE VESSELS	11
A. CRITERIA DEVELOPMENT	11
1. Initial Design Criteria	11
2. Metal Shell Fabrication Process Studies	11
3. Design Optimization Studies	17
4. NASA Redirection	24
B. DESIGN	32
C. FABRICATION	41
1. Aluminum Liner Assemblies	41
2. Kevlar/Aluminum Pressure Vessels	57

TABLE OF CONTENTS (continued)

	<u>Page</u>
D. TEST PROGRAM	60
1. Instrumentation and Test Plan	60
2. Initial Test Result - Vessel Serial Number S-3	63
3. Redesign Effort	74
4. Final Test Results	84
5. Evaluation of Test Results	89
III. DESIGN, FABRICATION, AND TEST OF KEVLAR-49 OVERWRAPPED CRYOFORMED 301 STAINLESS STEEL PRESSURE VESSELS	93
A. DESIGN	93
B. FABRICATION	104
1. Stainless Steel Liner Assemblies	104
2. Kevlar/Stainless Steel Pressure Vessels	106
C. TEST PROGRAM	113
1. Instrumentation and Test Plan	113
2. Performance Test Results	115
3. Evaluation of Test Results	127
IV. CONCLUDING REMARKS	129
A. KEVLAR/301 STAINLESS STEEL PRESSURE VESSELS	129
B. KEVLAR/ALUMINUM PRESSURE VESSELS	130

TABLE OF CONTENTS (concluded)

	<u>Page</u>
APPENDICES	
A. Design Analysis, Kevlar Fiber Reinforced Aluminum Sphere	135
B. Sizing Test Procedure - Kevlar Fiber Reinforced 2219-T6 Aluminum Spheres-Part Number 1269382-1	187
C. SCI Specification 73-17 - 2219-T62 Aluminum Metal Shell, Part Number 1269381	219
D. Kevlar FR 2219 Aluminum Pressure Vessel Fabrication Process Specification	239
E. Test Procedure - Kevlar Fiber Reinforced Metal Spheres	255
F. Sizing and Performance Test Pressure/Strain Plots for Kevlar/Aluminum Pressure Vessels	287
G. Design Analysis - Composite Spherical Pressure Vessel Kevlar-49 Fiber Overwrapped Ardeform 301 Stainless Steel Liner	313
H. Kevlar FR 301 Stainless Steel Pressure Vessel Fabrication Process Specification	339
I. Performance Test Pressure/Strain Plots, Kevlar/ Stainless Steel Pressure Vessels	355
J. List of Symbols	381
REFERENCES	385

LIST OF TABLES

<u>Tables</u>	<u>Page</u>
I. Preliminary Design Criteria for Overwrapped 2219 Aluminum Pressure Vessels	12
II. 2219-T62 Aluminum Properties Used for Preliminary Design	18
III. Summary of Ultimate Design Allowable Filament Stresses for Preliminary Designs	19
IV. Life Analysis Summary for Preliminary S-Glass Overwrapped Aluminum Sphere Designs	25
V. Life Analysis Summary for Preliminary Kevlar Overwrapped Aluminum Cylinder Designs	26
VI. Final Pressure Vessel Design Criteria	31
VII. Material Properties Used for Kevlar/Aluminum Vessel Design	37
VIII. Kevlar-49 FR 2219-T6 Aluminum Pressure Vessel Design Parameter Summary	38
IX. 2219-T62 Aluminum Material Acceptance Test Results	44
X. 2219-T62 Aluminum Weld Process Test Results	48
XI. 2219 Aluminum Half-Shell Inspection Data Summary	53
XII. 2219-T62 Aluminum Liner Assembly Inspection Data Summary	58
XIII. Kevlar-49 Overwrapped 2219-T62 Aluminum Pressure Vessel Fabrication Data Summary	62
XIV. Kevlar-49 Overwrapped 2219-T62 Aluminum Pressure Vessel Performance Test Data Summary	85
XV. Material Properties Used for Kevlar/Stainless Steel Vessel Design	98

LIST OF TABLES (concluded)

<u>Table</u>		<u>Page</u>
XVI.	Kevlar-49 FR Cryoformed 301 Stainless Steel Pressure Vessel Design Parameters Summary	105
XVII.	Liner Fabrication Data Summary - Cryoformed 301 Stainless Steel Spheres	107
XVIII.	Fabrication Data Summary - Kevlar Fiber Reinforced 301 Stainless Steel Sphres	111
XIX:	Test Data Summary - Kevlar Fiber Reinforced 301 Stainless Steel Spheres	117

LIST OF FIGURES

<u>Figure</u>	<u>Page</u>
1. Preliminary Design Configurations	13
2. 2219-T62 Aluminum Uniaxial Fracture Specimen	21
3. Uniaxial 2219-T62 Aluminum Base Metal, Ambient Temperature Failure Locus	22
4. Fatigue Crack Growth Rates for 2219-T62 Aluminum Base Metal at Ambient Temperature	23
5. Design Performance Curves for Kevlar FR 2219-T62 Aluminum Spheres	27
6. Design Metal Shell Thickness Curves for Kevlar FR 2219-T62 Aluminum Spheres	28
7. Design Stress Chart for Kevlar FR 2219-T62 Aluminum Spheres	29
8. SCI Drawing 1269381 - Liner Assembly 2219-T62 Aluminum Alloy Sphere	33
9. SCI Drawing 1269382 - Pressure Vessel Kevlar FR 2219 Aluminum Sphere	35
10. Ambient Stress/Strain Relationship for Kevlar-49 FR 2219-T62 Aluminum Sphere	39
11. Ambient Pressure/Strain Relationship for Kevlar-49 FR 2219-T62 Aluminum Sphere	40
12. 2219-T62 Aluminum Sphere Fabrication Plan, Half Shell Fabrication	42
13. 2219-T62 Aluminum Weld Test Specimen Configuration	46
14. 37.5-inch-diameter Aluminum Liner Assembly Used for Heat-Treatment Verification	49

LIST OF FIGURES (continued)

<u>Figure</u>		<u>Page</u>
15.	37.5-Inch-Diameter 2219 Aluminum Sphere Half-Shells	50
16.	Set of 2219 Aluminum Sphere Half-Shells	50
17.	37.5-Inch-Diameter 2219 Aluminum Half-Shell Assembly for Welding	55
18.	Overwrap Filament-Winding Development for 37.5-Inch-Diameter Sphere	59
19.	Kevlar Filament-Overwrapped 2219-T62 Aluminum Spheres, Serial Numbers S-3 and S-1	61
20.	Instrumentation Location	64
21.	Revised Test Plan and Vessel Assignment for Kevlar Fiber Reinforced 2219 Aluminum Spheres	65
22.	Kevlar-49 Filament Reinforced 2219-T62 Aluminum Pressure Vessel	66
23.	Strains From Longitudinally Oriented Strain Gages Obtained During Pressure Sizing of Kevlar/Aluminum Vessel S-3	67
24.	Strains From Circumferentially Oriented Strain Gages Obtained During Pressure Sizing of Kevlar/Aluminum Vessel S-3	68
25.	Strains From Great-Circle Extensometers Obtained During Pressure Sizing of Kevlar/Aluminum Vessel S-3	69
26.	Kevlar/Aluminum Vessel S-3 After Hydroburst	71
27.	Kevlar/Aluminum Vessel S-3 Port Areas After Hydroburst	72

LIST OF FIGURES (continued)

<u>Figure</u>		<u>Page</u>
28.	Strains From Great-Circle Extensometers Obtained During Hydraulic Burst of Kevlar/ Aluminum Vessel S-3	73
29.	End Closure Design Concepts (2 Sheets)	75
30.	Model of Port Region, Kevlar Reinforced Aluminum Sphere	78
31.	Tie-Rod/Boss Body Load Relations, Kevlar/ Aluminum Vessel	79
32.	Tie-Rod Design Parameters, Kevlar/Aluminum Vessel (2 Sheets)	80
33.	Effect of Rod Size on Shell Discontinuity Stresses, Kevlar/Aluminum Vessel	82
34.	Pressure/Strain Relation for Kevlar-Aluminum Vessel Tie-Rod Assembly.	83
35.	Predicted versus Measured Strains from Circum- ferentially Oriented Strain Gages During Pressure Sizing of Kevlar/Aluminum Vessel Serial Number S-1	86
36.	Predicted versus Measured Polar Strain During Pressure Sizing of Kevlar/Aluminum Vessel Serial Number S-1	88
37.	Kevlar/Aluminum Vessel Serial Number S-4 After Hydroburst	90
38.	Overwrapped Cryoformed 301 Stainless Steel Spheres- Pictorial Manufacturing Flow Plan	95
39.	ARDE Drawing J/N 51055 - Weldment Assembly Preform Sphere	99
40.	ARDE Drawing J/N 61055- Pressure Vessel Assembly, Ardeform - GFR	101

LIST OF FIGURES (concluded)

<u>Figure</u>		<u>Page</u>
41.	Subscale Kevlar-49/Cryoformed 301 Stainless Steel Spherical Pressure Vessels	103
42.	Cryoformed 301 Stainless Steel Liner Assemblies	108
43.	Kevlar-49 Overwrapping Cryoformed 301 Stainless Steel Spheres	109
44.	Completed Kevlar/Stainless Steel Pressure Vessel	110
45.	Test Setup, Kevlar Reinforced 301 Stainless Steel Pressure Vessel	114
46.	Revised Test Plan and Vessel Assignment for Kevlar Fiber Reinforced 301 Stainless Steel Spheres	116
47.	Kevlar Reinforced 301 Stainless Steel Vessel Serial Number 001 After Static Burst Test	118
48.	Kevlar/Stainless Steel Vessel Serial Number 003 After 1045 Pressure Cycles to 2330 psi	120
49.	Serial Number 003 Metal Shell Failure Site, External Surface View	121
50.	Serial Number 003 Metal Shell Failure, Site, Internal Surface View	122
51.	Cross Sectional View of Serial Number 003 Metal Shell at Failure Site.	123

SUMMARY

The primary purpose of this full-scale hardware demonstration program was to verify and show the advantages of filament overwrapped metal pressure vessels for future flight vehicles, as well as demonstrate the technology readiness and suitability of the vessels for the application. The program objective was accomplished by fabricating and performance testing six vessels each of two different overwrapped metal designs; a 61 cm (24 inch) diameter Kevlar-49 filament reinforced cryoformed 301 stainless steel sphere, and a 97 cm (38 inch) diameter Kevlar-49 filament reinforced 2219-T62 aluminum sphere.

Program results for the Kevlar/cryoformed stainless steel construction vessels verified capability to achieve the specified service life and burst factor of safety requirements, and also demonstrated their weight saving advantage, the repeatability of fabrication processes, and the reliability of existing design techniques as follows:

- Kevlar/stainless steel vessels were successfully subjected to two different service life test evaluation conditions:

- At a design safety factor of 2.0, 1600 fatigue pressure cycles at a performance factor $p_o V/W$ of 101 J/g (406 000 in-lb/lbm) were obtained without failure. Actual burst factor of safety demonstrated after the fatigue cycling was 2.06 and $p_b V/W$ was 208 J/g (837 000 in-lb/lbm).
- At a design burst to operating pressure ratio of 1.5, 1000 fatigue pressure cycles were sustained without failure resulting in an operating performance factor $p_o V/W$ of 122 J/g (490 000 in-lb/lbm). Subsequent burst-to-operating safety factor was 1.72 and $p_b V/W$ achieved was 210 J/g (843 00 in-lb/lbm). In addition, a similar 1.5 design factor of safety vessel was subjected to three months of sustained pressurization at $p_o V/W$ of 121 J/g (487 000 in-lb/lbm) without failure or evidence of degradation.
- The foregoing operational and burst performance levels represent a 25-30% weight savings over a comparable 6Al-4V Titanium (solution treated and aged) spherical homogeneous metal pressure vessel.

Excellent repeatability of major manufacturing processes was demonstrated. The variation in Kevlar/epoxy composite thickness was within $\pm 2.7\%$; variation in total vessel weight was $\pm 1.2\%$. The range of relative volume changes during cryosizing was 0.96 to 1.00% compared to a design value of 1.00%.

A unique boss design, previously developed by ARDE, performed as designed during all performance testing conducted. The bosses were not failure sites even at the high stress level operating pressure evaluation condition.

● Kevlar/aluminum vessel results demonstrated the ability to design and fabricate large filament overwrapped vessels with load sharing liners. Important information obtained during vessel development and evaluation was as follows:

- The use of a bolted end-closure design for the large ported vessels was inadequate. The revised design, incorporating a tie-rod to carry the port load, provided a good solution for completing performance tests on existing vessels.
- The thickness tolerance obtained for 2219 aluminum half shells was excellent; many exceeded the established acceptance criteria and met the thickness tolerance "design objective".
- Heat treatment quenching of large volume aluminum liner assemblies can be accomplished in the required time period without distortion of the shell, but port areas of future liner assemblies with integral bosses should be initially machined "rough" and final machined after heat treatment.
- Maximum performance for the 97 cm (38 inch) diameter Kevlar/aluminum pressure vessel at failure $p_b V/W$ was 164 J/g (658 000 in-lb/lbm). Failure was of the tie-rod and not the vessel itself.

● Test results for both styles of vessels verified the anticipated leak-before-burst, non-fragmentation, and controlled failure mode features of composite vessels with metal liners. When the vessels were fatigue cycled to point of final failure, the failure mode was localized leakage of the metallic liner, without vessel rupture or fragmentation.

I. INTRODUCTION

A. BACKGROUND

Since the early 1950's when the first serious efforts were made with high-strength, light-weight filament-wound pressure vessels and rocket motor cases, significant successes have been achieved in the development of a technology base and reliable application of these composite structures to operational systems.

The potential of filament-wound tankage for space vehicle pressurant vessels and cryogenic storage has and continues to be demonstrated in a series of NASA-LeRC technology development programs conducted over the past fourteen years. Such vessels, with an appropriate sealant liner, offer considerable weight savings when compared with the best homogeneous metal constructions. Some types of composite tanks, because of their failure modes, offer system safety enhancement as an additional benefit.

Research and development has been concentrated on evaluation of constituent-material properties, evolution of effective pressure-vessel analytical methods and designs for combining a metal liner with the overwrapped filament composite, and evaluation testing of tanks at elevated to cryogenic temperatures under burst, fatigue, and sustained loading conditions. These past NASA-LeRC efforts, work by the Air Force and recently by NASA-JSC have demonstrated the performance capabilities of composite tankage, and identified workable designs and fabrication approaches, as well as special attention areas.

1. Load-Sharing Concept

Liners for filament-wound pressure vessels have been discussed at length in prior publications. Briefly, stressing of the filament-wound composite results in formation of some matrix cracks in the wall that can let the contained fluid leak out. To prevent this, a liner is required. Three classes of liners used are:

- elastomeric - for near ambient temperature applications where some permeability is permissible,

- thin metal bonded to the overwrap--the lightest weight vessel, but cyclic life limited, and
- load sharing metal

Filament-wound composite tanks with load-sharing metal liners are intermediate in weight saving performance between thin-metal/bonded liner composite tanks and homogeneous metal tanks, and do not require a bond between the metal shell and overwrap. For tanks with load-sharing liners, the filament stress-strain curve is linearly elastic out to the proof strain and even beyond to burst. However, on the first pressurization cycle, the metal stress-strain curve shows yield and plastic flow. As the vessel proof pressure is released, the liner, which has taken a permanent plastic set, is forced into compression by the filaments trying to return elastically to their original size. Thus, at zero pressure after proof, the metal is in compression and the filaments in tension. From that time on, the metal operates elastically from compression to tension while the filaments operate in a tension-tension mode. The terminology used to refer to this type of tank is "fiber-reinforced-metal" or "load-bearing metal liner" filament-wound composite pressure vessel concept.

The primary objective in designing a fiber reinforced metal pressure vessel is to obtain maximum operating performance at a minimum weight, and to provide safe-life design features. Design development is related to (1) load and strain compatibility of the two types of material, (2) constrictive wrap buckling strength of the metal shell, (3) prestress set up between the two materials during fabrication and proof-testing (sizing), (4) effects of prestress into the plastic region of the metal shell, (5) thermal contraction characteristics of the various construction materials, and (6) effects of cyclic and sustained loading on fatigue life and residual strength. Special attention areas include insuring (1) metal compressive stress at zero pressure after proof test does not exceed compressive yield, (2) metal shell compressive strength is adequate so that adhesive bonding is not required to prevent metal shell buckling, (3) design allowable operating stresses are not exceeded in the metal or overwrap at operating pressure, and (4) required burst factor of safety is provided prior to exceeding metal shell biaxial ductility capability. These criteria fix relative thicknesses of the metal and overwrapped composite structure. In general, the metal liner thickness ends up being 25 to 50% of the thickness required for a homogeneous metal vessel design.

2. Establishment of Designs

To develop filament-reinforced metal tank designs, filament safe-operating stress levels are used in conjunction with the metal shell safe-operating stress level to develop a configuration which makes maximum use of these allowable stresses at operating pressure and also which provides the required pressure vessel burst strength within material minimum ultimate strength capabilities. Since the minimum weight pressure vessel is the one with least metal, weight minimization dictates making the liner as thin as possible consistent with filament-reinforced metal tank design criteria. This means letting the metal have maximum allowable compression at zero pressure and maximum allowable operating stress at operating pressure and temperature. Design development entails parametric studies of constituent material stresses at conditions of interest and resultant weight for given operating and burst pressures.

For the composite windings, allowable stresses at operating and ultimate conditions are determined from subscale filament-wound pressure vessels subjected to cyclic fatigue, sustained loading, temperature, burst, etc., evaluation tests.

For liner design, yield and ultimate strength levels are established from handbook data, simple uniaxial specimens and in some cases from subscale pressure vessels. Allowable operating stresses are determined from fracture data for the specific alloy, thickness, and design conditions, as described below.

3. Fracture Mechanics of Metal Liner

The proof test fracture mechanics approach to pressure vessel design is a reverse process analysis. First, the flaw size in the metal liner that will cause vessel failure $(a/Q)_{cr}^*$ is determined from K_{IE}/σ_o curves; K_{IE} is the fracture toughness of the material and σ_o is the desired operating stress in the liner. Then, with a vessel requirement of N pressure cycles, cyclic flaw growth rates da/dN are used to determine the maximum size flaw

*Refer to Appendix J for complete definition of symbols.

that could exist prior to the first pressure cycle $(a/Q)_i$ without growing to failure during the vessel life, i.e., $(a/Q)_i = (a/Q)_{cr} - N da/dN$. The proof test stress condition is then set as $\alpha \cdot \sigma_0$ such that no flaw larger than $(a/Q)_i$ can exist after the proof test. This procedure must, of course, be modified by considering the instantaneous stress intensity K which changes as a function of a/Q as the flaw size increases during cycling. A detailed analysis of the procedures may be found in Reference 1.

Filament-reinforced pressure vessels undergo a sizing pressurization after fabrication as has been previously discussed. The metal liner is stressed beyond the yield stress in order to establish prestress and elastic load sharing between the liner and filament overwrap. Thus, the sizing cycle acts as an extremely efficient proof test of the metal liner since it is subjected to a stress well above yield ($\alpha \cdot \sigma_0$ is large). Smaller flaws can be screened than by normal proof testing of homogeneous metal pressure vessels which are normally not stressed beyond the elastic limit.

Unfortunately, an acceptable fracture mechanics analysis has not been developed for post-yield stresses. One must empirically determine the stress versus flaw size relationship in this region. This data establishes the maximum initial flaw size screened by the sizing cycle. One also needs service life data obtained from specimens which were first stressed to the verge of failure, (i.e., containing a nearly critical initial flaw) and then subjected to the service life conditions at a range of lower stresses. For establishing critical failure conditions at the operating stress, conventional linear-elastic fracture mechanics analysis can be applied since operating conditions are always within the elastic limit of the metal liner. In some cases, the operating stress may be greater than the original material yield strength, but the yielding which occurred during the sizing cycle work-hardened the material and increases the effective yield strength of the material.

The validity of this analysis was recently documented by Boeing/SCI under NASA-LeRC Contract NAS 3-14380; results are summarized in Reference 1. The program was designed to establish a fracture control method which would guarantee safe service life for composite tanks with load sharing liners. Given sizing stress and

cycle life requirement, data were generated for various flaw shapes (a/2c) to permit the following:

- Determination of size of surface flaw which causes liner failure during sizing operation
 - Generate failure stress versus flaw depth curve
 - Establish maximum initial flaw size that did not cause failure at given sizing stress
- Determination of maximum allowable operating stress for required cycle life
 - Generate cyclic stress versus cycles to failure curve for maximum initial flaw size
 - Establish maximum allowable operating stress that did not cause failure before required cyclic life.

A detailed discussion of findings from the Reference 1 program is beyond the scope of this report. Briefly, both flawed uniaxial specimens and biaxial pressure vessels were tested to obtain static fracture and cyclic flaw growth data. The experimental evaluation by Boeing included investigation of different size flaws in 2219-T62 aluminum, Inconel X-750 (STA), and cryoformed 301 stainless steel at ambient and cryogenic temperatures. A most significant finding was that as R ratio (minimum stress/maximum stress) decreases from positive to negative values, the flaw growth rates increase. In addition, negative R ratio test results for uniaxial specimens did correlate well with the biaxial tank results, and the uniaxial data can be used to predict overwrapped tank cyclic life.

4. Failure Modes

In several past programs, the safety enhancement feature of composite tanks with load sharing metal liners has been vividly shown. Due to the relatively thin metal liner (compared to the wall thickness of a comparable homogeneous metal tank) and the

relatively thick overwrapped composite elastic restraint, leak-before-burst is enhanced. The failure of tanks during an intentional burst test or fatigue pressure cycling test is by leakage through the wall with no fragmentation of the metal. This composite pressure vessel characteristic maximizes personnel safety and mission success in critical applications involving compressed gas storage with minimum container weight. Additionally, the reduced metal thickness presents an option for selecting a tough material that in itself shows leak-before-burst characteristics.

B. PROGRAM PLAN

1. Program Objective

The objective of this program was to verify and show the advantages of overwrapped metal pressure vessels for future flight vehicles, as well as demonstrate the technology readiness and suitability of the vessels for the application. The vessels that were designed, fabricated and tested were to be of significantly lighter weight than competing monolithic metal vessels and also incorporate controlled failure mode (non-fragmenting) features.

2. Scope of Work

The program objectives were accomplished by conducting a three task technical effort as summarized below:

Task I- Design: This task covered the development of detailed designs, fabrication drawings, fabrication process specifications, and inspection procedures for two different configurations of Kevlar-49/epoxy composite-reinforced-metal-pressure vessels. The two designs (a) were spherical in shape and had the same cyclic life requirements, a burst factor of safety greater than 1.5, similar multiangular wrap patterns, but (b) utilized different metal liners (2219-T62 aluminum and cryoformed 301 stainless steel), operating and burst pressures, and vessel internal volumes.

Task II - Fabrication: This task included (a) fabrication and inspection of six complete liner assemblies for each of the two pressure vessels designs; (b) filament overwrapping and cure of the liner assemblies; and (c) instrumentation, inspection, and pressure sizing of the resultant vessels. Strains were recorded for each vessel during the application of the sizing cycle and the data submitted to NASA for evaluation.

Task III - Testing: This task included (a) the design, fabrication, procurement of required test hardware and instrumentation, and (b) the performance of burst, sustained loading, and cycle tests at ambient temperature on the twelve vessels fabricated and pressure-sized under Task II. The vessels were instrumented with strain-gauge rosettes, extensometers, and pressure sensors prior to testing.

II. DESIGN, FABRICATION, AND TEST OF KEVLAR-49 OVER-WRAPPED 2219 ALUMINUM PRESSURE VESSELS

A. CRITERIA DEVELOPMENT

The following paragraphs present applicable information obtained during the initial phase of this program which formulated the final criteria used to establish vessel designs, fabrication processes, and test requirements.

1. Initial Design Criteria

At the inception of the technical effort, the program objectives were to be accomplished utilizing two different design configurations of composite reinforced 2219 aluminum pressure vessels - an S-Glass filament reinforced (FR) spherical vessel, and a Kevlar-49 FR cylindrical vessel. The two designs were to have the same pressure, volume, operating temperature and cyclic life requirements, but were to incorporate different winding patterns which depended on each vessel's shape (sphere or closed-end cylinder). The specific initial criteria selected for establishing the two designs are summarized in Table I, and schematics of the preliminary configurations are shown in Figure 1.

Based on the preliminary design criteria, studies were initiated to (a) establish effects of fabrication processes on vessel design details, (b) parametrically evaluate vessel geometric details to provide weight optimized configurations, and (c) evaluate and apply concurrent fracture mechanics data being developed under NAS 3-14380 (Reference 1) to provide "safe-life" for the specified cyclic fatigue requirement. Results of the studies, which had an effect on selection of the final design criteria, are briefly discussed below.

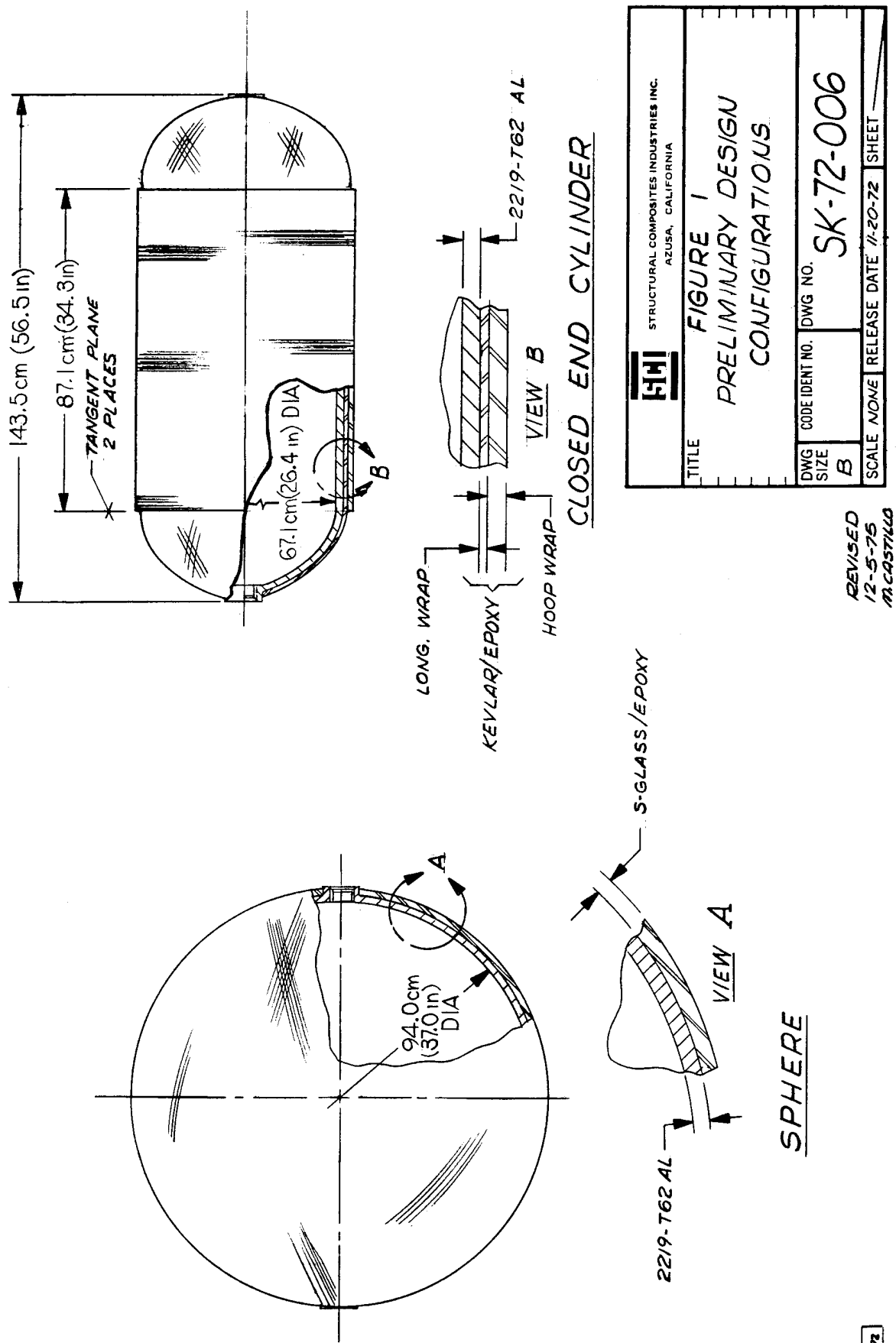
2. Metal Shell Fabrication Process Studies

a. Forming Methods

The various methods of forming pressure vessel heads were thoroughly investigated during precontract efforts and the initial design phase. It was concluded that deep drawing was generally advantageous over the forging or spinning methods in terms of controlling process variables, metallurgical and mechanical properties, and cost considerations. A primary reason machined

TABLE I
PRELIMINARY DESIGN CRITERIA
FOR OVERWRAPPED 2219 ALUMINUM PRESSURE VESSELS

<u>Parameter</u>	<u>Vessel 1</u>	<u>Vessel 2</u>
Volume,	$0.434 \text{ m}^3(26\ 500 \text{ in.}^3)$	$0.434 \text{ m}^3(26\ 500 \text{ in.}^3)$
Shape	Sphere	Closed-end cylinder with L/D = 2 and semi-oblate heads
Inside Diameter (nominal)	94.0cm (37.0 in.)	67.1cm (26.4 in.)
Overall Length (nominal)	96.5cm (38.0 in.)	143.5cm (56.5 in.)
Boss Openings	Two places, axially opposed	Two places, axially opposed
Materials	2219 aluminum S-glass/epoxy complete overwrap	2219 aluminum Kevlar-49/epoxy complete bidirectional overwrap
	117 to 344K (-250 to 160°F)	117 to 344K (-250 to 160°F)
Operating Temperature		
Pressure	1475 N/cm ² (2140 psi) to be determined	1475 N/cm ² (2140 psi) to be determined
Operating	2950 N/cm ² (4280 psi)	2950 N/cm ² (4280 psi)
Sizing		
Burst		
Operating Cyclic Life including Scatter Factor		
Pressure Cycles	690 to 1475 N/cm ² (1000 to 2140 psig) 0 to 1475 N/cm ² (2140 psig)	4000 1000
		4000 1000



HII		STRUCTURAL COMPOSITES INDUSTRIES INC.
AZUSA, CALIFORNIA		
FIGURE 1		
PRELIMINARY DESIGN		
CONFIGURATIONS		
DWG SIZE B	CODE IDENT NO. DWG NO.	SK-72-006
SCALE NONE	RELEASE DATE	11-20-72 SHEET

REVISED
12-5-75
MCASTLE

CASTLE 11-20-72

forgings were preferred over deep drawn heads, in spite of higher costs, concerned integral bosses. The integral boss feature permits the strain distribution in the boss-membrane transition region of filament reinforced metal tank heads to be more uniform during pressure testing. Loads in the metal shell are carried by homogeneous parent material unmarred by possible weld-associated strain discontinuities caused by mismatch, shrinkage, undercut, drop through, etc. Conventional drawn heads require welding separate bosses and the attendant risks involved.

However, the method selected for fabricating heads in this program eliminated this tradeoff, while achieving the best features of both machined forgings and draw formings. The method consists of draw forming the heads from starting blank plate material in which the boss configuration and membrane thickness has been premachined in the flat. Thus, the better microstructure, process control, and lower costs associated with deep drawing are retained, while incorporating the desired integral-boss feature of a machined forging. There is no expensive tracer or numerical controlled machining after deep drawing as is required on a forging to obtain the necessary contour and thickness. Also, the drawn heads made from annealed plate and formed at room temperature retain the wrought properties of plate as opposed to the larger grain size and variable microstructure of a forging (which is generally poorest at the equator where girth welding is to be performed).

A final draw is applied to "set" the shape precisely and minimize diameter mismatch for welding. After girth welding, the units are solution treated and aged to the -T62 condition. Forged heads would be in the -T6 or T852 condition after heat treatment and exhibit much lower transverse elongation than drawn heads in the -T62 condition. Comparative mechanical properties given in the Aloca Green Letter, Reference 2, are listed on the following page:

2219 Aluminum Alloy			
- T62 <u>Plate</u>	- T6 <u>Die Forging</u>	- T852 <u>Die Forging</u>	
Tensile Strength, MN/m² (ksi)			
Longitudinal	372 (54)	400 (58)	427 (62)
Transverse	372 (54)	386 (56)	414 (60)
Yield Strength, MN/m² (ksi)			
Longitudinal	248 (36)	262 (38)	345 (50)
Transverse	248 (36)	248 (36)	317 (46)
Elongation, %			
Longitudinal	8	8	6
Transverse	8	4	3

Based on the technical aspect of the preceding discussion and SCI's precontract proposal efforts, the deep draw process as outlined above was selected for forming the heads of both vessel configurations.

b. Thermal Treatment

Alloy 2219 is an age-hardenable alloy of aluminum with CuAl₂ as the sole precipitation hardener. The T62 temper, solution treated and age hardened, was selected for this configuration because of the excellent weld efficiency, approaching 100 percent that of the parent metal. Alcoa recommends a solution treatment of 808 K (995°F) and cold water quench followed by aging at 464K (375°F) for 36 hours to yield the T62 temper. However, to be consistent with concurrent fracture mechanics studies (Reference 1), it was decided to employ the T62 temper parameters recommended by Boeing Specification BAC5602 which differs only in that a 96 hour natural age precedes the artificial age treatment.

In order to minimize part distortion during the above heat treatment, it is necessary to control the quench delay time.

The quench delay period begins when the first corner of the part emerges from the solution treatment bath and ends when the last corner of the part is immersed in the quench fluid. Boeing Specification BAC5620 prescribes a 25 second maximum quench delay period for material thicknesses greater than 0.635cm (0.250 inch). In order to insure that the allowable quench period was not exceeded for the present application, a flow rate versus tank port diameter study was initiated.

The volume of both the spherical and cylindrical tanks, defined by the initial criteria, was 434 liters (115 gallons); the corresponding weight of the spherical aluminum shell was approximately 52.2 kg (115 pounds). Two "55 gallon drums" were welded together to form a test specimen which met volume and weight requirements (approximately 114 gallons and 85 pounds). Each end of the test specimen had provision for varying the port opening from 7.6 to 10.2cm (3 to 4 inch) diameters. The test specimen was set up in the actual heat treat area (specified for use during the program) and the quench process simulated for the 7.6 and 10.2cm (3 and 4 inch) port diameters. The following table lists the results:

Port Diameter, D_p <u>cm (inch)</u>	Port Area, A_p <u>cm² (inch²)</u>	Time to Fill <u>(second)</u>	Average Flow	
			Rate, \bar{Q} <u>liters/sec</u> (gal/second)	\bar{Q} / A <u>liters sec⁻¹ cm⁻²</u> (gal. sec ⁻¹ in ⁻²)
7.6 (3.0)	45.6 (7.07)	72	5.98 (1.58)	0.131 (0.223)
10.2 (4.0)	81.3 (12.6)	40	10.8 (2.85)	0.133 (0.226)

Based on an extrapolated \bar{Q} / A value 0.135
liters sec⁻¹ cm⁻² and a required flow rate of

$$\bar{Q} = 434 \text{ liters} / 25 \text{ second} = 17.37 \text{ liters/sec} (4.60 \text{ gal/sec}),$$

the necessary port diameter was calculated to be

$$D_p = \left[\frac{4\bar{Q}}{\pi(\bar{Q}/A)} \right]^{1/2} = 12.8 \text{ cm (5.04 in)}$$

It was concluded from this study that 12.8cm (5 in) I.D. ports were required for both the spherical and cylindrical vessels.

3. Design Optimization Studies

In order to establish weight-optimized designs for both the S-Glass overwrapped sphere and the Kevlar overwrapped cylindrical vessel, parametric studies were conducted to fix composite and metal shell thicknesses and stresses. The methods defined in Reference 3 were used to establish the design variables, and calculations were performed using the NASA Computer Program, Reference 4. Properties of the 2219-T62 aluminum, S-901 glass filaments and Kevlar 49 filaments were reviewed and revised (where necessary) to reflect design service requirements and recent data generated on "in-house" programs. Resultant design properties used in the parametric studies for the aluminum are presented in Table II, and allowable filament stresses for both fibers are presented in Table III. The following table lists values for significant parameters associated with each of the resultant preliminary designs:

<u>Parameter</u>	<u>Glass Filament Reinforced Sphere</u>	<u>Kevlar Filament Reinforced Cylinder</u>
Metal Shell Thickness, cm (inch)	0.635 (0.250)	0.833 (0.328)
Composite Wall Thickness, cm (inch)	0.719 (0.283)	0.808 (0.318)
Cylinder Hoop, cm (inch)	--	0.612 (0.241)
Cylinder Longo, cm (inch)	--	0.196 (0.077)
Ambient Sizing Pressure, N/cm ² (psi)	2082 (3020)	2273 (3296)
Ambient Sizing Stress in metal shell, MN/m ² (ksi)	317 (45.9)	325 (47.2)
Operating Pressure, N/cm ² (psi)	1475 (2140)	1475 (2140)
Operating Stress in Metal Shell, MN/m ² (ksi) at 297K (+ 70°F)	145 (21.0)	178 (25.8)
at 344K (+ 160°F)	134 (19.5)	165 (24.0)
at 117K (- 250°F)	186 (27.0)	252 (36.5)
Minimum Burst Pressure, N/cm ² (psi)	2950 (4280)	2950 (4280)

TABLE II

PROPERTIES OF ALUMINUM ALLOY 2219-T62^a
USED FOR PRELIMINARY DESIGN

Property	Temperature, K (°F)		
	117 (-250)	297 (75)	409 (160)
Density, g/cm ³ (1bm/in. ³)	--	2.82 (0.102)	--
Coefficient of thermal expansion, μ / K (in/in/°F x 10 ⁻⁶)			
297 to 78 K (75 to -320 °F)	--		
293 to 373 K (68 to 212 °F)(b)		16.05 (8.915) 22.3 (12.4)	--
Tensile yield strength, MN/m ² (ksi)			
Parent metal			
Typical	358 (51.9)	293 (42.5)	276 (40.0)
Minimum(b)	278 (40.3)	248 (36.0)	239 (34.6)
Weld metal			
Typical	358 (51.9)	293 (42.5)	276 (40.0)
Minimum(b)	278 (40.3)	248 (36.0)	239 (34.6)
Tensile ultimate strength, MN/m ² (ksi)			
Parent metal (minimum)(b)	421 (61.0)	372 (54.0)	361 (52.4)
Weld metal (minimum)(b)	404 (58.6)	357 (51.8)	347 (50.3)
Elastic Modulus, GN/m ² (psi x 10 ⁶)	--	72.4 (10.5)	--
Plastic Modulus, GN/m ² (ksi)	--	2.76 (400)	--
Poisson's Ratio	--	0.325	--
Compressive Stress (90% of yield), MN/m ² (ksi)	--	269 (39.0)	--

^a Reference 1, except as noted^b MIL-HDBK-5 "A", Reference 5

TABLE III

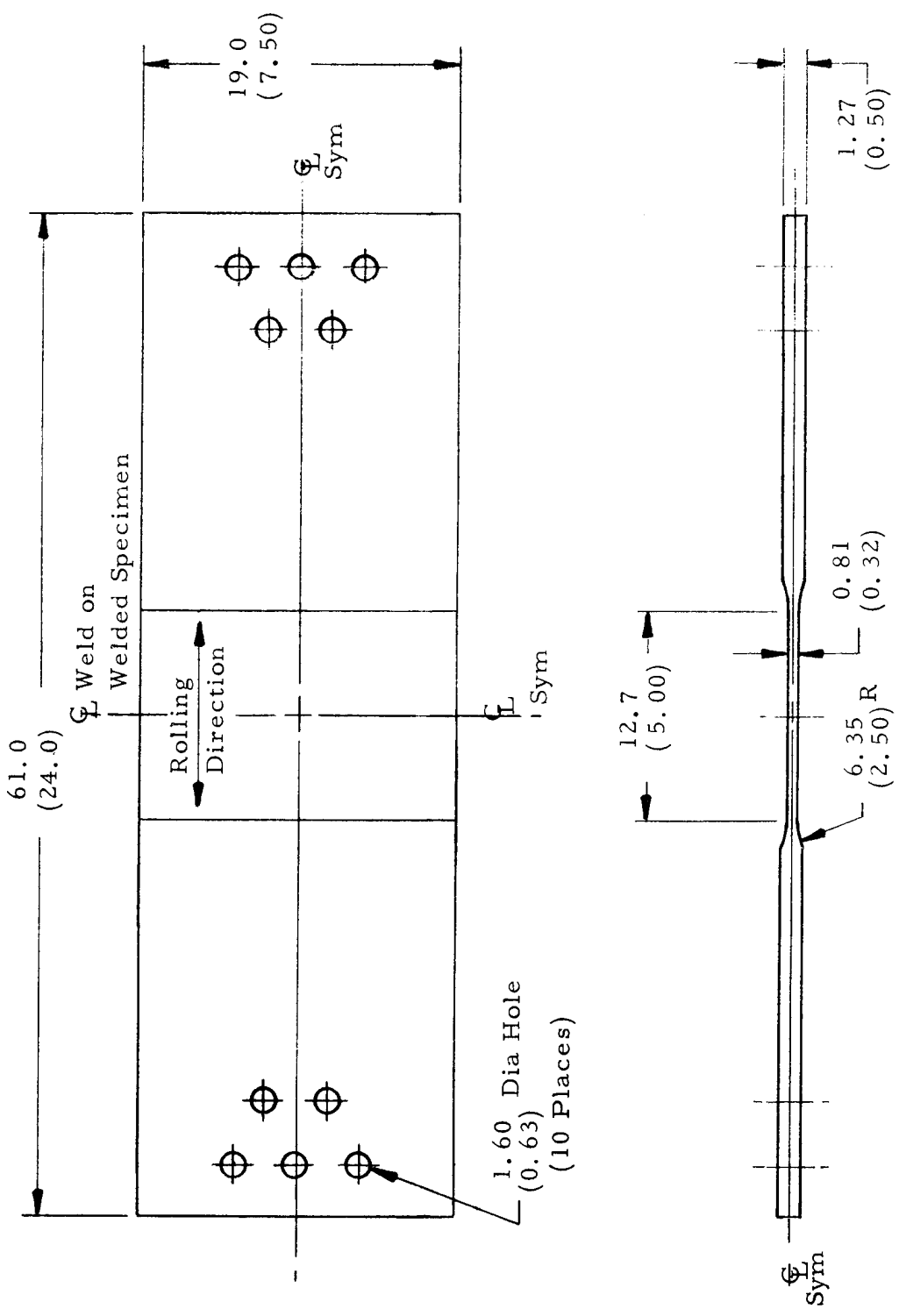
SUMMARY OF ULTIMATE DESIGN ALLOWABLE
FILAMENT STRESSES FOR PRELIMINARY DESIGNS

Minimum Projected Design Allowable, MN/m ² (ksi)	Temperature, K (°F)		
	78 (-320)	297 (75)	344 (160)
S-901 Glass/epoxy			
Hoop Filaments	2830 (410)	2260 (328)	2230 (324)
Longitudinal Filaments	2560 (372)	2050 (297)	1970 (286)
Average	2700 (391)	2150 (312)	2100 (305)
Kevlar-49			
Hoop Filaments	2100 (305)	2100 (305)	1880 (272)
Longitudinal Filaments	1720 (250)	1720 (250)	1680 (243)
Average	1920 (278)	1920 (278)	1780 (258)

Ambient operating stress levels in the metal shells (defined in the above table) were compared to the allowable values extrapolated from cyclic flaw growth data reported in Reference 1. In both cases, the cyclic life data indicated the design operating stress σ_0 had to be further decreased to a value of 138 MN/m^2 (20.0 ksi) to meet the minimum design cyclic life. The primary cause for the low value for allowable operating stress was the conservative approach which had to be used to extrapolate the cyclic life data from the known 0.457cm (0.180 inch) metal thickness value to values corresponding to preliminary design thickness requirements. Based on these results and their effects on vessel weight, more fracture data was required in this thickness range to eliminate excessive conservatism.

In order to supplement the existing service life data reported in Reference 1, two 0.813cm (0.32 inch) thick 2219-T62 aluminum uniaxial surface flawed (flaw shape ~ 0.20) specimens were fabricated by SCI and tested by The Boeing Company to determine the failure loci and fatigue flaw growth rates for the thicker base metal (BM) aluminum material. One of the 61-cm-long by 19-cm-wide (24-inch-long by 7.5-inch-wide) specimens is shown in Figure 2. The static fracture test result is shown in Figure 3 along with the 0.229 and 0.457cm (0.090 and 0.180 inch) thick base metal results from Reference 1. This specimen was loaded directly to failure at ambient temperature. Figure 4 shows the fatigue flaw growth rates obtained from the cyclic specimen tested in addition to data from Reference 1 for the 0.229 and 0.457cm (0.090 and 0.180 inch) thick results. This specimen was first sized to a stress, σ_s , of 317 MN/m^2 (45.9 ksi) and then cycled to flaw breakthrough at 207 MN/m^2 (30 ksi) and ambient temperature. The cyclic test was conducted at a $\sigma_{\min}/\sigma_{\max}$ (R ratio) of zero and a test frequency of 60 cpm. It appeared from the results presented in Figure 4 that the fatigue flaw growth rates for the 0.813cm (0.320 inch) thick material were essentially equal to the 0.457cm (0.180 inch) thick results.

The preceding test results and those reported in Reference 1 were used to determine the maximum flaw that could exist in the liner after sizing. It was assumed that this flaw then grows due to the operating cycles until it penetrates the liner thickness. The flaw growth rates presented in Figure 4 and Reference 1 were then used to determine the number of cycles required for the flaw to grow through-the-thickness. Allowances were made for the base metal and weld metal, R ratio effects and temperature effects.



DIMENSIONS GIVEN IN CENTIMETERS (INCHES)

FIGURE 2: 2219-T62 Aluminum Uniaxial Fracture Specimen

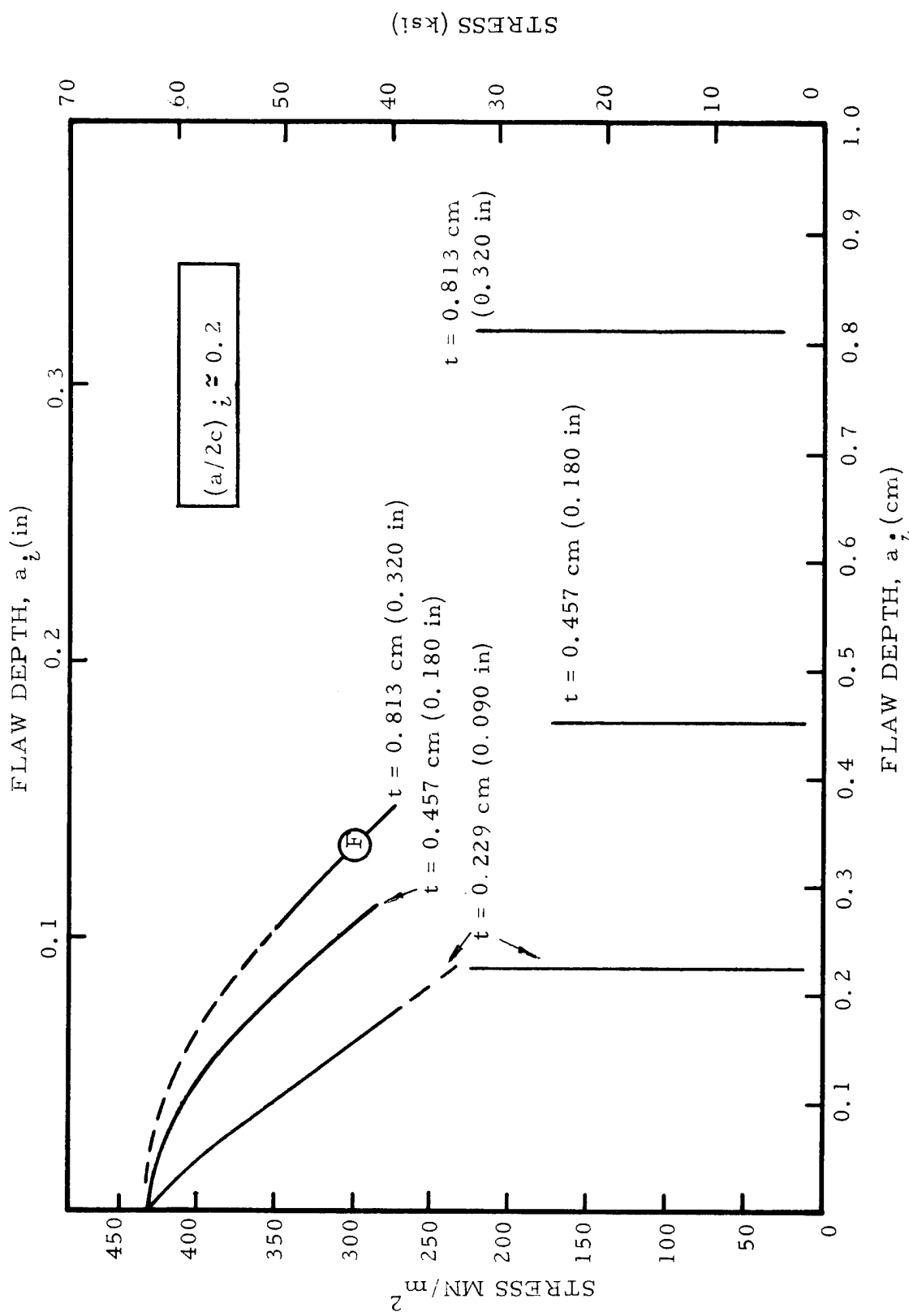


FIGURE 3: Uniaxial 2219-T62 Aluminum Base Metal,
Ambient Temperature Failure Locus

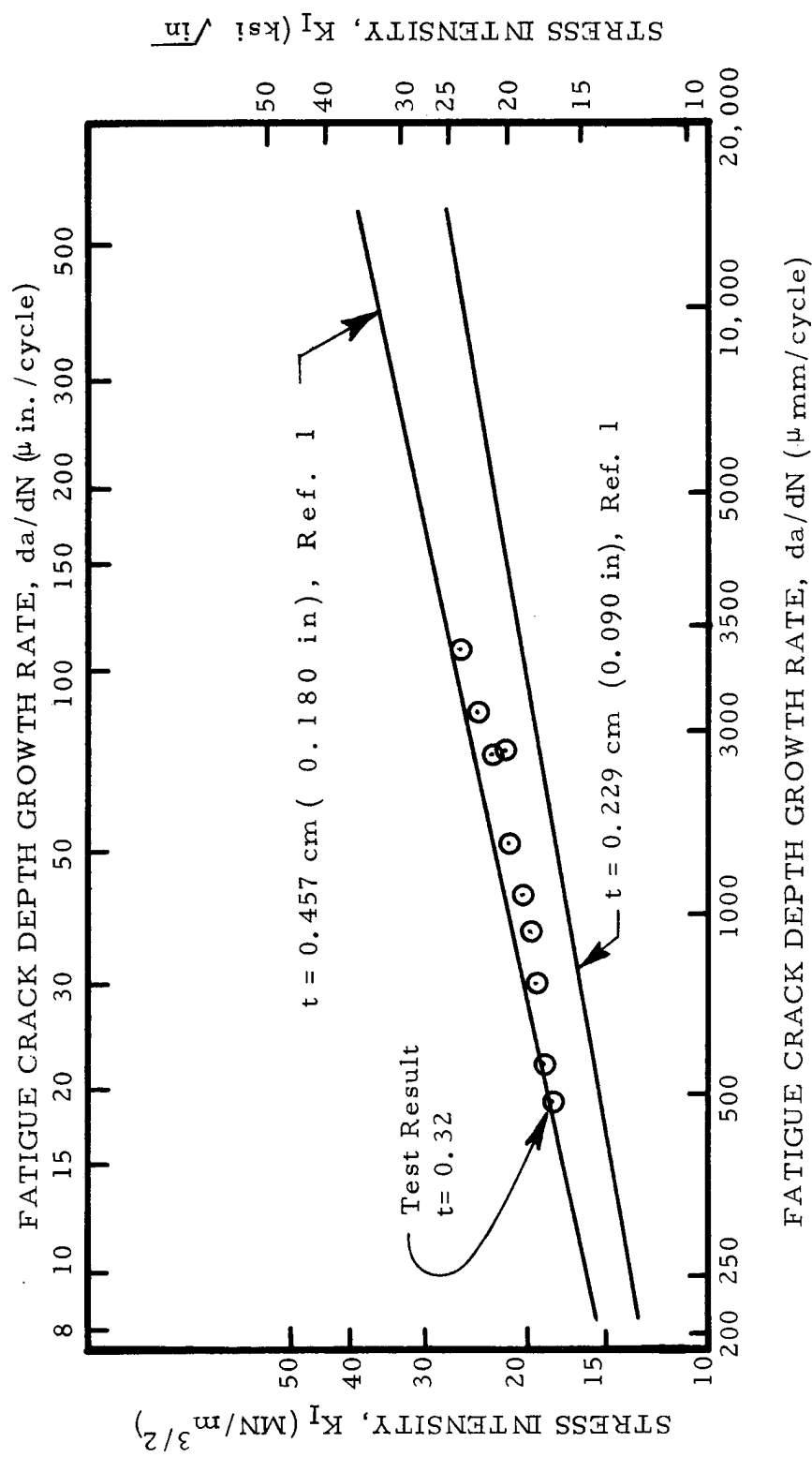


FIGURE 4: Fatigue Crack Growth Rates for 2219-T62 Aluminum
Base Metal at Ambient Temperature

Results of the analysis are presented in Tables IV and V, in terms of number of cycles to leakage, for the preliminary Glass FR sphere and Kevlar FR cylinder designs, respectively. Inspection of the values for cycle life over the temperature range indicated design adjustments had to be made to provide full required cyclic life capability (1000 full pressure cycles and 4000 partial pressure cycles per Table I).

4. NASA Redirection

At this point in the technical effort the original work statement for this program was being reevaluated by NASA to insure that program objectives reflected current space program requirements (i.e. necessity for increased weight reduction and changes in design factors of safety and pressure cycling requirements). Concurrent with the NASA evaluation, an additional parametric study was conducted by SCI to further optimize vessel designs under evaluation on this program. Previous optimization studies had indicated Kevlar fibers in combination with the spherical shape resulted in the greatest weight saving potential; thus, a Kevlar FR 2219-T62 aluminum sphere was selected as a study focal point. Data trends were established which related vessel weight, burst factor of safety and operating conditions in the aluminum and Kevlar overwrap. These curves, Figures 5 through 7,* were then used to establish values for cycle life dependent parameters for a representative number of specific design points. These data were then transmitted to The Boeing Company, prime contractor on Contract NAS 3-14380, for their use in establishing the corresponding cycle life (based on fracture control) for each design point.

An extensive detailed analysis of the various data was conducted to establish the further relationship between vessel weight, burst factor of safety, and vessel cycle life guaranteed by the proof (sizing) test. Based on the general data a specific design point was selected and, with NASA approval, a detailed preliminary design analysis, engineering drawings, and a metal shell fabrication specification were prepared and sent to NASA to aid in their evaluation. The table on page 30 lists significant parameters associated with the preliminary Kevlar FR aluminum sphere design:

*See List of Symbols, Appendix J

TABLE IV
LIFE ANALYSIS SUMMARY FOR PRELIMINARY
S-GLASS OVERWRAPPED ALUMINUM SPHERE DESIGNS

Thickness, cm (Inch)	Material Condition (b)	Sizing Stress, MN/m ² (ksi)	Operating Stress, MN/m ² (ksi)	Stress at Zero Pressure, MN/m ² (ksi)	Maximum Operating Pressure, N/cm ² (psi)	Temperature, K (°F)	Cycle Life (a)
0.635 (0.25)	Base Metal BM	317 (45.9)	145 (21.0)	273 (-39.6)	1476 (2140)	Ambient	5323(c)
	Weld Metal, WM		179 (25.9)	273 (-39.6)	1476 (2140)	78 (-320)	22 800

a 80% of the cycles; 690 to 1476 N/cm² (1000 to 2140 psi)
20% of the cycles; 0 to 1476 N/cm² (0 to 2140 psi)

b WM data base not as firm as BM

c BM critical if operated at RT

d WM critical if operated at 78 K (-320°F)

TABLE V

LIFE ANALYSIS SUMMARY FOR PRELIMINARY
KEVLAR OVERWRAPPED ALUMINUM CYLINDER DESIGNS

Thickness cm (Inch)	Stress Direction	Material Condition (b)	Sizing Stress MN/m ² (ksi)	Operating Stress, MN/m ² (ksi)	Stress at Zero Pressure, MN/m ² (psi)	Maximum Operating Pressure, N/cm ² (psi)	Temperature K (°F)	Cycle Life (a)
(0.833)	Hoop	Base Metal, BM	325 (47.2)	126 18.3	243 -35.3	1476 (2140)	RT	10 230
				252 36.5	123 -17.8	1476 (2140)	78 (-320)	3880(d)
		Weld Metal WM	325 (47.2)	252 36.5	123 -17.8	1476 (2140)	78 (-320)	3760(d)
	Long	Base Metal, BM	322 (46.7)	178 25.8	88.3 -12.8	1476 (2140)	RT	4630(c)
				241 35.0	26.9 -3.9	1476 (2140)	78 (-320)	Not Critical

a 80% of the cycles at 690 to 1476 N/cm² (1000 to 2140 psi);
20% of the cycles at 0 to 1476 N/cm² (0 to 2140 psi)

b WM data base not as firm as BM

c BM longo, critical if operated at RT

d BM and WM, Hoop critical if operated at 78 K (-320°F)

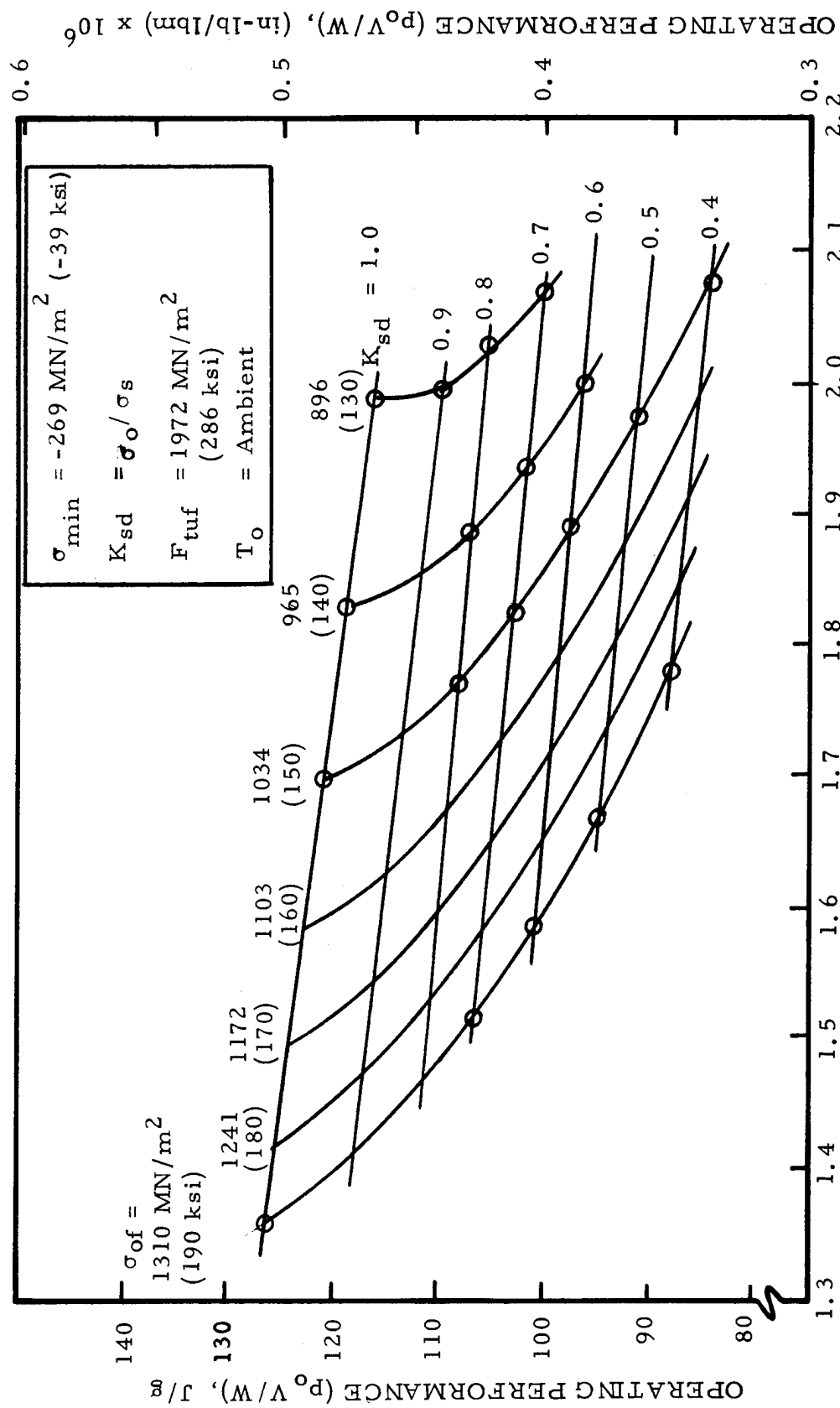


FIGURE 5: Design Performance Curves for Kevlar FR 2219-T62 Aluminum Spheres

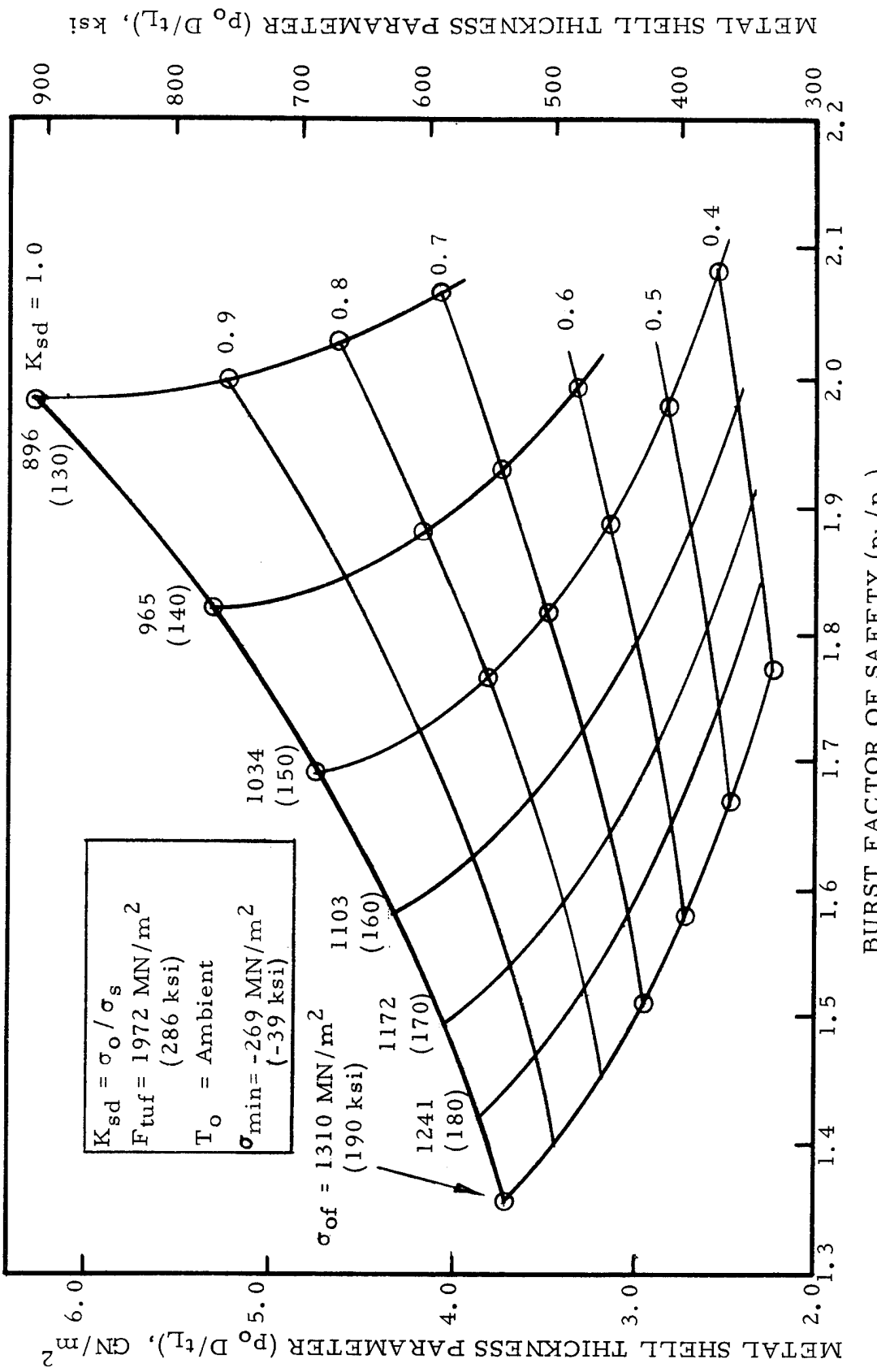


FIGURE 6: Design Metal Shell Thickness Curves For
Kevlar FR 2219-T62 Aluminum Spheres

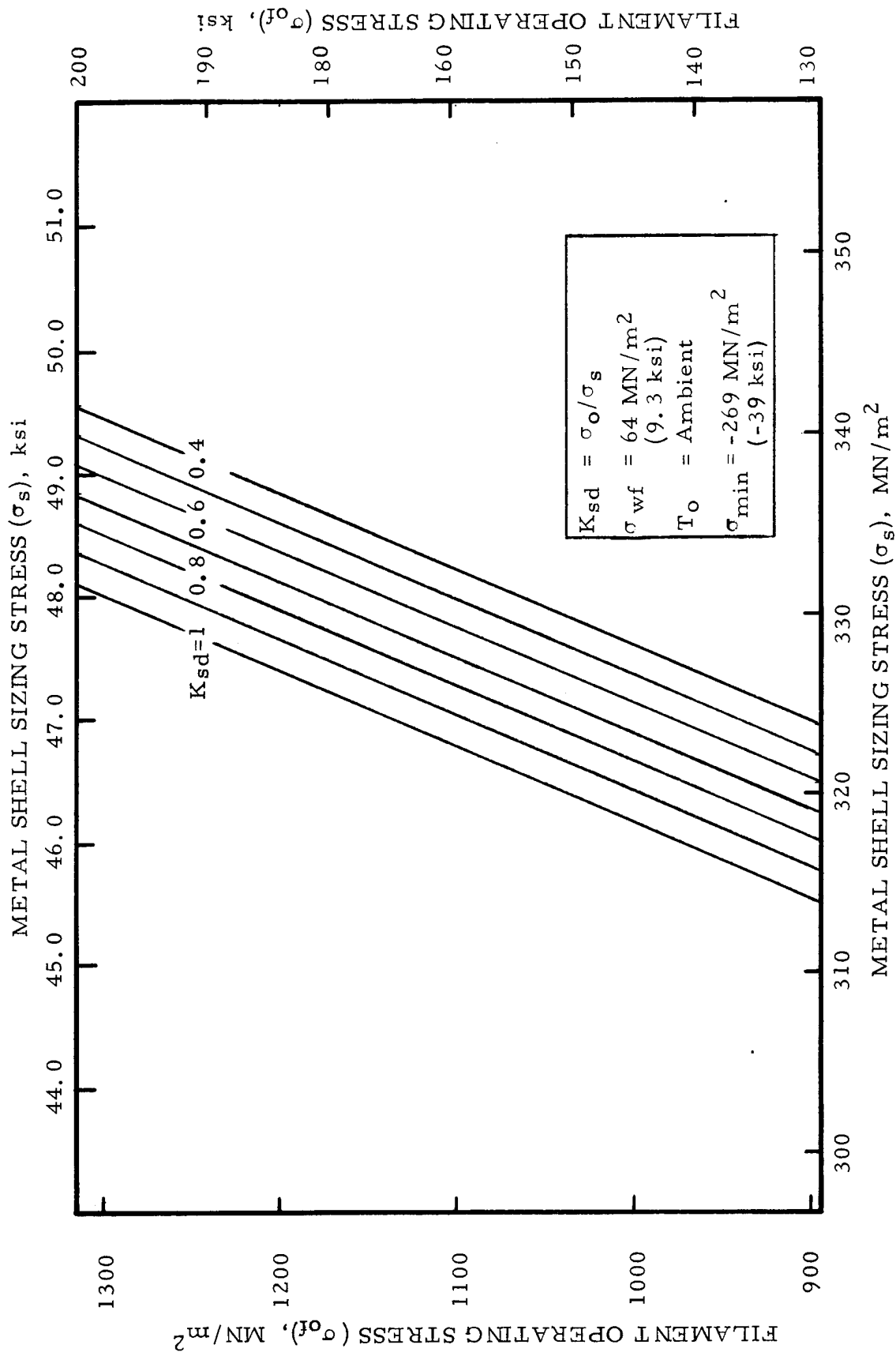


FIGURE 7: Design Stress Chart For
Kevlar FR 2219-T62 Aluminum Spheres

<u>Parameter</u>	<u>Value</u>
Vessel Weight (W)	54.4 kg (120 lbm)
Internal Volume (V)	0.434 m ³ (26 500 in ³)
Burst Pressure (p _b)	2206 N/cm ² (3200 psi)
Burst Factor of Safety	1.5
Operational Cycles Guaranteed by Proof Test.	418
Sizing Pressure	1586 N/cm ² (2300 psi)
Aluminum Sizing Stress	330 MN/m ² (47.9 ksi)
Aluminum Operating Stress.	288 MN/m ² (41.7 ksi)
Filament Operating Stress	2230 MN/m ² (178 ksi)
Aluminum Shell Thickness	0.390cm (0.154 inch)
Kevlar/epoxy Composite Thickness	0.615cm (0.242 inch)
Burst Performance Factor, p _b V/W	174 J/g (697 000 in-lb/lbm)

Based on NASA's reevaluation of program objectives coupled with the weight reduction associated with the above sphere design, the program scope of work was revised to provide for a Kevlar FR aluminum sphere design. Additionally, the design effort on the Kevlar FR aluminum cylindrical vessel was terminated; this vessel was replaced by a more efficient Kevlar FR cryoformed 301 stainless steel sphere. The tasks of designing the Kevlar/stainless steel pressure vessel and fabrication of the required metal liner assemblies were delegated to ARDE, Incorporated and are further discussed in Section III of this report. Final design criteria for the two Kevlar FR metal spheres are contained in Table VI. All further discussions contained in this section (II) of the report address the Kevlar/aluminum sphere only.

TABLE VI
FINAL PRESSURE VESSEL DESIGN CRITERIA

<u>Parameter</u>	<u>Vessel 1</u>	<u>Vessel 2</u>
Volume	$0.434 \pm 0.008 \text{ m}^3 (26.500 \pm 500 \text{ in}^3)$	$0.123 \pm .008 \text{ m}^3 (7500 \pm 500 \text{ in}^3)$
Shape	Sphere	Sphere
Outside Diameter (nominal)	96.5 cm (38.0 in.)	63.5 cm (25.0 in.)
Overall Length (nominal)	99.1 cm (39.0 in.)	66.0 cm (26.0 in.)
Boss Opening Inside Diameter (2 places axially opposed)	12.7 cm (5.00 in.)	1.91 cm (0.75 in.)
Materials	2219-T62 Aluminum Kevlar-49/ epoxy Axisymmetric, Multiangular	Cryoformed 301 stainless steel Kevlar-49/epoxy Axisymmetric, Multangular
Operating Temperature	Ambient	Ambient
Pressure	1240 to 1450 N/cm ² (1800 to 2100 psi) To be determined	1380 to 1725 N/cm ² (2000 to 2500 psi) To be determined
Operating (p _o)	$> 1.5 \text{ p}_o$	$> 1.5 \text{ p}_o$
Sizing		
Burst		
Operating Cyclic Life (0 to p _o) ^a	400 Minimum	400 Minimum

^aService requirement is 400 cycle life, but vessels are to be subjected to 1600 pressure cycles (400 cycles x scatter factor of 4) during qualification.

B. DESIGN

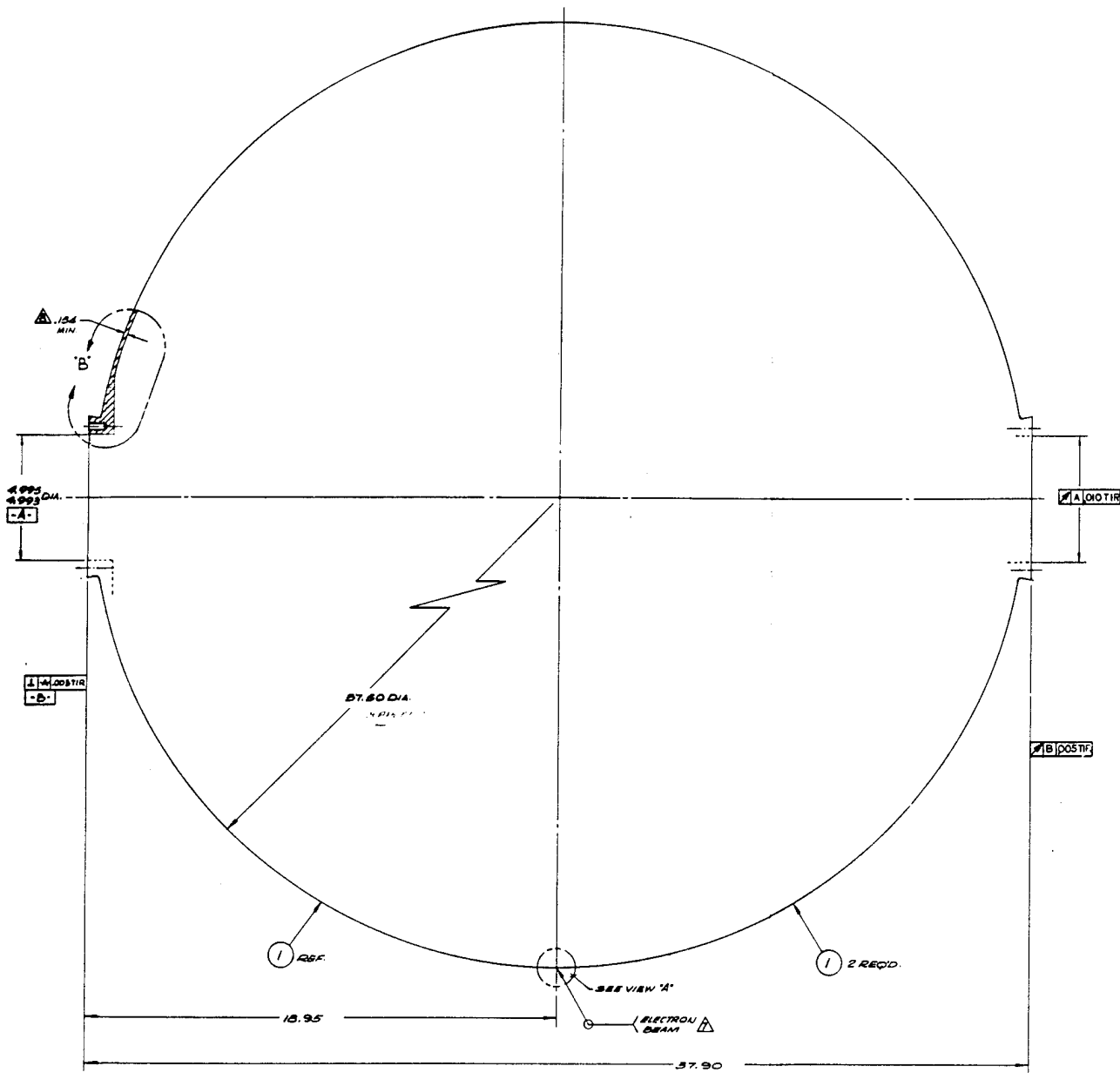
The Kevlar FR aluminum vessel is fabricated from an impermeable, load-bearing 2219-T62 aluminum alloy liner that is solution-treated and aged and subsequently overwrapped with epoxy impregnated Kevlar-49 roving and cured. After fabrication, the vessel is pressure-sized/proof-tested at ambient temperature to obtain the desired shell prestresses and screen preexisting flaws in the metal-shell.

Final design of this vessel was based on the fabrication process studies, design optimization studies, and the final design criteria (Table VI) discussed in Section II A. Material allowables, vessel membrane and boss analyses, cycle-life calculations, and winding pattern details are contained in the design analysis included as Appendix A. Engineering drawings of the 2219-T62 aluminum liner assembly (Part Number 1269381) and the Kevlar FR spherical vessel (Part Number 1269382) are shown in Figures 8 and 9, respectively.

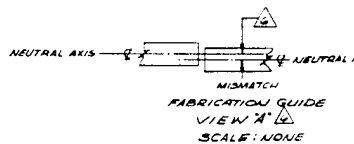
As noted in Appendix A, the design analysis was based on minimum thicknesses of 0.391cm (0.154 inch) and 0.711cm (0.280 inch) for the aluminum and Kevlar/epoxy shells, respectively. Based on the shell thickness tolerances shown in Figures 8 and discussed in Appendix A, the expected average thicknesses for the aluminum and Kevlar/epoxy shells were determined to be 0.439 and 0.787cm (0.173 and 0.310 inches), respectively. Since the behavior of the vessel during performance testing can be better approximated using average rather than minimum thickness values, the design of Appendix A was re-analyzed to obtain pressure/stress values based on the average thickness values. Table VII (from Appendix A) presents a summary of the mechanical properties used for the design analysis. A summary of final vessel design parameters for the Kevlar/aluminum vessel is given in Table VIII. The resultant vessel design stress-strain relationship is presented in Figure 10, and the design pressure versus strain curve is presented in Figure 11. Greater detail may be found in the Sizing Test Procedure included as Appendix B.

Two additional documents which were established under this design task and subsequently approved by NASA are the Metal Shell Fabrication Specification and the Composite Process Procedure included as Appendices C and D, respectively. These documents are discussed in the following section.

ZONE	LTR	DESC
	A	SEE OCN
	B	SEE OCN
	C	SEE OCN



0.75 DIA. (REF.



2	-2	SHELL	1&2 THK PL 2215 AL
1-1 (RTW#)	SYM CODE IDENT	PART OR IDENTIFYING NO.	NOMENCLATURE OR DESCRIPTION
LIST OF MATERIALS			
UNLESS OTHERWISE SPECIFIED			
DIMENSIONS ARE IN INCHES		TOLERANCE OR DECIMALS	
SIMILAR TO		AS: 2"	
JOGS & DRAWS			
DO NOT SCALE DRAWING			
TREATMENT			
FINISH			
SIMILAR TO ACT. W/TODAY WT.			
CONTACT NO. 2003		DRAWN BY C. SWAMBO DATE 9/15/73	
DESIGNER J. L. COLEMAN DATE 5-22-73		EFFECTIVE DATE G-20-73	
MATERIALS 100% ALUMINUM DATE 6/24/73		PREPARATION	
DESIGN ACTIVITY APPD J. L. COLEMAN DATE 6/24/73		DRAFTS B/E CODE IDENT E/B 00625	
SUBSCRIBER		SCALE 1/2" 1"	

1

4

3

2

1

REVISIONS		DATE APPROVED	
ZONE	LTR	DESCRIPTION	
	A	SEE OCN	2-3-23
	B	SEE OCN	10-22-23
	C	SEE OCN	5-6-23

1

G

F

三

9

1

57.50 DIA.

1 Page

- 18.95

4

11

2

1

2	- 2	SHELL	1/8" THK PLATE 2219 AL. ALY.	AMB-4051		1			
QTY NEEDED	SYN CODE IDENT	PART OR IDENTIFYING NO.	NOMENCLATURE OR DESCRIPTION	MATERIAL	SPECIFICATION	UNIT WT.	ZONE	ITEM NO.	
LIST OF MATERIALS									
UNLESS OTHERWISE SPECIFIED DIMENSIONS ARE IN INCHES TOLERANCES .005 UNLESS INDIVIDUALS XX = .03 XXX = .010 DO NOT SCALE DRAWING			CONTRACT NO. 2005	MANUFACTURER G-77-73	STRUCTURAL COMPOSITES INDUSTRIES INC. ALUMINA CALIFORNIA				
TREATMENT			DESIGNER G-22-73	DESIGNER G-29-73	TITLE LINER ASSEMBLY				
FINISH			STRUCTURE G-29-73	STRUCTURE G-29-73	2219-T62 AL. ALY				
PART NUMBER			PRODUCER G-74-72	PRODUCER G-74-72	SPHERE				
NEXT ASSY USED ON			ARMED ACTION NO. 1/18/73	ARMED ACTION NO. 1/18/73	DRAW. NO. SW625				
APPLICATION			SIZE E	CODE IDENT NO. 1269381	REL. DATE 6-28-73				
DRAWING LEVEL			SCALE 1/2	SNLCT					

8

7

6

H

G

F

E

D

C

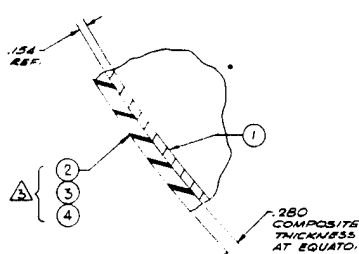
B

A

NOTES:
1. REMOVE ALL BURRS AND SHARP EDGES
2. INTERPRET DRAWINGS PER MIL-D-4500
3. APPLY WINDINGS AND PROCESS PER
SCI SHOP ORDER 1269382-1

(1)

35



SECTION A
SCALE 1:1

(6)

7

6

5

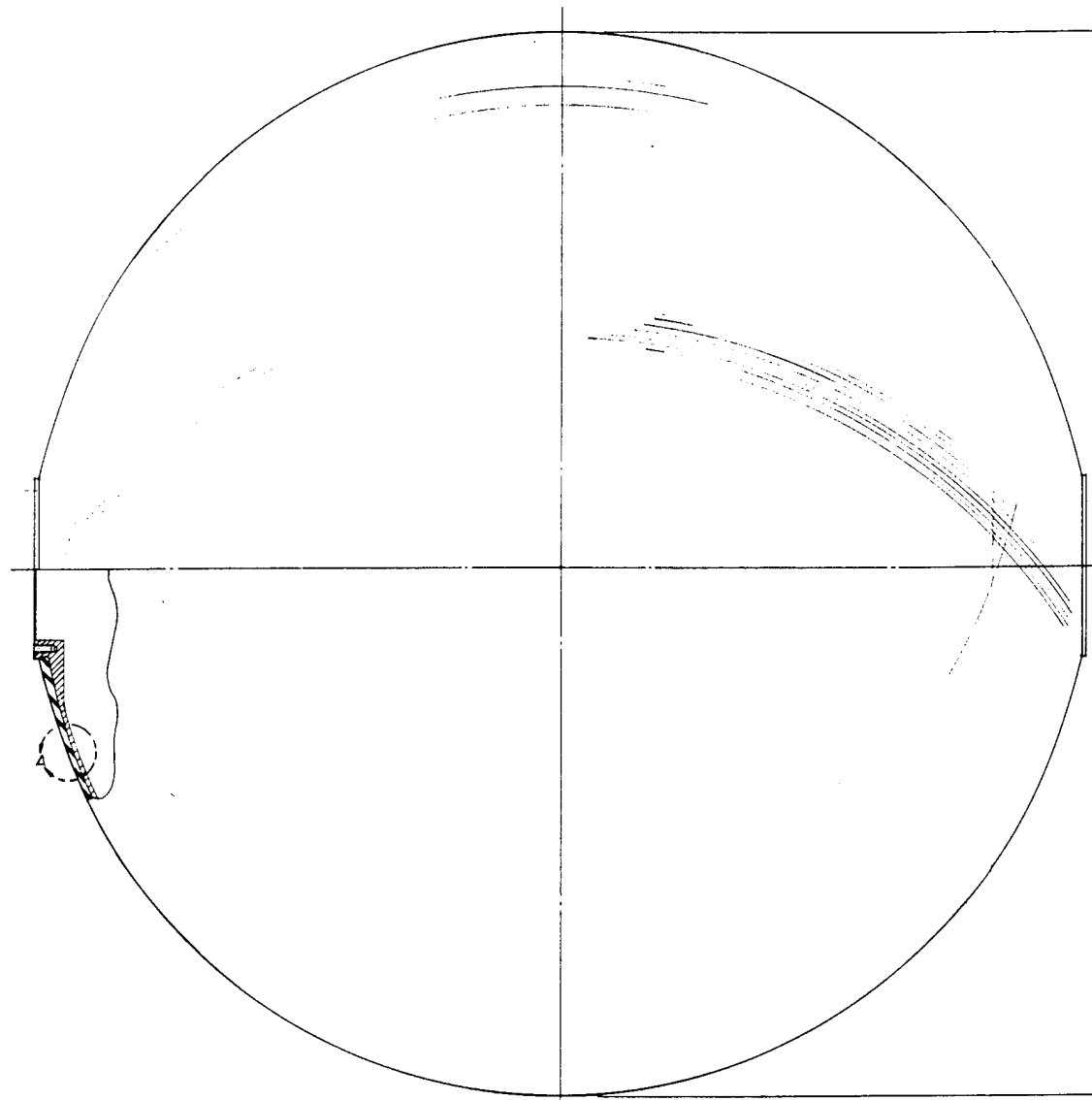
4

11

2

1

Q



.280
COMPOSITE
THICKNESS
AT EQUATO.

		3		AR			
		3		AR			
		3		AR			
				I		12693	
				(-)		SYM	CODE IDENT
				QTY REC		PART C IDENTIFICATION	
UNLESS OTHERWISE SPECIFIED							
DIMENSIONS ARE IN INCHES							
TOLERANCE ON DECIMAL DIMENSIONS IS .005							
XX ± .03							
± .005							
DO NOT SCALE DRAWING							
TREATMENT							
FINISH							
-1-1-1-		FINAL		-			
PART NEXT FINAL		NEXT ASSY		USED ON			
DRAWING NO.		NO. OF ASSY		APPLICATION		SIMILAR TO	
DRAWING LEVEL				<input type="checkbox"/>		INT. W/ TACIC C/W	

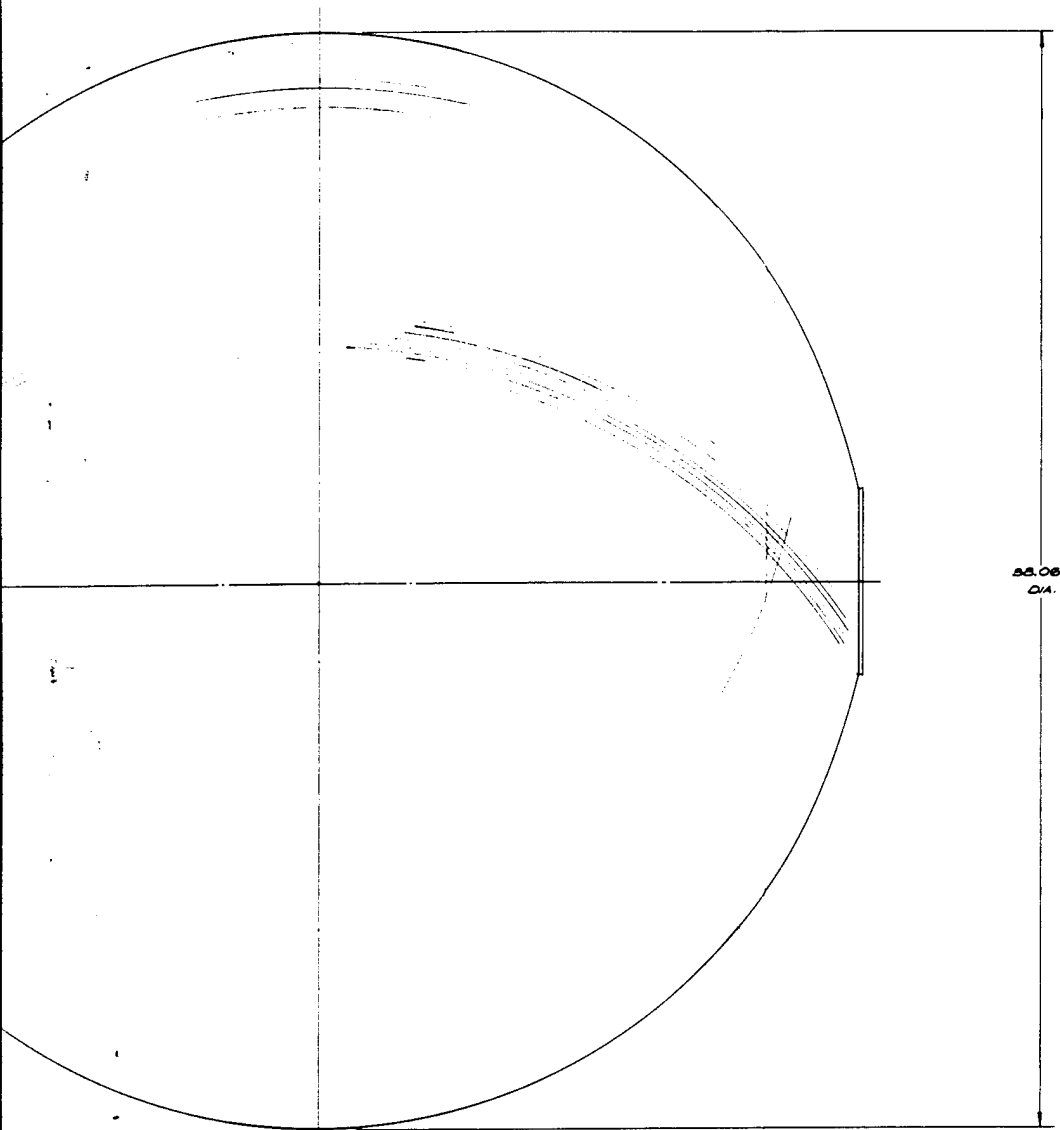
5

4

3

2

1



REVISIONS			
ZONE	LTR	DESCRIPTION	DATE APPROVED
A	SEE DCN		1269382 6-26-73

H
G
F
E
D [1269382] A
C COPY
B
A

△	AR		HARDENER	EPICURE 655	4
△	AR		EPOXY RESIN	DER 352	5
△	AR		PRD ROVING	4 END PRO 49 TYPE III	2
	I	1269382-I	LINER		1
-1	SYM	CODE IDENT	PART OR IDENTIFYING NO.	NOMENCLATURE OR DESCRIPTION	MATERIAL SPECIFICATION UNIT WT ZONE ITEM NO.
QTY 1000					

LIST OF MATERIALS

UNLESS OTHERWISE SPECIFIED	COMPANY	2005	STRUCTURAL COMPOSITES HOLDINGS INC. ALISO, CALIFORNIA
DIMENSIONS ARE IN INCHES	DESIGNER	G. SHAMBO G-26-73	
THICKNESS OF MATERIALS	CHECKED	J. S. JONES 6-26-73	
±0.03	APPROVED	R. F. Fender 6-26-73	
±0.010	DATE	6-26-73	
DO NOT SCALE DRAWING	TITLE	PRESSURE VESSEL PRD-FR	
		2219 ALUMINUM SPHERE	
TREATMENT	STRESS TESTED	TESTED BY: L. H. LEWIS 6-26-73	
	TESTED	TESTED BY: L. H. LEWIS 6-26-73	
	TESTER	TESTER: L. H. LEWIS 6-26-73	
	PRODUCT	PRODUCT: L. H. LEWIS 6-26-73	
FINISH	DESIGN ACTIVITY APPD	DESIGN ACTIVITY APPD: L. H. LEWIS 6-26-73	
	FINISH	FINISH: L. H. LEWIS 6-26-73	
	MANUFACTURER	MANUFACTURER: L. H. LEWIS 6-26-73	
	CUSTOMER	CUSTOMER: L. H. LEWIS 6-26-73	

3

5 FINAL

PART NUMBER: 1269382
NEXT ASSY: 1269382
USED ON: 1269382
DASH/WHITE: 1269382
NO. PER ASSY: 1
APPLICATION: 1269382

DRAWING LEVEL: 0

UNITS: INCHES

NOTES: 1. DASH/WHITE: 1269382
2. NO. PER ASSY: 1
3. APPLICATION: 1269382

1269382
E SH625
DRAWING NO. 1269382
SCALE: 1/2 REL DATE 6-26-73 SHEET 1

TABLE VII
MATERIAL PROPERTIES USED FOR KEVLAR/ALUMINUM VESSEL DESIGN

<u>Property</u>	<u>Aluminum 2219-T62</u>	<u>Kevlar/Epoxy</u>
Density, g/cm ³ (lbm/in ³)	2.82 (0.102)	1.36 (.049)
Coefficient of Thermal Expansion, μ/K (in/in/ $^{\circ}F$)	16.05 (8.915×10^{-6})	-3.573 (- 1.985×10^{-6})
Tensile Yield Strength, MN/m ² (ksi)	293 (42.5)	--
Derivative of Yield Strength with Respect to Temperature N/cm ² /K (psi/ $^{\circ}F$)	-36.1 (-29.1)	--
Elastic Modulus, GN/m ² (psi)	72.4 (10.5×10^6)	128 (18.6×10^6) ^(a)
Derivative of Elastic Modulus with Respect to Temperature GN/m ² /K (psi/ $^{\circ}F$)	-0.0311 (-2510)	-0.030 (-2410) ^(a)
Plastic Modulus, GN/m ² (psi)	2.76 (400 000)	--
Derivative of Plastic Modulus with Respect to Temperature MN/m ² /K (psi/ $^{\circ}F$)	-2.66 (-214)	--
Poisson's Ratio	0.325	--
Maximum Allowable Operating Compressive Stress at ambient Temp, MN/m ² (ksi)	273 (-39.6)	--
Volume Fraction Filament		.65

^aFilament Value

TABLE VIII

KEVLAR-49 FR 2219-T62 ALUMINUM
PRESSURE VESSEL DESIGN PARAMETER SUMMARY

<u>Parameter</u>	<u>Value</u>
Shape	Sphere
Volume, m ³ (in ³)	0.444 (27 100)
Outside Diameter, cm (in.)	97.10 (38.23)
Thicknesses, cm (in.).	
Liner.	0.439 (0.173)
Filament-Wound Composite	0.787 (0.310)
Weight, kg (lbm)	67.3 (148.4)
Pressures, N/cm ² (psi)	
Operating	1396 (2024)
Sizing	1871 (2714)
Burst (minimum).	2787 (4042)
Burst Factor of Safety	2.0
Operating Stresses, MN/m ² (ksi)	
Liner	172 (25.0)
Filaments	1000 (145.0)
Operating Cycles, Including	
Scatter Factor.	1600
Failure Stresses, MN/m ² (ksi)	
Liner	359 (52.0) 52 000
Filaments	1972 (286.0) 286 000
Performance factor, pV/W, J/g (in-lb/lbm)	
Operating	92 (370 000)
Burst	184 (740 000)

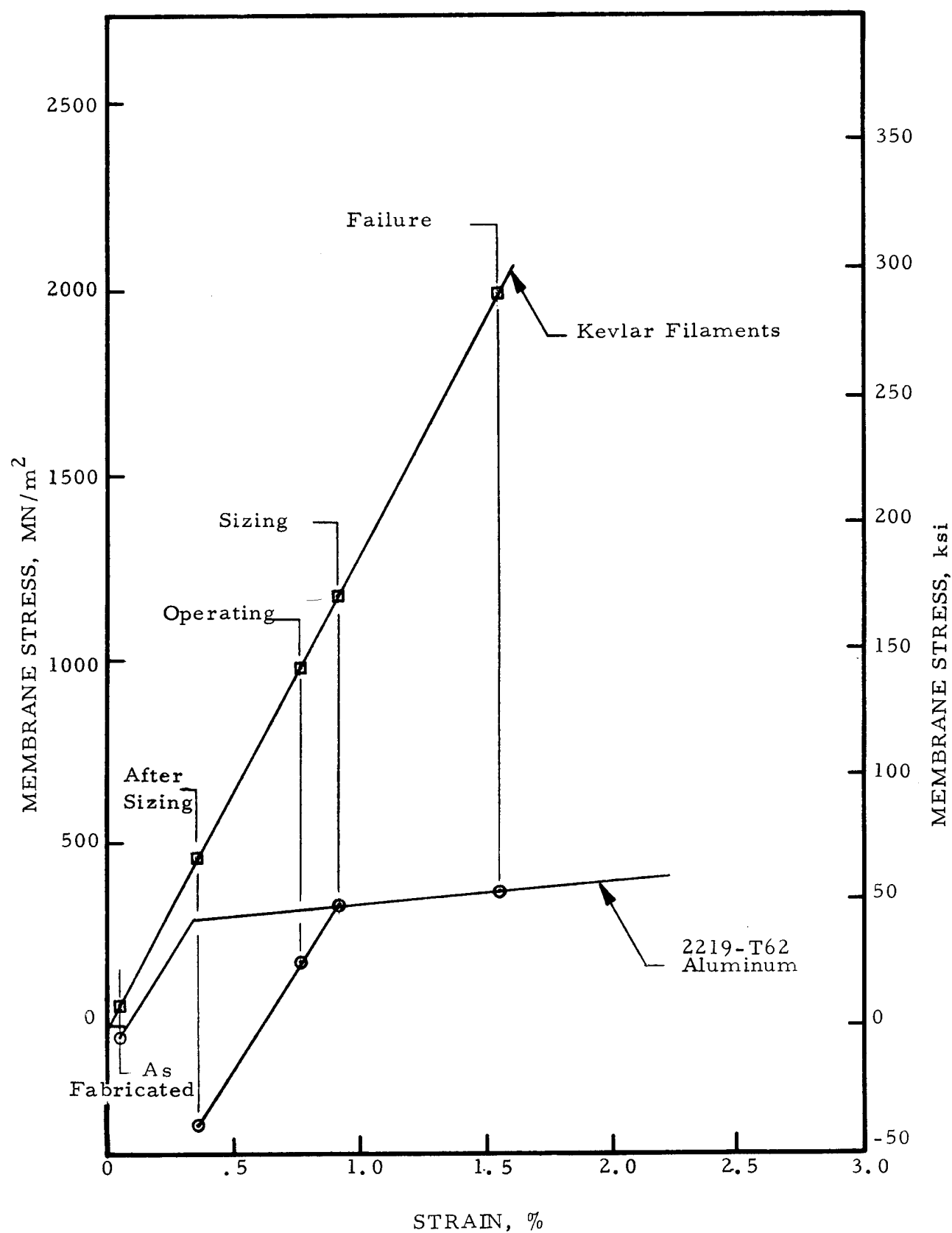


FIGURE 10: Ambient Stress/Strain Relationship
For Kevlar-49 FR 2219-T62 Aluminum Sphere

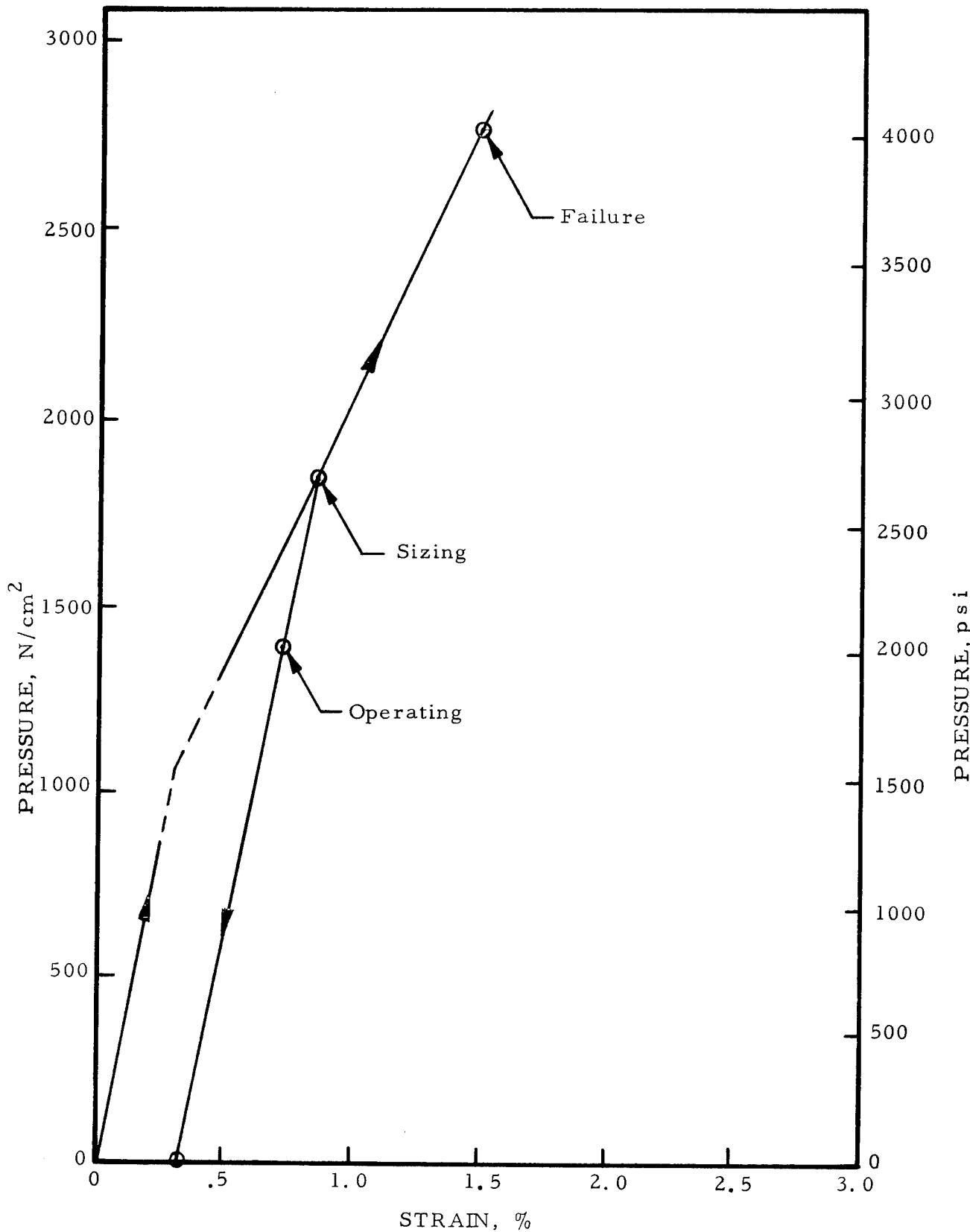


FIGURE 11: Ambient Pressure/Strain Relationship For Kevlar-49 FR 2219-T62 Aluminum Sphere

C. FABRICATION

1. Aluminum Liner Assemblies

Prior to metal shell manufacturing, a detailed fabrication flow chart was prepared to define fabrication processes, engineering and inspection requirements, and tooling and support functions for all half-shell and liner assembly operations. The fabrication plan, Figure 12, was then used to establish a metal shell fabrication specification covering all requirements for the 2219-T62 aluminum liner assemblies; this document is included as Appendix C. Based on the fabrication specification and the process studies conducted under the design task, critical processes were selected for further pre-manufacturing verification.

a. Material and Process Verification Studies

(1) Material Properties

In order to verify the structural properties of the heat and thickness of 2219 aluminum obtained for the program, tensile specimens were fabricated in accordance with Federal Test Method Standard Number 151. All specimens were fabricated from stock 2219-0 aluminum plate machined to the required 0.391cm (0.154 inch) thickness. Additionally, half the specimens were machined from 0.391cm (0.154 inch) thick aluminum which had been previously Electron Beam (EB) fusion-butt welded together. Four specimens (two parent-two welded) were selected from the lot and subsequently solution heat treated and aged to the T-62 condition. These four specimens were then tested in tension; results of the tests are recorded in Table IX. All test values exceeded the minimum allowable property requirements (Reference 5) as defined in the following table:

	<u>Parent Metal</u>	<u>Weld(94% Efficiency)</u>
Ultimate Tensile Strength, Minimum	372 MN/m ² (54.0 ksi)	352 MN/m ² (51.0 ksi)
Yield Strength (0.2% offset)	248 MN/m ² (36.0 ksi)	241 MN/m ² (35.0 ksi)
Elongation in 2-inch, %	7	6

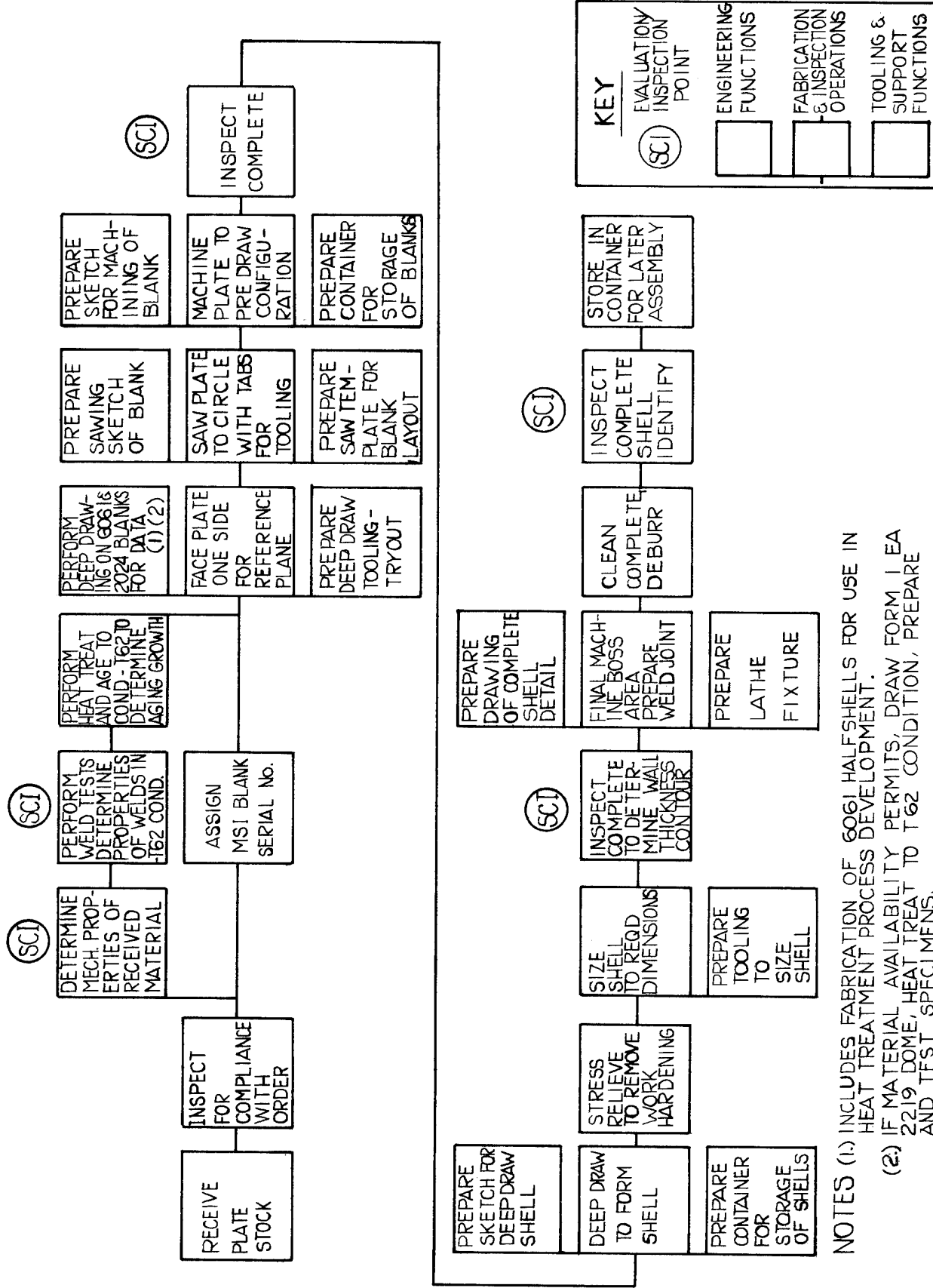
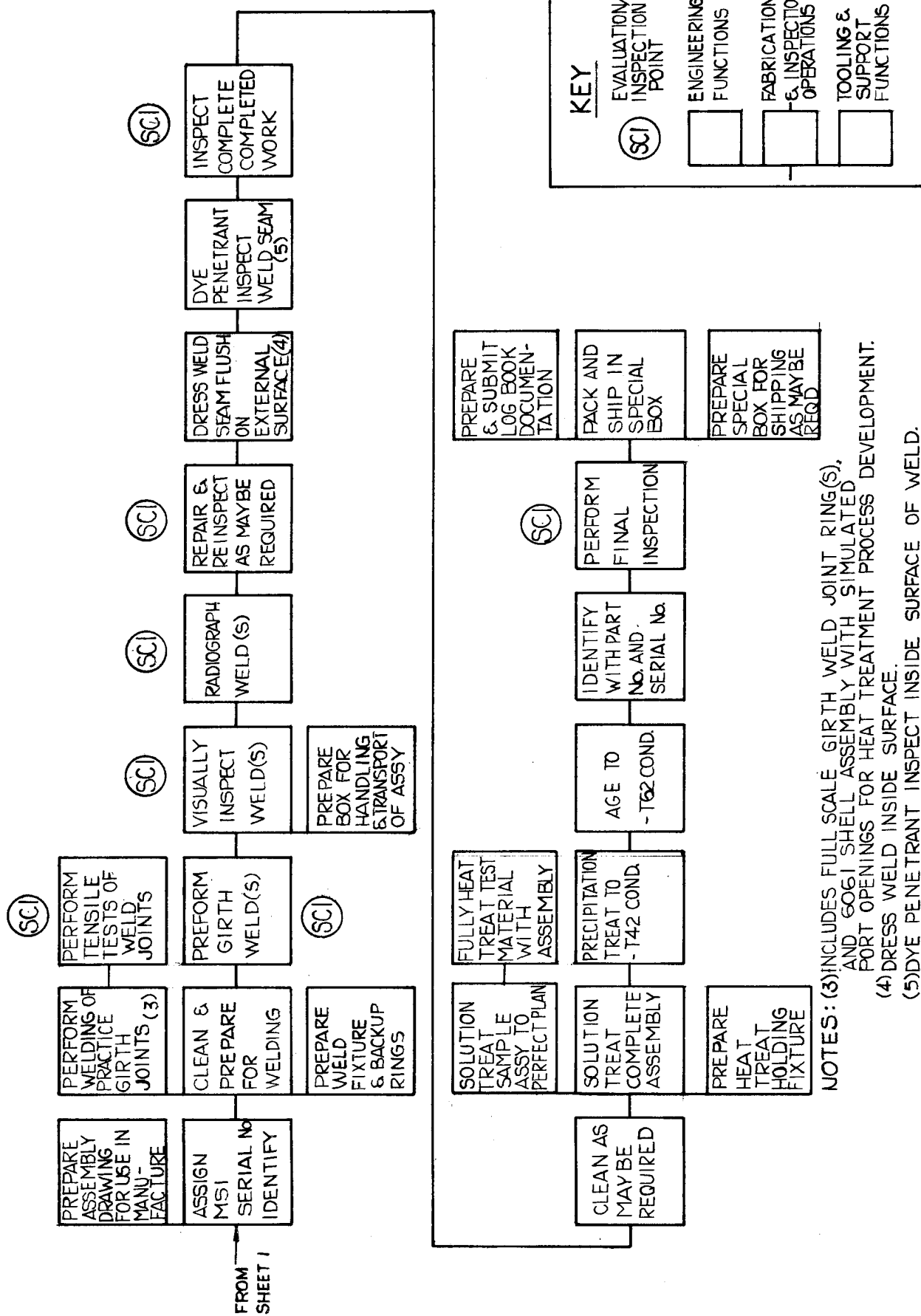


FIGURE 12: 2219-T62 ALUMINUM SPHERE FABRICATION PLAN

SHEET 1 - HALF SHELL FABRICATION



NOTES: (3) INCLUDES FULL SCALE GIRTH WELD JOINT RING(S),
AND 6061 SHELL ASSEMBLY WITH SIMULATED
PORT OPENINGS FOR HEAT TREATMENT PROCESS DEVELOPMENT.
(4) DRESS WELD INSIDE SURFACE.
(5) DYE PENETRANT INSPECT INSIDE SURFACE OF WELD.

FIGURE 12: 2219-T62 ALUMINUM SPHERE FABRICATION PLAN
SHEET 2 - ASSEMBLY FABRICATION

TABLE IX

MATERIAL ACCEPTANCE TEST RESULTS FOR 2219-T62 ALUMINUM

Specimen Type <u>(b)</u>	Strength MN/m ² (ksi)		Elongation, %	
	<u>Yield</u>	<u>Ultimate</u> <u>(c)</u>	5.08 cm (2.0-inch) Gage Length	1.27 cm (0.5-inch) Gage Length
Parent Metal	268 (38.8)	403 (58.4)	9.0	N. A.
	268 (38.8)	405 (58.7)	9.5	N. A.
E. B. Welded	284 (41.2)	405 (58.8)	9.0	16.0
	270 (39.2)	400 (58.0)	9.0	20.0

^a Fabricated and tested in accordance with Federal Test Method Standard Number 151

^b Specimen thickness 0.406 ± 0.015 cm ($0.160 \pm .006$ inches)

^c Location of fracture in parent metal

(2) Forming Development

Verification of the draw forming process parameters and the preliminary half-shell (preform) thickness profile was obtained using pre-machined blanks of aluminum alloys 6061 and 2024. The 6061 aluminum blanks were used, initially, to check the tooling, forming process, and resultant shell geometry. The formed hemispheres were subsequently EB girth welded together [preliminary weld process check for 0.391cm (0.154 inch) thick material], subjected to heat treatment (to reveal any shell distortional effects), and the resultant liner assembly used as a mandrel for winding pattern verification. It should be noted that alloy 6061 is not a good forming simulator for 2219 aluminum and was not used to verify thickness profile.

Alloy 2024 is an excellent forming simulator for 2219 aluminum and was used, subsequent to the 6061 forming, to verify the 2219 half shell thickness profile. Several draws were required to shape the parts to the full depth, and a stress relief was performed after each required draw. It was concluded from this study that no problems were anticipated in forming the 2219 aluminum half-shells or obtaining the desired shell thickness profile.

(3) Girth Weld Process

As discussed above, satisfactory results were obtained for EB welded joints prepared from design thickness flat 2219 aluminum stock. Girth welding of the 6061 aluminum half-shells provided additional information on weld process details for specimens with curvature.

Final verification of the welding process was obtained utilizing full-diameter girth weld simulators. This work was accomplished with 37.5 inch-diameter 2219 aluminum hemispheres which had been formed to include an excess prolongation of material at the equatorial diameter. The specimens were used to checkout half-shell fitup and weld tooling as well as the EB welding schedule.

Fitup was good, and joint welding easily accomplished. After welding, the prolongation was machined from the welded assembly, and the full-diameter ring X-rayed; the weld joint passed the established acceptance criteria. Portions of the full-diameter girth weld ring were solution-treated and aged to the-T62 condition, and mechanical test specimens prepared to the configuration shown in Figure 13.

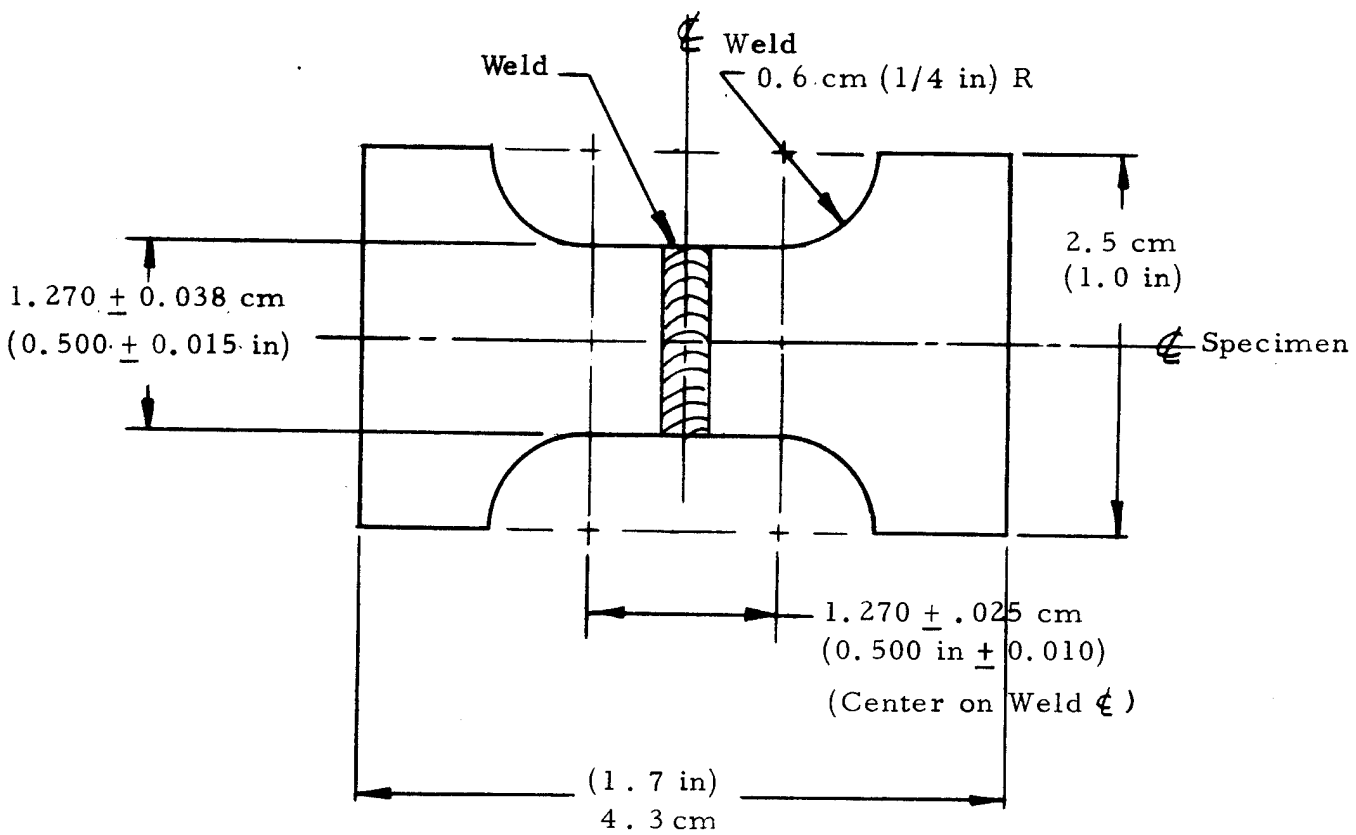


FIGURE 13: 2219-T62 Aluminum Weld Test Specimen Configuration

Mechanical test results are given in Table X. Properties were in excess of design values, and all failures occurred in parent metal. Results of this study indicated no problems were anticipated for the welding process or welded material properties.

(4) Heat Treatment Procedure

Aluminum 6061 preform blanks (used in the aluminum half-shell forming process verification) were deep-draw formed into hemispheres with approximate design wall thickness, girth-welded together, and subsequently used to evaluate the heat-treat process. The unit was heated to the solution treatment temperature, then subjected to water quench. Results of the heat-treat evaluation of this unit confirmed that the 12.7cm (5 inch) diameter ports were of sufficient size to allow the unit to be quenched in the required 15-second* period. Inspection with contour templates indicated there was no distortion of the metal sphere during the solution treatment and subsequent water quench. Figure 14 shows the full-scale metal shell after heat treatment process verification.

b. Half-Shell Fabrication

Based on the initial process verification studies, sixteen 142cm (56.0 inch) diameter by 2.95cm (1.16 inch) thick 2219-0 aluminum blanks were machined to the established preform thickness profile and subsequently draw-formed into the half-shell configuration per Drawing Number 1269381 (Figure 8). Twelve of the sixteen half-shells were final machined at the equatorial girth weld joint area and inside and outside surfaces polished; four units were lost during the machining/forming process. Four of the acceptable units required minor rework prior to final machining. Figures 15 and 16 show some of the half-shells at this point in the fabrication process.

The half-shells were then visually inspected for surface cracks, scratches, and defects and dimensionally inspected per the criteria of Appendix C and the metal shell drawing, 1269381. Thickness measurements were obtained at sixty-four locations, on each half-shell using Vidigage equipment. In order to verify that thickness

*Required period for material thickness of 0.390cm (0.154 inch)

TABLE X

WELD PROCESS TEST RESULTS FOR 2219-T62 ALUMINUM^a

<u>Specimen Number</u>	<u>Thickness, cm (in.)</u>	<u>Width, cm (in.)</u>	<u>Ultimate Tensile Stress, MN/m² (ksi)</u>	<u>Elongation in 1.27 cm (0.5 in.) %</u>	<u>Failure Location</u>
1	0.414 (0.163)	1.288 (0.507)	377 (54.7)	6	Parent Metal
2	0.434 (0.171)	1.290 (0.508)	365 (53.0)	11	Parent Metal
3	0.406 (0.160)	1.196 (0.471)	425 (61.7)	6	Parent Metal
4	0.409 (0.161)	1.240 (0.488)	405 (58.7)	8	Parent Metal
5	0.411 (0.162)	1.234 (0.486)	402 (58.3)	9	Parent Metal

^a(Electron-beam welded specimen per Figure 13, solution-treated and aged after welding; weld transverse to direction of loading)

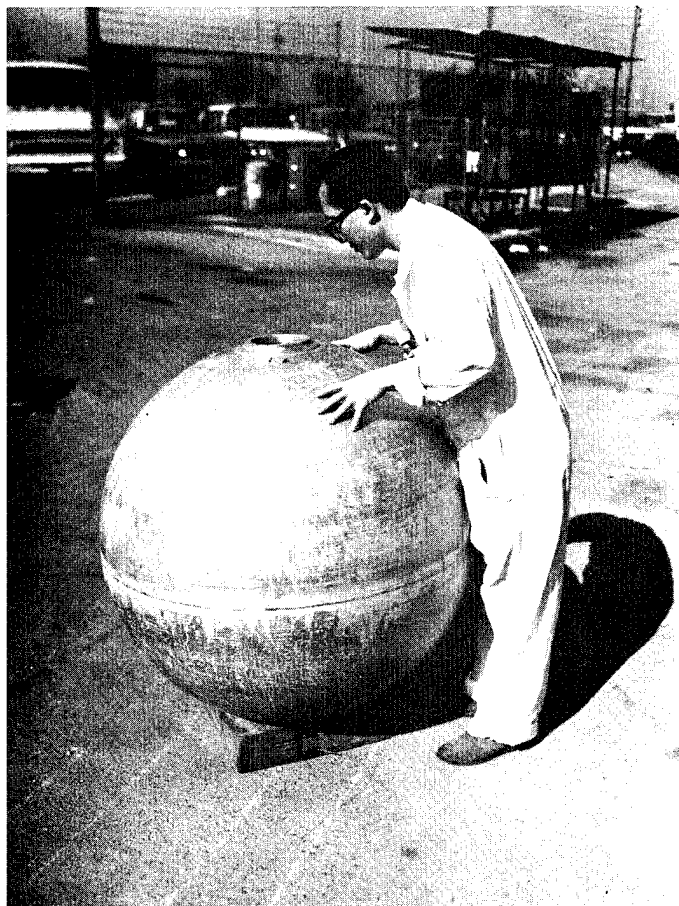


FIGURE 14: 95.3 cm (37.5-Inch) Diameter Aluminum Liner
Assembly Used for Heat-Treatment Verification

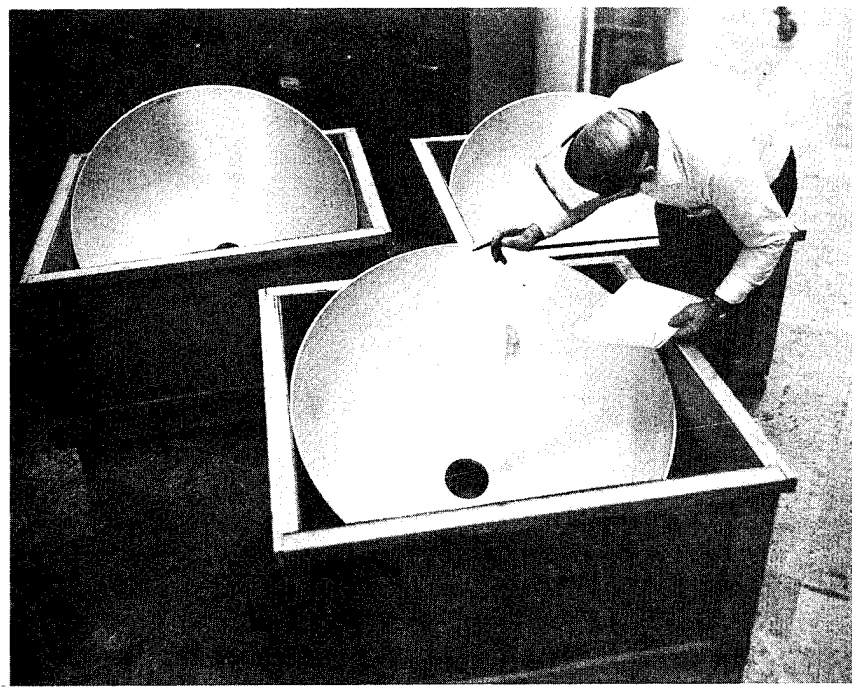


FIGURE 15: 95.3 cm (37.5 Inch) Diameter 2219 Aluminum Sphere Half-Shells

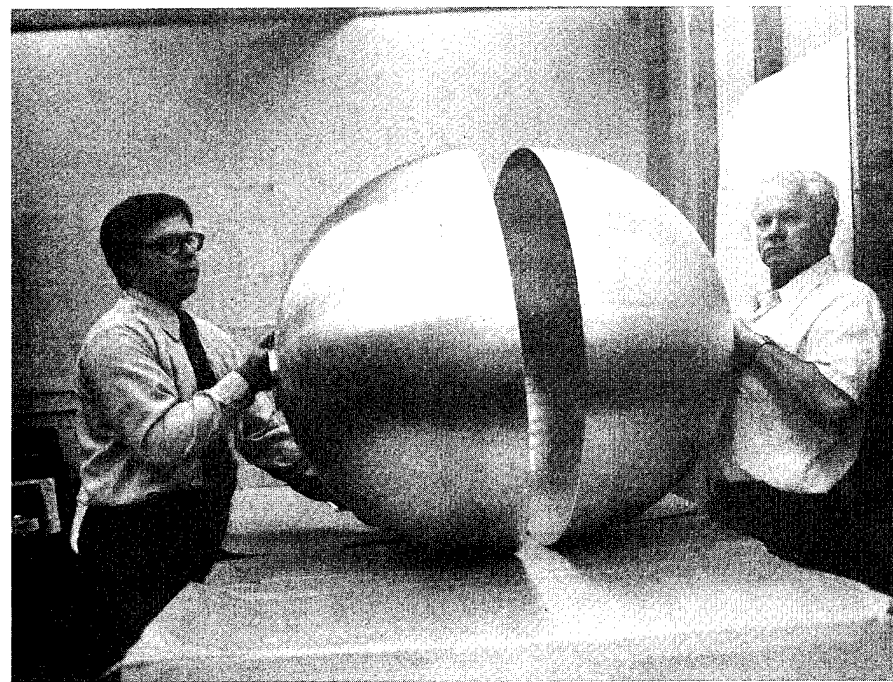
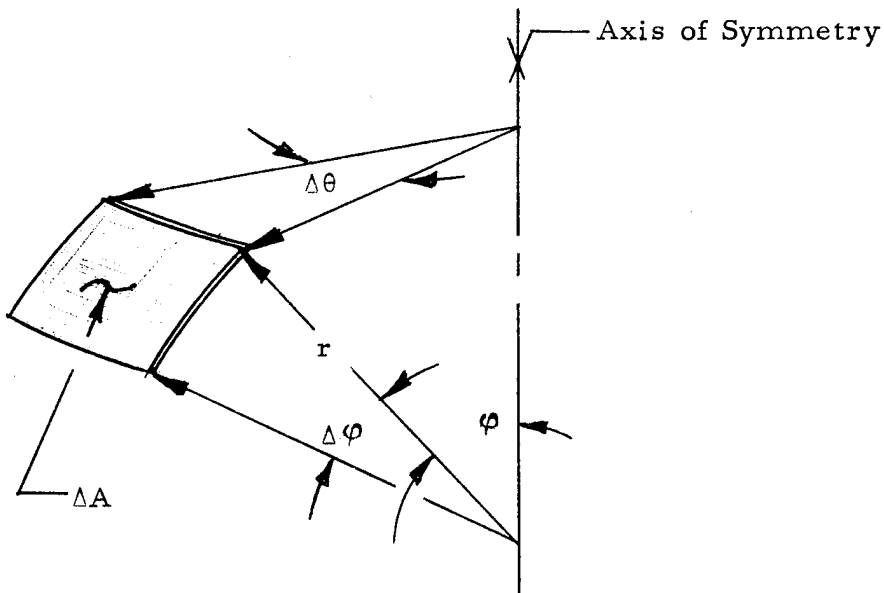


FIGURE 16: Set of 2219 Aluminum Sphere Half-Shells

tolerances were maintained over the dome contour, the half-shell was divided into surface area elements (for analysis) per the sketch below.



The equation for each surface area element is

$$\Delta A = r^2 \sin \phi \Delta \phi \Delta \theta$$

where, $\Delta \theta$ (defined by eight meridians) was selected as $\pi/4$ radians (45°) and $\Delta \phi$ was determined from eight circumferential circles defined by ϕ values which were $\pi/18$ radians (10°) apart (i.e. $\phi = 90, 80, 70, \dots, 20$ degrees).

To determine the percentage $(\%)_i$ of the total surface area (A) which was in a specific tolerance range (i) , the following relation was used:

$$(\%)_i = \frac{100}{A} \sum_{\phi}^{90} N_i \Delta A$$

where,

N_i = number of surface area elements at ϕ in thickness tolerance range i

The six applicable thickness tolerance ranges obtained from the metal shell drawing (1269381) are:

Range Symbol (i)	Thickness		% of Total Surface Area in Indicated Tolerance Range	
	Tolerance cm	Range (in)	Design Objective	Acceptance Criteria
1	<.391	(<.154)	0	0
2	.391 to .442	(.154 to .174)	80	-
3	.443 to .467	(.175 to .184)	10	80
4	.468 to .493	(.185 to .194)	10	10
5	.494 to .518	(.195 to .204)	-	10
6	>.518	(>.204)	0	0

Results for calculated area percentages are contained in Table XI along with other selected inspection data for each half-shell.

As noted in the table, three half-shells (Serial Numbers 5, 7, and 8) did not meet the established acceptance criteria for shell thickness tolerance; the variation of Serial Number 7 was minor. Because of the unavailability of spare half-shells (the four spares had to be scrapped during the preform-machining/forming processes), the under thickness units were accepted and assigned to the dome liner assembly (Serial Number S-6). The thickness tolerance and other geometric parameters for all other half-shells was excellent; many actually exceeded the acceptance criteria and met the thickness tolerance "design objective".

Assignment of half-shells to liner assemblies was based on the following criteria:

- (1) Equatorial diameter match
- (2) Equatorial thickness match
- (3) Half-Shell average thickness match
- (4) Visual defects and/or geometric discrepancies

The prime consideration was an equatorial diameter/thickness match which was necessary to minimize fitup problems during welding. The resulting liner assembly assignments based on the above criteria, are contained in Table XI.

ORIGINAL PAGE IS
OF POOR QUALITY

TABLE XI
2219 ALUMINUM HALF-SHELL INSPECTION DATA SUMMARY

Half Shell Serial Number	% of Total Half Shell Surface Area in Indicated Thickness Tolerance Range (a)			Average Thickness cm (in)	Average Thickness At Equator cm (in)	Outside Diameter At Equator cm (in)	Liner Assembly Assignment S/N	Remarks
	1	2	3	4	5	6		
16	0	53	29	18	0	0	0.442 (0.174)	0.432 (0.170)
15	0	77	23	0	0	0	0.434 (0.171)	0.437 (0.172)
11	0	71	9	0	0	0	0.422 (0.166)	0.437 (0.172)
14	0	74	25	1	0	0	0.439 (0.173)	0.440 (0.173)
4	0	62	35	3	0	0	0.439 (0.173)	0.437 (0.172)
7	2	69	29	0	0	0	0.432 (0.170)	0.445 (0.175)
1	0	96	4	0	0	0	0.422 (0.166)	0.422 (0.166)
9	0	60	25	10	5	0	0.445 (0.175)	0.432 (0.170)
12	0	62	35	3	0	0	0.439 (0.173)	0.437 (0.172)
13	0	54	42	4	0	0	0.437 (0.172)	0.419 (0.165)
5	33	67	0	0	0	0	0.401 (0.158)	0.386 (0.152)
8	31	69	0	0	0	0	0.399 (0.157)	0.389 (0.153)

^a Thickness Tolerance Ranges per Drawing Number 1269381:

1. < 0.191 cm (< .154 in.)
2. .391 to .442 cm (.154 to .174 in)
3. .445 to .467 cm (.175 to .184 in)
4. .470 to .493 cm (.185 to .194 in)
5. .495 to .518 cm (.195 to .204 in)
6. > 0.518 cm (> .204 in)

^a Thickness Tolerance Ranges per Drawing Number 1269381:

Pit/inclusion on ID surface repaired with 2319 weld wire and dressed flush (S/N 16). Pin Pore 2.008 cm (.003 in) deep at equatorial weld zone sanded out (S/N 15).

Very slight waviness on S/N 11 ID surface in equatorial area. No visual discrepancies on S/N 14.

Both half-shells in excellent condition. Very localized thin spot on S/N 7 at 20 to 40° zone.

Local thin area, approx. 0.381 cm (.150 in.) thick; slight ripple on external surface at 25° zone (S/N 1). Local thin area at 75° zone on S/N 9.

One tapped hole with bad thread, retapped for S/N 12.

No visual defects on S/N 13.

Both half-shells under thickness; 0.363 cm (.143 in.) min. thickness for S/N 5 and 0.348 cm (.137 in.) min. thickness for S/N 8. Sharp "ding" on OD of S/N 5 required w/2319 weld wire and dressed.

c. Final Assembly

Final manufacture (welding/heat treating) of the six aluminum liner assemblies was conducted in two lots of three assemblies each. The first lot consisted of Assembly Serial Number S-1 (half-shells 15 and 16), Assembly Serial Number S-2 (half-shells 11 and 14), and Assembly Serial Number S-3 (half-shells 4 and 7). These first three assemblies were EB girth welded according to the preestablished weld-schedule/process without incident. Figure 17 shows a half shell assembly prior to welding. Subsequent radiographic and dye-penetrant inspections indicated that Assemblies S-1 and S-3 were acceptable and free from any significant defects. Radiographic inspection of Assembly S-2 revealed excessive porosity, probably in the weld-drop-through. This unit was rewelded using a previously established repair weld procedure consisting of full penetration and cosmetic passes. Subsequent X-rays and dye-penetrant inspections showed a "clear" defect free weld joint.

Following welding, the three assemblies were solution-treated and aged to the -T62 condition without any visible distortion, and were submitted for final inspection. Dimensional inspection of the port area of the three liner assemblies revealed that the boss bore and bolt-hole-pattern had decreased in size. The following table summarizes the inspection results:

Half Shell S/N	Bolt Circle Diameter <u>Min/Max Dimensions</u>		Boss Bore Diameter <u>Min/Max Dimensions</u>	
	cm	(in)	cm	(in)
16	14.171/14.221	(5.579/5.599)	11.598/12.642	(4.960/4.977)
15	14.201/14.254	(5.591/5.612)	12.631/12.652	(4.973/4.981)
11	14.229/14.252	(5.602/5.611)	12.657/12.670	(4.983/4.988)
14	14.188/14.227	(5.586/5.601)	12.606/12.649	(4.963/4.980)
7	14.221/14.239	(5.599/5.606)	12.649/12.667	(4.980/4.987)
4	14.173/14.209	(5.580/5.594)	12.593/12.606	(4.958/4.963)

The pre-heat treatment value (obtained from half-shell inspection logs) for the bolt-circle-diameter was 14.288cm (5.625 inch) and for the boss-bore-diameter was 12.705cm (5.002 inch) per the drawing. This permanent contraction had not been noted in the process verification studies since (1) a more massive welded-in "work horse" boss had been used, and (2) concern with distortional effects had been concentrated on

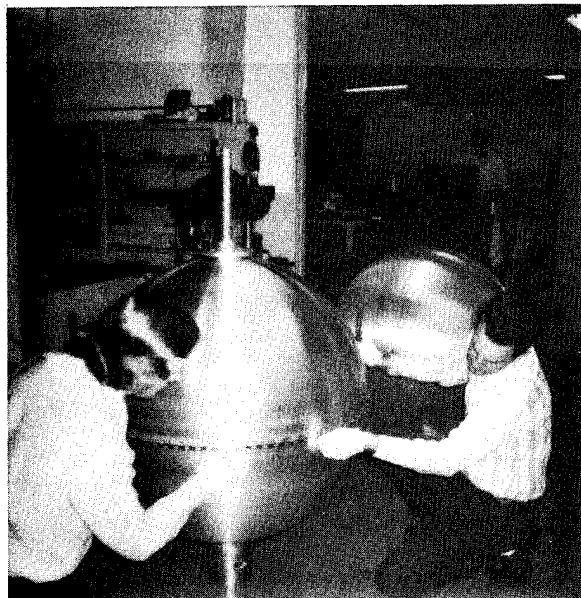


FIGURE 17: 95.3 cm (37.5 Inch) Diameter 2219 Aluminum Half-shell Assembly for Welding

the shell rather than the port. The permanent contraction had, obviously, occurred during the high temperature solution heat treatment and subsequent water quench.

In addition to the general shrinkage of the ports, each assembly contained one port (half-shell Serial Numbers 16, 14 and 4) with local inward permanent distortions around each of four opposed bolt holes. A reexamination of heat treatment procedures indicated that the local distortions around each of the bolt holes had been caused by four steel bolts used to fixture the liner assembly during furnace aging and the subsequent cool down period (solution treatment was eliminated as a cause because a different method of fixturing was employed). Apparently, differential thermal expansion/contraction between the aluminum boss and the steel bolt/fixture had caused large localized radial loads at the bolt holes. The effect was permanent inward deformation in the local area of each of the four holes. This method of fixturing was revised prior to heat treatment of the second lot of liner assemblies.

Since all half shell ports had been final machined prior to the heat treatment process and no additional units were available, the two ports on each of the three liner assemblies were rebored to a new common inside diameter of 12.682/12.687cm (4.993/4.995 inch) and accepted "as-is". Corresponding test closure plates were redesigned using this value and a new common bolt circle diameter of 14.214cm (5.596 inch) per Revision C of Drawing 1269381. It was concluded that any future liner assemblies manufactured according to the above processes should be initially machined "rough" in the port area and final machined (drill/tap and bore) after heat treatment.

The second lot of three liner assemblies consisted of Assembly Serial Number S-4 (half-shells 1 and 9), Assembly Serial Number S-5 (half-shells 12 and 13), and Assembly Serial Number S-6 (half-shells 5 and 8). These assemblies were EB girth welded according to the preestablished weld-schedule/process with only one minor incident. Alignment of half-shells 12 and 13 over the entire girth diameter (prior to welding) was very difficult in that these units had the greatest mismatch in diameter and thickness at the girth. As a result, the final welded assembly, Serial Number S-5, exhibited a 0.157cm (0.062 inch) mismatch over a 10° area of the girth weld. Subsequent radiographic and dye-penetrant inspection of this unit, as well as Serial Number S-4 and S-6, indicated that all three units were acceptable and free from defects, except as noted.

Based on the earlier heat treatment information obtained for the first three liner assemblies, the second lot of three liner assemblies was solution treated and aged to the -T62 condition without incident. The general shrinkage of the bolt-hole pattern and boss bore did occur (this was expected and could not be prevented), but no local deformation around bolt holes was indicated during final inspection of the units. Both ports on each of the three assemblies were bored to the new 12.682/12.687cm (4.993/4.995 inch) inside diameter as previously discussed. Table XII contains dimensional inspection data characterizing all six 2219-T62 aluminum liner assemblies.

2. Kevlar/Aluminum Pressure Vessels

Pressure vessel fabrication consisted of overwinding completed 2219-T62 aluminum liner assemblies with a predetermined uniaxial multiangular pattern composite of epoxy impregnated four-end Kevlar-49 roving; following the overwrap process the resulting composite material was oven cured. The composite fabrication task for this program focused on the development of an optimum filament winding pattern; most other fabrication process parameters had been previously established under other development programs.

a. Kevlar Overwrap Pattern Development

Concurrent with this program, an "in-house" study was conducted by SCI to optimize the filament winding pattern for spherical vessels utilizing Kevlar-49 continuous roving. The vessels used for this effort were elastomer lined 40.6cm (16.0 inch) diameter spheres incorporating "molded-in" metal bosses. In order to verify that the resultant subscale geometric winding parameters could be used on full-scale hardware, a pattern development study was conducted. This study utilized the full-scale heat-treat-development 6061 aluminum sphere discussed in Section IIC 1a and, additionally, provided a checkout of all filament winding tooling. Figure 18 shows overwrapping of the "work horse" 6061 aluminum liner assembly. Results of the study verified the geometric scale-up and established final composite processing details. The resultant composite fabrication process procedure is included as Appendix D.

TABLE XII
2219-T62 ALUMINUM LINER ASSEMBLY
INSPECTION DATA SUMMARY

Assembly Serial Number	Average Shell Thickness, cm(in)	Outside Diameter, cm(in)			Overall Axial Length, cm(in)	Maximum Weld Joint Shrinkage, cm(in)	Internal Volume, m ³ (in ³)	Weight, kg(lb)	Remarks
		Polar	45°	Equator					
S-1	0.439 (0.173)	95.402 (37.560)	95.466 (37.585)	95.377 (37.550)	96.360 (37.937)	0.020 (0.008)	(a)	36.9 (81.4)	Local bolt hole deformations (4 places); rebore of port caused minimum wall thickness from edge of thread to edge of bore=0.381cm(.150in).
S-2	0.432 (0.170)	95.387 (37.554)	95.334 (37.533)	95.372 (37.548)	96.363 (37.938)	0.023 (0.009)	0.4393 (26.810)	36.4 (80.2)	Local bolt hole deformations (4 places); rebore of port caused minimum wall thickness from edge of thread to edge of bore=0.401 cm (.158 in)
S-3	0.437 (0.172)	95.415 (37.565)	95.293 (37.517)	95.314 (37.525)	96.360 (37.937)	0.010 (0.004)	(a)	37.8 (83.3)	Local bolt hole deformations (4 places); rebore of port caused minimum wall thickness from edge of thread to edge of bore=0.381cm (.150 in)
S-4	0.434 (0.171)	95.395 (37.557)	95.324 (37.529)	95.250 (37.500)	96.342 (37.930)	0.010 (0.004)	0.4380 (26.810)	36.7 (81.0)	Minor handling damage to shell exterior (slight dings and depressions)
S-5	0.439 (0.173)	95.169 (37.468)	95.344 (37.537)	95.286 (37.514)	96.215 (37.880)	0.028 (0.011)	0.4380 (26.730)	37.2 (82.0)	Weld mismatch of approximately 0.157 cm (0.062 in) over 10° zone
S-6	0.401 (0.158)	95.275 (37.510)	95.273 (37.509)	95.255 (37.502)	96.203 (37.875)	0.013 (0.005)	0.4402 (26.860)	33.5 (73.9)	Thin-wall unit.

a Data either invalid or not recorded.

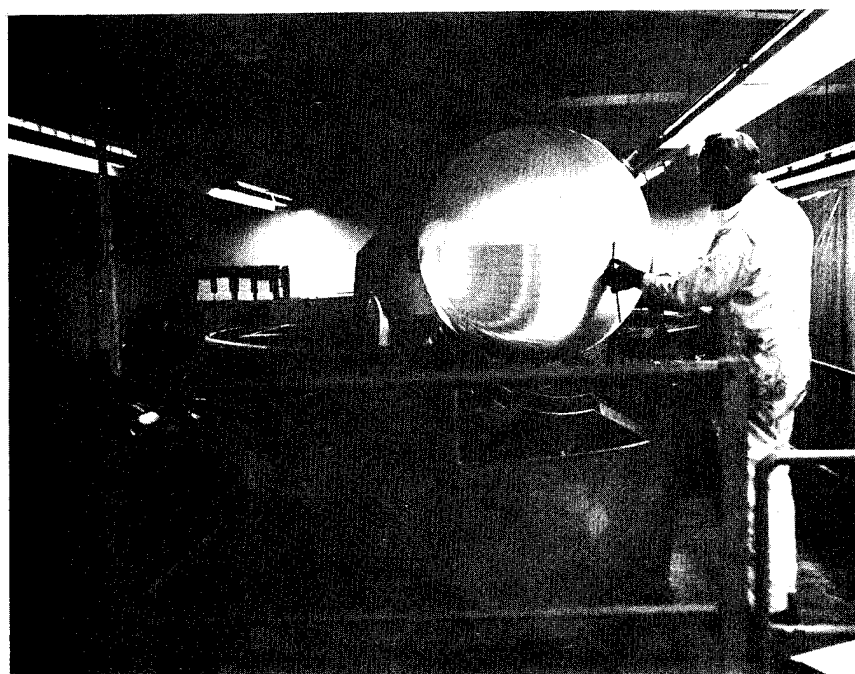


FIGURE 18: Overwrap Filament-Winding Development
for 95.3 cm (37.5 Inch) Diameter Sphere

b. Filament Winding

The established filament-winding procedures, Appendix D, were used to initially overwrap three of the aluminum liner assemblies (Serial Number S-1, S-2, and S-3) to form pressure vessels as defined by Drawing Number 1269382 (refer to Figure 9). The actual winding pattern used on these three units did not contain steps 11 through 14 as defined in Appendix D.

Based on the performance test result obtained for Vessel S-3, discussed later in Section IID2, the initial winding pattern was modified. Since Vessels S-1 and S-2 had already been fabricated according to the initial pattern (including cure of the composite material), a supplemental winding operation was utilized on these two units to comply with the final (four additional steps) pattern requirements. After the supplemental winding operation and subsequent (second) cure, the visual appearance of these two vessels was slightly different than the first vessel, or subsequent vessels.

The final three liner assemblies (S-4, S-5, and S-6) were overwrapped with epoxy impregnated Kevlar-49 roving according to the revised pattern, defined in Appendix D, and oven cured. Two of the three completed vessels are shown in Figure 19.

No special problems were encountered during the overwrap/cure processes for any of the six vessels fabricated. Table XIII presents a summary of fabrication data obtained for each of the vessels.

D. TEST PROGRAM

Prior to performance testing, each vessel was pressure-sized (proof tested) to screen preexisting flaws in the metal shell and also fix the required prestresses in both the metal and filament-wound composite shells. Detailed procedures for the pressure sizing operation are contained in Appendix B.

1. Instrumentation and Test Plan

Primary instrumentation consisted of pressure and strain sensors, transducers, and recording equipment necessary to (a) verify achievement of prescribed shell stresses during the sizing cycle, and (b) provide pressure/strain data documenting performance tests.

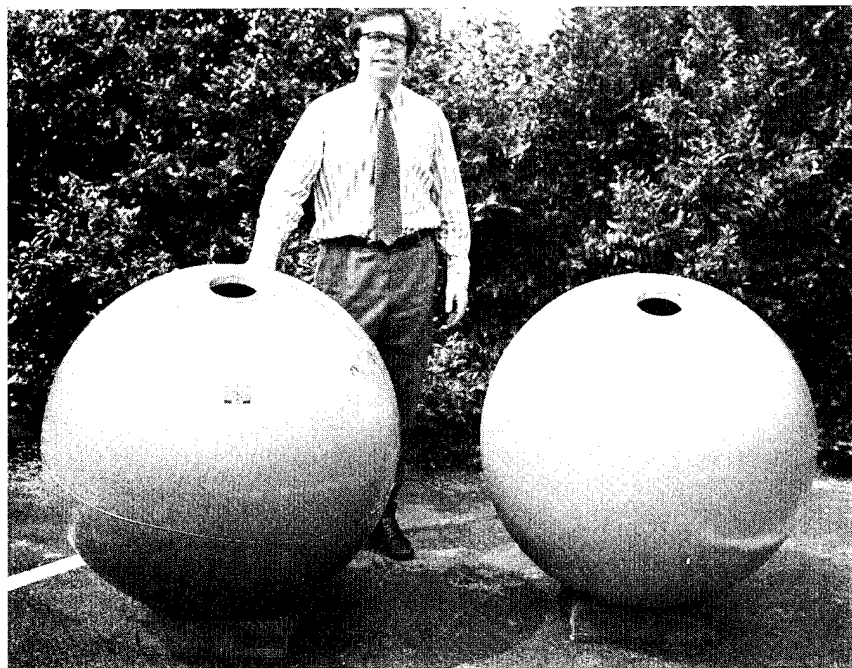


FIGURE 19: Kevlar Filament-Overwrapped 2219-T62
Aluminum Spheres, S/N S-3 and S-1

TABLE XIII
KEVLAR-49 OVERWRAPPED 2219-T62 ALUMINUM
PRESSURE VESSEL FABRICATION DATA SUMMARY

Vessel Serial Number	Weights, kg (lb)			Internal Volume, m ³ , (in. ³)	Outside Diameter, cm (in.)	Fiber Content Volume % (b)	Remarks
	Liner Assembly	Composite Fiber Resin	Vessel (e)		Polar 45° Equator		
S-1 (81.4)	36.9 (55.0)	25.0 (27.2)	12.3 (163.6)	74.2 (c)	74.4 (c)	0.4387 (26.770)	Vessel wrapped to initial pattern and cured. Secondary (4 rev.) wrap added and cured later.
S-2 (80.2)	36.4 (55.9)	25.4 (27.9)	12.6 (164.0)	74.4 (c)	74.4 (c)	0.4387 (26.770)	" " "
S-3 (83.3)	37.8 (52.0)	23.6 (19.9)	9.0 (155.2)	70.4 (26.810)	97.229 (38.235)	97.396 (38.345) (38.370)	Vessel wrapped to initial winding pattern only; single cure
S-4 (81.0)	36.7 (54.2)	24.6 (25.3)	11.5 (160.5)	72.8 (26.810)	97.485 (38.380) (38.305)	97.295 (38.315) (38.320)	0.547 " " "
S-5 (82.0)	37.2 (55.0)	24.9 (28.0)	12.7 (165.0)	74.8 (26.630)	0.4364 (38.325)	97.282 (38.300) (38.330)	1.021 (0.402) 0.554 " " "
S-6 (73.9)	33.5 (54.4)	24.7 (29.2)	13.2 (157.5)	71.5 (26.820)	0.4395 (38.315)	97.320 (38.255) (38.360)	1.021 (0.406) 0.560 " " "

a Calculated values based on difference between average shell diameters before and after overwrapping

b Calculated values based on total turns of fiber applied to vessel

c Data either invalid or not recorded

d Vessel wrapped using original winding pattern

e Tie-rod weight of 10 pounds not included

The strain gage selected for this application was Micro-Measurement's Gage Number EA-06-250TG-350. This gage is a polyimide backed, general purpose, 2-element 90° tee rosette with a strain range of $\pm 5\%$. Four rosettes were bonded to the external surface of each vessel at the locations defined in Figure 20.

The linear displacement transducers selected for measurement of the vessel circumferential expansion were designed and fabricated by SCI. The major component was a Duncan Series 220 Slideline Control with a single linear 1 K ohm resistive element. The control had a functional mechanical travel of 2.54cm (1.0 inch), infinite resolution, and 3% tracking. Three "great circle" extensometers, located on the external surface of the vessel in the orientations shown in Figure 20, were connected to the linear displacement transducers to provide the expansion data.

Detailed test procedures were established, and approved by NASA, prior to initiation of the performance test program. These procedures are contained in Appendix E, and the final (revised) test plan is shown in Figure 21.

2. Initial Test Result Vessel Serial Number S-3

Kevlar/aluminum Vessel S-3 was fully instrumented, according to the procedures of Appendix B, in preparation for sizing and a subsequent hydraulic burst test. Figure 22 shows two views of the vessel, including the bonded strain gage rosettes, prior to the sizing test. During the sizing test, pressure/strain data were monitored at 345 N/cm^2 (500 psi) increments up to a sizing pressure of 1586 N/cm^2 (2300 psi).

At this pressure, extensometer data indicated the desired sizing strain had been reached and further pressurization to the design value of 1862 N/cm^2 (2700 psi) might induce excessive stresses in the metal shell. Figures 23 through 25 are plots of the vessel strain data required during the sizing test. Figures 23 and 24 show longitudinal and hoop strains, respectively, obtained from the biaxial strain gages bonded to the exterior surface of the vessel; the hoop leg of gage SG-2 was lost during pressurization. Figure 25 indicates the strains in three planes obtained from the "great circle" extensometers.

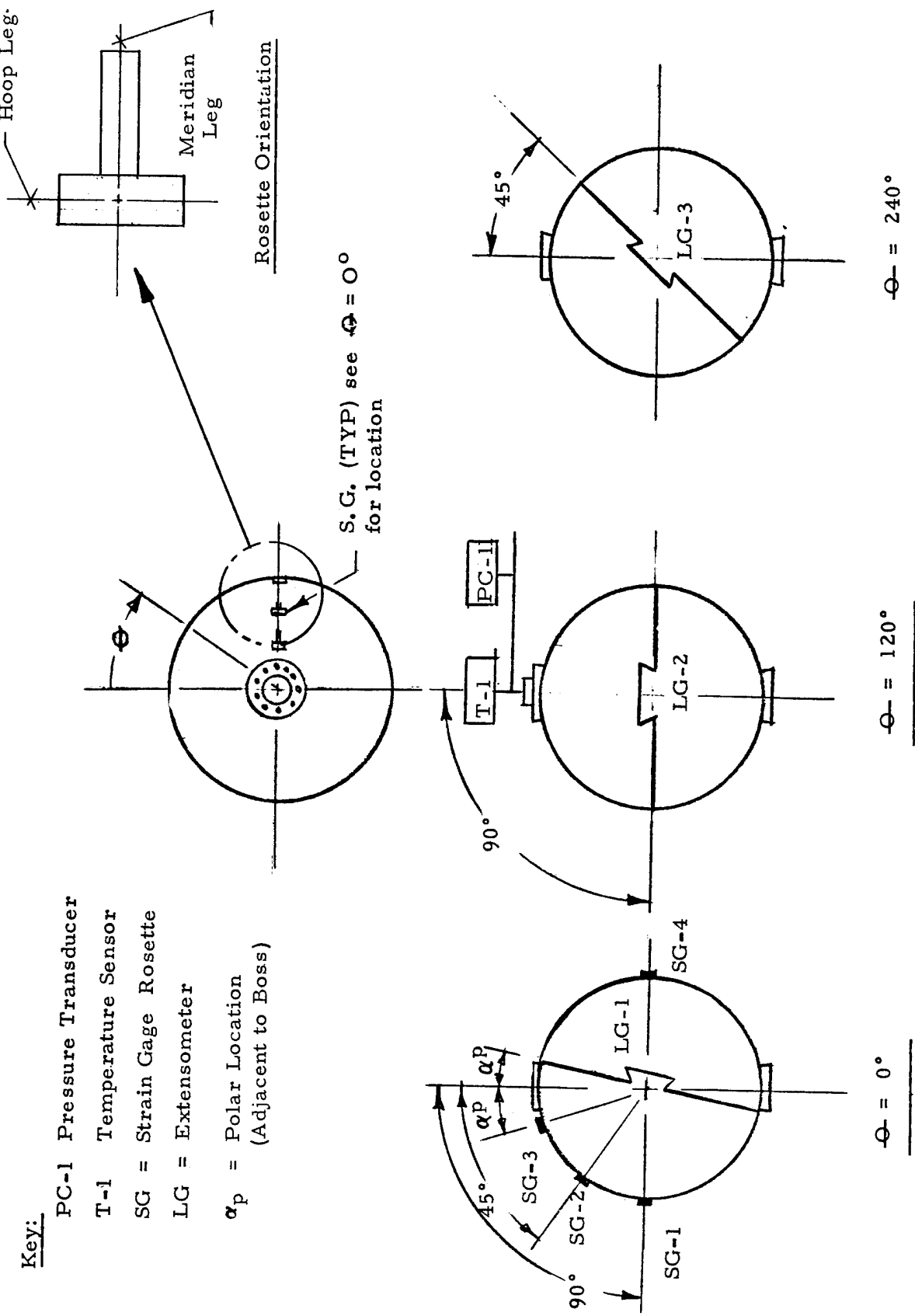
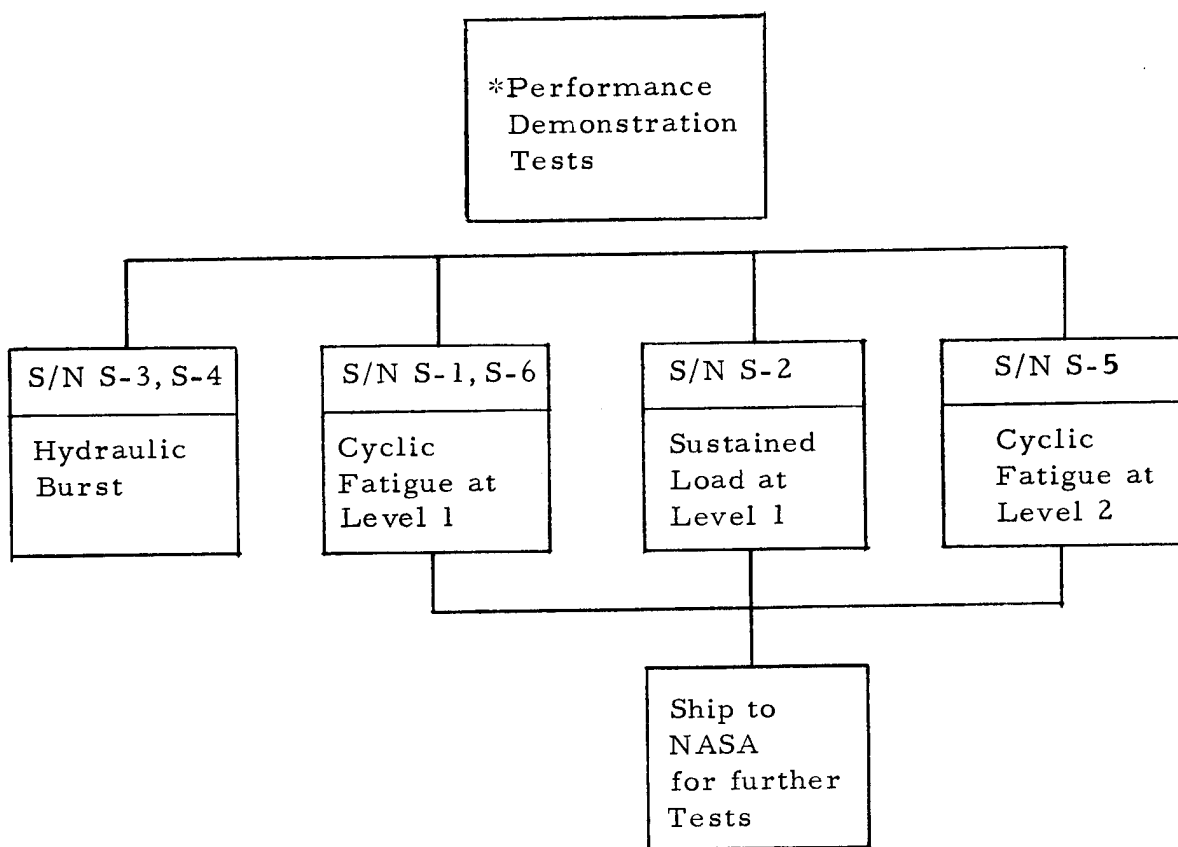


FIGURE 20: Instrumentation Location



<u>*Key</u>	<u>Level Number</u>	<u>Operating Pressure, N/cm², (psi)</u>	<u>Number of Fatigue Cycles</u>	<u>Period at Sustained Loads, Hrs.</u>
	1	1396 (2024)	1600	96 (minimum)
	2	1620 (2350)	1000	96 (minimum)

FIGURE 21: Revised Test Plan and Vessel Assignment
For Kevlar Fiber Reinforced 2219 Aluminum Spheres

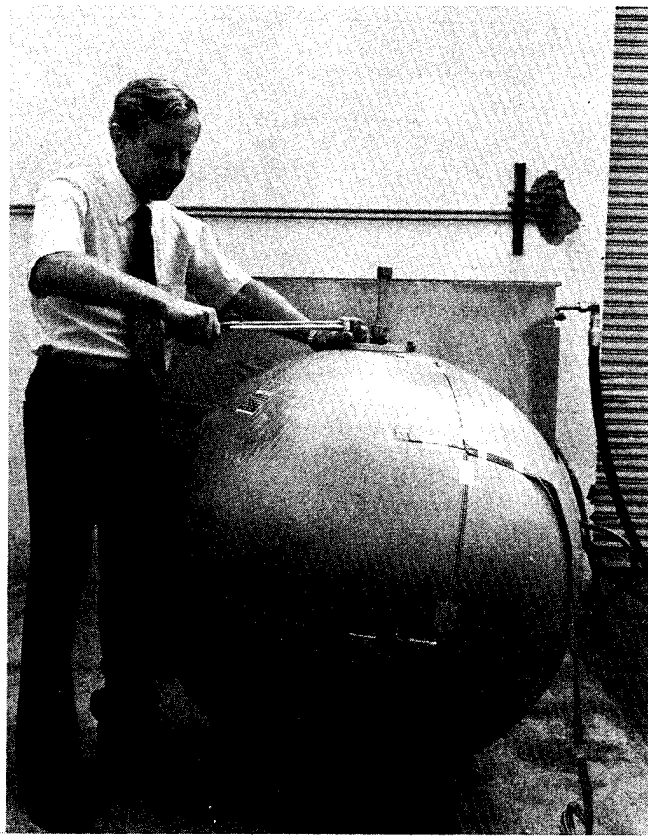
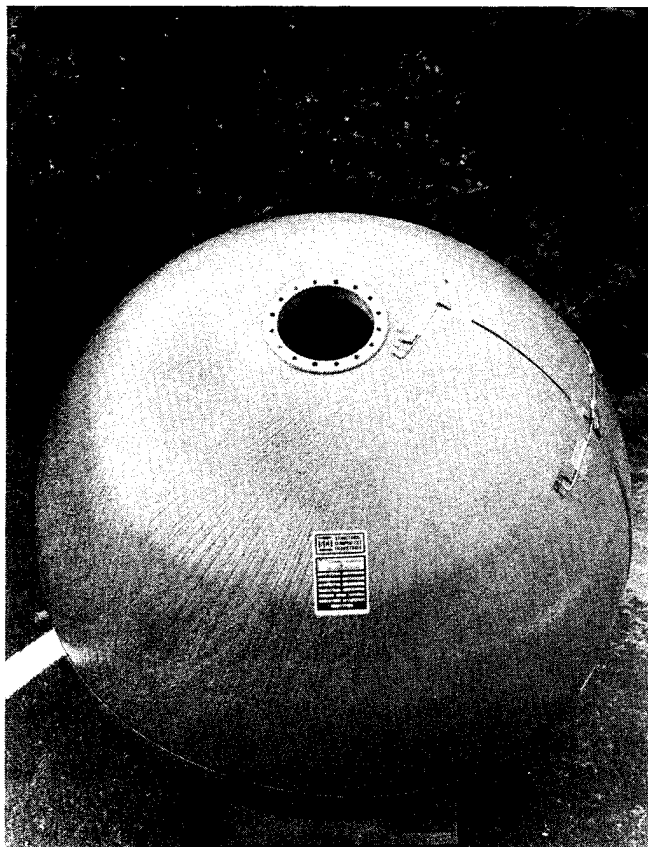


FIGURE 22 KEVLAR-49 FILAMENT REINFORCED 2219-T62 ALUMINUM PRESSURE VESSEL

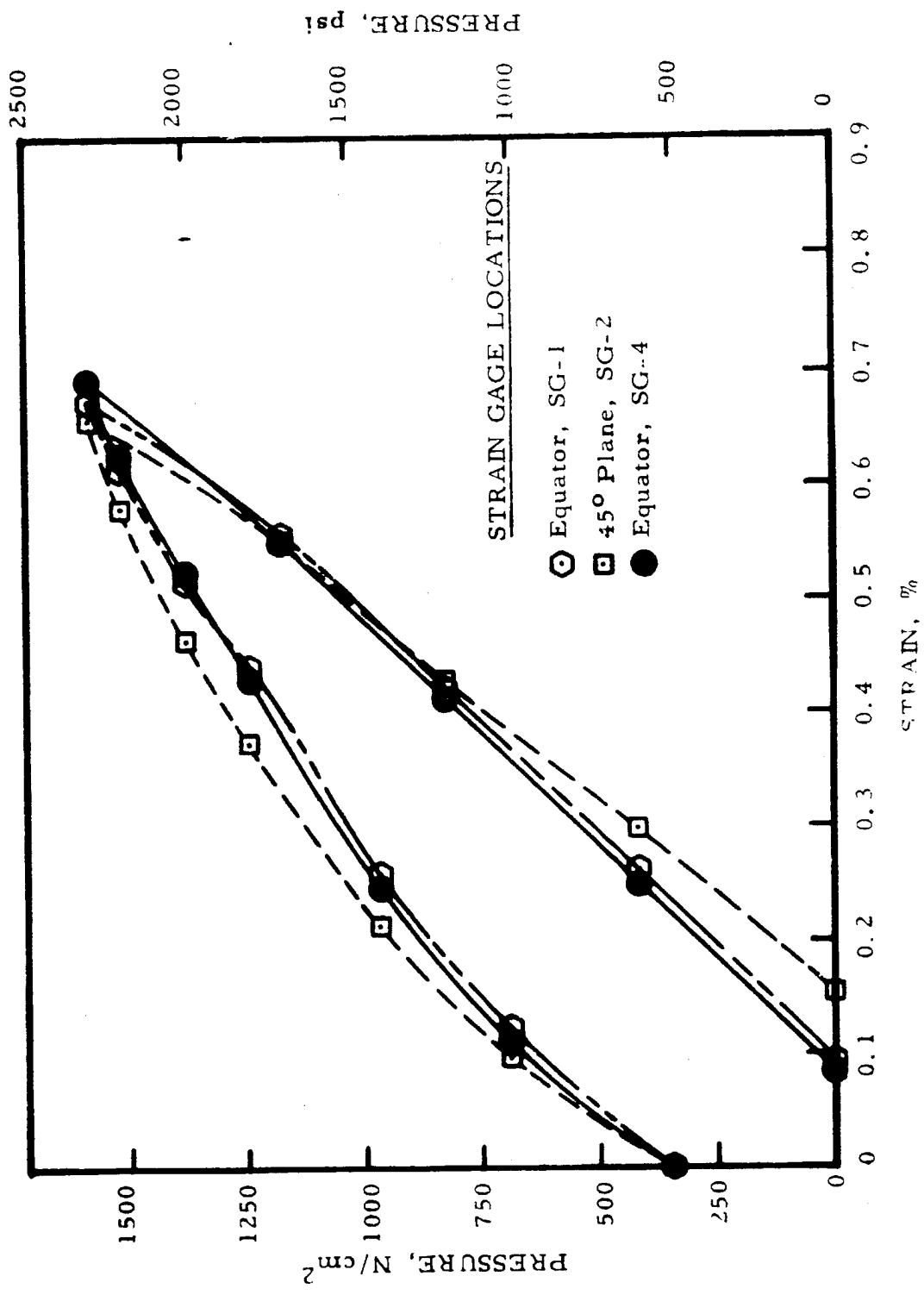


FIGURE 23: Strains Obtained From Longitudinally Oriented Strain Gages During Pressure Sizing of Kevlar/Aluminum Vessel S-3

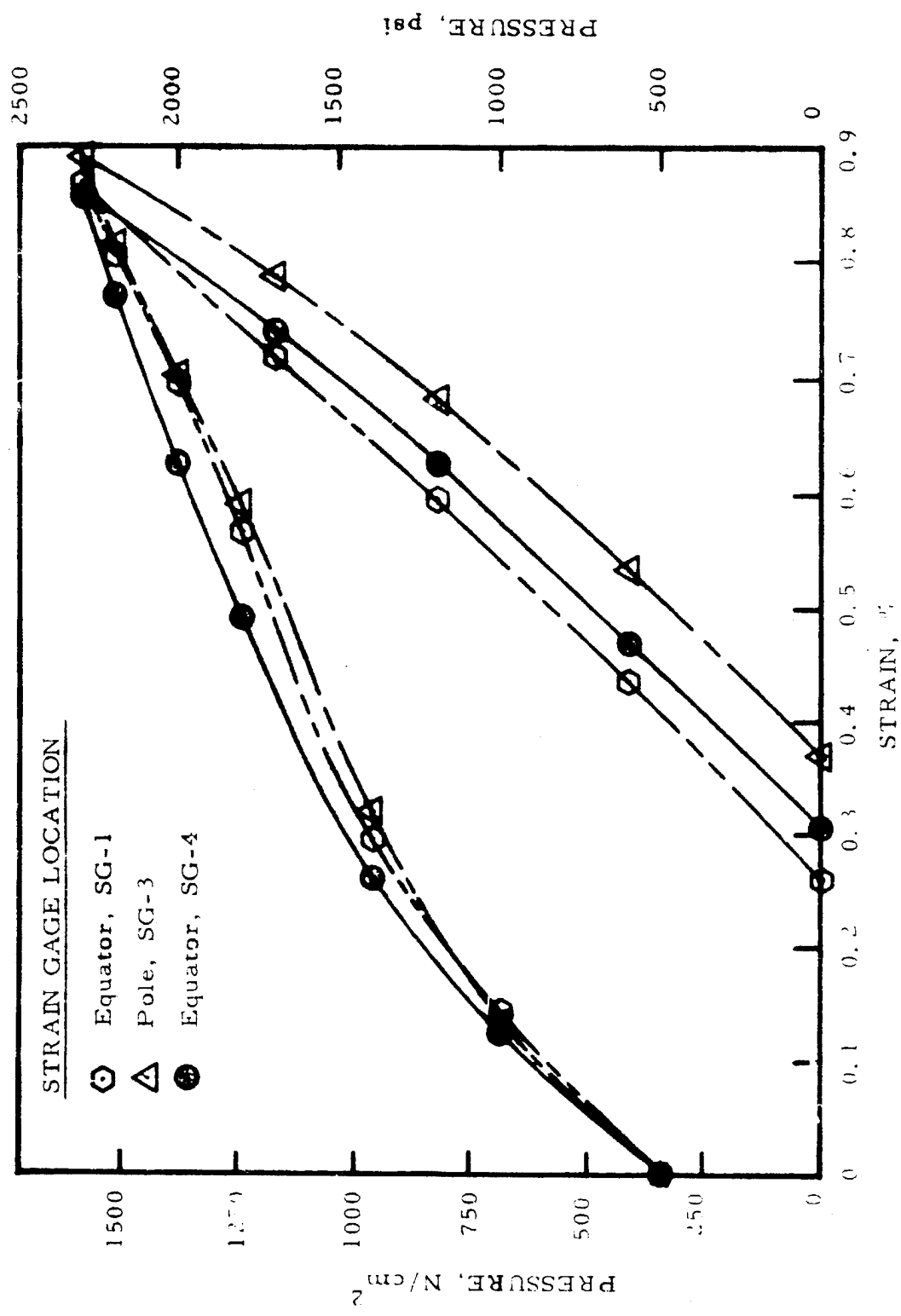
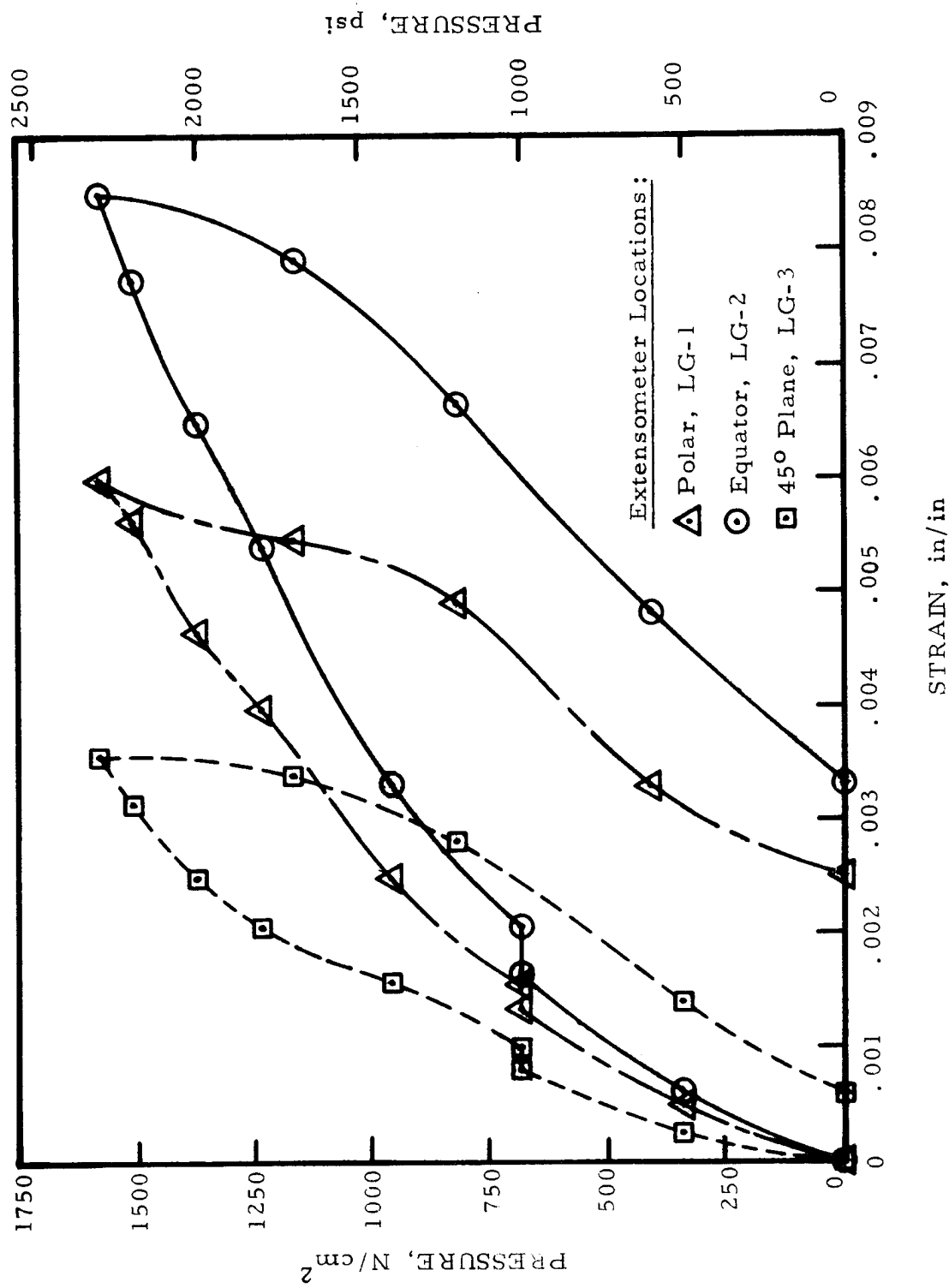


FIGURE 24. Strains Obtained From Circumferentially Oriented Strain Gages During Pressure Sizing of Kevlar-Aluminiun Vessel S-3



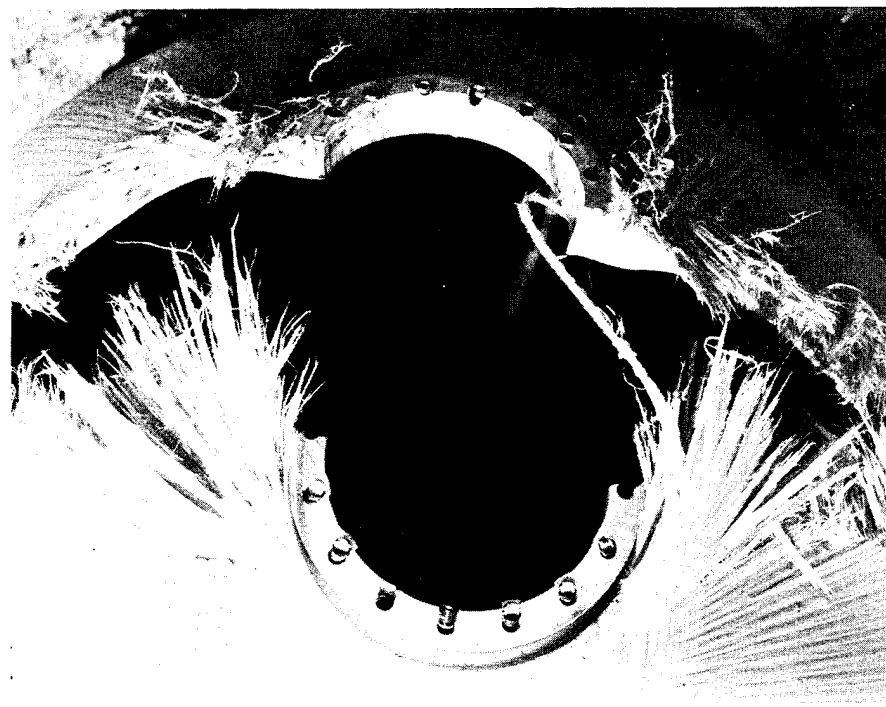
Following the sizing test, Vessel S-3 was subjected to a hydraulic burst test per the procedures of Appendix E. The minimum expected burst pressure for this series of vessels was 2787 N/cm^2 (4042 psi); the vessel failed, permanently, at a pressure of 1793 N/cm^2 (2600 psi). The failure initiated at the upper aluminum port in the region where the mating steel end closure bolts to the boss body; the failure consisted of a meridional split in the upper hemisphere traversing through the girth weld on either side of the shell and terminating in the lower hemisphere. Figure 26 shows the vessel after hydroburst, and Figure 27 shows close-up views of the upper (failure location) and lower port areas. Strain data obtained during the hydrotest from "great circle" extensometers are plotted in Figure 28.

A complete structural analysis of the vessel failure region was performed by both NASA and SCI. The following conclusions/observations resulted from the analysis:

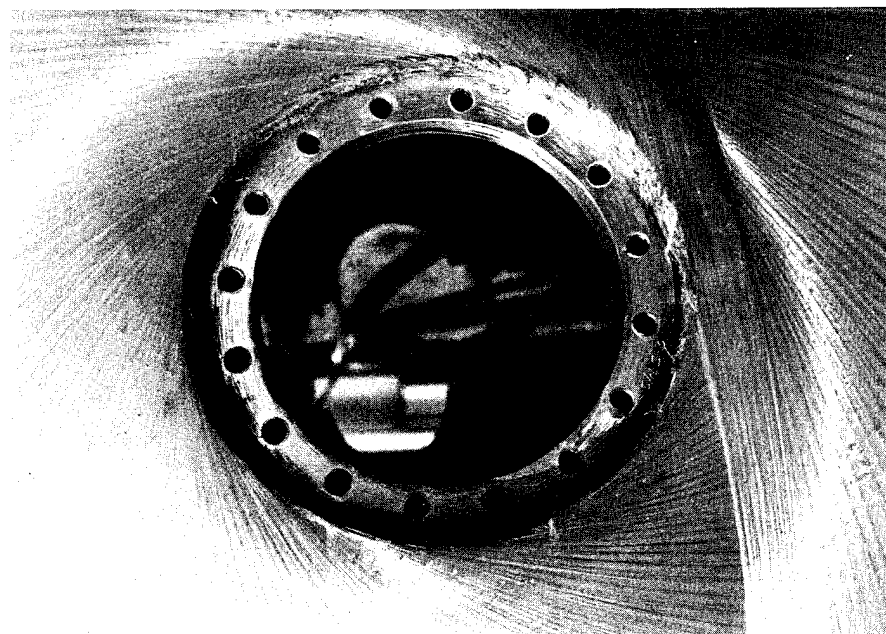
- Radial restraint of the aluminum boss/shell by the rigid, bolted, end closure induced large radial loads on the bolts. Effect of the radial bolt loads was a high bearing stress induced in the aluminum boss-body which was sufficiently large to cause local plastic flow. Plastic flow reduced the effective cross-section (bolt holes alone caused stress concentrations in boss body) of the boss body available for supporting applied hoop loads. The result was a hoop stress that exceeded the strength of the material and caused the meridional split in the shell.
- The large axial port load was transferred through the bolted closure as a vertical shear load reacting at the boss-body/shell juncture. The resultant couple induced high meridional bending stresses at the discontinuity. If relaxation of the rigid radial restraint at the bolt holes had not occurred, calculations indicate a bending failure would have occurred at the boss-body/shell juncture.



Figure 26: Kevlar/Aluminum Vessel S-3 After Hydroburst



(a) Upper Port



(b) Lower Port

Figure 27: Vessel S-3 Port Areas After Hydroburst

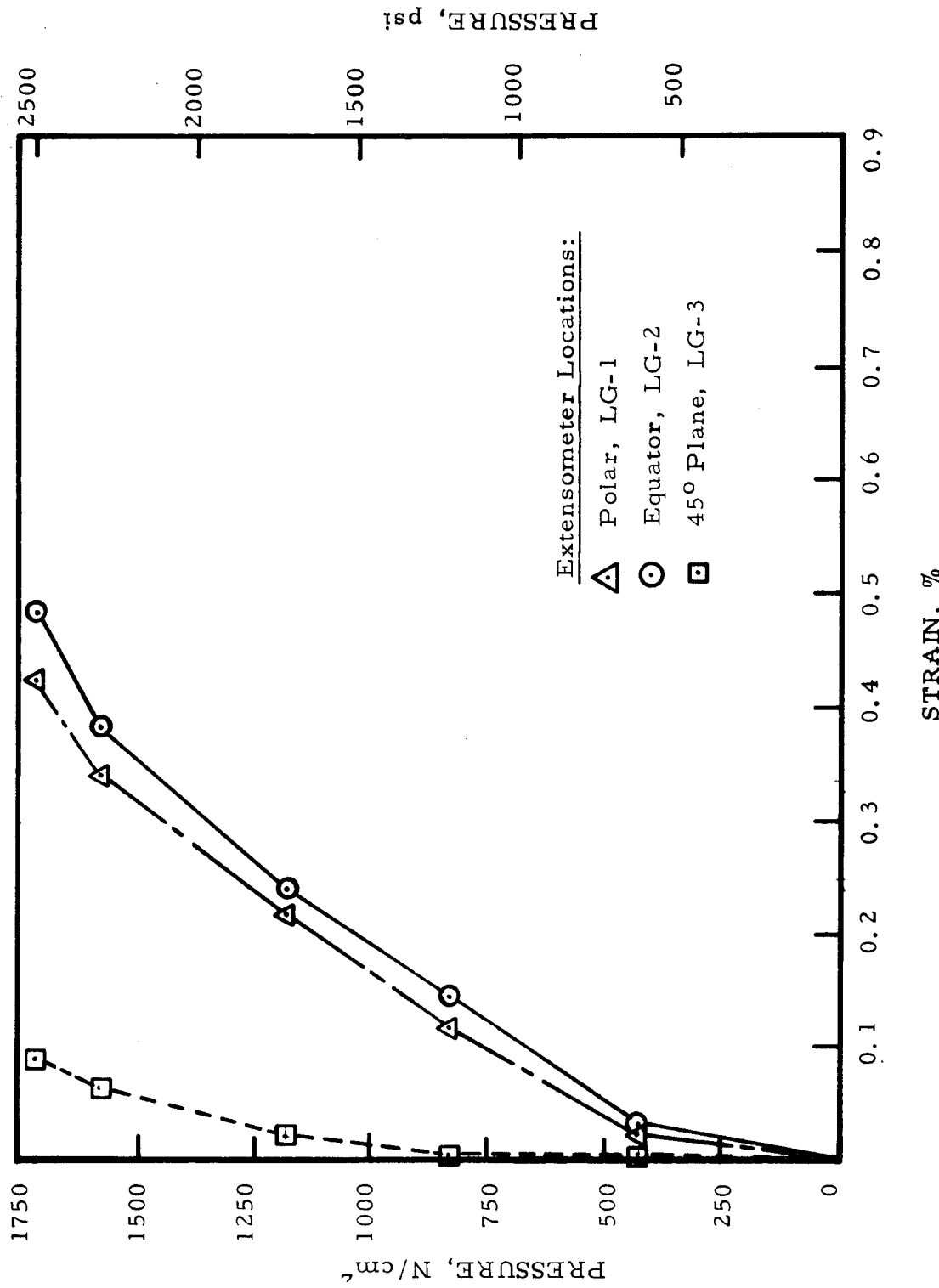


FIGURE 28: Strains Obtained From Great-Circle Extensometers During Hydraulic Burst of Kevlar/Aluminum Vessel S-3

- The major conclusion resulting from the analysis was to not only eliminate the radial bolt load, but also to substantially reduce the induced vertical shear load at the boss-body/shell juncture. The effect would be to allow natural expansion/rotation of the shell in the area of the port.

3. Redesign Effort

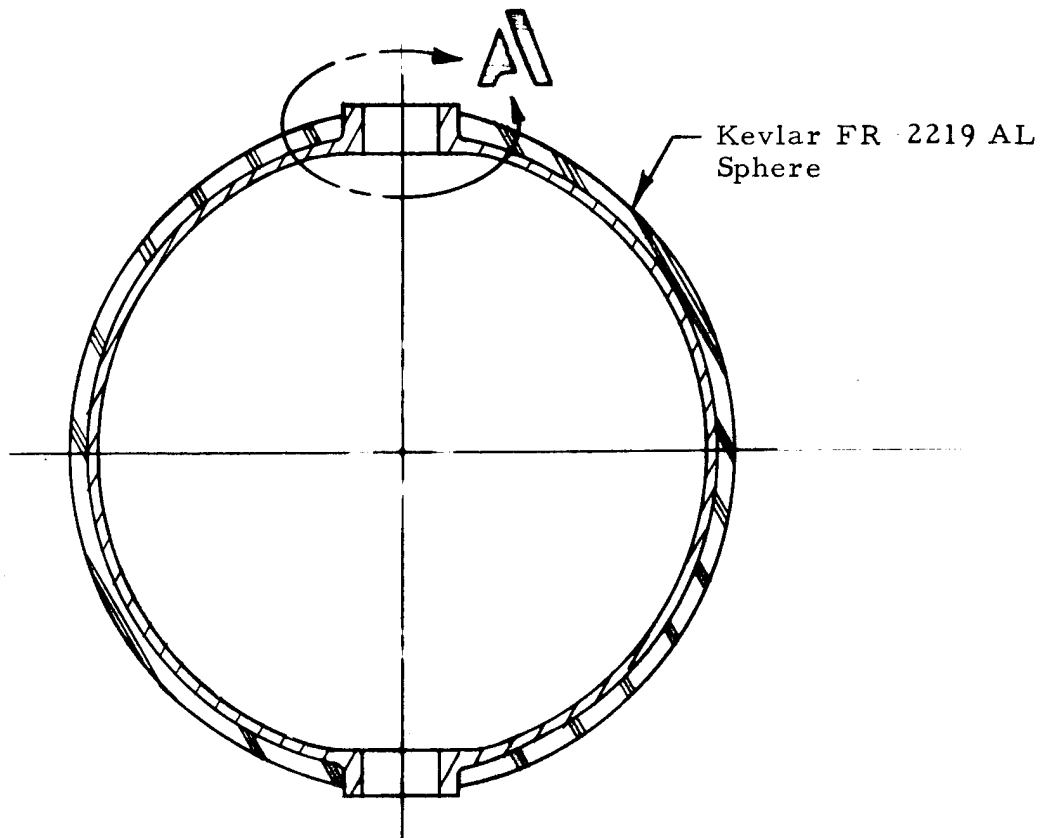
a. Port End-Closure

Based on conclusions from the preceding analysis and the desire to redesign the end-closure and not the vessel itself (liners had already been fabricated and machined), several design concepts were evaluated. Three of the concepts are shown schematically in Figure 29 and discussed below.

The Dished Closure of Figure 29a is a standard end-closure concept used in the static testing of large opening rocket motor cases. The closure is designed to allow natural rotation of the port and a corresponding control of both radial and axial bolt loads. In order to function properly, the vessel boss body, as well as the dish itself, must be designed as a unit. Since redesign of vessel porting details and refabrication was beyond the scope of the current program, this concept was discarded. The concept is noted for possible use in future efforts.

Figure 29b is a schematic of a Piston Tie-Rod, which was conceived under Contract NAS 3-13318. The piston-rod assembly is designed to carry the entire port load and acts independent of the shell itself. Calculations, based on utilization of this concept, indicated that the concept would allow sizing and pressure cycling of the vessel, but achievement of the desired burst pressure would be marginal. Counter rotation of the boss body (i.e., further reduction of the induced discontinuity moment) was required to sufficiently reduce stresses.

The end-closure concept finally selected for further design evaluation, termed Rigid Tie-Rod, is shown schematically in Figure 29c. The concept utilizes the piston feature of the Figure 29b design and also includes a method for application of counter rotation loads to the boss body. The gap (sizing gap) between the boss body and



A. DISHED CLOSURE

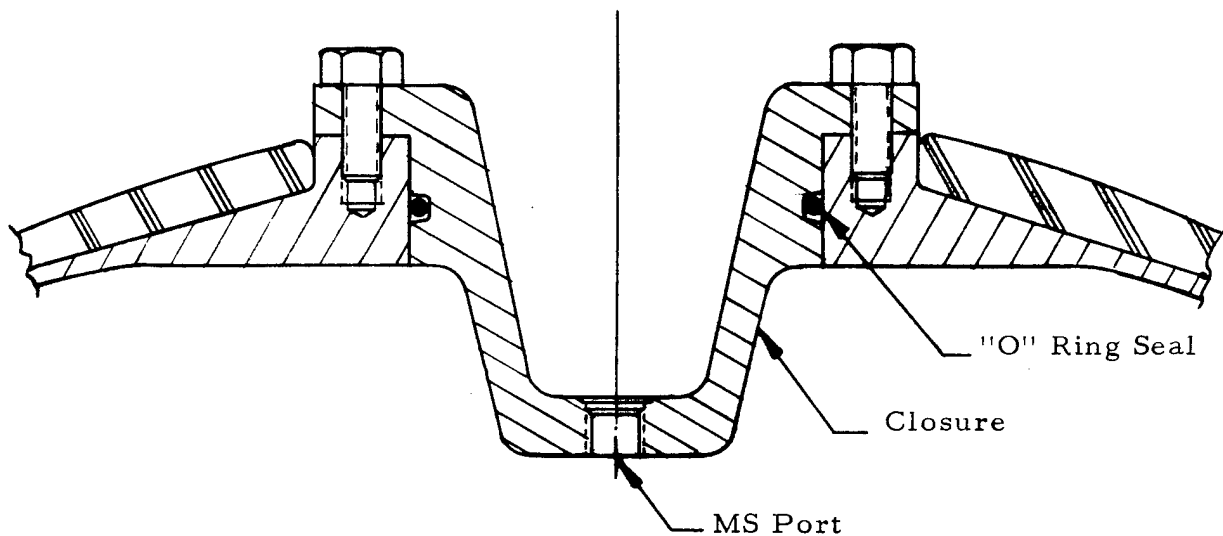
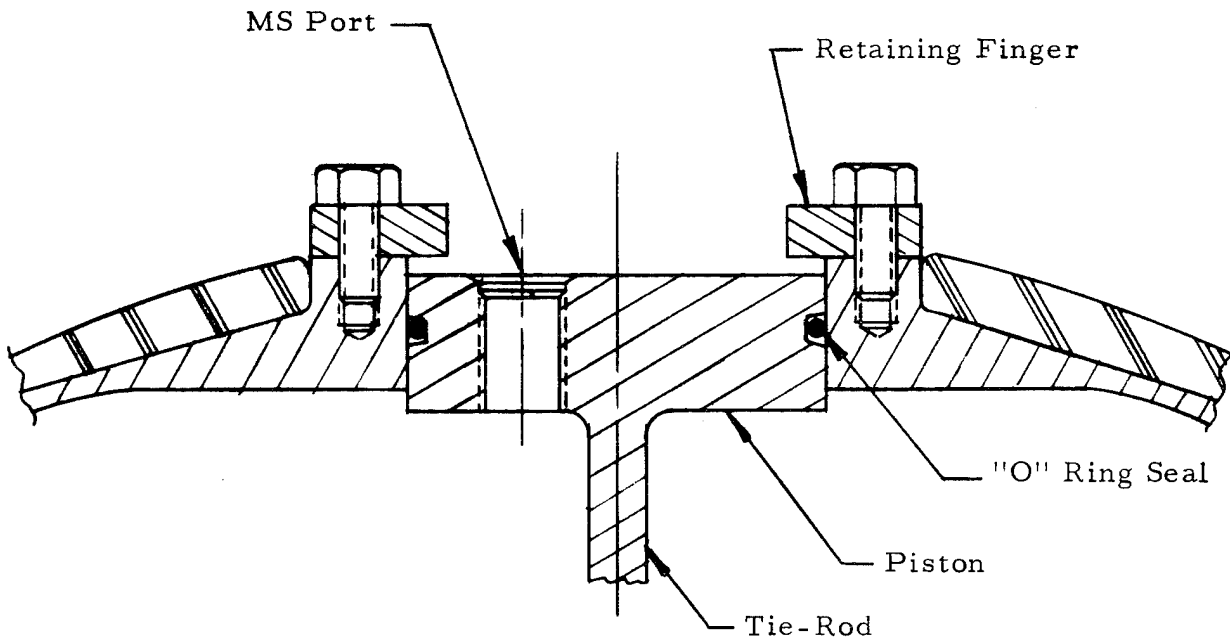


FIGURE 29: End Closure Design Concepts

B. PISTON TIE-ROD



C. RIGID TIE-ROD

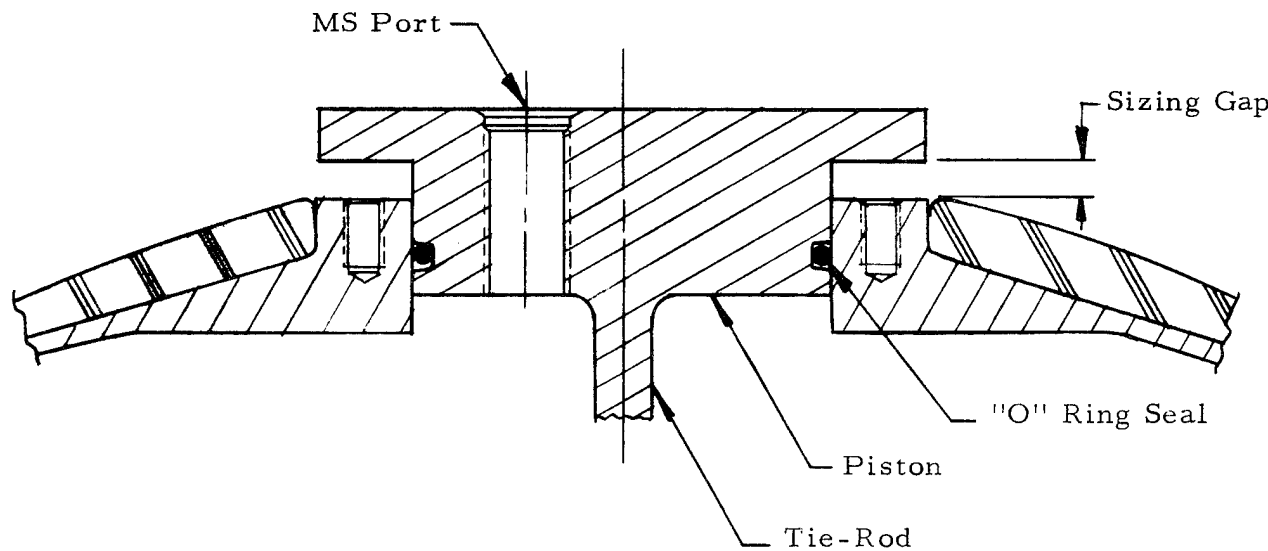


FIGURE 29: Concluded

piston flange can be varied to allow loading to occur at any point during vessel pressurization.

A brief parametric study was performed to optimize the rigid tie-rod design. Figure 30 is a schematic of the model used for the parametric study; the model was originally used during the conduct of the failure analysis effort. For the case of a rigid tie-rod, the closure is not bolted ($P_{HB} = 0$) and the axial "flange" load V_B is directionally reversed during pressurization of the vessel. The effect of the resultant compressive load V_B on the tank is a reversal of the induced vertical shear load V_D and a correspondent damping of the discontinuity moments M_D and M_S . Flange load effects on tank vertical shear load and also total rod load P_R are shown in the curves of Figure 31. It should be noted that the curves of Figure 31 represent loading per unit (tank) pressure.

Since both tank and rod-loading are a function of rod cross-sectional area (actually stiffness, but material is assumed to be steel), rod radius was used as the independent variable for construction of the design curves presented as Figure's 32 and 33. Figure 32 shows rod weight, stress, and strain as a function of rod radius. Also included in the figure is a table of materials (steels), their corresponding strengths, and allowable stresses. Possible design points are included in the figure. It should be noted in Figure 32 that tank axial strain is also depicted by the rod strain curve since axial strain compatibility was maintained in the study. Figure 33 indicates the effect of each specific rod on the stress distribution in the metal shell at the discontinuity (refer to radius r_s in Figure 30).

Inspection of the shell stresses of Figure 33, in conjunction with rod weight/stress values shown in Figure 32, lead to the selection of a 1.37 cm (0.54 inch) radius 200 grade maraging steel rod heat treated to 1930 MN/m^2 (280 ksi). This size rod was expected to reduce the bending stresses at shell discontinuities sufficiently to allow sizing, operation, and burst testing of the tank without overstressing the rod itself. The resultant predicted pressure versus axial strain of the tank/rod system is shown in Figure 34; this curve is referred to in later discussions of the test program conducted on these vessels.

b. Wrap Pattern Modification

One additional design modification which resulted from sizing test data obtained for Vessel S-3 concerns the Kevlar wrap pattern. Comparison of hoop and longitudinal strain data obtained

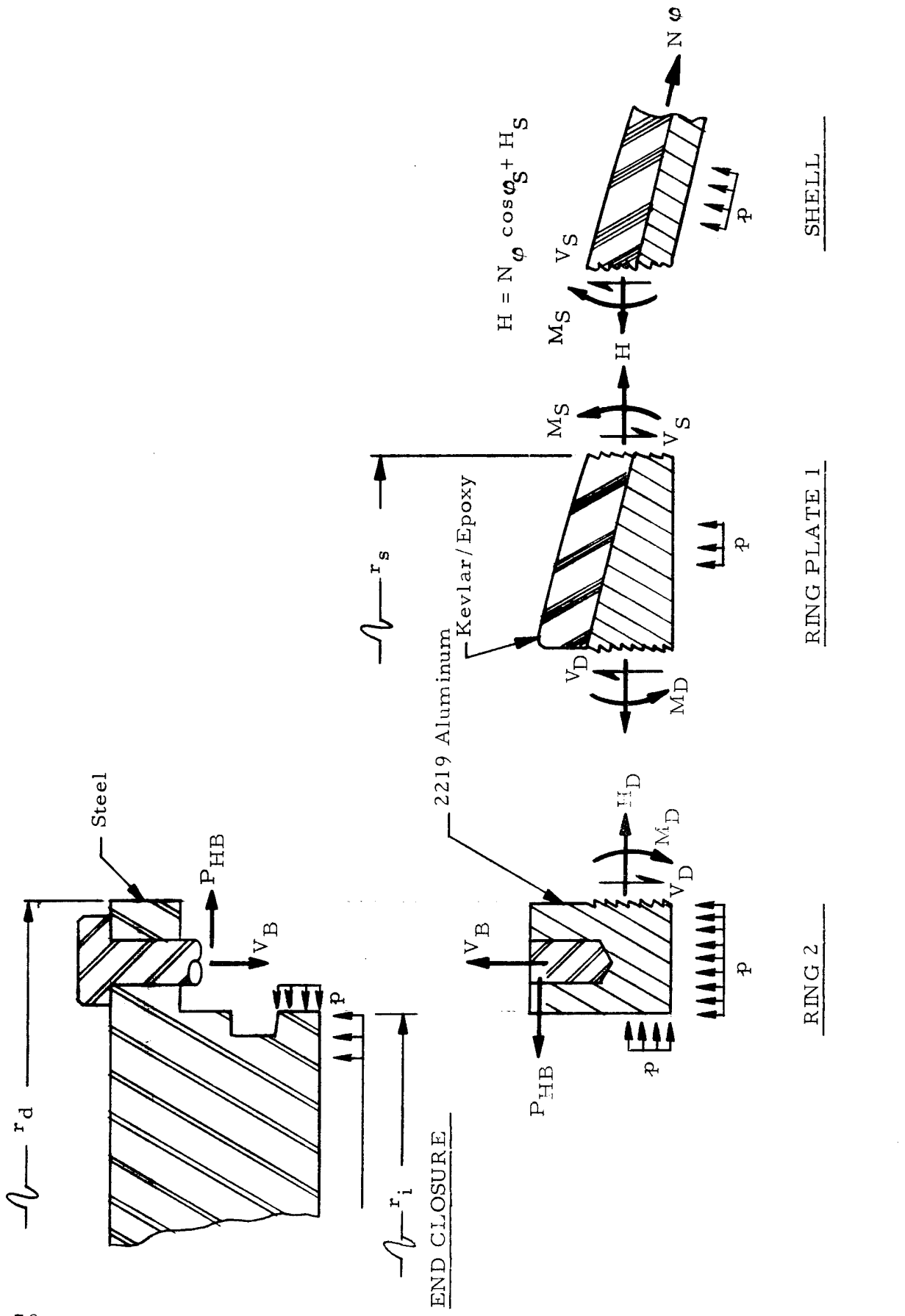


FIGURE 30: Model of Port Region, Kevlar Reinforced Aluminum Sphere

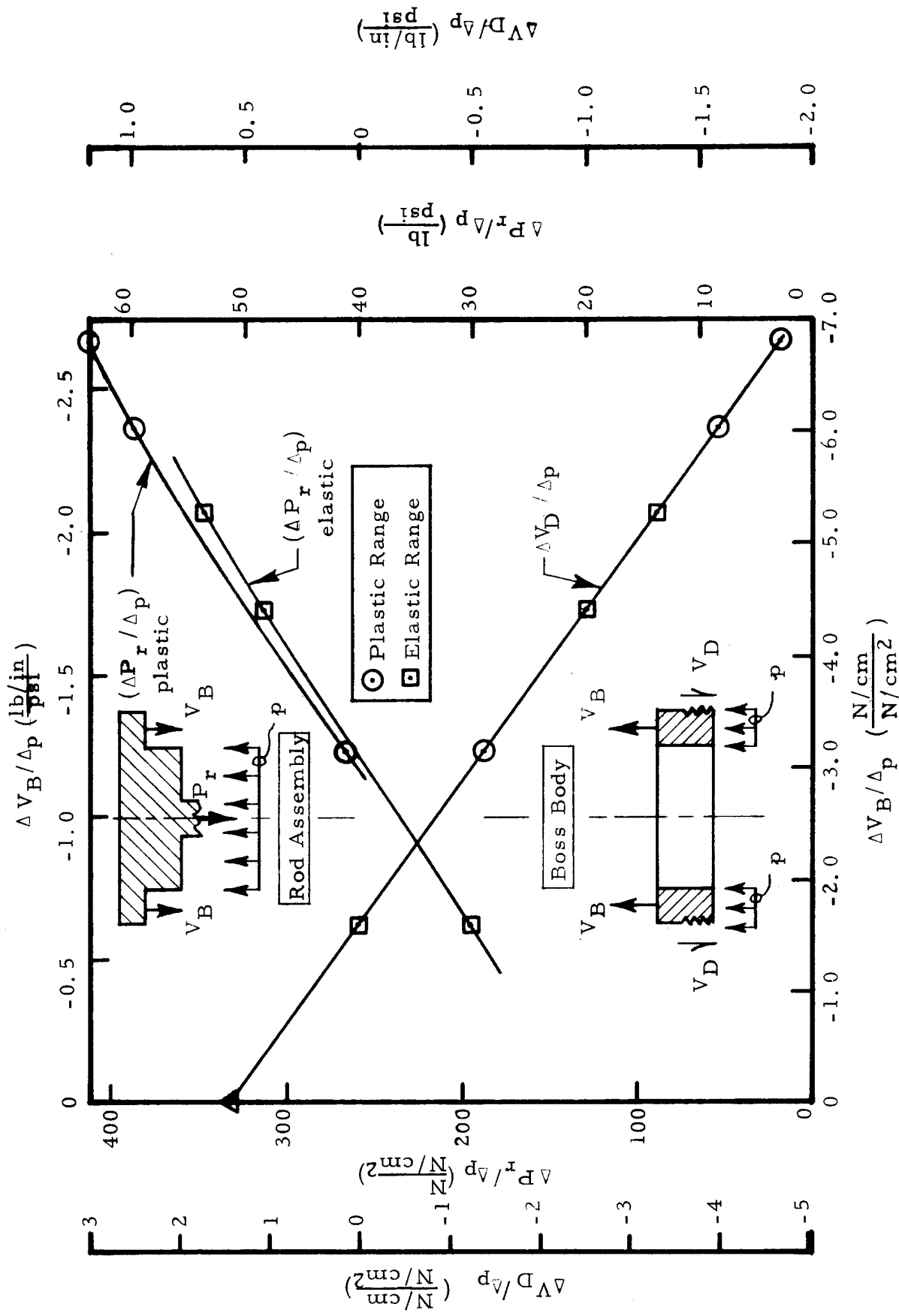


FIGURE 31: Tie-Rod/Boss Body Load Relations,
Kevlar/Aluminum Vessel

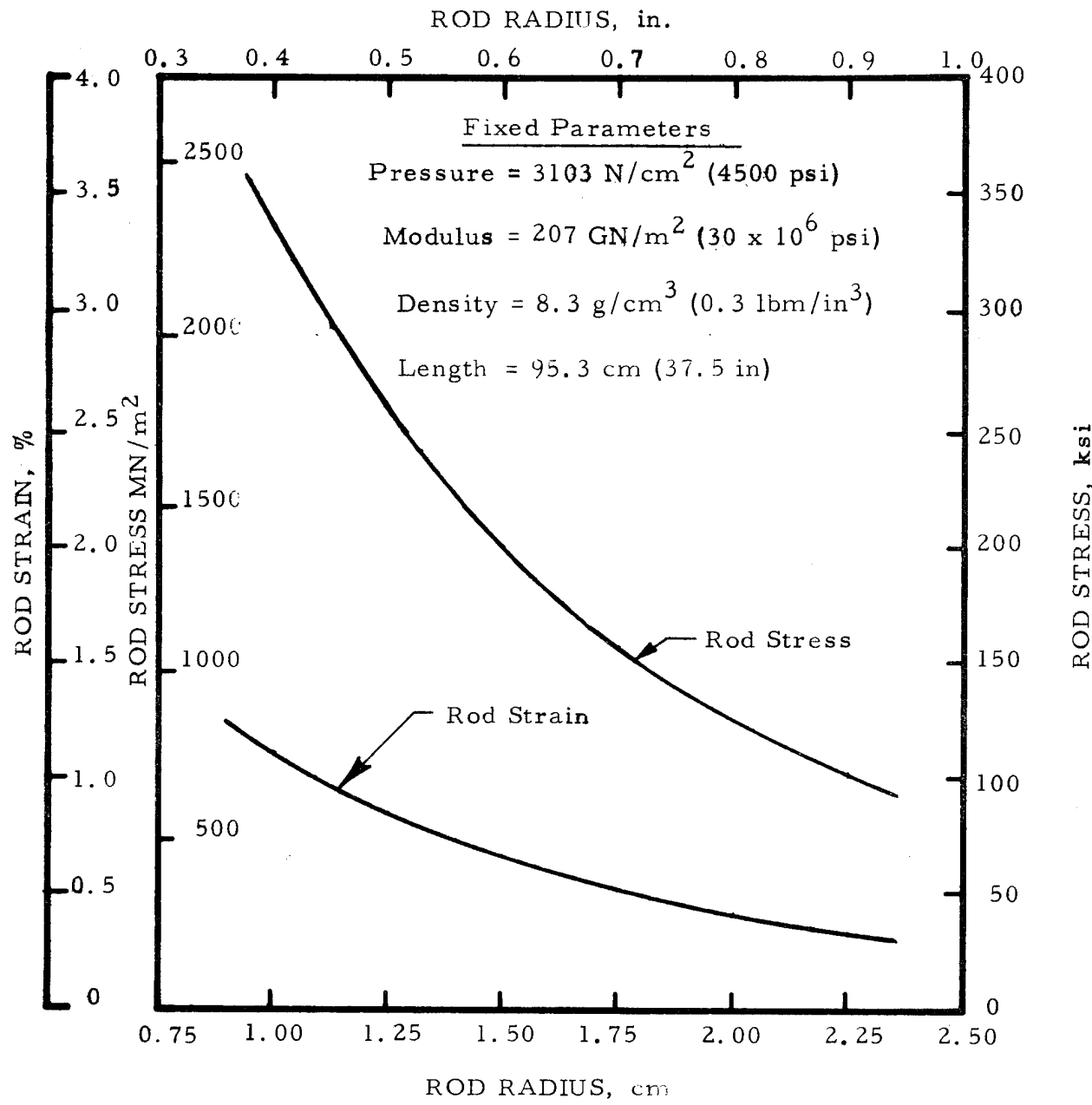


FIGURE 32: Tie Rod Design Parameters,
Kevlar/Aluminum Vessel

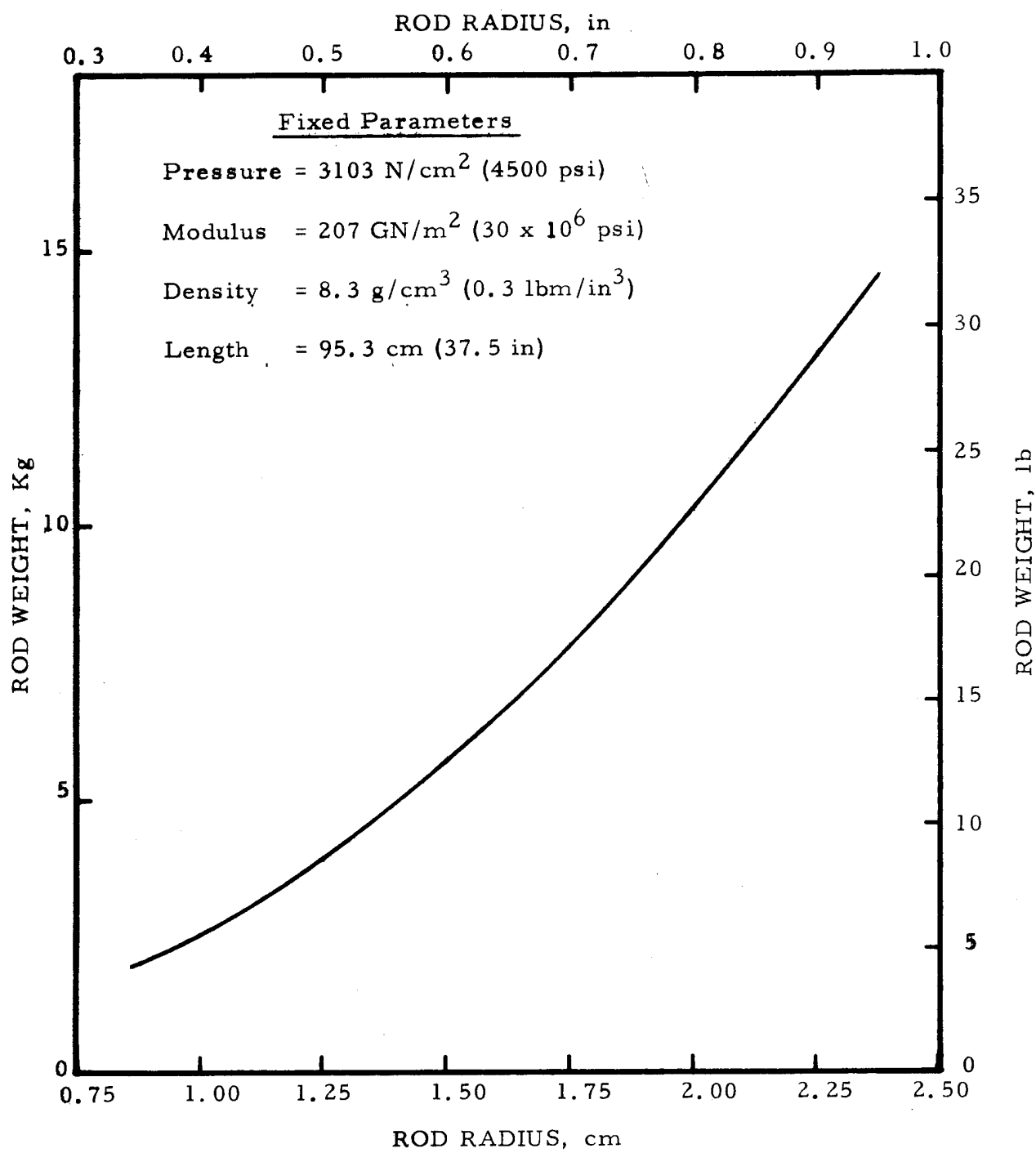


FIGURE 32 (Concluded): Tie-Rod Design Parameters
Kevlar/Aluminum Vessel

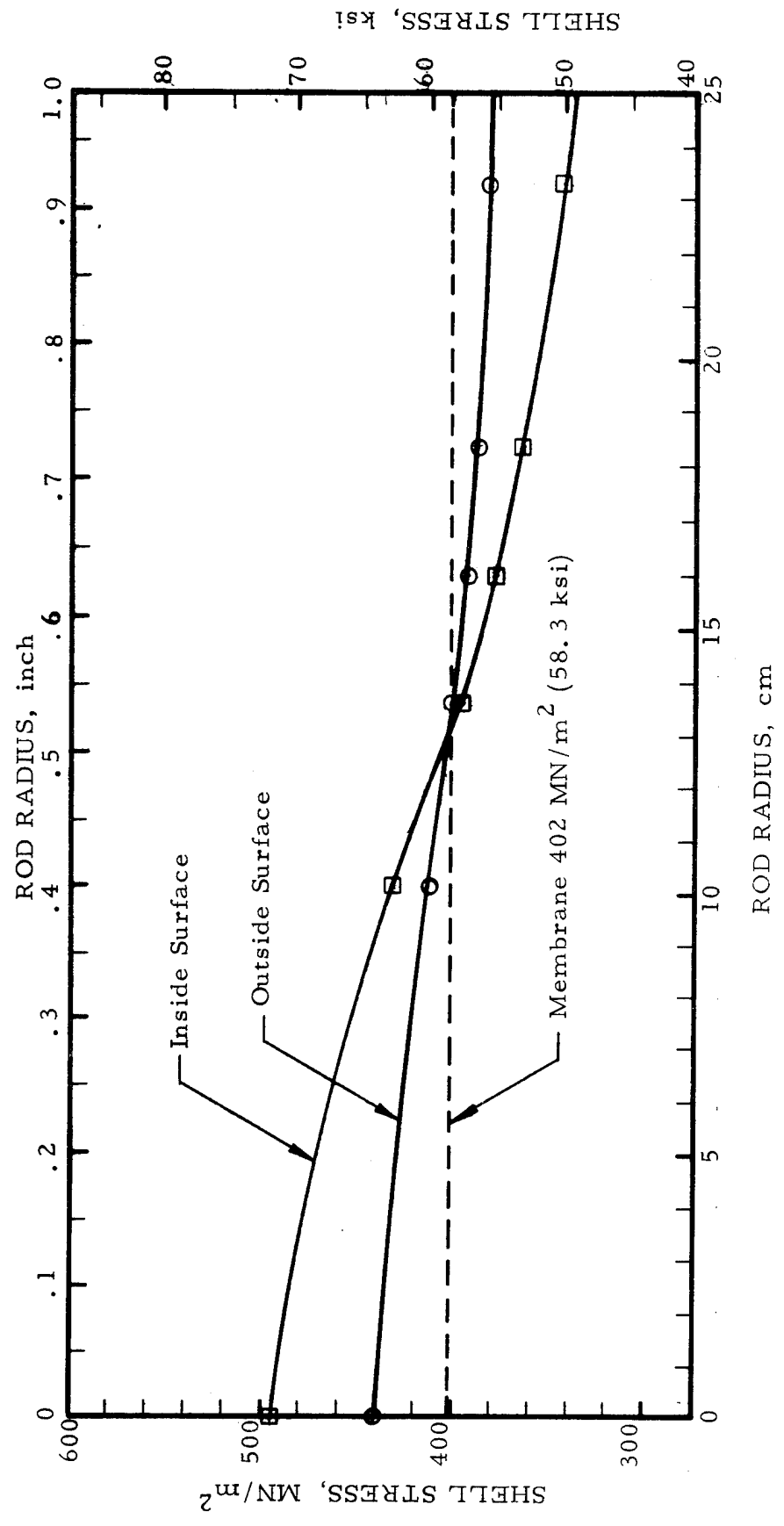


FIGURE 33: Effect of Rod Size on Shell Discontinuity Stresses, Kevlar/Aluminum Vessel

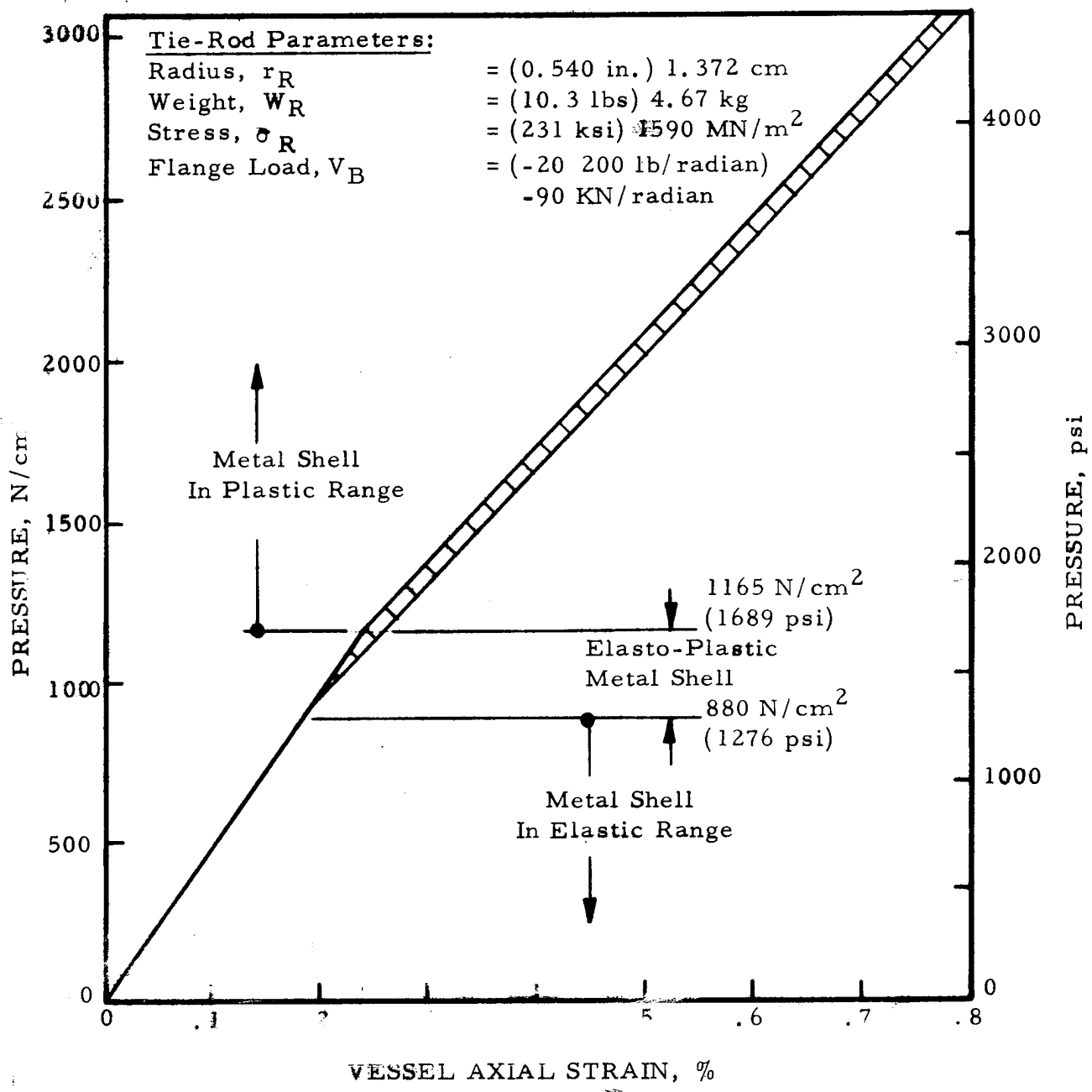


FIGURE 34- Pressure/Strain Relation for
Kevlar-Aluminum-Vessel Tie-Rod Assembly

at the equator during pressure sizing of the vessel (Figures 22 and 23) indicated an 11% deviation from the average. In order to better approach a 1:1 strain (stress) field in the metal shell during testing, additional hoop stiffness was required in the equatorial region. (It should be noted that the initial wrap pattern for this series of vessels was based on tests of vessels with non-structural liners, Section IIC 2a). Analysis of the existing pattern indicated that four additional revolutions at near-equatorial wrap angles (i.e. 2 revolutions each at 2 different angles) should produce a 1:1 stiffness ratio at the equator without disrupting strain ratios at other regions in the spherical shells. Thus, all vessels fabricated subsequent to Vessel S-3 contained the four additional revolutions as defined in the final winding pattern of Appendix D.

4. Final Test Results

Performance test results for all six Kevlar/aluminum vessels are summarized in Table XIV. The table indicates sizing data, the type of performance test conducted, the load level used for fatigue and sustained load testing, pressure cycles or sustained load period achieved, the failure pressure, modes of failure, and pertinent remarks. Pressure/strain curves depicting both the sizing test and performance tests are contained in Appendix F for the last five Kevlar/aluminum vessels tested. Comments regarding individual tests, amplifying the data recorded in Table XIV, are given below:

a. Cyclic Fatigue

Cyclic fatigue tests were conducted by increasing the vessel internal pressure to the design operating level and then reducing the pressure to zero. Per the test plan, Figure 21, two vessels were subjected to the Level 1 test of 1600 pressure cycles to 1396 N/cm^2 (2024 psi), and one vessel was subjected to the Level 2 test of 1000 pressure cycles to 1620 N/cm^2 (2350 psi).

The first Kevlar/aluminum vessel scheduled for cyclic fatigue testing, Vessel S-1, was successfully sized at the required pressure of 1862 N/cm^2 (2700 psi) utilizing the tie-rod assembly designed for this series of vessels. Strain gauge readings at the sizing pressure indicated nominal strains of 0.9% in the hoop and longitudinal direction at the equator and the 45° plane. Residual strain at zero pressure after sizing (permanent set) was approximately 0.3%. Figure 35 compares measured hoop

TABLE XIV
KEVLAR-49 OVERWRAPPED 2219-T62 ALUMINUM PRESSURE VESSEL
PERFORMANCE TEST DATA SUMMARY

Sequence of Testing	Vessel Serial Number	Sizing Pressure, N/cm ² (psi)	Final Internal Volume, m ³ (in ³)	Type of Performance Test	Operating Pressure, N/cm ² (psi)	Number of Pressure Cycles	Sustained Pressure- ization Period, hours	Failure Pressure, N/cm ² (psi)	Remarks
1	S-3 ^a	1586 (2300)	0.4413 (26 928)	Single Cycle Hydroburst	N.A.	N.A.	N.A.	1793 (2600)	Vessel tested with bolted end-closure. Failure occurred in upper port at a pressure of 1793 N/cm ² (2600 psi).
2	S-1	1862 (2700)	0.4431 (27 040)	Cycle Fatigue	1396 (2024)	1600	N.A.	N.A.	Tie-rod used during sizing and fatigue testing. Back up ring leak at cycle No. 335; no leaks after installation of new ring.
3	S-6	1862 (2700)	(c)	Cycle Fatigue	1396 (2024)	1600	N.A.	N.A.	Tie-rod used during sizing and fatigue testing with no problems or failure.
4	S-5	1862 (2700)	0.4423 (26 988)	Cycle Fatigue	1620 (2350)	124	N.A.	1620 (2350)	Vessel exhibited leak failure at girth weld during fatigue cycling test. Tie-rod used during all tests.
5	S-2	1862 (2700)	0.4423 (26 988)	Sustained Load	1396 (2024)	N.A.	172	N.A.	Tie-rod used during sizing and sustained load testing with no problems, leaks, or failure.
6	S-4	1862 (2700)	0.4440 (27 095)	Single Cycle Hydroburst	N.A.	N.A.	N.A.	2689 (3900)	Tie-rod failed at 2689 N/cm ² (3900 psi) during hydroburst test. Vessel exhibited no damage.

^a This vessel was not in same fabrication or test population.

^b Vessels did not fail during performance testing; additional tests to be conducted by NASA

^c Data not recorded

86

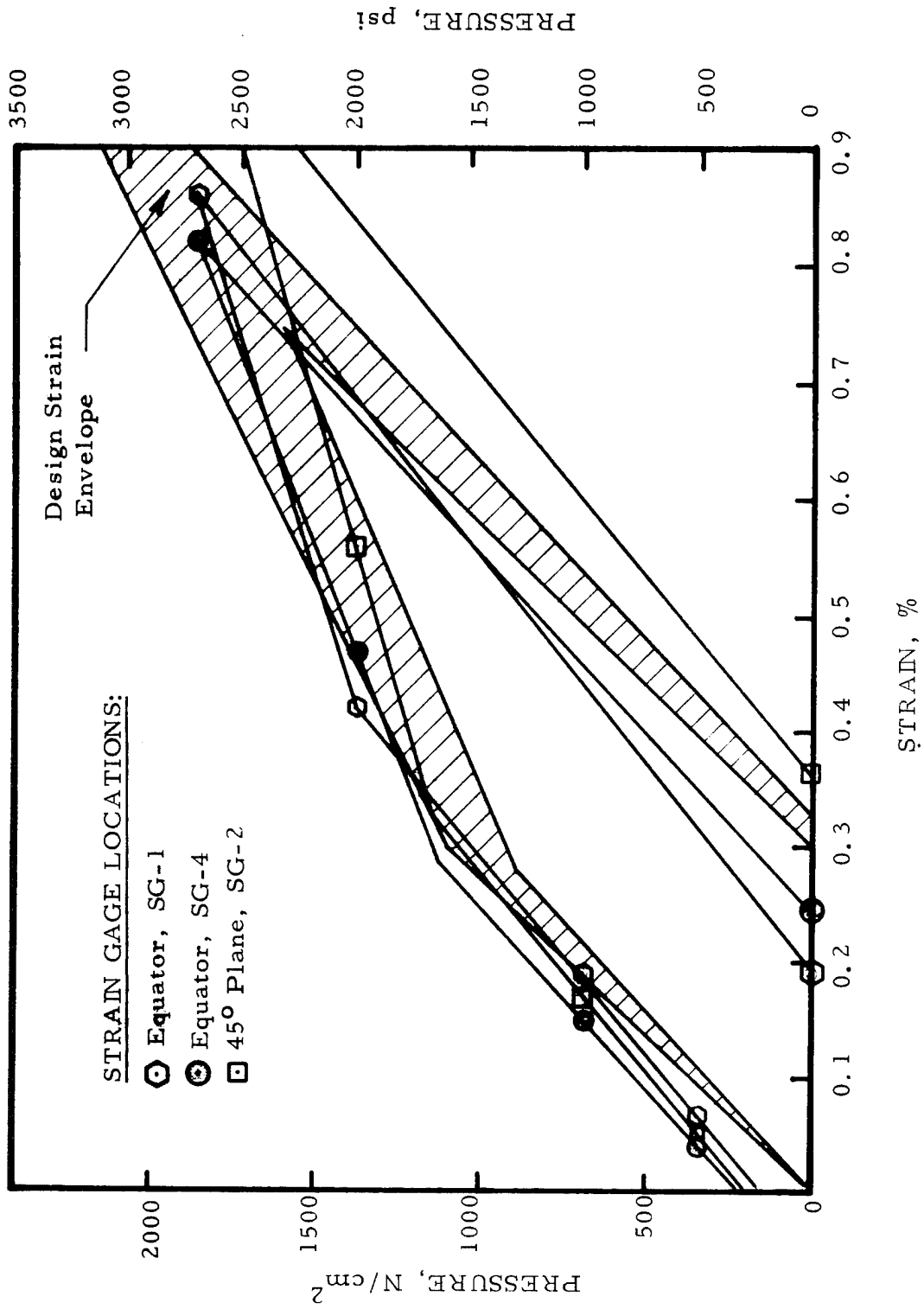


FIGURE 35: Predicted versus Measured Strains From Circumferentially Oriented Strain Gages During Pressure Sizing of Kevlar/Aluminum Vessel Serial Number S-1

strains, obtained from Appendix F, with the predicted "design strain envelope" from Appendix B. Due to the stiffening effect of the tie-rod, the nominal polar strain was approximately 0.4% at 1862 N/cm^2 (2700 psi). Recorded polar strain is compared to the predicted "polar strain envelope" in Figure 36.

Following the successful sizing operation, Level 1 pressure cycling was initiated for Vessel S-1 and after 335 cycles, a leak was observed at the test-plate/boss interface. Cause of the leak was an extruded back-up ring which was replaced and cycling reinitiated. No other problems were encountered during the additional 1265 cycles, and the vessel successfully passed the prescribed test without failure or any additional leakage. Figures F- 1 through F- 3 of Appendix F show the pressure/strain relations obtained for this vessel during fatigue testing.

Kevlar/aluminum Vessel S-6 was successfully sized at the required pressure of 1862 N/cm^2 (2700 psi) and, also, subjected to 1600 pressure cycles to the Level 1 operating pressure of 1396 N/cm^2 (2024 psi). No problems or leaks were encountered during the conduct of this test; pressure/strain relations for the vessel are shown in Figures F-22 through F- 24 of Appendix F. Following the Level 1 fatigue tests, both vessels S-1 and S-6, were shipped to NASA LeRC for additional performance tests.

In order to obtain cyclic fatigue data at higher operating stress levels, the prescribed operating pressure for Vessel S-5 was increased to the Level 2 value. Following the sucessful sizing of this unit to 1862 N/cm^2 (2700 psi), the vessel was subjected to pressure cycling between zero and 1620 N/cm^2 (2350 psi). At pressure cycle number 124, test fluid leakage through the Kevlar composite shell was observed. The leakage was in the region of the equator,rather than the boss,suggesting failure of the girth weld. It should be noted that this vessel had the 0.157 cm (.062 in) weld mismatch as discussed in Section IIC 1c. The test was terminated at this point and the vessel shipped to NASA LeRC for additional investigation of the failure location. Pressure/strain relations for the vessel are plotted in Figures F-16 through F-21 of Appendix F.

b. Sustained Pressurization

Sustained load tests were conducted by increasing the vessel internal pressure to the design operating level

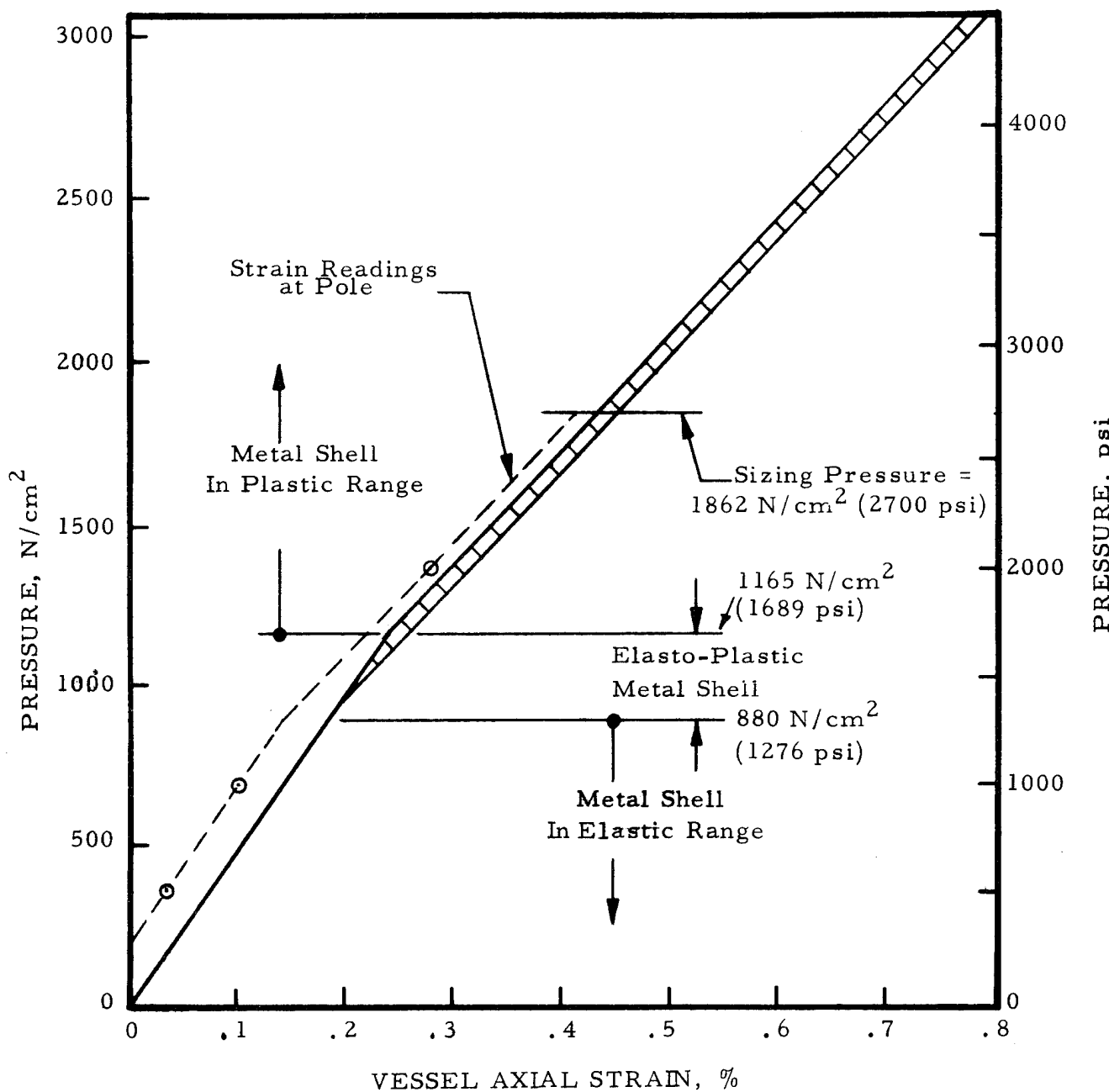


FIGURE 36- Predicted versus Measured Polar Strain During Pressure Sizing of Kevlar/Aluminum Vessel S/N S-1

and holding this level for the prescribed time period. The single vessel scheduled for sustained pressurization, Vessel S-2, was successfully sized at 1862 N/cm^2 (2700 psi) and subjected to a Level 1 sustained load of 1396 N/cm^2 (2024 psi) for a period of 172 hours. No evidence of leakage or degradation was observed during the entire period, and the vessel was subsequently shipped to NASA LeRC for further testing. Pressure/strain relations for the vessel are shown in Figures F- 4 through F- 9 of Appendix F.

c. Single Cycle Hydroburst

The last vessel in this series, Vessel S-4, was successfully sized at a pressure of 1862 N/cm^2 (2700 psi) and subjected to a hydroburst test. At a pressure of 2689 N/cm^2 (3900 psi), the tie-rod failed in tension at the first thread; no apparent damage was sustained by the vessel. Figure 37 shows the vessel and the tie-rod/test-plate after the hydroburst test. Figures F-10 through F- 15 of Appendix F show the pressure/strain relations obtained for this vessel.

5. Evaluation of Test Results

a. Sizing Test Data

Measured values of internal volume obtained for the Kevlar/aluminum vessels, after the sizing operation, were within 0.3% of each other and the average measured value of 0.4424 m^2 ($27\ 000 \text{ inch}^3$) deviated from the design value of 0.4441 m^2 ($27\ 100 \text{ inch}^3$) by only 0.4%.

At the sizing pressure of 1862 N/cm^2 (2700 psi), the range in recorded vessel strain obtained from (1) biaxial strain gages was 0.60 to 0.90%, and from (2) extensometers was 0.40 to 0.60%; the design strain range at this pressure (Appendix B) was 0.80 to 0.95%. At zero pressure after the sizing operation, the recorded strains were in a range of 0.15 to 0.35% compared to the design value of 0.30%. The general lower range of strain values obtained from the extensometers (refer to Appendix F) was probably caused by the three "great circle" wires binding on each other during vessel pressurization. Although Teflon channel-guides were utilized to minimize binding, recorded strains indicated this frictional effect was not eliminated.

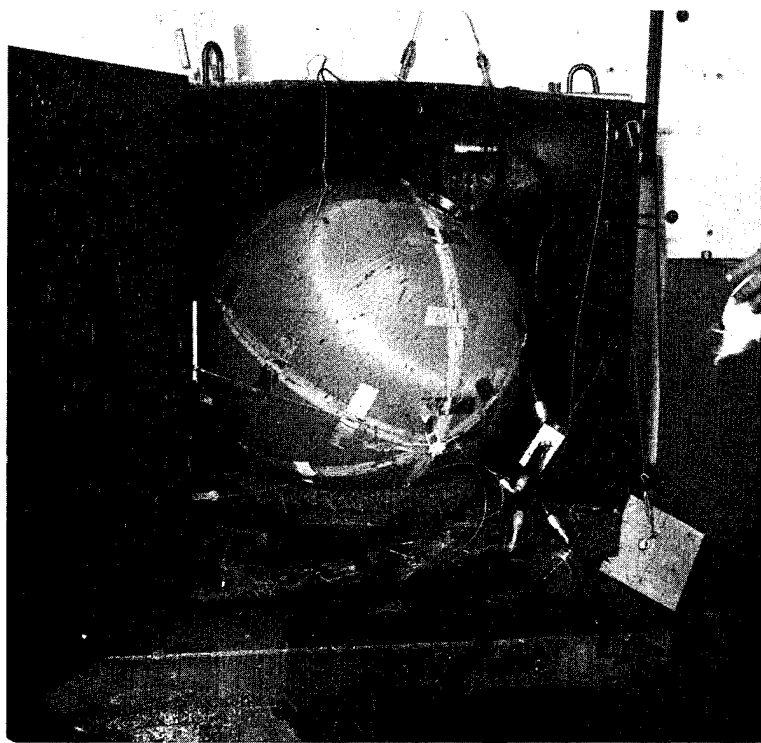


Figure 37: Kevlar/Aluminum Vessel Serial S-4
after Hydroburst

It was concluded that the good comparison of measured data (i.e. strains and volumetric expansions) with design values verified the validity of the analytic method used to predict shell stresses.

b. Port End-Closures

Test results for Kevlar/aluminum Vessel S-3 clearly indicated the inadequacy of the original relatively large diameter bolted test closure design (the large diameter was required due to the need to meet 2219-T62 heat treating requirements, as previously discussed). The revised design, incorporating a tie-rod to carry the port load, provided a good solution for completing performance tests on the existing vessels but it did not allow burst testing of a vessel. The premature failure of the tie-rod (13% below design) was probably due to the inherent brittle behavior of the required ultra-high-strength steel coupled with the load history prior to burst testing (i.e. cyclic fatigue of three units at two levels plus sustained load on the fourth unit). For future applications, the ability to initially design the tie-rod and porting details as a unit might allow the use of lower strength (greater ductility) rod materials and also greater design margins of safety. However, the best solution is more detailed and complete design analysis on the metal boss and bolted closure (acting as a unit) than was employed for original design development in this program.

c. Performance Test Data

Since all vessels subjected to cyclic fatigue and sustained loading were not burst tested, the effect of these load conditions on vessel performance is not known. Strain data presented in Appendix F, indicate there is very little change in vessel operating characteristics with either time or pressure cycling. The leak type failure of Vessel S-1 did verify the inherent safety of filament-reinforced metal pressure vessels, and the known fact that built-in geometric discontinuities, especially in the weld zone, can lead to premature failure of a vessel.

Neglecting the weight of the tie-rod, the operating performance factor ($p_0 V/W$) for both vessels subjected to Level 1 tests was 83.4 J/g (335 000 in-lb/lbm); the Level 2 operating performance factor was 95.7 J/g (384 000 in-lb/lbm). Kevlar/aluminum Vessel S-5 demonstrated a performance factor of

164 J/g (658 000 in-lb/lbm) at the rod failure pressure of 2689 N/cm² (3900 psi), and the potential performance factor at the predicted burst pressure of 3137 N/cm² (4550 psi) was calculated to be 191 J/g (768 000 in-lb/lbm).

III. DESIGN, FABRICATION, AND TEST OF KEVLAR-49 OVER-WRAPPED CRYOFORMED 301 STAINLESS STEEL PRESSURE VESSELS

Section IIA discussed the evolution of design criteria which lead to the selection of the Kevlar-49 overwrapped cryoformed 301 stainless steel (Kevlar/stainless steel) pressure vessel for further evaluation. Prime basis for the selection was the excellent weight saving potential offered by the combination of Kevlar-49 fibers and cryoformed 301 stainless steel (References 3 and 6). For clarity, a brief explanation of the cryoforming process and its use for the current application is given below:

The cryogenic stretch forming process (cryoforming), as pictorially depicted in Figure 38, consists of plastically straining a closed undersize metal preform at liquid nitrogen temperature in order to achieve a high degree of work hardening (lattice structure change) without changing the chemical composition of the material. The net result is a strong metallic material (yield strength increased by a factor of approximately seven) that is exceptionally tough and is compatible with severe environments.

The strengthened liner is then overwrapped with resin impregnated fibers, cured, put back into the liquid nitrogen bath and "sized" to form the required pressure vessel. The sizing operation further strengthens the metal in addition to establishing the desired prestress conditions (fibers in tension/metal in compression).

The cryoforming process described above was developed by ARDE Incorporated and is currently being used by them to manufacture homogenous metal pressure vessels as well as fiber reinforced metal vessels. As stated in Section IIA, the tasks of designing the Kevlar/stainless steel vessel for this program and fabrication of the required metal liner assemblies were delegated to ARDE.

A. DESIGN

Initial criteria, which formed the basis for preliminary design of the Kevlar/301 pressure vessel, established the vessel burst-to-operating pressure ratio (safety factor) at 2:1 and the vessel fatigue cycle life at 1600 operating pressure cycles. Both of these criteria reflected the then current space program design criteria. Additional design criteria provided to ARDE are summarized on the following page:

(1)

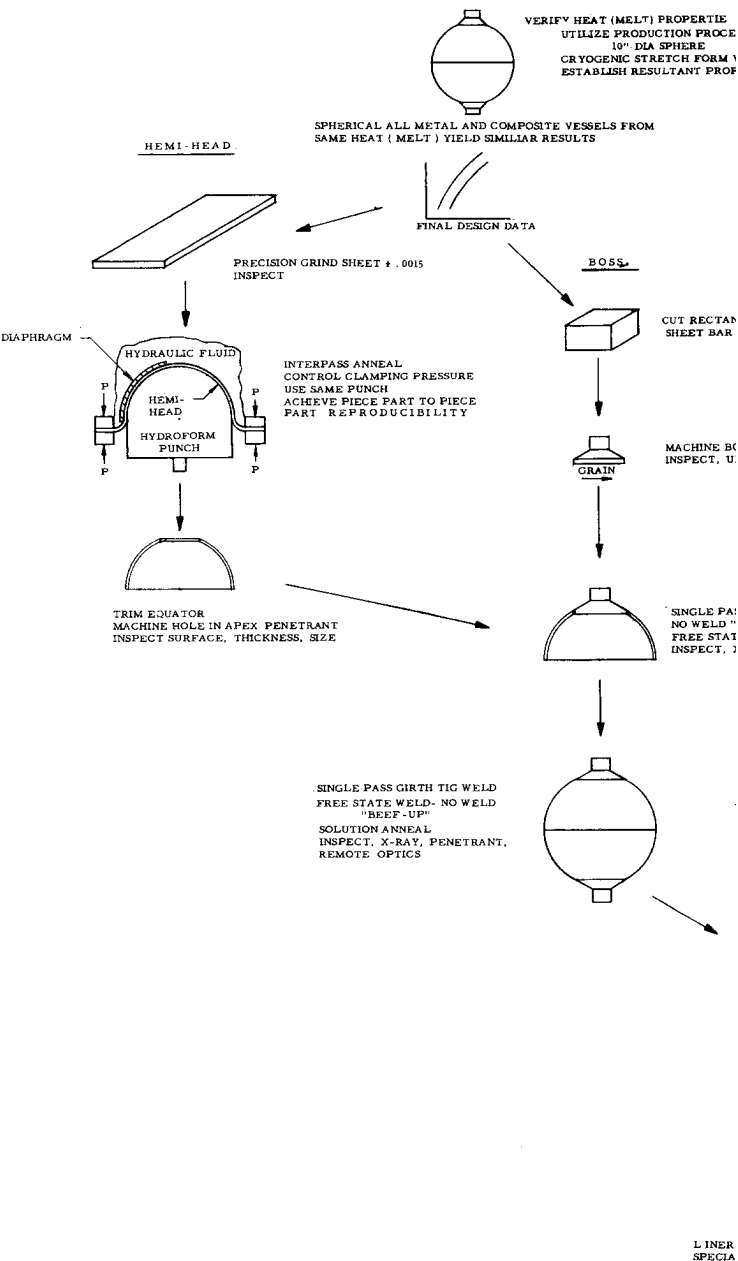
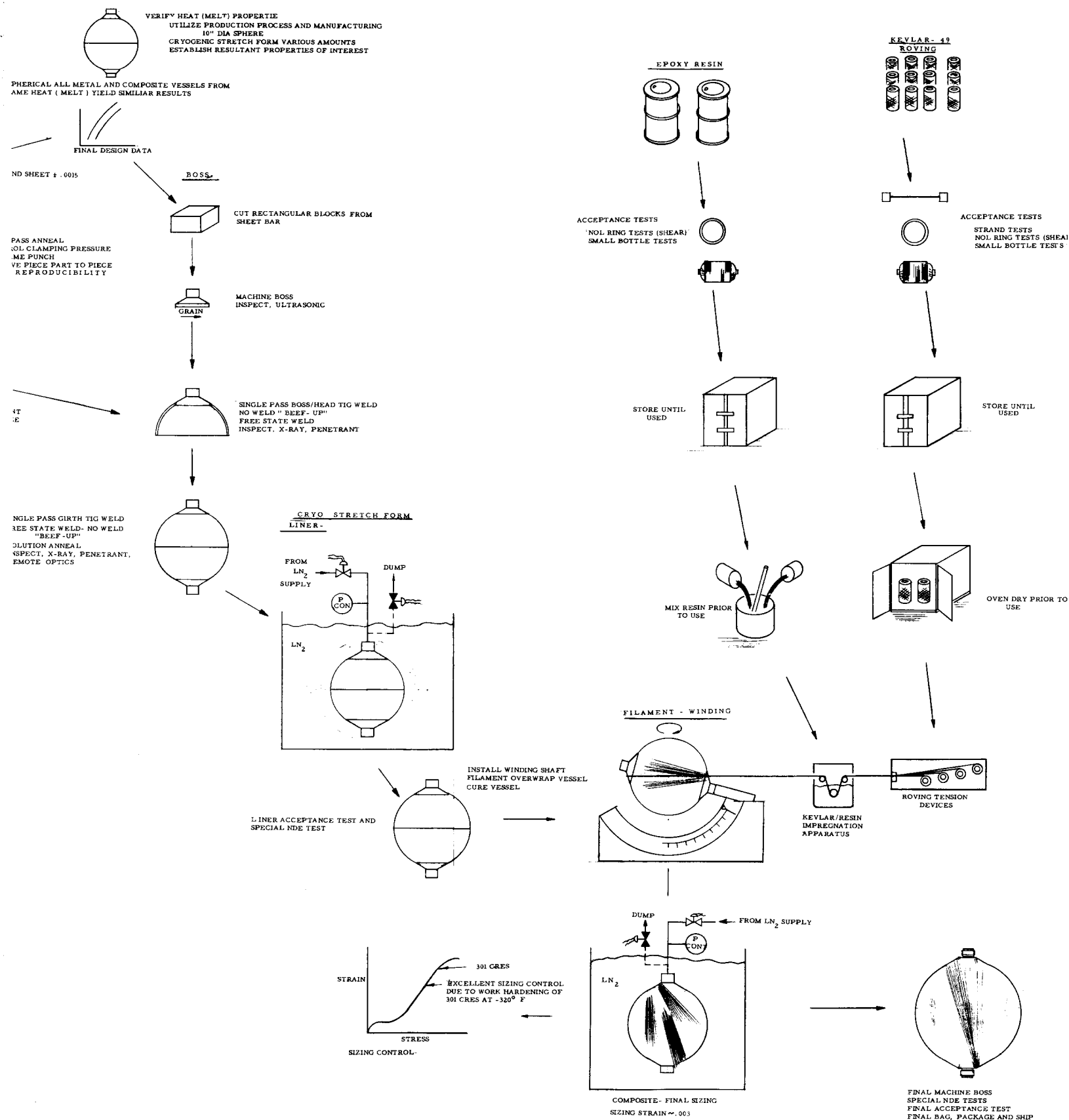


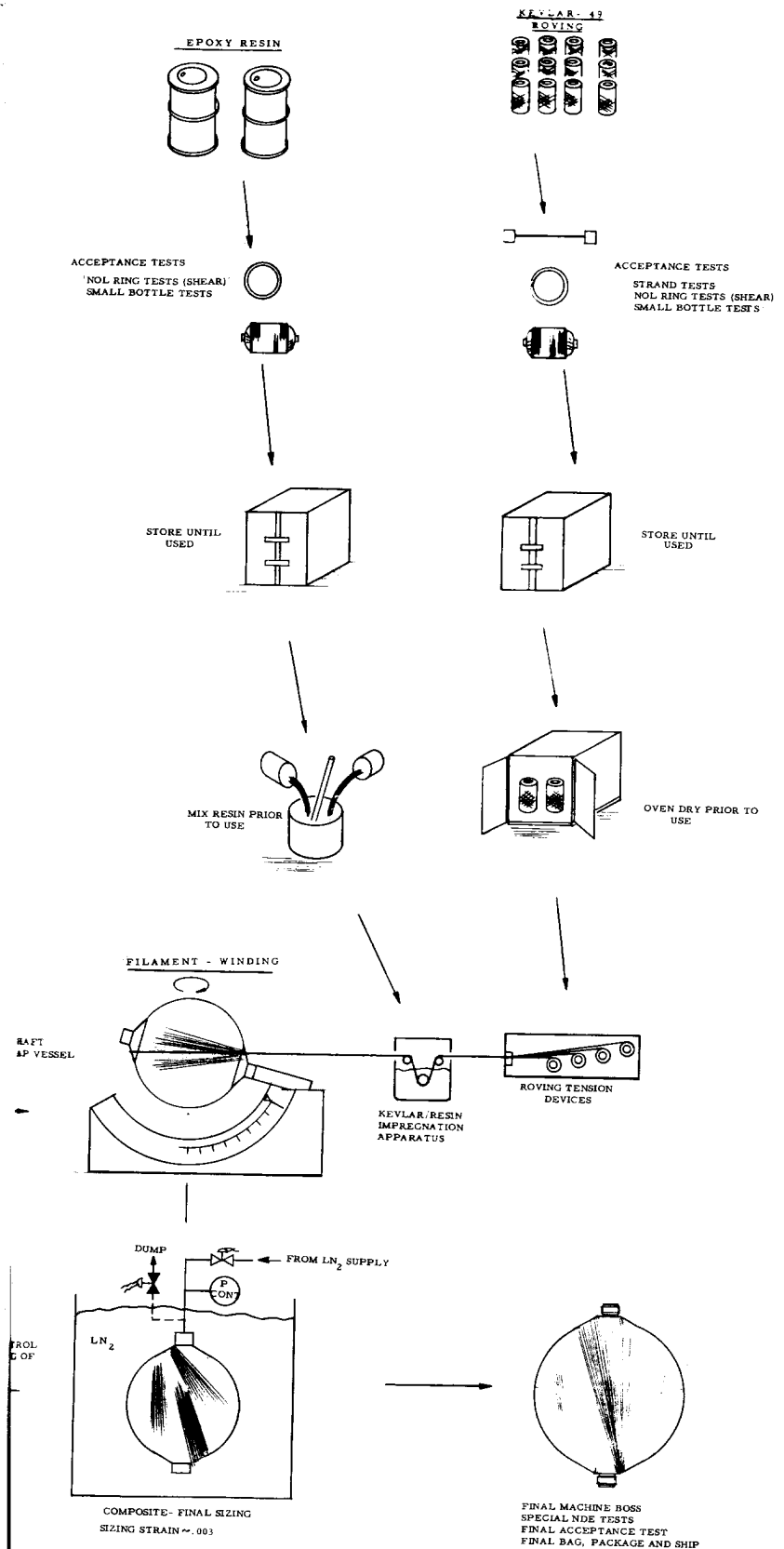
FIGURE 38: Pictorial Manufa
301 Stainless Ste

(2)



JRE 38: Pictorial Manufacturing Flow Plan Overwrapped Cryoformed 301 Stainless Steel Spheres

(S)



rapped Cryoformed

<u>Parameter</u>	<u>Valve</u>
Shape	Sphere
Vessel Weight	TBD (minimum)
Vessel Volume, Nominal	0.115 to 0.123 m ³ (7000 to 7500 in ³)
Outside Diameter.	61.0 to 63.5 cm (24.0 to 25.0 in.)
Metal Shell Thickness	0.102 to 0.127 cm (0.040 to .050 in.)
Kevlar/epoxy Composite Thickness.	TBD
Operating Pressure.	TBD
Metal Operating Stress	690 MNm ² / (100 ksi)
Fiber Operating Stress	986 MN/m ² (143 ksi)
Burst Performance Factor	TBD

Material properties used for the design are presented in Table XV, and the resultant preliminary design analysis, provided by ARDE, is included as Appendix G. Engineering drawings of the welded 301 stainless steel liner assembly (ARDE Part Number D3895) and the Kevlar FR spherical vessel (ARDE Part Number D3898) are shown in Figures 39 and 40, respectively.

As noted in Appendix G, the design analysis defines the operating and design burst pressure of the vessel as 1790 N/cm² (2600 psi) and 3580 N/cm² (5200 psi), respectively. Subsequent to preparation of the analysis, an "in-house" subscale vessel effort was conducted by ARDE/SCI to verify the Appendix G design. The vessel utilized for the study was a 20.3 cm (8.0 inch) diameter scale model of the full scale Kevlar/301 vessel. Figure 41 shows two views of the subscale vessel. Based on the test results obtained during this effort, the vessel design operating and burst pressures were revised to 1610 N/cm² (2330 psi) and 3220 N/cm² (4660 psi), respectively.

TABLE XV

MATERIAL PROPERTIES USED FOR KEVLAR/STAINLESS STEEL VESSEL DESIGN

<u>Property</u>	<u>Cryoformed 301 Stainless Steel</u>	<u>Kevlar-49/Epoxy</u>
Density, g/cm ³ (lbm/in ³)	7.89 (0.285)	1.36 (0.049)
Coefficient of thermal expansion, μ/K (in/in/ $^{\circ}F$)	8.26 (4.59×10^{-6})	-3.573 (-1.985 $\times 10^{-6}$)
Tensile yield strength, MN/m ² (ksi)	1276 (185)	
Derivative of yield strength with respect to temperature, N/cm ² /K (psi/ $^{\circ}F$)	-117 (-94.3)	
Elastic modulus, GN/m ² (psi)	131 (19.0×10^6)	128 (18.6×10^6) ^(a)
Derivative of elastic modulus with respect to temperature, GN/m ² /K (psi/ $^{\circ}F$)	-0.207 (-16 700)	-0.030 (-2410) ^(a)
Plastic modulus, GN/m ² (psi)	4.10 (600 000)	
Derivative of plastic modulus with respect to temperature, MN/m ² /K (psi/ $^{\circ}F$)	-0.78 (-63)	
Poisson's ratio	0.280	
Maximum allowable operating compressive stress, MN/m ² (ksi)		
At 297 K (+ 75 $^{\circ}F$)	-900 (-130)	
At 78 K (- 320 $^{\circ}F$)	-1160 (-169)	
Ultimate tensile strength, MN/m ² (ksi), minimum 1380 (200)		1972 (286)
Volume fraction filament		0.65

^aFilament Value

8 | 7 | 6 | 5

D

C

B

A

(1)

(2)

(1)

(2) (3)

5



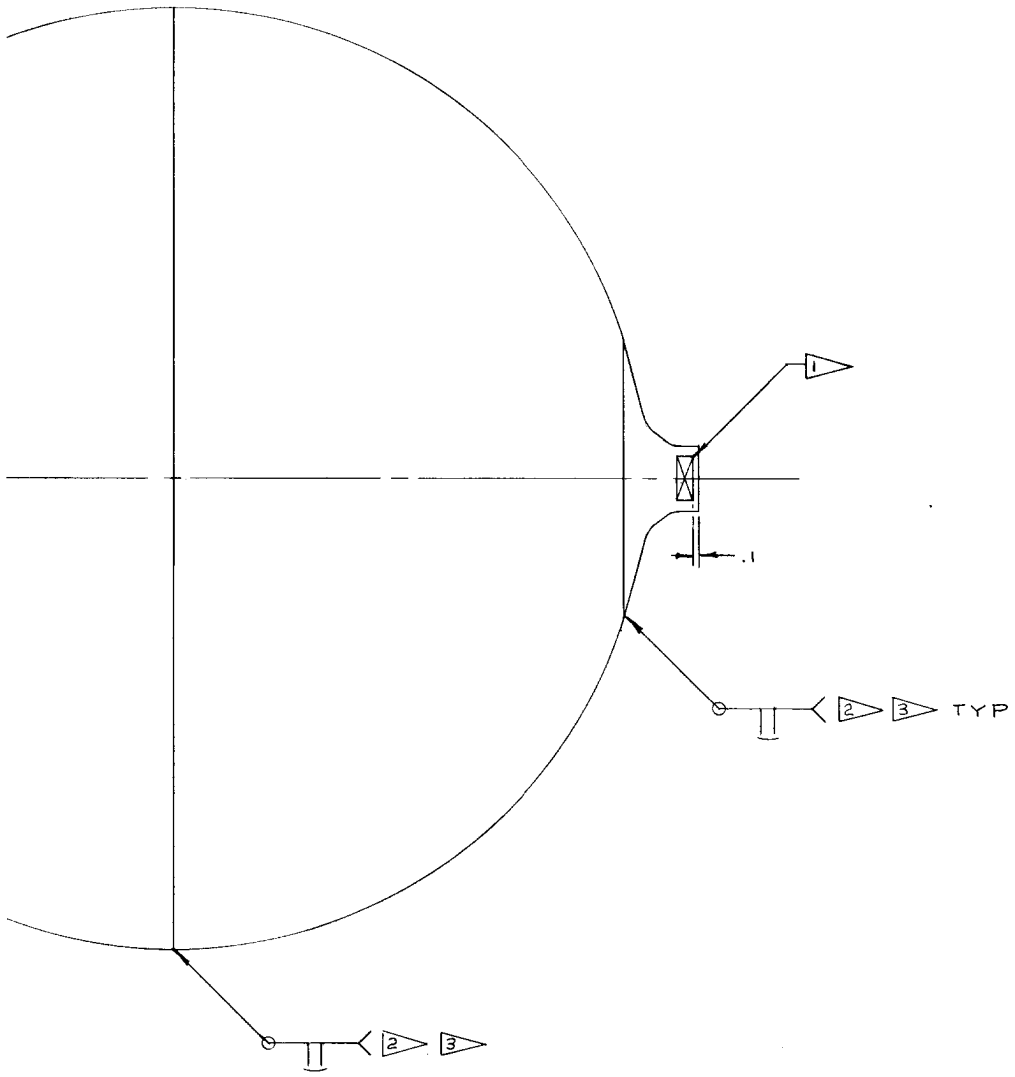
4

3

2

ZONE	LTR

(2)



2	2	C104705	BOSS, POR
2	1	D104698	HEAD, HEMI
-1	ITEM NO.	CODE IDENT	PART OR IDENTIFYING NO.

LIST OF MATERIAL OR PARTS

UNLESS OTHERWISE SPECIFIED DIMENSIONS ARE IN INCHES TOLERANCES X = ± .030, XX = ± .010, XXX = ± .005 ANGULAR ± 30° BREAK SHARP EDGES .03-.015 ALL SMALL FILLETS .020-.040 THREADED PER TED, HNDBK H-28 AND SHEET ELENTS	DRAWN BY <i>DM</i> 3-21-74
CHECKER <i>BB</i> 3/21/74	TITLE
STRESS ENG'R <i>BB</i> 3/21/74	WE
METALLURGY <i>MM</i> 3-22-74	
DES. ENG'R <i>BB</i> 4/2/74	
PROJ. ENG'R <i>MM</i> 3-22-74	
MFG <i>BB</i> 4/3/74	
QUAL. CONTROL <i>BB</i> 4-3-74	
NEXT ASSEMBLY <i>D 3896</i>	SIZE CO
	D C
	SCALE 1

4

3

2

1

REVISIONS

ZONE	LTR	DESCRIPTION	DATE	APPROVED

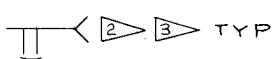
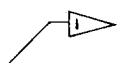
(2)

D

NOTES:

- 1. SERIALIZE CONSECUTIVELY AND IDENTIFY PER ARDE SPEC AES 601 METHOD 'D' IN THE AREA INDICATED
- 2. WELD PER ARDE SPEC AES 501
- 3. INSPECT WELDS PER ARDE SPEC AES 550
- 4. CLEAN PER ARDE SPEC AES 253
- 5. PICKLE PER ARDE SPEC AES 251
- 6. SOLUTION ANNEAL PER ARDE SPEC AES 351 WITH AIR ATMOSPHERE EXTERNALLY AND ARGON ATMOSPHERE EXTERNALLY
- 7. PICKLE PER ARDE SPEC AES 250 AFTER ANNEALING

C



B

95
88
D32

		2	2	C104705	BOSS, PORT		
		2	1	D104698	HEAD, HEMISPER		
QTY REQD PER DASH NO.		-1	ITEM NO.	CODE IDENT	PART OR IDENTIFYING NO.	NOMENCLATURE OR DESCRIPTION	MATERIAL

LIST OF MATERIAL OR PARTS LIST

UNLESS OTHERWISE SPECIFIED DIMENSIONS ARE IN INCHES TOLERANCES $X = \pm .030$, $XX = \pm .010$, $XXX = \pm .005$ ANGULAR $\pm 30'$ BREAK SHARP EDGES .003-.015 ALL SMALL FILLETS .020-.040R THREADS ARE FED. HNDBK H-28 AND JIS ELENEMENTS	DRAWN BY <i>Dm</i> 3-21-74	CHECKER <i>JW</i> 3-21-74	STRESS ENG'R <i>JW</i> 4-13-74	METALLURGY <i>Fm</i> 3-22-74	DES. ENG'R <i>JW</i> 4-13-74	PROJ. ENG'R <i>Fm</i> 3-22-74	MFG <i>af</i> 4-13-74	QUAL. CONTROL <i>af</i> 4-3-74	ARDE, INC. PARAMUS, N. J.	TITLE WELDMENT ASSEMBLY PRE FORM SPHERE - COMPOSITE
NEXT ASSEMBLY D3896									D 05980	D 3895
								SCALE 1/2 WT		SHEET

J/N 51055

(3)

8

7

6

5

D

C

B

A



5

4

3

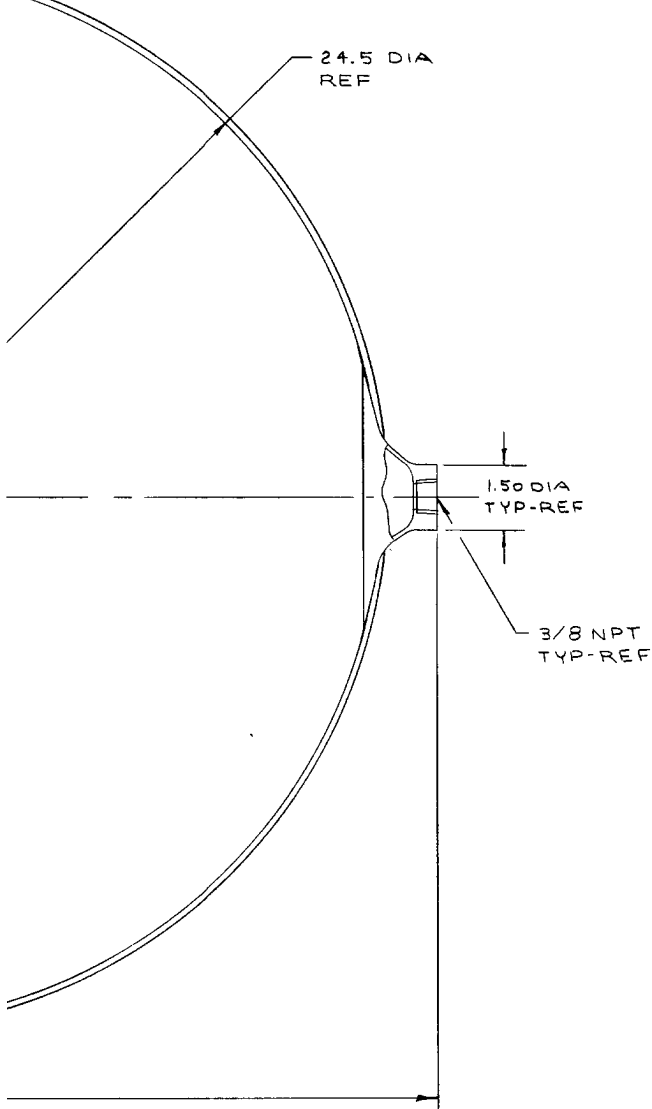
2

1

REVISIONS

ZONE	LTR	DESCRIPTION	DATE

(2)



NOTES:

1. CRYOGENICALLY STRETCH FORM PER ARDE S AES 353

2> SERIALIZE CONSECUTIVELY AND IDENTIFY PER A SPEC AES 601 METHOD 'D' IN THE AREA INDICATED WITH THE FOLLOWING INFORMATION

S/N —
P/N D3898 REV —

ITEM NO.	CODE IDENT	PART OR IDENTIFYING NO.		NOMENCLATURE OR DESCRIPTION	MATERIAL	SPECIFICATION
LIST OF MATERIAL OR PARTS LIST						
UNLESS OTHERWISE SPECIFIED DIMENSIONS ARE IN INCHES TOLERANCES: Δ = $\pm .030$, $\Delta\Delta$ = $\pm .010$, $\Delta\Delta\Delta$ = $\pm .005$ ANGULAR $\pm 30'$ BREAK SHARP EDGES .003-.015 ALL SMALL FILLETS .020-.040R THREADS PER FED. HNDBK H-28 AND S-147-74 DIMENSIONING PER MIL-STD-8 WELD SYMBOLS PER JAN-STD-19 SURFACE ROUGHNESS SYMBOLS PER MIL-STD-10 ALL FINISHED SURFACES 125	DRAWN BY	DM	3-25-74	ARDE, INC. PARAMUS, N.J.		
CHECKER	AB	1/17/74				
STRESS ENG'R	AB	1/17/74	- TITLE	VESSEL ASSEMBLY		
METALLURGY	FM	7-17-74		PRESSURE		
DES. ENG'R	AB	1/17/74		COMPOSITE, ARDEFORM-G		
PROJ. ENG'R	FM	7-17-74				
MFG	ef	1/17/74				
QUAL. CONTROL	AB	1/17/74				
NEXT ASSEMBLY						
	D	05980		D 3898		
	SCALE	1/2	WT			

J/N 51

2

4

3

2

1

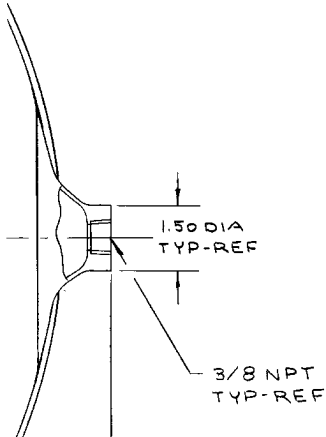
REVISIONS

ZONE	LTR	DESCRIPTION	DATE	APPROVED

D

4.5 DIA
.EF

NOTES:

1. CRYOGENICALLY STRETCH FORM PER ARDE SPEC
AES 8532. SERIALIZE CONSECUTIVELY AND IDENTIFY PER ARDE
SPEC AES 601 METHOD 'D' IN THE AREA INDICATED
WITH THE FOLLOWING INFORMATIONS/N —
P/N D3898 REV —

C

B

D3898
00000000

LIST OF MATERIAL OR PARTS LIST

ITEM NO.	CODE IDENT	PART OR IDENTIFYING NO.	NOMENCLATURE OR DESCRIPTION	MATERIAL	SPECIFICATION
UNLESS OTHERWISE SPECIFIED					
DIMENSIONS ARE IN INCHES	DRAWN BY	TDM	3-25-74	ARDE, INC.	
X = ± .030, Y = ± .010, Z = ± .005 ANGULAR ± 30°	CHECKER	AL	1/17/74	PARAMUS, N. J.	
BREAK SHARP EDGES .003-.015	STRESS ENG'R	DT	1/17/74	TITLE	
ALL SMALL FILLETS .020-.040R	METALLURGY	FM	7-17-74	VESSEL ASSEMBLY	
THICKNESS PER FED. HANDBK H-28 AND SUPPLEMENT	DES. ENG'R	JH	1/17/74	PRESSURE	
DIMENSIONING PER MIL-STD-8	PROJ. ENG'R	FM	7-17-74	COMPOSITE, ARDEFORM-GFR	
WELD SYMBOLS PER JAN-STD-19	MFG	AL	7-17-74		
SURFACE ROUGHNESS SYMBOLS PER MIL-STD-13	QUAL. CONTROL	AL	1/17/74		
ALL FINISHED SURFACES 125					
NEXT ASSEMBLY					

SIZE CODE IDENT NO. D 05980 D 3898

SCALE 1/2 WT SHEET

J/N 51055

A

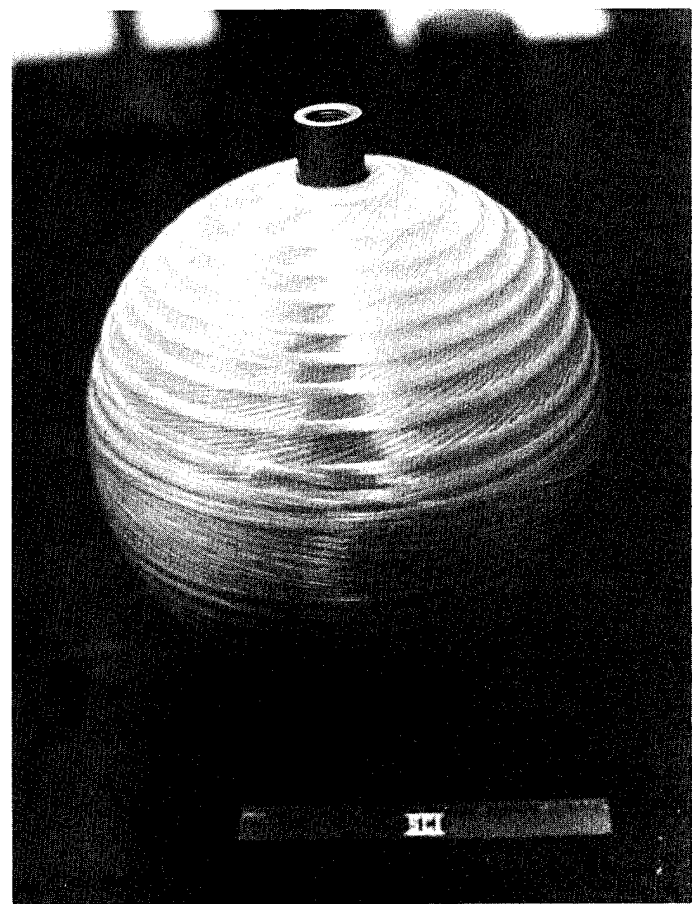
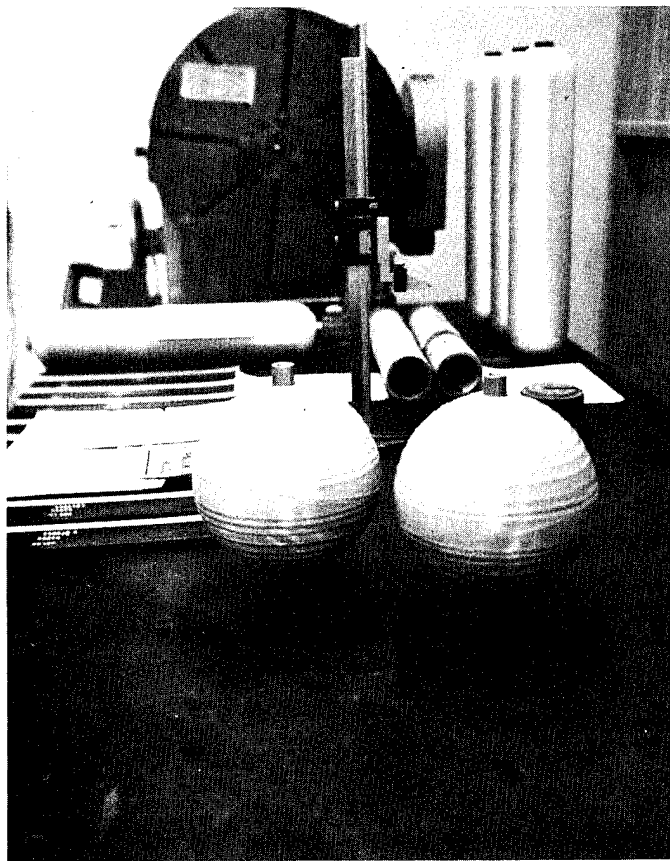


FIGURE 41: Subscale Kevlar-49/Cryoformed 301
Stainless Steel Spherical Pressure Vessels

A summary of final vessel design parameters for the Kevlar/stainless steel vessel is given in Table XVI.

Additional design requirements imposed on ARDE included the establishment of (1) a vessel port design which would allow the structural components (metal boss and composite shell) to operate as a unit during vessel pressurization, and (2) a method to predict vessel strains (plastically induced prestresses) during the sizing operation.

ARDE developed a unique boss design to satisfy the porting requirements using previously computerized plasticity relations. The computerized analysis technique not only accounted for induced stresses in vessel port components but also defined shape (geometry) changes which occur during vessel pressurization. The resultant port design was verified initially utilizing the 20.3 cm (8.0 inch) diameter subscale vessels previously discussed.

The method for strain prediction during the sizing operation had previously been developed by ARDE since the technique is inherent in their established cryosizing procedures. Briefly, vessel volumes are measured before and after cryosizing, and the average vessel strain ϵ is calculated from the volume change ΔV data according to the expression $3\epsilon = \Delta V/V$.

B. FABRICATION

1. Stainless Steel Liner Assemblies

Six cryoformed 301 stainless steel liner assemblies were fabricated according to existing ARDE fabrication process specifications and inspection procedures. The primary operations included (a) hydroforming hemispherical shells from 301 stainless steel sheet material, (b) fabrication of bosses and subsequent welding into each hemisphere, (c) girth welding the hemispherical shells together, and (d) cryoforming each of the six resulting liner assemblies to a predetermined internal volume.

The as-rolled 301 stainless steel sheet material, from which the liner assemblies were fabricated, did not meet ARDE's specification for a 2B/2D finish and was unacceptable for standard flight hardware. Due to funding and time limitations and the desire to use the same heat of material supplied for fracture control data

TABLE XVI

KEVLAR-49 FR CRYOFORMED 301 STAINLESS STEEL
PRESSURE VESSEL DESIGN PARAMETER SUMMARY

<u>Parameter</u>	<u>Value</u>
Shape	Sphere
Volume, m ³ (in ³)	0.116 (7075) min.
Outside Diameter, cm (in)	61.98 (24.40)
Materials	
Metal Shell	Cryoformed 301 Stainless Steel
Overwrap	Kevlar-49/epoxy
Thicknesses, cm (in)	
Liner	0.107 (0.042)
Filament-Wound Composite	0.544 (0.214)
Weight, kg (lbm)	19.4 (42.7) max.
Pressures, N/cm ² (psi)	
Operating	1607 (2330)
Sizing at 78 K (-320 °F)	2551 (3700)
Burst	3213 (4660) min.
Burst Factor of Safety	2.0
Operating Stresses, MN/m ² (ksi)	
Liner	69.0 (100)
Filaments	986 (143)
Operating Stresses, Including Scatter Factor	1600
Performance Factor, pV/W, J/g (in-lb/lbm)	
Operating	96.2 (836 000)
Burst	192.3 (772 000)

(NAS 3-14380), a decision was made to hand polish the liner heads after hydroforming. The result was an abnormal thickness variation, and an improved but abnormal surface finish. Subsequent performance test results and metallurgical examinations of metal from hydroburst vessels (discussed in later sections of this report) indicated the material abnormalities had no effect on vessel performance.

Table XVII contains dimensional inspection data characterizing the initial and final cryostretch operations for all six stainless steel liner assemblies. A picture of two of the completed liner assemblies is shown in Figure 42; the winding shaft has been installed in one of the liners in preparation for filament-winding. It should be noted that even though the incoming material was out of specification no 301 stainless steel liners had to be scrapped during the entire manufacturing process (including initial hydroforming, boss and girth welding, and two cryoforming operations).

2. Kevlar/Stainless Steel Pressure Vessels

Pressure vessel fabrication consisted of overwinding completed 301 stainless steel liner assemblies with a predetermined uniaxial multi-angular pattern composed of epoxy impregnated four-end Kevlar-49 roving; the resulting composite material was then oven cured. Following cure, the vessels were shipped to ARDE for a final cryosizing operation.

The established filament-winding procedures, Appendix H, were used to overwrap six ARDE liner assemblies (Serial Number 001 through 006) to form pressure vessels defined by Drawing Number D3898 (refer to Figure 40). Figure 43 shows a liner assembly at two stages in the winding process and Figure 44 shows a completed pressure vessel. Table XVIII presents a summary of the fabrication data obtained for the six vessels, and the following paragraphs discuss problems encountered during fabrication efforts and the resultant solutions.

a. Vessel 001

Analysis of cryosizing data obtained for the first Kevlar/stainless steel vessel, Serial Number 001, indicated a measuring system accuracy problem. As previously discussed, vessel strain (and prestresses) during cryosizing was based on ΔV data. The volumes were obtained by the "weight of water" method which requires

TABLE XVII
LINER FABRICATION DATA SUMMARY
CRYOFORMED 301 STAINLESS STEEL SPHERES^a

Weldment Assembly ARDE P/N D 3895	Liner Assembly, ARDE P/N D 3896									
	After Initial Cryostretch		After Final Cryostretch		Internal		External		Weight	
Liner Serial Number	Outside Diameter cm	Internal Volume m ³	External Diameter cm	Internal Volume m ³	Cryostretch Pressure N/cm ² (psi)	Membrane Thickness cm	Diameter cm	Volume m ³	(in ³)	kg (lbm)
001	54.71 21.54	.08431 5145	1000 1450	57.81 22.76	0.09955 6075	930 1350	0.107 0.042	60.78 23.93	(b)	10.5 23.1
002	54.71 21.54	.08432 5146	1000 1450	57.79 22.75	0.09973 6086	1000 1450	0.107 0.042	61.16 24.08	0.1183 7219	10.4 23.0
003	54.71 21.54	.08431 5145	1005 1460	57.86 22.78	0.09984 6093	1105 1600	0.107 0.042	61.54 24.23	0.1204 7350	10.6 23.3
004	54.69 21.53	.08426 5142	965 1400	58.06 22.86	0.1011 6168	1080 1570	0.104 0.041	61.82 24.34	0.1222 7460	10.6 23.3
005	54.69 21.53	.08428 5143	965 1400	58.09 22.87	0.1011 6168	1080 1570	0.102 0.040	61.87 24.36	0.1227 7487	10.1 22.2
006	54.69 21.53	.08428 5143	965 1400	57.81 22.76	0.09974 6087	1089 1570	0.102 0.040	61.49 24.21	0.1206 7358	10.1 22.3

^a All cryosizing was conducted at Liquid Nitrogen Temperature.

^b Values not recorded or in error.

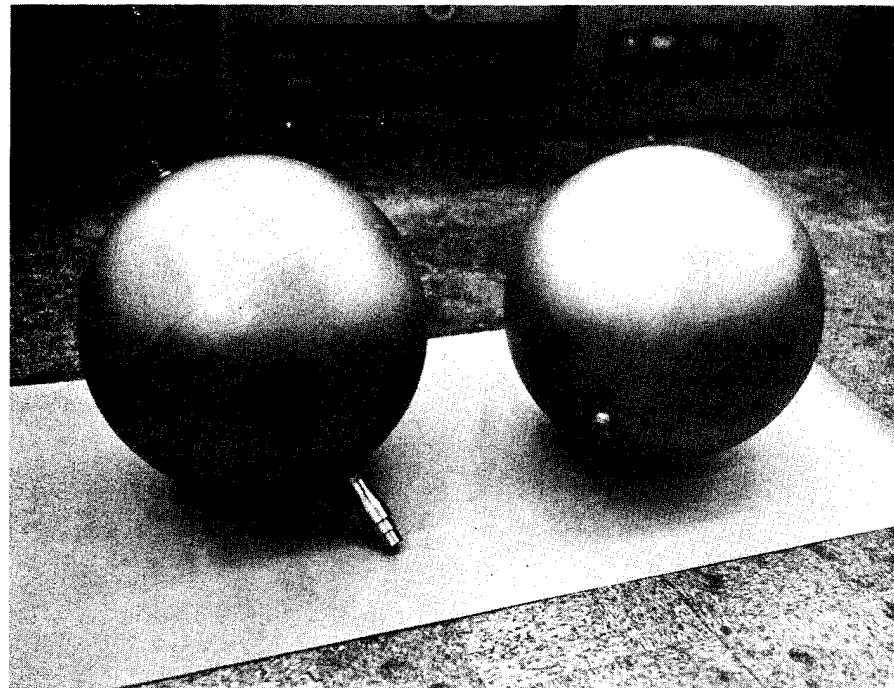
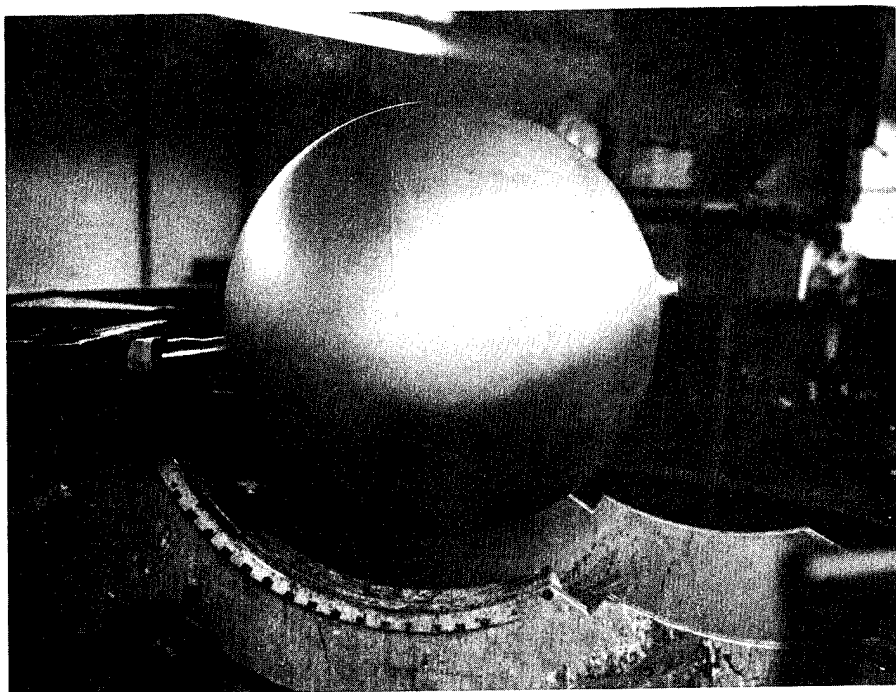
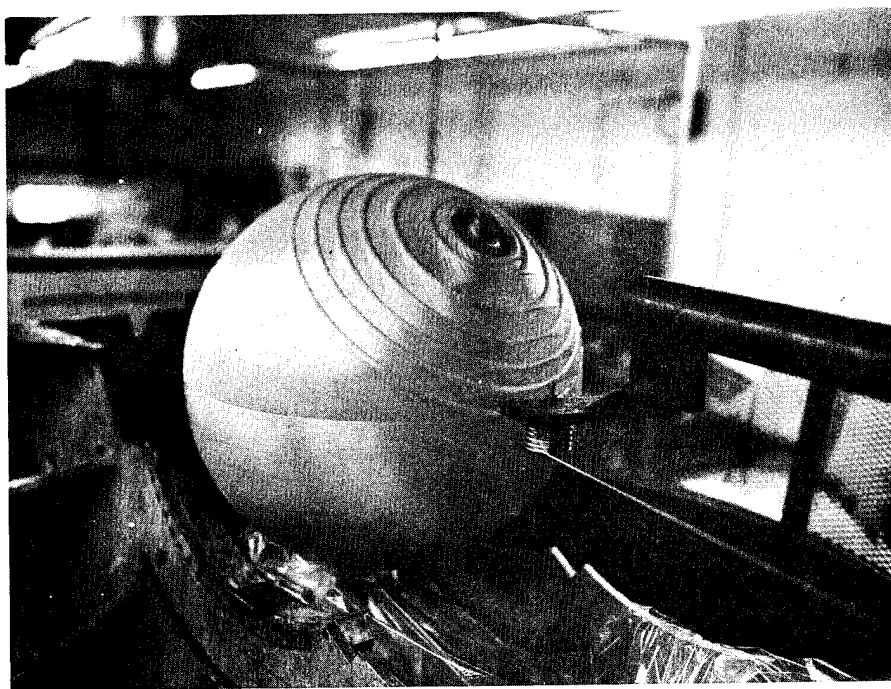


Figure 42: Cryoformed 301 Stainless Steel Liner Assemblies



(a) Liner Assembly Prior to Overwrap



(b) Partially Overwrapped Liner Assembly

Figure 43: Kevlar-49 Overwrapping Cryoformed 301
Stainless Steel Spheres



Figure 44: Completed Kevlar/Stainless Steel Pressure Vessel

TABLE XVIII
FABRICATION DATA SUMMARY
KEVLAR FIBER REINFORCED 301 STAINLESS STEEL SPHERERS^a

Vessel Serial Number	Pressure N/cm ² (psi)	Sizing Parameters ^b			Thickness, cm (in)			Weights, kg (lbm)		
		Specific Volume (ΔV/V), %	Residual Stresses at Ambient Temp MN/m ² , (ksi)		Final Internal Volume, m ³ (in. ³)	Outside Diameter At Equator, cm (in.)	Kevlar/ epoxy Composite	301 SS Liner Assembly	Kevlar Fiber	Epoxy Resin
			301, SS Liner	Filaments						
001	2606 (3780)	(d)	(d)	(d)	0.1189 (7204) ^c	62.13 (24.46)	0.544 (0.214)	0.107 (0.042)	6.03 (13.3)	2.18 (4.8)
002(e)	3137 (4550)	.96 (-111)	-765 (66)	455 (66)	0.1194 (7289)	62.48 (24.60)	0.566 (0.223)	0.107 (0.042)	6.22 (13.7)	2.31 (5.1)
003(f)	3068 (4450)	1.2 (-123) ^f	848 (77) ^f	531 (7439)	0.1219 (7439)	63.04 (24.82)	0.635 (0.250)	0.107 (0.042)	10.57 (23.3)	5.99 (13.2)
004	3158 (4580)	.98 (-106)	731 (63)	434 (7534)	0.1234 (24.88)	63.20 (24.88)	0.572 (0.225)	0.104 (0.041)	10.57 (23.3)	6.35 (14.0)
005	3185 (4620)	.99 (-110)	758 (64)	441 (7562)	0.1239 (24.89)	63.22 (24.89)	0.559 (0.220)	0.102 (0.040)	10.07 (22.2)	6.35 (14.0)
006	3275 (4750)	1.0 (-110)	758 (64)	441 (7433)	0.1218 (24.75)	62.87 (24.75)	0.554 (0.218)	0.102 (0.040)	10.12 (22.3)	6.26 (13.8)

^a General Notes: Stainless steel sheet as rolled did not meet ARDE, Inc. Specification for 2B/2D finish. Decision was made to hand polish heads after hydroforming. Result was abnormal thickness variation and improved, but abnormal, surface finish. Vessels 002, 004, 005 and 006 were fabricated to same criteria; see special notes regarding Vessels 001 and 003.

^b Sizing operation conducted at 78 K (-320 °F). Volumes and changes in volumes (ΔV) obtained by weight-of-water method. Residual Stresses (Prestresses) are calculated values based on volume changes during sizing.

^c Calculated values based on before and after wrap diameter differences.

^d Inaccurate data: Scale used to obtain weights for volume calculations had reading accuracy of one-half pound. A one-half pound error represents 20% of ΔV value and is unacceptable. Weights for subsequent vessels obtained from scale with accuracy of .01 pound.

^e The measuring system accuracy problem with Vessel 001 was verified by initially stretching Vessel 002 to the same sizing pressure as Vessel 001 and ascertaining that sizing strains were low. Flexibility of process and value of stress-strain plasticity equations and material evaluation was demonstrated by use of additional cryostretch (i.e., incremental cryostretch can be accomplished without degradation). Stretch pressure band established as 3137/3275 N/cm² (4550/4750 psi). This range is accepted by others as standard and is analogous to heat treat spread allowed for Titanium (i.e., 110,000 to 124,000 N/cm² or 160,000 to 180,000 psi).

^f Modified wrap tool was evaluated concurrent with overwrapping of this vessel. Tooling checkout problems caused a local thin spot (approximately 7% less than requirement) in winding pattern at polar boss area; and, resulted in extended wrap period (24 hours versus 8 hours) leading to a "resin rich" composite. Also, higher prestresses were intentionally induced in this vessel during sizing as an oversize checkout for this diameter-to-thickness ratio.

accurate weight measurements for precise volume calculations. The scale utilized for weight measurements of Vessel 001 was readable to 1/2 lb. increments. A 1/2 lb. error represents 20% of the delta volume and is unacceptable (as evidenced by relatively low burst pressure obtained for this unit). Based on this analysis, a scale with a reading accuracy of 0.10-lb was utilized during cryosizing of subsequent units.

b. Vessel 002

The measuring system accuracy problem with Vessel 001 was verified by initially cryosizing Vessel 002 to the same sizing pressure, 2606 N/cm^2 (3780 psi), as Vessel 001 and ascertaining that strains were too low. Based on the strain data, the unit was subjected to an additional cryostretch at a sizing pressure of 3137 N/cm^2 (4550 psi). Performance test results for the vessel, discussed in the following section, were very successful and verified that incremental cryostretching can be accomplished without any vessel degradation; flexibility of the cryostretch process was demonstrated.

The successful cryostretch and performance test results obtained for Vessel 002 established an allowable cryostretch pressure band for subsequent units at 3137 to 3275 N/cm^2 (4550/4750 psi). This range is accepted by others as standard and is analogous to heat-treat strength ranges established for other alloys (e.g., Titanium: 1103 to 1241 MN/m^2 or 160 to 180 ksi).

c. Vessel 003

Problems associated with the overwrap process were experienced on the third Kevlar/stainless steel Vessel 003. Although the total amount of Kevlar roving applied to Vessel 003 was within 1.5% of the requirement (compare Kevlar fiber weights in Table XVIII), a local thin spot (approximately 7% less than the requirement) in the winding pattern at the polar boss area occurred. The deviation in winding pattern was caused by a tooling modification which, by necessity, was being evaluated concurrent with the winding operation.

A further deviation caused by the tooling modification was the increase in elapsed time required to wrap Vessel 003. The unit was partially wrapped during the first day, allowed to sit overnight, and the wrap completed during the second day. The effect of this extended wrap period was a "resin rich" composite which resulted in a slightly

overweight vessel (compare resin and composite weights for Vessel 003 with the other five units in Table XVIII).

Although no problems were experienced during the cryosizing of Vessel 003, an intentional deviation in established cryostretch process procedures did occur. The unit was subjected to a special stretch pressure (see Table XVIII), somewhat lower than normal due to the light fiber weight, but high enough to induce higher prestress in the metal. The overstress condition was desired to obtain information on the sensitivity of this specific vessel design (diameter-to-thickness ratio) to metal wrinkling (diamond buckels) during cryosizing, subsequent warming to ambient temperature, and performance testing. No buckles or diamond wrinkles were observed during visual inspection of the internal and external surface after cryosizing prior to performance testing. A buckle did develop in this unit during performance testing, and details are discussed in Section III C2 of this report.

d. Vessels 004 through 006

Kevlar/stainless steel Vessels 004, 005, and 006 were fabricated according to established process procedures without deviation. There were no problems associated with the major vessel process operations of filament-winding, cure or cryosizing. Comparison of fiber/resin weight data and composite thickness data recorded in Table XVIII indicates the excellent control achieved during the filament-winding process. Excellent control was also achieved by ARDE during the cryosizing operation as is apparent from the relative volume change ($\Delta V/V$ is 1%). Resultant metal/filament prestresses after cryosizing (based on $\Delta V/V$ data) were consistently reproducible.

C. TEST PROGRAM

1. Instrumentation and Test Plan

Prior to testing, all vessels were instrumented with three "great circle" extensometers and four biaxial strain gages according to the detailed test procedures of Appendix E. Figure 45 shows a typical test setup of a fully instrumented Kevlar/stainless steel vessel.

Preliminary performance test assignments for the six Kevlar/stainless steel vessels are shown in the test plan of Appendix E. As discussed in the following section on test results, this plan was

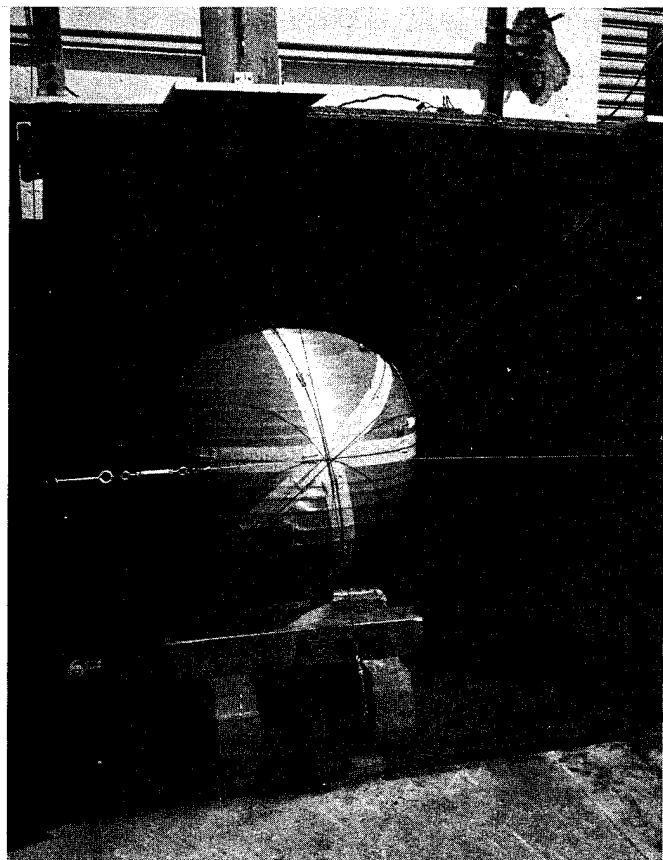


Figure 45: Test Setup, Kevlar
Reinforced 301 Stainless Steel Pressure Vessel

modified with NASA concurrence; the revised test plan is shown in Figure 46.

2. Performance Test Results

Performance test results for all six Kevlar/stainless steel vessels are summarized in Table XIX. The table indicates sizing data, type of performance test given, the load level used for fatigue and sustained load testing, pressure cycles or sustained load period achieved, the failure pressure, and pertinent remarks. Pressure/strain data obtained during the performance tests are presented as plots in Appendix I. The following paragraphs briefly describe individual test results.

a. Vessel 001- Hydraulic Burst

Kevlar/stainless steel Vessel 001 was subjected to a static burst test; the resultant burst pressure was 3000 N/cm^2 (4350 psi), which was 93% of the design burst pressure. A photograph of the vessel after burst testing is shown in Figure 47. Inspection of the photo indicates the basis for the failure-mode term "flower burst". Pressure/strain plots for the vessel are contained in Appendix I.

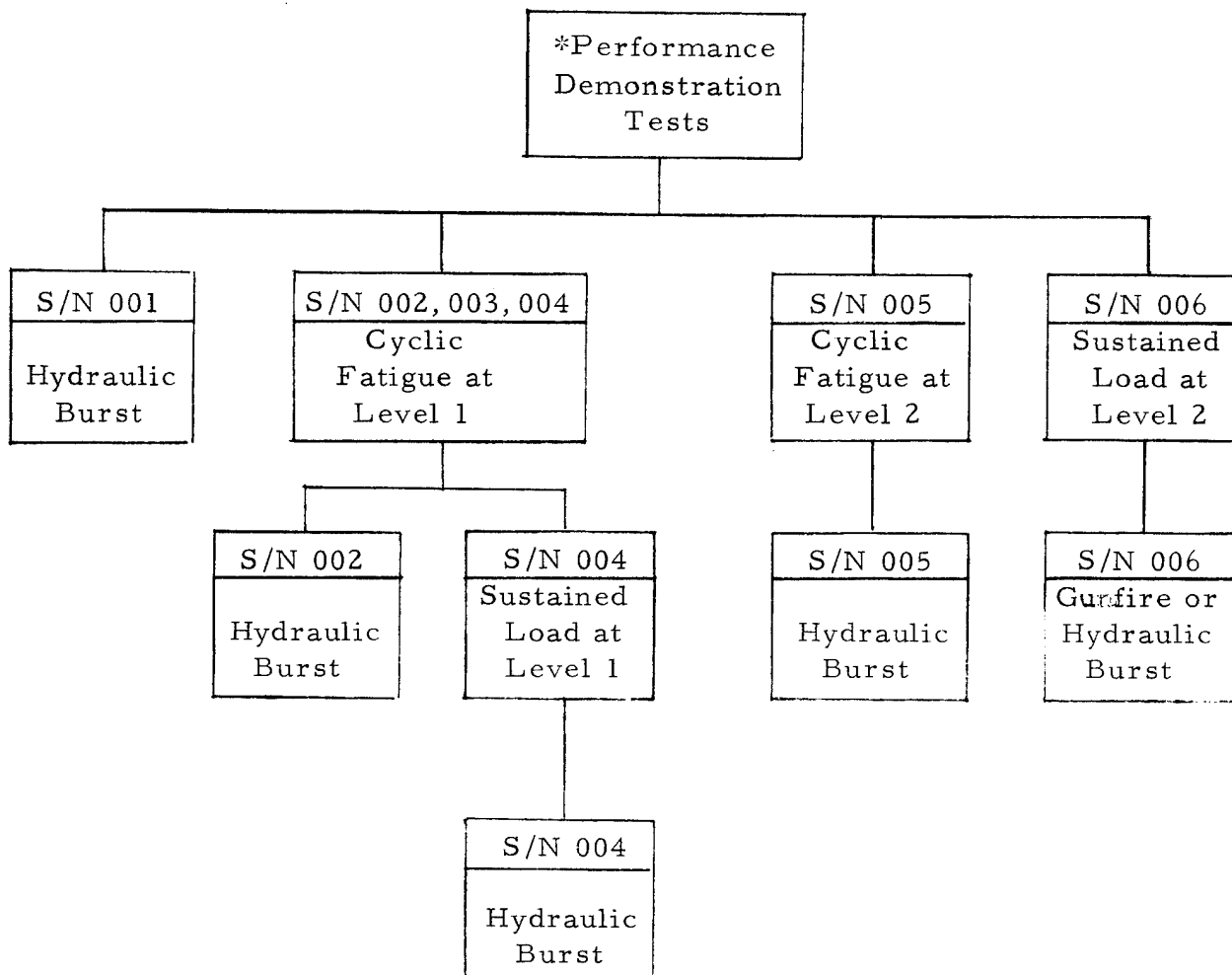
b. Vessel 002 - Cyclic Fatigue

Kevlar/stainless steel Vessel 002 was subjected to a cyclic fatigue test. The test consisted of pressure cycling the vessel 1600 times from zero to 1607 N/cm^2 (2330 psi) to zero, followed by pressurization to burst. The vessel successfully passed the pressure cycling test and subsequently demonstrated a burst pressure of 3310 N/cm^2 (4800 psi). The resultant safety factor was 2.06, and the corresponding performance factor ($p_b V/W$) was 208 J/g (837 000 in-lb/lbm). The failure mode was a "flower burst" similar to Vessel 001.

Appendix I contains the pressure/strain plots for both the fatigue and burst test conducted on this vessel. The data is plotted in "bar form" at several different selected cycles to indicate the changes in operating strain range as cycling progressed.

c. Vessel 003 - Cyclic Fatigue

Kevlar/stainless steel Vessel 003 was subjected to the same cyclic fatigue test as prescribed for Vessel 002.



<u>* Key:</u>	<u>Level Number</u>	<u>Operating Pressure N/cm², (psi)</u>	<u>Number of Fatigue Cycles</u>	<u>Period at Sustained Load, Hrs.</u>
	1	1607 (2330)	1600	96 (minimum)
	2	1862 (2700)	1000	96 (minimum)

FIGURE 46: Revised Test Plan and Vessel Assignment for Kevlar Fiber Reinforced 301 Stainless Steel Spheres

TABLE XIX
TEST DATA SUMMARY
KEVLAR FIBER REINFORCED 301 STAINLESS STEEL SPHERES

Vessel Serial Number	Final Internal Volume, m^3 (in. ³)	Total Vessel Weight kg (lbm)	Type of Performance Test	Operating Pressure N/cm^2 (psi)		Stress at Operating Pressure, MN/m^2 (ksi) Fiber	Number of Pressure Cycles	Sustained Pressurization Period, Hours	Failure Pressure N/cm^2 (psi)	Safety Factor Demonstrated	Performance Factor, J/g (in-lb/lbm) P_o/P_b
				Test	N/cm^2 (psi)						
001	0,1181 (7204)	18.7 (41.2)	Single Cycle Hydroburst	1607 (2330)	N.A.	N.A.	N.A.	3000 (4350) (a)	1.87	N.A.	(761 000)
002	0,1194 (7289)	19.0 (41.8)	Cycle Fatigue	1607 (2330)	1083 (157)	490 (71)	1616	N.A.	3310 (4800)	2.06	101 (406 000)
003 (b)	0,1219 (7439)	19.8 (43.6)	Cycle Fatigue	1607 (2330)	1145 (166)	434 (63)	1045 (b)	N.A.	(b)	99 (398 000)	208 (837 000)
004	0,1235 (7534)	19.1 (42.1)	Cycle Fatigue plus Sustained Load	1607 (2330)	1069 (155)	545 (79)	1600	150	3137 (4550)	1.95	104 (417 000)
005 (c)	0,1239 (7562)	18.9 (41.7)	Cycle Fatigue	1862 (2700)	1207 (175)	772 (112)	1000	N.A.	3206 (4650)	1.72 (c)	122 (490 000)
006 (c)	0,1218 (7433)	18.7 (41.2)	Sustained Load	1862 (2700)	1220 (177)	800 (116)	N.A.	2230	(d)	121 (487 000)	(d)

a Measurement error of volume resulted in low sizing pressure and strain with consequent low burst pressure.
b Leak failure during pressure cycling; low fatigue life was result of fabrication problem identified prior to test (light fiber wrap/high prestrain)

c Off-limit tests; operating pressure increased to 1862 N/cm² (2700 psi).

d Vessel not tested to failure



Figure 47: Kevlar Reinforced 301 Stainless Steel Vessel
After Static Burst Test

During the fatigue test, the vessel was checked for leaks at 690 N/cm^2 (1000 psi) every 100 cycles, including the 1000th cycle, with no observable leakage. After the 1000 cycle leak check, cycling continued for 45 more cycles at which time a slight pressure decay was indicated by the recording equipment. Cycling was discontinued and a 690 N/cm^2 (1000 psi) vessel leak check performed; results of the check indicated a leak type failure in the area of the polar fitting. The test was terminated at this point, and the vessel shipped to NASA LeRC for metallurgical examination. Figure 48 is a photograph of the failed vessel prior to the examination.

Photographic coverage of the metallurgical examination conducted by NASA LeRC is contained in Figures 49 through 51. Information obtained during the failure analysis is summarized in the following paragraphs.

- Leakage failure of the vessel was due to a localized 3.8-cm (1.5-inch) long crack in the metal membrane (through the thickness in several places) located approximately 1.3-cm (0.5-inches) away from one boss weld and oriented parallel to the weld (see Figure 49 and 50).
- The through crack was oriented along the center line of a very localized inward buckle in the metal shell, 5.1-cm by 10.2-cm (2-inch by 4-inch area). There was no evidence of buckling at any other location on the vessel.
- A significant flat spot was observed on the inside surface of the filament-wound composite material precisely over the area of the metal liner buckle. The area of composite involved was approximately 10.2-cm by 15.2 cm (4-inch by 6-inch).
- There was no evidence of thinning of the metal membrane in the failure area.

Localized leakage in area shown

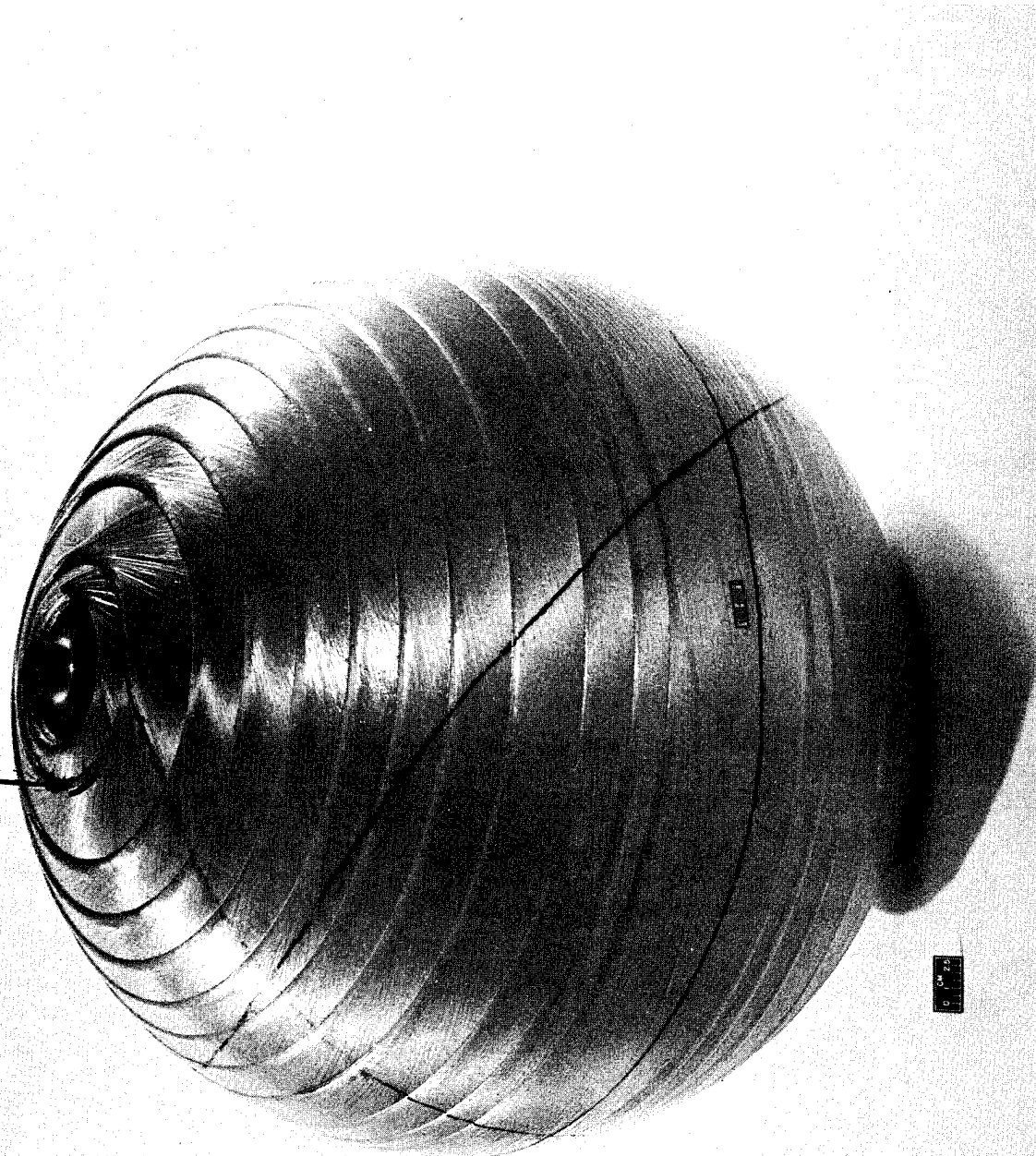


FIGURE 48: Kevlar/Stainless Steel Vessel 003 After 1045 Pressure Cycles to 1607 N/cm^2 (2330 psi)

NASA
C-75-732

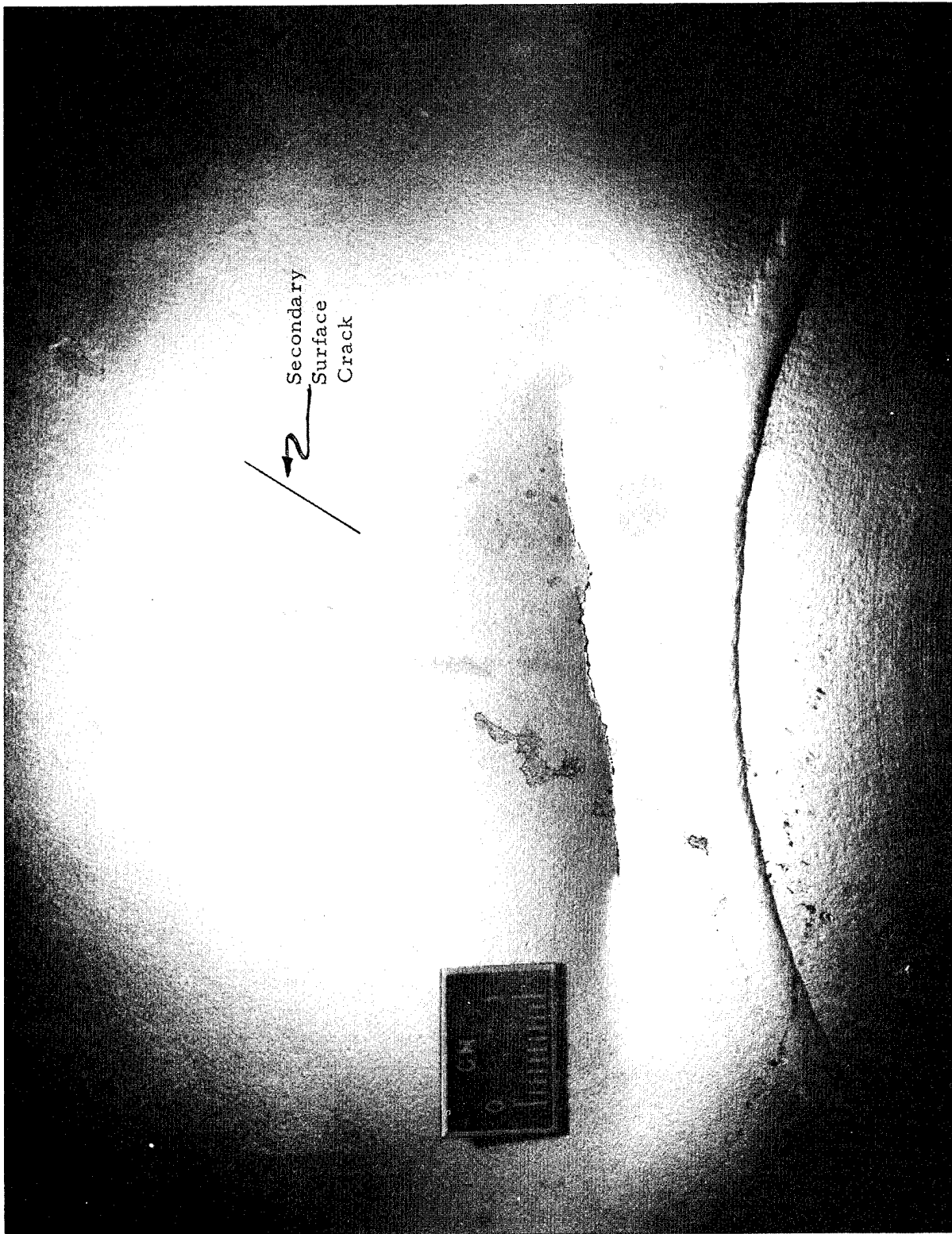


FIGURE 49: Vessel 003 Metal Shell Failure Site External Surface View

NASA
C-75-731

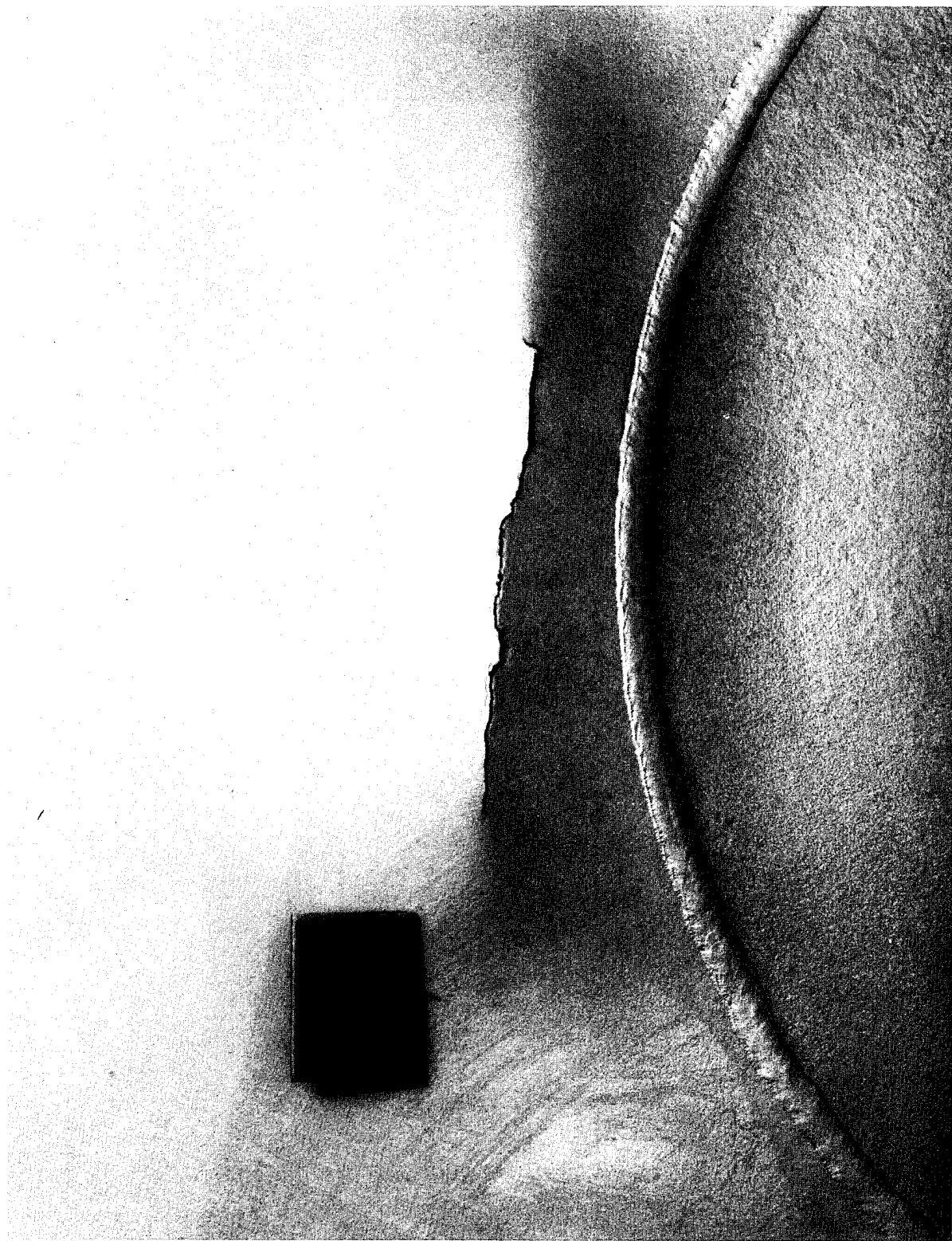
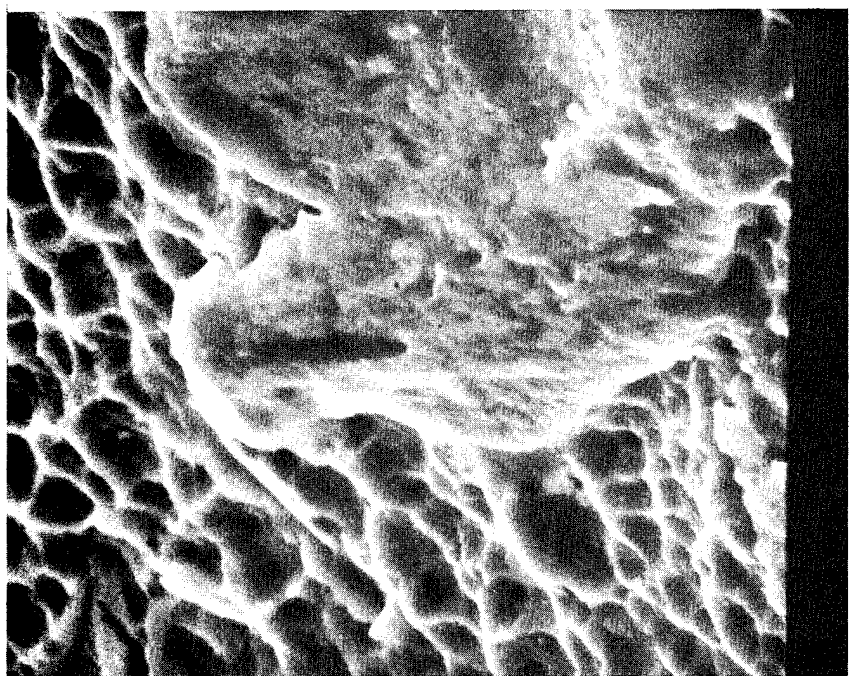


FIGURE 50: Vessel 003 Metal Shell Failure Site Internal Surface View

(b) 3000X Magnification



(a) 100 X Magnification



FIGURE 51: Cross Sectional View of Vessel 003 Metal Shell at Failure Site

- A second external surface crack was observed approximately 3.8-cm (1.5-inch) away from the boss weld, starting approximately at the edge of the buckles, and oriented at 45° to the weld (Figure 49).
- Branching of both the through-the-thickness crack and the surface crack was major (Figure 51).
- Ductile cleavage type failure was observed in two areas on the inner edge of the through crack and in two areas on the outer edge of the surface crack (Figure 51).

A review of the fabrication process and inspection records for Vessel 003 produced the following additional information:

- No buckles in the metal shell were observed during visual inspection of the internal and external surface at various steps in fabrication prior to testing.
- This vessel had a local "thin spot" in the Kevlar/epoxy overwrap material (approximately 7% less than the requirements) at the polar boss area near the liner buckle (refer to Section IIIB2c).
- Higher prestresses (metal compression, filament tension) were intentionally induced in this unit during cryosizing as an overstress checkout for this diameter-to-thickness ratio (Refer to Section IIIB2c).

Based on the above failure analysis and fabrication information, the details leading to failure could only be speculated. One explanation was: At some point during the overwrap operation (prior to or during cure of the vessel) a local flat area developed (or was induced) in the metal shell. This flat spot was not visually apparent

during in-process inspections of the overwrapped vessel. During the metal compression part of the fatigue cycle test, the flat area caused debonding of the metal from the composite and resultant buckling. The metal snap-through capability was probably amplified by the thin region of composite material and/or higher prestresses existing in this unit. Subsequent fatigue cycling caused local bending of the buckled section, a high stress concentration, crack initiation, and failure.

Since the final three vessels had already been fabricated (with excellent process control), the only applicable recommendation resulting from the above analysis was to perform an additional examination of the interior of vessels for flat spots, buckles, and flaws.

d. Vessel 004 - Cyclic Fatigue and Sustained Loading

Kevlar/stainless steel Vessel 004 was subjected to the recommended additional interior examination - no defects were found. The vessel was instrumented and subsequently pressure cycled 1600 times from zero to 1607 N/cm^2 (2300 psi) to zero. Following the fatigue test, the vessel was subjected to sustained pressurization for 150 hours at 1607 N/cm^2 (2330 psi). The vessel successfully passed both these tests without leakage or failure and was subsequently pressurized to a burst pressure of 3137 N/cm^2 (4550 psi). The resultant performance factor ($p_b V/W_t$) for this vessel was calculated to be 203 J/g ($814\,000 \text{ in-lb/lbm}$) with corresponding factor of safety, based operating pressure, of 1.95. Failure mode of this vessel was a "flower burst" similar to Vessels 001 and 002. Pressure/strain plots depicting both the fatigue and sustained load tests are contained in Appendix I.

e. Vessel 005 - Off Limit Cyclic Fatigue

The criteria for performance testing of Kevlar/stainless steel Vessel 005 were reevaluated and revised at this point in the test program. The options which were considered during the evaluation were (1) to continue the test program as planned, which would have included pressure cycling at 1607 N/cm^2 (2330 psi) or half of design burst pressure as was the case for Vessels 002, 003, and 004, or (2) to perform an off-limit test with the current vessel design in order

to obtain more cyclic fatigue data at higher metal stress levels to develop stress versus cycles to failure trends.

Option (1), the original contract requirement, would have provided addditional vessel data at the same test conditions as before, and if successful, would have emphasized the repeatability of the Kevlar/stainless steel vessel design and fabrication. On the other hand, the baseline for the current space vehicle composite vessels had changed to a 1.5 factor of safety; the test results to date did not give full scale Kevlar/stainless steel vessel pressure cycling data at this revised design condition. Option (2), the use of a higher operating pressure for cyclic fatigue testing, would provide this data.

The problem with Option (2) was that the unreinforced metal bosses were designed for 1600 cycles of fatigue at 1607 N/cm^2 (2330 psi). Increasing the tank operating pressure significantly increases maximum stress in the metal bosses. After preliminary design type analyses (without computer program aid as was used in developing the original design) SCI/ARDE concluded that increasing the operating pressure to 1862 N/cm^2 (2700 psi) for a 1000 cycle test might not push the design too far. However, since there is a large scatter in fatigue tests, a degree of risk existed in attempting to obtain this performance increase with a metal boss design intended for a lower operating stress.

Option (2) was recommended by SCI/ARDE, and NASA concurred with the recommendation. Following the decision, Vessel 005 was pressure cycled 1000 times from zero to 1862 N/cm^2 (2700 psi) to zero. The vessel successfully passed the cyclic fatigue test without leakage or failure and was subsequently pressurized to a burst pressure of 3206 N/cm^2 (4650 psi). The resultant performance factor ($p_b \text{ V/W}$) for this vessel was calculated to be 210 J/g ($843 \text{ 000 in-lb/lbm}$) with a corresponding 1.72 factor of safety based on the 1862 N/cm^2 (2700 psi) operating pressure. Failure mode for the vessel was of the "flower burst" type. Pressure/strain plots for the fatigue and burst tests are contained in Appendix I.

f. Vessel 006 - Off Limit Sustained Loading

The final Kevlar/stainless steel Vessel 006, was placed under sustained pressurization at the same "off limit" operating pressure utilized for the fatigue testing of Vessel 005. Pressurization of

the vessel was maintained for 2230 hours (93 days) without any evidence of leakage or failure. During the test, day and night temperature variations induced a pressure variation of $\pm 70 \text{ N/cm}^2$ ($\pm 100 \text{ psi}$). This fluctuation was controlled but since full-time observation was impractical, the pressure actually reached 2070 N/cm^2 (3000 psi) on several occasions during the test. Upon completion of the test at SCI, the vessel was shipped to NASA LeRC. Subsequent testing by NASA included 1000 cycles from 0 to 1862 N/cm^2 (2700 psi) followed by 800 cycles from 0 to 1607 N/cm^2 (2330 psi); the failure mode was leakage through the wall.

3. Evaluation of Test Results

The validity of computerized plasticity relations used to analyze the port area and the resultant boss design itself were both verified during the test program. The bosses were not failure sites even at the "off-limit" cyclic fatigue operating pressure of 1862 N/cm^2 (2700 psi).

Neither cyclic fatigue nor sustained loading had an effect on the hydraulic burst pressure of the vessels. In fact, the highest value of burst pressure, 3310 N/cm^2 (4800 psi), was obtained from a unit (Vessel 002) which had initially been subjected to 1600 operating pressure cycles prior to hydroburst. Although the exact series of events which lead to the failure of Vessel 003 during fatigue cycling could not be pinpointed, the vessel still sustained 1045 operating pressure cycles before failure occurred; further, the failure mode was leakage through the wall and not catastrophic failure.

Vessel 005 demonstrated a performance factor of 210 J/g ($843\,000 \text{ in-lb/lbm}$) at the burst pressure of 3206 N/cm^2 (4650 psi). This remarkably high factor was achieved after the vessel had been subjected to 1000 fatigue cycles at an off-limit operating pressure of 1862 N/cm^2 (2700 psi). The average operating performance factor at the design operating pressure of 1607 N/cm^2 (2330 psi) was 101 J/g ($407\,000 \text{ in-lb/lbm}$); the average performance factor at the off-limit operating pressure of 1862 N/cm^2 (2700 psi) was 122 J/g ($489\,000 \text{ in-lb/lbm}$). The variation of operating performance factors was within $\pm 2\%$.

IV. CONCLUDING REMARKS

The principle program objective -- to verify the advantages of overwrapped metal pressure vessels for future flight vehicles, as well as demonstrate the technology readiness and suitability of the vessels for the application -- was accomplished. Both the 61 cm (24-inch) diameter Kevlar-49/cryoformed 301 stainless steel sphere and the 97 cm (38-inch) diameter Kevlar-49/2219 aluminum sphere, which were developed and tested under this program, were of lighter weight than competing monolithic metal vessels and incorporated controlled failure mode features.

A. KEVLAR/301 STAINLESS STEEL PRESSURE VESSELS

The reliability of existing design techniques and repeatability of fabrication processes utilized for the Kevlar/stainless steel vessel was demonstrated as summarized below:

- A unique boss design, previously developed by ARDE, performed as designed during all performance testing conducted. The bosses were not failure sites even at the off-limit operating pressure of 1862 N/cm^2 (2700 psi).
- The validity of existing computerized plasticity relations used for design of the vessel (and ports) was verified during both the cryosizing operation and the performance test effort.
- Excellent repeatability of major manufacturing processes was demonstrated. The variation in Kevlar/epoxy composite thickness was within $\pm 2.7\%$; variation in total vessel weight was $\pm 1.2\%$ (non-representative Vessel 003 has been excluded).
- Excellent control during the cryosizing operation was also achieved as evidenced by relative volume change $\Delta V/V$ values obtained; the range in $\Delta V/V$ was from 0.96 to 1.0%, excluding non-representative Vessels 001 and 003.

The weight advantage of Kevlar/stainless steel construction and the reliability of pressure vessels during operation was demonstrated as summarized below:

- Maximum performance at burst $p_b V/W$ achieved during the test program was 210 J/g (843 000 in-lb/lbm). This represents a 35% weight savings over the lightest weight, 6Al-4V Ti (STA), homogeneous metal pressure vessel.
- Technology readiness and suitability of full-scale hardware for flight vehicle application was demonstrated. Vessels achieved a burst-to-operating safety factor of 1.72 after 1000 fatigue cycles at an operating performance factor $p_o V/W$ of 222 J/g (489 000 in-lb/lbm).
- Anticipated non-fragmentation and controlled failure mode features of composite vessels were demonstrated. When failure occurred during fatigue cycling (Vessel 003), the mode was localized leakage and not catastrophic.

B. KEVLAR/ALUMINUM PRESSURE VESSELS

The ability to design and fabricate large filament over-wrapped vessels with load bearing liners was verified by the manufacture of the 97 cm (38-inch) diameter Kevlar/aluminum spheres. Information obtained during the design/fabrication phases of vessel development is summarized below:

- The use of bolted end-closure design for the large ported vessels was inadequate. The revised design, incorporating a tie-rod to carry the port load, provided a good solution for completing performance tests on existing vessels.
- The thickness tolerance obtained for aluminum half shells was excellent; many exceeded the established acceptance criteria and met the thickness tolerance "design objective" defined in SCI Drawing 1269381.
- Port areas of future liner assemblies with integral bosses should be initially machined "rough" and final machined after heat treatment.

- Quenching of large volume aluminum liner assemblies can be accomplished in the required 15 second time period without distortion of the part.

Information obtained during testing of the Kevlar/aluminum vessels is summarized below:

- The good comparison of measured strains and volumetric expansions with design values verified the validity of the analytic method used to predict shell stresses. Measured values of internal volume after the sizing operation were within 0.3% of each other. A typical recorded strain range for a vessel after sizing was 0.15 to 0.35% compared to the design value of 0.30%.
- The leak type failure of Vessel S-5 during fatigue cycling verified the anticipated safety (controlled failure mode and leak-before-burst) of filament-reinforced metal pressure vessels.
- Maximum performance for the 97 cm (38-inch) diameter Kevlar/aluminum pressure vessel at failure ($p_b V/W$) was 164 J/g (658 000 in-lb/lbm). Failure was of the tie-rod and not the vessel itself. The potential performance factor for this vessel (Serial Number S-4) at the predicted burst pressure of 3137 N/cm² (4550 psi) was calculated to be 191 J/g (768 000 in-lb/lbm).

REFERENCES

1. Bixler, W. D.; "Fracture Control Method for Composite Tanks With Load Sharing Liners", NASA CR 134758, Boeing Company, July 1975.
2. Mayer, L. W.: "Alcoa Aluminum Alloy 2219", Alcoa Green Letter, June 1967
3. Landes, R. E.; "Glass Fiber Reinforced Metal Pressure Vessel Design Guide", NASA CR 120917, July 1972
4. Darms, F. J. and Landes, R. E.; "Computer Program for the Analysis of Filament-Reinforced Metal-Shell Pressure Vessels" NASA CR-72124, Aerojet-General Corporation, Rev. May 1972.
5. "Metallic Materials and Elements for Aerospace Vehicle Structures", MIL-HDBK- 5B, September 1971
6. Gleich, D.; "Development of a Filament-Overwrapped Cryoformed Metal Pressure Vessel", NASA CR-72753, January 1971, Arde, Inc.

APPENDIX A

DESIGN ANALYSIS KEVLAR FIBER REINFORCED ALUMINUM SPHERE*

Special Report 7331, Revision A

January 1974

Prepared for

NASA LEWIS RESEARCH CENTER

CLEVELAND, OHIO

Prepared by

E. E. Morris
R. E. Landes

STRUCTURAL COMPOSITES INDUSTRIES, INC.

6344 North Irwindale Avenue
Azusa, California 91702
213-334-8221

* Presentation of this Design Analysis in S.I. units would reduce the clarity of this Appendix. The report is presented in the original form as written by the authors.

TABLE OF CONTENTS

	<u>Page</u>
I. DESIGN CRITERIA	141
II. MATERIAL PROPERTIES	142
III. VESSEL DESIGN	145
IV. WINDING PATTERN	158
V. BOSS ANALYSIS	162
REFERENCES	165

TABLES

	<u>Page</u>
AI MATERIAL PROPERTIES USED IN DESIGN ANALYSIS	166
AII MATERIAL DESIGN ALLOWABLES	167
AIII CYCLE LIFE CALCULATION, PRD/2219-T62	168
AIV PRD FR 2219-T62 ALUMINUM SPHERE MEMBRANE STRESS SUMMARY	169
AV PRD FR 2219-T62 ALUMINUM SPHERE SUMMARY DESIN PARAMETERS	170
AVI PRD FR ALUMINUM SPHERE WINDING PATTERN	171

FIGURES

	<u>Page</u>
A1 Weight Relationship, PRD FR 2219 Aluminum Spheres	172
A2 Metal Shell Thickness Relationship, PRD FR 2219 Aluminum Spheres	173
A3 Metal Shell Stress Relationship, PRD FR 2219 Aluminum Spheres	174
A4 Critical Flaw Size	175
A5 Schematic Representation of Growth-on-Loading	176
A6 Growth-on-Loading as a Function of Thickness	177
A7 Shape Parameter Curves for Surface and Internal Flaws	178
A8 Deep Flaw Magnification Curves	179
A9 Effect of R Ratio on Service Life of 0.090-in-Thick 2219-T62 Aluminum	180
A10 Flaw Growth Rate Data as a Function of R Ratio and Tensile Stress	181
A11 Relative Effects of α_{Max} and R Ratio	182
A12 Fatigue Crack Growth Rates for 2219-T62 Aluminum Base Metal at RT	183
A13 2219-T62 Mode of Failure as a Function of Stress and Thickness	184
A14 Ambient Stress/Strain Relationship for PRD FR Aluminum Sphere	185
A15 Ambient Pressure-Strain Relationship for PRD FR Aluminum Sphere	186

LIST OF SYMBOLS

A_f	Cross sectional area of 4-end PRD roving, inches ²
$A_{s,f}$	Surface area of filaments, inches ²
\bar{D}	Average spherical diameter, inches
D_b	Boss diameter, inches
D_{bc}	Bolt circle diameter, inches
D_c	Inside diameter of sphere, inches
E_L	Primary modulus (computer value), psi
E_l	Secondary modulus (computer value), psi
F_{tu}	Ultimate strength, psi
F_{ty}	Yield strength, psi
K_{sd}	Metal shell operating to sizing stress ratio, dimensionless
$K_1, \dots K_6$	Design factors defined in text, dimensionless
L_b	Bolt load, pounds
L_1	Thread grip length, inches
N_b	Number of bolts, dimensionless
N_R	Number of mandrel revolutions, dimensionless
N_2	Number of rovings per tape, dimensionless
N_3	Number of tape turns per mandrel revolution, dimensionless
P_{vf}	Filament fraction in composite, dimensionless
\mathcal{P}	Internal Pressure, psi
T	Temperature, degrees F
t	Thickness, inches
V	Volume, inches ³
W	Flange load, pounds
W_f	Strand width, inches

LIST OF SYMBOLS (continued)

w_1	Winding tape width, inches
α	Wrap angle, degrees
α_f, α_L	Coefficients of thermal expansion, inches/inches/ $^{\circ}$ F
β_{22}	Influence coefficient, dimensionless
$\Delta\gamma$	Angle defined in text, radians
Δe	Change in strain, inches/inches
ν	Poisson's ratio, dimensionless
σ	Stress, psi
σ_b	Bending stress, psi
σ_{st}	Thread shear stress, psi

SUBSCRIPTS

b	Burst condition
c	Refers to composite
e	Refers to equator
f	Refers to filaments
L	Refers to metal shell
N	"new" condition
O	"old" condition
o	Operating condition
p	Refers to pole
s	Sizing condition
wf	Filament winding condition

DESIGN ANALYSIS
PRD* FIBER REINFORCED
ALUMINUM SPHERE

This report covers the design and analysis of a 37.5-inch-diameter spherical PRD Fiber Reinforced (PRD FR) aluminum pressure vessel to be used in a test program which will demonstrate the suitability of this type of vessel for future flight vehicles.

I. DESIGN CRITERIA

The PRD FR aluminum pressure vessel design, shown in the reference drawings, was prepared according to the following criteria:

Shape:	Spherical
Size:	37.0-inch inside diameter
Metal Shell:	2219 T-62 aluminum
Fiber Reinforcement:	Continuous four-end PRD-49-III Roving
Resin Matrix:	Epoxy (to be determined)
Winding Pattern:	Axisymmetric, Multiangular, in-plane pattern
Ports:	Five-inch ID, two places axially opposed
Operating Temperature:	Ambient
Operating Pressure:	1820 psi
Burst Factor of Safety:	2.0
Operating Cyclic Life:	400 operating cycles from 0 to 1820 psi to meet service life requirements (1600 operating cycles for qualification)
Reference Drawings:	Pressure Vessel-SCI Drawing 1269382 Liner Assembly-SCI Drawing 1269381 "B" change

*Kevlar-49 roving was formerly designated as PRD-49-III Roving.

II. MATERIAL PROPERTIES

This section covers the mechanical properties required for (1) design of the pressure vessel, and (2) structural analysis of the resulting design.

A. DESIGN VALUES

Table AI presents a summary of the mechanical properties used for the design of the PRD FR aluminum sphere in terms of ambient values and their derivatives with respect to temperature. Since the design equations, described in Section III, require a bi-linear form for the metal shell stress/strain relation, the tabulated values for yield strength and "plastic" modulus of the aluminum are different from the conventional values; the method outlined in Reference A1 was used to obtain these values. The remainder of the mechanical properties listed in Table AI were obtained from Reference A2 (recent verification of the values is reported in Reference A3).

The value for maximum allowable compressive stress in the metal shell listed in Table AI is equivalent to the tensile proportional limit of the material at the stated temperature. This value was selected to minimize any hysteresis effects in the metal shell during pressure cycling.

B. ALLOWABLE STRENGTHS

Table AII presents a summary of allowable tensile strengths selected for use in the structural analysis. Strength levels at cryogenic and elevated temperature are included for reference only.

1. 2219 T-62 Aluminum

The minimum values for both ultimate and yield strength of parent 2219 T-62 aluminum were obtained from MIL-HDBK 5A Reference A4).

The 2219 T-62 aluminum weld metal ultimates were based on typical weld joint efficiencies developed in References A2 and A3 applied to the MIL-HDBK 5A minimums. Reference A3 indicates no reduction in yield strength is expected for 2219 T-62 aluminum weldments, thus tabulated values for yield strength apply to both parent and weld metal.

2. PRD 49 Filaments

Aerojet/SCI has developed a systematic approach to the design of filament-wound vessels (Reference A5) and is using it in a number of applications. The method involves the use of pressure-vessel design factors, corresponding to a range of dimensional parameters, to determine the allowable strength for each configuration. The factors are based on data collected over the past 10 years from tests on several thousand of pressure vessels; these vessels ranged in diameter from 4 to 74 inches and had significant variations in their design parameters. Included as factors used for the selection of design-allowable values are the strength of the roving, resin content, envelope dimensions (length and diameter), internal pressure level, axial port diameters, temperature, sustained loading requirements, and cyclic loading requirements. The method was used in this analysis to establish realistic values for the allowable ultimate tensile strength of PRD-49-III filaments for the 37.5-inch diameter PRD FR aluminum sphere.

The allowable filament strength is given by the relation

$$F_{tu,f} = K_1 K_2 K_3 K_4 K_5 (\sec^2 \alpha) F_f \quad (A1)$$

Where the design factors (K_i), from Reference A5, are based on the specific vessel parameters:

<u>Parameter</u>	<u>Design Factor</u>
$D_c = 37.5$ inches	$K_1 = 0.77$
$D_b/D_c = 0.167$	$K_2 = 1.01$
No cylinder	$K_3 = 1.00$
$t_f/D_c \approx 0.0025$	$K_4 = 0.92$
$T = 75^{\circ}\text{F}$	$K_5 = 1.00$

For Type III PRD-49 filaments, the minimum ultimate tensile strength, $F_{tu,f}$, is 400 ksi, and because the sphere utilizes a multiangular wrap pattern the $\sec^2\alpha$ term approaches one. Thus, the single-pressure-cycle minimum allowable filament strength is

$$F_{tu,f} = 0.77 (1.01) (1.00) (0.92) (1.00) 400 \text{ ksi}$$

$$= 286 \text{ ksi}$$

This value converts to a PRD/epoxy composite wall strength of

$$F_{tu,c} = 0.5 P_{vf} F_{tu,f}$$

$$= 0.5 (.65) (286)$$

$$F_{tu,c} = 93.0 \text{ ksi}$$

It should be noted that the design factors used in the above method were developed for S-Glass filament-wound pressure vessels. Since a large quantity of dimensionally different PRD filament-wound vessels have not been fabricated by industry, including SCI, the validity of the factors for PRD FR vessels has not been substantiated. Other evaluations of PRD composites which have been done at SCI indicate the factors are conservative and will not compromise this current vessel design.

The degree of conservatism can be seen by comparing recent test results for SCI PRD/epoxy filament-wound spheres which have produced an average ultimate filament stress of about 330 ksi, or 107 ksi composite wall strength.

III. VESSEL DESIGN

A. DESIGN METHODS

Stresses, pressures, and dimensional parameters not fixed by the design criteria (Section I) or material allowables (Section II) were established from previously developed compatibility and equilibrium equations reported in Reference A2. Since the sphere maintains a 1:1 bi-axial stress state for all combinations of pressure and temperature, the equations of Reference A2 were simplified as described in the following paragraphs.

Stress and strain equations for the PRD/epoxy shell were based on netting theory which assumes constant stress along the filament path and negligible structural contribution from the resin matrix. The resultant equation for the change in filament strain from a condition "old" (o) to a condition "new" (N) is

$$\Delta \epsilon_f = (\tau_f / E_f)_N - (\tau_f / E_f)_o + \alpha_f (T_N - T_o) \quad (A 2)$$

As in Reference A2, a bi-linear form for the metal shell stress/strain relation was used for analysis of the sphere. The resultant general (elastic/plastic) strain equation for the metal shell is

$$\Delta \epsilon_L = \left[\frac{(\tau - F_{ty})(1-\nu_p)}{E_1} + \frac{F_{ty}(1-\nu)}{E_L} \right]_N - \left[\frac{(\tau - F_{ty})(1-\nu_p)}{E_1} + \frac{F_{ty}(1-\nu)}{E_L} \right]_o + \alpha_L (T_N - T_o) \quad (A 3)$$

For stresses in the elastic range ($\tau \leq F_{ty}$), $E_1 = E_L$, $\nu_p = \nu$, and F_{ty} is set equal to zero. Poisson's ratio in the plastic range, ν_p , was assumed to be 1/2, and values for the other material properties are recorded in Table AI and AII.

Strain compatibility between the metal shells was maintained in the analysis by the requirement that

$$\Delta\epsilon_f = \Delta\epsilon_L \quad (A4)$$

for all combinations of temperature (T) and pressure (p). Further, load equilibrium was maintained by the membrane stress relation

$$\sigma_f t_e + \sigma_L t_L = \rho \bar{D}/4 \quad (A5)$$

The parameter t_e is the equivalent thickness of PRD in the vessel and is defined by the relation

$$t_e = P_{vf} t_c / 2 \quad (A6)$$

B. PARAMETRIC STUDY

In order to establish a weight-optimized design for the PRD FR aluminum sphere, a parametric study was performed according to the following procedure:

1. Fix all parameters defined by the design criteria (Section I) and the material properties (Section II).

2. Select a value for filament operating stress (σ_{of}), subject to the criteria

$$\sigma_{of} \leq \sigma_{ftu}/1.5 \leq 190 \text{ ksi}$$

3. Select several values for the metal shell operating to sizing stress ratio ($K_{sd} \equiv \sigma_o/\sigma_s$), where

σ_s = initial sizing stress in metal

σ_o = operating stress in metal

4. Solve equations (2) through (6) for the unknown design parameters, and then calculate vessel weight and burst factor of safety, for each value of K_{sd} .

5. Repeat Steps 2 through 4 to establish vessel weight trends.

Figure A1 presents the results of this study for a burst factor of safety range between 1.4 and 2.0. Stress curves have been included in the design range to provide a method for evaluating specific design points. Also included as Figures A2 and A3 are curves relating aluminum thickness, sizing stress, and operating stress for use in establishing vessel cycle life.

C.

ADDITIONAL DATA NEEDED FOR ESTABLISHING VESSEL CYCLE LIFE GUARANTEED BY PROOF TEST

To establish the cycle life guaranteed by proof test of specific vessel designs, values of aluminum thicknesses, sizing stresses, and operating stresses must be established. Figures A2 and A3 present the range of these parameters which correspond to the previously defined weight and factor of safety range. The method used to establish values for the necessary parameters for a specific design was as follows:

- Aluminum thickness was fixed at 0.154-in-minimum, based on preliminary design analysis and metal liner manufacturing plans for this program
- Based on results obtained on contract NAS 3-14380 (Development of a Fracture Control Method for Composite Tanks with Load Sharing Liners) and preliminary fracture control design calculations, Ksd was chosen as approximately 0.55.
- Using a safety factor P_b/P_o of 2, diameter (D) of 37.5-in, operating pressure (P_o) of 1820 psi, and liner thickness (t_L) of 0.154-in, filament operating stress (σ_{of}) was determined from Figure A2.
- From Figure A1 $P_o V/W$ was determined.
- Aluminum sizing stress (σ_s) was determined from Figure A3 based on Ksd and σ_{of} .
- Aluminum operating stress (σ_{oL}) was calculated from the expression
$$\sigma_{oL} = Ksd \sigma_s$$

Specifics are summarized as follows

D, in	37.5 (OD liner)
t_L , in	0.154
V, in ³	26,935
P_b/P_o	2.0
P_o , psi	1820

p_b , psi	3640 (Minimum)
$\frac{p_o D}{t_L}$, psi	444,000
σ_{of} , psi	145,000 (Figure A2)
K_{sd}	0.53 (Figure A2)
σs_L , psi	47,500 (Figure A3)
σo_L , psi	25,175
$p_o V/W$, in	370,000 (Figure A1)
$p_b V/W$, in (min)	740,000
W , lbs	132.5
$R \frac{\sigma_{min}}{\sigma_{max}} = \frac{-39,600}{25,175}$	-1.57

D. DETERMINATION OF VESSEL CYCLIC LIFE GUARANTEED BY PROOF TEST

It should be mentioned at the onset of this analysis that numerous assumptions were made during the course of developing the procedures, and the data on which these assumptions were made are limited in nature. Because of this, the results presented herein should be considered only rough estimates and should be used primarily to establish data trends. As more data comes in from NAS 3-14380 work in progress, much firmer estimates of cyclic life guaranteed by proofing will be possible.

Reference A3 data show basically that for 2219-T62 aluminum, flaw size screened by sizing/proof testing is almost identical between base metal and weld metal*. Also, for 0.180-inch material, flaw growth rates for base metal and weld metal were almost identical. These trends are expected to hold as more data are developed, and base metal data (which is believed to be slightly conservative) will be used for the analysis. Also RT proofing was no less effective than cryogenic proofing with respect of flaw size screening.

* Actually, a smaller flaw is screened in weld metal than based metal; and calculations based on base metal result in least cyclic life.

The first step in the analysis was to establish the maximum flaw size that could exist in the liner after the sizing cycle. Reference A3 static fracture results showed (1) that for the same failure stress the flaw depth causing failure was larger for the actual tank tests (biaxial stress field) compared to the uniaxial tests, and (2) no flaw extension occurred for the actual tank tests during sizing as it did in uniaxial tests. However, this biaxial data was developed for only one liner thickness. For the analysis presented herein, it was assumed that the flaw depth existing in an overwrapped tank after sizing could be approximated by using uniaxial static fracture and growth-on-loading results. If more tank test data were available for various liner thicknesses this assumption would not have been necessary.

The uniaxial static fracture data were cross-plotted to generate a family of curves for constant sizing stresses relating the initial flaw depth that will cause failure (a_{cr}) to the liner thickness. This relationship is presented in Figure A4. The initial flaw depth is the flaw depth present in the liner prior to sizing and it is assumed that the flaw shape ($a/2c$) associated with the initial flaw is 0.20. For a given liner thickness and sizing stress, Figure A4 was used to determine the initial flaw depth that would have failed a uniaxial specimen. Uniaxial growth-on-loading data generated in Reference A3 is schematically illustrated in Figure A5. As the figure indicates, the amount of flaw depth growth-on-loading occurring is greater for larger initial flaw depths and asymptotically approaches the initial flaw depth that will cause failure. Because of the nature of the flaw growth-on-loading, it was necessary to select an initial flaw depth that was less than the one that would cause failure during sizing. For this analysis a flaw depth of 90% of the uniaxial a_{cr} was arbitrarily assumed as the initial flaw depth prior to sizing. The flaw dimensions after sizing (as subscript) are defined by the equations below:

$$0.90 \frac{(a_{cr})}{t} t + \Delta a_s = a_{as} \quad (A7)$$

$$5 \left[0.90 \frac{(a_{cr})}{t} t \right] = 2c_{as} \quad (A8)$$

where Δa_s = growth-on-loading, and the factor of 5 in Equation (A8)

is based on an assumed initial flaw shape ($a/2c$) of 0.20.

Only a limited amount of growth-on-loading data is available on 2219-T62 aluminum. The relationships used in this analysis are presented in Figure A6 and are based upon data generated in Reference A3. It was assumed that these curves were independent of sizing stress but, in reality, a family of curves as a function of sizing stress would exist.

The second step in the life analysis was to determine how many operating cycles it takes to grow the flaw (after sizing) to a point where either the liner leaks or fails. Liner leakage occurs when the flaw depth equals the liner thickness. Failure in the base metal was assumed to occur when the combination of flaw depth and operating stress level equals an apparent stress intensity value of 31.7 ksi $\sqrt{\text{in.}}$ This value was based upon RT base metal data of Reference A3. The stress intensity equation used is presented below.

$$K = 1.1 \sigma \sqrt{\frac{\pi a}{Q}} M_K \quad (\text{A9})$$

where K = stress intensity factor

Q = flaw shape parameter (Figure A7)

M_K = deep flaw magnification factor (Figure A8)

A numerical integration technique was used to determine the number of operating cycles required to grow the flaw from its state after sizing to the cutoff condition (leakage or failure, whichever occurs first). This flaw growth potential was divided into increments of Δa and the number of cycles required to grow Δa is $\frac{\Delta a}{da/dN}$: these N's are then summed to give the total cyclic life. It was assumed that the flaw length remains constant until the flaw shape reaches 0.35 and then the flaw shape remains constant; this is based on observations of flaw growth behavior in 2219 aluminum.

Uniaxial data must be modified as applied to overwrapped tanks. Overwrapped liners operate from compression to tension during a zero-to-full pressure

For this analysis, σ_{ys} was assumed equal to σ_s for Q determination

cycle. From data presented in Reference A3, it was evident that rate data is a function of R ratio ($\sigma_{\min}/\sigma_{\max}$) and this should be accounted for. Very recently, data were run to determine the influence of $\sigma_{\min}/\sigma_{\max}$ (R ratio) on cyclic life of surface flawed 0.090-inch material as related to overwrapped metal vessel. Results of some of the preliminary tests are shown in Figure A9, giving the variation in relative cyclic life as a function of R value with σ_{\max} of 36.1 ksi. The correlation appears excellent especially where negative R ratios are concerned. The failure mode was leakage for all tests conducted.

Additional data are given in Figures A10 and A11 for 2219-T62 aluminum tested at R ratios up to -2.0, with σ_{\max} values of 36.1, 24.1 and 18 ksi, further confirming and correlating the results.

The value of da/dN for each increment of Δa growth was determined from the data presented in Figure A12 for $\sigma_{\max} = 36$ ksi, $R = 0$, $t_{\ell} = 0.180$ -in (close to 0.154-in). Stress intensity for these calculations was based on equation (3) without the M_K . Then data of Figure A11 were used to adjust results for the tank design $R = -1.57$ and $\sigma_0 = 25.2$ ksi.

Sample calculations and results for the tank design of interest with $K_{sd}=0.53$ are given in Table AIII. Based on the foregoing assumptions and data for $a/2c = 0.2$, cycle life guaranteed by a proof test is about 570 cycles; this meets the 400 cycle operating requirement.

E. REASONABLE TANK REPROOFING INTERNAL

It is desirable that tanks be suitable for 400 flight service cycles, and considering data scatter, the qualification program would then require demonstration of a 1600 cycle capability. The greatest cycle life that can be guaranteed by the conservative fracture mechanics approach would be 570 cycles. Thus, it might be possible to pass the 1600 cycle test during vessel qualification, since it is unlikely that any given tank would contain an undetected flaw as large as a_{cr} after proof. However, it is recommended that for this design, for both flight and qualification hardware, a reproof be made after every 500 cycles.

F. METAL SHELL MODE OF FAILURE

The Reference A3 specimens (up to 0.320-in thick) were subjected to a sizing (proof) stress in the plastic range of the material and subsequently cycled to failure at various stresses below the sizing stress. The mode of failure was the leak type for all specimens tested (i.e. the leak mode failure exhibits no visual structural damage; the fail mode of failure is more energetic and results in rapid crack propagation in the aluminum).

In order to provide a conservative estimate of the fail mode crack depth for a given thickness and cyclic operating stress level, the following assumptions were made:

- (1) K_{Ic} (as modified by plasticity effects) has a value of 31.7 ksi $\sqrt{\text{in.}}$ This was the minimum value obtained during static fracture testing.

(2) When the stress intensity, as defined by the relation

$$K = 1.95 \sigma \left(\frac{a}{q} \right)^{1/2} M_K$$

reaches K_{Ic} , fail mode of failure will occur.

(3) The surface flaw is initially defined by $a/2c = 0.2$,

and the primary flaw growth is in the depth direction. As the flaw approaches the back surface (flaw depth = thickness), the flaw shape is defined by $a/2c = 0.35$. The corresponding deep flaw magnification factor (M_K) is approximately 1.25.

(4) Equating the stress intensity (K) to the value of K_{Ic} , the relation may be solved for the critical thickness ($a = t_{cr}$) which will cause fail mode of failure (as opposed to leak mode) for a given operating stress ($\sigma = \sigma_o$).

The results are depicted in the fail/leak curve of Figure A13. For both modes of failure, destruction or fragmentation of the composite overwrap is not expected (based on ambient test results obtained under Contract NAS 3-14380). For the designs of interest, thicknesses and operating stresses are well within the leak mode of failure regime.

G. FILAMENT-WOUND COMPOSITE THICKNESS

The equivalent thickness of PRD is

$$t_e = \frac{\frac{P_o D}{4} - \sigma_o L t_L}{\sigma_{of}} = 0.091 \quad (A5a)$$

and, the composite thickness is

$$t_c = \frac{2t_e}{P_{vf}} = 0.280 \text{ in} \quad (\text{A6a})$$

where

$$P_{vf} = 0.65 \text{ for PRD/Epoxy}$$

H. LOAD BALANCE CHECK

The operating condition has been checked above.

For the burst pressure condition

$$\begin{aligned} \frac{P_{bR}}{2} &= F_{tu,L} t_L + F_{tu,f} t_e \\ &= 34,125 \text{ lb/in} \end{aligned} \quad (\text{A5b})$$

where

$$F_{tu,L} = 51,800 \text{ psi}$$

$$F_{tu,f} = 286,000 \text{ psi}$$

The liner carries 24% of the load and the filament-wound composite 76%.

I. LOAD-DUMP CHECK

This refers to the capability of the FWC to sustain the entire applied operating pressure load if the metal should fail and have no load carrying capability whatsoever.

$$\begin{aligned} \frac{P_o R}{2} &= 17,063 \text{ lb/in} = \sigma_f t_e \\ \sigma_f &= \frac{17,063 \text{ lb/in}}{0.091} = 187,505 \ll 286,000 \text{ psi} \end{aligned} \quad (\text{A5c})$$

J. WEIGHT DATA

Mid-Diameter Liner, D_L = 37.346 in

Mid-Diameter FWC, D_c = 37.780 in

Outside Diameter Vessel = 38.060 in

Vessel Membrane Weight, W_M , is determined from

$$W_M = 12.57 \left[\left(\frac{D_L}{2} \right)^2 t_L \rho_L + \left(\frac{D_C}{2} \right)^2 t_C \rho_C \right] \quad (A 10)$$

$$= 68.84 + 61.54 = 130.38 \text{ lbs}$$

where

$$\rho_L = 0.102 \text{ lb/in}^3 \quad t_L = 0.154\text{-in}$$

$$\rho_C = 0.049 \text{ lb/in}^3 \quad t_C = 0.280\text{-in}$$

Total Weight (minimum design) 130.38 lbs

Tolerance Contingency and Bosses 17.12 lbs

Total 147.50 lbs

The weight contingency is divided as follows. For the metal liner, the 0.154-in thickness is design minimum, with a permissible tolerance of -0.000 / + 0.030 in; actual metal shell weights, including tolerances and the polar boss fittings are expected to be 10.46 lbs over the computed minimum values. The filament wound composite can be fabricated to 0.280-in nominal thickness at the equator, but there is a thickness increase up the shell from the equator to the polar bosses which is expected to add 6.66 lbs to the computed minimum values.

K. Performance Efficiencies

Based on the foregoing data, pressure vessel performance efficiencies are as follows for 1820 psi operating, 3640 psi minimum burst, and 26,935 in³ volume.

	<u>Vessel Weight, lbs</u>	
	<u>130.381</u>	<u>147.50</u>
$\frac{\rho_{ov}}{W}$, in	375,830	332,350
$\frac{\rho_{bv}}{W}$, in, minimum	749,840	664,700

Expected burst pressure is greater than minimum design. Using

$$p_b = \frac{4}{D} [F_{tu, L} t_L + F_{tu, f} t_e] = 4161 \text{ psi} \quad (\text{A5d})$$

with the following typical properties

$$F_{tu, L} = 58,000 \text{ psi}$$

$$F_{tu, f} = 330,000 \text{ psi}$$

$$t_L = 0.154 \text{ in}$$

$$t_e = 0.091 \text{ in}$$

Expected $p_b V/W$ based on 147.50 lb weight is

$$\frac{p_b V}{W} = \frac{(4161)(26,935)}{147.5} = 759,840 \text{ in}$$

Weight savings are expected to range from 11% minimum to 26% when compared to 6Al-4 V Ti (STA) spherical pressure vessels at $p_b V/W = 600,000$ in.

L. STRESS VERSUS STRAIN DIAGRAM

Detailed calculations were performed to establish stresses and strains at various conditions. Figure A14 presents the vessel stress-strain diagram. Membrane stresses in the PRD/epoxy and aluminum shells are summarized in Table AIV.

M. PRESSURE VERSUS STRAIN DIAGRAM

Figure A15 gives the vessel design pressure versus strain curve.

N. SUMMARY DATA

Table AV lists summary data for the pressure vessel design.

IV. WINDING PATTERN

Winding patterns for FR metal pressure vessels require the application of a specific quantity of roving in predetermined orientations in order to obtain the desired burst and/or operating pressure. Unlike the filament-wound oblate spheroidal vessel, whose head shape depends upon a single in-plane winding pattern, the head shape of a spherical vessel is fixed, and the pattern is designed to complement the shape.

The basis for establishing a winding pattern for the sphere is the uniform stress field induced in the wall of a sphere when the vessel is subjected to pressure. Efficient filament loading is obtained if filaments are oriented in a balanced multiangular pattern within the wall. SCI has developed semi-empirical, axisymmetric, multiangular, winding patterns for spherical vessels based on these considerations.

A. EQUATOR OF HEAD

All oriented layers of fiber pass thru the equator of the head, and the filament thickness per layer of 4-end PRD-49 roving may be determined from the expression

$$t_f = A_f / W_f \quad (A\ 11)$$

where

$$\begin{aligned} A_f &= \text{cross sectional area of 4-end roving} \\ &= 5.380 \times 10^{-4} \text{ inches}^2 \end{aligned}$$

$$W_f = \text{single strand width, fixed at 0.130 inches}$$

Thus, the filament thickness per layer is

$$t_f = 5.380 \times 10^{-4} / 0.130 = 0.00414 \text{ inches}$$

Two layers are formed for each revolution of the winding mandrel. A value of 21 revolutions (N_R) of the winding mandrel was selected for this pattern, and for a volume fraction (P_{vf}) of PRD at the vessel equator equal to 0.62*, the resultant thickness at the equator is

$$t_{ce} = 2N_R t_f / P_{vf} \\ = 2(21) (.00414) / 0.62$$
(A 12)

$$t_{ce} = 0.280 \text{ inches}$$

B. ADJACENT TO POLE

Experience gained in testing GFR metal spheres has indicated that a 10 to 15% buildup of composite material is necessary as a reinforcement in the area of the port. The average composite thickness adjacent to the pole resulting from one revolution of butt windings at the equator may be calculated from the expression

$$t_{cp} = \frac{V_f}{\pi P_{vf} W_1 (D_b + W_1)} \quad (A 13)$$

The volume of fiber (V_f) contributing to the buildup is

$$V_f = N_3 A_{s,f} t_f \quad (A 14)$$

The surface area of fiber ($A_{s,f}$) contributed by each tape (turn) may be found from the expression

$$A_{s,f} = \left(\frac{D_b + 2W_1}{2} \right)^2 \left[\Delta\gamma - \frac{\sin 2\Delta\gamma}{2} \right] \quad (A 15)$$

Where,

$$\Delta\gamma = \cos^{-1} \left(\frac{D_b}{D_b + 2W_1} \right) \quad (A 16)$$

$$W_1 = \text{winding tape width} = N_2 W_f$$

*Based on actual measurements P_{vf} average for a PRD/ Epoxy vessel is 0.65, with 0.62 locally at the equator.

N_2 = number of rovings per tape

D_b = diameter of boss = 6.25 inches

The number of turns per revolution (N_3) is related to the tape width by the expression

$$N_3 = \frac{\pi D_c \cos \alpha_p}{W_1} \quad (A 17)$$

where, the polar in-plane angle (α_p) is

$$\alpha_p = \sin^{-1} \left(\frac{D_p + W_1}{D_c} \right) \quad (A 18)$$

and

D_c = diameter of sphere = 37.5 inches

Calculations were performed using equations (A13) thru (A18) to arrive at values of composite thickness adjacent to the boss as a function of four different tape widths. Results of the calculations are presented in the following table.

N_2	W_1 (inches)	α_p (degrees)	N_3	$\Delta\delta$ (radians)	$A_{s,f}$ (inches ²)	V_f (inches ³)	t_{cp} (inches)
12	1.56	12.0	74	0.841	7.546	2.312	0.093
10	1.30	11.5	89	0.787	5.611	2.067	0.103
8	1.04	11.2	111	0.722	3.925	1.804	0.117
6	0.78	10.8	148	0.643	2.489	1.525	0.136

Inspection of the above table coupled with practical considerations during winding, lead to the selection of a polar pattern consisting to two revolutions of 12-strand tapes and one revolution of 6-strand tapes. This pattern results in a total composite thickness adjacent to the port of

$$t_{cp} = 2(0.093) + 0.136 = 0.322 \text{ inches}$$

which is 1.15 times the composite thickness at the equator. This value is within the required 10 to 15% buildup range.

C. ADDITIONAL PARAMETERS

In addition to the three revolutions of windings adjacent to the pole, two circuits consisting of 9 revolutions (steps) each of 12-strand tapes was selected to complete the winding pattern; the total pattern contains the required 21 revolutions of two-layer windings selected in Section IV A. The circuit consists of windings placed at wrap angles (or steps) incremented by the expression

$$\alpha_i = \alpha_1 + \Delta\alpha_{12} + (i-2) \Delta\alpha \quad (A 19)$$

Where,

$$i = 2, 3, \dots, 10$$

α_1 = polar wrap angle for 12-strand tape = 12.0 degrees

$\Delta\alpha_{12}$ = angular increment of polar step to second step, selected as

3.5 degrees

$\Delta\alpha$ = angular increment, selected as 6.5 degrees

The number of turns per revolution for the i'th wrap angle is given by the expression

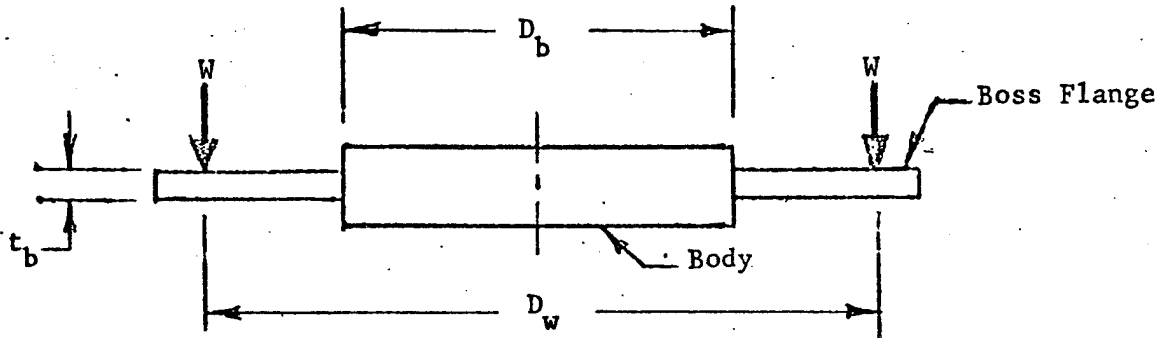
$$N_{3,i} = \pi D_c \cos \alpha_i / N_2 W_f \quad (A 20)$$

Calculations were performed using equations (A 19) and (A 20) at values for the wrap pattern variables. Results of the calculations are presented in Table AVI.

V. BOSS ANALYSIS

A. FLANGE BENDING

Only the most critical section of the boss, located at the base of the flange, was analyzed. Stresses there were determined by using the conservative assumption that the flange is a flat plate with a concentrated annular load and a fixed inner edge (the body).



The end-for-end wrap pattern of the polar longitudinal filaments produces a rigid band around the boss that supports the flange. The load applied (W) is the reaction of the boss flange bearing against the composite structure. The total load is therefore equivalent to the pressure acting over the area within the reaction circle. The diameter at which the load is assumed to act (D_w) is

$$D_w = D_b + W_1$$

where

$$D_b = \text{boss diameter} = 6.250 \text{ inches}$$

$$W_1 = \text{polar winding tape width} = 0.780 \text{ inches}$$

The bending stress at the juncture of the flange and boss (σ_b) is calculated in accordance with formulas for loading on a flat plate (Reference A6, Case 22, p. 223):

$$\sigma_b = \frac{\beta_{22} W}{t_b^2} \quad (\text{A } 21)$$

$$W = \frac{\pi P_b D_w^2}{4} \quad (\text{A } 22)$$

$$\beta_{22} \approx \frac{D_w}{D_b} - 1$$

t_b = flange thickness = 0.600 inches

Solving the relationships

$$D_w = 6.250 + 0.780 = 7.030 \text{ inches}$$

$$W = \pi (3640) (7.030)^2 / 4 = 141,215 \text{ pounds}$$

$$\beta_{22} = \frac{7.030}{6.250} - 1 = 0.125$$

The bending stress is

$$\sigma_b = 0.125 (141,215) / (0.600)^2 \\ = 49,033 \text{ psi}$$

and, the margin of safety is

$$M.S. = \frac{F_{tu}}{\sigma_b} - 1 = \frac{54}{49} - 1 = \underline{\underline{+0.10}}$$

B. BOLT STRENGTH

The load per bolt (L_b) was calculated from the expression

$$L_b = \pi D_{bc}^2 p_b / 4N_b \quad (A 23)$$

where

D_{bc} = bolt circle diameter = 5.625 inches

N_b = number of bolts = 16

Thus,

$$L_b = \pi (5.625)^2 (3640) / 4(16) \\ = 5651 \text{ pounds}$$

For 5/16-24 bolts with an ultimate tensile strength of 170,000, the ultimate tensile load per bolt (L_{tu}) is 9800 pounds. The margin of safety is

$$M.S. = \frac{9.8}{5.65} - 1 = + \underline{\underline{0.73}}$$

C. FLANGE THREAD SHEAR

The shear stress in the threads (τ_{st}) was determined from the expression

$$\tau_{st} = \frac{L_b}{.5\pi D_b L_t} \quad (A 24)$$

Where, L_t = thread grip length = 0.470 inches

$$\begin{aligned}\tau_{st} &= \frac{5651}{.5\pi (5.625)(.470)} \\ &= 1361 \text{ psi}\end{aligned}$$

The ultimate shear strength of 2219-T62 aluminum (Reference A4) is 32 ksi, and the margin of safety is

$$\text{M.S.} = \frac{32}{1.36} - 1 = \underline{\underline{\text{HIGH}}}$$

REFERENCES

- A1. Landes, R. E.; "Glass Fiber Reinforced Metal Pressure Vessel Design Guide", NASA CR-120917, Structural Composites Industries, July 1972.
- A2. Morris, E. E., et. al.; "Parametric Study of Glass-Filament-Reinforced Metal Pressure Vessels", NASA CR 54-855, Aerojet-General Corporation, April 1966.
- A3. Bixler, W. D.; "Development of a Fracture Control Method for Composite Tanks with Load Sharing Liners", (Interim Report), NASA CR-120918, Boeing Aerospace Company, March 1973.
- A4. Metallic Materials and Elements for Aerospace Vehicle Structures, MIL-HDBK-5A, Department of Defense, February 1966.
- A5. Structural Materials Handbook, Aerojet-General Corporation, February 1964.
- A6. Roark, R. J.; "Formulas for Stress and Strain", 4th Edition, McGraw-Hill Book Company, 1965.

TABLE AI

MATERIAL PROPERTIES USED FOR VESSEL DESIGN

<u>Property</u>	<u>Aluminum 2219-T62</u>	<u>PRD/Epoxy</u>
Density, lb/inch ³	0.102	.049
Coefficient of Thermal Expansion, inch/inch -°F at +75 to -423°F	8.915×10^{-6}	-1.985×10^{-6}
Tensile Yield Strength, psi	42,000	-
Derivative of Yield Strength with Respect to Temperature, psi/°F	-29.1	-
Elastic Modulus, psi	10.5×10^6	18.6×10^6
Derivative of Elastic Modulus with Respect to Temperature, psi/°F	-2,510	-2,410
Plastic Modulus, psi	400,000	-
Poisson's Ratio	0.325	-
Derivative of Poisson's Ratio with Respect to Temperature, 1/°F	-0.2005×10^{-4}	-
Maximum Allowable Operating Compressive Stress at +75°F, psi	39,600	-
Volume Fraction Filament		.65

[FH]

TABLE AII

MATERIAL DESIGN ALLOWABLES

Material	Property	Temperature, °F		
		-250	+75	+160
2219 T-62 Aluminum	Tensile Yield Strength, ksi			
	Typical (a)	51.9	42.5	40.0
	Minimum (b)	40.3	36.0	34.6
	Minimum Ultimate Tensile Strength, ksi			
	Parent Metal (b)	61.0	54.0	52.4
	Weldment (c)	58.6	51.8	50.3
	Ultimate Shear Strength, ksi	—	32.0(b)	—
PRD 49-III Filaments	Minimum ultimate tensile strength, ksi	—	286 330	277 320
	Typical ultimate tensile strength, ksi	—	—	—

(a) Data from References A2 and A3.

(b) Data from Reference A4.

(c) Based on weld joint efficiency of 96% from References A2 and A3.

TABLE AIII

CYCLE LIFE CALCULATION, PRD / 2219-T62 (K_{sd} = 0.53)

PARAMETERS			
$t_L = 0.154\text{-in}$	$a_{cr}/t_L = 0.51$	$2c_{as} = (0.071) 5 = 0.355 \text{ in}$	
$\sigma_s = 47,400 \text{ psi}$	$a_{cr} = 0.079 \text{ in}$	$\sigma_o/\sigma_s = 0.53$	
$\sigma_o = 25,175 \text{ psi}$	$0.90a_{cr} = 0.071 \text{ in}$		
$\sigma_c = 39,600 \text{ psi}$	$\Delta a_{as} = 0.020 \text{ in}$	$R = -\frac{39,600}{25,175} = -1.57$	
	$a_{as} = 0.091 \text{ in}$		

$a, \text{ in}$	$2c, \text{ in}$	CALCULATIONS BASED ON $\sigma_o = 36,000 \text{ psi}$		$K = 1.95 \sigma_o \sqrt{\frac{a}{Q}} \text{ ksi, in.}$	$\frac{da/dn[R=o]}{\sigma_o = 36 \text{ ksi}}$	ΔN
		$\frac{a}{Q}$	$\frac{a}{Q}$			
0.092	0.355	0.259	1.36	0.068	.261	18, 322
0.100	0.282	0.282	1.44	0.0695	.264	18, 533
0.110	0.310	0.310	1.55	0.071	.266	18, 673
0.120	0.388	0.388	1.64	0.073	.270	18, 954
0.130	0.350	0.350	1.69	0.0769	.277	19, 445
0.140	0.350	0.350	1.69	0.0828	.288	20, 218
0.150	0.350	0.350	1.69	0.0888	.298	20, 920
0.154	0.350	0.350	1.69	0.0911	.302	21, 200
						$\Sigma \frac{77}{1597}$
						28
						286
						344
						333
						333
						285
						250
						222
						45
						52

Adjusting to $\sigma_o = 25,175 \text{ psi}$, $R = -1.57$, Relative flaw growth rate is 2.80.

$$\frac{1597 \text{ cycles}}{2.80 \text{ Relative Life}} = 570 \text{ cycles to Leak}$$

TABLE AIV
PRD FR 2219-T62 ALUMINUM SPHERE MEMBRANE

STRESS SUMMARY

Condition	Pressure, psi	Filament Stress, ksi	Metal Shell Membrane Stress, ksi
As Fabricated.	0	7.4	-4.3
Sizing	2447	172	47.5
After Sizing	0	67.1	-39.6
Operating	1820	145	25.1
Failure	3640	286	52.3

TABLE AV

PRD FR 2219-T62 ALUMINUM SPHERE SUMMARY

DESIGN PARAMETERS

PARAMETER	VALUE
Diameters, in	
Inside	37.192
Outside	38.060
Volume, in ³	26,935
Thicknesses, in	
2219-T62 Liner	0.154
Filament-Wound Composite (Equator)	0.280
Weight, lbs	147.5
Pressures, psi	
Operating	1820
Sizing	2447
Burst (Minimum)	3640
Burst (Expected)	4161
Burst Factor of Safety	2.0
Operating Stresses, psi	
2219-T62 Liner	25,175
PRD Filaments	145,000
Operating Cycles Guaranteed by Proof Test	570
Performance Factor, $\phi_{V/W}$, in	
Operating	332,350
Minimum Burst	664,700
Expected Burst	759,840

TABLE AVI
PRD FR ALUMINUM SPHERE WINDING PATTERN

Step No.	Tape Width W_1 (inches)	Wrap Angle α (degrees)	No. turns per revolution, N_3
1	1.56	12.0	74
2		15.5	73
3		22.0	70
4		28.5	66
5		35.0	62
6		41.5	57
7		48.0	51
8		54.5	44
9		61.0	37
10		67.5	29
11		67.5	29
12		61.0	37
13		54.5	44
14		48.0	51
15		41.5	57
16		35.0	62
17		28.5	66
18		22.0	70
19		15.5	73
20	1.56	12.0	74
21	.78	11.0	148

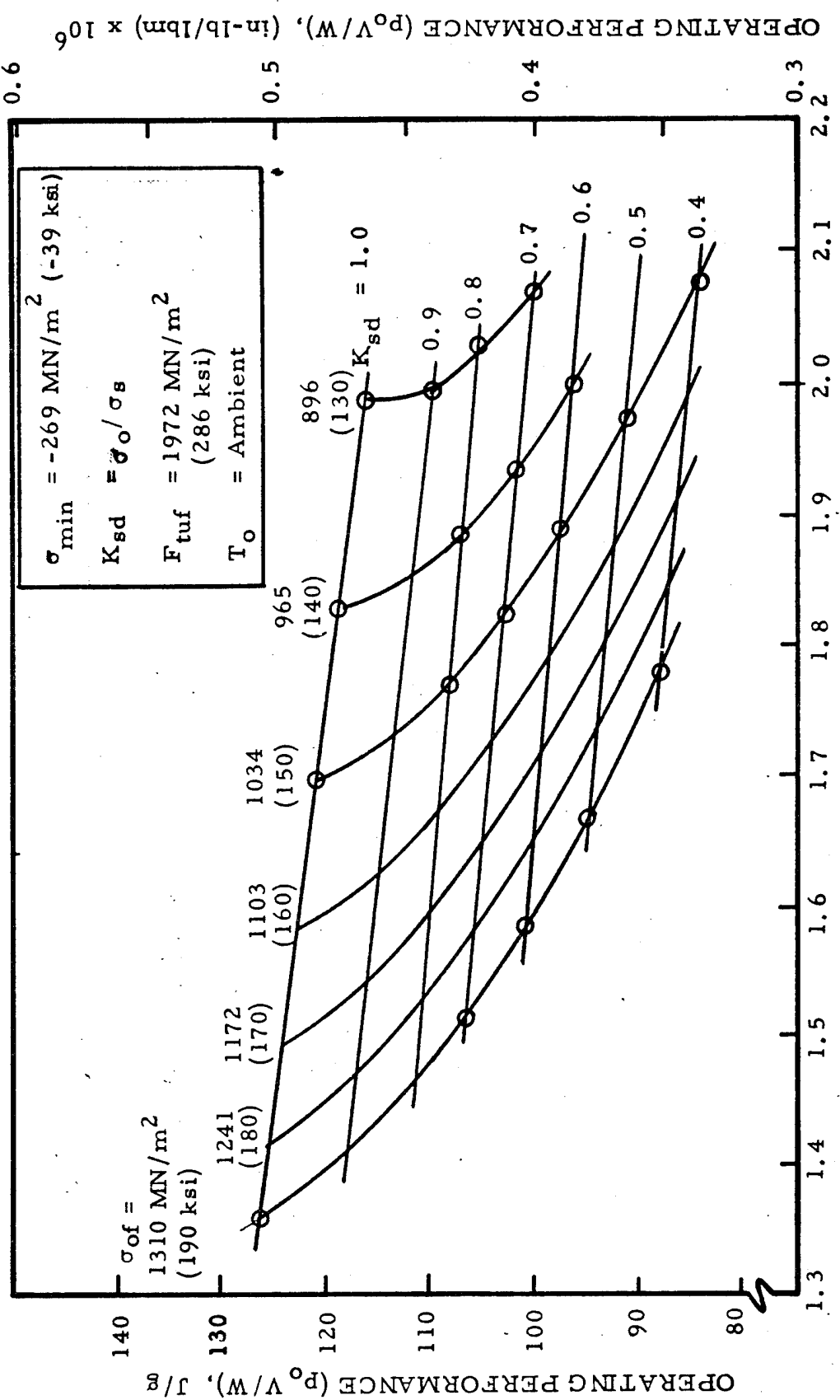


FIGURE A1: Design Performance Curves for
Kevlar FR 2219-T62 Aluminum Spheres

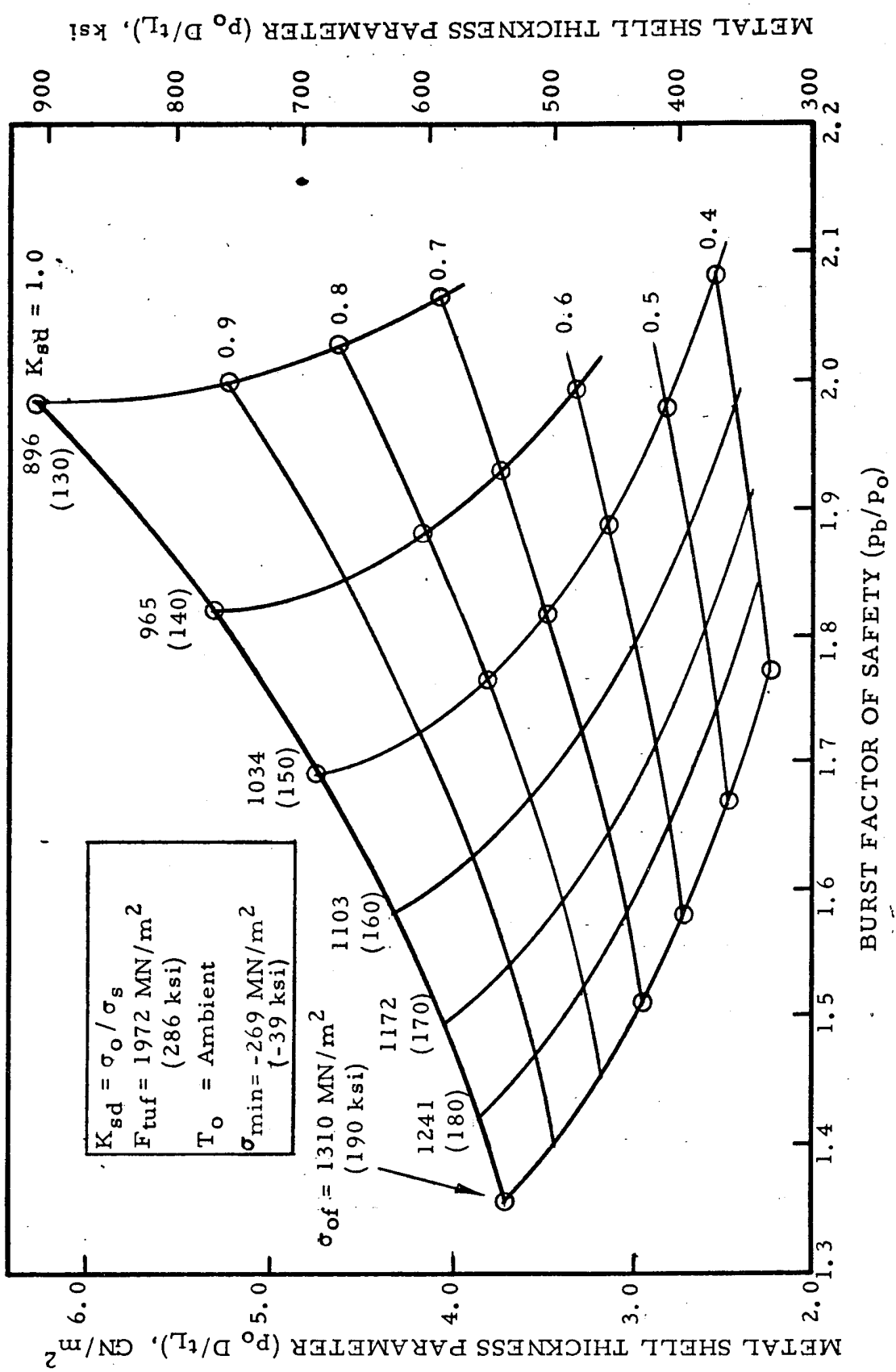


FIGURE A2: Design Metal Shell Thickness Curves For
Kevlar FR 2219-T62 Aluminum Spheres

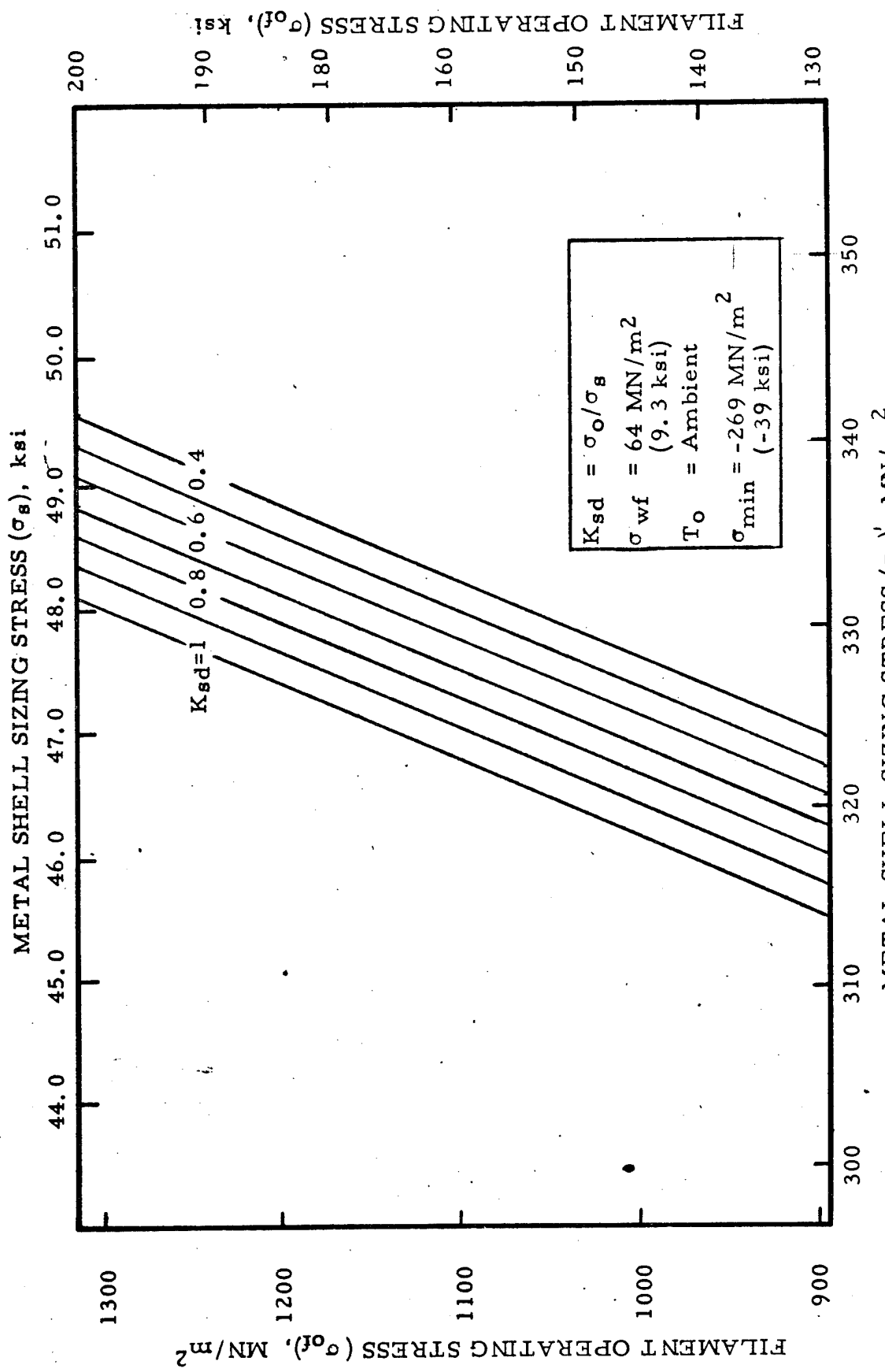


FIGURE A3: Design Stress Chart For
Kevlar FR 2219-T62 Aluminum Spheres

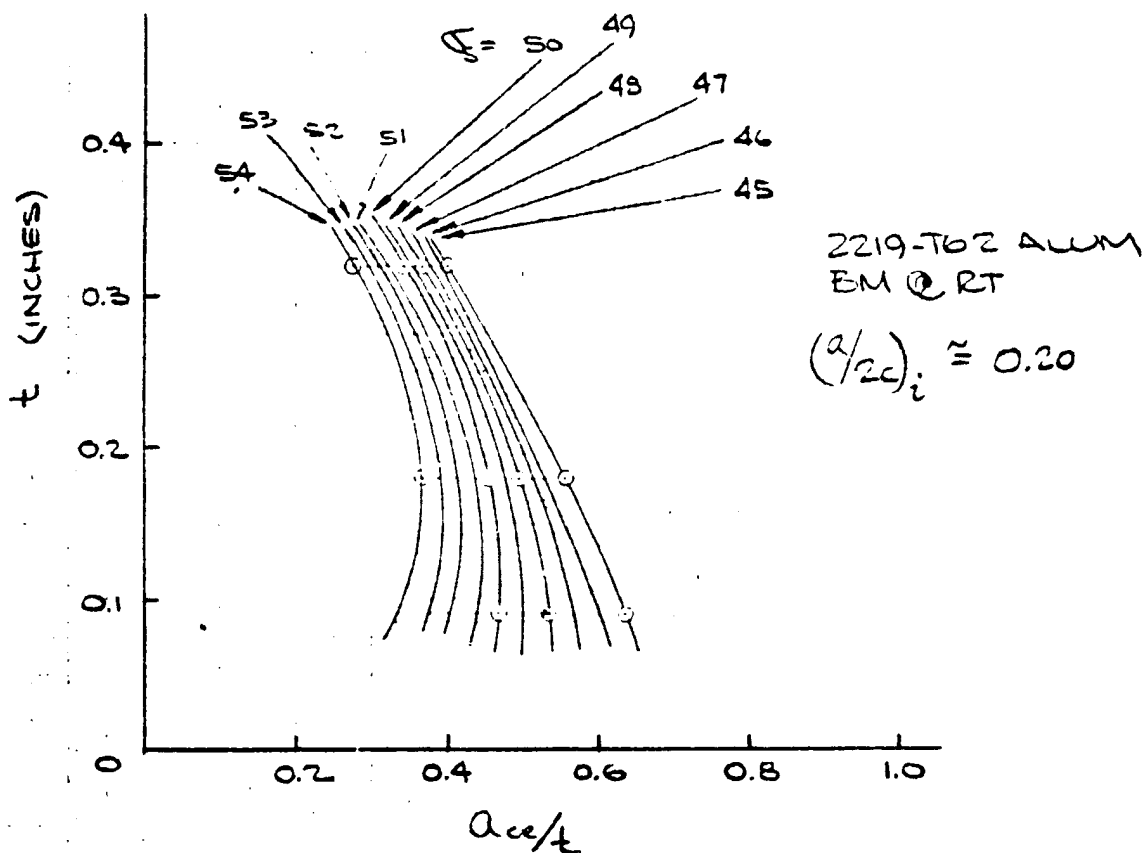
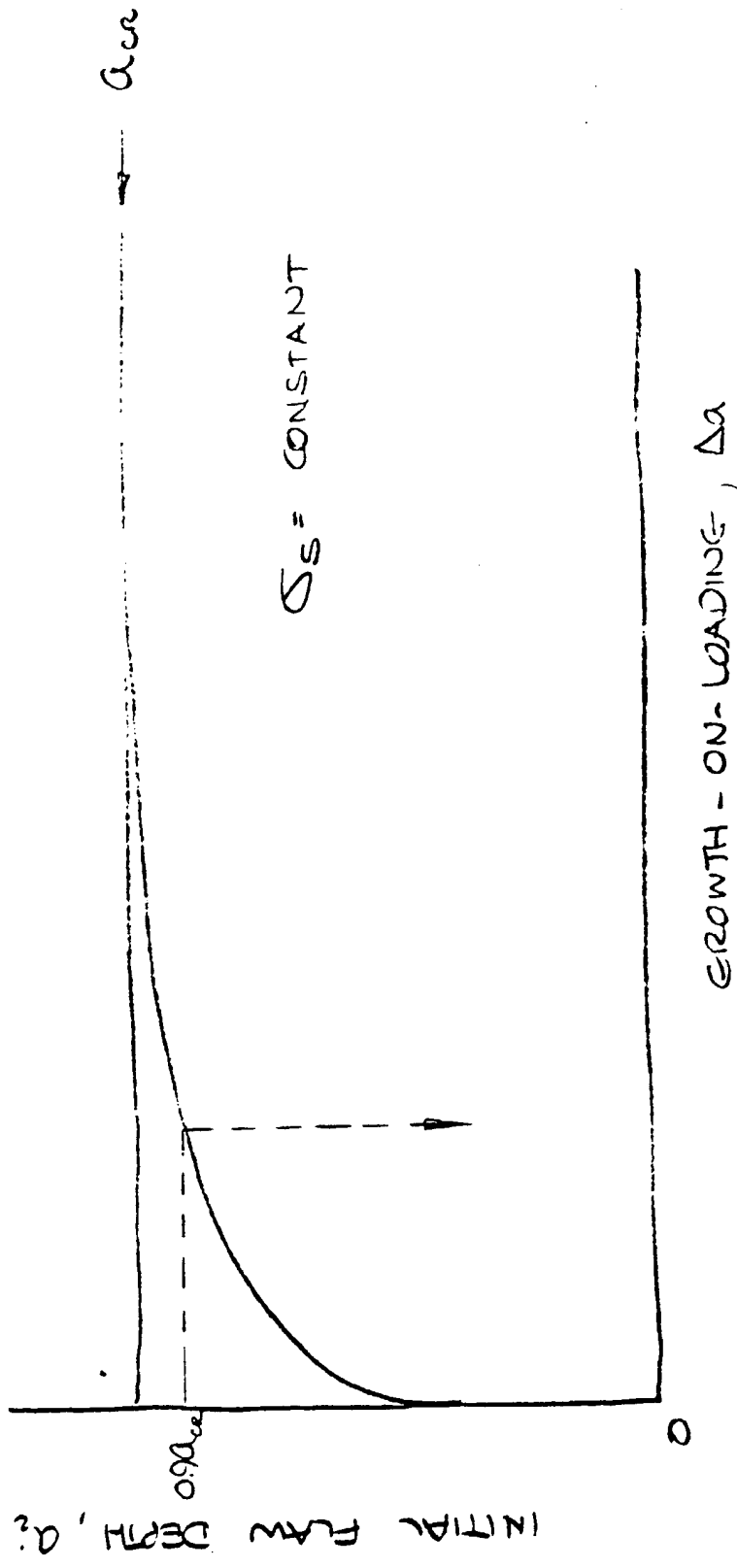


FIGURE A4 CRITICAL FLAW SIZE

GROWTH - ON - LOADING, Δa

Schematic representation of growth-on-loading

Figure A5



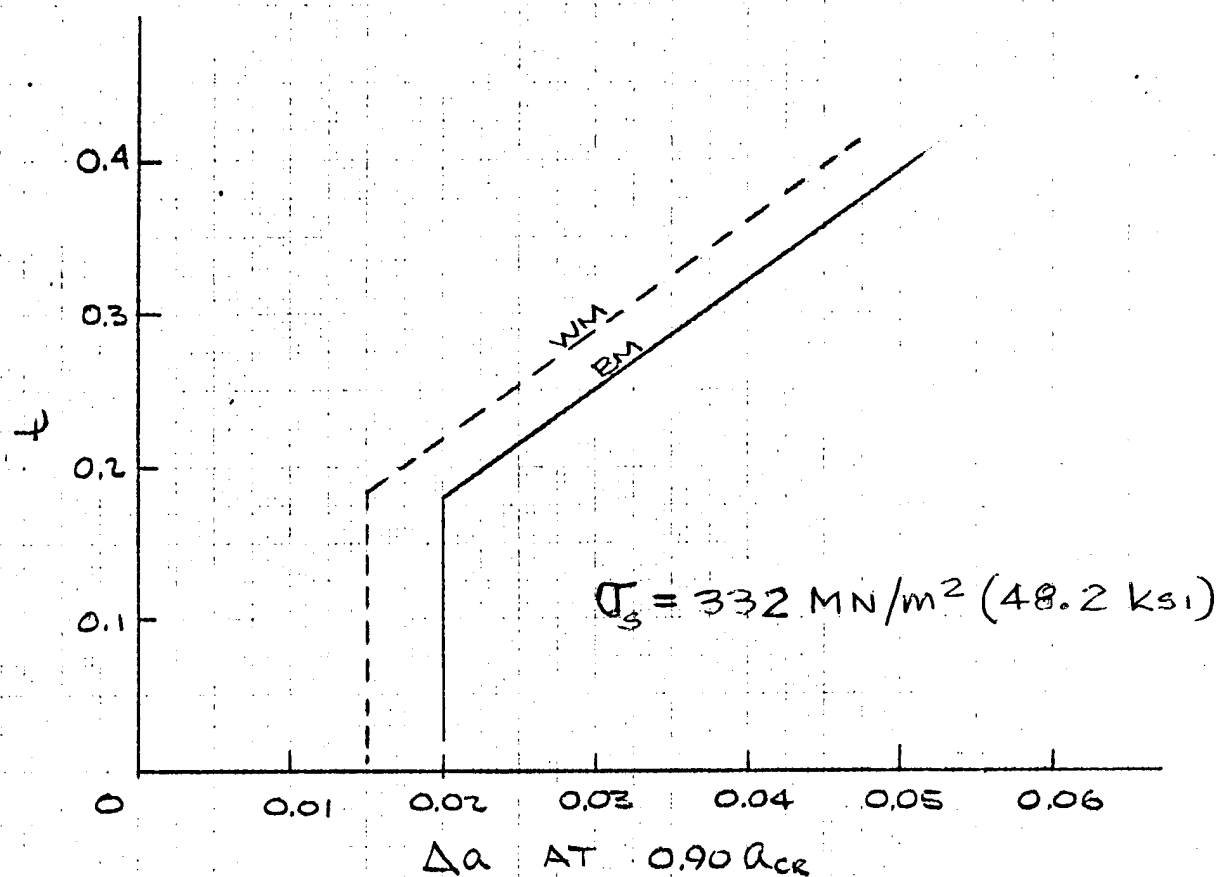
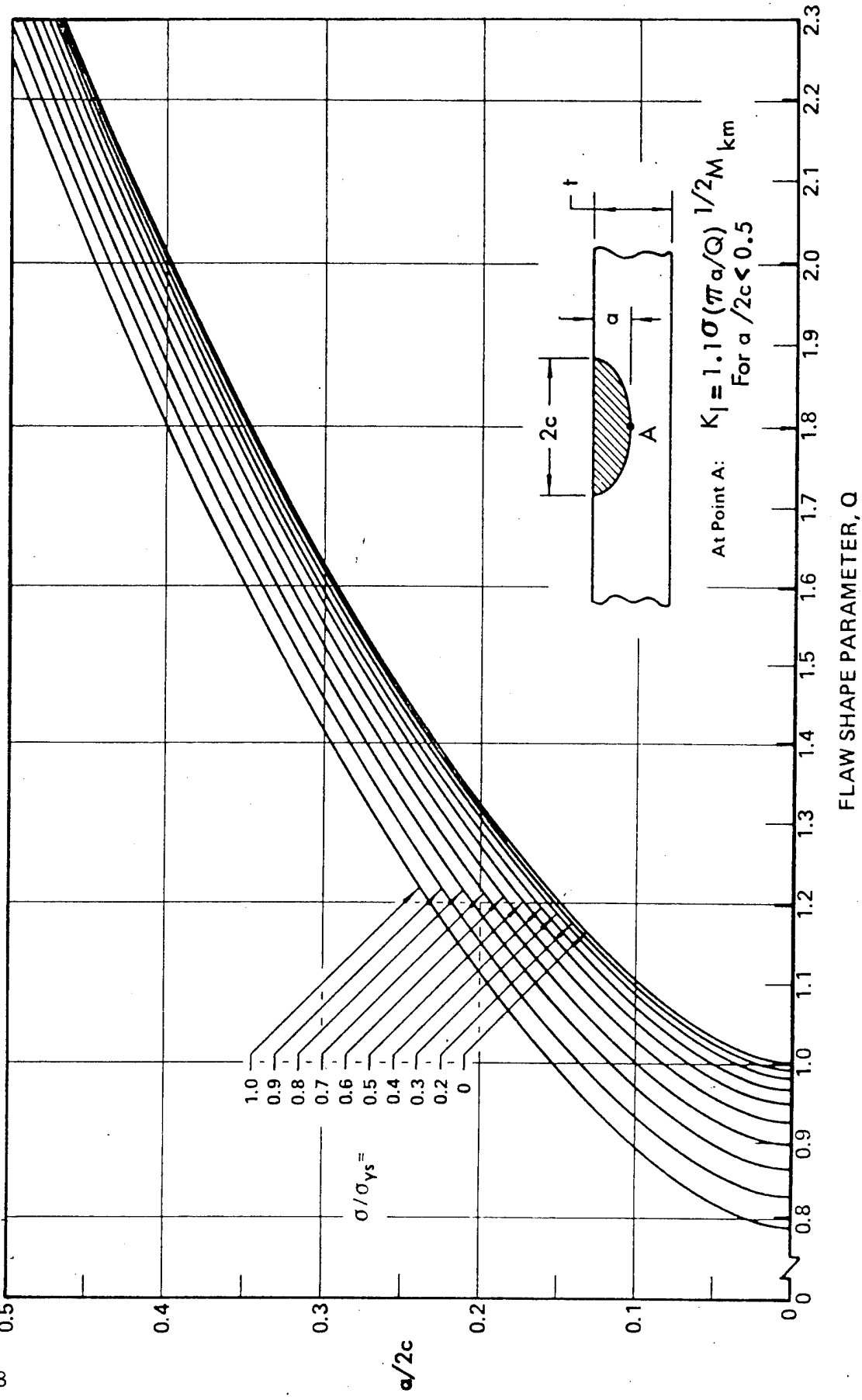


FIGURE A6

GROWTH-ON-LOADING AS A FUNCTION OF THICKNESS



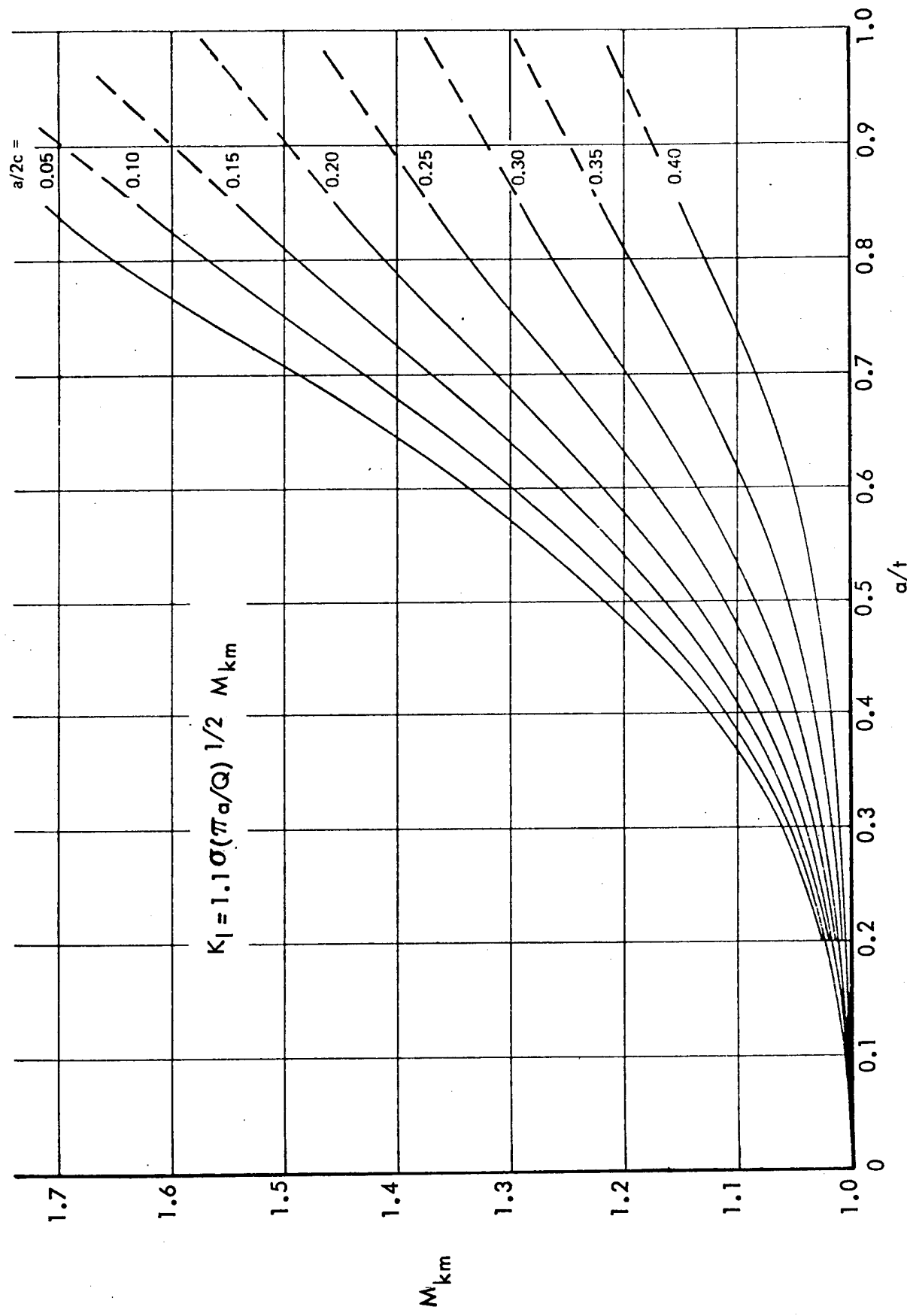
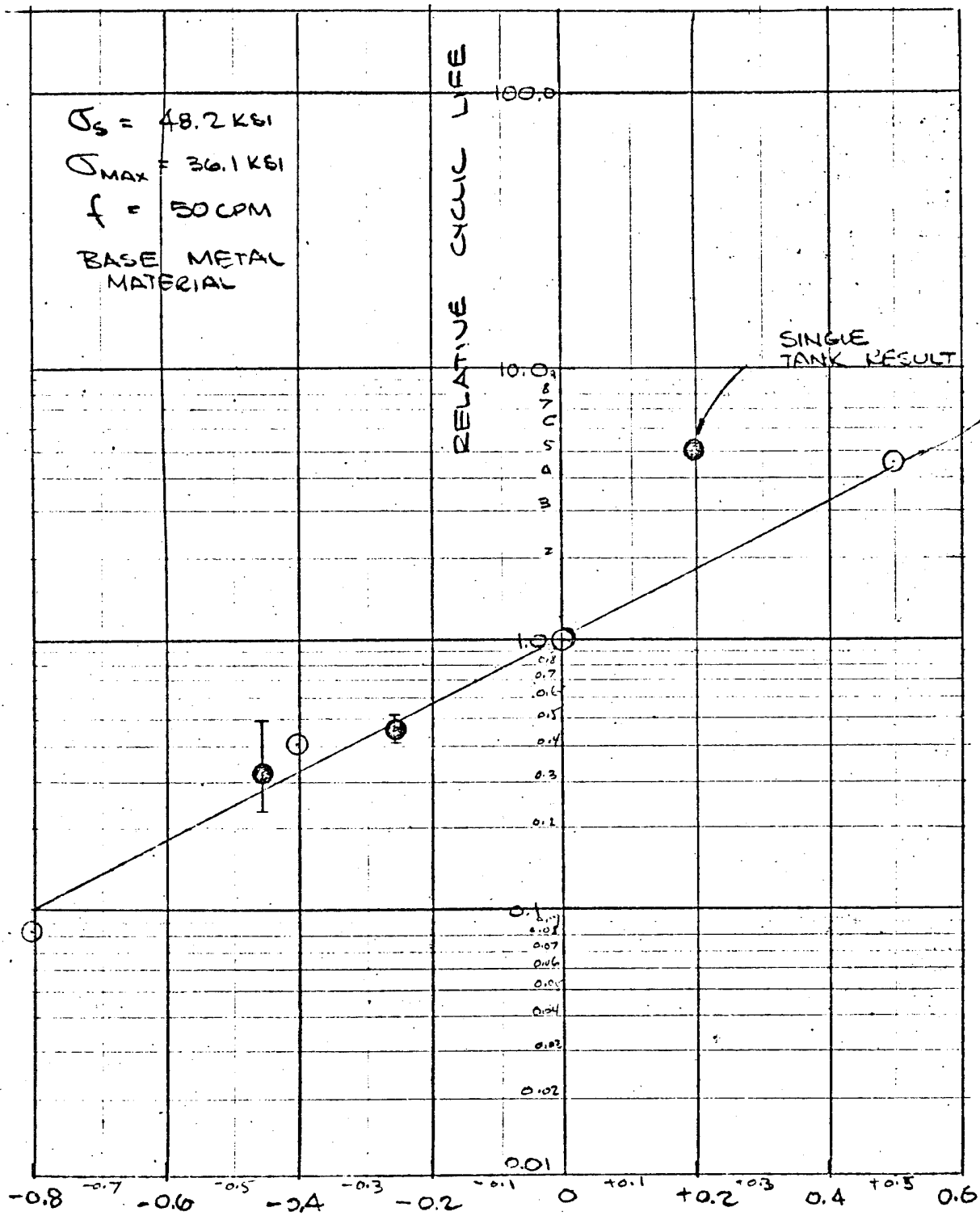


FIGURE A8: DEEP FLAW MAGNIFICATION CURVES

- DATA GENERATED ON ON-GOING PROGRAM
(UNIAXIAL WITH TENSION/COMPRESSION CAPABILITY)
- AVERAGE OF DATA GENERATED IN NASA CR-120918
(BIAXIAL WITH HOOP GFR)



R RATIO ($\sigma_{\text{MIN}}/\sigma_{\text{MAX}}$)

FIGURE A9

EFFECT OF R RATIO ON SERVICE LIFE
OF 0.090" THICK 2219-T62 ALUMINUM

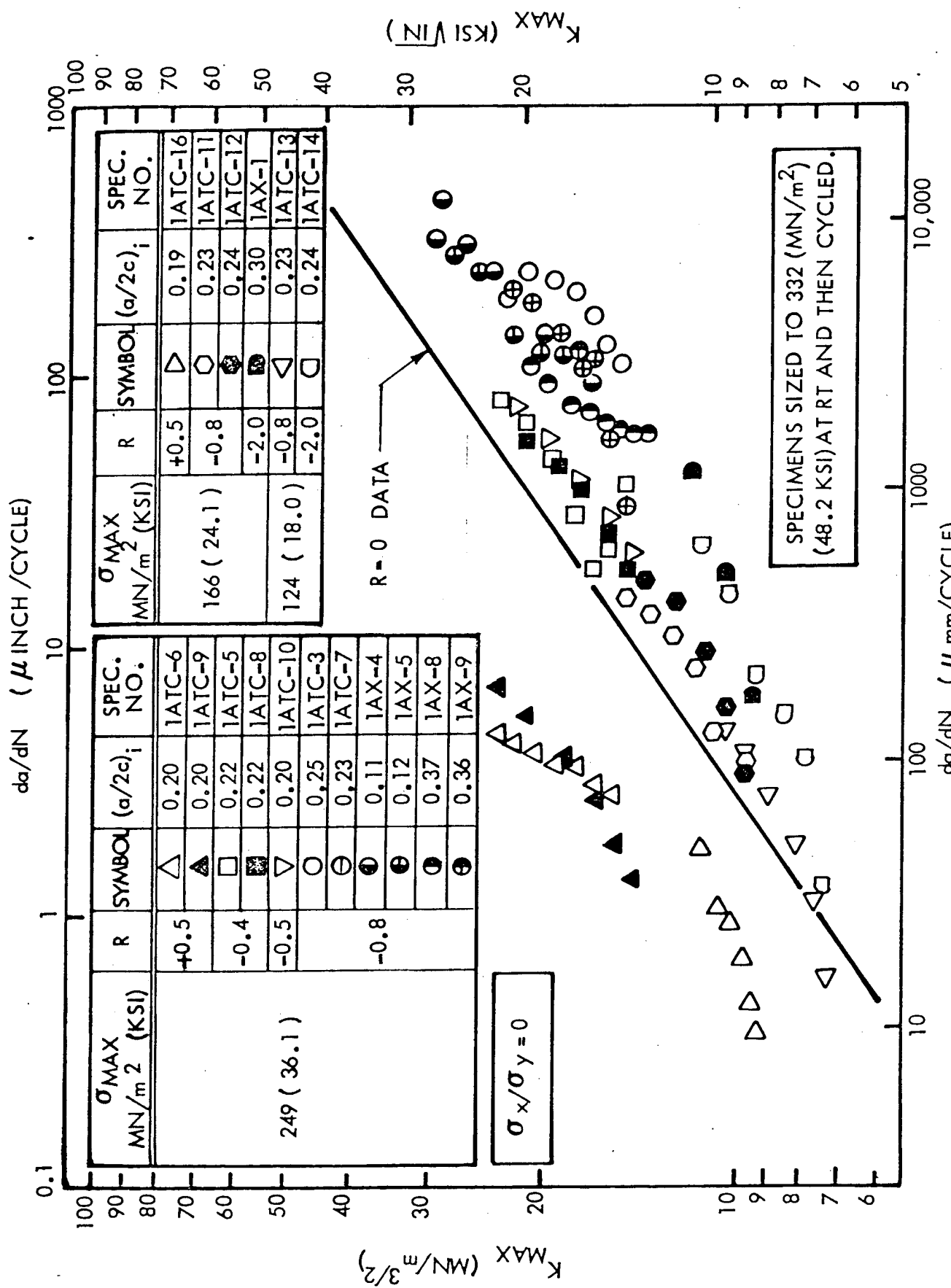
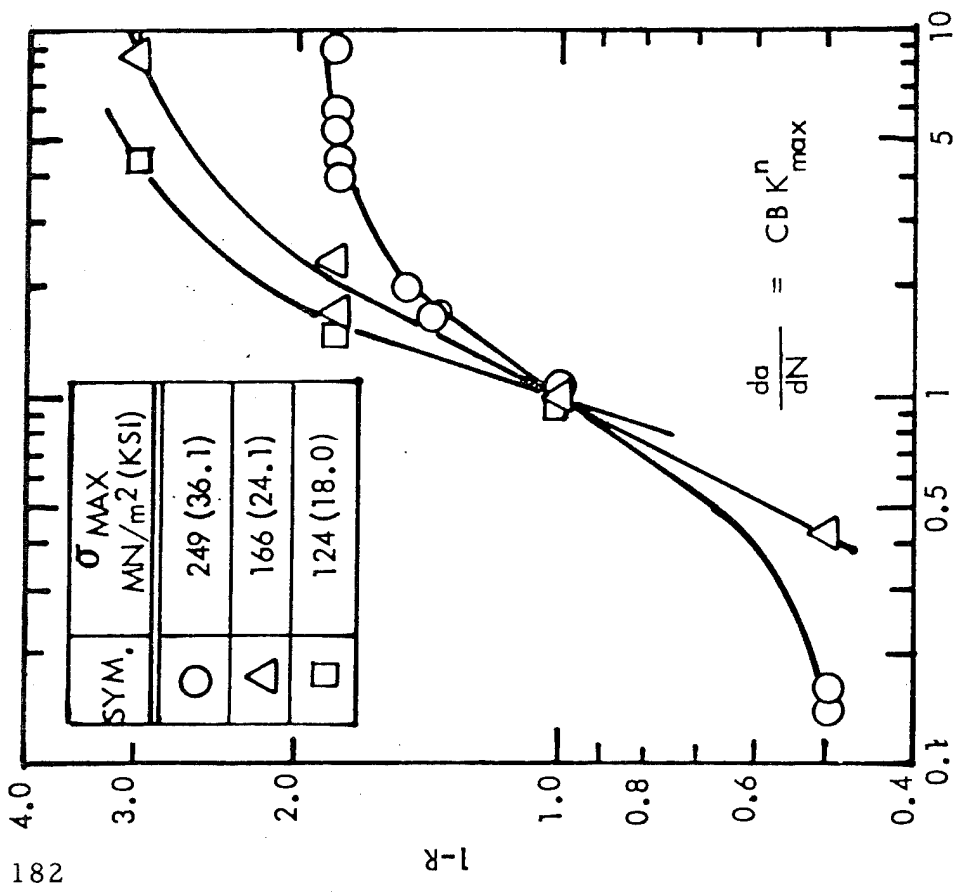
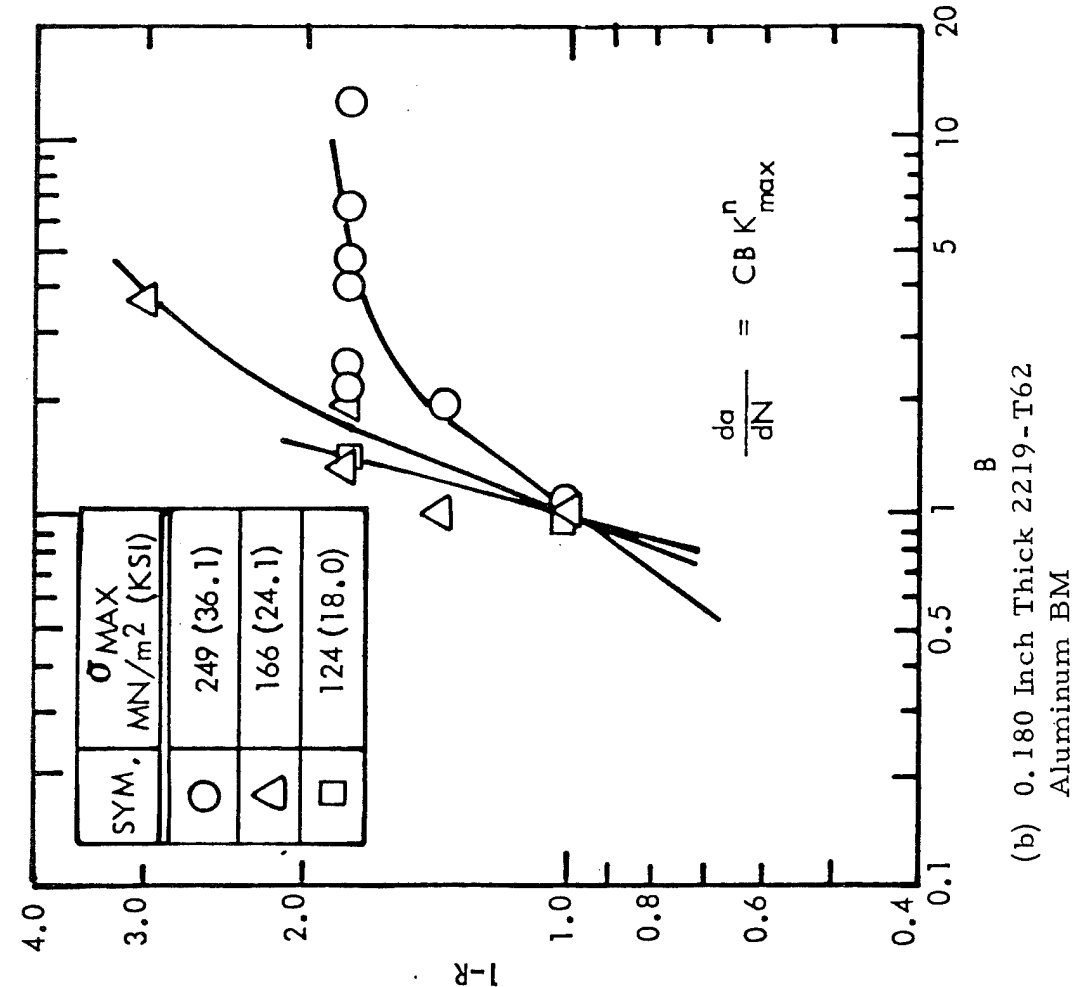


FIGURE A10: CYCLIC CRACK GROWTH RATES FOR 2.29 mm (0.090 INCH) THICK 2219-T62 ALUMINUM BM AT 295K (72°F) AND VARIOUS R RATIOS.



(a) 0.090 Inch Thick 2219-T62
Aluminum BM

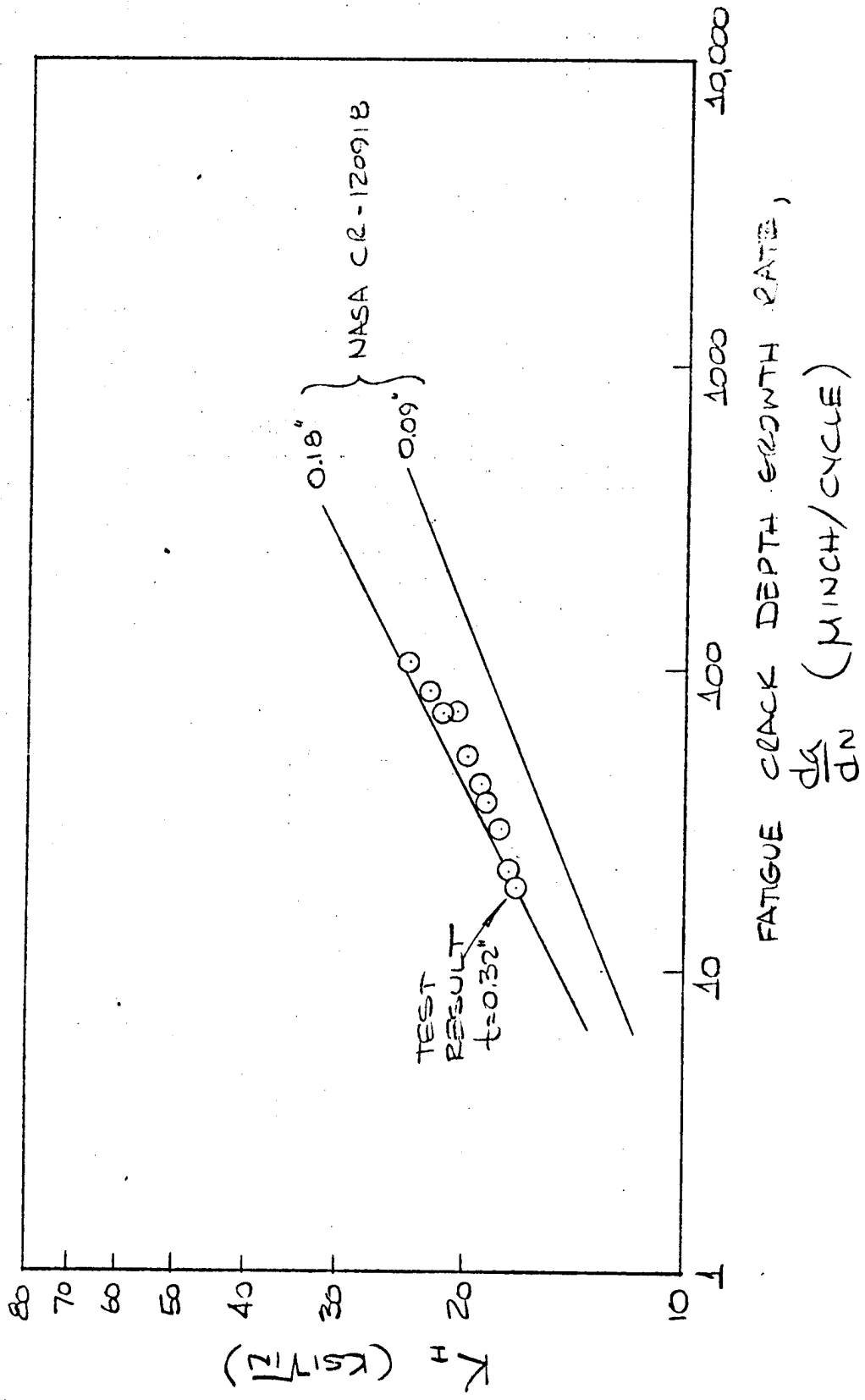


(b) 0.180 Inch Thick 2219-T62
Aluminum BM

FIGURE A11: Relative Effects of σ_{max} and R Ratio

FIGURE A 12

FATIGUE CRACK GROWTH RATES FOR 2219-T62
ALUMINUM BASE METAL AT 25 ($\alpha_{rc} \approx 0.20$)



2219-T62 Aluminum
METAL SHELL MODE
OF FAILURE
NAS 3-16770

METAL SHELL OPERATING STRESS (σ), ksi

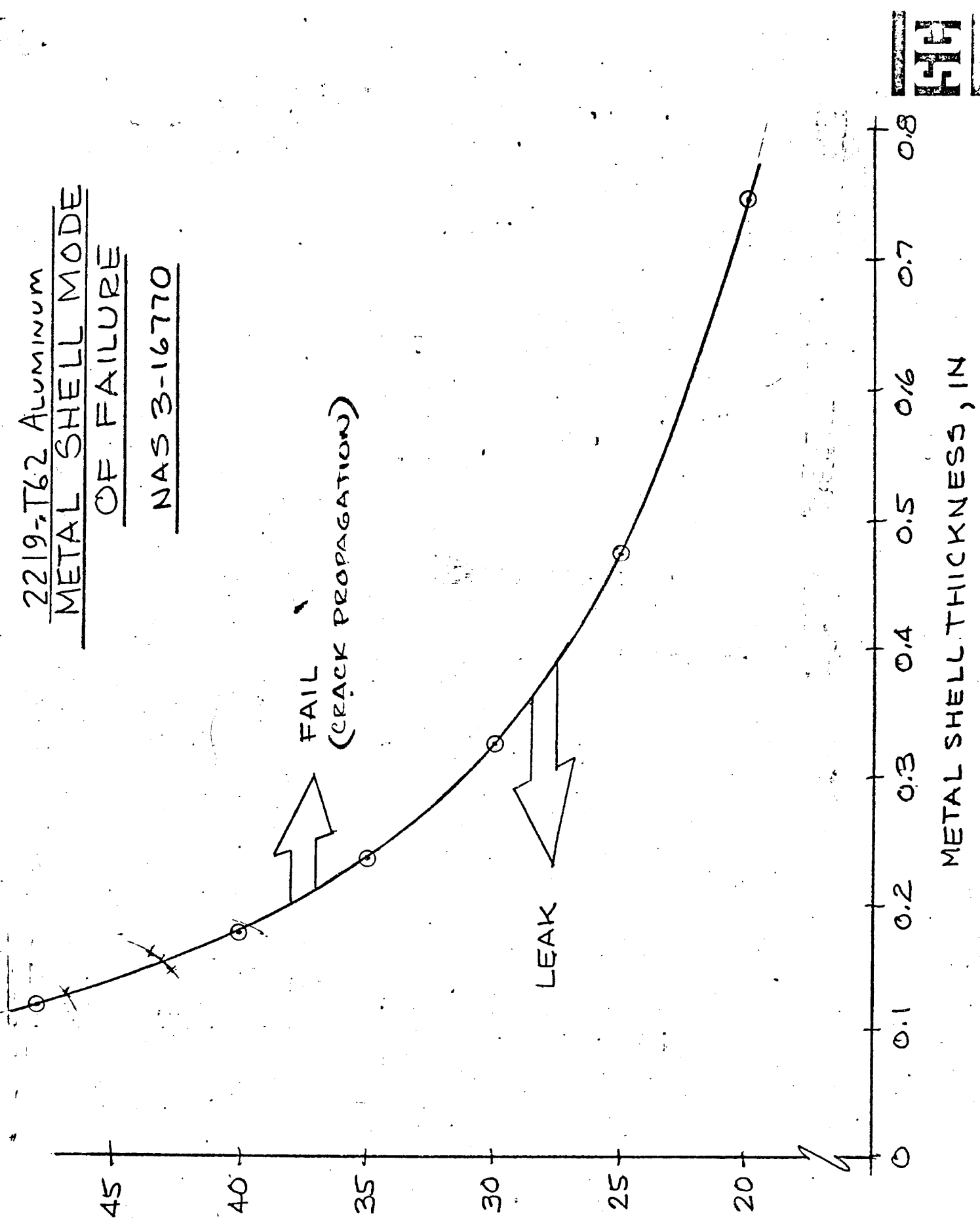


FIGURE A 13
2219 T-62 MODE OF FAILURE AS A
FUNCTION OF STRESS AND THICKNESS

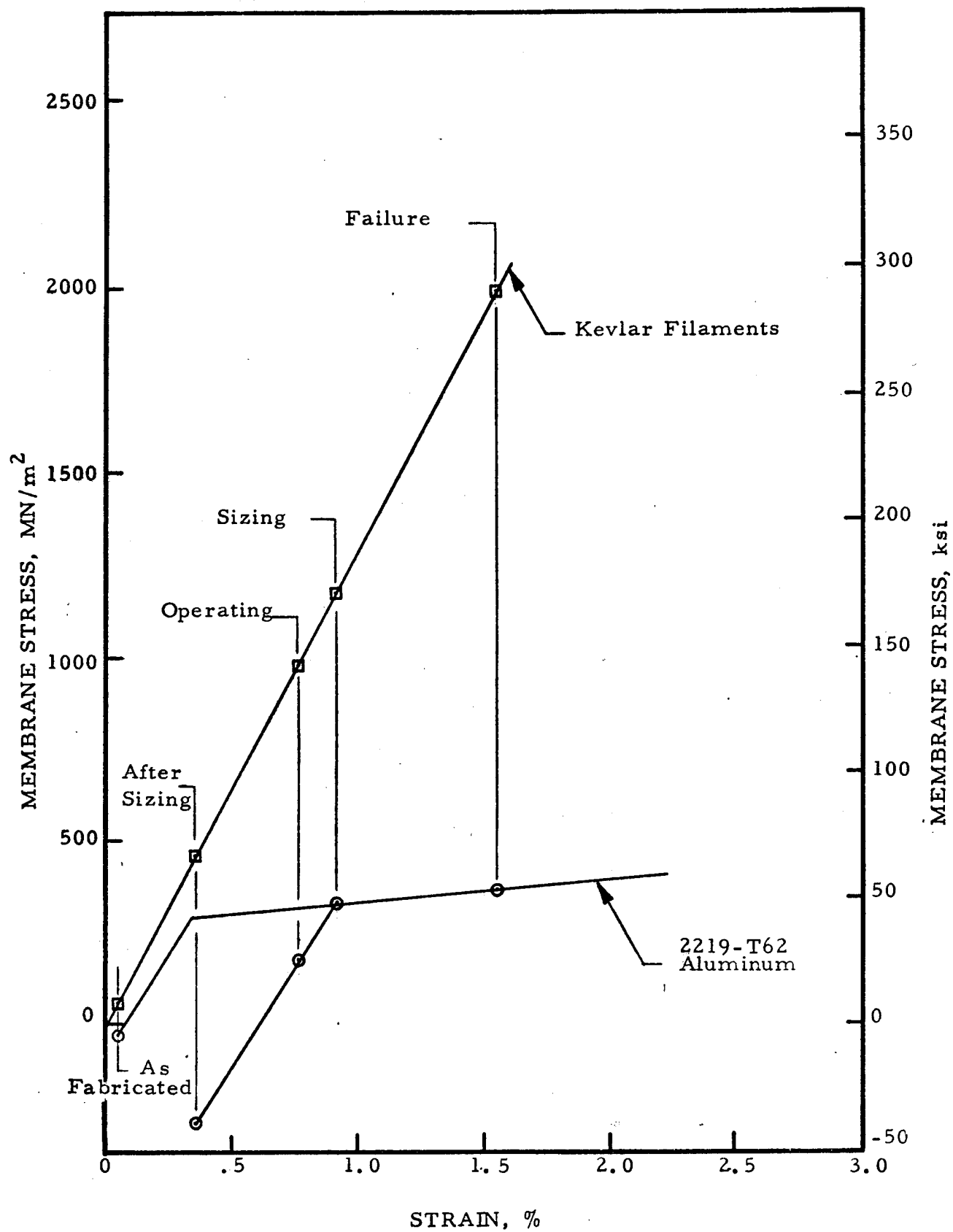


FIGURE A14: Ambient Stress/Strain Relationship
For Kevlar-49 FR 2219-T62 Aluminum Sphere

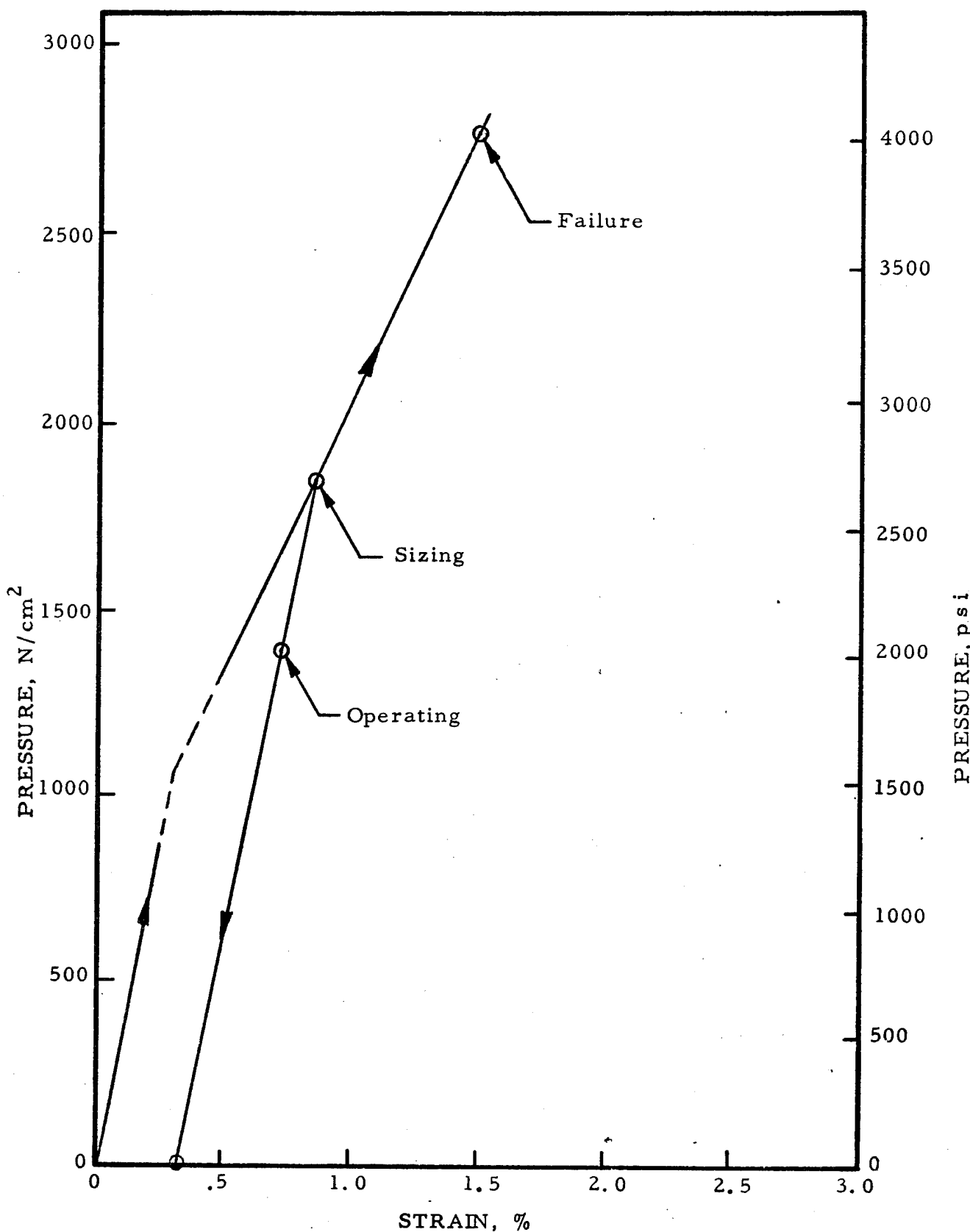


FIGURE A15: Ambient Pressure/Strain Relationship For
Kevlar-49 FR 2219-T62 Aluminum Sphere

APPENDIX B

SIZING TEST PROCEDURE*
KEVLAR FIBER REINFORCED
2219-T62 ALUMINUM SPHERES
PART NUMBER 1269382-1

SCI Specification 74-45,

March 1974

Prepared for

NASA LEWIS RESEARCH CENTER

CLEVELAND, OHIO

Prepared by

R. E. Landes

STRUCTURAL COMPOSITES INDUSTRIES, INC.

6344 North Irwindale Avenue
Azusa, California 91702

* Presentation of this procedure in S.I. Units would reduce the clarity of this Appendix. The procedure is presented in the original form as written by the author.

TABLE OF CONTENTS

	<u>Page No.</u>
1.0 SCOPE	190
2.0 REFERENCE DOCUMENTS	191
3.0 DESCRIPTION OF TEST SPECIMENS	192
4.0 TEST SPECIMEN DESIGN CONSIDERATIONS	193
5.0 GEOMETRIC DATA ACQUISITION	195
6.0 STRAIN DATA ACQUISITION	196
7.0 TEST REQUIREMENTS AND PROCEDURES	197
7.1 Test Setup	197
7.2 Test Procedure	197
7.3 Instantaneous Data Plots	198
 TABLE BI - PROBABLE VARIATION IN GEOMETRIC AND MATERIAL PROPERTIES	200
 TABLE BII - EXPECTED TEST VALUES FOR SENSOR CALIBRATION	201
 FIGURE B1 - METAL SHELL STRESS/STRAIN ENVELOPE (PRD FILAMENT MODULUS = 18.6×10^6 psi)	202
 FIGURE B2 - METAL SHELL STRESS/STRAIN ENVELOPE (PRD FILAMENT MODULUS = 20×10^6 psi)	203
 FIGURE B3 - PRESSURE/STRAIN ENVELOPE FOR PRD FR ALUMINUM SPHERE	204
 FIGURE B4 - INSTRUMENTATION LOCATIONS	205
 FIGURE B5 - HYDRAULIC TEST SYSTEM	206

TABLE OF CONTENTS
(cont.)

	<u>Page</u>
ENCLOSURE B1 TEST SPECIMEN DATA SHEETS	207
ENCLOSURE B2 EQUATIONS FOR CALCULATION OF TEST SPECIMEN GEOMETRIC DATA	212
ENCLOSURE B3 EXTENSOMETER CALIBRATION PROCEDURE	216

1.0

SCOPE

1.1

The purpose of this test procedure is to present the detailed methods and instrumentation to be used for establishing the required filament and metal prestress conditions in the spherical*PRD Fiber-Reinforced (PRD FR) 2219-T62 Aluminum pressure vessels, P/N 1269382-1.

* Kevlar-49 Roving was formerly designated as PRD-49-III Roving

2.0 REFERENCE DOCUMENTS

NOTE: Latest changes apply to all documents.

- 2.1 SCI Drawing Number 1269382-1, titled: Pressure Vessel PRD-FR 2219 Aluminum Sphere
- 2.2 SCI Drawing Number 1269381-1, titled: liner Assembly 2219-T62 Aluminum Sphere
- 2.3 SCI Drawing Number T-1400138 Revision C, titled: Test Plate
- 2.4 Design Analysis-PRD Fiber Reinforced Aluminum Sphere, SCI Special Report 7331 (Rev. A), dated January 1974
- 2.5 Fabrication Procedure for PRD FR 2219 Aluminum Sphere SCI Shop Order Number 1269382-1
- 2.6 Micr-Measurements Strain Gage Installation Procedure, Instruction Bulletin B-137, October 1970.
- 2.7 SCI Drawing Number T-1400264, titled: Tie-Rod
- 2.8 SCI Drawing SK-75-001, titled: Tie-Rod Assembly

3.0

DESCRIPTION OF TEST SPECIMENS

3.1

The six (6) test specimens are spherical 38.0-inch-diameter PRD FR 2219-T62 aluminum pressure vessels fabricated as SCI Part Number 1269382-1 and serialized as S-1 thru S-6.

4.0

TEST SPECIMEN DESIGN CONSIDERATIONS

4.1

The test specimen Design Analysis document of Paragraph 2.4 presents calculated values of stresses, strains, and pressures including the resultant stress-strain and pressure-strain relations for sizing, operating, and bursting the test specimens. The calculations are based on average values for geometric parameters and material properties.

4.1.1

Manufacturing tolerances inherent in the fabrication of the test specimens and normal variations in basic properties of the materials of construction can strongly influence the predicted test results. The probable variations in these parameters are shown in Table BI.

4.1.2

A variation between predicted values for stresses (strains) and actual stresses (strains) achieved during pressure testing could have a strong influence on the performance of the test specimen. This is especially true during the sizing test since this operation fixes the stress states between the metal shell and overwrap and the strain range available for later operation of the test specimen. Values for the most critical stress conditions which must be predictably achieved, if the specimen is to perform according to the Design Analysis, are:

(1) Metal Shell Sizing Stress (σ_s) 47.5 ksi

(2) Metal Shell Prestress
after sizing (F_c) -39.6 ksi

(3) Metal Shell Operating Stress
(σ_o) 25.1 ksi

Note: The metal shell sizing stress (Item 1) may vary slightly with negligible effects on performance.

4.2

Stress/strain and pressure/strain envelopes were prepared to indicate the probable variation in parameters which could be expected during the sizing operation.

4.2.1

The stress/strain envelopes were based on equations from the Design Analysis (Paragraph 2.4), the metal shell material property range of Table BI, and expected values for composite

4.2.1 thickness ($t_C = 0.310$) and metal shell thickness ($t_L = 0.173$). Figures B1 and B2 indicate the stress/strain envelopes based on filament modulii of 18.6×10^6 psi (minimum value) and 20.0×10^6 psi (maximum value), respectively. Included in each figure is a (canted) pressure scale for establishing the value of pressure for a given stress/strain condition.

4.2.2 Figure B3 is the expected pressure/strain envelope based on the combined stress/strain envelopes of Figures B1 and B2. Several specific pressure/strain curves corresponding to different fixed combinations of material properties have been included in the figure. The procedure for using this figure to establish the correct sizing pressure during test of a specific vessel (which fixes the desired operating strain range) is covered in Paragraph 7.0.

5.0

GEOMETRIC DATA ACQUISITION

5.1

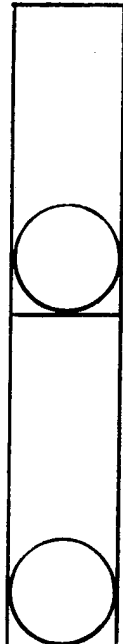
As discussed in Paragraph 4.1.1, manufacturing tolerances cause variations in test specimen geometry, not only from the expected design value, but also from unit to unit. Since geometry was **not** included as a variable in the parameter envelopes of Figures B1 through B3, expected versus actual comparative data are required for each test specimen prior to test.

5.1.1

Expected values for selected geometric parameters associated with the Liner Assembly, PN 1269381, are recorded on Data Sheet Number 1. Actual values for those parameters which can be measured shall be transferred from the Shop Order, Paragraph 2.5 to Data Sheet Number 1. The remainder of the parametric values shall be calculated using the equations of Enclosure B2 and entered on Data Sheet Number 1.

5.1.2

Expected values for selected parameters associated with the Pressure Vessel, PN 1269382, are recorded on Data Sheet Number 2. Actual values recorded on the Shop Order, Paragraph 2.5, shall be entered on Data Sheet Number 2. The remainder of the required values shall be calculated using the equations of Enclosure B2 and entered on Data Sheet Number 2.



6.0

STRAIN DATA ACQUISITION

6.1

Strain gage and extensometer output will be used to fix the location of the individual pressure/strain curve within the envelope of Figure B3 during the sizing operation performed on each test specimen. Expected test values for sensor calibration are recorded in Table BII.

6.2

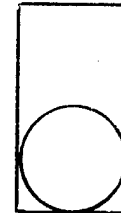
Strain Gage Rosettes

6.2.1

The strain gage selected for this application is Micro-Measurements Gage No. EA-06-250TG-350. This gage is a polyimide backed, general purpose, 2-element 90° tee rosette with a strain range of $\pm 5\%$.

6.2.2

Four strain gages shall be located on the external surface of the test specimen at the locations defined in Figure B4. The gages shall be banded with M-Bond AE-10 adhesive according to the procedure outlined in the document of Paragraph 2.6



6.3

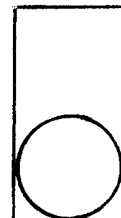
Extensometers

6.3.1

The linear displacement transducers selected for measurement of the vessel circumferential expansion were designed and fabricated by SCI. The major component is a Duncan Series 220 Slideline Control with a single linear 1 K ohm resistive element. The control has a functional mechanical travel of 2.5-inches, infinite resolution, and 3% tracking.

6.3.2

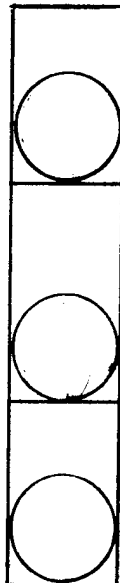
Three extensometers shall be located on the external surface of the vessel in the orientations shown in Figure B4. The extensometers shall be calibrated according to the procedure outlined in Enclosure B3.



7.0 TEST REQUIREMENTS AND PROCEDURES

7.1 Test Setup

7.1.1 "O" Rings and Backup rings shall be installed on each test plate, T-1400138, and the test plates secured to the vessel bosses. The test plates shall be coupled together with a tie-rod, T-1400264, per SK-75-001.



7.1.2 A pretest leak check of all fittings and equipment shall be performed on the pressurization system adjusted to a dead-end condition. The test specimen shall be isolated from the system during the leak test.

7.1.3 The test specimen, filled with hydraulic fluid per MIL H-5606-C and bled of all entrapped air, shall be installed in a hydraulic test system as illustrated in Figure B5.

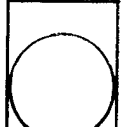
7.2 Test Procedure

7.2.1 Fluid pressure in the test specimen shall be increased to 500 psi at rate of approximately 2000 psi/min.



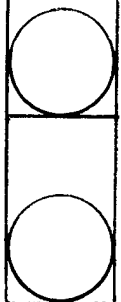
7.2.2 Pressure shall be maintained at 500 psi while strain data is observed and selected values recorded on Data Sheet Number 3.

7.2.3 Fluid pressure shall be increased to 1000 psi at a rate of approximately 2000 psi/min.



7.2.4 Pressure shall be maintained at 1000 psi while strain data is observed and selected values recorded on Data Sheet Number 3.

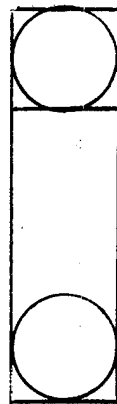
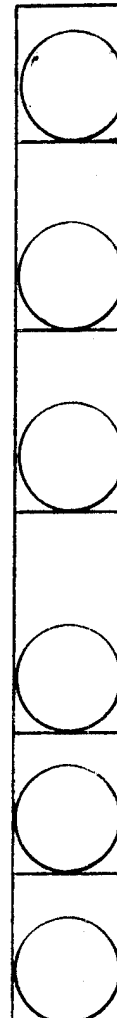
7.2.5 Fluid pressure shall be increased at a rate of 2000 psi/min to a value (approximately 1800 psi) determined by the Cognizant Project Engineer per Paragraph 7.3.4



- 7.2.6 Pressure shall be maintained at the value of Paragraph 7.2.5 while pressure and selected strain data are recorded on Data Sheet Number 3.
- 7.2.7 Fluid pressure shall be increased at a rate of 1000 psi/min to a 2nd value (approximately 2000 psi) determined by the Cognizant Project Engineer per Paragraph 7.3.4.
- 7.2.8 Pressure shall be maintained at the value of Paragraph 7.2.7 while pressure and selected strain data are recorded on Data Sheet Number 3.
- 7.2.9 Fluid pressure shall be increased at a rate of 1000 psi/min to the sizing pressure as determined by the Cognizant Project Engineer (see Paragraph 7.3), and subsequently reduced to zero at a rate of approximately 2000 psi/min.
- 7.2.10 The value for sizing pressure and any additional observations shall be recorded on Data Sheet Number 3.
- 7.2.11 Data Sheet Number 3 and all additional raw data shall be maintained on file in the Quality Control Department.

7.3 Instantaneous Data Plots

- 7.3.1 All instantaneous data plots constructed during the sizing test shall be the sole responsibility of the Cognizant Engineer or his delegate.
- 7.3.2 The two data points of Paragraphs 7.2.2 and 7.2.4 shall be recorded on Figure B3 and subsequently connected by a straight line extending above 2000 psi (approximate). This line defines the tensile biaxial elastic modulus of the test specimen and indicates the probable compressive biaxial elastic modulus.



- 7.3.3** The location of the tensile elastic curve, relative to preplotted E_f/E_L curves, shall be noted and used to define the probable location of the compressive elastic curve in the compressive (depressurization) envelope. A straight line shall be drawn on Figure B3, at the selected location within the depressurization envelope, having the same slope as the tensile elastic curve. The curve shall extend from zero pressure to approximately 3000 psi.
- 7.3.4** Establishment of the pressure hold points of Paragraphs 7.2.5 and 7.2.7 shall be based on strain data indications that (1) the test specimen has experienced metal yielding (definite change in slope of pressure/strain curve), but (2) has not approached the probable sizing strain limit point.
- 7.3.5** The two data points of Paragraphs 7.2.6 and 7.2.8 shall be recorded on Figure 3 and subsequently connected by a straight line extending between the constructed tensile and compressive elastic curves. This line defines a linear approximation of the biaxial "plastic" modulus of the test specimen. The intersection of this biaxial "plastic" modulus curve with the compressive elastic curve defines the sizing pressure. This value is required as input for the operation defined in Paragraph 7.2.9.
- 7.3.6** Figure B3 curve plots for each specific test specimen shall remain with the corresponding data package on file in the Quality Control Department.

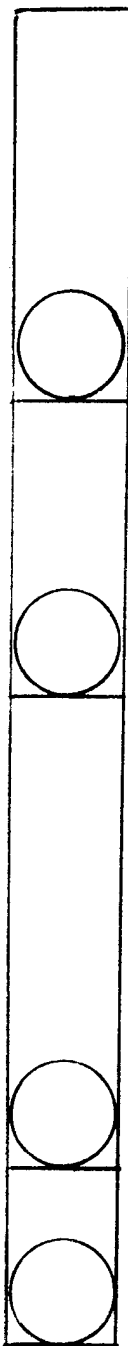


TABLE BI PROBABLE VARIATION IN GEOMETRIC AND MATERIAL PROPERTIES

Design Parameter	Range of Values		
	Minimum	Maximum	Expected
<u>PRD/Epoxy Composite Shell</u>			
Thickness (t_c), in	0.280	0.322	0.310
Filament Molulus (E_f), 10^6 psi	18.6	20.0	18.6
<u>Aluminum Shell</u>			
Thickness (t_L), in	0.154	0.214	0.173
Elastic Modulus (E_L), 10^6 psi	9.7	11.5	10.5
Plastic Modulus (E_i) 10^6 psi	0.38	0.45	0.40
Linearized Yield Stress (SYL), ksi	36.0	46.5	42.5
(1) Biaxial Elastic Modulus (E_L^1), 10^6 psi	14.4	17.0	15.6
(2) Biaxial Plastic Modulus (E_i^1), 10^6 psi	0.76	0.90	0.80

1) $E_L^1 \equiv E_L / (1 - \nu_L)$, where $\nu_L = 0.325$

2) $E_i^1 \equiv E_i / 0.5$, ν_p is assumed to be 1/2

TABLE BII EXPECTED TEST VALUES FOR SENSOR CALIBRATION

<u>Test Parameter</u>	<u>Expected Value</u>
<u>As Fabricated</u>	
Outside Diameter, in	38.11
Internal Volume, in ³	26,800
<u>At Sizing Pressure</u>	
Pressure, psi	2714
Volumetric Expansion, in ³	715
Circumferential Expansion, in	1.05
Strain, %	0.88
<u>After Sizing (zero pressure)</u>	
Outside Diameter, in	38.23
Internal Volume, in ³	27,100

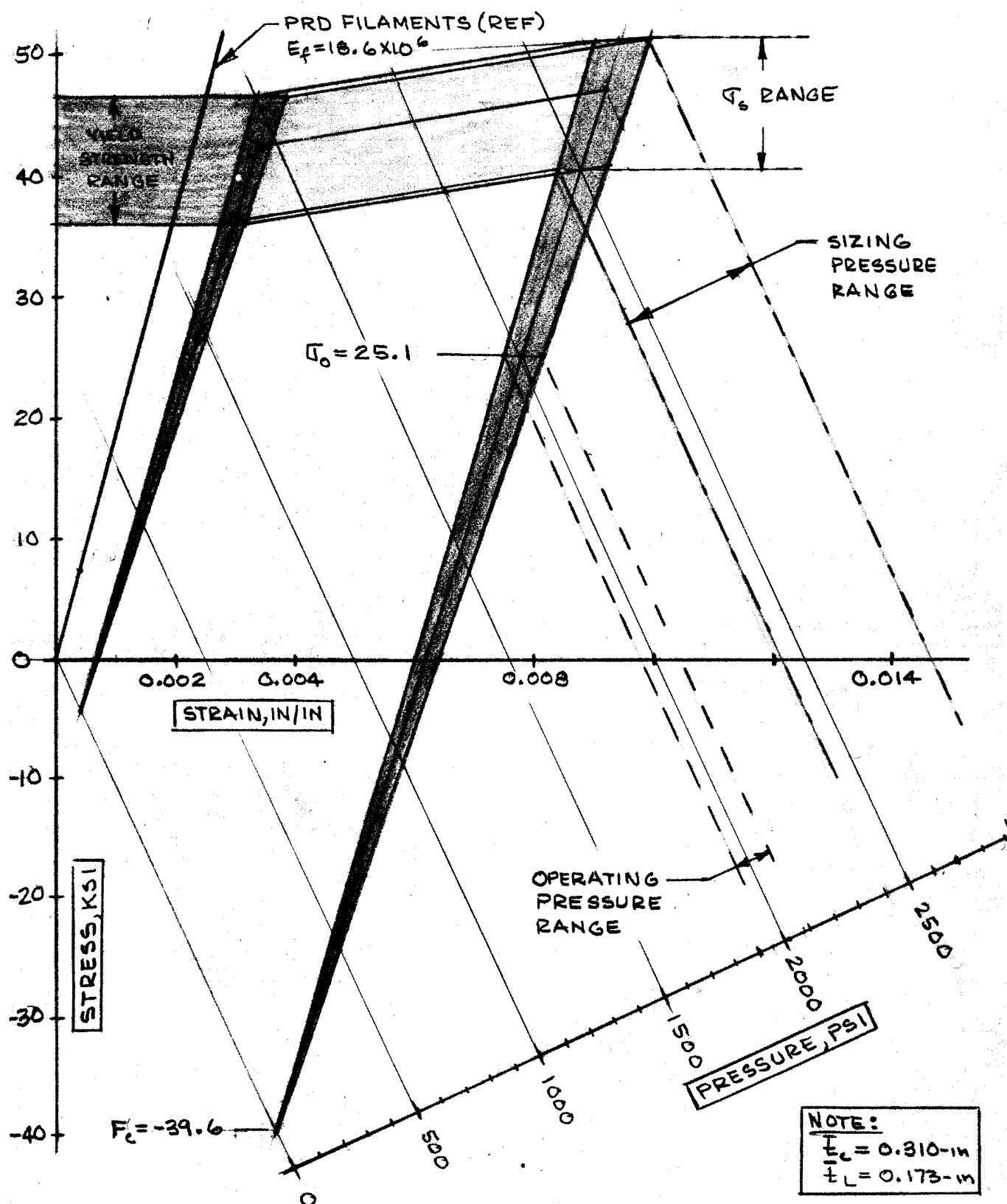


FIGURE B1 METAL SHELL STRESS/STRAIN ENVELOPE
 (PRD FILAMENT MODULUS = 18.6×10^6 psi)

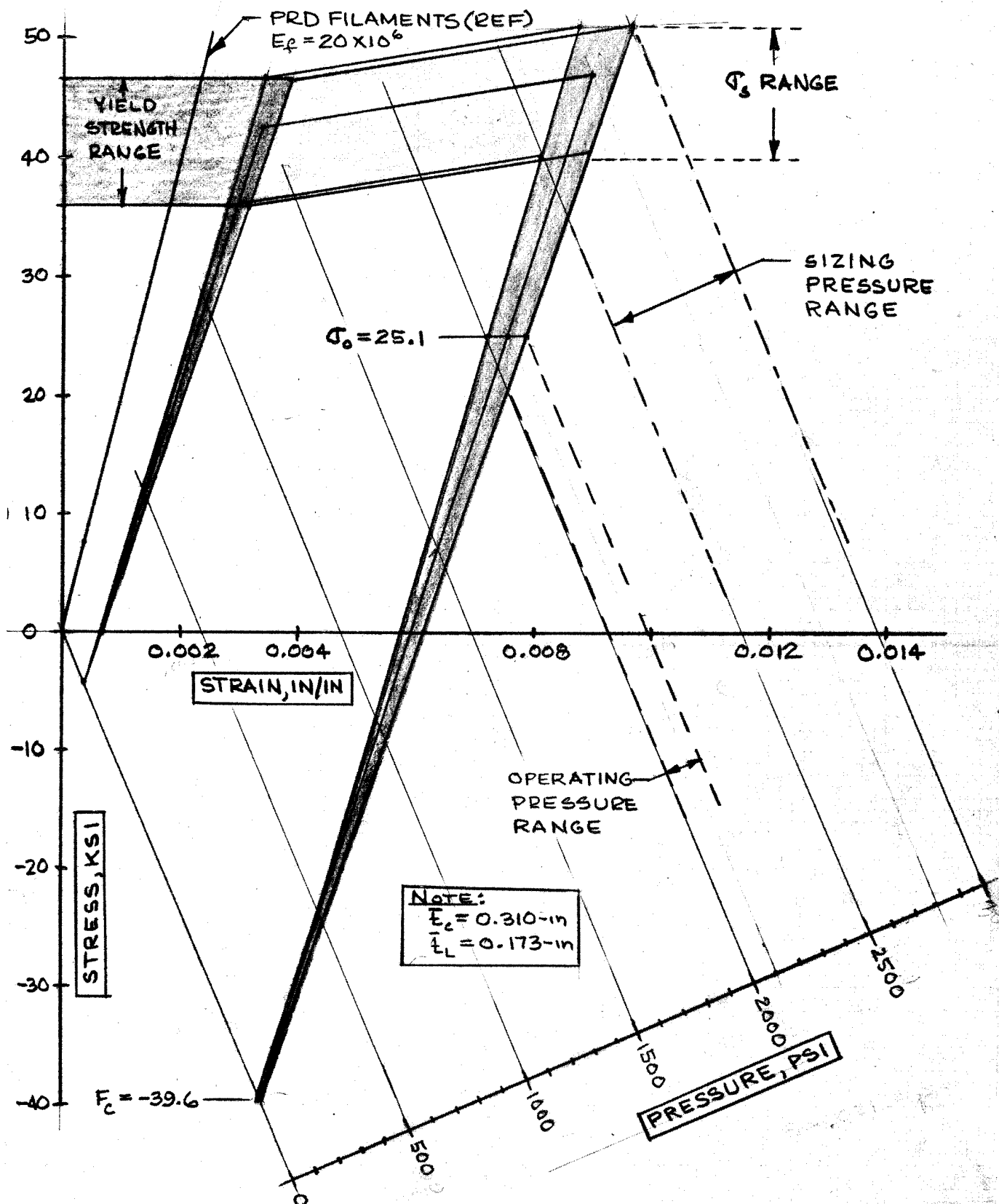
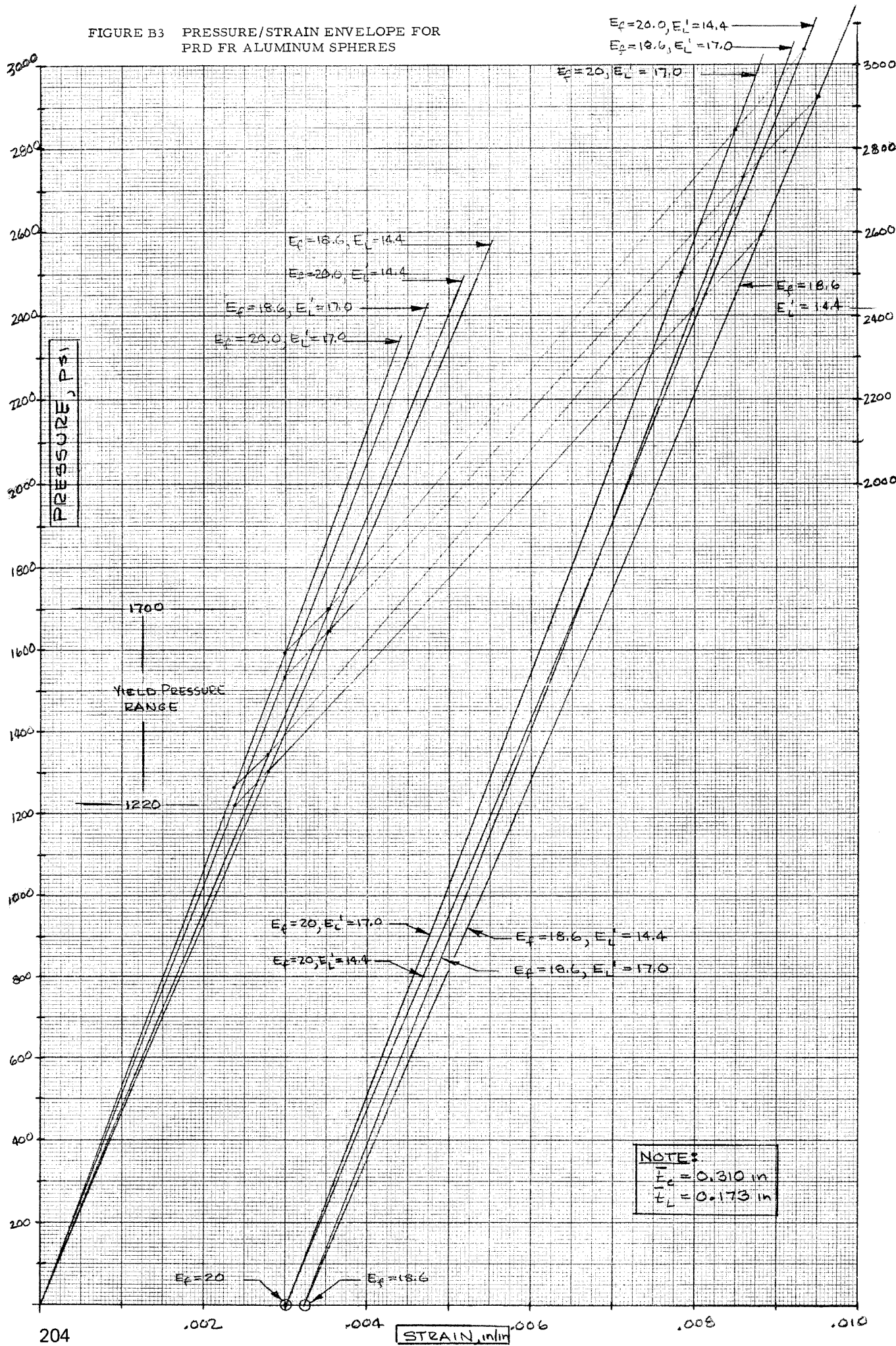


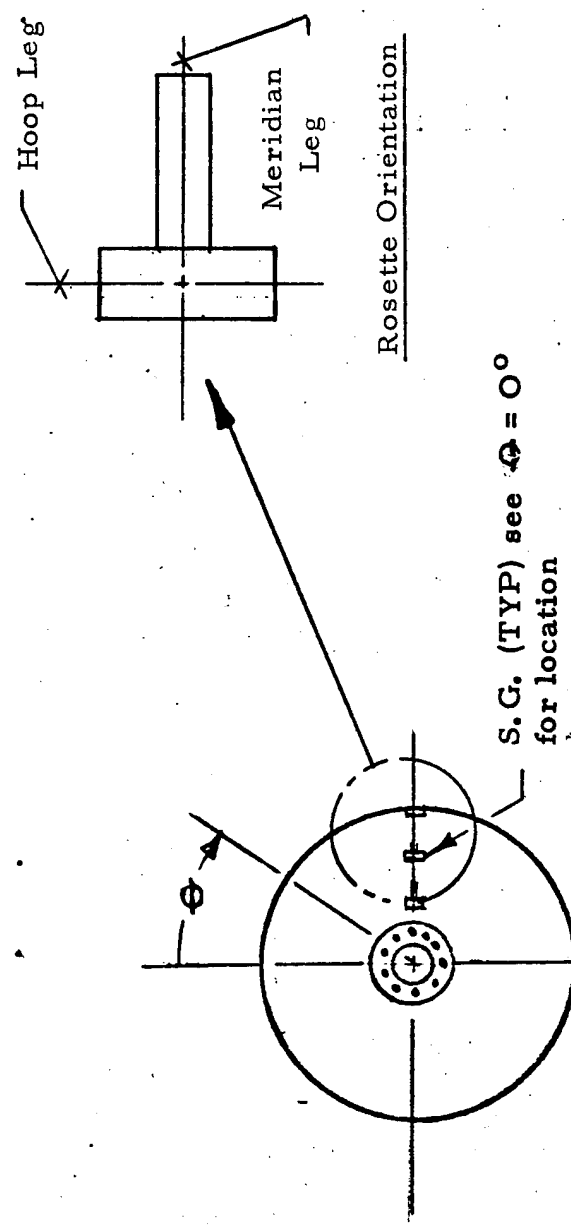
FIGURE E2- METAL SHELL STRESS/STRAIN ENVELOPE
 (PRD FILAMENT MODULUS = 20.0×10^6 psi)

FIGURE B3 PRESSURE/STRAIN ENVELOPE FOR
PRD FR ALUMINUM SPHERES



Key:

- PC-1 Pressure Transducer
- T-1 Temperature Sensor
- SG = Strain Gage Rosette
- LG = Extensometer
- α_p = Polar Location
(Adjacent to Boss)



S.G. (TYP) see $\phi = 0^\circ$
for location

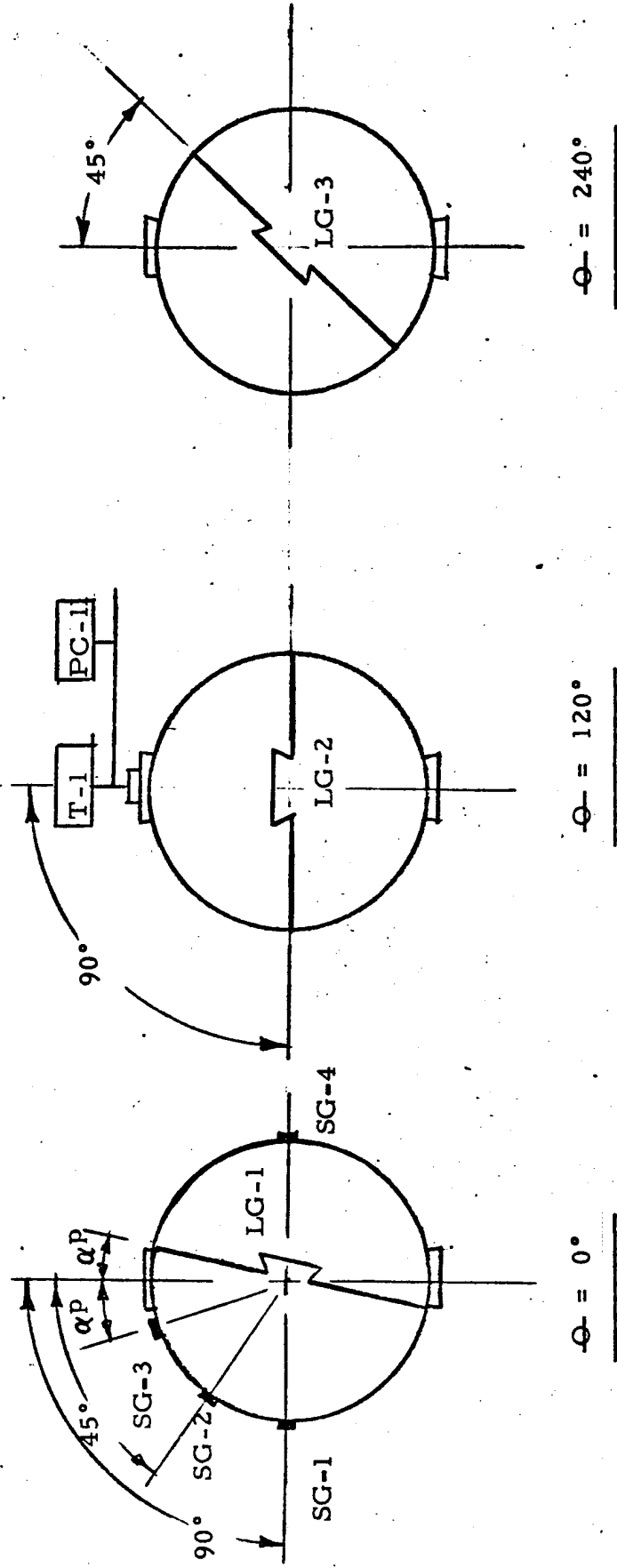
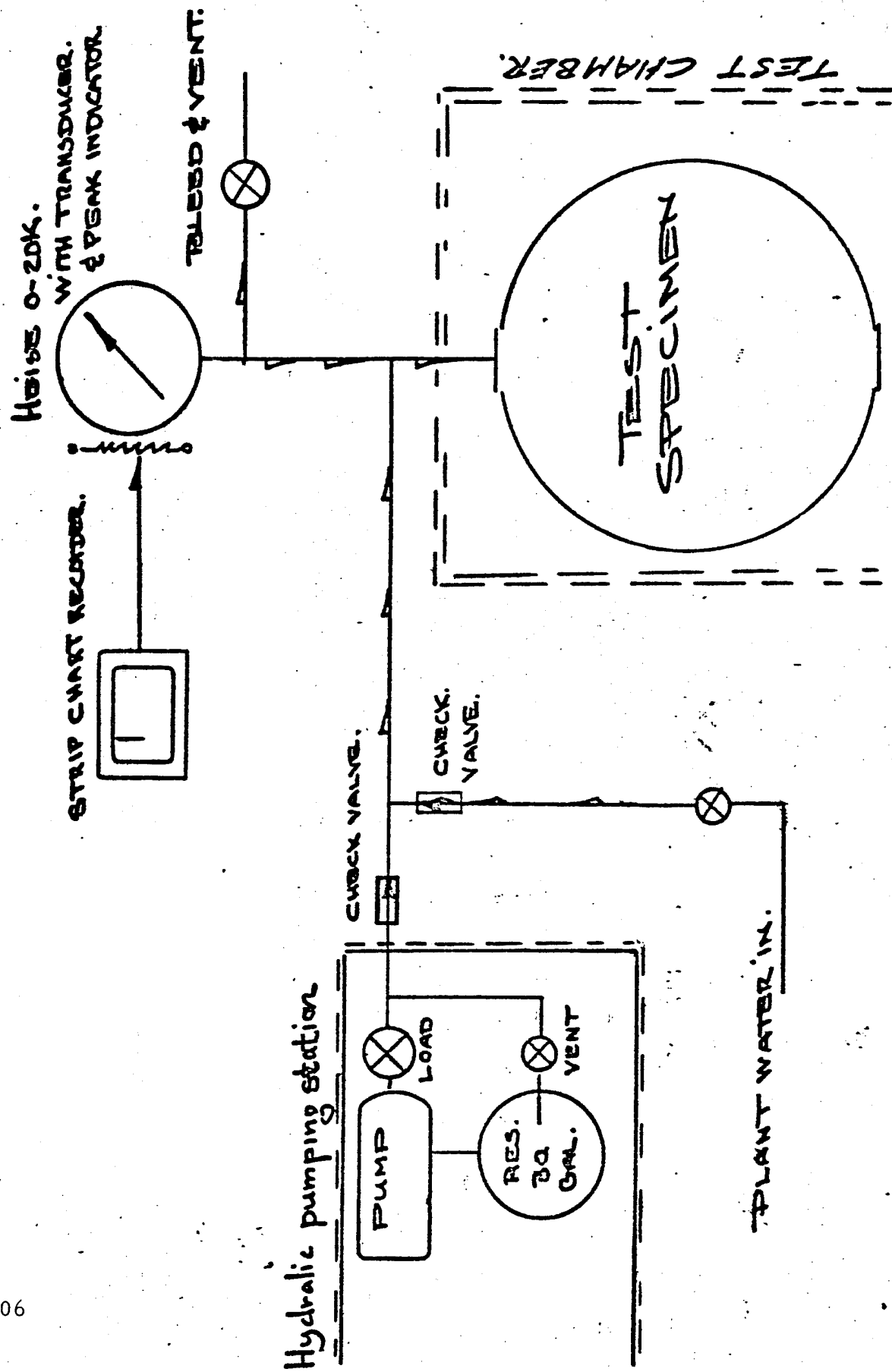


FIGURE B4: Instrumentation Location



ENCLOSURE B1

TEST SPECIMEN DATA SHEETS

DATA SHEET NUMBER 1

PART NUMBER 1269381

TEST SPECIMEN NUMBER:

LINER GEOMETRIC DATA, Paragraph 5.1.1

<u>Parameter</u>	<u>Expected</u>	<u>Actual</u>
Internal Volume (V_L)	26,850 in ³	_____ in ³
Weight (W_L)	80.2 lb	_____ lb
Inside Diameter (\bar{D}_{iL})	37.15 in	_____ in
Thickness (t_L)	0.173 in	_____ in
Outside Diameter (\bar{D}_{oL})	37.50 in	_____ in

DATA SHEET NUMBER 2

PART NUMBER 1269382

TEST SPECIMEN NUMBER:

VESSEL GEOMETRIC DATA, Paragraph 5.1.2

<u>Parameter</u>	<u>Expected</u>	<u>Actual</u>
Internal Volume (V_T)	26,830 in ³	_____ in
Vessel Weight (W_T)	148.4 lb	_____ lb
Composite Weight (W_C)	68.2 lb	_____ lb
Fiber Weight (W_f)	49.1 lb	_____ lb
Inside Diameter (D_i)	37.14 in	_____ in
Composite Thickness (t_c)	0.310 in	_____ in
Outside Diameter (D_o)	38.11 in	_____ in
Weight Fraction Resin (P_{wr})	0.28	_____
Volume Fraction Filaments (P_{vf})	0.65	_____

SCI Specification 74-45
Date: _____

DATA SHEET NUMBER 3

PART NUMBER 1269382

TEST SPECIMEN NUMBER:

VESSEL SIZING DATA, Paragraph 7.2

<u>Parameter</u>	<u>Expected</u>	<u>Actual</u>
Test Media	Inhibited Water	_____
Pressure Rise Rate	2000 psi/min	_____ psi/min
Hold Pressure	500 psi	_____ psi
Strain (SG-1)	0.0010 in/in	_____ in/in
Strain (SG-4)	0.0010 in/in	_____ in/in
Pressure Rise Rate	2000 psi/min	_____ psi/min
Hold Pressure	1000 psi	_____ psi
Strain (SG-1)	0.0020 in/in	_____ in/in
Strain (SG-4)	0.0020 in/in	_____ in/in
Pressure Rise Rate	2000 psi/min	_____ psi/min
Hold Pressure	1800 psi	_____ psi
Strain (SG-1)	0.0045 in/in	_____ in/in
Strain (SG-4)	0.0045 in/in	_____ in/in
Pressure Rise Rate	1000 psi/min	_____ psi/min
Hold Pressure	2000 psi	_____ psi
Strain (SG-1)	0.0055 in/in	_____ in/in
Strain (SG-4)	0.0055 in/in	_____ in/in
Pressure Rise Rate	1000 psi/min	_____ psi/min
Sizing Pressure	2714 psi	_____ psi

Date: _____

DATA SHEET NUMBER 3 (cont)

PART NUMBER 1269382

TEST SPECIMEN NUMBER:

Test Observations _____

Tested By _____ Date _____

Witness _____ Date _____

ENCLOSURE B2

EQUATIONS FOR

CALCULATION OF TEST SPECIMEN

GEOMETRIC DATA

Average Liner Inside Diameter (\bar{D}_{iL})

Given

Internal Volume (V_L)

Value or Source

Para 2.5

$$\bar{D}_{iL} = (6V_L / \pi)^{1/3}$$

(1)

Average Liner Thickness (\bar{t}_L)

Given

Liner Weight (W_L)

Value or Source

Para 2.5

Density Aluminum (ρ_L)

0.102 lb/in³

Boss Weight (W_B)

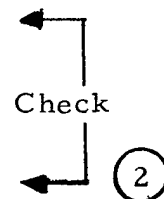
3.0 lb

$$W_S = W_L - W_B$$

$$\text{Assume: } \bar{t}_L = 0.173$$

$$\bar{D}_L = \bar{D}_{iL} + \bar{t}_L$$

$$\bar{t}_L = W_S / \pi \bar{D}_L^2 \rho_L$$



Average Liner Outside Diameter (\bar{D}_{oL})

$$\bar{D}_{oL} = \bar{D}_{iL} + 2\bar{t}_L$$

(3)

Composite Weight (W_c)

Given

Vessel Weight (W_T)

Value or Source

Para 2.5

$$W_c = W_T - W_L$$

(4)

Vessel Inside Diameter (\bar{D}_i)

Given

Vessel Internal Volume (V_T)

$$\bar{D}_i = (6V_T/\pi)^{1/3}$$

Value or Source

Para 2.5

(5)

Resin Weight Fraction (\bar{P}_{Wr})

Given

Fiber Weight (W_f)

$$\bar{P}_{Wr} = (W_c - W_f) / W_c$$

Value or Source

Para 2.5

(6)

Fiber Volume Fraction (P_{Vf})

Given

Fiber S.G. (ρ_f)

1.51

Resin S.G. (ρ_r)

1.10

Void Content (ρ_{vv})

~ 0

$$\bar{P}_{vf} = \rho_r (1 - \bar{P}_{wr}) / \left[\rho_f - (1 - \bar{P}_{wr}) (\rho_f - \rho_r) \right]$$

(7)

Average Composite Thickness (\bar{t}_c)

Given

Total Single Strand Turns ($\sum_i N_s N_T$)

Value or Source

Para 2.5

Boss Diameter

6.25 in

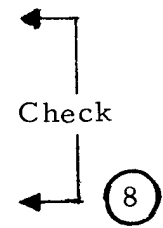
Fiber Cross Sectional Area (A_f)

$5.38 \times 10^{-4} \text{ in}^2$

$$\text{Assume: } \bar{t}_c = 0.310$$

$$\bar{D}_c = \bar{D}_i + \bar{t}_c + 2\bar{t}_L$$

$$\bar{t}_c = \bar{D}_c A_f \sum_i N_s N_T / P_{vf} (\bar{D}_c^2 - D_b^2 / 2)$$



Average Vessel Outside Diameter (\bar{D}_o)

$$\bar{D}_o = \bar{D}_i + 2\bar{t}_L + 2\bar{t}_c$$

(9)

SCI Specification 74-45
5 April 1974



STRUCTURAL COMPOSITES INDUSTRIES INC.

6344 NORTH IRWINDALE AVENUE AZUSA, CALIFORNIA 91702 (213) 334-8221

ENCLOSURE B3

EXTENSOMETER CALIBRATION PROCEDURE

CALIBRATION PROCEDURE

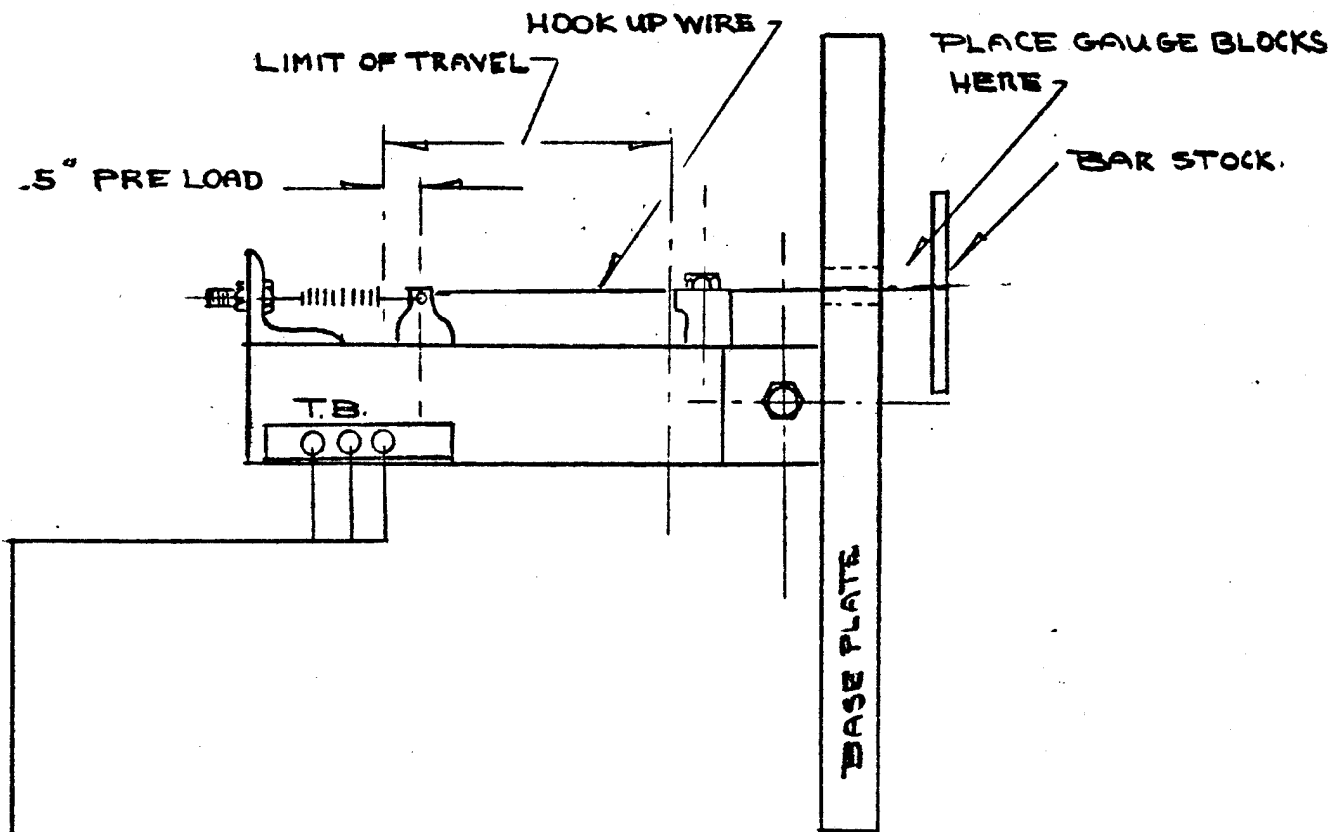
EXTENSOMETER

LINEAR DISPLACEMENT TRANSDUCER

1. Set up the extensometer and data acquisition equipment in accordance with attached figure.
2. Using gauge blocks or precision ground stock, preload an extensometer 0.5 inches relative to full mechanical stop: Record preload displacement on the attached data sheet.
3. Zero recording equipment through use of attenuator and position controls.
4. Use gauge blocks or precision ground stock to displace extensometer arm in small increments to expected circumferential expansion as noted in Test Procedure. Adjust gain and balance of recorder preamplifier for desired deflection on chart read out.

EXTENSIOMETER CALIBRATION

W.O. _____
 TEST UNIT. _____
 DATE _____



SANBORN 350-1300
 D.C. COUPLING
 PREAMPLIFIER

EIGHT CHANNEL
 SANBORN CHART RECORDER

1.5 VDC.
 P.S.

EXTENSIOMETER SN. _____

EXTENSIOMETER DISPLACEMENT	RECORDER DEFLECTION

MAX. EXPECTED DISPLACEMENT _____
 AMOUNT OF PRELOAD _____

2.5 INCH MAX.

RECORDED BY _____

APPENDIX C

**SCI SPECIFICATION 73-17 FOR
FABRICATION OF 2219-T62 ALUMINUM METAL SHELL**

REVISIONS										
REV. LTR.	DESCRIPTION	DATE	AUTHOR	DESIGN	STRESS	M & P ENG.	MFG. ENG.	QC	CUST.	DOC. REL.
None	Original Issue Work Order 2003	6-18-73								
REVISION										
SHEET										
AUTHORITY	INITIAL	DATE	ENGINEERING PROCESS SPECIFICATION							
AUTHOR	<i>ZSM</i>	6/25/73	TITLE 2219-T62 Aluminum Metal Shell, P/N 1269381 Contract NAS3-16770							
DESIGN	<i>KF</i>	6/26/73								
STRESS	<i>TK</i>	6/26/73								
M & P ENG.	<i>ZSM</i>	6/25/73								
MFG. ENG.	<i>ZSM</i>	6/25/73								
PURCH.										
Q.C.	<i>TP</i>	6/28/73								
CUST.			NUMBER SCI Specification 73-17							
DOC. REL.			SHEET 1 OF 19							

CONTENTS

	<u>Page</u>
1.0 SCOPE	5
2.0 APPLICABLE DOCUMENTS	5
3.0 FABRICATION PLAN SUMMARY	6
4.0 REQUIREMENTS	7
4.1 Materials	7
4.1.1 Component Parts	7
4.1.2 Components, Heat Treatment	7
4.1.2.1 Partial Annealing Heads	7
4.1.3 Test Coupons	7
4.1.3.1 Parent Metal	7
4.1.3.2 Weld Metal	8
4.1.3.3 Test Coupons Disposition	8
4.1.3.4 Post-Heat-Treatment Disposition of Test Coupons	9
4.2 Handling	9
4.3 Forming and Machining	9
4.4 Assembly Procedure	9
4.5 Welding Requirements	9
4.5.1 Welding Method	9
4.5.2 Weld Schedule Development and Qualification	10
4.5.3 Weld Schedule Approval	10
4.5.4 Cleaning	10
4.5.5 Weld Beads	10
4.5.6 Mismatch	11
4.6 Weld Repairs	11



STRUCTURAL COMPOSITES INDUSTRIES INC.
6344 NORTH IRWINDALE AVE.
AZUSA, CALIFORNIA 91702
P.O. BOX 904

ENGINEERING PROCESS SPECIFICATION

NUMBER	REV.	DATE	SHEET	OF
SCI Spec. 73-17		6/18/73	2	19

CONTENTS

	<u>Page</u>
4.6.1 Permitted Repair	11
4.6.2 Repair to be Authorized by SCI	11
4.6.3 Repair of Weld Defects	11
4.6.3.1 Defect Location	11
4.6.3.2 Defect Removal Procedure	11
4.6.3.3 Cleaning	11
4.6.3.4 Repair Welding	12
4.6.3.4.1 Filler Wire	12
4.6.3.4.2 Inert Gas	12
4.6.3.4.3 Inert Gas Purge for TIG Welding	12
4.6.3.5 Records	12
4.6.4 Repair of Welds on Age-Hardened Material	12
4.7 Heat Treating Operations	12
4.7.1 Solution Heat Treatment	12
4.7.2 Precipitation Heat Treatment	13
4.7.3 Additional Precipitation (Aging) Treatment	13
4.8 Identification of Shell Assembly	13
4.9 Workmanship	13
5.0 QUALITY ASSURANCE PROVISIONS	13
5.1 Suppliers Responsibility	13
5.1.1 Acceptance Criteria	13
5.1.2 Cognizant SCI Personnel	14
5.2 Dimensional Inspection	14
5.3 In-Process Acceptance Inspection	14
5.3.1 Inspection During Assembly	14



STRUCTURAL COMPOSITES INDUSTRIES INC.
6344 NORTH IRWINDALE AVE.
AZUSA, CALIFORNIA 91702
P.O. BOX 904

ENGINEERING PROCESS SPECIFICATION

NUMBER	REV.	DATE	SHEET	OF
SCI Spec. 73-17		6/18/73	3	19

CONTENTS

	<u>Page</u>
5.3.1.1 Weld Inspection	14
5.3.1.1.1 Dye-Penetrant Inspection	14
5.3.1.1.2 Radiographic Inspection	15
5.3.2 Inspection of Shell Assembly Prior to Heat Treatment	15
5.3.3 Inspection of Shell Assembly after Heat Treatment	15
5.3.3.1 Test Coupons	15
5.3.3.1.1 Basis for Rejection	15
5.4 Final Inspection	16
6.0 PREPARATION FOR DELIVERY	16
6.1 Packing	16
6.2 Log Books	16
7.0 NOTES	16
7.1 Intended Use	16

 <p>STRUCTURAL COMPOSITES INDUSTRIES INC. 6344 NORTH IRWINDALE AVE. AZUSA, CALIFORNIA 91702 P.O. BOX 904</p>	ENGINEERING PROCESS SPECIFICATION			
	NUMBER SCI Spec. 72-17	REV. 	DATE 6/18/73	SHEET 4
				OF 19

1.0 SCOP E

1.1 This specification establishes the requirements for the metal shell assembly (2219 alloy) per SCI Drawing 1269381 for a Filament Reinforced (FR) Pressure Vessel for structural test evaluation. Fabrication, inspection, and testing procedures related to fabrication are included in this specification.

2.0 APPLICABLE DOCUMENTS

2.1 Government Documents

Unless otherwise specified, the following standards, of the issue in effect on the date of invitation for bids, shall form a part of this specification to the extent specified herein:

STANDARDS

Military

MIL-STD-453 - Inspection, Radiographic

Federal

Fed. Test Method Std. No. 151, Metals; Test Methods

2.2 Other Documents

Unless otherwise specified, the following documents, of the issue in effect on the date of invitation for bids, shall form a part of this specification to the extent specified herein:

PUBLICATIONS

Military Specification

MIL-W-46132

Welding, Fusion, Electron Beam Process For

MIL-A-8920A-1

Aluminum Alloy 2219 Sheet and Plate

MIL-I-6866B

Inspection, Penetrant, Method of



STRUCTURAL COMPOSITES INDUSTRIES INC.
6344 NORTH IRWINDALE AVE.
AZUSA, CALIFORNIA 91702
P.O. BOX 904

ENGINEERING PROCESS SPECIFICATION

NUMBER	REV.	DATE	SHEET	OF
SCI Spec. 73-17		6/18/73	5	19

Aerospace Materials Specifications

AMS 4031

Aluminum Alloy 2219-0,
Sheet and Plate

AMS 4191A

Rod and Wire, Welding,
Aluminum Alloy 2319

2.3 Structural Composites Industries' Documents

Unless otherwise specified, the following drawings of the issue in effect on the date of invitation for bids, forms a part of this specification to the extent specified herein:

DRAWINGS

1269381

2219-T62 Aluminum Sphere

1269382

Kevlar FR Aluminum Pressure
Vessel

2.4 Boeing Company Documents

Unless otherwise specified, the following specifications, of the issue in effect on the date of invitation for bids, shall form a part of this specification to the extent specified herein:

SPECIFICATIONS

BAC 5602

Heat Treatment of Aluminum
Alloys

BAC 5765

Cleaning and Deoxidizing
Aluminum Alloys

BAC 5915

Radiographic Inspection

BAC 5935

Fusion Welding of Aluminum

2.5 This specification establishes the specific requirements for all work to be performed during 2219-T62 Aluminum Sphere assembly manufacturing. Where instances occur of differences in requirements between this specification and the applicable documents listed herein, this specification will be considered the guiding authority, superceding such requirements of the listed sources.

3.0 FABRICATION PLAN SUMMARY

Figure C1 depicts the fabrication plan for the 2219-T62 Aluminum Alloy Sphere Assembly. Specific requirements are delineated in Sections 4.0, 5.0, and 6.0.



STRUCTURAL COMPOSITES INDUSTRIES INC.
6344 NORTH IRWINDALE AVE.
AZUSA, CALIFORNIA 91702
P.O. BOX 904

ENGINEERING PROCESS SPECIFICATION

NUMBER	REV.	DATE	SHEET	OF
SCI Spec. 73-17		6/18/73	6	19

4.0 REQUIREMENTS

4.1 Materials

Fabrication of the metal shell assembly shall be governed by the following requirements:

4.1.1 Component Parts

Components of the assembly consist of two hemispheres with integral boss configuration, initially machined, then deep drawn from aluminum alloy 2219, condition O, plate stock conforming to Specification AMS 4031. This material shall be furnished by the government, and upon receipt shall be visually, and dimensionally inspected for compliance with AMS 4031. All surface defects which will be eliminated by subsequent processing shall be noted as such and shall not be cause for rejection. Formed hemispheres shall be final machined prior to welding into a serialized part number. Care shall be exercised to insure that the serial number shall not become disassociated from the part at any stage of shell assembly. Written records identifying these serial numbers with the shell assembly shall be maintained and delivered to SCI with the shell assembly and test coupons.

4.1.2 Components, Heat Treatment

4.1.2.1 Partial Annealing Heads

To remove cold work incident to forming, head assemblies shall be charged into an oven preheated to 650°F, held at temperature for sixty minutes and air cooled in accordance with Boeing Specification BAC 5602.

4.1.3 Test Coupons

4.1.3.1 Parent Metal

Tensile Test Coupon blanks shall be cut longitudinal to the direction of rolling from each heat of the Mill stock from which head sections are made. Specimen configurations and disposition shall be as follows:



STRUCTURAL COMPOSITES INDUSTRIES INC.
6344 NORTH IRWINDALE AVE.
AZUSA, CALIFORNIA 91702
P.O. BOX 904

ENGINEERING PROCESS SPECIFICATION

NUMBER	REV.	DATE	SHEET	OF
SCI Spec. 73-17		6/18/73	7	19

<u>Number of Specimens</u>	<u>Configuration</u>	<u>Disposition</u>	<u>Identification</u>
Four initial samples from plate stock.	Fed. Test Method Std. No. 151, Method 211.1, F2 Specimen	Deliver to SCI at time of initial fabrication work.	Serialize by metal stamping one end of specimen.
Four witness samples for each sphere assembly.	(As above)	Heat treat with respective sphere assembly, deliver to SCI.	Serialize with respect to each metal shell assembly by metal stamping on one end of specimen; maintain records relating serial numbers to each assembly.

4.1.3.2 Weld Metal

Weld tensile test coupons shall be obtained during the weld schedule development effort detailed under 4.5.2, with disposition as follows:

<u>Number of Specimens</u>	<u>Configuration</u>	<u>Disposition</u>	<u>Identification</u>
Four initial specimens from EB welding of simulated joint from flat stock.	Fed. Test Method Std. No. 151, Method 211.1, F2 Specimen	Deliver to SCI for verification testing early in weld development effort.	Serialized by metal stamping one end of specimen.
Four specimens Per Figure C2 from full scale girth weld simulation joint.		Deliver to SCI for verification testing as soon as completed.	Serialized by metal stamping one end of specimen.
Four witness samples for each sphere assembly.	As above	Heat treat with respective sphere assembly, deliver to SCI.	Serialize with respect to each metal shell assembly by metal stamping on one end of specimen; maintain records relating serial numbers to each assembly.

4.1.3.3 Test-Coupons Disposition

When shell assemblies are ready for the final heat-treatment operation per 4.7, the four each parent metal and weld witness coupons of paragraphs 4.1.3.1 and 4.1.3.2 shall accompany each shell assembly through the entire heat-treating operation.



STRUCTURAL COMPOSITES INDUSTRIES INC.
6344 NORTH IRWINDALE AVE.
AZUSA, CALIFORNIA 91702
P.O. BOX 904

ENGINEERING PROCESS SPECIFICATION

NUMBER	REV.	DATE	SHEET	OF
SCI Spec. 73-17		6/18/73	8	19

4.1.3.4 Post-Heat-Treat Disposition of Test Coupons

Upon completion of the heat-treatment operation, the test coupons shall remain with the shell assembly they represent and accompany it on its delivery to Structural Composites Industries. When tensile specimens are machined from the coupons and tested in accordance with Fed. Test Method Std. No. 151, the results of the tests for both parent metal and weld specimens shall comply with the following values:

	<u>Parent Metal</u>	<u>Weld (94% Efficiency)</u>
Ultimate Tensile Strength, psi	54,000 min	51,000 min
Yield Strength (0.2% offset), psi	36,000 min	34,000 min
Elongation in 2-inch, %	7 min	6 min

4.2 Handling

All handling of the shell assembly or its components in the uncrated condition shall be performed using maximum care because of the susceptibility of the material to damage during all stages of fabrication. Components shall be kept in suitable protective containers except when they are being worked.

4.3 Forming and Machining

During forming process development, dimensions shall be recorded for blank starting parameters (such as thickness profiles) and formed shell parameters. These data shall be used as a control of starting blank dimensions used for deliverable hardware. Prior to forming blanks to make deliverable half-shells, dimensions of blanks shall be submitted to SCI for comparison with forming development program data. Machining of the shell-assembly components shall conform to the requirements of the SCI Drawings referenced in 2.3. After final machining, solvent cleaning shall be employed to insure complete freedom from machining residue, shavings and cuttings. Cutting tools shall be maintained at proper sharpness to prevent burnishing of the metal surface.

4.4 Assembly Procedures

The shell shall be assembled in accordance with SCI Drawing 1269381.

4.5 Welding Requirements

4.5.1 Welding Method

Welding of girth welds shall be electron beam fusion welding per MIL-W-46132.



STRUCTURAL COMPOSITES INDUSTRIES INC.
6344 NORTH IRWINDALE AVE.
AZUSA, CALIFORNIA 91702
P.O. BOX 904

ENGINEERING PROCESS SPECIFICATION

NUMBER	REV.	DATE	SHEET OF
SCI Spec. 73-17		6/18/73	9 19

4.5.2 Weld Schedule Development and Qualification

Welders, welding equipment, and procedures shall be demonstrated to be satisfactory by means of test coupons from weld blanks similar to the configurations of the joint to be welded. SCI acceptance of representative girth weld schedules developed by the weld source shall constitute acceptance of electron beam welding operators qualification and certification.

In addition to welding simulated joints from flat stock, for girth weld schedule development two hemispheres with an excess prolongation of material at the diameter of the girth weld shall be prepared for welding as a typical metal shell girth weld and welded per the established schedule for the specific configuration. The specific electron beam welding parameters of established weld schedule and tolerances shall be documented in writing and submitted to SCI Quality Control. SCI project engineering shall witness the girth weld demonstration(supplier to provide notification to SCI) and the weld shall be inspected per 5.3.1 and accepted by SCI Quality Control. Following inspection and acceptance, the weld shall be removed as a ring, salvaging the respective hemisphere shells for remachining to the applicable drawing and use as deliverable components of an assembly.

The removed ring shall be used to prepare transverse weld coupons required under 4.1.3.2; four specimens will be heat treated and tested as specified in 4.1.3.2 and 4.1.3.4 to verify compliance with requirements.

Acceptance by SCI of the welding schedule development and qualification task of 4.5.2 shall be in writing and shall be considered appropriate evidence of operator certification and equipment qualification for performing the related work of this specification.

4.5.3 Weld Schedule Approval

The weld schedule development task of 4.5.2 shall be completed and accepted by SCI Quality Control in writing prior to any welding on deliverable parts. All welding on deliverable hardware shall be in accordance with the documented established weld schedule of 4.5.2.

4.5.4 Cleaning

Cleaning shall be in accordance with BAC 5765 and MIL-W-46132. The use of dust or sand blasting is prohibited.

4.5.5 Weld Beads

Weld bead thickness shall be uniform and shall not exceed the height indicated on SCI Drawing 1269381. Severe sharpness in the weld contour, such as may contribute to a "notch" effect, shall be removed insofar as is possible, provided there is no filing into the parent metal. Other weld surface discontinuities shall be dressed as required to provide smooth blending with the adjacent parent metal surfaces.



STRUCTURAL COMPOSITES INDUSTRIES INC.
6344 NORTH IRWINDALE AVE.
AZUSA, CALIFORNIA 91702
P.O. BOX 904

ENGINEERING PROCESS SPECIFICATION

NUMBER	REV.	DATE	SHEET	OF
SCI Spec. 73-17		6/18/73	10	19

4.5.6 Mismatch

Mismatch in the weld joints shall not exceed that shown on SCI Drawing 1269381.

4.6 Weld Repairs

Weld repairs shall be performed in accordance with the following requirements.

4.6.1 Permitted Repair

Repair of an electron beam weld may be performed where practicable, using the same weld schedule originally developed for the respective weld. This repair procedure involves no removal and replacement of weld material, only a subsequent fusion of material in place.

4.6.2 Repair to be Authorized by SCI

Weld corrective effort considered impracticable to be performed under 4.6.1 above, or unsuccessful after attempt per 4.6.1 above, may be repaired, subject to approval by SCI in writing of the specific repair procedure, after consideration of the nature and location of the defect and the specific procedure proposed to correct the defect.

4.6.3 Repair of Weld Defects-Procedure

The following repair procedure shall be performed.

4.6.3.1 Defect Location

Locate defect areas from the radiographic film or dye-penetrant inspection.

4.6.3.2 Defect Removal Procedure

If there is no surface indication of the defect, remove the weld bead in progressive stages of 1/32 inch in depth. Dye penetrant inspect the weld after each stage of metal removal. Proceed in this manner until the defect itself has been located and removed.

4.6.3.3 Cleaning

Prior to repair welding, the groove and areas around and on both sides of the groove shall be cleaned by flushing with clean, uncontaminated isopropyl alcohol; any substitute shall be subject to approval by SCI. This operation shall be followed by thorough brushing with a clean austenitic stainless steel wire brush. Do not wipe the cleaned area with cloth or similar material.



STRUCTURAL COMPOSITES INDUSTRIES INC.
6344 NORTH IRWINDALE AVE.
AZUSA, CALIFORNIA 91702
P.O. BOX 904

ENGINEERING PROCESS SPECIFICATION

NUMBER	REV.	DATE	SHEET	OF
SCI Spec. 73-17		6/18/73	11	19

4.6.3.4 Repair Welding

Weld per Boeing Specification BAC 5935 by manual tungsten inert gas welding process using Type 2319 weld filler rod.

4.6.3.4.1 Filler Wire

As required, filler wire shall be Aluminum Alloy 2319 in accordance with Specification AMS 4191A.

4.6.3.4.2 Inert Gas

All TIG welding operations shall be performed with inert gas backup. Inert gas used shall be argon.

4.6.3.4.3 Inert Gas Purge for TIG Welding

Prior to TIG welding the root side of the weld shall be purged for a minimum period of three (3) minutes to insure the exclusion of ambient air. During welding the gas flow rate shall be maintained at 3 to 5 cubic feet per hour. If the gas flow is interrupted during welding, the welding operation shall be discontinued. The root side of the weld shall be repurged prior to resuming the welding operation.

4.6.3.5 Records

Records shall be maintained by the supplier and included in the log for each metal shell assembly. Such records shall indicate location, nature, repair conducted, number of repairs conducted, and inspection results.

4.6.4 Repair of Welds on Age-Hardened Material

Weld repairs shall not be permitted on articles which have undergone solution heat treatment and/or aging.

4.7 Heat Treatment Operations

The welded shell assembly shall be solutionheat treated and aged in accordance with Boeing Specification BAC 5602 and the following procedure:

4.7.1 Solution Heat Treatment

Charge the shell assembly into a furnace or salt bath previously heated to 995°F and soak the shell assembly at a temperature of 985 - 1005°F for a period of four (4) hours. Quench in water as required by Boeing Specification BAC 5602.

 STRUCTURAL COMPOSITES INDUSTRIES INC. 6344 NORTH IRWINDALE AVE. AZUSA, CALIFORNIA 91702 P.O. BOX 904	ENGINEERING PROCESS SPECIFICATION				
	NUMBER SCI Spec. 73-17	REV.	DATE 6/18/73	SHEET 12	OF 19

4.7.2 Precipitation Treatment

Hold shell assembly at room temperature for 96 hours to obtain condition - T42.

4.7.3 Additional Precipitation (Aging) Treatment

Charge the shell assembly into a furnace previously heated to 375°F and soak the shell assembly at a temperature of 365 - 385°F for a period of 36 hours to obtain condition - T62.

4.8 Identification of Component Parts and Shell Assembly

The shell assembly shall be assigned serial numbers S1, S2, S3, etc., which shall be marked by vibratory pencil on the external side of the boss neck as indicated on the SCI Drawings. The serial number shall relate to the supplier's fabrication, heat treatment, and inspection records which shall be incorporated into a log book accompanying each assembly upon delivery to SCI.

Non-permanent marking on the parts and assemblies, such as part number, serial number, weld identification, and in-process serialization shall be made on suitable areas using felt marking pen, waterproof type, or equivalent.

4.9 Workmanship

The shell assembly, including all component parts, shall be fabricated, heat-treated, finished, and tested in a thoroughly workmanlike manner. Particular attention shall be given to neatness and thoroughness in the forming and welding of the component parts.

5.0 QUALITY ASSURANCE PROVISIONS

5.1 Supplier's Responsibility

The supplier shall be responsible for the fabrication, heat treatment, and inspection of the shell assembly in accordance with all of the requirements, reference documents, and procedures of this specification. No deviation from fabrication, heat treatment, inspection and testing requirements, and procedures of this specification shall be allowed except in the form of an amendment to this specification or to the purchase order. Test data, letters of conformance, and other pertinent information affecting shell fabrication shall be forwarded without delay to the cognizant Structural Composites project engineer and Structural Composites inspection department.

5.1.1 Acceptance Criteria

Acceptance of the shell assembly shall be based upon compliance with the requirements herein as verified by a series of in-process acceptance



STRUCTURAL COMPOSITES INDUSTRIES INC.
6344 NORTH IRWINDALE AVE.
AZUSA, CALIFORNIA 91702
P.O. BOX 904

ENGINEERING PROCESS SPECIFICATION

NUMBER	REV.	DATE	SHEET	OF
SCI Spec. 73-17		6/18/73	13	19

tests (see 5.3) and final inspection (see 5.4) of the finished product. Detailed inspection records shall be maintained to insure that all requirements of this specification have been met.

5.1.2 Cognizant SCI Personnel

As required, Structural Composites Industries, Inc., personnel, such as the project engineer, welding engineer, metallurgical engineer, stress engineer, inspector, etc., shall be permitted to observe those phases of work at their discretion.

5.2 Dimensional Inspection

Maintaining dimensional and other requirements of the components and assemblies, as required by SCI Drawing 1269381 is of prime importance and will be thoroughly inspected by SCI Quality Control upon receipt of the units. Dimensional inspections shall be conducted during fabrication of the components and assemblies to insure meeting the SCI Drawing requirements, and submitted with each shell assembly in its log book. The supplier shall submit to SCI Quality Control his in-process and final assembly dimensional inspection plan and standard forms for recording these data for approval before initiating metal shell assembly operations.

5.3 In-Process Acceptance Inspection

All requirements of this specification shall be assured through inspection. Inspection tests shall be performed in accordance with the requirements specified herein.

5.3.1 Inspection During Assembly

5.3.1.1 Weld Inspection

All joints shall be visually inspected for compliance with the requirements of 4.5 and the applicable drawings, and shall be inspected in accordance with the following:

5.3.1.1.1 Dye-Penetrant Inspection

Dye-penetrant inspection in accordance with MIL-I-6866, Type II, Method A shall be performed on all welds. After inspection, welds shall be cleaned thoroughly, and the welded surface and adjacent area brushed with a stainless steel wire brush. The welds and heat-affected zones shall be free of external cracks or propagating defects.

 STRUCTURAL COMPOSITES INDUSTRIES INC. 6344 NORTH IRWINDALE AVE. AZUSA, CALIFORNIA 91702 P.O. BOX 904	ENGINEERING PROCESS SPECIFICATION			
	NUMBER SCI Spec. 73-17	REV.	DATE 6/18/73	SHEET 14 OF 19

5.3.1.1.2 Radiographic Inspection

Radiographic inspection shall be performed on all welds in accordance with Boeing Specification BAC 5915. Radiographs shall be subject to final interpretation and acceptance by designated SCI quality control and project representatives. Radiographic film shall be numbered to coincide with the identification markings of the shell assembly. Felt-tip-ink pen shall be used for marking weld identifications on parts so that the exact location of weld areas with corresponding radiographs may be easily identified. All radiographic film shall become the property of SCI. All welds shall meet the requirements of Boeing Specification 5935, Class A, Tables XI and XII, with the following additional acceptance criteria:

- a. Porosity smaller than .005 inches diameter shall be considered fine porosity and not be considered a defect.
- b. Aligned fine porosity shall be subject for acceptance per Note 8 of Table XI and/or Table XII of BAC 5935 and shall not be considered as aligned defects under Note 7 of Table XI.
- c. Aligned defects (4 or more) shall not be accepted when the spacing between each of the four or more defects in line is less than three times the longest distance of the smallest defect.

5.3.2 Inspection of Shell Assembly Prior to Heat Treatment

The shell assembly shall be free of oil, grease, paper, or any type of carbonaceous material prior to heat treatment.

5.3.3 Inspection of Shell Assembly After Heat Treatment

5.3.3.1 Test Coupons

After heat treatment of the shell assembly, the test coupons may be tested by Structural Composites Industries, Inc., to verify compliance with 4.1.3.4.

5.3.3.1.1 Basis for Rejection

Failure to meet the tensile-test requirements of 4.1.3.4 shall be the basis for rejection.



STRUCTURAL COMPOSITES INDUSTRIES INC.
6344 NORTH IRWINDALE AVE.
AZUSA, CALIFORNIA 91702
P.O. BOX 904

ENGINEERING PROCESS SPECIFICATION

NUMBER	REV.	DATE	SHEET	OF
SCI Spec. 73-17		6/18/73	15	19

5.4 Final Inspection

The completed shell assembly shall be subjected to surface inspection, with visual examination for imperfections and finish. Fissures or other defects that are likely to weaken strength or reduce ductility of the pressure vessel are not permitted and shall be cause for rejection. The parent metal macrostructure shall exhibit uniform grain flow and uniformly fine-grain size as revealed by lightly macroetching locations on the finished vessel subjected to the most severe deformation and temperature during fabrication. The surface shall be such that the removal of scratches or other surface imperfections shall not reduce the thickness of the metal below the minimum specified on the drawing. A reasonably smooth and uniform surface finish is required. Inspection of workmanship shall conform to 4.9. Measurements of dimensions (with attention to SCI drawing tolerances) shall be included in this inspection.

6.0 PREPARATION FOR DELIVERY

6.1 Packing

The shell assembly shall be crated and firmly supported to avoid damage during shipping.

6.2 Log Book

A log book shall be assembled incorporating all in-process fabrication and inspection data required by this specification, as well as other pertinent information as may be required or desirable to fully document each deliverable part.

7.0 NOTES

7.1 Intended Use

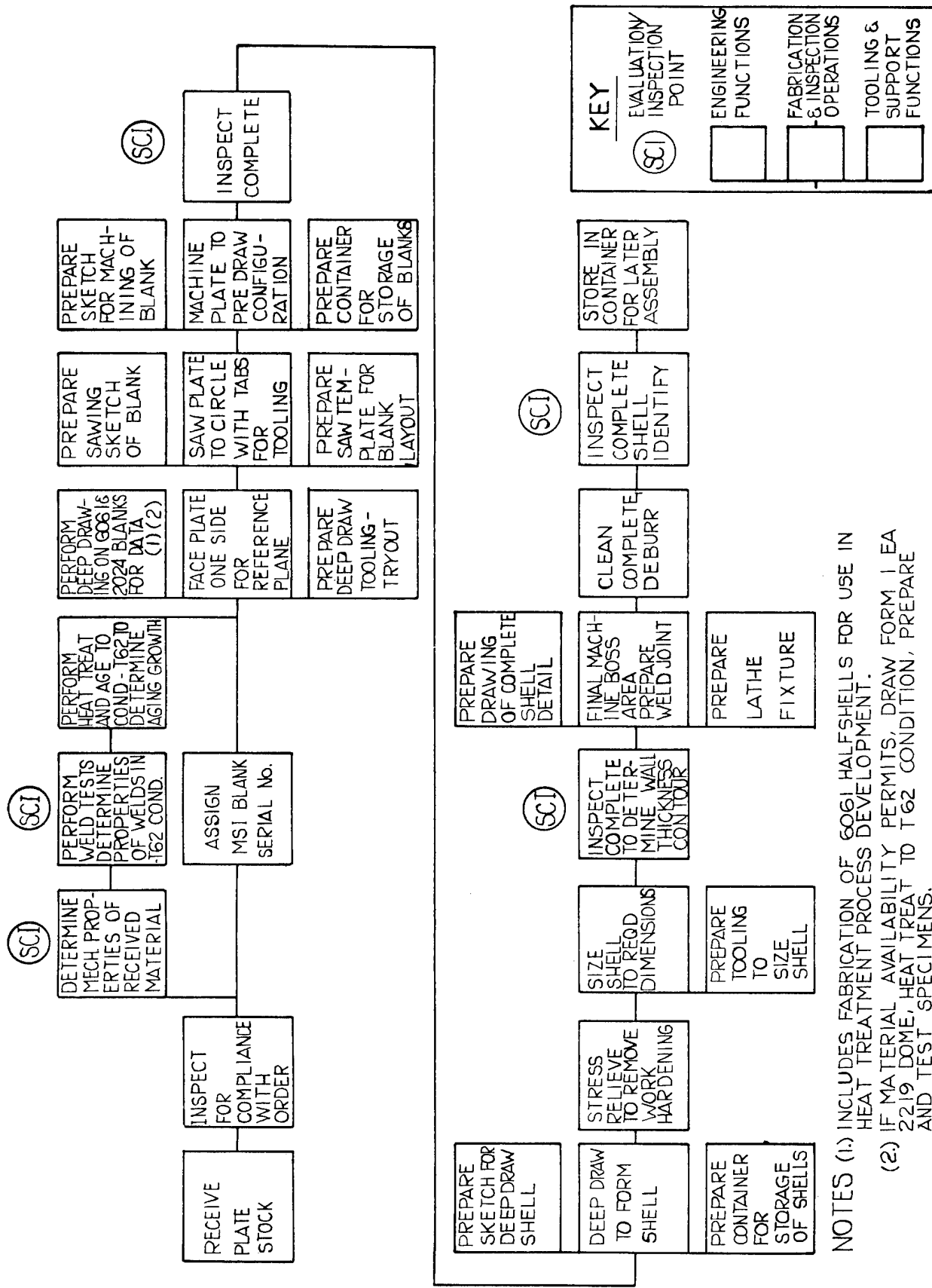
This metal-shell assembly will be used for filament-reinforced-metallic tankage for storage of pressurized fluids.



STRUCTURAL COMPOSITES INDUSTRIES INC.
6344 NORTH IRWINDALE AVE.
AZUSA, CALIFORNIA 91702
P.O. BOX 904

ENGINEERING PROCESS SPECIFICATION

NUMBER	REV.	DATE	SHEET	OF
SCI Spec. 73-17		6/18/73	16	19



NOTES
 (1) INCLUDES FABRICATION OF G661 HALFSHELLS FOR USE IN HEAT TREATMENT PROCESS DEVELOPMENT.
 (2) IF MATERIAL AVAILABILITY PERMITS, DRAW FORM 1 EA 2219 DOME, HEAT TREAT TO T62 CONDITION, PREPARE AND TEST SPECIMENS.

FIGURE C1 : 2219-T62 ALUMINUM SPHERE FABRICATION PLAN
SHEET I - HALF SHELL FABRICATION

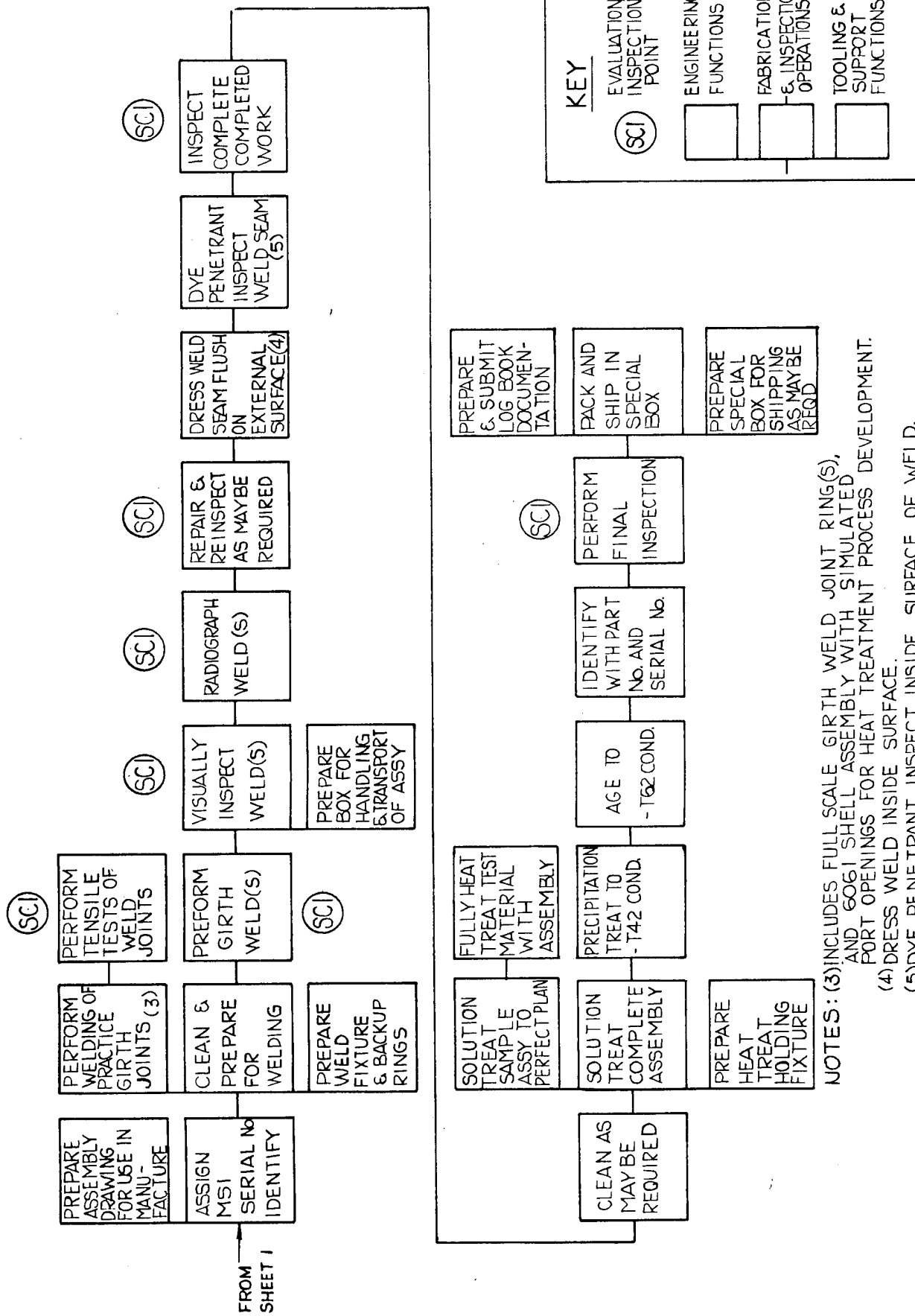


FIGURE C1: 2219-T62 ALUMINUM SPHERE FABRICATION PLAN
SHEET 2 - ASSEMBLY FABRICATION

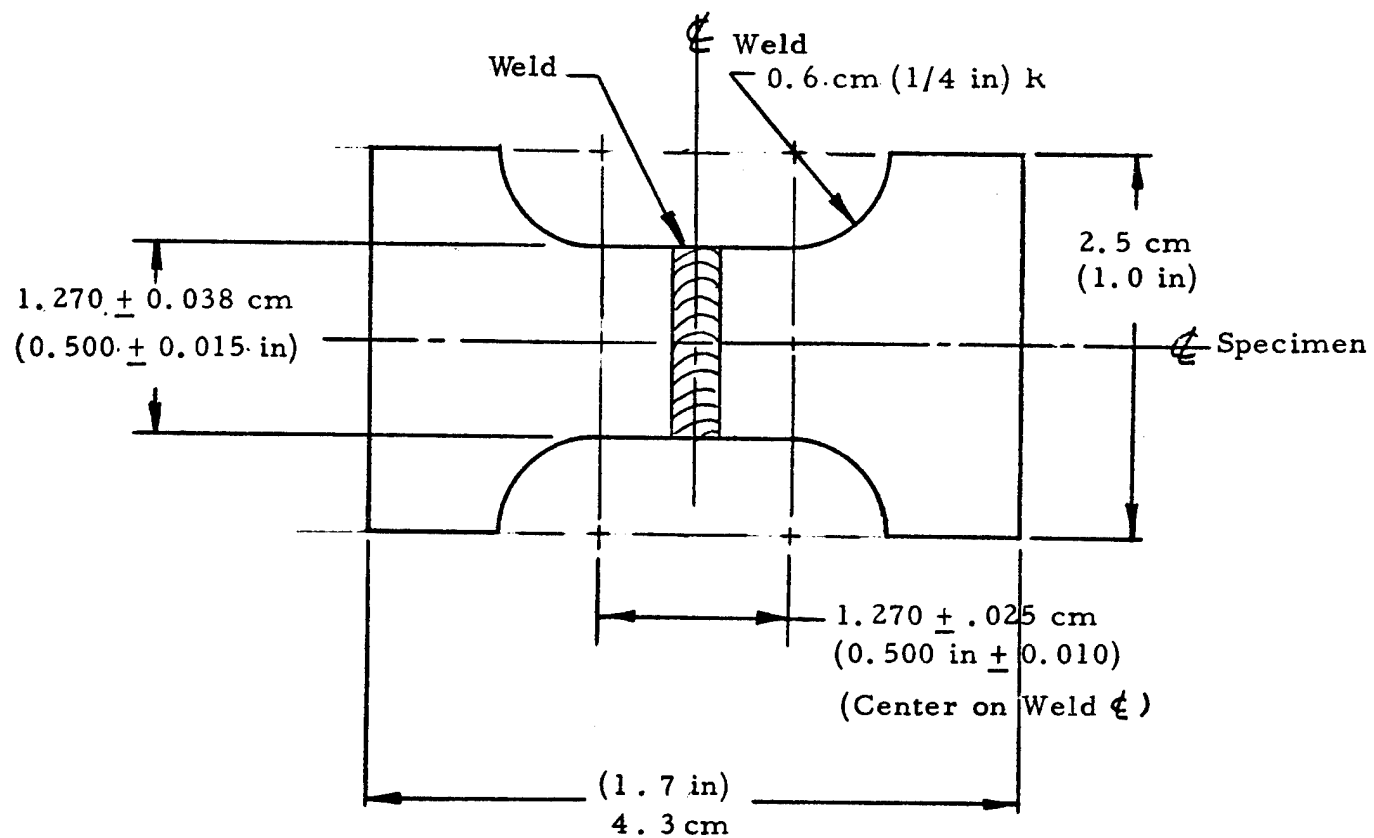


FIGURE C2: 2219-T62 Aluminum Weld Test Specimen Configuration

APPENDIX D

KEVLAR*FR 2219 ALUMINUM PRESSURE VESSEL FABRICATION PROCESS SPECIFICATION

* Kevlar-49 Roving was formerly designated as PRD-49-III Roving

SHOP ORDER NO.	SPLIT REFERENCE	COMPLETION DATE	PART DESCRIPTION		PART NUMBER	DATE
			MONTH	DAY		
1269382-1			Pressure Vessel, PRD-FR		1269382-1	
WORK CHARGE NUMBER	QTY.	SERIALIZATION	MATERIAL AVAILABILITY	E.O'S	N/C	A
2003-	1		MONTH DAY	YEAR		
TIME CARD CHARGE NO.	RELEASED BY	PLANNED BY	DATE	DATE	MASTER B.I.L. NO.	NEXT ASSY NO.
CHECK ONE □ shop order no. & oper. no. □ work charge no.	R. Landes	R. Landes	2-4-74	2-7-74	1269382	Final
MATERIAL DESCRIPTION	REVISED BY	REVIEWED BY	DATE	DATE	IN.P.	CHECK C.H.C.
See Parts List Requisition (PLR)	R. Landes	R. Landes	7-7-75	7-8-75	IN.P.	MAINTENANCE
C. OPER. STA. NO.	OPERATION DESCRIPTION	I.W.A. NO.	REVIEW AUTHORITY	IN.P.	IN.P.	TOOL NAME AND NUMBER
C. OPER. STA. NO.	OPR. DOW.	PROD.	PERF.	IN.P.	SET UP TIME	TOOL NAME AND NUMBER
2	1. All inspection stop points, as indicated by a circle in the inspection stamp column, will be verified and work will not proceed until verification by Quality Control is made by placing a Q.C. stamp at all points indicated.					
2	2. All quality engineering stop points, as indicated by a circle in the production stamp column, will be observed and work will not proceed until verification by the assigned Quality Engineer is made by placing a Q.C. stamp at all points indicated.					
2	3. Any discrepant inspection requirement or departure from the Shop Order instructions shall be documented on an Inspection Report (IR). Inspection will advise of action to be taken.					
2	4. No changes, alterations, or additions to Shop Order Traveler shall be honored by Inspection unless stamped by the Inspection Planner and Manufacturing Planner, and approved.					

SHOP ORDER CONTINUATION SHEET

SHOP ORDER NO.				SPLIT REFERENCE			COMPLETION DATE		PART DESCRIPTION		DATE			SHEET 2 OF 8	
SHOP ORDER NO.	STARTING AREA	SPLIT NO.		MONTH	DAY	YR.	C	P	Pressure Vessel, PRD-FR	1269382-1	DWG. REV.	PLAN. REV.	DWG. RESP.	PLAN. RESP.	
C	OPER. NO.	STA. NO.		OPERATION DESCRIPTION			OPR.	STAMP	SET UP C	SET UP R	TOOL NAME AND NUMBER	TOOL NAME AND NUMBER	N/C	A	
				OVR.	PROD.	INSP.									
2				2	5.	All entries on this Shop Order must be in ink.			.	.					
2				2	0103	Withdraw all productive materials and record traceability data on		○	1.0	1					
2				2		Process Control Record (PCR), Figure D1.			.	.					
2				2					.	.					
2				2	0203	PREPARATION FOR WINDING		○	3.0	2					
2				2		1. Record serial number and acceptance tag number of liner assembly,			.	.					
2				2		P/N 1269381 on PCR, Figure D1.			.	.					
2				2					.	.					
2				2		2. Measure liner assembly length, diameters (Pi-Tape), weight, and volume; record values on PCR, Figure D2.			.	.					
2				2					.	.					
2				2		3. Apply resin release to all connecting surfaces (threads, flange face, etc.) of winding shaft assembly, T-1400136-101, which must be disassembled after winding. Secure the winding shaft to the liner assembly.			.	.	Winding Shaft T-1400136-101				
2				2					.	.					
2				2					.	.					
2				2		4. Secure the liner/shaft assembly into the Spherical Winding Machine.			.	.	Sphere Winder E-100413				
2				2					.	.					
2				2		5. Install collimation and payoff roller system, T-1400165, to obtain the required 1.56-in-wide tape from (12) spools of roving.			.	.	Payoff System T-1400165				
2				2					.	.					

SHOP ORDER CONTINUATION SHEET

SHEET 3 OF 8

SHOP ORDER NO.	STARTING ATICK	SPLIT REFERENCE	COMPLETION DATE	P	PART DESCRIPTION		PART NUMBER	DATE		DWG. REV.	PLAN. REV.	PLAN. RESP.		
					MONTH	DAY	YR.	1269382-1	1269382-1					
C	OPER. NO.	STA. NO.	OPERATION DESCRIPTION							OPR. DWG.	STAMP	SET UP C	TOOL AVAIL. DATE	
C	OPER. NO.	STA. NO.								PROD.	INSP.	RUN TIME	TOOL NAME AND NUMBER	
2	0203	Cont	6.	Oven dry twelve (12) spools of 4-end PRD 49-III roving for 16 hours at 150°F. Record cure cycle and retain chart.						.	.	.		
2			7.	Weight twelve (12) spools of 4-end PRD 49-III roving and enter the weights on Figure D 3.						.	.	.		
2			8.	Set up twelve (12) spools of 4-end roving for winding on the eddy-current tensioning devices.						.	.	.		
2			9.	Thread the twelve (12) 4-end rovings through all sets of collimation rollers and secure to winding machine.						.	.	.		
2			10.	Preset static winding tension to 3.0 lb. on each of the 12 spools of roving.						.	.	.		
2			11.	Run the winding machine and check machine settings and pattern per Quality Engineer instructions.						.	.	.		
2			12.	Protect liner assembly with plastic sheet if next operation is not to be performed immediately.						.	.	.		
2				INSPECTION										
2			1.	Verify that all data required for Operation 0203 was recorded.						.	.	.		
2			2.	FILAMENT WINDING						.	.	.		
2			1.	Wipe exterior surface of liner assembly with MEK, using clean cheesecloth and air dry.						.	.	.		
2			2.											

SHOP ORDER CONTINUATION SHEET

PART DESCRIPTION										PART NUMBER			DATE			SHEET			
SHOP ORDER NO.		SPLIT REFERENCE		COMPLETION DATE		P	C	Pressure Vessel, PRD-FR		1269382-1			N / C	A	DWG. REV.	PLAN. REV.	PLAN. RESP.	4	8
C	OPER. STA. NO.	NO.		MONTH	DAY	YR.		OPERATION DESCRIPTION		STAMP	SET UP	R	SET UP	R	TOOL NAME AND NUMBER	AVAIL. DATE			
1	1269382-1							OPE. DWG.	PROD.	INSP.	RUN TIME	C	SET UP	R	TOOL NAME AND NUMBER	AVAIL. DATE			
2	0403 Cont.	2.	Prepare a single batch of resin mix in a one-gallon can as follows:																
2		2.	Epoxy Resin, DER 332 = 500 gm (100 parts)																
2		2.	Hardener, Epicure 855 = 425 gm (85 parts)																
2		2.	NOTE: This resin mix has a fairly short pot life at room temperature (approximately 2 hours). Prepare mix only after winding setups have been completed. Prepare second batch of resin mix, as above, when resin viscosity has increased noticeably. Prepare a resin cure witness sample for each batch of resin used.																
2		2.	3. Install the resin impregnation container (one-gallon can) at the appropriate position in the payoff system.																
2		2.	4. Adjust the machine to the settings for Step 1 per Figure D5, and thread the 12 four-end rovings over the payoff head tangent to the liner boss and secure them to the liner.																
2		2.	5. Adjust the static tension to 4.0 lbs / roving at the final payoff between the final payoff and liner assembly. Record tensions on Figure D4.																
2		2.	6. Set the turn counter to zero.																
2		2.	7. Proceed to wind rovings Steps 1 thru 25, per Figure D5 changing																
2		2.																	

SHOP ORDER CONTINUATION SHEET

SHOP ORDER NO.	STARTING AREA	SPLIT REFERENCE	COMPLETION DATE		P	PART DESCRIPTION	DATE	PART NUMBER	DWG. REV.	PLAN. REV.	C.F. 8
			MONTH	DAY							
1269382-1						Pressure Vessel, PRD-FR 2219 Aluminum Sphere	1269382-1				
C OPER. NO.	STA. NO.					OPERATION DESCRIPTION		OPR. DWG. STAMP	SET UP C	TOOL NAME AND NUMBER	TOOL AVAIL. DATE
2	0403 Cont.					wrap angles, machine settings, payoff heights, and RPM to obtain the required number of turns for each step in the wrap pattern.		DWG. PROD. INSP.	RUN TIME E		
2						Record the actual turn counts on Figure D5.			W		
2											
2						GENERAL NOTE: Stop overwrapping and notify Quality Engineering if any of the following should occur: (a) filament breakage.					
2						(b) loss of roving or rovings on guide rollers, (c) loss of roving tension, (d) winding pattern gapping, or (e) excessive variation of winding tape width. Retain any excess roving not used in winding but included in the initially recorded roving-spool weights; weigh it and record the weight on PCR, Figure D3.					
2											
2						8. Wipe all excess resin from the vessel surface with clean cheese-cloth or Kemwipes after every step (revolution) is completed.					
2						9. Measure the static tension on each roving at the final payoff after completion of the 5th, 10th, 15th, and 20th Steps (revolutions); record the data on Figure D4, then adjust the tension to obtain the required 4.0 lbs/roving.					
2						10. After completion of Step 24, Figure D5, cut and remove the three upper and three lower rovings from the winding tape. Proceed to wind the six roving tape under tension per Step 25 of Figure D5.					
2						11. At the conclusion of winding (after Step 25), tie off the rovings by					

SHOP ORDER CONTINUATION SHEET

SHOP ORDER NO.	STARTING AREA	SPLIT REFERENCE	COMPLETION DATE		PART DESCRIPTION		DATE	SHEET	DWG. PLAN.		REV. RESP.	
			MONTH	DAY	YR.	Pressure Vessel, PRD-FR			OPR. DWG.	STAMP	SET UP	TOOL NAME AND NUMBER
C	OPER. N.	STA. N.			OPERATION DESCRIPTION		N/C	A				
1269382-1												
2	0403	Cont.	burying the ends under two or three turns of winding.									
2			12. Wipe off excess resin from the exterior surface of the filament-wound vessel and from the shaft/boss mating surfaces. Continue wiping vessel surface every 15 minutes until gelation occurs.									
2			13. Transfer vessel from the sphere winder to the cure cart, SK-73-041.									
2			14. Remove the spools of roving from the tension devices, weigh each spool, and record the weights on Figure D3; return the spools to Material Control. Weigh all scrap roving, retained in plastic bag, and record weight on Figure D3.									
2			15. Protect the vessel with plastic sheet if next operation is not to be performed immediately.									
2												
2	0506		INSPECTION						0.2	1		
2			1. Verify that tension was maintained and recorded on Figure D4.									
2			2. Verify that the number of winding turns for each Step (Steps 1 thru 25) was recorded on Figure D5.									
2			3. Verify weight of roving (including scrap) was recorded on Figure D3.									
2	0603		OPEN CURE AND CLEANUP									
2			1. Install the wound-vessel/cure-cart assembly and resin witness									

SHOP ORDER CONTINUATION SHEET

SHOP ORDER NO.				SPLIT REFERENCE	COMPLETION DATE	P	C	PART DESCRIPTION		PART NUMBER		DWG. REV.	PLAN. REV.	PLAN. RESP.	
C	OPER. NO.	STA. NO.	OPERATION DESCRIPTION		MONTH	DAY	YR.	Pressure Vessel, PRD-FR 2219 Aluminum Sphere		1269382-1		N/C	A	TOOL AVAIL. DATE	
2	0603	Cont.	sample (op. 0403-2) in oven preheated to 125° F.												
2			2. Install a new (circular) oven cure chart in temperature recorder.												
2			3. Maintain oven temperature at 125° F for a period of 8 hours. Wipe off excess resin at 1/4-hour intervals (or lesser intervals, as necessary) until gelation occurs. Rotate position of the sphere periodically during this period to prevent uneven surface resin buildup.												
2			4. Remove the cured vessel from the oven. Obtain oven cure chart and attach to PCR.												
2			5. Disassemble tooling from cured vessel and return to tool control.												
2			6. Clean all visible metal surfaces with MEK to remove any resin.												
2			Care should be exercised so that internal metal "O" Ring surface is not defaced.												
2			7. Measure cured vessel length, diameters (Pi-Tape), weight, and volume; record values on PCR, Figure D2.												
2			8. Deliver the vessel to the inspection area.												
2	0706		INSPECTION									0 . 2	1		
2			1. Verify cure cycle from cure record.												
2			2. Verify record of dimensions.												
2			3. Inspect for handling damage.												
2			Deliver vessel to test area.												

SALVADOR URQUET-PAJAS LIST REQUISITUM

EFFECT RATE

REV. 12-64)

EXCERPT

卷之三

DATA

PROCESS CONTROL RECORD

FIGURE D1: MATERIAL TRACEABILITY

Part No. 1269382-1 Date Started _____

Part Name F/W Pressure Vessel W.O. No. 2003-

Serial No. _____ Shop Order No. 1269382-1 _____

Operation

<u>No.</u>	<u>Description of Data Required</u>	<u>Inspector</u>
------------	-------------------------------------	------------------

0103 Record traceability data of the following:

Mfg. Lot No. Accept. Tag No.

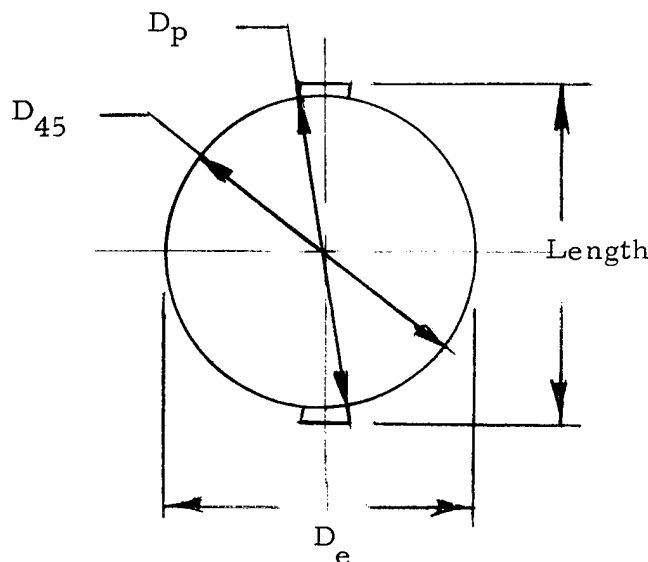
1. PRD Roving, 4-End, _____ _____
Type III
2. Epoxy Resin, DER 332 _____ _____
3. Hardener, Epicure 855 _____ _____

0203-1 Record traceability data of aluminum liner assembly, P/N 1269381-1

Accept Tag No. _____ S/N _____

PROCESS CONTROL RECORDFIGURE D2: DIMENSION/WEIGHT RECORDPart No. 1269 382-1 Date Started _____Part Name F/W Pressure Vessel W.O. No. 2003-

Serial No. _____ Machine Operator _____



Operation No.

0203-20603-7Before WrapAfter Cure

Vessel Length = _____ inch _____ inch

Diameters

D_e = _____ inch _____ inchD_p = _____ inch _____ inchD₄₅ = _____ inch _____ inch

Vessel Weight = _____ lbs _____ LBS.

Internal Volume = _____ in³ _____ in³
(See Sheet 2)

PROCESS CONTROL RECORD (cont.)FIGURE D2: DIMENSION / WEIGHT RECORDInternal Volume Calculations

	<u>Before Wrap</u>	<u>After Cure</u>
A. Dry Weight (w/ Tare)	_____ lbs.	_____ lbs.
B. Filled Weight (w/ Tare)	_____ lbs.	_____ lbs.
C. Subtract B-A=W	_____ lbs.	_____ lbs.
D. Water Temperature	_____ °F	_____ °F
E. Specific Gravity (SG)*	_____ in ³	_____ in ³
F. Calculated Volume (V)**	_____ in ³	_____ in ³

* TABLE OF SPECIFIC GRAVITY (SG) vs. TEMPERATURE

<u>°C</u>	<u>°F</u>	<u>SG</u>	<u>°C</u>	<u>°F</u>	<u>SG</u>
17	62.6	.99880	25	77.0	.99707
18	64.4	.99862	26	78.8	.99681
19	66.2	.99843	27	80.6	.99654
20	68.0	.99823	28	82.4	.99626
21	69.8	.99802	29	84.2	.99597
22	71.6	.99780	30	86.0	.99567
23	73.4	.99756	31	87.8	.99537
24	75.2	.99732	32	89.6	.99505

**Calculated Volume

27.68W

V = $\frac{W}{SG}$

PROCESS CONTROL RECORD

FIGURE D3: MATERIAL USAGE RECORD

Part No. 1269382-1 Date Started _____

Part Name F/W Pressure Vessel W.O. No. 2003-

Serial No. _____ Shop Order No. 1269382-1

<u>Operation No.</u>	<u>Description of Data Required</u>	<u>Inspector</u>
<u>0203-6</u>	Record PRD roving usage	

Brake No.	Roll No.	Weight, gm			Usage
		Start	End		
1					
2					
3					
4					
5					
6					
7					
8					
9					
10					
11					
12					

0403-14

Total Usage: _____

Scrap _____

Net Usage: _____

[$\frac{1}{4}$ 454 = _____ lb.]

PROCESS CONTROL RECORD

FIGURE D4: TENSION RECORD

Part No. 1269382-1 Date Started
Part Name F/W Pressure Vessel W.O. No. 2003-
Serial No. Shop Order No. 1269382-1

Brake NO.	STEP NO.				
	1	5	10	15	20
1					
2					
3					
4					
5					
6					
7					
8					
9					
10					
11					
12					
Oper. No.	0403-5	0403-9			

NOTE: Record the static tension before adjustment to 4.0 lb/roving is made

PROCESS CONTROL RECORD

FIGURE D5: WINDING PATTERN

Part No. 1269382-1 Date Started _____
 Part Name F/W Pressure Vessel W.O. No. 2003-
 Serial No. _____ Shop Order No. 1269382-1
 Machine Operator _____

Twelve Strand Pattern Except as Noted

Step No.	Degree Setting	Machine Setting	Payoff Arm Setting	RPM	TURNS	
					Req'd.	Actual
1	12.0	7663	12.900	8	74	
2	15.5	7660	12.025		73	
3	22.0	7642	10.150		70	
4	28.5	7631	8.350		66	
	35.0	7620	6.600		62	
6	41.5	7595	5.225		57	
7	48.0	7560	3.800		51	
8	54.5	7517	2.500		44	
9	61.0	7455	1.350		37	
10	67.5	7337	0.475		29	
11	74.0	7150	1.100		21	
12	79.5	7085	.775	**	19	
13	79.5	7085	.775		19	
14	74.0	7150	1.100		21	
15	67.5	7337	0.475		29	
16	61.0	7455	1.350		37	
17	54.5	7517	2.500		44	
18	48.0	7560	3.800		51	
19	41.5	7595	5.225		57	
20	35.0	7620	6.600		62	
21	28.5	7631	8.350		66	
22	22.0	7642	10.150		70	
23	15.5	7660	12.025		73	
24	12.0	7663	12.900		74	
* 25	11.0	7765	14.000	8	148	

*Six - Strand Pattern

** - Setting are with payoff head stock
all the way up.

APPENDIX E

TEST PROCEDURE *
KEVLAR FIBER REINFORCED
METAL SPHERES

SCI Specification 74-44

February 1974

Prepared for

NASA LEWIS RESEARCH CENTER

CLEVELAND, OHIO

Prepared by

R. E. Landes

STRUCTURAL COMPOSITES INDUSTRIES, INC.
6344 North Irwindale Avenue
Azusa, California 91702

* Presentation of this procedure in S. I. units would reduce the clarity of this Appendix. The procedure is presented in the original form as written by the author.

TABLE OF CONTENTS

	<u>Page</u>
1. 0 SCOPE	257
2. 0 REFERENCE DOCUMENTS	258
3. 0 DESCRIPTION OF TEST SPECIMENS	259
4. 0 SEQUENCE OF TESTING	260
5. 0 TEST CONDITIONS AND EQUIPMENT	261
6. 0 TEST ADMINISTRATION AND DATA	263
7. 0 TEST REQUIREMENTS AND PROCEDURES	265
7. 1 Hydraulic Burst Test	265
7. 2 Pneumatic Burst Test	266
7. 3 Cyclic Fatigue Test	267
7. 4 Hydraulic Sustained Load Test	268
7. 5 Gaseous Hydrogen Sustained Load Test	269
7. 6 Gunfire Test	270
TABLE EI - SEQUENCE OF TESTING	272
TABLE EII - EXPECTED TEST VALUES FOR SENSOR CALIBRATION	273
FIGURE E1 - INSTRUMENTATION LOCATION	274
FIGURE E2 - HYDRAULIC TEST SYSTEM	275
FIGURE E3 - PNEUMATIC TEST SYSTEM	276
FIGURE E4 - FATIGUE CYCLE TEST SYSTEM	277
FIGURE E5 - GUNFIRE TEST SYSTEM	278
ENCLOSURE EI TEST DATA SHEETS	279

1.0 SCOPE

- 1.1 The purpose of this test procedure is to present the detailed test methods, conditions, and equipment to be used for demonstrating the performance of spherical*PRD Fiber-Reinforced (PRD FR) metal pressure vessels.
- 1.2 In the event of conflict between this procedure and any other procedure or document, this procedure shall govern.

* Kevlar-49 Roving was formerly designated PRD-49-III Roving

2.0 REFERENCE DOCUMENTS

NOTE: Latest changes apply to all documents.

2.1 Structural Composites Industries Documents as follows:

2.1.1 Drawing Number 1269382-1, titled: Pressure Vessel PRD-FR 2219 Aluminum Sphere

2.1.2 Drawing Number 1269381-1, titled: Liner Assembly 2219-T62 Aluminum Sphere

2.1.3 Drawing Number T-1400138, titled: Test Plate

2.1.4 Sizing Test Procedure, SCI Specification 74-45

2.1.5 Drawing Number T-1400264, titled: Tie-Rod

2.1.6 Drawing SK-75-001, titled: Tie-Rod Assembly

2.2 ARDE Incorporated Documents as follows:

2.2.1 Drawing Number D3898 , titled: Pressure Vessel PRD FR 301 Stainless Steel Sphere

2.2.2 Drawing Number D3895 , titled: Arde form 301 Stainless Steel Liner

2.3 Military Specification Number MIL-T-25363C, titled: Tank, Pneumatic Pressure, Aircraft, Glass Fiber.

2.4 NASA Technical Memorandum TMX-52454, titled: Hydrogen Safety Manual (issued by Lewis Research Center, Cleveland Ohio).

3.0 DESCRIPTION OF TEST SPECIMENS

- 3.1** The test specimens are six (6) pressure vessels each of two (2) different designs as follows:
- 3.1.1** Specimen Serial Numbers S-1 through S-6 are 38.0-inch-diameter PRD FR Aluminum Spheres fabricated as SCI Part Number 1269382-1 and pressure sized according to SCI Specification 74-45.
- 3.1.2** Specimen Serial Numbers 001 through 006 are 25.0-inch-diameter PRD FR Stainless Steel Spheres fabricated as ARDE Part Number D3898 and cryogenically pressure sized according to ARDE Specifications.
- 3.2** Each test specimen will be supplied with four (4) strain gage rosettes bonded to the external surface of the vessel.

- 4.0 SEQUENCE OF TESTING
- 4.1 The test specimens shall be subjected to Performance Demonstration Tests in accordance with Table EI of this test procedure after Sizing Tests have been performed.
- 4.2 The test requirements for each test, and the test procedures to be used, are presented in Paragraph 7.0 of this test procedure.
- 4.3 The Sizing Test Procedures are defined in the documents of Paragraphs 2.1.4 for the S series vessels and by ARDE Specifications for the 00x series vessels

5.0 TEST CONDITIONS AND EQUIPMENT

5.1 Ambient Conditions

5.1.1 Unless otherwise specified herein, all tests required by this procedure shall be performed with the test specimens at standard laboratory conditions; defined as a temperature between 60° and 80°F, a relative humidity of less than 85%, and a barometric pressure between 27.9 and 31.9 inches of Mecury absolute.

5.2 Primary Instrumentation

5.2.1 The primary test instrumentation, as a minimum, shall consist of sensors, transducers, signal conditioning equipment, and recording equipment for recording the following specimen test parameters within the indicated tolerance range:

Pressure $\pm 0.5\%$ of indication
Strain/Displacement $\pm 0.5\%$ of indication

5.2.2. Quantity and location of sensors shall be as defined in Figure E1.

5 2-3 Deleted

5.3 Equipment Log and Calibration

5.3.1 A test equipment log shall be maintained during the test program described in this test procedure. The test equipment log shall state equipment description, manufacturer, range, accuracy, and calibration date (where applicable).

5.3.2 All test equipment used shall conform to applicable standards with regard to appropriateness, accuracy, and calibration interval.

5.3.3 Each item of test equipment shall be checked prior to use to insure that the instrument has been calibrated (if applicable) according to its specified schedule and that the instrument is functioning within the accuracy range required.

- 5.3.4 All pressure transducers shall be laboratory calibrated at 90 day intervals or sooner as required. The instrumentation systems shall be calibrated by closed loop pressurization to the values of Table EII prior to each test.
- 5.3.5 All extensometers shall be calibrated in place on the vessel prior to test using the expected deflection ranges of Table EII.
- 5.3.6 All strain gage rosettes shall be individually shunt calibrated over the strain ranges of Table EII prior to each test.
- 5.3.7 All calibration information shall be maintained on file in the Quality Control Department and shall be available for inspection by cognizant SCI and NASA personnel.

- 6.0 TEST ADMINISTRATION AND DATA
- 6.1 Program Management
- 6.1.1 The overall conduct of the test program shall be coordinated between the cognizant project engineer and the test engineer. All questions, problems and other matters of a technical nature shall be directed to the cognizant project engineer or his representative.
- 6.2 Test Witnessing
- 6.2.1 Testing shall be witnessed by the cognizant project engineer who shall be present to perform any required operational checks during the test program. The cognizant project engineer may elect to waive witnessing requirements, but in any event, he shall be notified prior to the beginning of any test.
- 6.3 Test Data
- 6.3.1 During the test program, complete data sheets shall be maintained documenting the test progress to that point.
- 6.3.2 Deleted.
- 6.3.3 Raw data acquisition shall consist of permanent records of pressure versus time and extensometer/strain gage output versus time for all sensors of Paragraph 5.2.2.
- 6.3.3.1 For burst tests, data shall be recorded continuously as the vessel is pressurized to failure.
- 6.3.3.2 For cyclic fatigue tests, data shall be recorded for the first, 10th, 50th, 100th, 500th, and each additional 500th pressure cycle concluding with a record of the final pressure cycle.
- 6.3.3.3 For sustained load tests, data shall be recorded for the initial pressurization cycle, the final depressurization cycle, and (as a minimum) at time intervals of 12 ± 2 hours. Any observed pressure decay shall be recorded prior to a system adjustment.

6.3.4 Data reduction shall consist of reducing the raw data of Paragraph 6.3.3 to plots of pressure versus strain for all sensors of Paragraph 5.2.2 for each specific test.

7.0 TEST REQUIREMENTS AND PROCEDURES

7.1 Hydraulic Burst Test

7.1.1 Deleted.

7.1.2 Instrumentation shall be installed per Figure E1 and calibrated per Paragraph 5.3.

7.1.3 "O" Rings and Backup rings shall be installed on each test plate, T-1400138, and the test plates secured to the vessel bosses. The test plates shall be coupled together with the tie-rod, T-1400264, per SK-75-001. This operation shall apply to the test specimens of Paragraph 3.1.1 only.

7.1.4 A pretest leak check of all fittings and equipment shall be performed on the pressurization system adjusted to a dead-end condition. The test specimen shall be isolated from the system during the leak test.

7.1.5 The test specimen, filled with inhibited water and bled of all entrapped air, shall be installed in a hydraulic test system as illustrated in Figure E2.

7.1.6 Fluid pressure in the test specimen shall be increased to the expected burst pressure (EBP) at pressurization rate defined on Data Sheet Number 1.

7.1.7 The pressure shall be maintained at the EBP value for three (3) minutes and subsequently increased at a rate per Data Sheet Number 1 until specimen failure occurs.

7.1.8 All test data obtained during the burst test shall be recorded on Data Sheet Number 1.



7.1.9 Data Sheet Number 1, and the additional raw data of Paragraph 6.3 shall be maintained on file in the Quality Control Department.



7.2 Pneumatic Burst Test

7.2.1 The high speed motion picture camera shall be located, set up, and checked out prior to initiation of test.

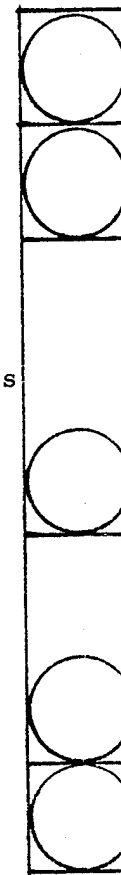
7.2.2 Instrumentation shall be installed per Figure E1 and calibrated per Paragraph 5.3.

7.2.3 "O" Rings and Backup rings shall be installed on each test plate, T-1400138, and the test plates secured to the test specimen. The test plates shall be coupled together with the tie-rod, T-1400264, per SK-75-001. This operation shall apply to the test specimens of Paragraph 3.1.1 only.

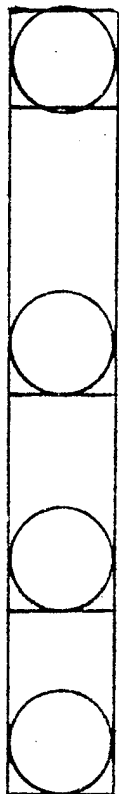
7.2.4 A pretest leak check of all fittings and equipment shall be performed on the pressurization system adjusted to a dead-end condition. The test specimen shall be isolated from the system during the leak test.

7.2.5 The test specimen shall be installed in a pneumatic test system as illustrated in Figure E3.

7.2.6 The test specimen shall be pressurized with gaseous nitrogen per MIL-P-27401, at the pressure rate defined on Data Sheet Number 2, until specimen failure occurs. Fluid temperature shall not exceed 160°F during this test.



- 7.2.7 All test data obtained during the burst test shall be recorded on Data Sheet Number 2.
- 7.2.8 **Data Sheet Number 2**, and the additional raw data of Paragraph 6.3 shall be maintained on file in the Quality Control Department.
- 7.3 Cyclic Fatigue Test
- 7.3.1 Instrumentation shall be installed per Figure E1 and calibrated per Paragraph 5.3.
- 7.3.2 "O"Rings and Backup rings shall be installed on each test plate, T-1400138, and the test plates secured to the vessel bosses. The test plates shall be coupled together with the tie-rod, T-1400264, per SK-75-001. This operation shall apply to the test specimens of Paragraph 3.1.1 only.
- 7.3.3 A pretest leak check of all fittings and equipment shall be performed on the pressurization system adjusted to a dead-end condition. The test specimen shall be isolated from the system during the leak test.
- 7.3.4 The test specimen, filled with hydraulic fluid per MIL H-5606-C and bled of all entrapped air, shall be installed in a hydraulic pressure cycle test system as illustrated in Figure E4.
- 7.3.5 The test specimen shall be subjected to 1600 operating pressure cycles at a rate of 1 to 2 cycles per minute. Each pressure cycle shall consist of the following:
- 7.3.5.1 Increase the test specimen pressure to the mean operating pressure (MOP) \pm 50 psig and hold for 10 seconds.
- 7.3.5.2 Decrease the test specimen pressure to 50 psig or less.



7.3.5.3 The test shall be terminated if the test specimen exhibits signs of leakage or rupture prior to completion of the 1600 pressure cycles.

7.3.6 The test specimen shall be visually inspected for damage and these observations, including all test data, recorded on Data Sheet Number 3.

7.3.7 Data Sheet Number 3 and the additional raw data of Paragraph 6.3 shall be maintained on file in the Quality Control Department.

7.4 Hydraulic Sustained Load Test

7.4.1 Instrumentation shall be installed per Figure E1 and calibrated per Paragraph 5.3.

7.4.2 A pretest leak check of all fittings and equipment shall be performed on the pressurization system adjusted to a dead-end condition. The test specimen shall be isolated from the system during the leak test.

7.4.3 The test specimen, filled with inhibited water and bled of all entrapped air, shall be installed in a hydraulic test system as illustrated in Figure E2.

7.4.4 Fluid pressure in the test specimen shall be increased, at the rate defined on Data Sheet Number 4, to the mean operating pressure (MOP) \pm 50 psig and the load/vent valves locked in the closed position.

7.4.5 Pressure in the test specimen shall be maintained at the MOP value for a minimum period of 96 hours. Any pressure decay during the period shall first be recorded per 6.3.3.3 and then adjusted to the MOP value.

7.4.6 After completion of the 96 hour period, pressure in the test specimen shall be decreased to zero at a rate defined in Data Sheet Number 4. The test specimen shall be visually in-



spected for damage and these observations, including all test data, recorded on Data Sheet Number 4.

7.4.7 Deleted.

7.4.8 Fluid pressure in the test specimen shall be increased at the rate defined on Data Sheet Number 4 until specimen failure occurs.

7.4.9 Additional data associated with the burst test shall be recorded on Data Sheet Number 4; Data Sheet 4, and the data of Paragraph 6.3 shall be maintained on file in the Quality Control Department.

7.5 Gaseous Hydrogen Sustained Load Test

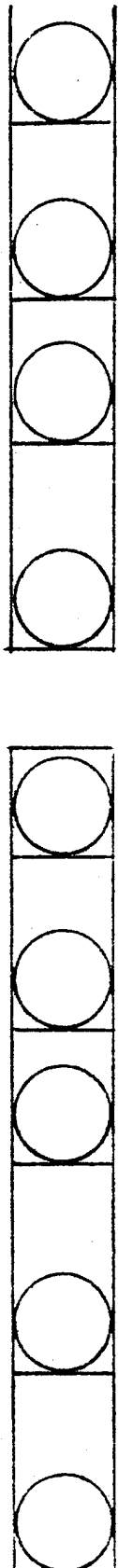
7.5.1 The Hydrogen Safety Manual, Paragraph 2.4, shall be reviewed prior to the initiation of any efforts on this test.

7.5.2 For this test, a volume-filling material may be used to reduce the test specimen internal volume. If used, the material designation and quantity shall be recorded on Data Sheet Number 5.

7.5.3 Instrumentation shall be installed on the test specimen per Figure E and calibrated per Paragraph 5.3.

7.5.4 "O" Rings and Backup rings shall be installed on each test plate, T-1400138, and the test plates secured to the vessel bosses. The test plates shall be coupled together with the tie-rod, T-1400264, per SK-75-001.

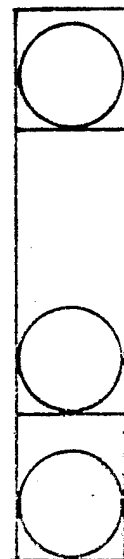
7.5.5 A pretest leak check of all fittings and equipment shall be performed on the pressurization system adjusted to a dead-end condition. The test specimen shall be isolated from the system during the leak test.



- 7.5.6 The test specimen shall be installed in a pneumatic test system as illustrated in Figure E 3
- 7.5.7 The test specimen shall be pressurized with gaseous hydrogen per MIL P-27201A at the rate defined on Data Sheet Number 5, to the mean operating pressure (MOP) \pm 50 psig and the load valve locked in the closed position. During pressurization fluid temperature shall not exceed 160°F.
- 7.5.8 Pressure in the test specimen shall be maintained at the MOP value for a minimum period of 96 hours. Any pressure decay during the period shall first be recorded per 6.3.3.3 and then adjusted to the MOP value.
- 7.5.9 After completion of the 96 hour period, pressure in the test specimen shall be decreased to zero at a rate per Data Sheet Number 5. The test specimen shall be purged of all residual gaseous hydrogen.
- 7.5.10 The test specimen shall be visually inspected for damage and these observations, including all test data, recorded on Data Sheet Number 5.
- 7.5.11 Data Sheet Number 5 and the additional raw data of Paragraph 6.3 shall be maintained on file in the Quality Control Department.

7.6 Gunfire Test

- 7.6.1 Deleted.
- 7.6.2 "O" Rings and Backup rings shall be installed on each test plate, T-1400138, and the test plates secured to the test specimen bosses. The test plates shall be coupled together with the tie-rod, T-1400264, per SK-75-001. This operation shall apply to the test specimens of Paragraph 3.1.1 only.
- 7.6.3 The test specimen shall be restrained in a mounting fixture at the gun range as illustrated in Figure E5.



- 7.6.4 The test specimen shall be pressurized with gaseous nitrogen per MIL-P-27401, at the rate defined in Data Sheet to the mean operating pressure (MOP) \pm 50 psig.
- 7.6.5 A gunfired 50 caliber armor piercing projectile with a muzzle velocity of 2800 ± 100 feet per second shall be caused to tumble and strike the test specimen at the location shown in Figure E5. (Reference MIL-T-25363C, Paragraph 2.3). The range of gunfire shall be 50 yards maximum.
- 7.6.6 After gunfire, the test specimen shall be examined and the extent of structural damage recorded on Data Sheet Number 6 along with all other test data.
- 7.6.7 Data Sheet Number 6 shall be maintained on file in the Quality Control Department.



TABLE EI
SEQUENCE OF TESTING

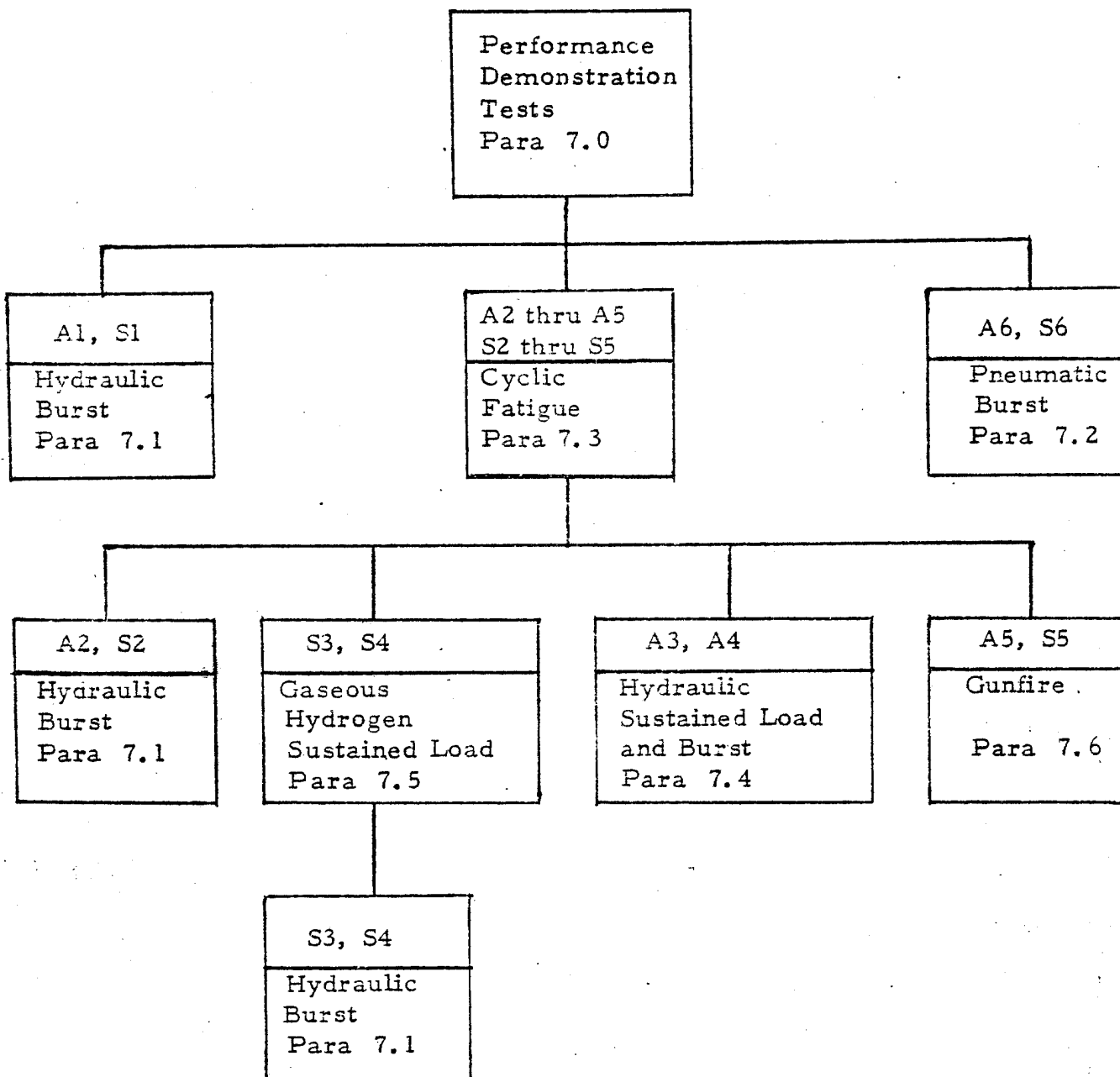
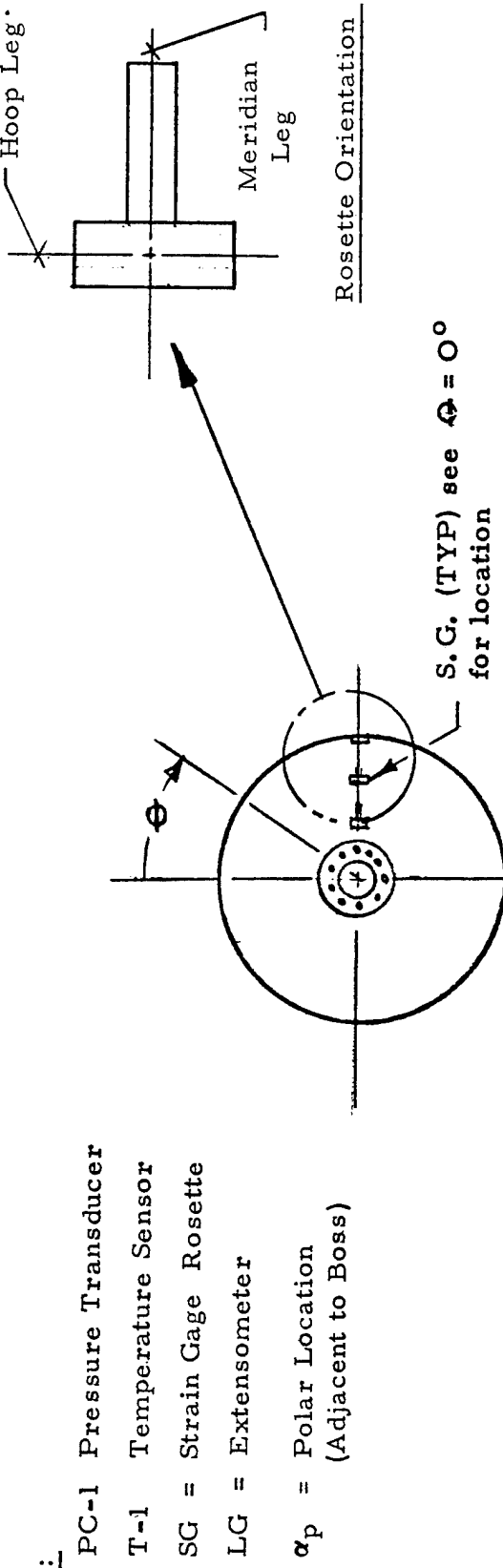


TABLE EII

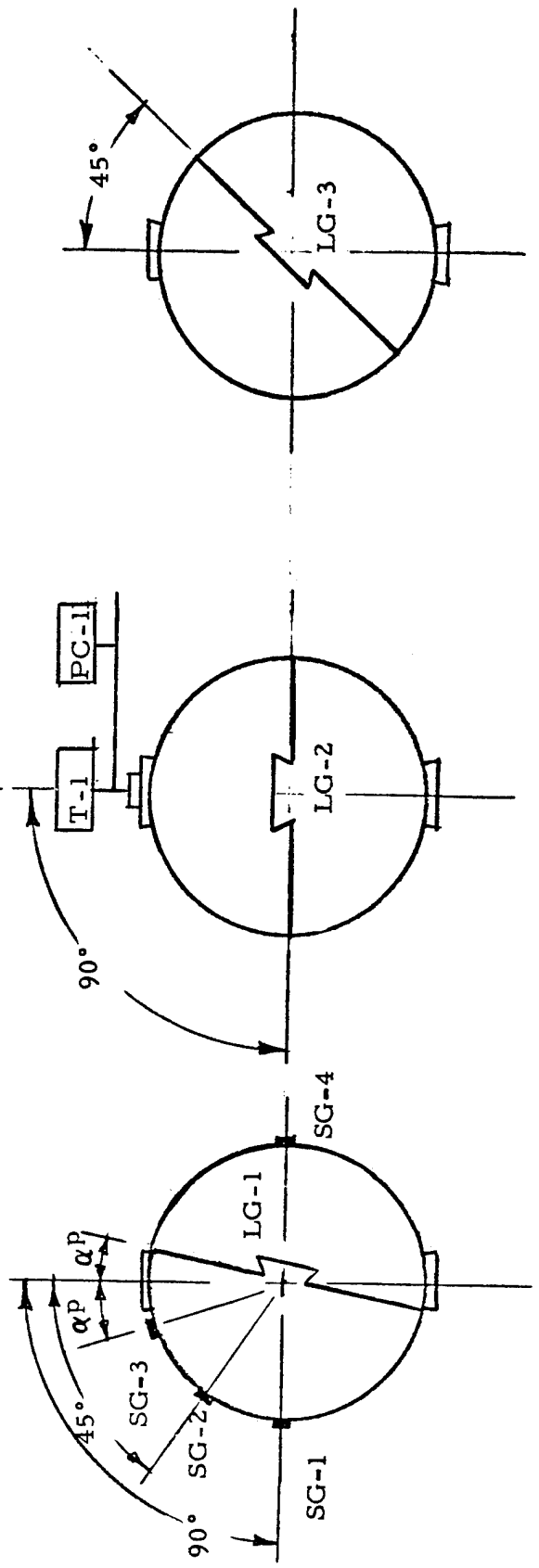
EXPECTED TEST VALUES FOR SENSOR CALIBRATION

Test Parameters	Vessel Series	
	S	00X
<u>Pretest Condition</u>		
Outside Diameter, in	38.23	26.04
Internal Volume, in ³	27,100	7204
<u>Operating Condition (Para 7.3, 7.4, 7.5, 7.6)</u>		
Pressure (MOP), psi	2024	2330
Volumetric Expansion, in ³	340	107
Circumferential Expansion, in	0.5	0.4
Strain, %	0.41	0.50
<u>Burst Condition (Para 7.1, 7.2, 7.4)</u>		
Pressure (EBP), psi	4042	4660
Volumetric Expansion, in ³	964	270
Circumferential Expansion, in	1.4	1.0
Strain %	1.17	1.25

Hoop Leg.



Rosette Orientation



$\Theta = 240^\circ$

$\Theta = 120^\circ$

$\Theta = 0^\circ$

FIGURE E1: Instrumentation Location

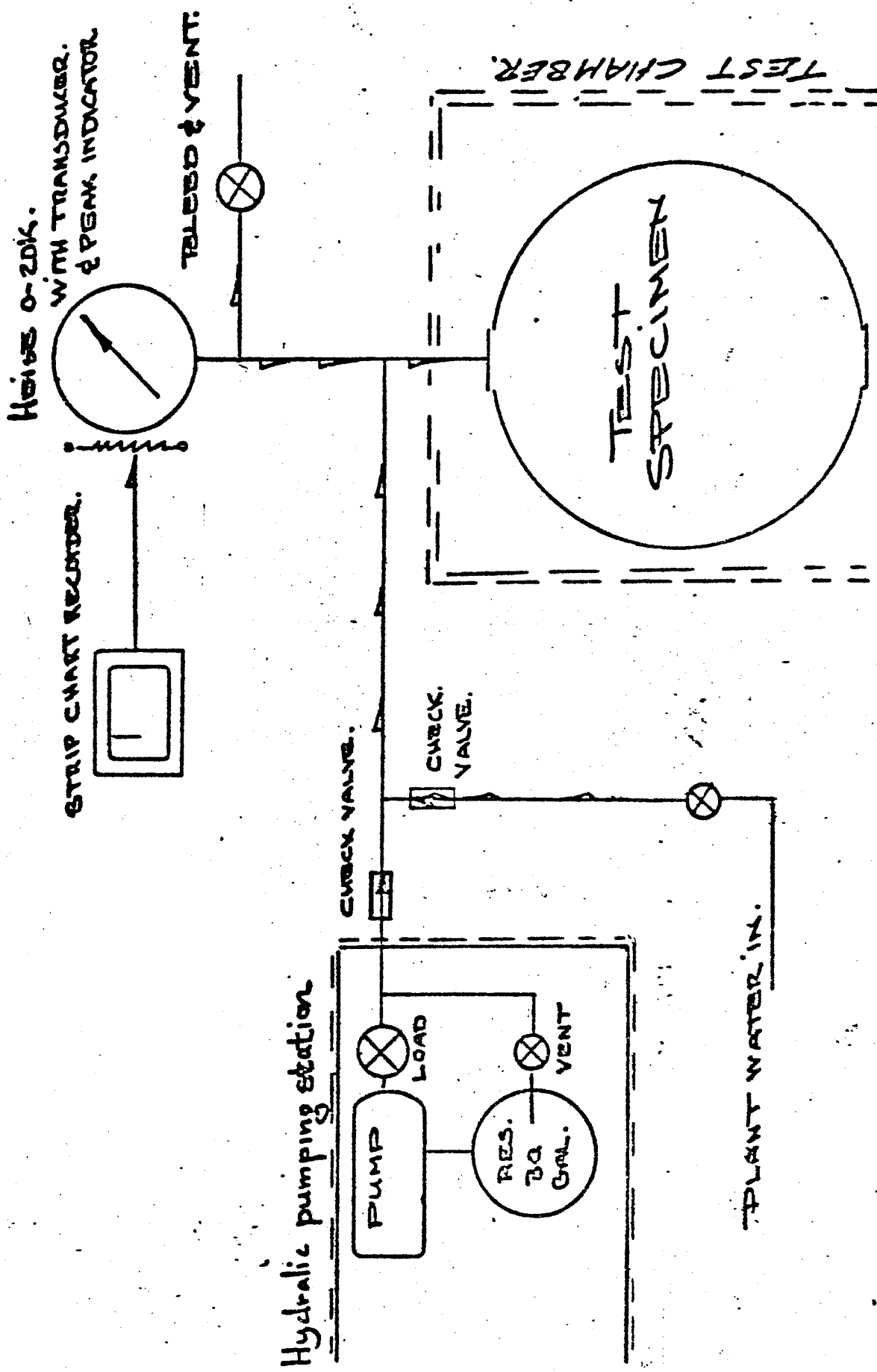


FIGURE E2
 HYDRAULIC TEST SYSTEM

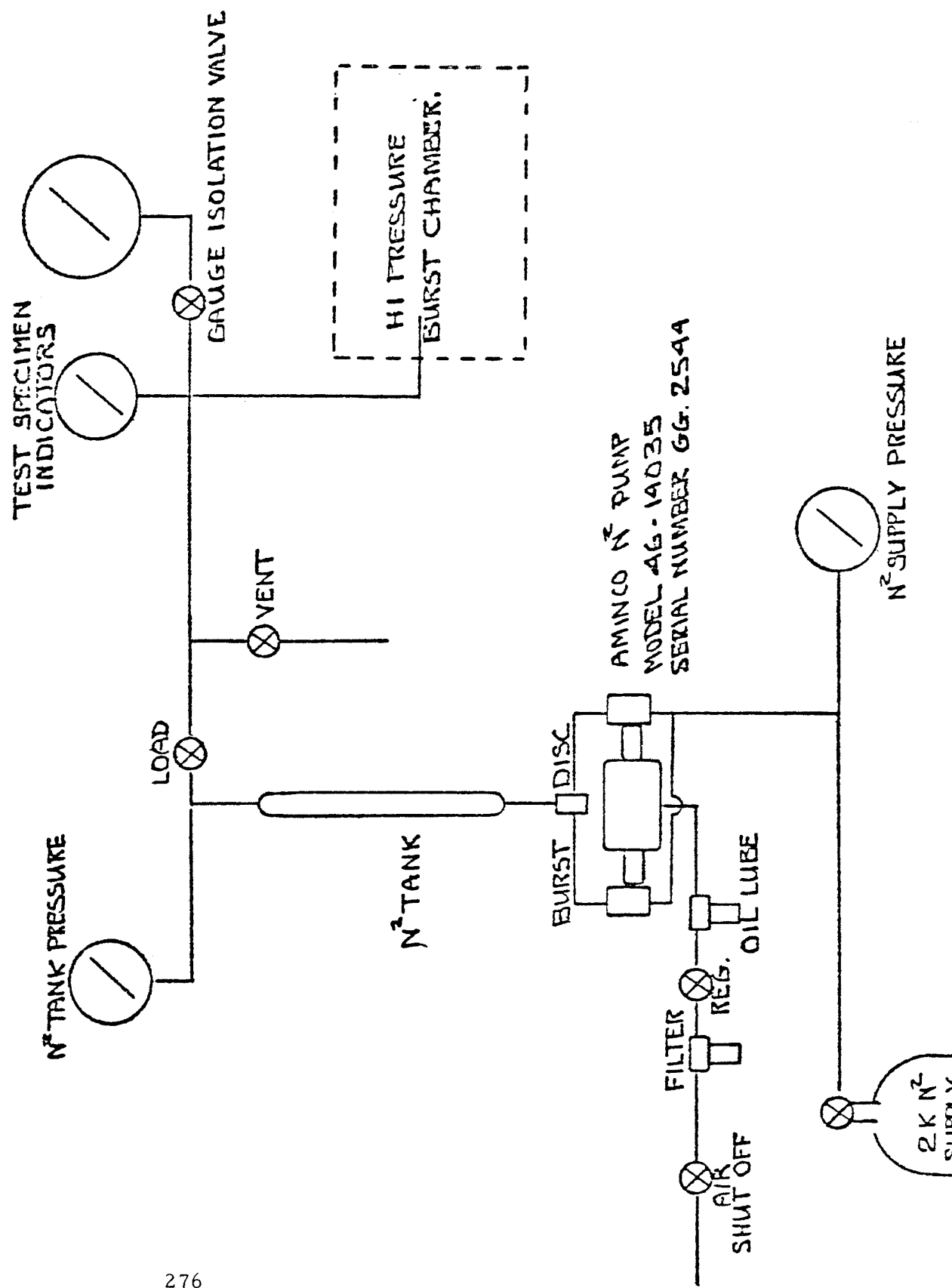


FIGURE E3
PNEUMATIC TEST SYSTEM

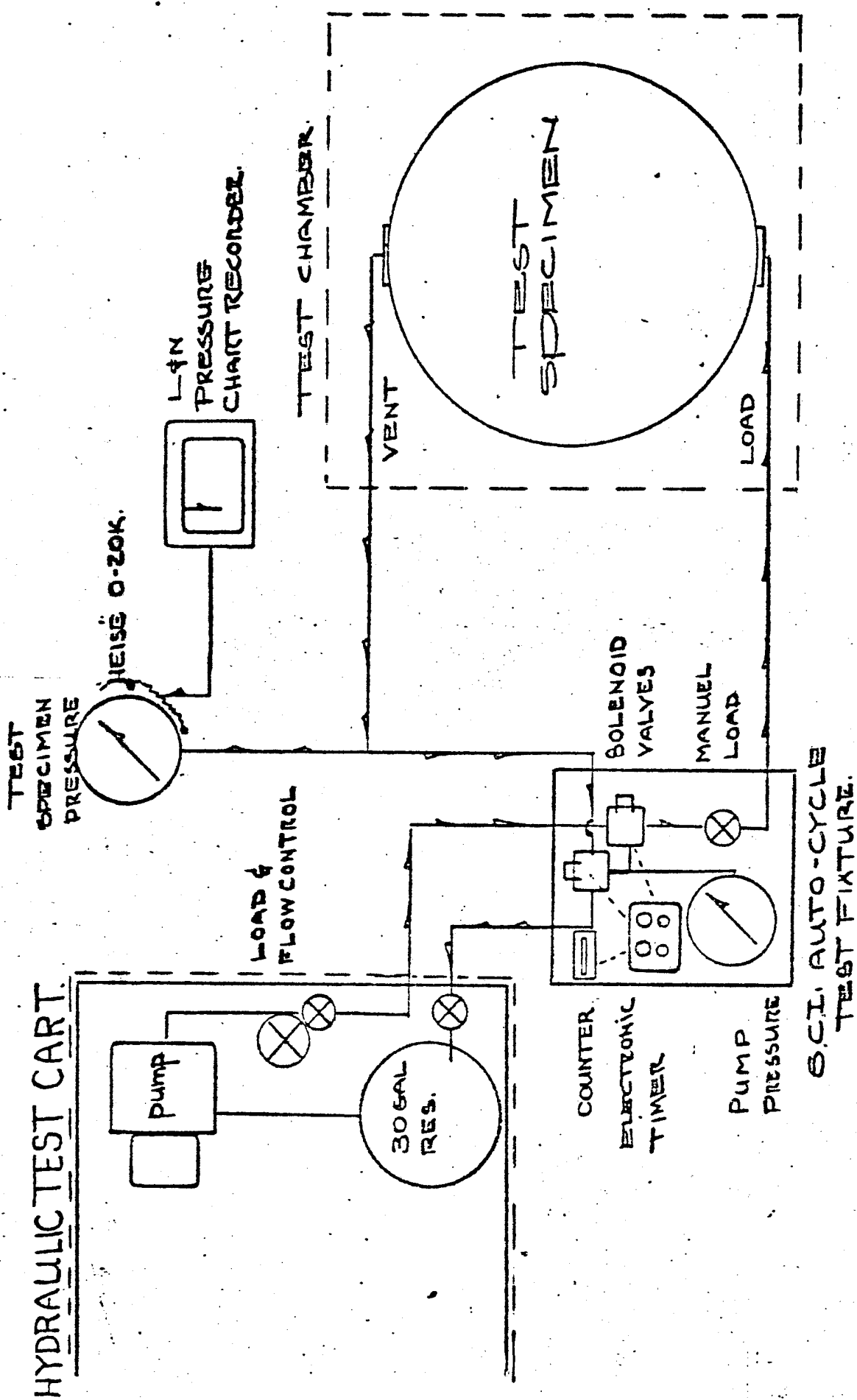


FIGURE E4
FATIGUE CYCLE TEST SYSTEM

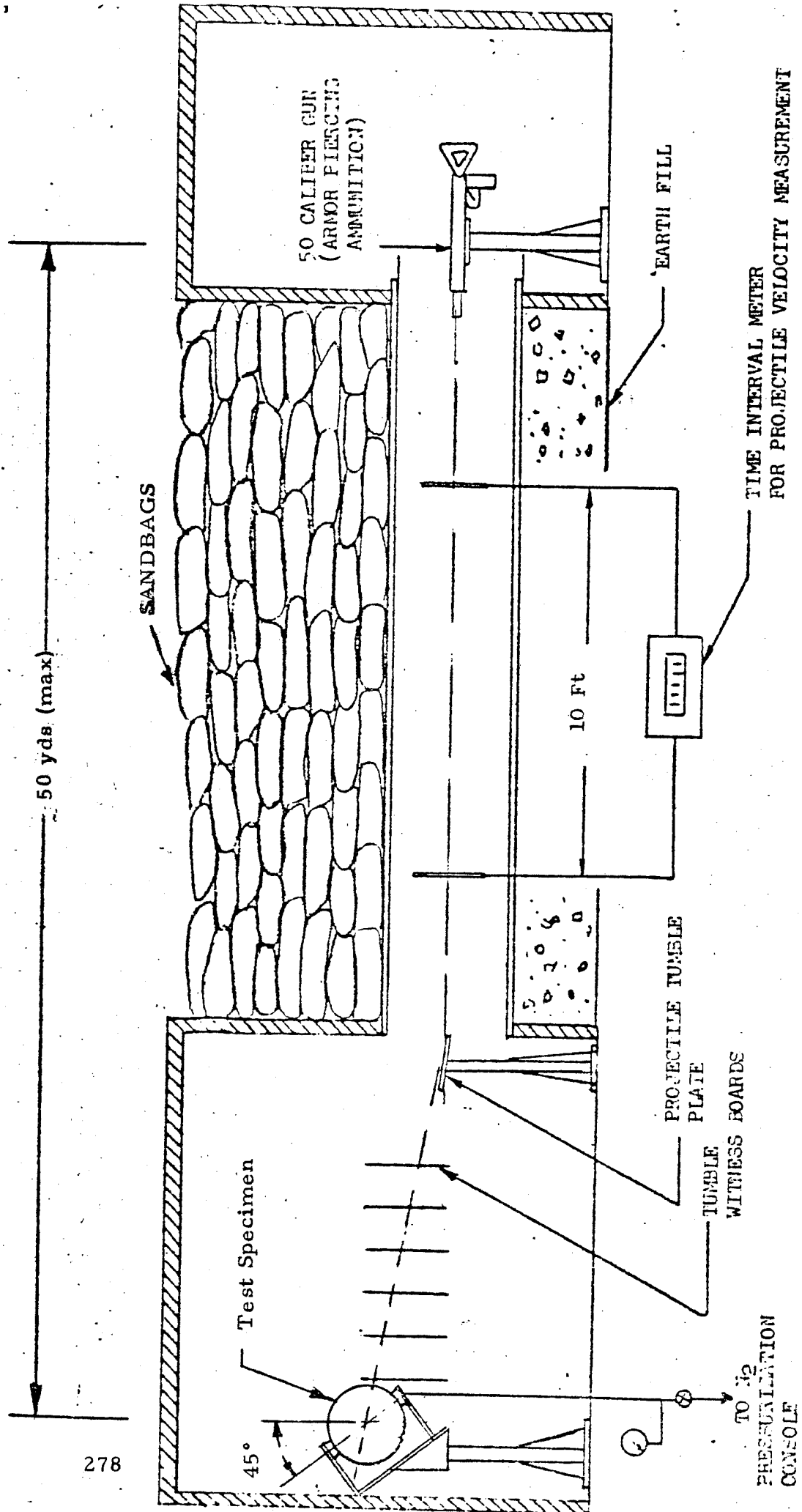


FIGURE E5
 GUNFIRE TEST SYSTEM

SCI Specification 74-44

Date: _____

ENCLOSURE EI

TEST DATA SHEETS

Date: _____

DATA SHEET NUMBER 1

PART NUMBER: _____

TEST SPECIMEN NUMBER: _____

HYDRAULIC BURST TEST, Paragraph 7.1

<u>Parameter</u>	<u>Required</u>	<u>Actual</u>
Test Media	Inhibited Water	_____
Pressure Rise Rate		_____ psi/min
Expected Burst Pressure (EBP)		_____ psig
Time at EBP	3 minutes	_____ min
Pressure Rise Rate		_____ psi/min
Failure Pressure	As Measured	_____ psig

Mode of Failure _____

Tested By _____ Date _____

Witness _____ Date _____

Date: _____

DATA SHEET NUMBER 2

PART NUMBER: _____

TEST SPECIMEN NUMBER: _____

PNEUMATIC BURST TEST, Paragraph 7.2

<u>Parameter</u>	<u>Required</u>	<u>Actual</u>
Test Media	Gaseous Nitrogen	_____
Pressure Rise Rate		psi/min
Fluid Temperature (shall not exceed)	160°F	°F
Failure Pressure	As Measured	psig

Mode of Failure _____

Tested By _____ Date _____

Witness _____ Date _____

Date: _____

DATA SHEET NUMBER 3

PART NUMBER: _____

TEST SPECIMEN NUMBER: _____

CYCLIC FATIGUE TEST, Paragraph 7.3

<u>Parameter</u>	<u>Required</u>	<u>Actual</u>
Test Media	Hydraulic Fluid	_____
Operating Pressure (MOP)		_____ psig
Hold Period	10 sec	_____ sec
Cyclic Rate	1 to 2 cpm	_____ cpm
Cycles	2000	_____

Vessel Examination _____

Tested By _____ Date _____

Witness _____ Date _____

Date: _____

DATA SHEET NUMBER 4

PART NUMBER: _____

TEST SPECIMEN NUMBER: _____

HYDRAULIC SUSTAINED LOAD TEST, Paragraph 7.4

<u>Parameter</u>	<u>Required</u>	<u>Actual</u>
Test Media	Inhibited Water	_____
Pressure Rise Rate	_____	psi/min
Operating Pressure (MOP)	_____	psi
Time at MOP	96 hours	hours
Depressurization Rate	_____	Psi/min
Vessel Examination	_____	_____
Pressure Rise Rate	_____	psi/min
Failure Pressure	As Measured	psig

Date _____

DATA SHEET NUMBER 4 Cont.

PART NUMBER: _____

TEST SPECIMEN NUMBER: _____

Mode of Failure _____

Tested By _____ Date _____

Witness _____ Date _____

Date _____

DATA SHEET NUMBER 5

PART NUMBER: _____

TEST SPECIMEN NUMBER: _____

GASEOUS HYDROGEN SUSTAINED LOAD TEST, Paragraph 7.5

<u>Parameter</u>	<u>Required</u>	<u>Actual</u>
Test Media	Gaseous Hydrogen	_____
Volume Filling Material	As Necessary	_____
Weight of Material	As Necessary	_____ pounds
Pressure Rise Rate	_____	psi/min
Operating Pressure(MOP)	_____	psi
Fluid Temperature (shall not exceed)	160°F	_____ °F
Time at MOP	96 hours	_____ hours
Depressurization Rate	_____	psi/min
Fluid Temperature (shall not exceed)	160°F	_____ °F
Vessel Examination	_____	_____
Tested By _____	Date _____	_____
Witness _____	Date _____	_____

Date _____

DATA SHEET NUMBER 6

PART NUMBER: _____

TEST SPECIMEN NUMBER: _____

GUNFIRE TEST, Paragraph 7.6

<u>Parameter</u>	<u>Required</u>	<u>Actual</u>
Test Media	Gaseous Nitrogen	_____
Pressure Rise Rate		_____ psi/min
Operating Pressure (MOP)		_____ psi
Gun Distance	<50 yards	_____ yards
Projectile	50 Caliber AP	_____
Muzzle Velocity	2800 ± 100 fps	_____ fps

Mode of Failure _____

Tested By _____ Date _____

Witness _____ Date _____

APPENDIX F

**SIZING AND PERFORMANCE TEST
PRESSURE/STRAIN PLOTS FOR
KEVLAR/ALUMINUM PRESSURE VESSELS**

APPENDIX F

FIGURE INDEX

Figure Number	Vessel Serial Number	Type of Test	Page Number
F -1	S -1	Sizing	289
F -2			290
F -3			291
F -4	S -2	Sizing	292
F -5			293
F -6			294
F -7		Sustained Load	295
F -8			296
F -9			297
F -10	S -4	Sizing	298
F -11			299
F -12			300
F -13		Hydroburst	301
F -14			302
F -15			303
F -16	S -5	Sizing	304
F -17			305
F -18			306
F -19		Cyclic Fatigue	307
F -20			308
F -21			309
F -22	S -6	Sizing	310
F -23		Cyclic Fatigue	311
F -24			312

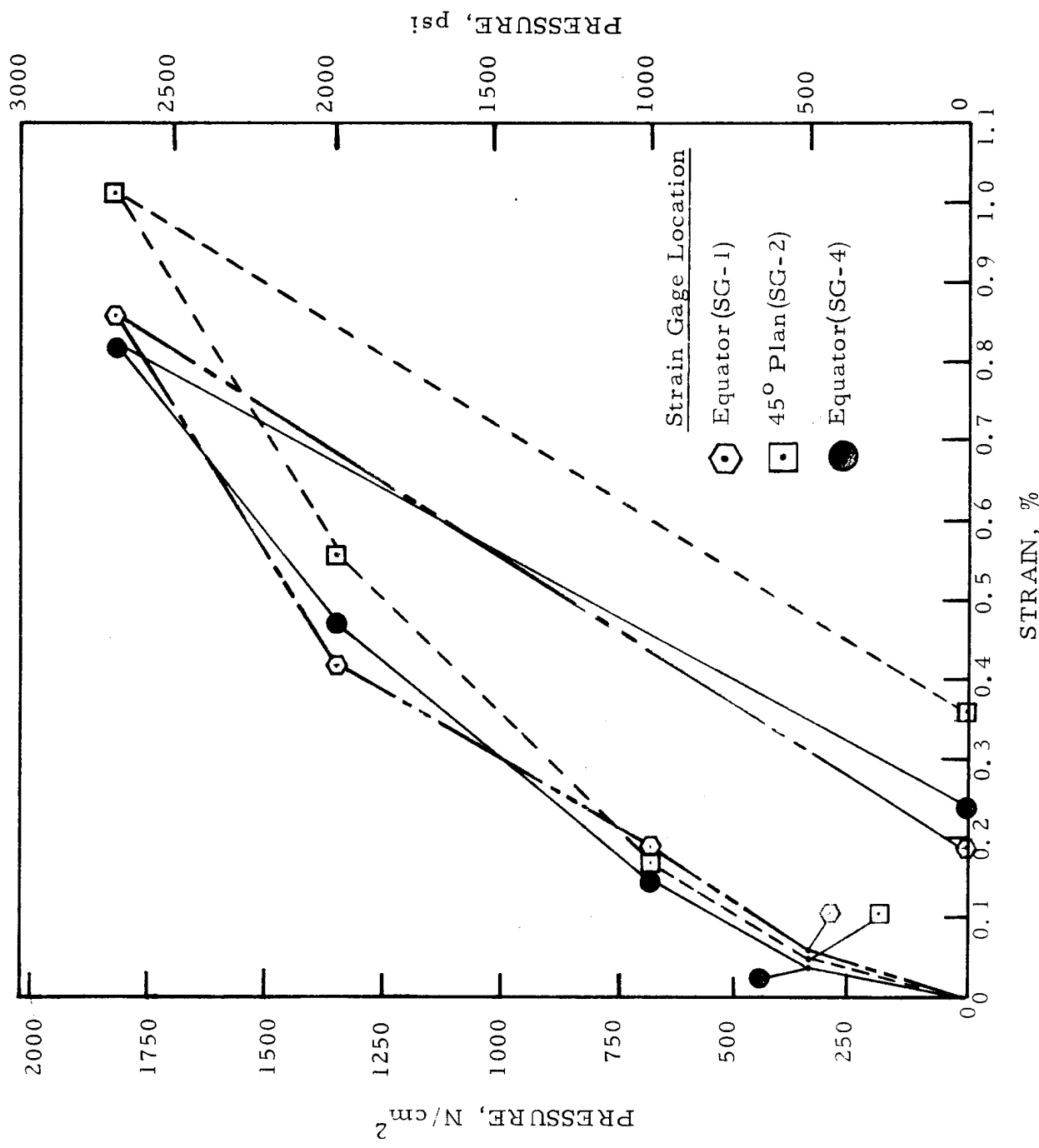


FIGURE F-1: Strains Obtained From Circumferentially Oriented Strain Gages During Pressure Sizing of Keviar/Aluminum Vessel S-1

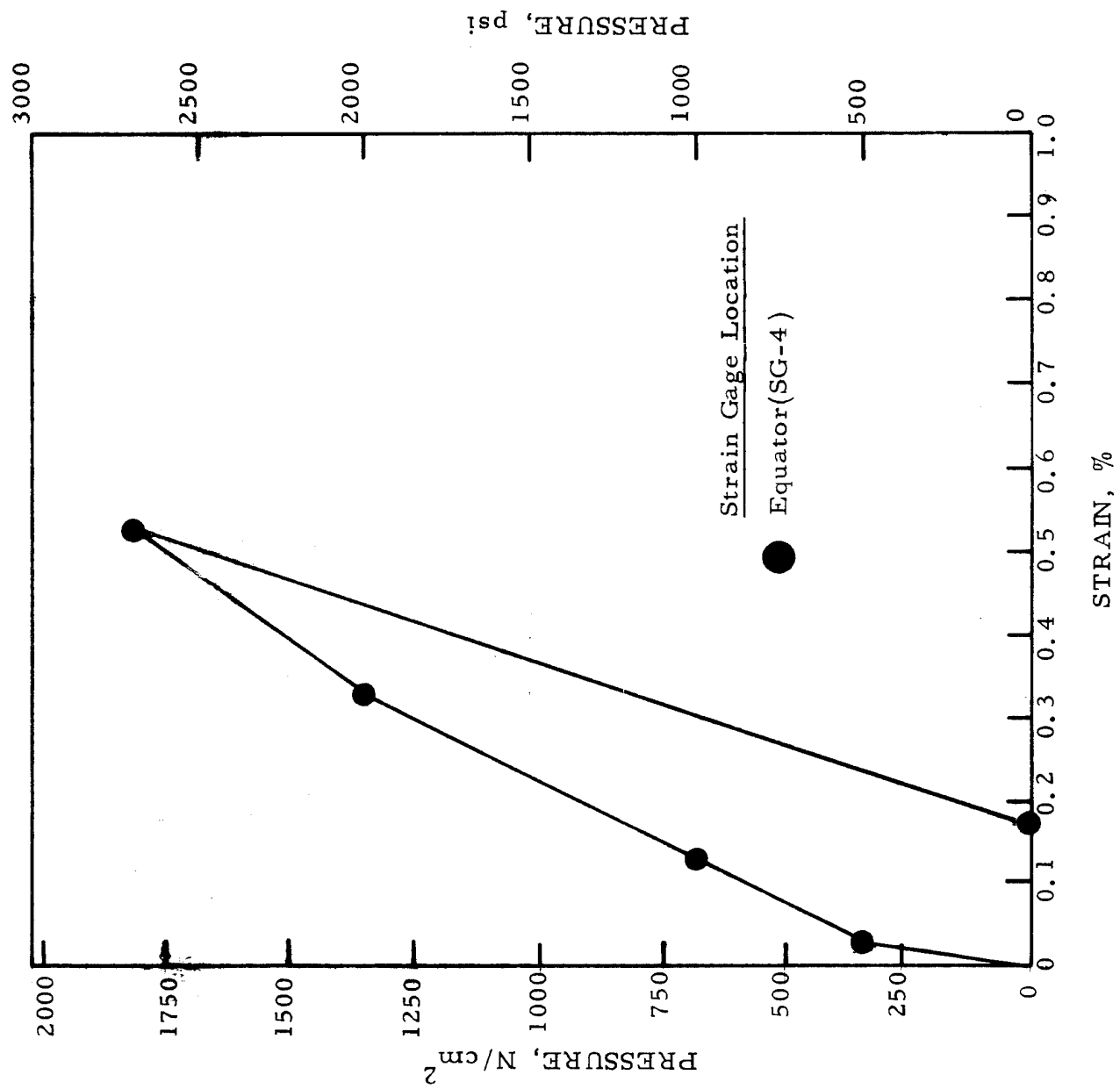


FIGURE F-2: Strains Obtained From Longitudinally Oriented Strain Gages During Pressure Sizing of Kevlar/Aluminum Vessel S-1

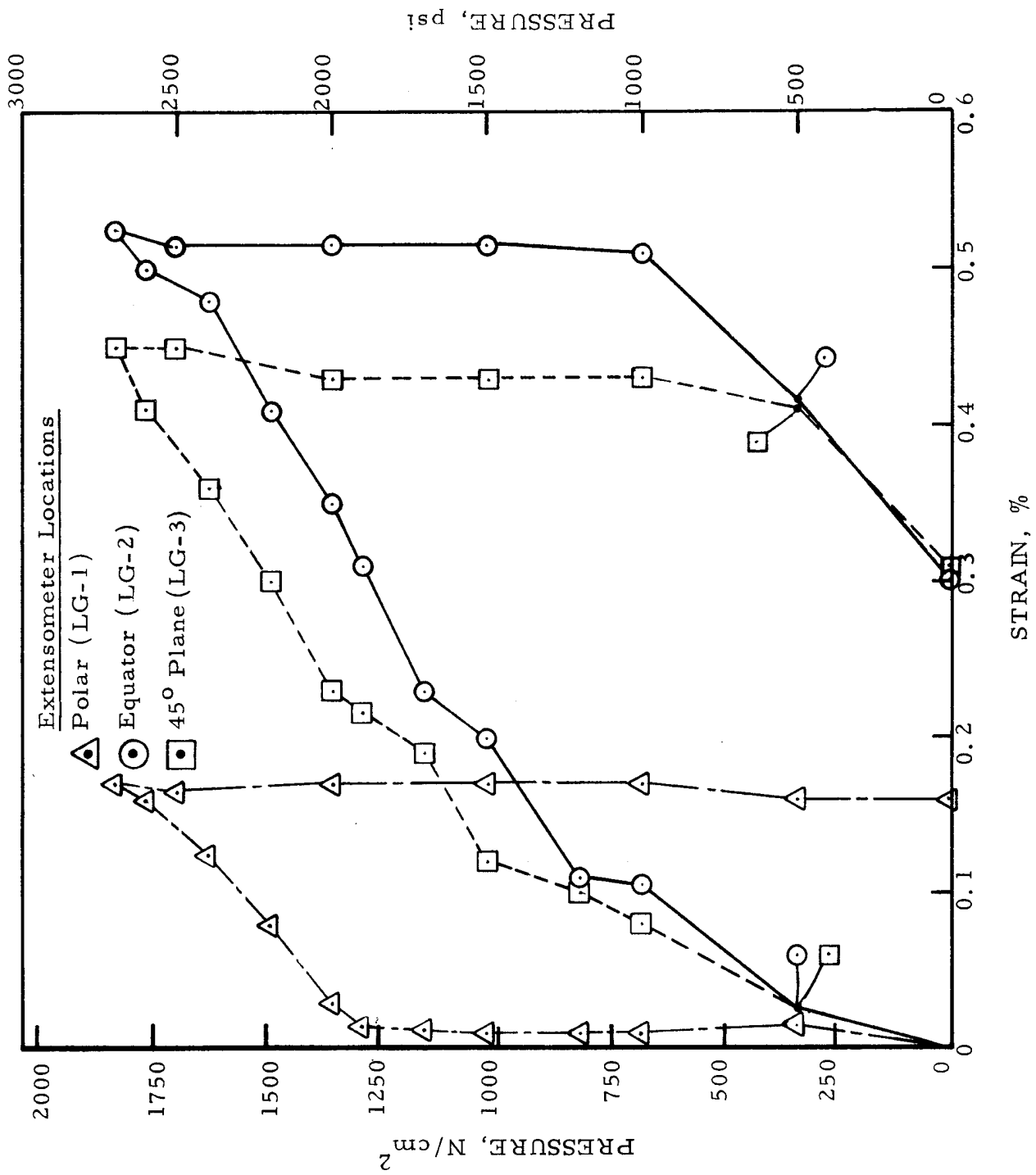


FIGURE F-3: Strains Obtained From Great Circle Extensometers During Pressure Sizing of Kevlar / Aluminum Vessel S-1

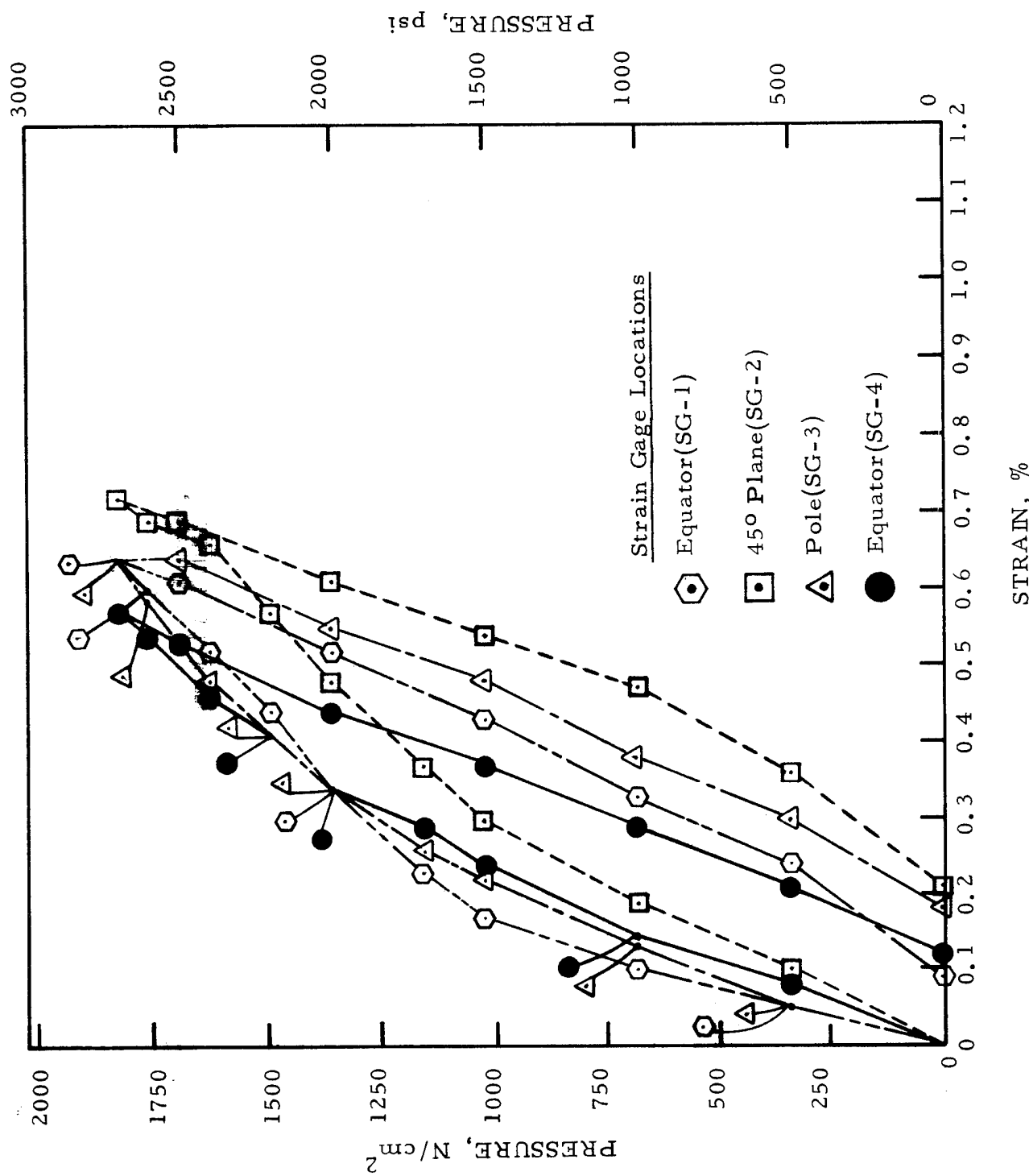


FIGURE F-4: Strains Obtained From Circumferentially Oriented Strain Gages During Pressure Sizing of Kevlar/Aluminum Vessel S-2

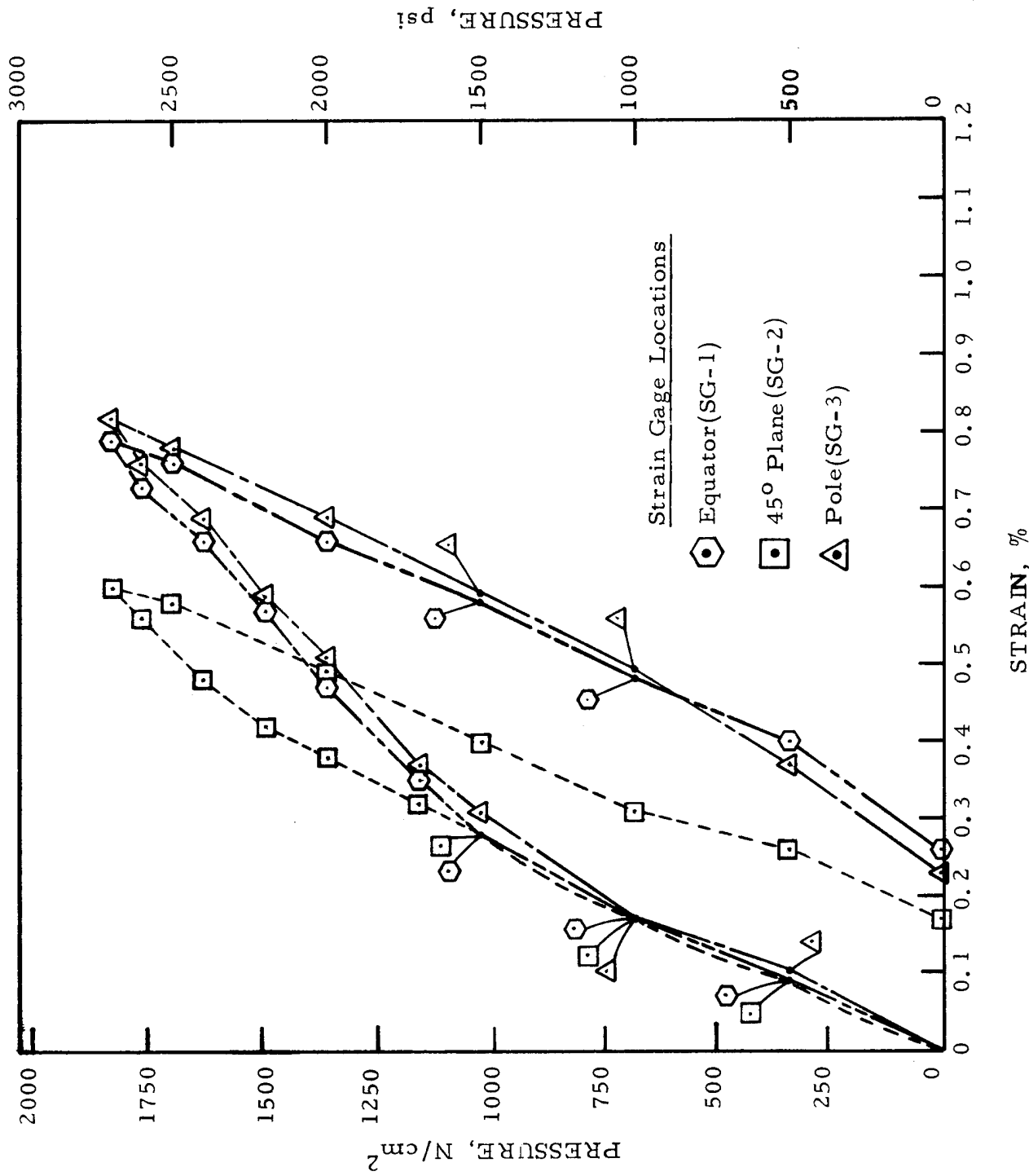


FIGURE F-5: Strains Obtained From Longitudinally Oriented Strain Gages During Pressure Sizing of Keviar/Aluminum Vessel S-2

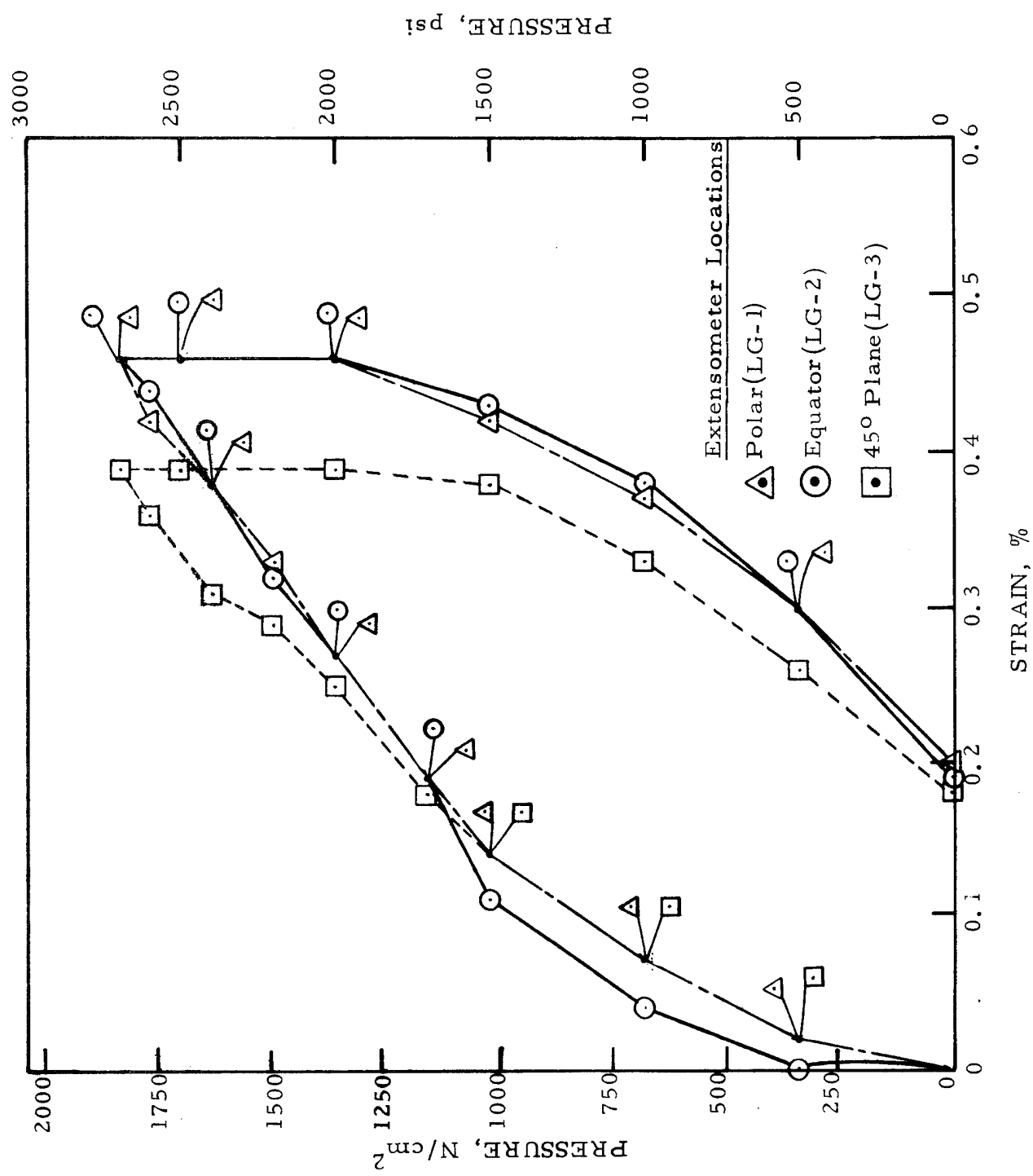


FIGURE F-6: Strains Obtained From Great Circle Extensometers During Pressure Sizing of Kevlar/ Aluminum Vessel S-2

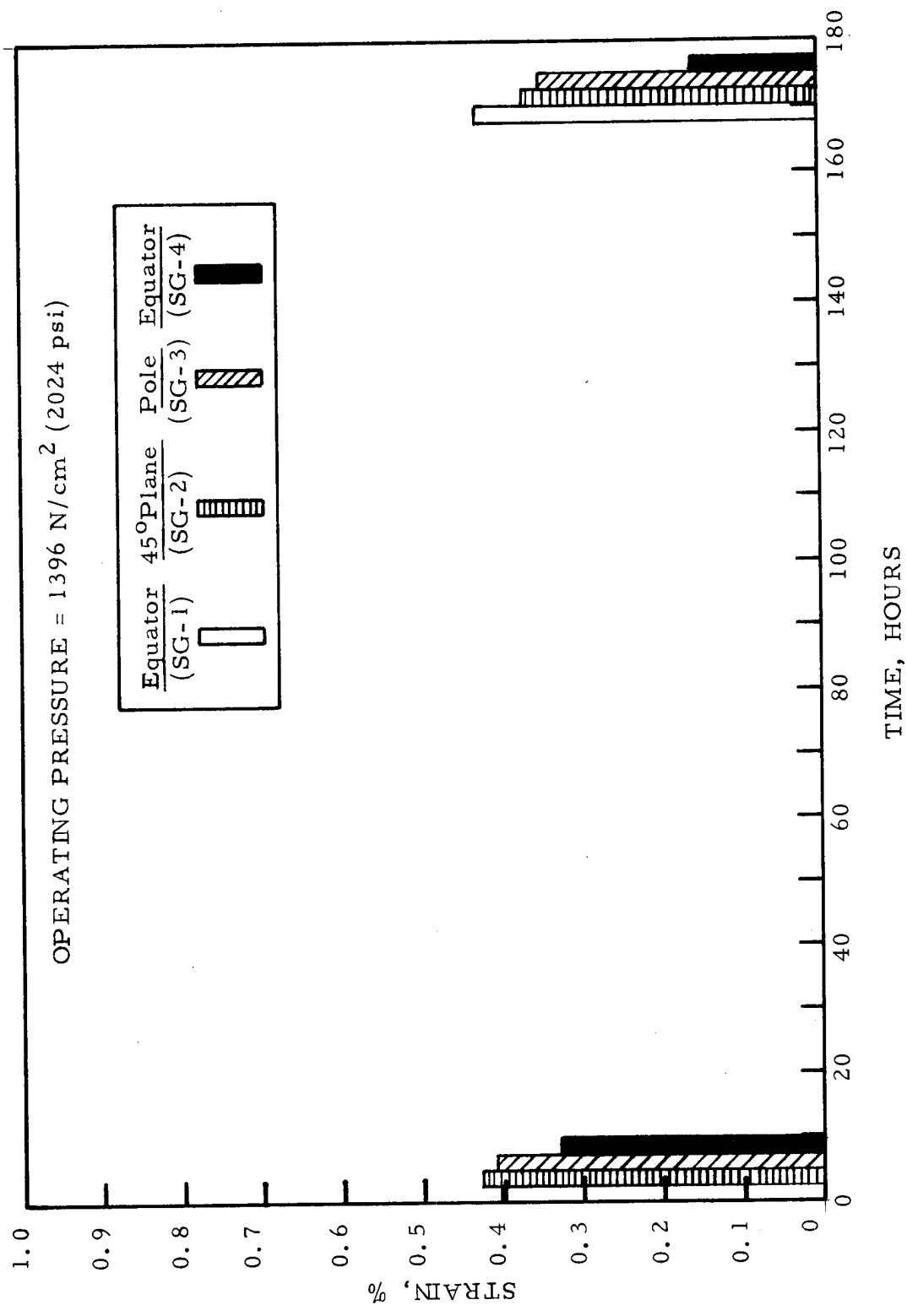


FIGURE F-7: Strains Obtained From Circumferentially Oriented Strain Gages During Sustained Load Test of Kevlar/Aluminum Vessel S-2

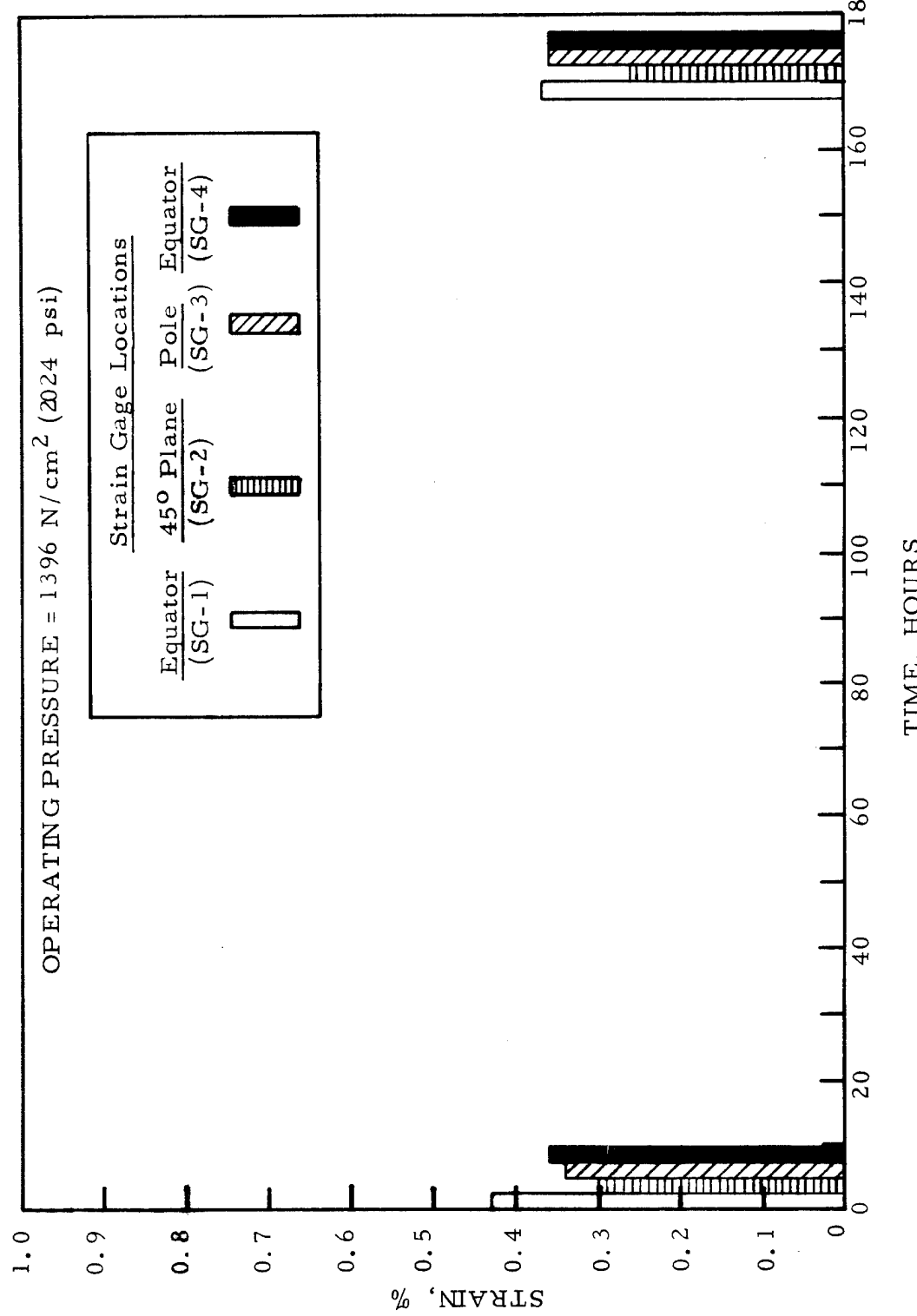


FIGURE F-8: Strains Obtained From Longitudinally Oriented Strain Gages During Sustained Load Test of Kevlar/Aluminum Vessel S-2

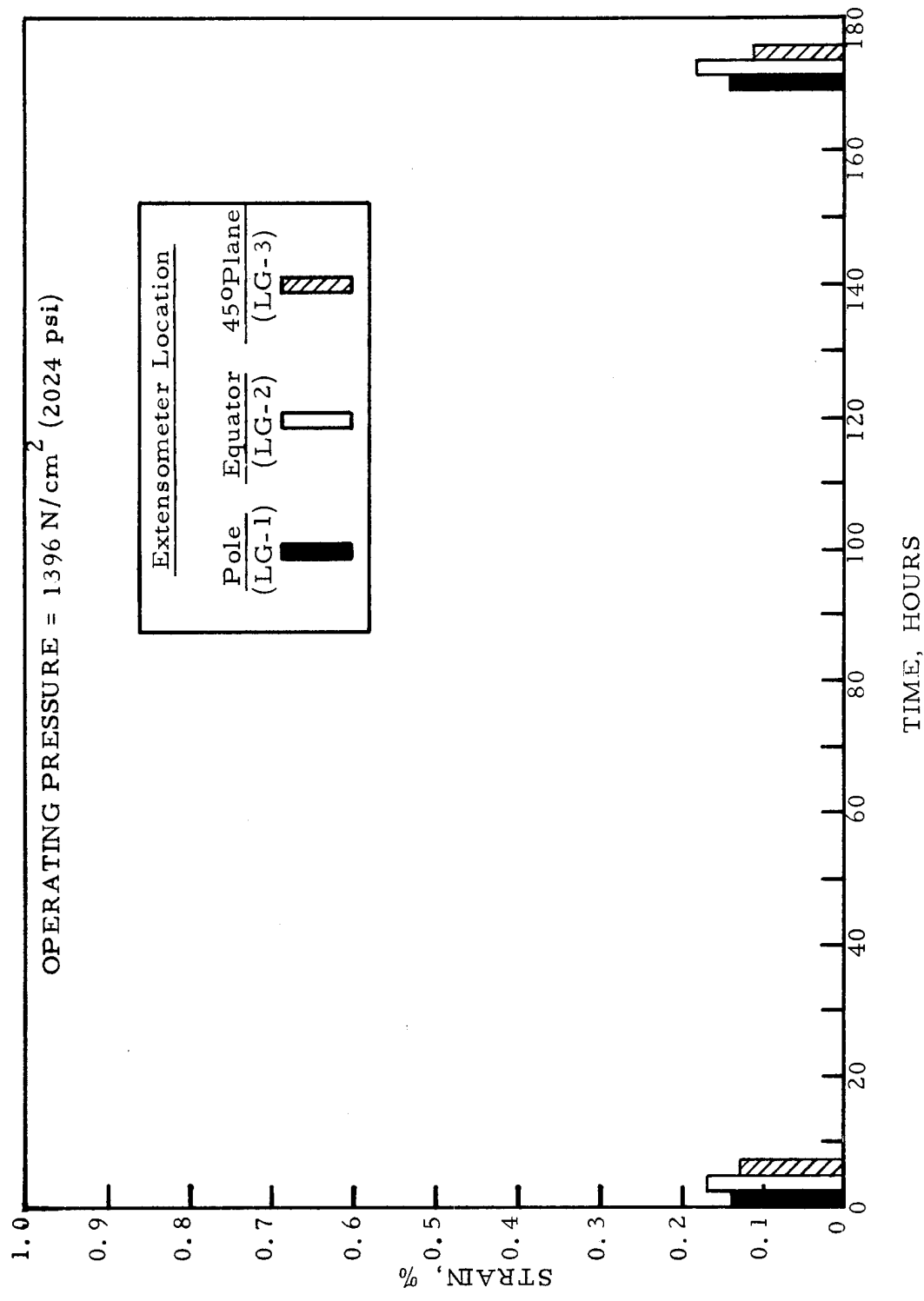


FIGURE F-9: Strains Obtained From Great Circie Extensometers During Sustained Load Test of Kevlar/Aluminum Vessel S-2

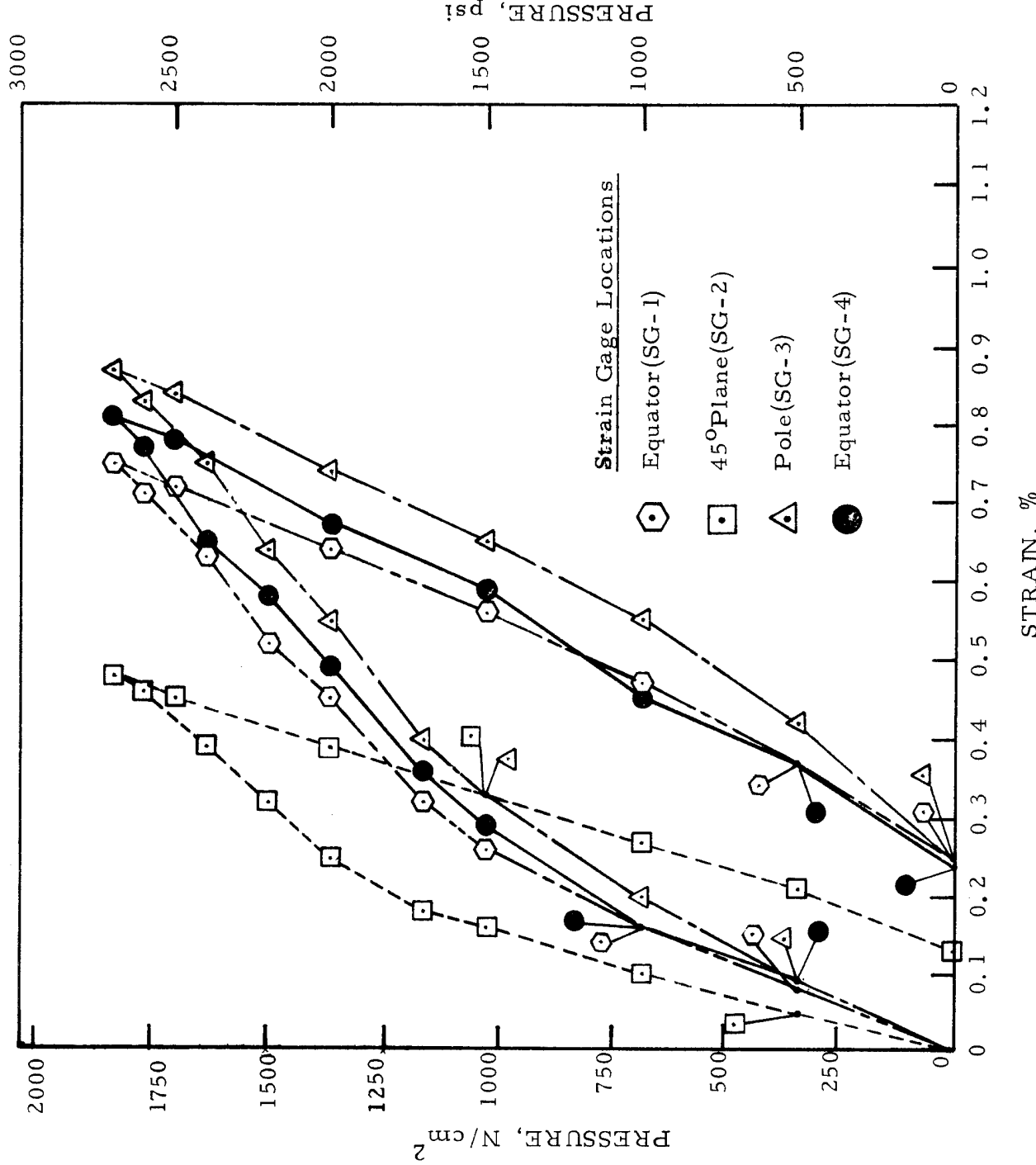


FIGURE F-10: Strains Obtained From Circumferentially Oriented Strain Gages During Pressure Sizing of Kevlar/Aluminum Vessel S-4

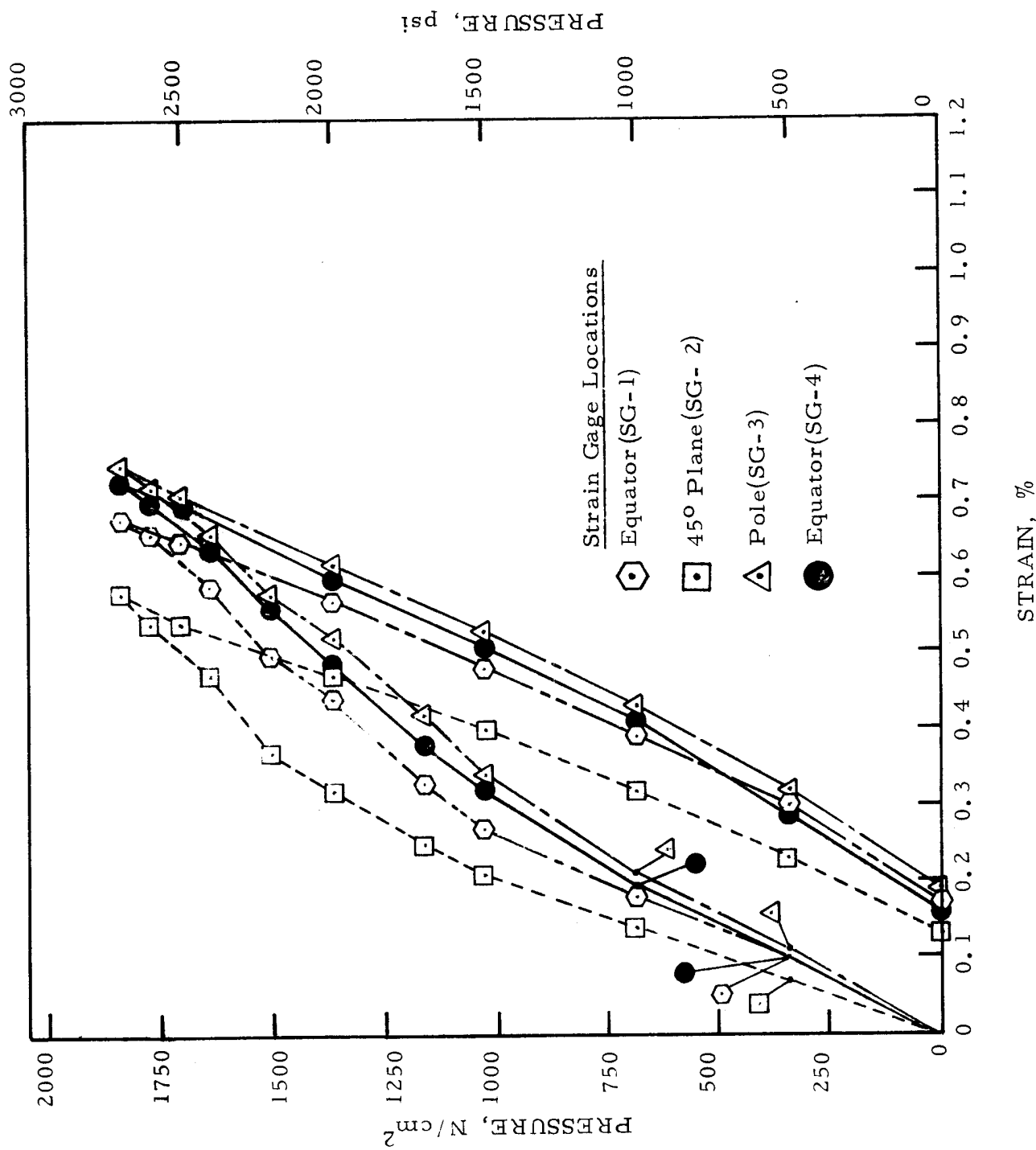


FIGURE F-11: Strains Obtained From Longitudinally Oriented Strain Gages During Pressure Sizing of Keviar/Aluminum Vessel S-4

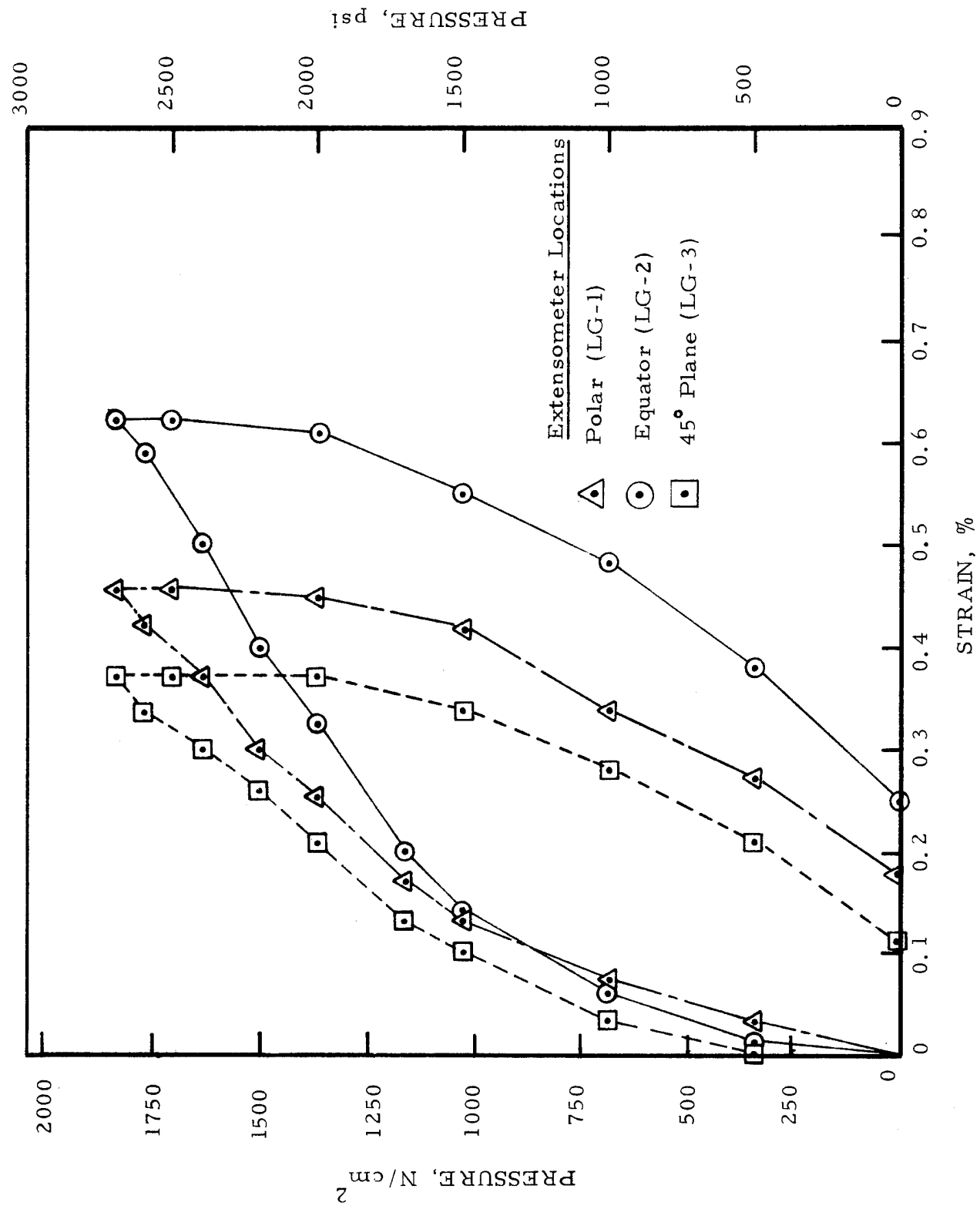


FIGURE F-12: Strains Obtained From Great Circle Extensometers During Pressure Sizing of Kevlar/Aluminum Vessel S-4

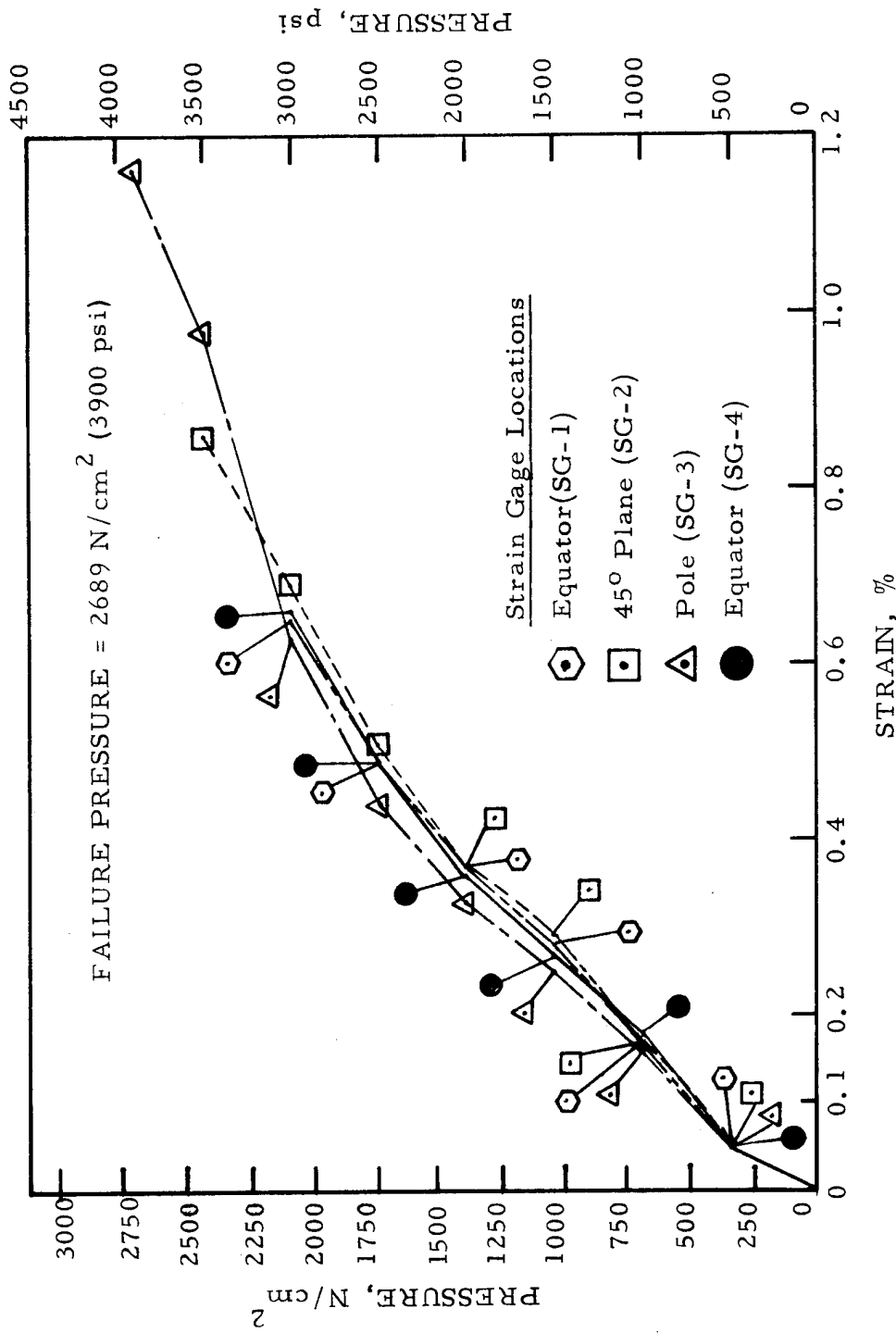


FIGURE F-13: Strains Obtained From Circumferentially Oriented Strain Gages During Hydraulic Burst of Kevlar/Aluminum Vessel S-4

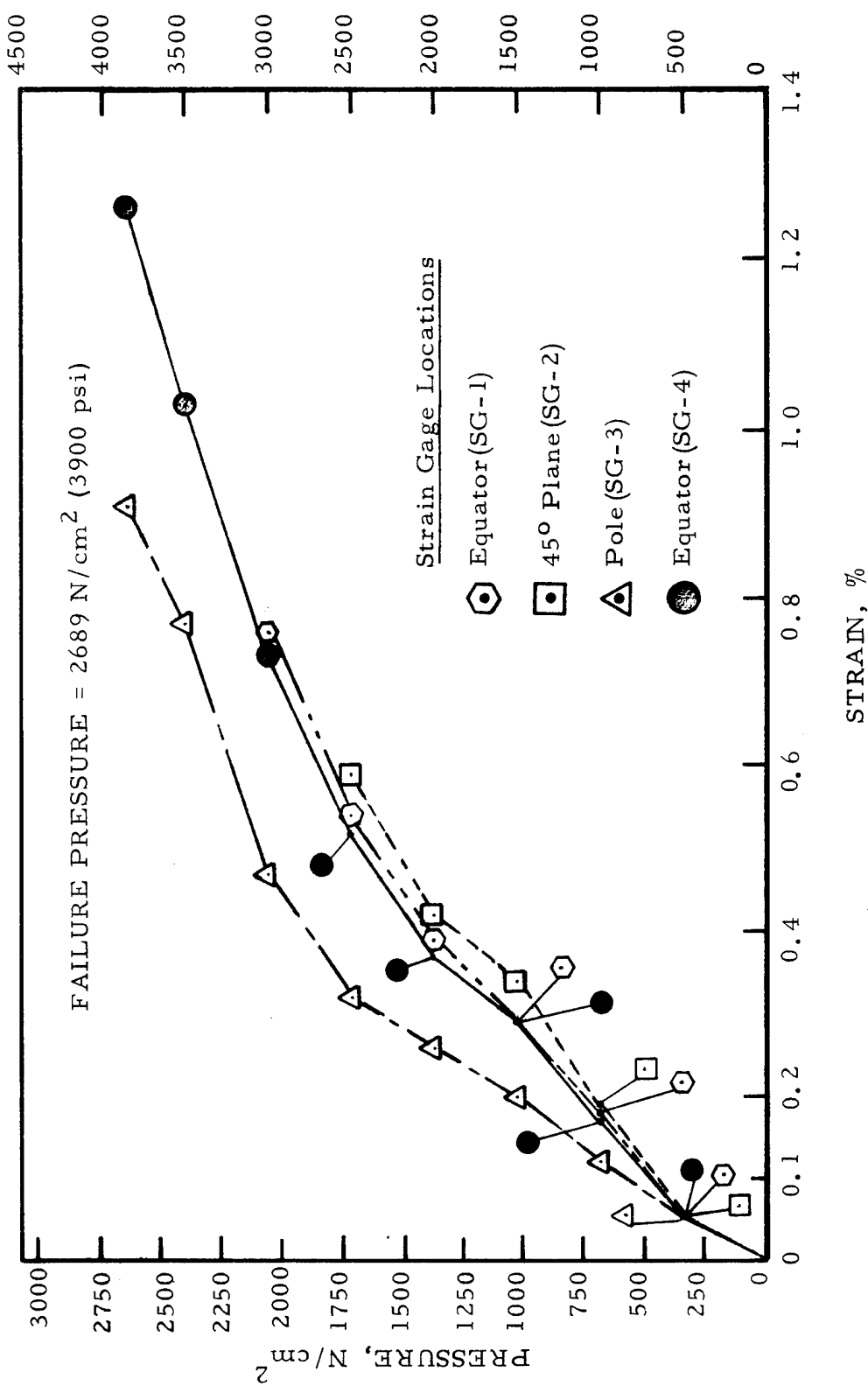


FIGURE F-14: Strains Obtained From Longitudinally Oriented Strain Gages During Hydraulic Burst of Kevlar/Aluminum Vessel S-4

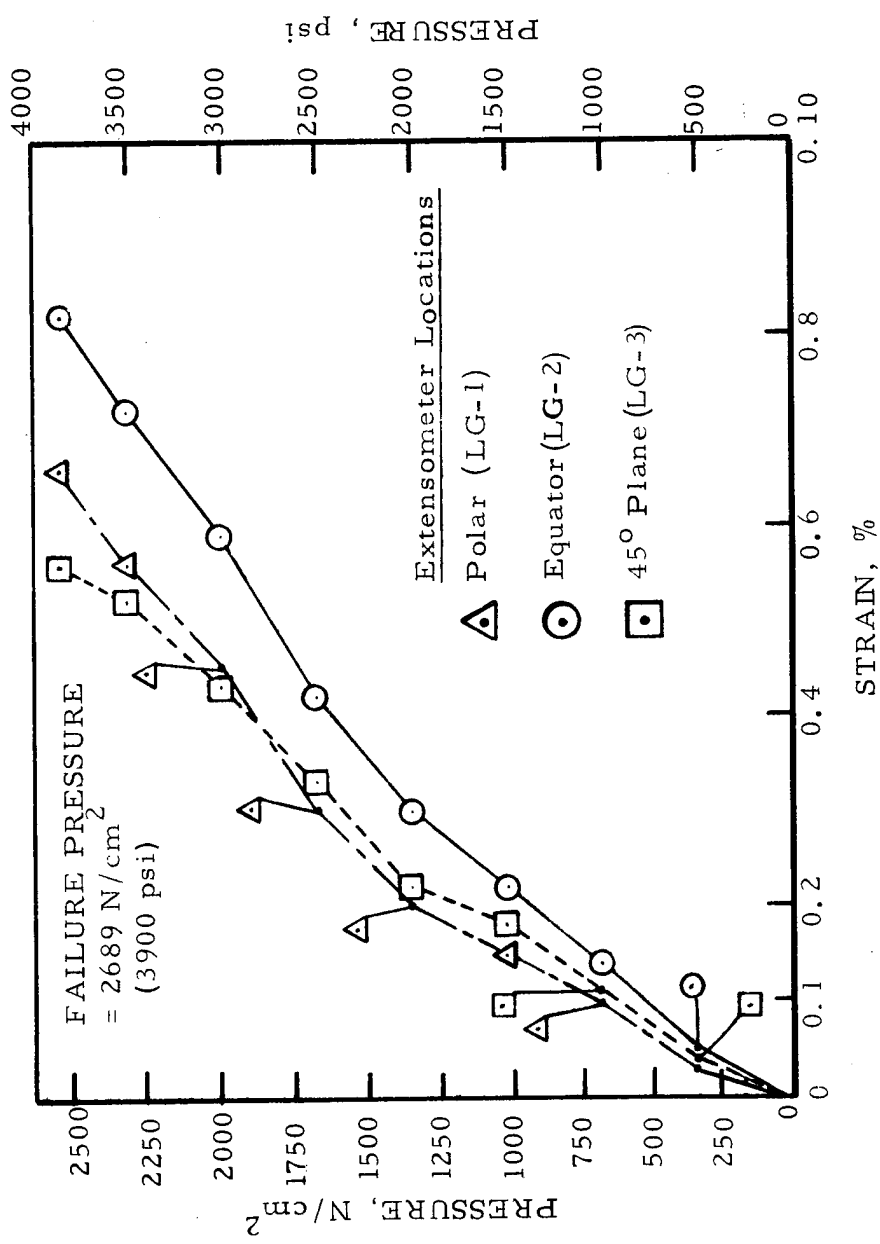


FIGURE F-15: Strains Obtained From Great Circle Extensometers During Hydraulic Burst of Kevlar/Aluminum Vessel S-4

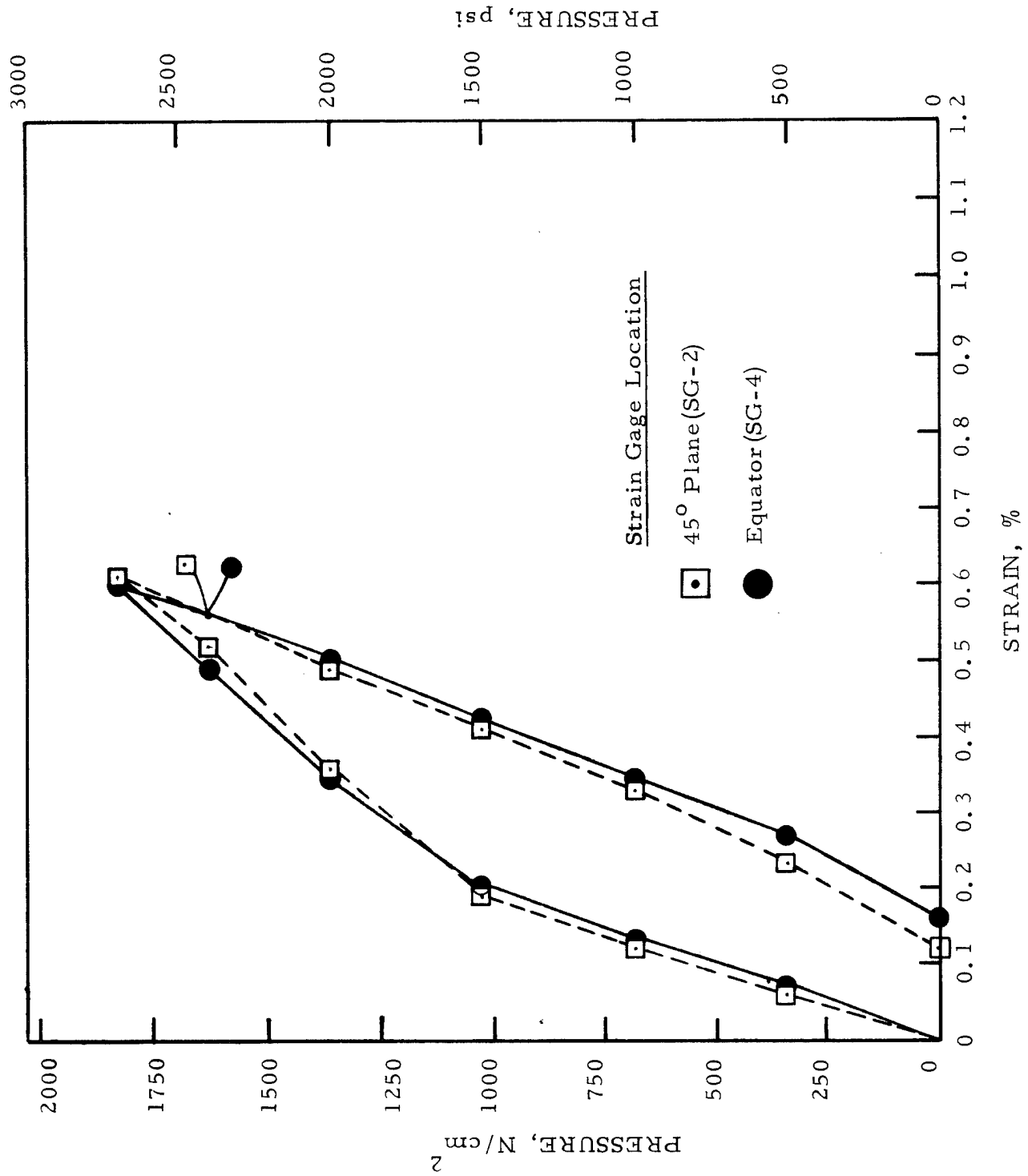


FIGURE F-16: Strains Obtained From Circumferentially Oriented Strain Gages During Pressure Sizing of Kevlar/Aluminum Vessel S-5

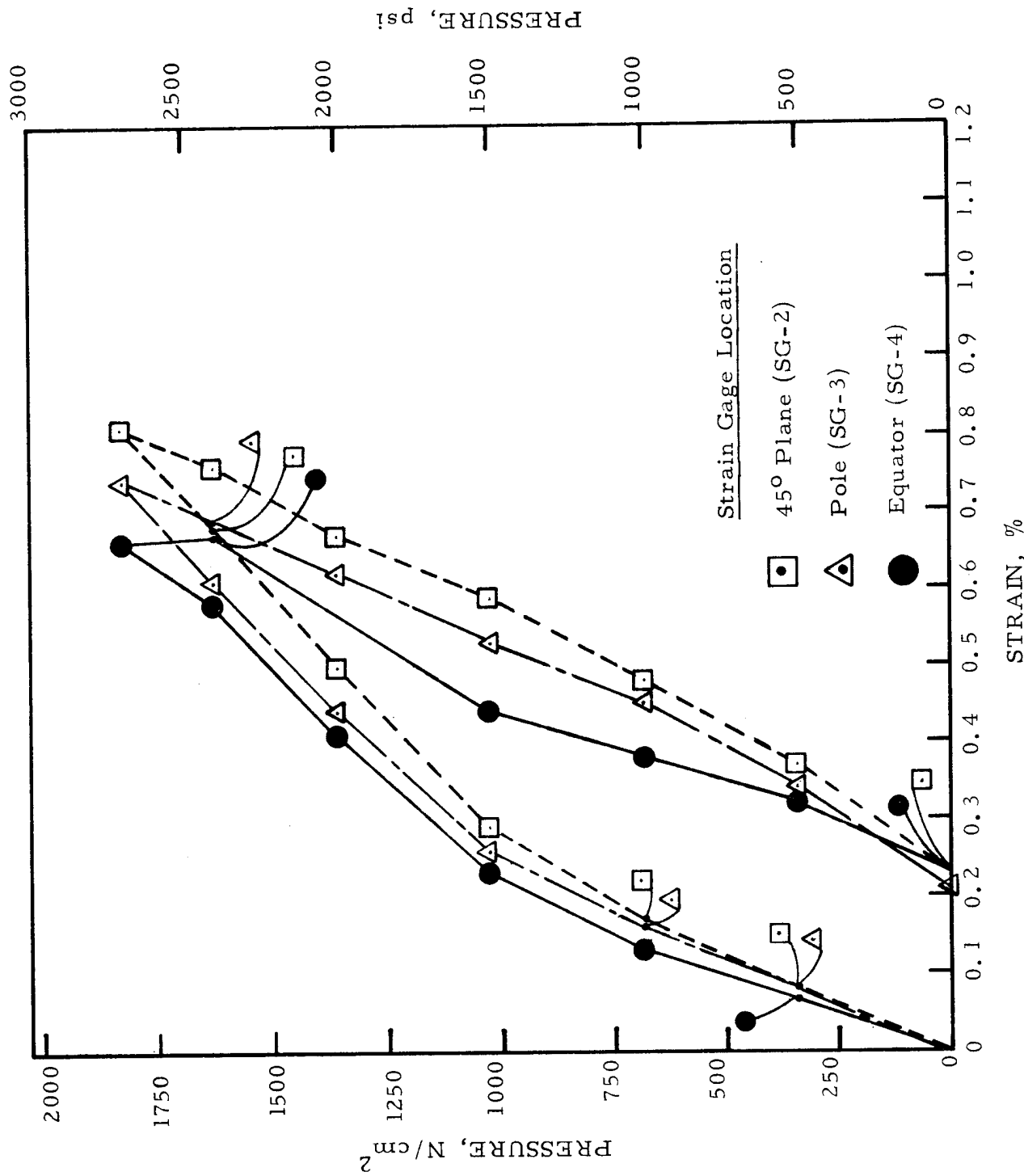


FIGURE F-17: Strains Obtained From Longitudinally Oriented Strain Gages During Pressure Sizing of Kevlar/Aluminum Vessel S-5

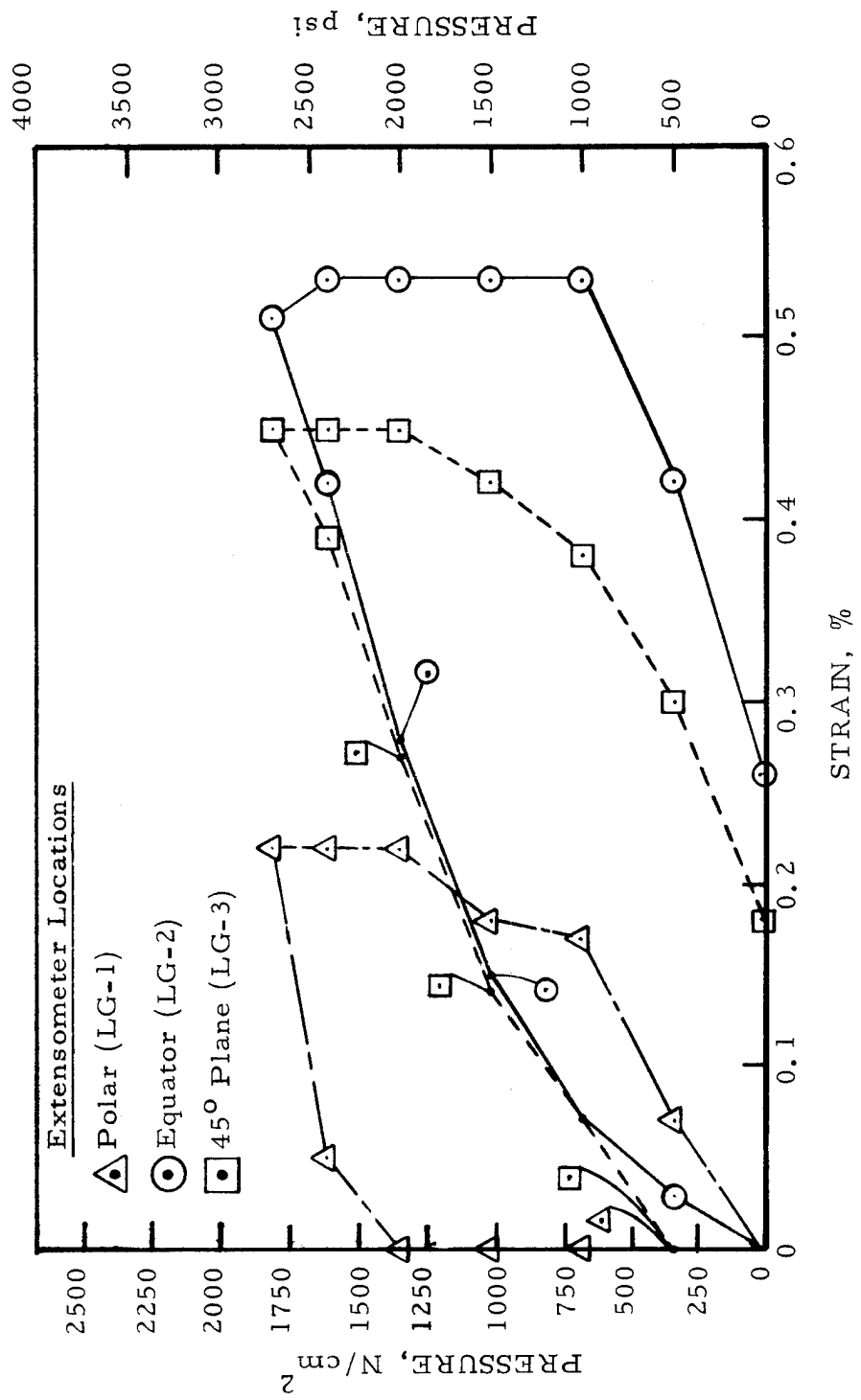


FIGURE F-18: Strains Obtained From Great Circle Extensometers During Pressure Sizing of Kevlar/Aluminum Vessel S-5

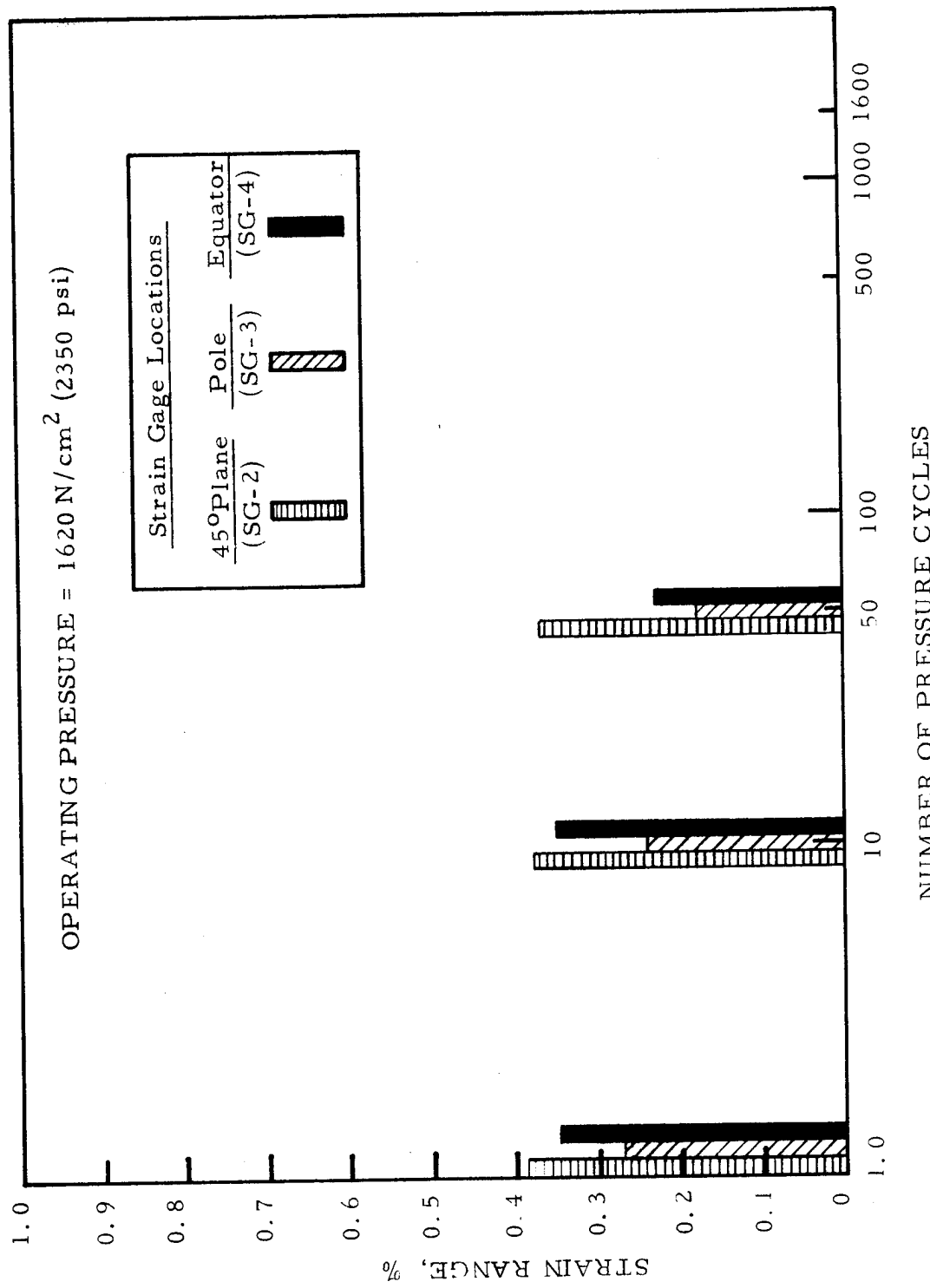


FIGURE F-19: Strains Obtained From Circumferentially Oriented Strain Gages During Cyclic Fatigue of Kevlar/Aluminum Vessel S-5

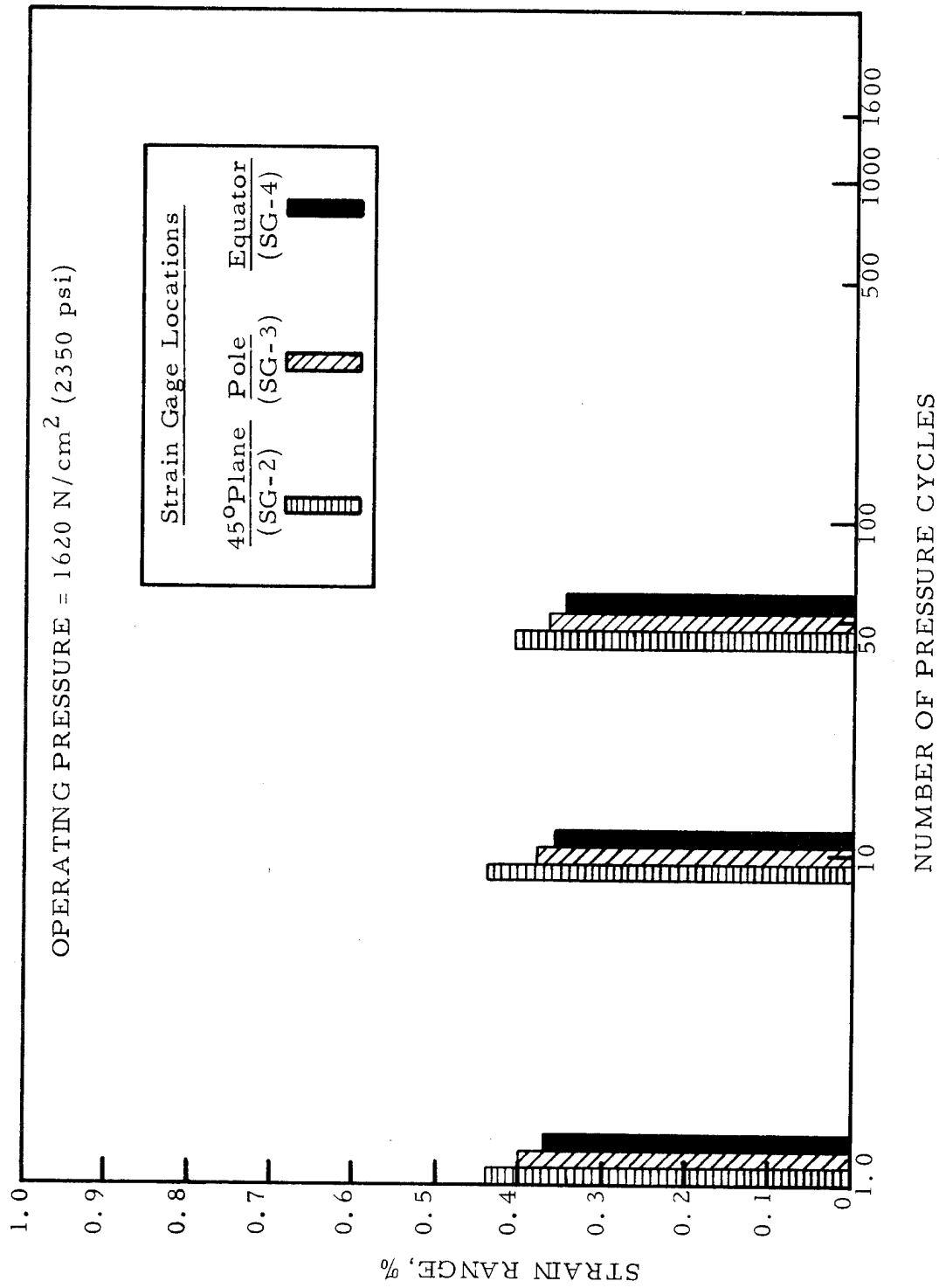


FIGURE F-20: Strains Obtained From Longitudinally Oriented Strain Gages During Cyclic Fatigue of Kevlar/Aluminum Vessel S-5

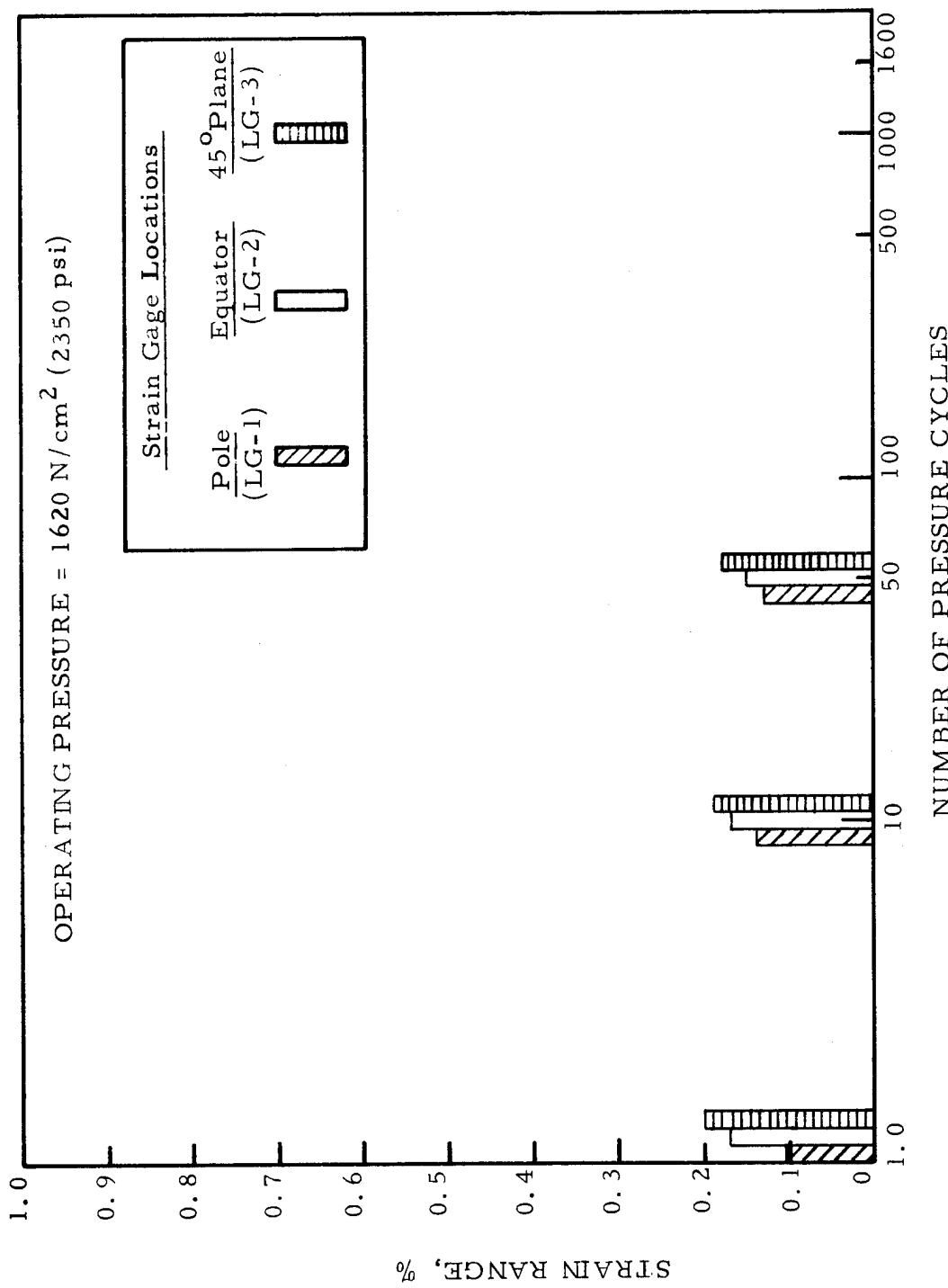


FIGURE F-21: Strains Obtained From Great Circle Extensometers During Cyclic Fatigue of Kevlar/Aluminum Vessel S-5

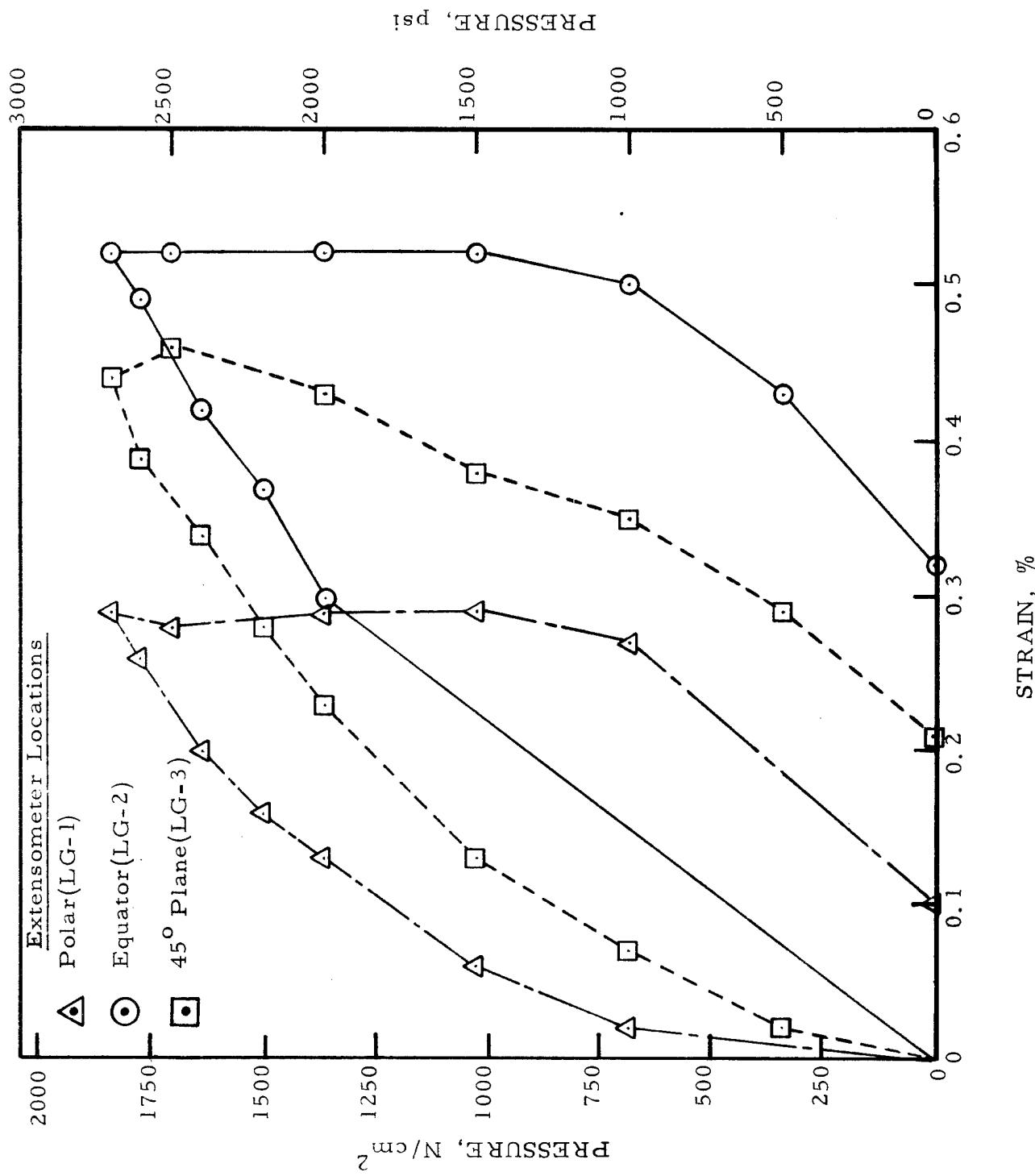


FIGURE F-22: Strains Obtained From Great Circles Extensometers During Pressure Sizing of Kevlar/Aluminum Vessel S-6

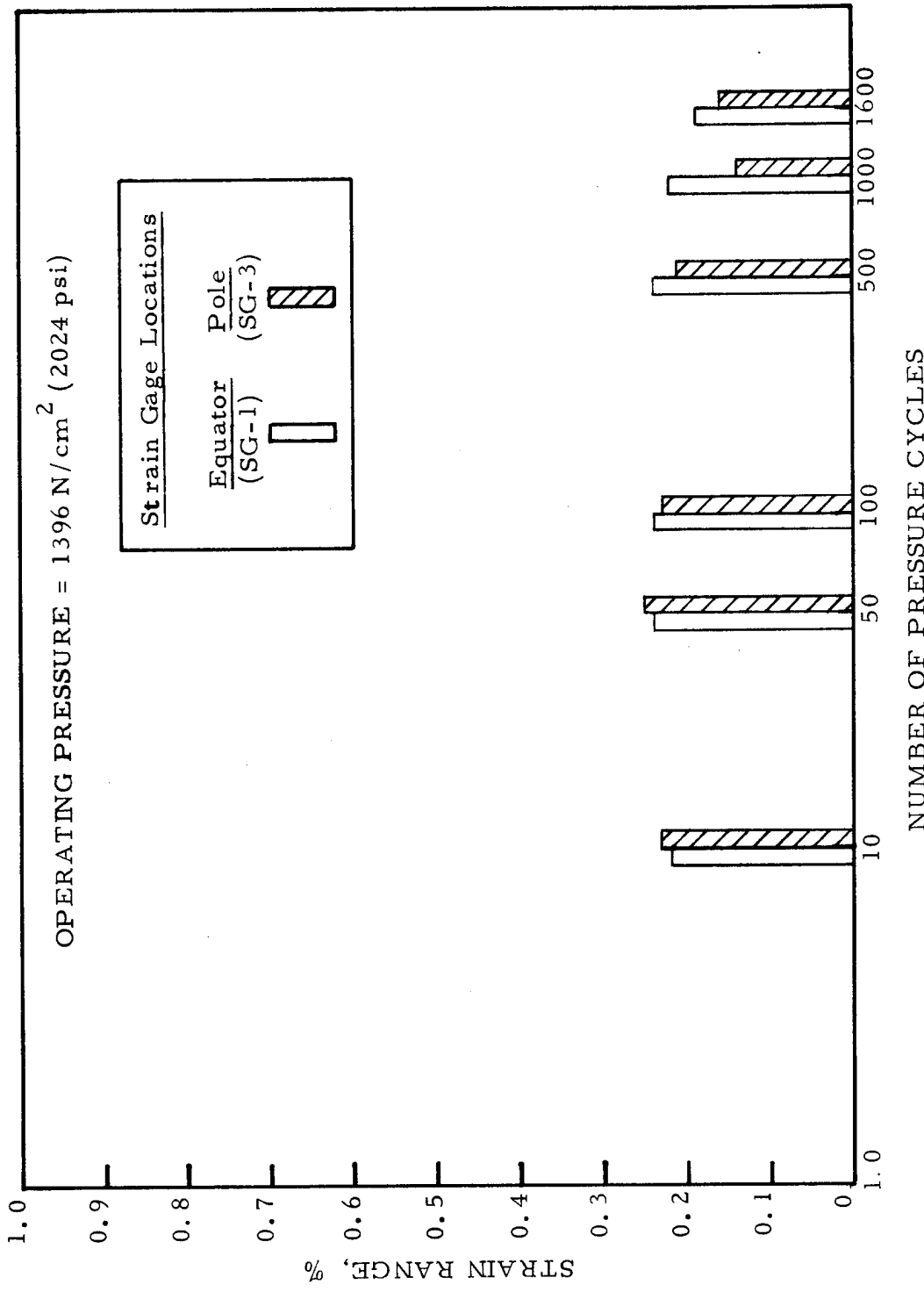


FIGURE F-23: Strains Obtained From Longitudinally Oriented Strain Gages During Cyclic Fatigue of Kevlar/Aluminum Vessel S-6

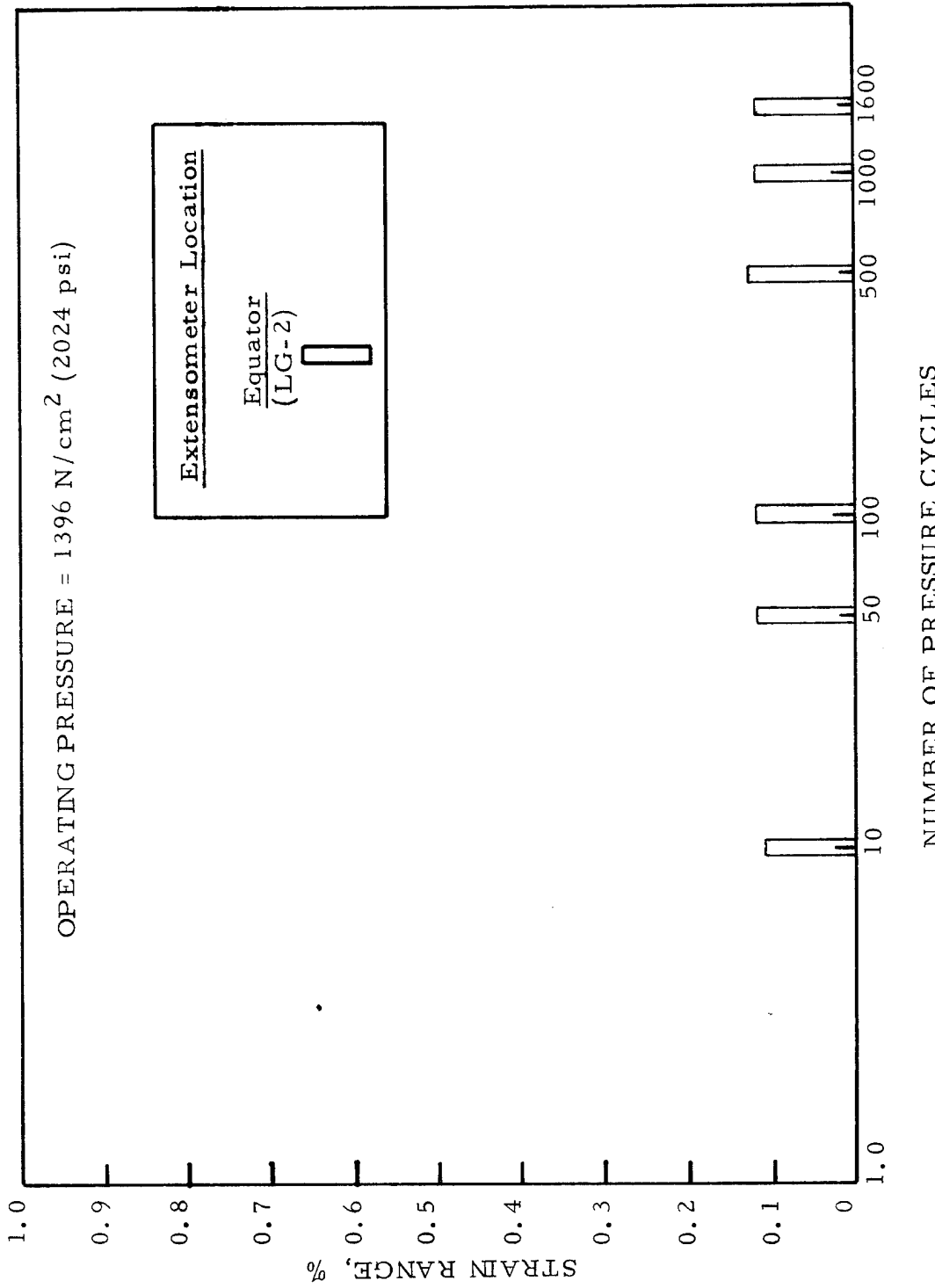


FIGURE F-24: Strains Obtained From Great Circle Extensometers During Cyclic Fatigue of Kevlar/Aluminum Vessel S-6

AR 510551
Feb. 1974

APPENDIX G

DESIGN ANALYSIS*
COMPOSITE SPHERICAL PRESSURE VESSEL
KEVLAR FIBER OVERWRAPPED ARDEFORM 301
STAINLESS STEEL LINER

Prepared for:
Structural Composites Industries, Inc.
Azusa, Cal. 91702

P.O. 9431, 9432

Prepared by: D. Gleich
D. Gleich



* Presentation of this Design Analysis in S.I. units would reduce the clarity of this Appendix. The report is presented in the original form as written by the author.

1. INTRODUCTION AND SUMMARY

An analysis of the selected design configuration for the PRD*49 III fiber overwrapped ARDEFORM 301 stainless steel liner composite spherical pressure vessel is presented herein in accordance with the requirements of Task I of the SCI purchase order (ref.G1).

Selection of the design point was based on SCI purchase order requirements supported by ARDE test data coupled with recent fracture mechanics flaw growth test results, generated by Boeing Aerospace Company on a current NASA LeRC program.

* Kevlar - 49 Roving was formerly designated as PRD-49-III Roving.

2. ANALYSIS

2.1. MATERIAL PROPERTIES

2.1.1 Ardeform 301 SST Liner (Heat 76235 Unaged)

REF. No.

G1, G2, G4

$$\sigma_{M0} = \text{room temp. operating stress} = 100 \text{ ksi}$$

$$S_y = .2\% \text{ offset yield point (room temp.)} \equiv \sigma_{My} = 185 \text{ ksi}$$

$$\sigma_{Mu} = \text{room temp. ult. tensile strength} = 200 \text{ ksi}$$

Stress - Strain Characteristics (Fig 1 - Sphere Design Chart Heat 76235)

$$E_{M1-V_M} = E_M^1 = \text{room temp. effective Young's Modulus} = \frac{27 \times 10^3}{.71} = 38 \times 10^3 \text{ ksi}$$

$$E_{M1-V_M}^1 = E_M^1 = \text{cryogenic } (-320^\circ F) \text{ effective Young's Modulus} = 1.1 \times 38 \times 10^3 \text{ ksi}$$

$$E_M^2 = \text{cure temp. (+300°F) effective Young's Modulus} = 36 \times 10^3 \text{ ksi}$$

$$\alpha_M = \text{Thermal expansion coeff. (R.T.} \rightarrow -320^\circ F) = 4.57 \times 10^{-6} \text{ (in/in°F)}$$

$$(R.T. \rightarrow +300^\circ F) \approx 9 \times 10^{-6} \text{ (in/in°F)}$$

$$= .285 \text{ in}^{-3}$$

2.1.2 Fibers (PRD-49 III)

REF. No.

G1, G3

$$\sigma_{f0} = \text{room temp. operating stress} = 143 \text{ ksi}$$

$$\sigma_{fu} = \text{room temp. ult. tensile stress} = 286 \text{ ksi}$$

$$E_f = \text{room temp. Young's Modulus} = 19 \times 10^3 \text{ ksi}$$

$$E_f^1 = \text{cryogenic } (-320^\circ F) \text{ Young's Modulus} = 22 \times 10^3 \text{ ksi}$$

$$E_f^2 = \text{cure temp. (+300°F) Young's Modulus} = 16 \times 10^3 \text{ ksi}$$

$$\alpha_f = \text{Thermal expansion coeff. (R.T.} \rightarrow -320^\circ F) = -1.985 \times 10^{-6} \text{ (in/in°F)}$$

$$(R.T. \rightarrow +300^\circ F) = -3.8 \times 10^{-6} \text{ (in/in°F)}$$

$$S_{fiber} = S_{resin} \approx .05 \text{ in}^{-3}$$

$$(V.R.)_f = \text{Fiber volume ratio} \approx 2/3$$

J. A. Leck
Revised 4/19/63

Heat 76235
Sphere Design Chart
Based on Actual Spheres

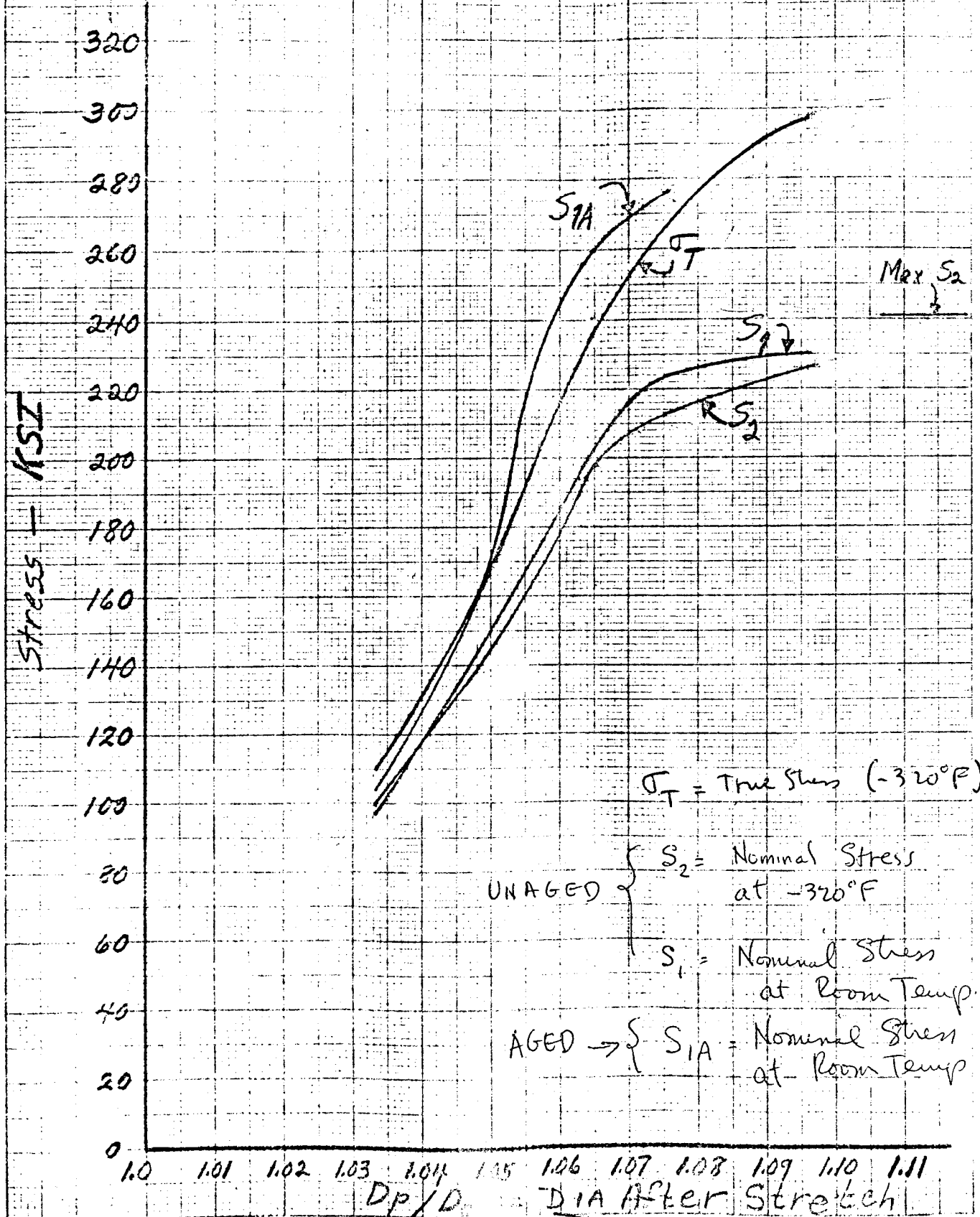


Figure G1

2.2 DIAMETER & THICKNESS Values

Avg. Starting Sheet Thickness = 55 mils ; Avg hydroforming Hydroformed Head I.D. = 21.4" thinout = 5%
 Avg Head Starting thickness = $(55/1.05)$ mils starting
 a) Apply 5% cryo-sizing strain (First Cryostrain)
 $(21.4)(1.05) = 22.47$ I.D.

$$t = \left\{ \left(\frac{55}{1.05} \right) \right\} \times \frac{1}{(1.05)^2} = 47.6 \text{ say } 48 \text{ mils}^* = t_0$$

$$\text{Mean } D = 22.47 + .05 = 22.52" = D_0$$

b) Anneal

c) Apply (in 2 steps) $\epsilon = 6\%$ { See Fig G1
 (2nd & Third cryostrains) Sphere Design Chart
 I.D. = $22.47 \times 1.06 = 23.82$ final { to obtain $S_y = 185$ ksi,
 R.T. 2% yield point

$$\text{Avg (final) } t_M = \frac{47.6}{(1.06)^2} = 42.3 \text{ say } 42 \text{ mils}^* \} \text{ Use these values for design calculation.}$$

$$(\text{final}) \text{ mean } D \equiv 23.82 + .04 = 23.86$$

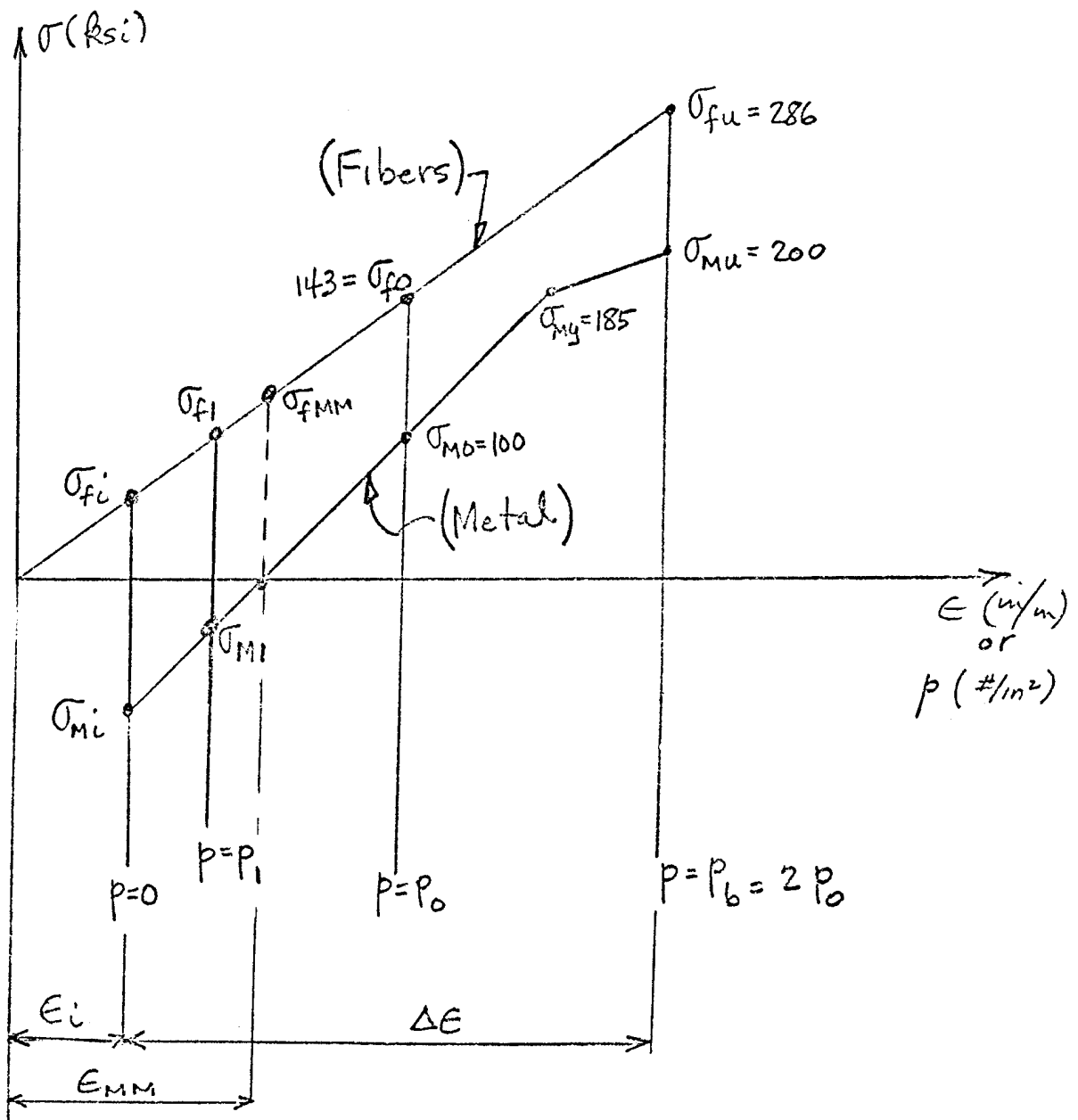
* For sphere, true thickness strain is twice true diametral strain

$$\ln \left(\frac{t}{t_0} \right) = -2 \ln \left(\frac{D}{D_0} \right) = -2 \ln (1+\epsilon)$$

$$\ln \left(\frac{t}{t_0} \right) = -\ln [(1+\epsilon)^2] \text{ or,}$$

$$\frac{t}{t_0} = \frac{1}{(1+\epsilon)^2}$$

2.3 Room TEMPERATURE STATE:



Equilibrium* at $p=0$, $p=P_0$ and $p=P_b$ requires:
 (note: eq.(2) valid at $P_b=2P_0$)

$$\sigma_{Mi}(t_M) + \sigma_{fi}\left(\frac{t_f}{2}\right) = 0 \quad \dots \text{(G1)}$$

$$100(t_M) + 143\left(\frac{t_f}{2}\right) = P_0 \times \frac{D}{4} \quad \dots \text{(G2)}$$

Strain Compatibility between $p=0$ and $p=P_0$
 yields from stress-strain relations and mat'l's properties,

$$\Delta\epsilon_f = \Delta\epsilon_m$$

$$\frac{(143 - \sigma_{fi})}{19} = \frac{(100 - \sigma_{Mi})}{38} \quad \dots \text{(G3)}$$

From (G1), (G2), (G3)

$$\sigma_{Mi} = \frac{-186}{\left\{1 + \frac{4}{(t_f/t_M)}\right\}} \quad \dots \text{(G4)}$$

$$\sigma_{fi} = -\frac{2}{(t_f/t_M)} \times \sigma_{Mi} \quad \dots \text{(G5)}$$

$$\left(\frac{P_0 D}{t_M}\right) = 400 + 286\left(\frac{t_f}{t_M}\right) \quad \dots \text{(G6)}$$

* Factor of $\frac{1}{2}$ used on t_f since there are two(2)
 fiber layers, one(1) resists hoop load and one(1) resists
 meridional load.

$$\text{Say : } \left(\frac{t_f}{t_M} \right) = 3.75 \quad \dots \text{ (G7)}$$

Then from (G4), (G5), (G7)

OK,
 low enough
 So that
 linear comp.
 yielding, buckling
 or fiber
 creep no
 problems

$$\left\{ \begin{array}{l} \sigma_{Mi} = \frac{-186}{1 + \left(\frac{4}{3.75}\right)} = -89.8 \text{ ksi} \quad \dots \text{ (G8)} \\ \sigma_{fi} = -\frac{2}{3.75} (-89.8) = 47.8 \text{ ksi} \quad \dots \text{ (G9)} \end{array} \right.$$

For $D = 23.86''$, $t_M = 42 \text{ mils}$ (See P.318)
 and $t_f = 3.75 t_M \approx 158 \text{ mils}$ we have from (G6),

$$P_o \times \frac{23.86}{42} = 400 + 286 \times 3.75$$

or,

$$P_o = 2590 \text{ psig} \quad \dots \text{ (G10)}$$

$$\text{and, } P_b = 2 P_o = \underline{\underline{5180 \text{ psig}}} \quad \dots \text{ (G11)}$$

$t_{fc} = \frac{t_f}{(VR)_f} = 1.5 t_f \quad \dots \text{ (G12)}$
 fiber composite thickness

Structural Efficiency Parameter :

$$\frac{P_o V}{W} = \frac{P_o \frac{\pi D^3}{6}}{\pi D^2 [285 t_M + .05 \times 1.5 t_f]} = \frac{P_o D/6}{[285 t_M + .075 t_f]} \quad \dots \text{ (G13)}$$

For $t_M = .042"$, $t_f = .158$, $D = 23.86$, $P_o = 2700$,
 $\underline{P_M = 285}$, $\underline{P_f = 95}$

$$\left(\frac{P_o V}{W} \right) = \frac{(2590) \left(\frac{23.86}{6} \right)}{285 \times .042 + .075 \times .158} = .43 \times 10^6 (\text{in}^{-1}) \quad \text{--- (G14)}$$

$$\left(\frac{P_b V}{W} \right) = 2 \times .43 = .86 \times 10^6 (\text{in}^{-1}) \quad \text{--- (G15)}$$

Between $p=0$ and $p=P_o$ (see p. 319)
the metal stress is,

$$\frac{\sigma_{Mi}}{\sigma_{Mo}} = \frac{\sigma_{Mi}}{\sigma_{Mo}} + \left(\frac{p_i}{P_o} \right) \left(1 - \frac{\sigma_{Mi}}{\sigma_{Mo}} \right) \quad \text{--- (G16)}$$

Taking $\left(\frac{p}{P_o} \right) = \frac{1}{11}$, compatible with projected shuttle design point we have,

$$\frac{\sigma_{Mi}}{\sigma_{Mo}} = -\frac{89.8}{100} + \frac{1}{11} (1 + .898)$$

$$\frac{\sigma_{Mi}}{\sigma_{Mo}} = -.725 \quad \text{--- (G17)}$$

Metal liner is cycled then between
 $p = p_i = \frac{P_o}{11}$ and $p = P_o$ at corresponding
stress levels of -72.5 ksi to $+100 \text{ ksi}$
 $(R = \frac{\sigma_{min}}{\sigma_{max}} = -.725)$

Total strain to rupture = $\Delta \epsilon$

(This strain required to achieve design burst pressure.)

$$\Delta \epsilon = \frac{\sigma_{fu} - \sigma_{fi}}{E_f} = \frac{286 - 47.8}{19 \times 10^3} \approx .0126 \text{ in/in}$$

$$\text{Metal elastic strain} = \Delta \epsilon_{me} = \frac{185 - (-89.8)}{38 \times 10^3} = .00723 \text{ in/in}$$

$$\text{Metal plastic strain} = \Delta \epsilon_{mp} = \Delta \epsilon - \Delta \epsilon_{me}$$

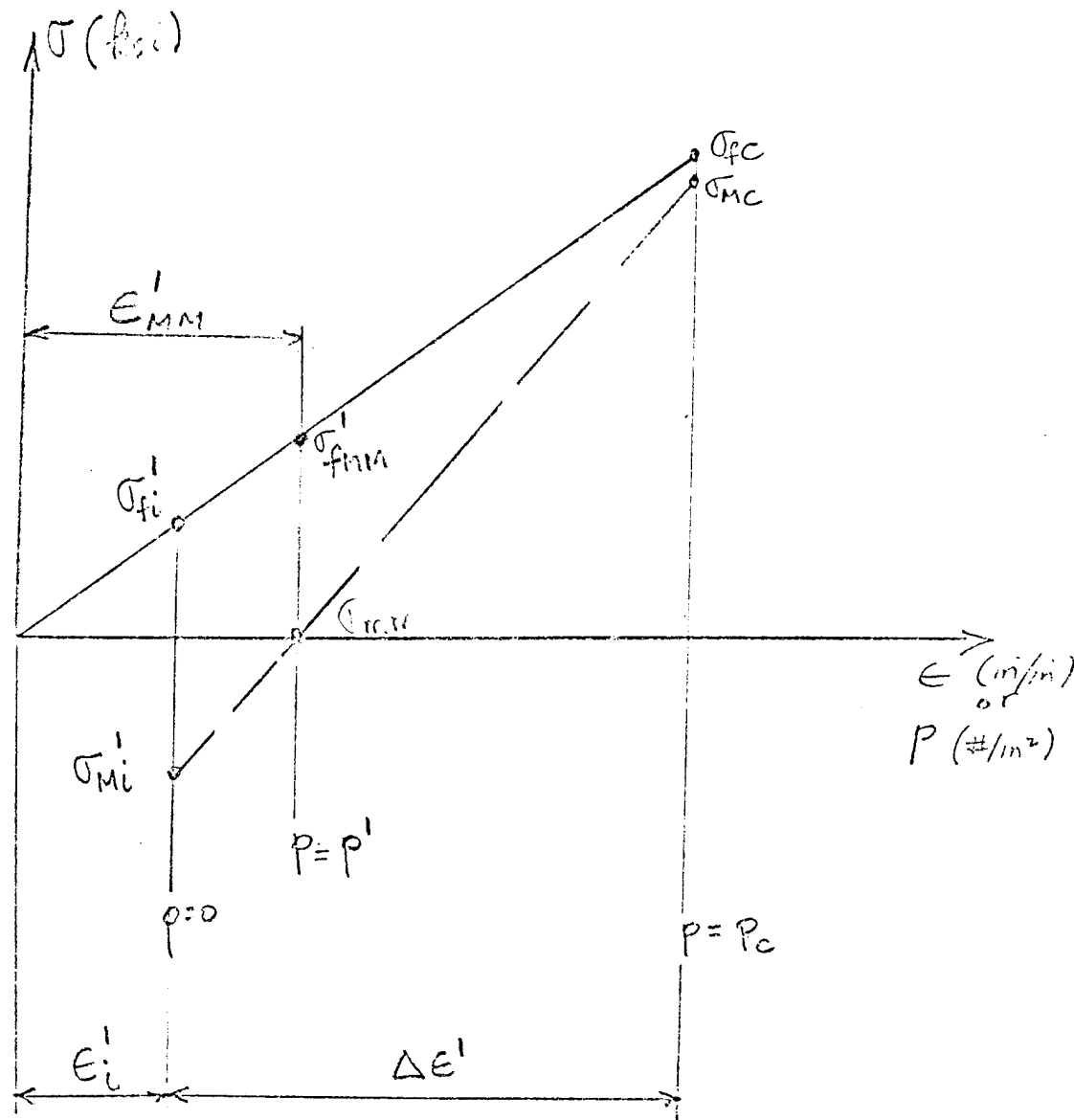
$$\Delta \epsilon_{mp} \approx .0054 \text{ in/in} \text{ (bi-axial plastic strain)}$$

$$\text{Equivalent uniaxial plastic strain} \approx \frac{.0054}{\sqrt{2}} \approx .0108 \text{ in/in}$$

(bi-axial to uniaxial
plastic strain factor
for sphere)

Thus, metal liner requires about 1%
uniaxial plastic strain capability to rupture
in order to load up fibers and
achieve design burst pressure.

2.4 CRYOGENIC STATE (-320°F)



Equilibrium at $p=0$:

$$\sigma_{fi}' \frac{t_f}{2} + \sigma_{Mi}' t_M = 0 \quad \dots \text{(G18)}$$

Strain Compatibility Between $p=0$ and $p=p'$:
(see p. 8)

$$\frac{\sigma_{fMM}' - \sigma_{fi}'^1}{E_f'} = - \frac{\sigma_{Mi}'^1}{\hat{E}_M'} \quad \dots \text{(G19)}$$

Noting that E_{MM}' (strain at -320°F for zero state of stress — cryogenic mismatch strain) is given by (see p. 324)

$$E_{MM}' = \frac{\sigma_{fMM}'}{E_f'} \quad \dots \text{(G20)}$$

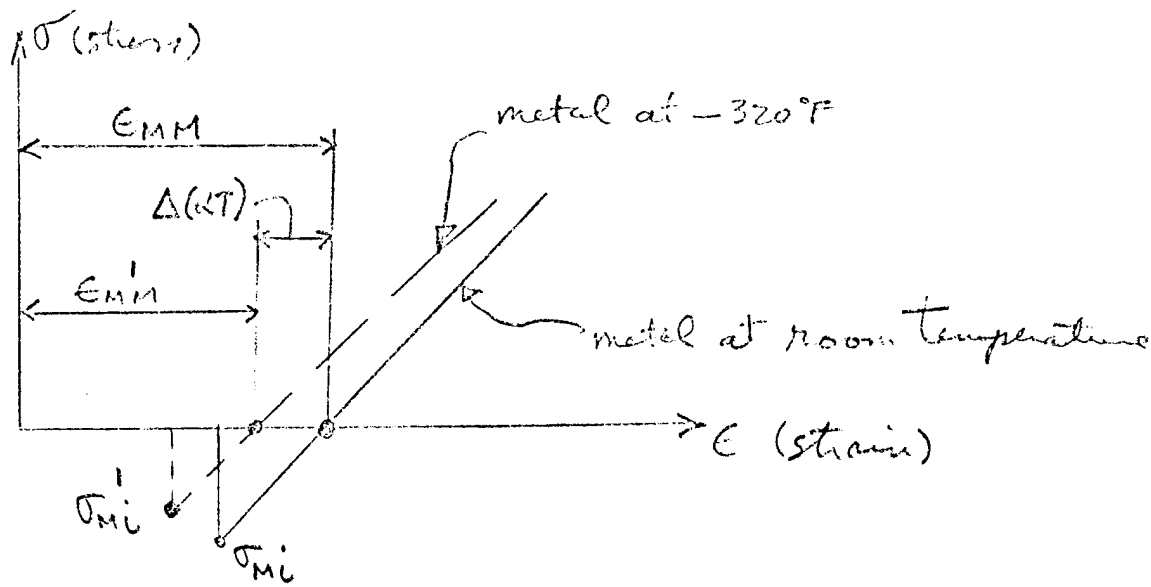
we obtain, using also (G18) and (G19), the cryogenic prestresses,

$$-\sigma_{Mi}' = \left(\frac{1}{1+\beta'} \right) \hat{E}_M' E_{MM}' \quad \dots \text{(G21)}$$

$$\sigma_{fi}' = \left(\frac{\beta'}{1+\beta'} \right) E_f' E_{MM}' = -\sigma_{Mi}' \left(\frac{t_M}{\frac{1}{2} t_f} \right) \dots \text{(G22)}$$

where β' , the metal to fiber cryogenic stiffness ratio, is

$$\beta' = \frac{\hat{E}_M' t_M}{E_f' \frac{t_f}{2}} \quad \dots \text{(G23)}$$



The cryogenic "mismatch" strain, ϵ_{MM}' , is related to the room temp. "mismatch" strain, ϵ_{MM} , by

$$\epsilon_{MM}' = \epsilon_{MM} - \Delta(\alpha T) \quad \text{--- (G24)}$$

with,

$$\Delta(\alpha T) = \Delta T (\alpha_M - \alpha_f) = 370 (\alpha_M - \alpha_f) \quad \text{--- (G25)}$$

and from stress-strain relations and diagram (see p. 319) we have,

$$\epsilon_{MM} = \frac{\sigma_f}{E_f} - \frac{\sigma_{Mi}}{E_M} \quad \text{--- (G26)}$$

Substituting appropriate numerical values in (G23) \Rightarrow (G26) gives,

$$\epsilon_{MM} = \frac{47.8}{19 \times 10^3} - \frac{(-89.8)}{38 \times 10^3} = 4.88 \times 10^{-3} \text{ (in/in)}$$

$$\Delta(\alpha T) = 390 \times 10^{-6} \{4.59 - (-1.785)\} = 2.56 \times 10^{-3} \text{ (in/in)}$$

$$\epsilon_{MM}' = (4.88 - 2.56) \times 10^{-3} = 2.32 \times 10^{-3} \text{ (in/in)}$$

$$\beta' = \frac{(1.1 \times 38)(42)}{(22)(\frac{158}{2})} = 1.01$$

Using these results in (G21) and (G22) yields
the cryogenic prestresses,

OK
low enough so that fiber compon. yielding, buckling or fiber creep no problems

$$\left\{ \begin{array}{l} \sigma_{MC}' = -\left(\frac{1}{2.01}\right)(1.1 \times 38 \times 2.32) = -48.2 \text{ ksi} \quad \dots \dots \text{(G27)} \\ \sigma_{fi}' = -(-48.2) \times \left(\frac{42}{\frac{1}{2} \times 158}\right) = 25.7 \text{ ksi} \quad \dots \dots \text{(G28)} \end{array} \right.$$

Strain compatibility between $p=0$
and $p=p_c$ requires,

$$\frac{\sigma_{fc} - \sigma_{fi}'}{E_f'} = \frac{\sigma_{MC} - \sigma_{Mi}'}{E_M'} \quad \dots \dots \text{(G29)}$$

From Fig G1 at $\epsilon = .06$ (corresponding to 185 ksi room temp yield) we obtain the required cryogenic true stress, $\sigma_T = \sigma_{MC} = 215 \text{ ksi}$. Substituting this and other appropriate numerical values in (G29) gives the fiber cryogenic stress at cryogenic stretch pressure, P_c , as

$$\sigma_{fc} = \frac{(22)}{(1.1 \times 38)} \left\{ 215 - (-48.2) \right\} + 25.7$$

$$\sigma_{fc} \approx 163 \text{ ksi} \quad \dots \text{(G30)}$$

Equilibrium at $p = P_c = P_{c3}$ (Third Cryostretch Pressure)
see p.

$$\sigma_{MC} t_m + \sigma_{fc} \frac{t_f}{2} = P_{c3} \frac{D}{4} \quad \dots \text{(G31)}$$

or,

$$P_{c3} = \frac{4}{23.86} \left\{ 215 \times 42 + 163 \times \frac{158}{2} \right\}$$

$$\underline{P_{c3} = 3670 \text{ psig say } 3700} \quad \dots \text{(G32)}$$

Vessel state prior to third cryostretch is
 pressure = stresses = 0
 temperature = ambient (R.T.)

When we cool vessel down to -320°F from R.T., a strain mismatch (gap) of $\Delta(\alpha T)$ is produced between the metal and fibers. Subsequent cryopressure and pressure unloading at -320°F produces a further strain mismatch of ϵ_{MP}' . In order for the vessel to satisfy compatibility (fit together) with the required prestresses, the metal liner must have been plastically strained an amount,

$$\Delta\epsilon_{MP}'' = \Delta(\alpha T) + \epsilon_{MP}' = \epsilon_{MM} \quad \text{---(G33)}$$

Using appropriate numerical values from p.327 gives,

$\Delta\epsilon_{MP}'' = 4.88 \times 10^{-3} \text{ in/in} \approx \frac{1}{2}\%$ metal bi-axial plastic cryostain during third cryostretch operation. Total strain (elastic + plastic) cryogenically is (see p.8) $\frac{163}{22 \times 10^3} = 7.42 \times 10^{-3} \text{ in/in}$

Since we require a total of 6% cryostain in metal liner to achieve the desired 185 psi

room temperature yield point (see p. 12) we must strain the metal liner plastically

$6 - \frac{1}{2} = 5\frac{1}{2}\%$ during the second cryostretch operation with the liner unwrapped.

From figure 1 (Sphere design chart) at

$$1 + \epsilon = D_p/D_o = 1.055, \text{ we have } S_2 = 160 \text{ ksc.}$$

Starting diameter and thickness are (see p. 3)

$$D_o = 22.52", t_o = 48 \text{ Mils.}$$

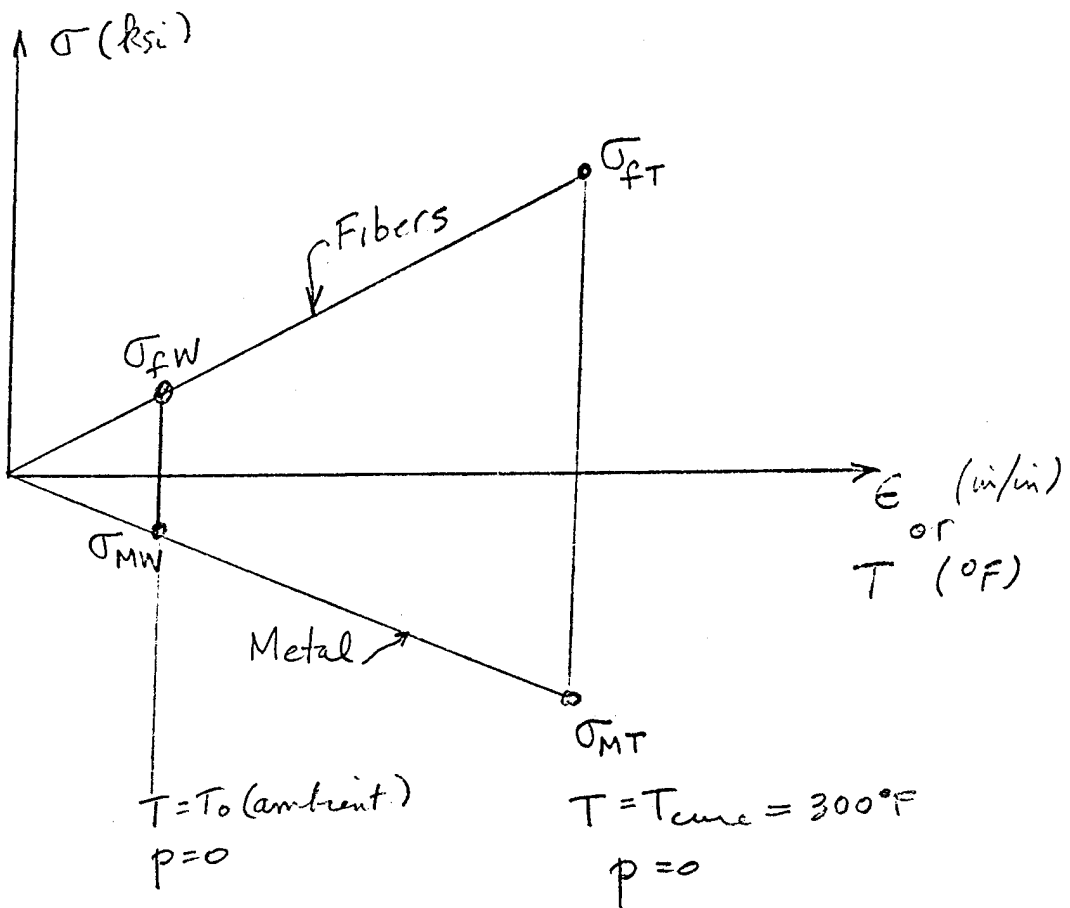
$$S_2 = \text{Nominal cryostress} = \frac{P_{cr} D_o}{4 t_o} \text{ and,}$$

$$P_{cr} = \frac{(160) \times 4 \times 48}{22.52} = 1376 \text{ say } 1380 \text{ ---(G34)} \text{ psig}$$

Second cryostretch pressure (metal alone)

2.5 CURE TEMPERATURE & NON-ZERO INITIAL FIBER WRAP TENSION EFFECTS:

2.5.1 Cure Mode



Equilibrium:

$$\left. \begin{aligned} \sigma_{fw}\left(\frac{t_f}{2}\right) + \sigma_{mw}(t_m) &= 0 \\ \sigma_{ft}\left(\frac{t_f}{2}\right) + \sigma_{mt}(t_m) &= 0 \end{aligned} \right\} \dots \text{(G35)}$$

$$\sigma_{ft}\left(\frac{t_f}{2}\right) + \sigma_{mt}(t_m) = 0$$

Strain Compatibility:

$$\frac{(\sigma_{ft} - \sigma_{fw})}{E_f''} + \alpha_f(T - T_0) = \frac{(\sigma_{mt} - \sigma_{mw})}{E_m''} + \alpha_m(T - T_0) \dots \text{(G36)}$$

From (G35) and (G36) we obtain,

$$(\sigma_{MT} - \sigma_{MW}) = \left(\frac{1}{1 + \beta''} \right) \left\{ \hat{E}_M'' (\alpha_f - \alpha_M) (T - T_0) \right\} \quad \dots \text{(G37)}$$

$$(\sigma_{fT} - \sigma_{fw}) = - \left(\frac{\beta''}{1 + \beta''} \right) \left\{ E_f'' (\alpha_f - \alpha_M) (T - T_0) \right\} = - \left(\sigma_{MT} - \sigma_{MW} \right) \frac{t_M}{t_{f/2}} \quad \dots \text{(G38)}$$

where, β'' , the cure temperature metal to fiber stiffness ratio is given by,

$$\beta'' = \frac{\hat{E}_M'' t_M}{E_f'' \frac{t_f}{2}} \quad \dots \text{(G39)}$$

Taking $\sigma_{fw} = 9 \text{ ksi}$ (SCI value for initial wrap tension)
and using appropriate numerical values
yields,

$$\beta'' = \frac{36 \times 42}{16 \times \frac{158}{2}} \cong 1.2$$

$$(\alpha_f - \alpha_M) (T - T_0) = -(3.8 + 9) \times 10^{-6} \times (300 - T_0) = -2.94 \times 10^{-3} \text{ (in/in)}$$

$$\sigma_{fT} - 9 = - \left(\frac{1.2}{2.2} \right) (-2.94 \times 17) = 22.7 \text{ ksi}$$

Effects are
present - $\left\{ \begin{array}{l} \sigma_{fT} = 31.7 \text{ ksi} \quad \dots \text{(G39)} \\ \sigma_{MT} = -31.7 \times \frac{158/2}{42} = -59.6 \text{ ksi} \quad \dots \text{(G40)} \end{array} \right.$

$$\sigma_{MW} = -9 \times \frac{158/2}{42} = -16.9 \text{ ksi} \quad \dots \text{(G41)}$$

2.5.2 Third Cryostretch Mode

A zero starting state of stress (corresponding to zero fiber wrap tension) has been assumed in the calculations of section 2.4.

The fibers actually are wrapped with a wrap tension of 9 kN (see section 2.5.1). However, when the vessel is cooled down to -320°F prior to application of the cryogenic stretch pressure, this fiber pretension is lost by fiber expansion and metal contraction as shown by comparison of thermal and fiber wrap strains. It is concluded that the assumption of zero starting stresses is valid.

$$\text{Thermal (fibers)} \quad \alpha_f \Delta T = -1.985 \times 10^{-6} (-390) = 773 \times 10^{-6} \text{ (expansion)}$$

$$\text{strain (metal)} \quad \alpha_m \Delta T = 4.59 \times 10^{-6} (-390) = -1790 \times 10^{-6} \text{ (contraction)}$$

$$\text{Thermal gap strain} = [773 - (-1790)] \times 10^{-6} \approx 2.56 \times 10^{-3} \text{ in/in}$$

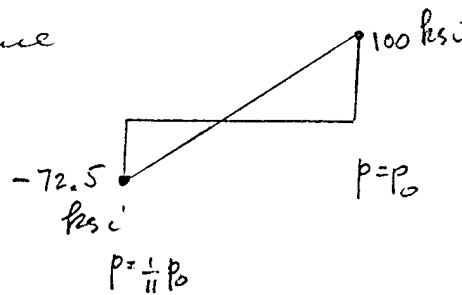
$$\text{fiber tension strain} = \frac{9}{19 \times 10^3} = .474 \times 10^{-3} \text{ in/in} \ll \begin{matrix} \text{thermal} \\ \text{gap} \\ \text{strain} \end{matrix}$$

Thus fiber wrap tension is lost on cool down.

2.6 FATIGUE & CREEP CONSIDERATIONS :

2.6.1 Metal Liner

a) Fatigue



$$\bar{\sigma}_{\text{mean}} = \frac{1}{2}(100 - 72.5) = 13.75 \text{ ksi} ; \bar{\sigma}_m/\bar{\sigma}_u = \frac{13.75}{200} \approx 0.069$$

$$\bar{\sigma}_{\text{alt.}} = 100 - 13.75 = \pm 86.25 \text{ ksi} ; \frac{\bar{\sigma}_a}{\bar{\sigma}_u} = \frac{86.25}{200} \approx 0.431$$

From Modified Goodman Diagram,

$$\left. \begin{array}{l} \text{Endurance} \\ \text{Limit for} \\ \text{Completely} \\ \text{Reversed} \\ \text{Loading} \end{array} \right\} \quad \frac{\bar{\sigma}_a}{\bar{\sigma}_u} = \left(\frac{\bar{\sigma}_r}{\bar{\sigma}_{uR=1}} \right) \left(1 - \frac{\bar{\sigma}_m}{\bar{\sigma}_u} \right) = \left(\frac{\bar{\sigma}_r}{\bar{\sigma}_{uR=1}} \right) (1 - 0.069) = 0.931 \left(\frac{\bar{\sigma}_r}{\bar{\sigma}_{uR=1}} \right) = 0.431$$

$$\left(\frac{\bar{\sigma}_r}{\bar{\sigma}_{uR=1}} \right) = \frac{0.431}{0.931} = 0.462 = \left(\frac{\bar{\sigma}_{\text{max}}}{\bar{\sigma}_u} \right)_{R=-1}$$

where, $R = \frac{\bar{\sigma}_m}{\bar{\sigma}_{\text{max}}}$

From Fig G2 (for $R=-1$) p. 335

$N \approx 12,000$ cycles

b) Creep

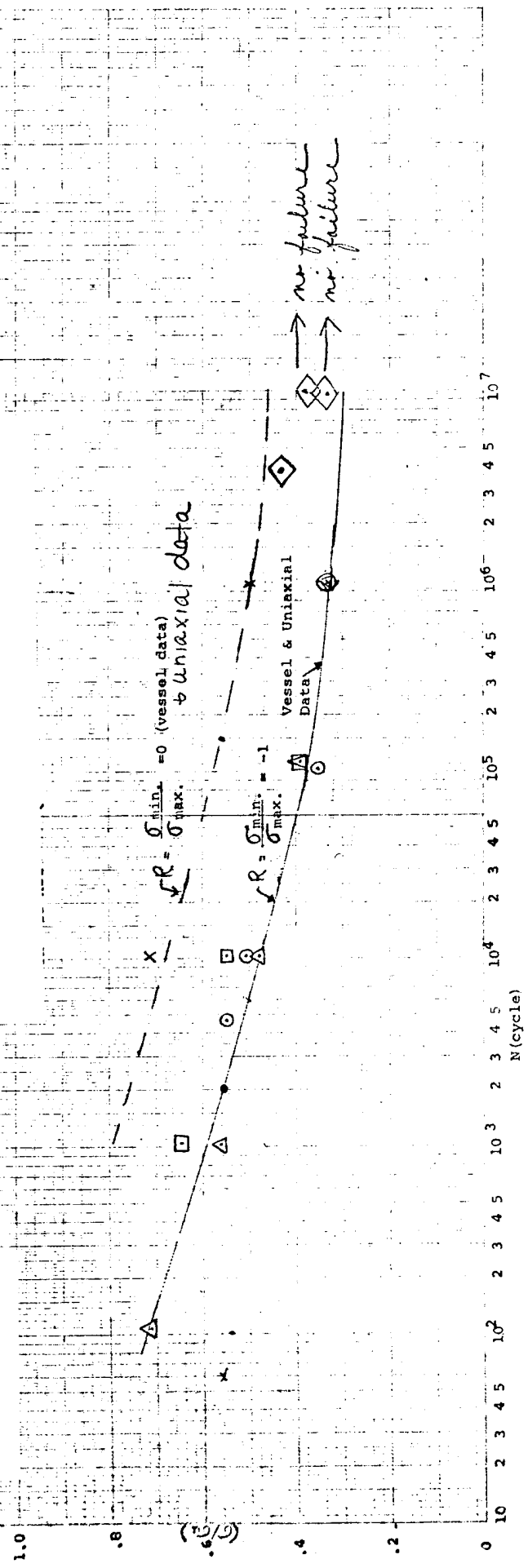
Liner creep does not occur for temp -57°C - -76°F . At lower temp values, it is exposed to $(-89.8 \text{ ksi at } R.T. - \text{long term strain})$ and $(-55 \text{ ksi at } +30^{\circ}\text{F} (4.5^{\circ}\text{C}))$.

FIGURE G2

Heat 76235

301 stainless steel

Rev. 12/19/73



Key:

- X Vessel Data ($R=0$) $\sigma_u = 220$ ksi (unaged Heat 76235, 301 SST - Ham Std Data)
- Vessel Data for $R=0$ Transformed to $R=-1$ by Modified Goodman Diagram ($\sigma_u = 220$ ksi).
- △ Tensile Data ($R=-1$) Annealed 301 SST, $\sigma_u = 90$ ksi, Ham. Std. Data (Transformed to $R=0$ using modified Goodman Diagram)
- ▽ Tensile Data ($R=-1$) Annealed 301 SST, $\sigma_u = 90$ ksi, Ham. Std. Data (Transformed to $R=0$ using modified Goodman Diagram)
- Tensile Data ($R=.10$) $\sigma_u = 220$ ksi, unaged 301 SST, Ham. Std. Data, Transformed to $R=-1$
- ×
- Tensile Data ($R=.10$) $\sigma_u = 220$ ksi, unaged 301 SST, Ham. Std. Data, Transformed to $R=0$
- Tensile Data ($R \approx 0$) Aged - 290 ksi, 301 SST { Heat 76235 - Tested by Nat. Labs for Research + Testing, Inc.
- Tensile Data ($R \approx 0$) Unaged - 230 ksi, 301 SST }

2.6.2 PRD-49 Fibers

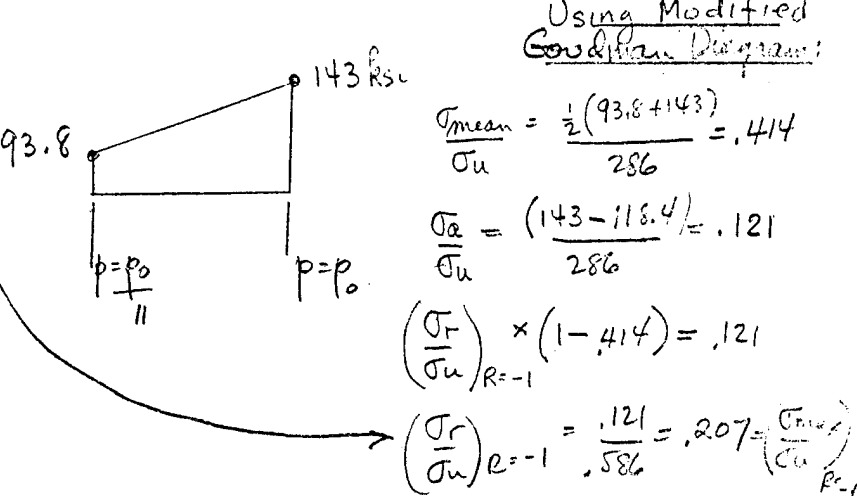
a) Fatigue

$$\left(\frac{\sigma}{\sigma_u}\right)_{R=0} = \frac{2(\sigma/\sigma_u)_{R=-1}}{1 + (\sigma/\sigma_u)_{R=-1}}$$

$$(\sigma/\sigma_u)_{R=0} = \frac{2 \times 207}{1.207} = .343$$

$$\left(\frac{\sigma}{\sigma_u}\right)_{R=1} = \frac{(\sigma/\sigma_u)_{R=0}}{.9 + .1(\sigma/\sigma_u)_{R=0}}$$

$$\left(\frac{\sigma}{\sigma_u}\right)_{R=1} = \frac{.343}{.9 + .1(343)} = .367$$



From Dupont Data
(Ref. G3) $\{ \begin{matrix} F_{cr} \\ R=0.10 \end{matrix} \}$

$$\sigma_{max} = (200) (.367) = 73 \text{ ksi}$$

\uparrow composite UTS

$N \rightarrow \infty$ (infinite cycle life)

(Fiber Fatigue not critical)

b) Creep

$$\sigma_{fi} = 44.9 \text{ ksi} \quad (\text{long term stress at R.T.})$$

$$\frac{\sigma_{fi}}{\sigma_{fu}} = \frac{44.9}{286} = .157 \quad \text{small, ok.}$$

Fiber Creep
not critical

$\left\{ \begin{array}{l} \text{stress rupture time} \rightarrow \infty \\ \text{creep elongation} \rightarrow 0 \end{array} \right\}$ From Dupont Data
(Ref. G3)

2.7. Fracture Mechanics Considerations

Metal lower cycle life are limited by
flaw growth effects (crack propagation).
to be determined by SIT (Borning).

3. REFERENCES

- G1. SCI Purchase Orders No. 9431 and 9432,
Amendment 02 (12/28/73)
-
- G2. ARDE, Inc. Test Data
- G3. DUPONT Data
"Kevlar" 49 Data Manual
- G4. International Nickel Co. Data

APPENDIX H

KEVLAR*FR 301 STAINLESS STEEL PRESSURE VESSEL FABRICATION PROCESS SPECIFICATION

* Kevlar-49 Roving was formerly designated as PRD-49-III Roving

SHOP ORDER NO.	SHIPPING AREA	SPLIT REFERENCE	COMPLETION DATE		PART DESCRIPTION		PART NUMBER	REV. N/C	LAST REV. N/C
			MONTH	DAY	YEAR	MATERIAL			
D3897							Pressure Vessel, PRD-FR		
WORK CHARGE NUMBER	QTY.	SERIALIZATION	AVAILABILITY				301 Stainless Steel		
TIME CARD CHARGE NO.	RELEASED BY	PLANNED BY	MONTH	DAY	YEAR				
CHECK ONE <input type="checkbox"/> SHOP ORDER NO. & OPER. NO. <input type="checkbox"/> WORK CHARGE NO.	R. Landes	R. Landes	7-24-74	14	1974				
MATERIAL DESCRIPTION			Q.C. APPROVAL	DATE	DATE		MASTER B.P.L. NO.	NEXT ASSY NO.	
See Parts List Requisition (PLR)							D3897	D3898	
OP. NO.	STA. NO.	OPERATION DESCRIPTION		I.W.A. NO.	REVIEW AUTHORITY	INSP. STAMP	SET UP TIME	GROSS TIME	TOTAL MANUFACTURE TIME
C	C	OPR. DWG.	PROD.	INSP.	NONE ER MR	OPR. DWG.	INSP.	INSP.	INSP.
2		1.	All inspection stop points, as indicated by a circle in the inspection stamp column, will be verified and work will not proceed until verification by Quality Control is made by placing a Q.C. stamp at all points indicated.						
2		2.	All quality engineering stop points, as indicated by a circle in the production stamp column, will be observed and work will not proceed until verification by the assigned Quality Engineer is made by placing a Q. E. stamp at all points indicated.						
2		3.	Any discrepant inspection requirement or departure from the Shop Order instructions shall be documented on an Inspection Report (IR). Inspection will advise of action to be taken.						
2		4.	No changes, alterations, or additions to Shop Order Traveler shall be honored by Inspection unless stamped by the Inspection Planner						

and Main Partitions Planner and approved

SHOP ORDER CONTINUATION SHEET

SHEET 2 OF 9

ITEM, ORDER NO. SPLIT REFERENCE	PART NUMBER	PART DESCRIPTION		ARDE P/N D3897	N/C/N/C
		COMPLETION DATE MONTH DAY YEAR	Pressure Vessel, PRD-FR Sphere		
OPER. NO.	SIA NO.	OPERATION DESCRIPTION		STAMP	TEST UP RUN TIME HR MIN SEC
ITEM, ORDER NO.	SIA NO.	OPN. OWN.	PROD. INGP.	TEST UP RUN TIME HR MIN SEC	TEST UP RUN TIME HR MIN SEC
2		5:	All entries on this Shop Order must be in ink.		
2					
2	0103	Withdraw all productive materials and record traceability date on Process Control Record (PCR), Figure H1.		○ 1.0 1	
2					
2	0203	PREPARATION FOR WINDING		○ 3.0 2	
2		1. Record serial number and acceptance tag number of liner assembly, D3896 on PCR, Figure H1.			
2					
2		2. Measure liner assembly length, diameters (Pi-Tape) and weight; record values on PCR, Figure H2.			
2					
2		3. Mix resin per operation 0403-1 in sufficient quantity for coating entire shell.			
2					
2		4. Mix Cab-O-Sil with a portion of the resin until paste consistency is obtained. Sweep paste mix over boss and girth, weld areas to smoothly blend weld crown to shell surface.			
2					
2		5. Coat remainder of metal shell surface, to be overwrapped, with unfilled resin; Gel resin coated metal shell in oven for 3 hours at 185°F.			
2					

SHOP ORDER CONTINUATION SHEET

PART DESCRIPTION

OAK
SACRED GROVE

SHEET 3 OF 9
SACRIFICE PLATES

EET 3 OF 9

EET 3 OF 9

卷之三

SHOP ORDER CONTINUATION SHEET

DATE: 9/10/68 SHEET: 4 OF 9

PART NUMBER: D3897

SPLIT REFERENCE: C CANCELLED DATE: MONTH DAY HRS.

PART DESCRIPTION: Pressure Vessel, PRD-FR Sphere

ARDE P/N D3897 N/C N/C

OPERATION DESCRIPTION

OPR. STA. NO. OPR. STA. NO.

T.O. AVAILABLE DATE

T.O. HAC AND NUMBER

T.O. UP TIME

OPR. INCR. PROD. INCR. PROD.

SET UP TIME

CURE TIME

- 2 0203 Cont. 13. Present static winding tension to 1.0 lb. on the spool of roving.
- 2 14. Run the winding machine and check machine settings and pattern per

Quality Engineer instructions.

- 2 15. Protect liner assembly with plastic sheet if next operation is not to be performed immediately.

- 2 0306 INSPECTION
- 2 1. Verify that all data required for Operation 0203 was recorded.

2 0403 FILAMENT WINDING

- 2 1. Prepare a single batch of resin mix in a one-gallon can as follows:

Epon	828 = 400 gm (100 parts)
DSA	= 463.6 gm (115.9 parts)
Empol	1040 = 80 gm (20 parts)
BDMA	= 4 gm (1 part)

Thoroughly mix the constituents.

- 2 2. Coat the previously gel-coated metal shell with the prepared resin mix.

PART FIFTH
SHEET 6 OF 9

FICP ORDER NO.	ITEM NO.	SPLIT REFERENCE	COMPLETION DATE		C	PART DESCRIPTION	N/C	N/C
			MONTH	DAY				
D3897						Pressure Vessel, PRD-FR		ARDE P/N D3897
						Sphere		
						OPERATION DESCRIPTION		
						OPR. STA. NO.	STAMP	SET UP
						NO.	PROD. ING.	HUN. TIME
2	0403	Cont.				GENERAL NOTE: Stop overwrapping and notify Quality Engineering		
1						if any of the following should occur: (a) filament breakage,	.	
2						(b) loss of roving or rovings on guide rollers, (c) loss of roving	.	
2						tension, (d) winding pattern gapping, or (e) excessive variation of	.	
2						winding tape width. Retain any excess roving not used in winding	.	
2						but included in the initially recorded roving-spool weights; weight it	.	
2						and record the weight on PCR, Figure H3.	.	
2					8.	Wipe all excess resin from the vessel surface with clean cheese-		
2					2	cloth or Kemwipes after every step (revolution) is completed.		
2					9.	Measure the static tension on each roving at the final payoff after		
2					2	completion of the each odd numbered Step (revolution); record		
2					2	the data on Figure H4, then adjust the tension to obtain the required		
2					1	1.0 lb/roving.		
1					10.	At the conclusion of winding, tie off the roving by		
1					1	burying the ends under two or three turns of winding.		
1					11.	Wipe off excess resin from the exterior surface of the filament-		
1					1	wound vessel and from the shaft/boss mating surfaces.		

SHOP ORDER CONTINUATION SHEET

DATE _____ SHEET 7 OF 9

SHOP ORDER NO.	SPLIT REFERENCE	PART DESCRIPTION		PART NUMBER	ARDE P/N D3897	N/C N/C
		COMPLETION DATE MONTH DAY	PART NO.			
D3897				Pressure Vessel, PRD-FR		
2 0403 Cont.	STA. NO.			Sphere		
				OPERATION DESCRIPTION		
2						
2				12. Transfer vessel from the sphere winder to the cure cart. SK-73-041.		
2						
2						
2				13. Remove the spool of roving from the tension device, weigh the spool, and record the weight on Figure H3; return the spool to Material Control. Weigh all scrap roving, retained in plastic bag, and record weight on Figure H3.		
2						
2				14. Protect the vessel with plastic sheet if next operation is not to be performed immediately.		
2						
2 0506				INSPECTION	0 . 2 . 1	
2				1. Verify that tension was maintained and recorded on Figure H4		
2				2. Verify that the number of winding turns for each Step was recorded on Figure H5.		
2				3. Verify weight of roving (including scrap) was recorded on Figure H3.		
1 0603				OVEN CURE AND CLEANUP	8 . 0 . 1	
1				1. Install the wound-vessel/cure-cart assembly in an oven at ambient temperature.		
1						

SHOP ORDER CONTINUATION SHEET

SHEET 8 OF 9

SPLIT REFERENCE	STARTING NUMBER AREA	SPLITTING ORDER NO.	C. OPER. NO.	STA. NO.	PART DESCRIPTION			PART NUMBER	ARDE P/N D3897	N/C	N/C	
					MONTH	DAY	YEAR	C.	C.	C.	C.	
D3897												
2	2	0603	Cont.	2.	Install a new (circular) oven cure chart in temperature recorder.							
2	2			3.	Install cam for curing unit 2 hours at 200°F plus 4 hours at 300°F and initiate cure cycle. Wipe off excess resin at 1/4-hour intervals (or lesser intervals, as necessary) until gelation occurs. Rotate position of the sphere periodically during this period to prevent uneven surface resin buildup.							
2	2			4.	Remove the cured vessel from the oven. Obtain oven cure chart and attach to PCR.							
2	2			5.	Disassemble tooling from cured vessel and return to tool control.							
2	2			6.	Clean all exposed metal surfaces with MEK to remove any resin. Care should be exercised so that internal metal "O" Ring surface is not defaced.							
2	2			7.	Measure cured vessel length, diameters (Pi-Tape), and weight; record values on PCR, Figure H2.							
2	2			8.	Deliver the vessel to the inspection area.							
2	2	0706			INSPECTION							
2	2			1.	Verify cure cycle from cure record.							
2	2			2.	Verify record of dimensions.							
2	2			3.	Inspect for handling damage.							
2	2		D		Deliver vessel to shipping							

PROCESS CONTROL RECORD

FIGURE H1: MATERIAL TRACEABILITY

Part No. D3897 Date Started _____

Part Name F/W Pressure Vessel W.O. No. 2003-

Serial No. _____ Shop Order No. D3897

<u>Operation No.</u>	<u>Description of Data Required</u>	<u>Inspector</u>
0103	Record traceability data of the following:	

	<u>Mfg. Lot No.</u>	<u>Accept. Tag No.</u>
1. PRD Roving, 4-End, Type III	_____	_____
2. Epon 828	_____	_____
3. DSA	_____	_____
4. Empol 1040	_____	_____
5. BDMA	_____	_____

0203-1 Record traceability data of aluminum liner assembly, P/N D3896

Accept Tag No. _____ S/N _____

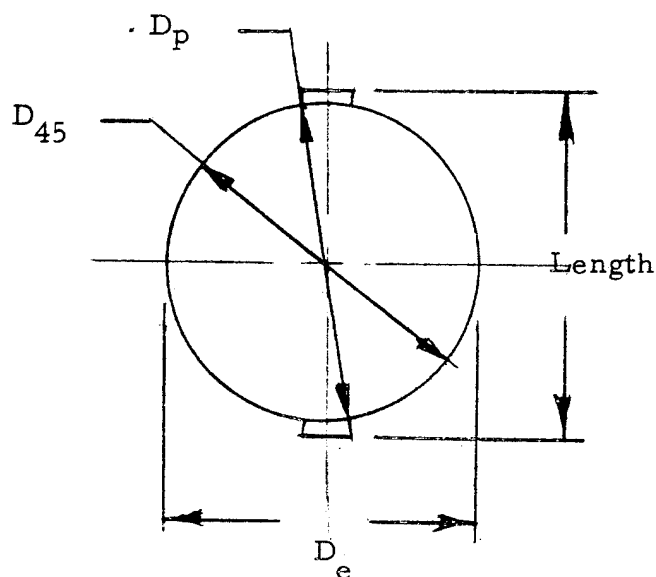
PROCESS CONTROL RECORD

FIGURE H2: DIMENSION/WEIGHT RECORD

Part No. D3897 Date Started _____

Part Name F/W Pressure Vessel W.O. No. 2003-

Serial No. _____ Machine Operator _____



Operation No. 0203-2 0603-7

Before Wrap After Cure

Vessel Length = _____ inch _____ inch

Diameters

D_e = _____ inch _____ inch

D_p = _____ inch _____ inch

D_{45} = _____ inch _____ inch

Vessel Weight = _____ lbs _____ LBS.

PROCESS CONTROL RECORD

FIGURE H3: MATERIAL USAGE RECORD

Part No. D3897 Date Started _____

Part Name F/W Pressure Vessel W.O. No. 2003-

Serial No. _____ Shop Order No. D3897

<u>Operation No.</u>	<u>Description of Data Required</u>	<u>Inspector</u>
<u>0203-10</u>	Record PRD roving usage	

Brake No.	Roll No.	Weight, gm		Usage
		Start	End	
1				
2				
3				
4				
5				
6				
7				
8				
9				
10				
11				
12				

0403-13

Total Usage: _____

Scrap _____

Net Usage: _____

[÷ 454 = _____ lb.]

PROCESS CONTROL RECORD

FIGURE H4: TENSION RECORD

Part No. D3897 Date Started _____
Part Name F/W Pressure Vessel W.O. No. 2003-
Serial No. _____ Shop Order No. D3897

Brake NO.	STEP NO.				
	1	3	6	9	13
1					
2					
3					
4					
5					
6					
7					
8					
9					
10					
11					
12					
Oper. No.	0403-5	0403-9			

NOTE: Record the static tension before adjustment to 1.0 lb/roving is made

PROCESS CONTROL RECORD

FIGURE H5: WINDING PATTERN

Part No. D3897 Date Started _____
Part Name F/W Pressure Vessel Work Order No. 2003-
Serial No. _____ Shop Order No. D3897
Machine Operator _____

<u>Step No.</u>	<u>Degree Setting</u>	<u>Machine Setting</u>	<u>Payoff Arm Setting</u>	<u>RPM</u>	<u>Turns</u>
					<u>Required</u> <u>Actual</u>

PROPRIETARY INFORMATION

APPENDIX I

**PERFORMANCE TEST PRESSURE/STRAIN
PLOTS KEVLAR/STAINLESS STEEL
PRESSURE VESSELS**

APPENDIX I

FIGURE INDEX

Figure Number	Vessel Serial Number	Type of Test	Page Number
I-1	001	Hydroburst	357
I-2			358
I-3			359
I-4	002	Cyclic Fatigue	360
I-5			361
I-6			362
I-7		Hydroburst	363
I-8			364
I-9	003	Cyclic Fatigue	365
I-10			366
I-11			367
I-12	004	Cyclic Fatigue	368
I-13			369
I-14			370
I-15		Sustained Load	371
I-16			372
I-17		Hydroburst	373
I-18			374
I-19			375
I-20	005	Cyclic Fatigue	376
I-21			377
I-22			378
I-23	006	Sustained Load	379

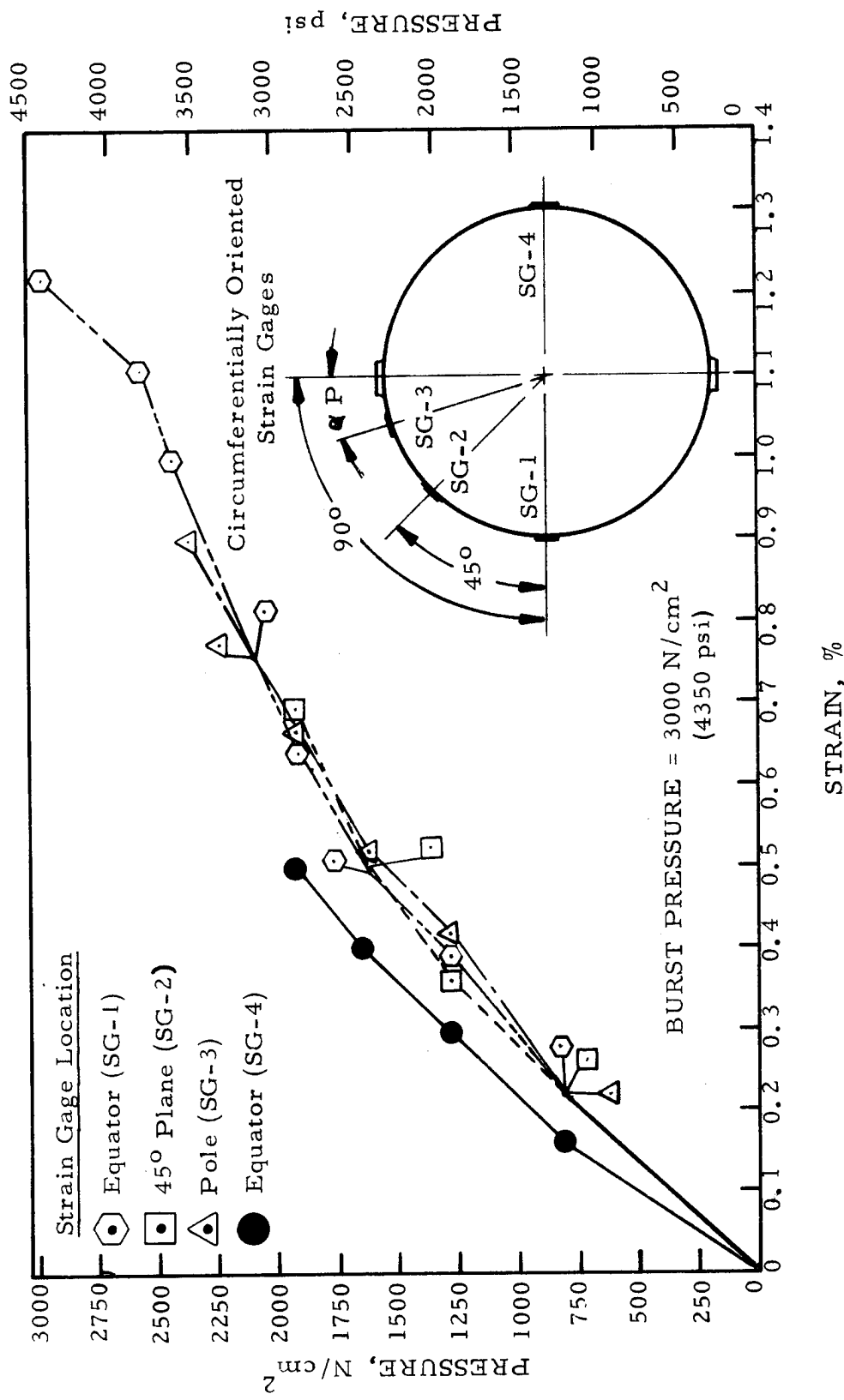


FIGURE I-1: Strains Obtained From Circumferentially Oriented Strain Gages During Hydraulic Burst of Kevlar/Stainless Steel Vessel 001

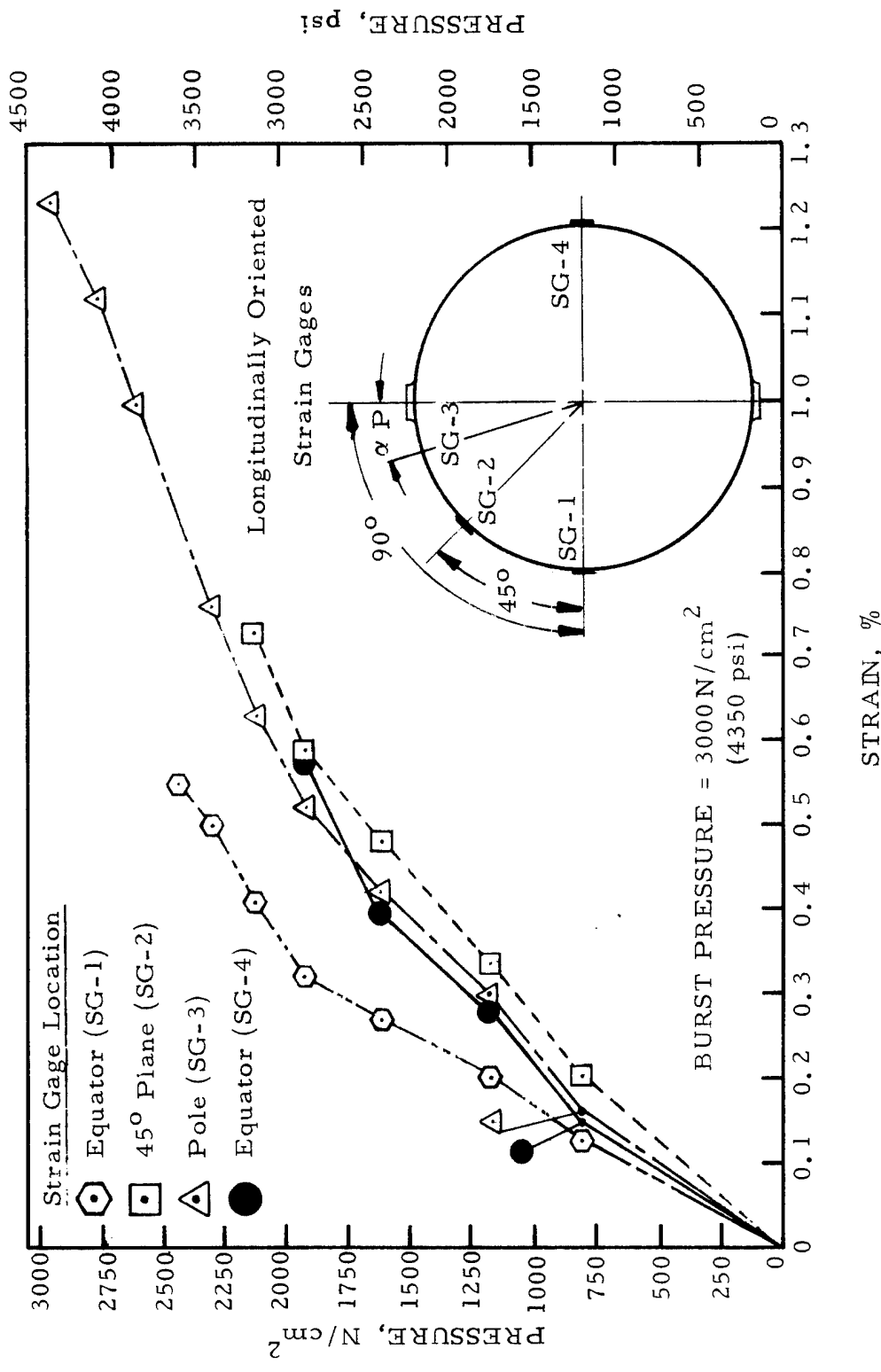


FIGURE I-2: Strains Obtained From Longitudinally Oriented Strain Gages During Hydraulic Burst of Kevlar/Stainless Steel Vessel 001

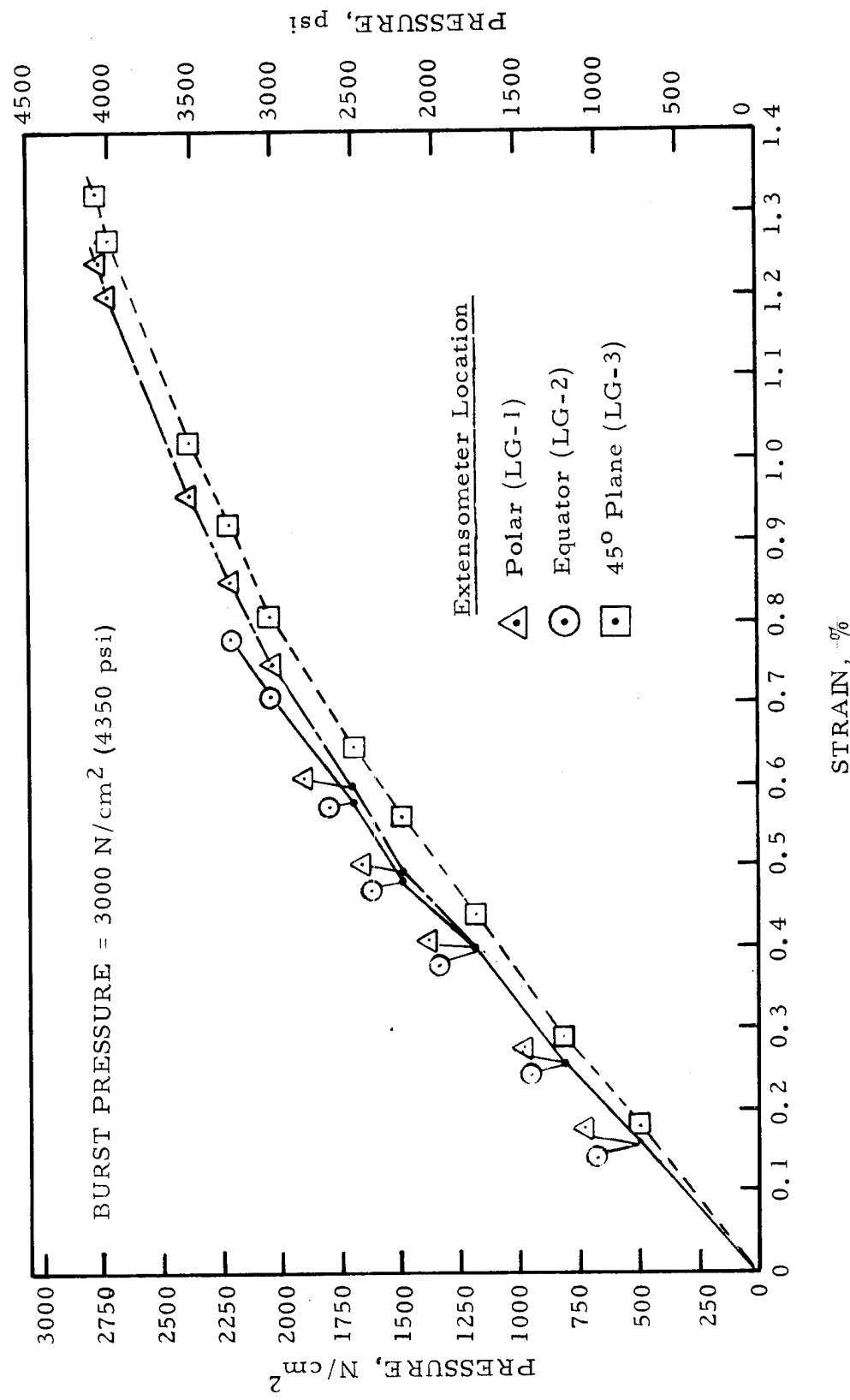
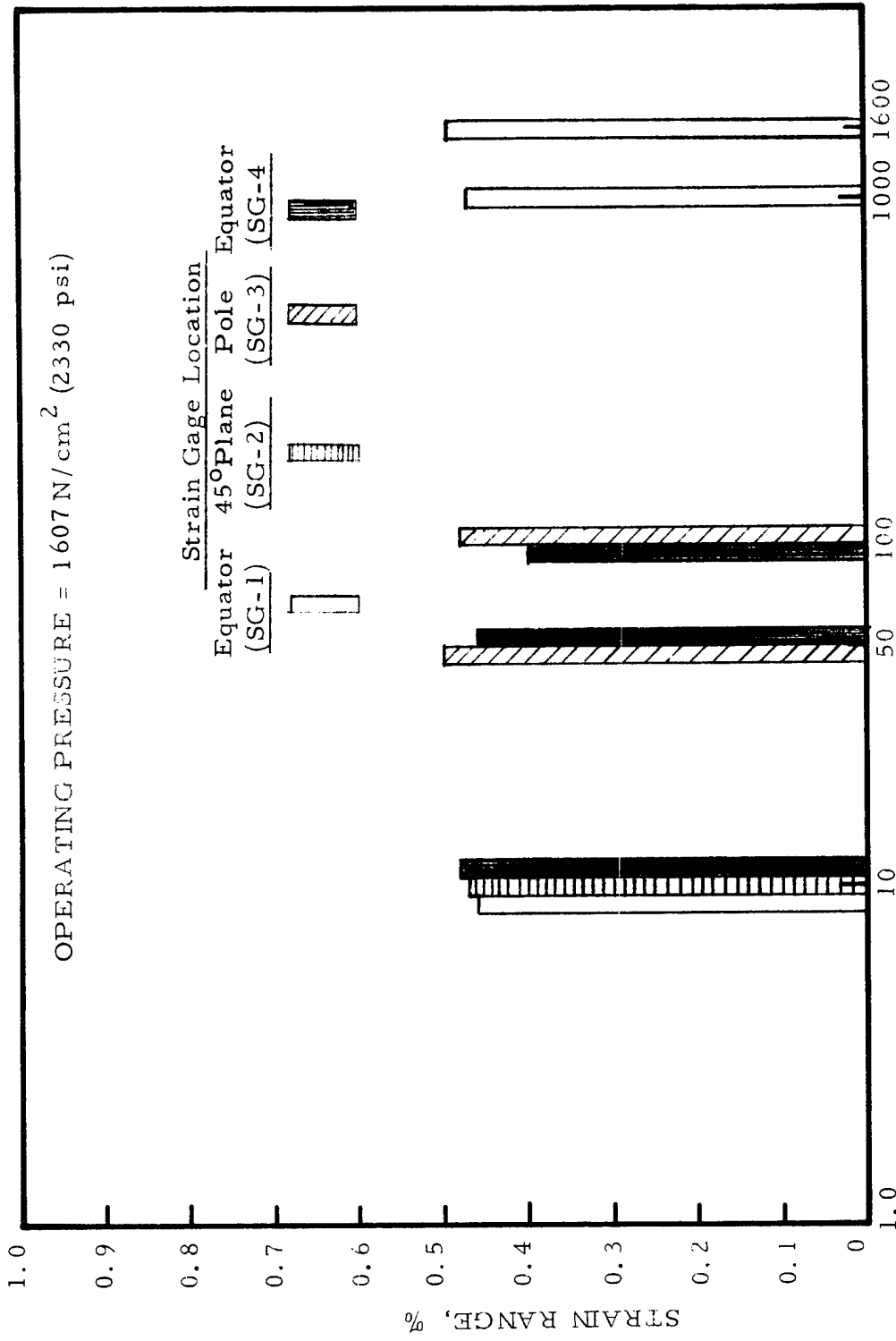


FIGURE I-3: Strains Obtained From Great Circle Extensometers During Hydraulic Burst of Kevlar/Stainless Steel Vessel 001

OPERATING PRESSURE = 1607 N/cm^2 (2330 psi)



NUMBER OF PRESSURE CYCLES

FIGURE I-4: Strains Obtained from Circumferentially Oriented Strain Gages During Cyclic Fatigue of Kevlar/Stainless Steel Vessel 002.

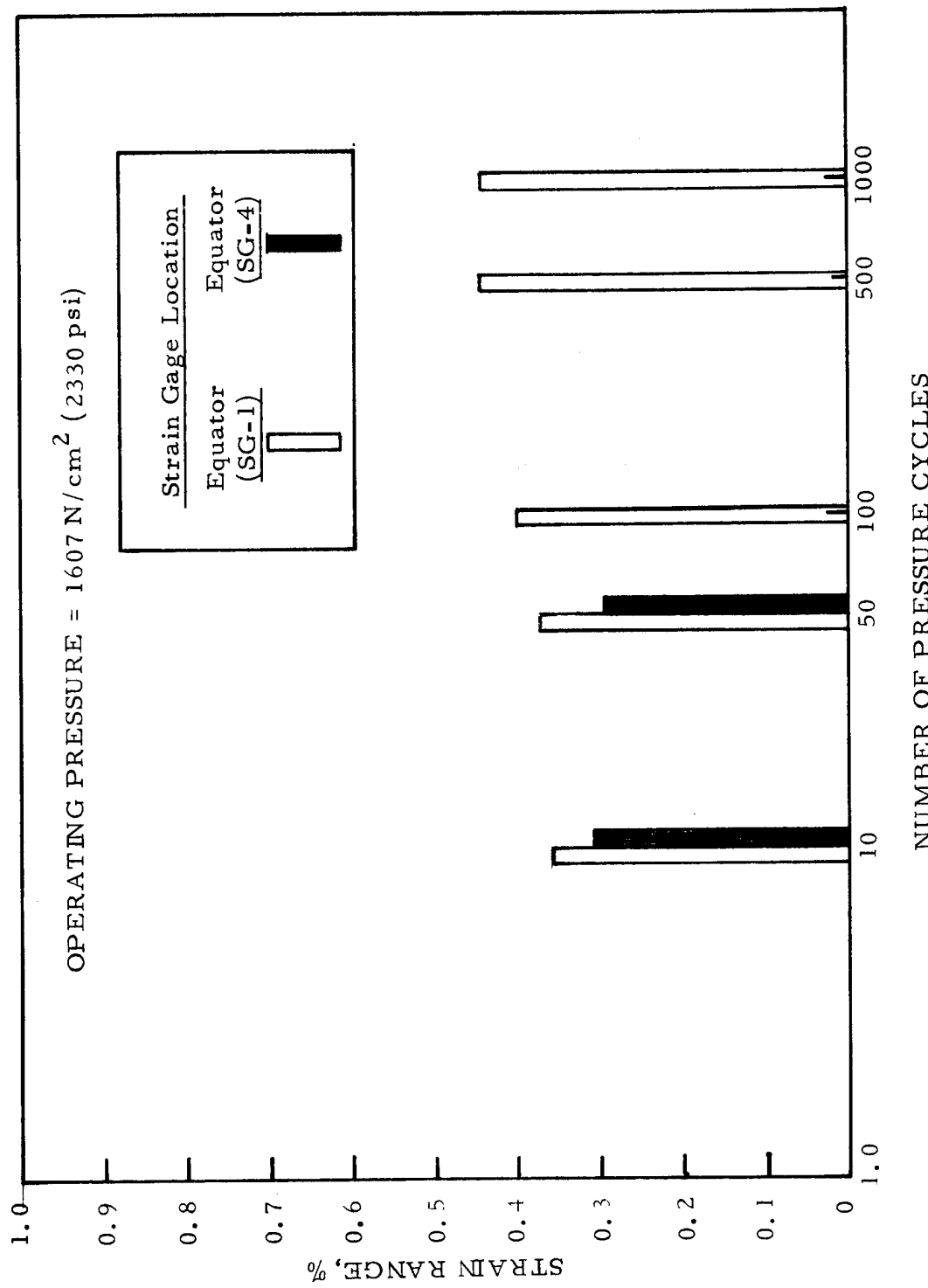
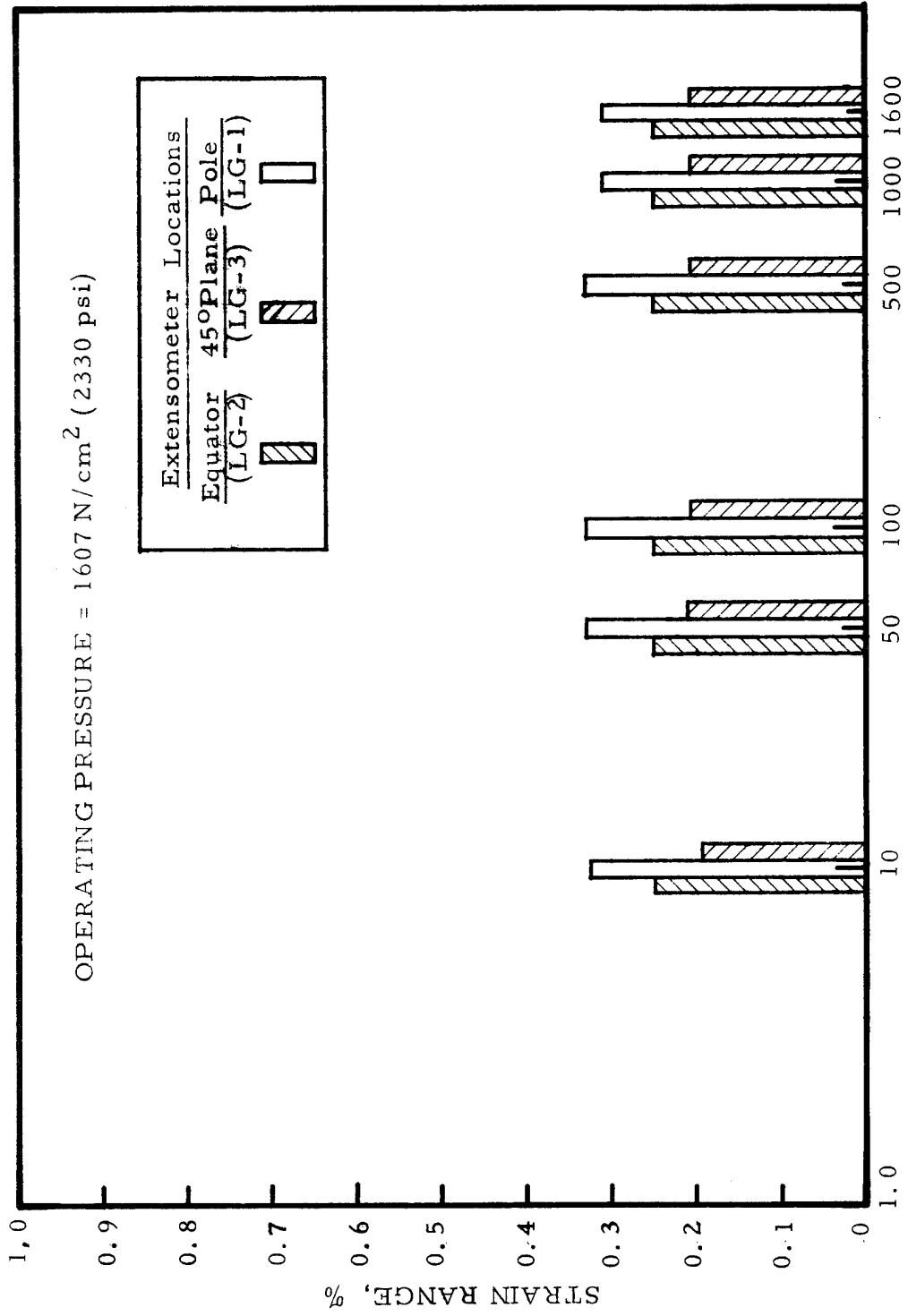


FIGURE I-5: Strains Obtained From Longitudinally Oriented Strain Gages During Cyclic Fatigue of Kevlar/Stainless Steel Vessel 002



NUMBER OF PRESSURE CYCLES

FIGURE I-6: Strains Obtained From Great Circle Extensometers During Cyclic Fatigue of Kevlar/Stainless Steel Vessel 002

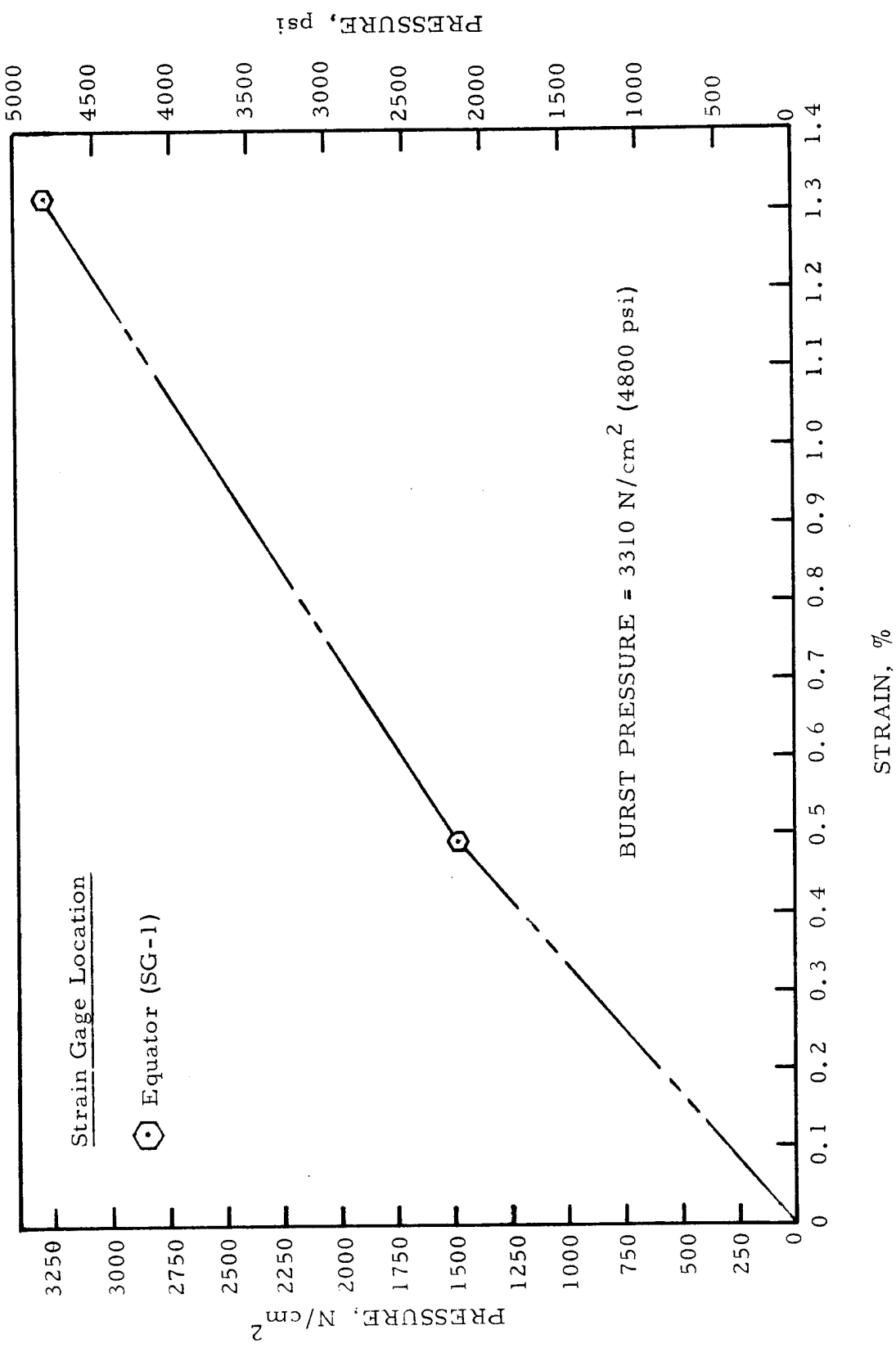


FIGURE I-7: Strains Obtained From Circumferentially Oriented Strain Gages During Hydraulic Burst of Kevlar / Stainless Steel Vessel 002

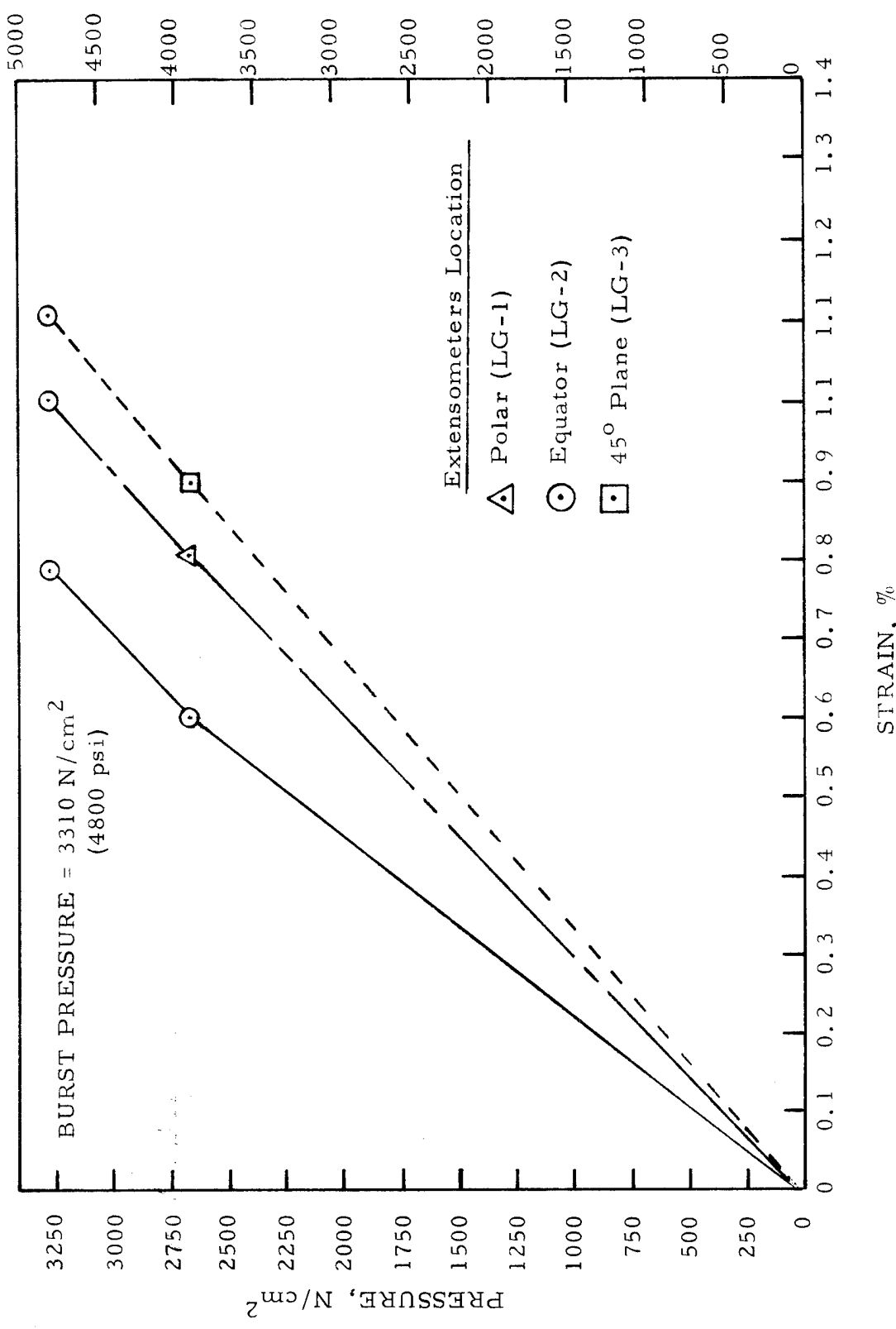


FIGURE I-8: Strains Obtained From Great Circle Extensometers During Hydraulic Burst of Kevlar/Stainless Steel Vessel 002

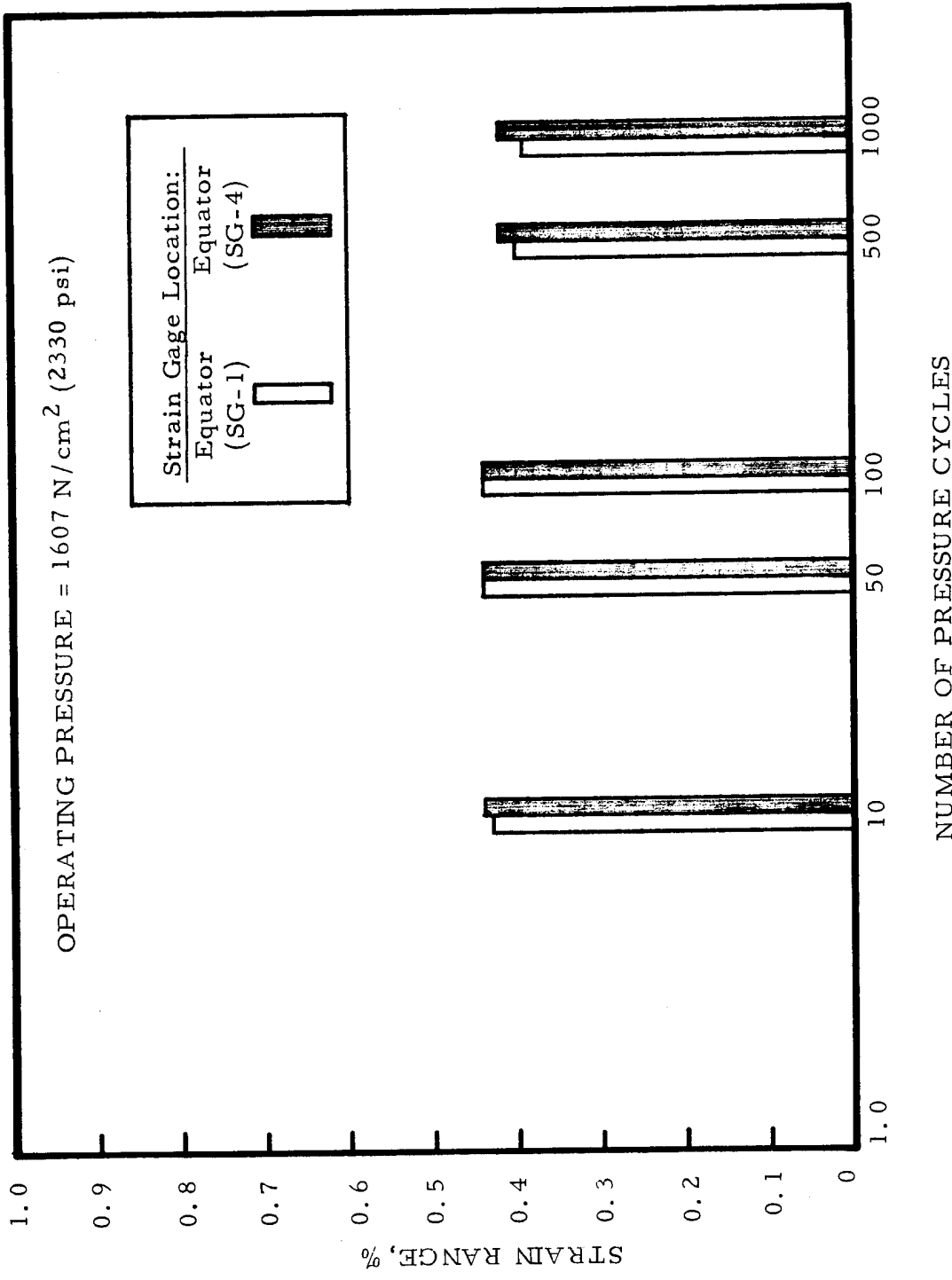
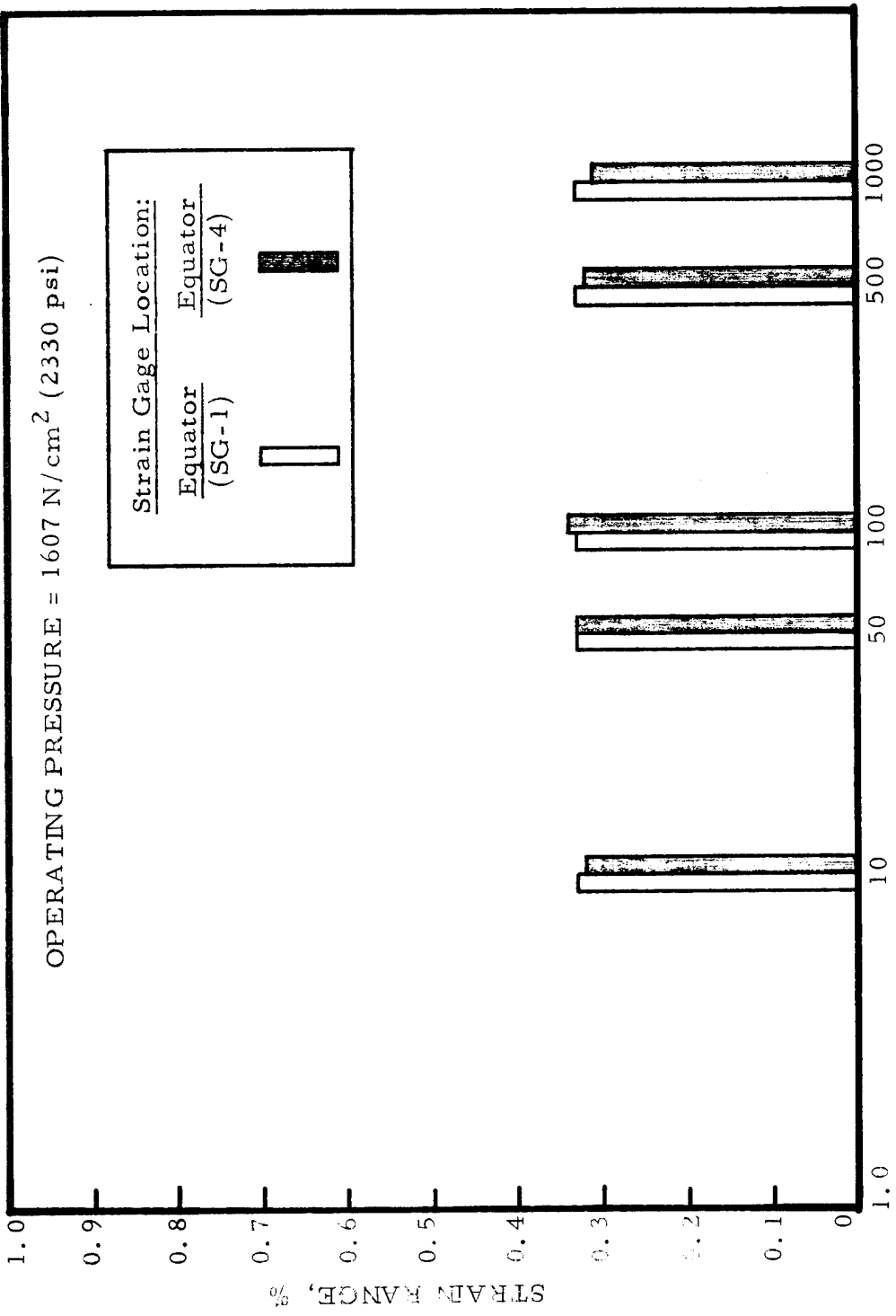


FIGURE I-9: Strains Obtained From Circumferentially Oriented Strain Gages During Cyclic Fatigue of Kevlar/Stainless Steel Vessel 003



NUMBER OF PRESSURE CYCLES

FIGURE I-10: Strains Obtained From Longitudinally Oriented
Strain Gages During Cyclic Fatigue of Kevlar/Stainless
Steel Vessel 003

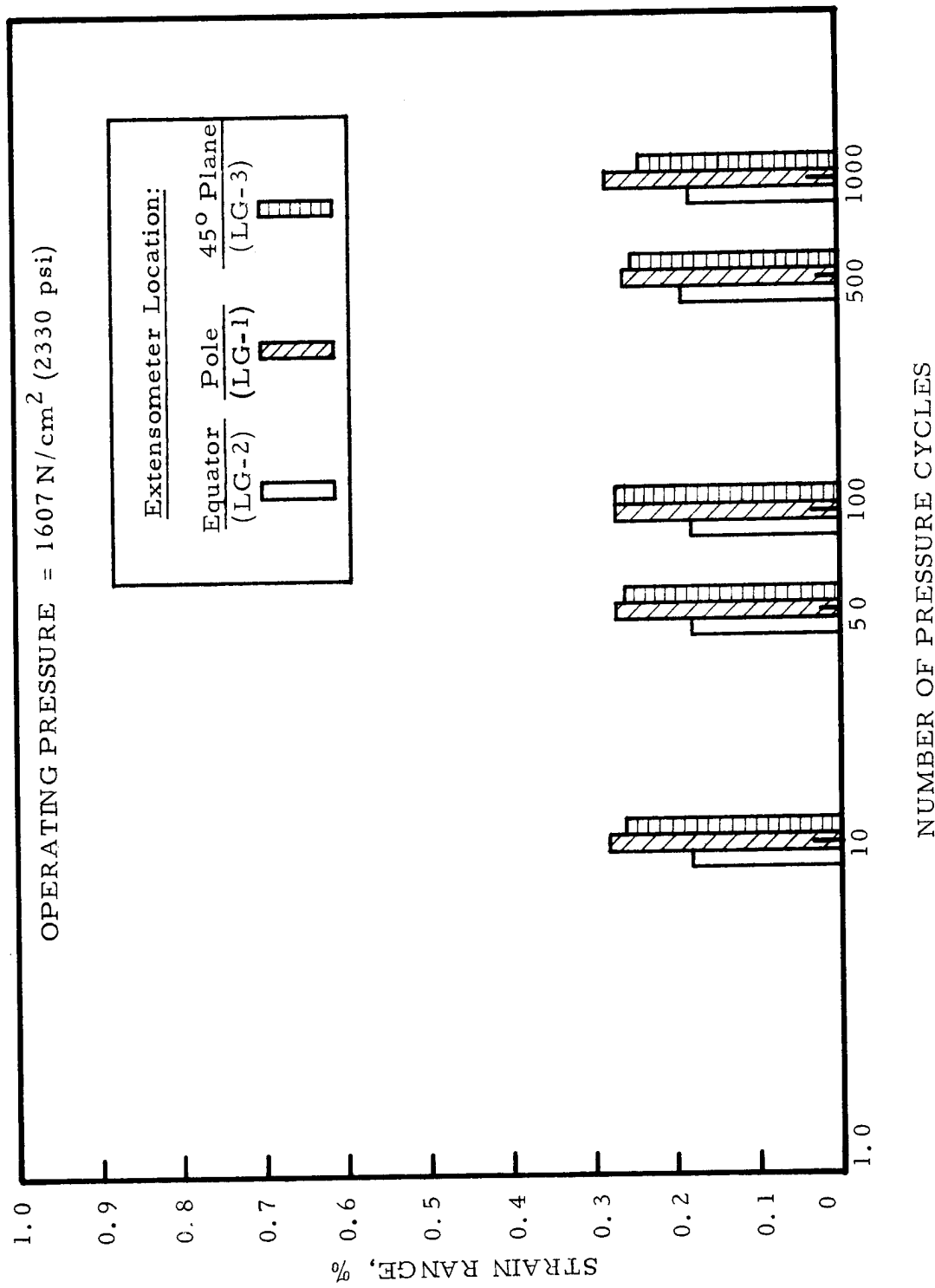


FIGURE I-11: Strains Obtained From Great Circle Extensometers During Cyclic Fatigue of Kevlar/Stainless Steel Vessel 003

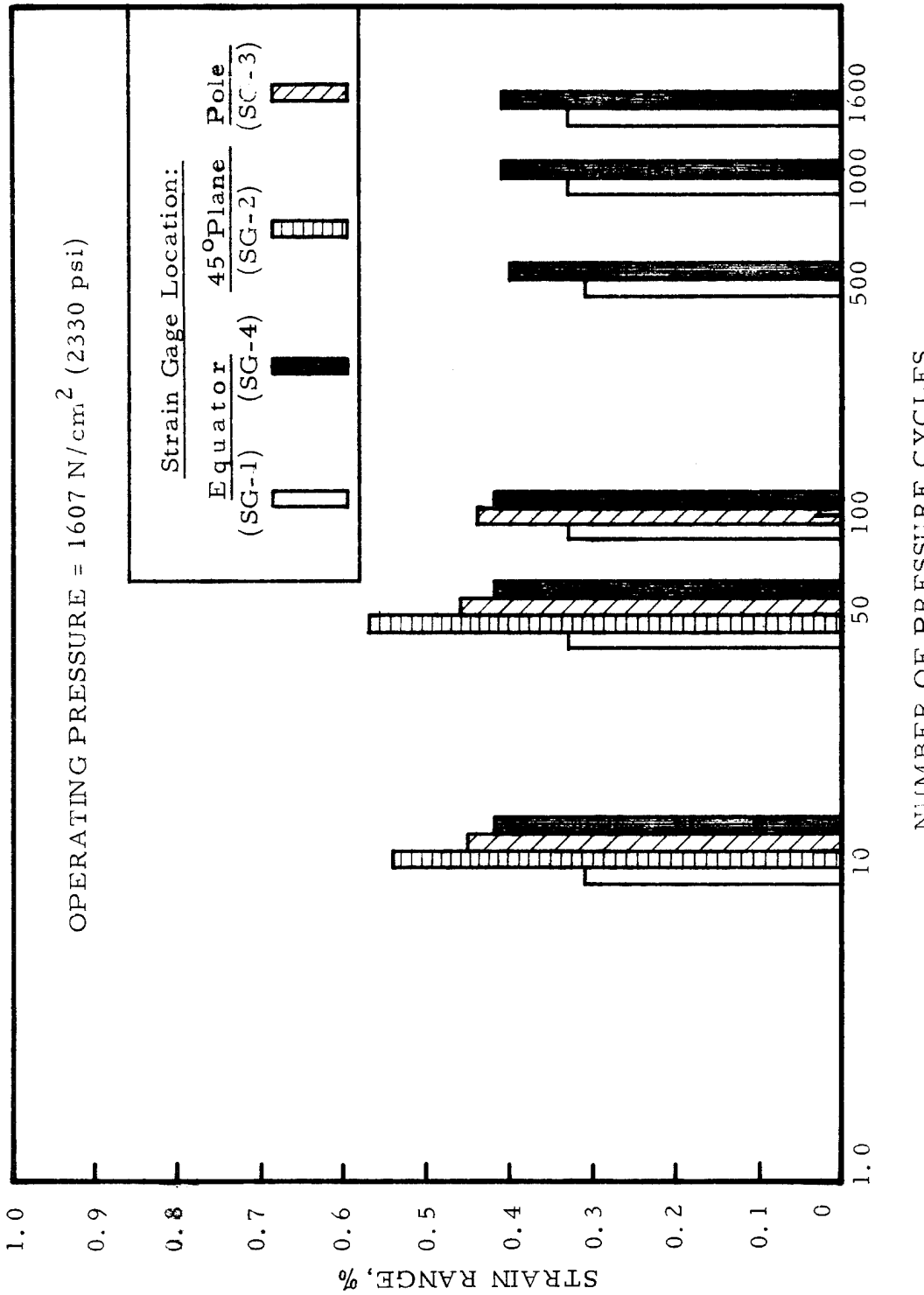


FIGURE I-12: Strains Obtained From Circumferentially Oriented Strain Gages During Cyclic Fatigue of Kevlar/Stainless Steel Vessel 004

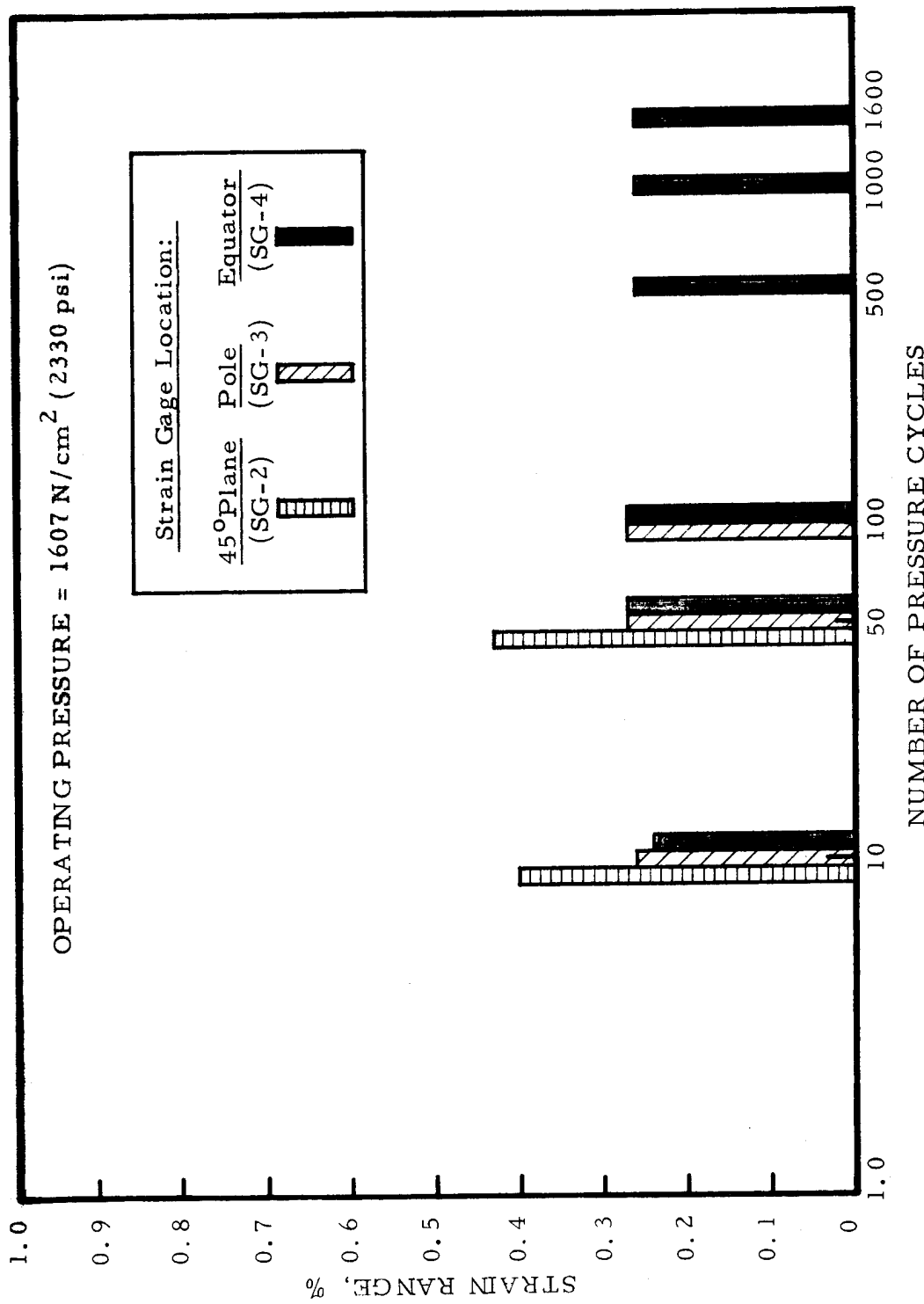


FIGURE I-13: Strains Obtained From Longitudinally Oriented Strain Gages During Cyclic Fatigue of Kevlar/Stainless Steel Vessel 004

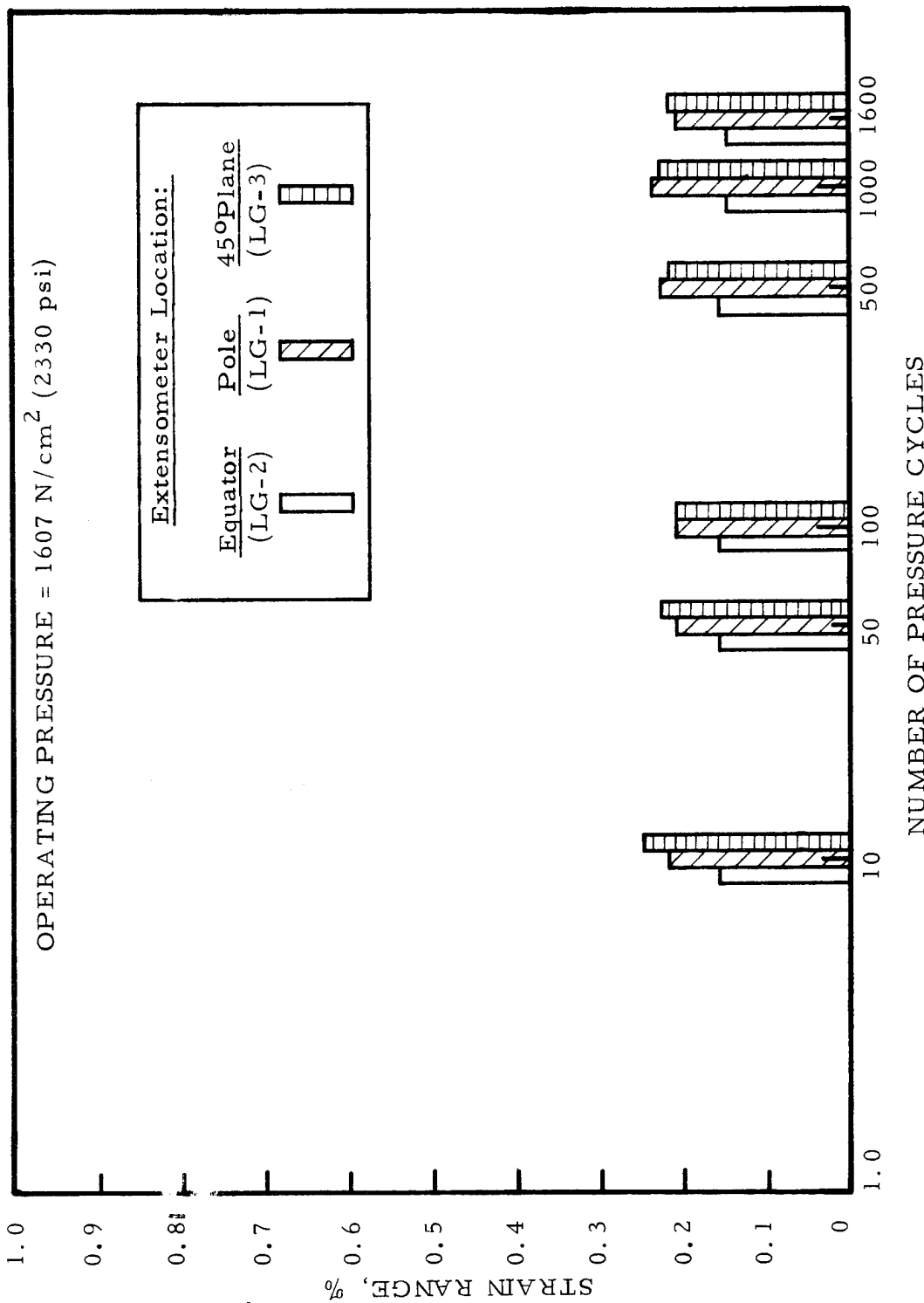


FIGURE I-14: Strains Obtained From Great Circle Extensometers During Cyclic Fatigue of Kevlar/Stainless Steel Vessel 004

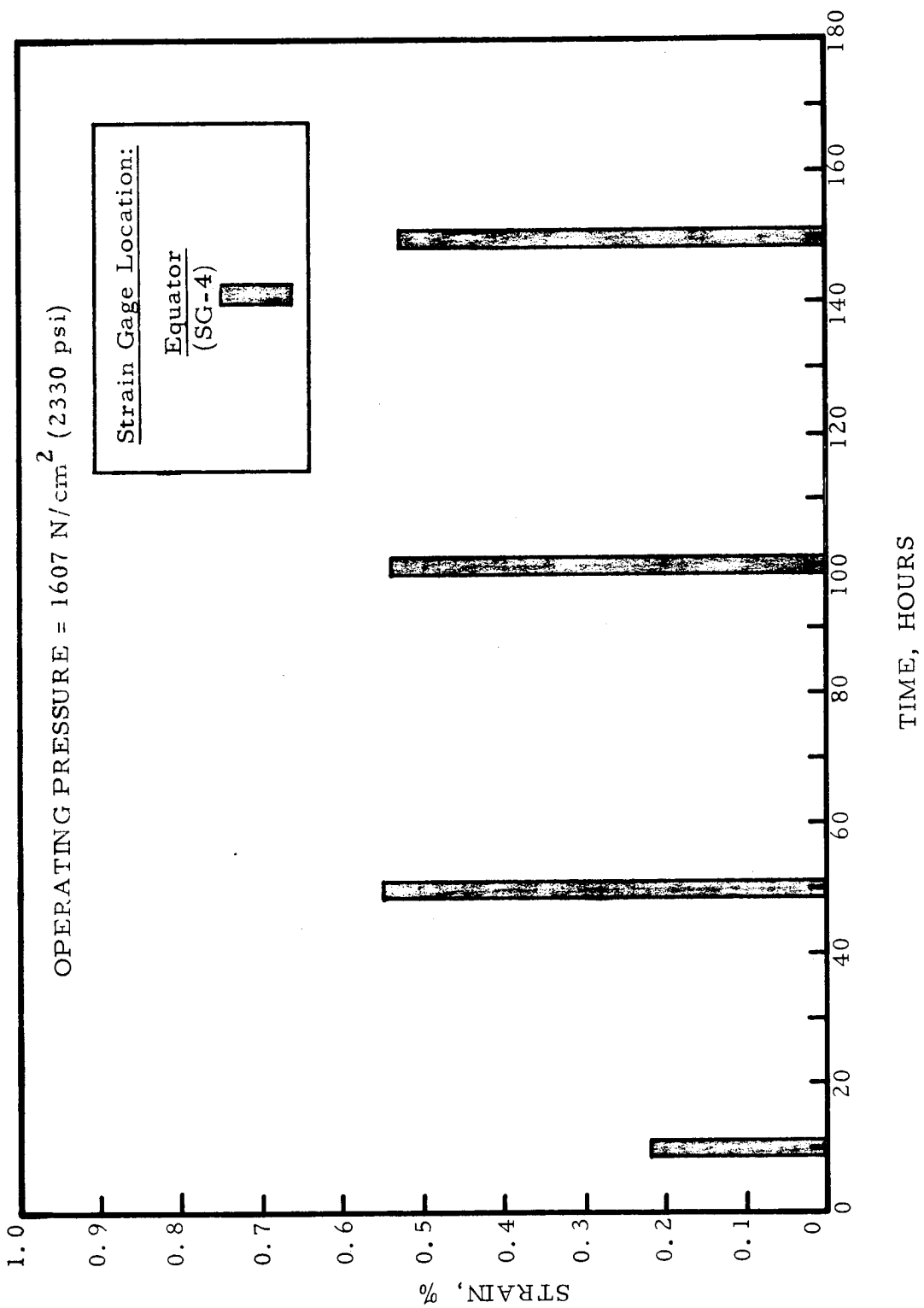


FIGURE I-15: Strains Obtained From Longitudinally Oriented Strain Gages During Sustained Load Test of Kevlar/Stainless Steel Vessel 004

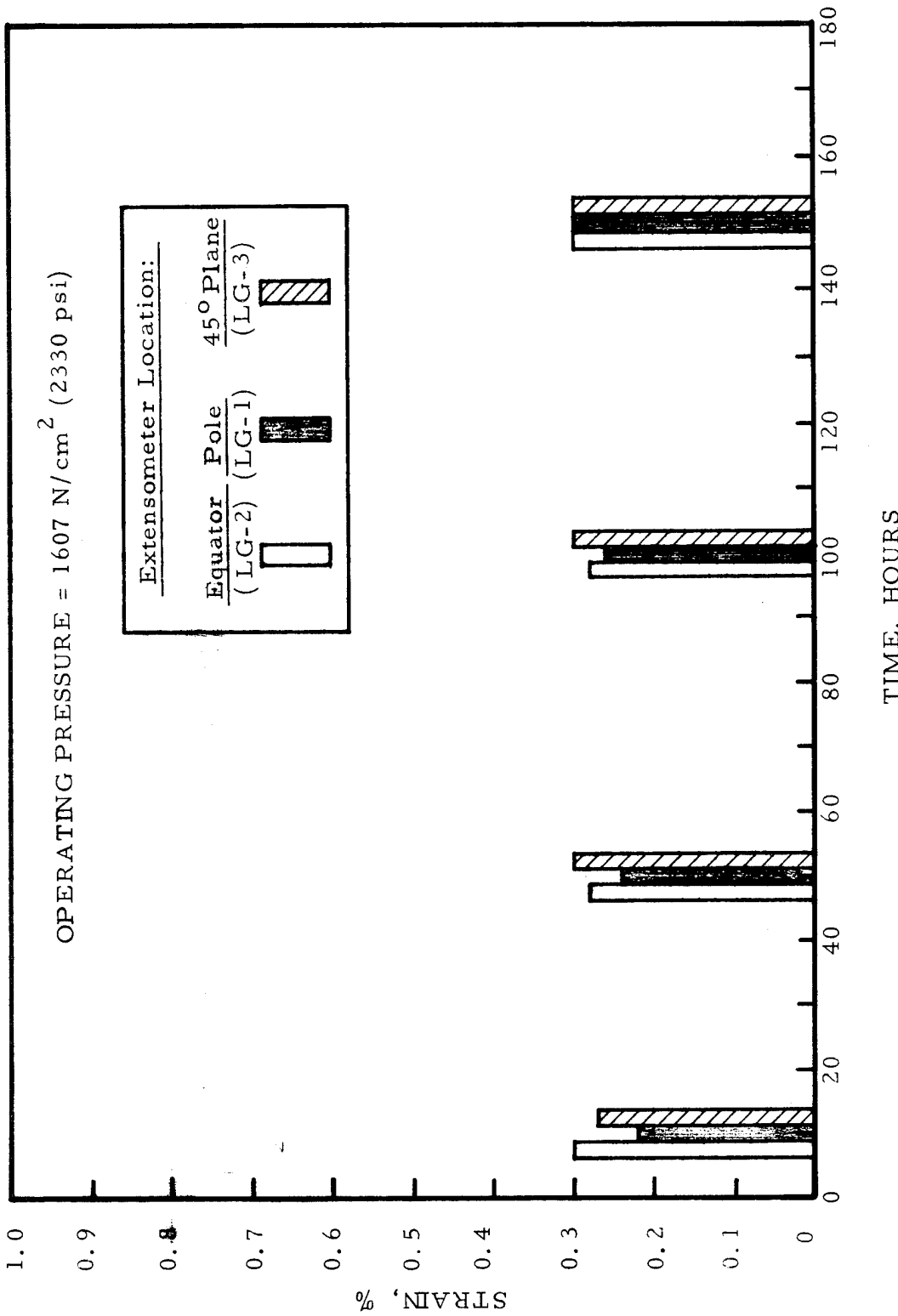


FIGURE I-16: Strains Obtained From Great-Circle Extensometers During Sustained Load Test of Kevlar/Stainless Steel Vessel 004

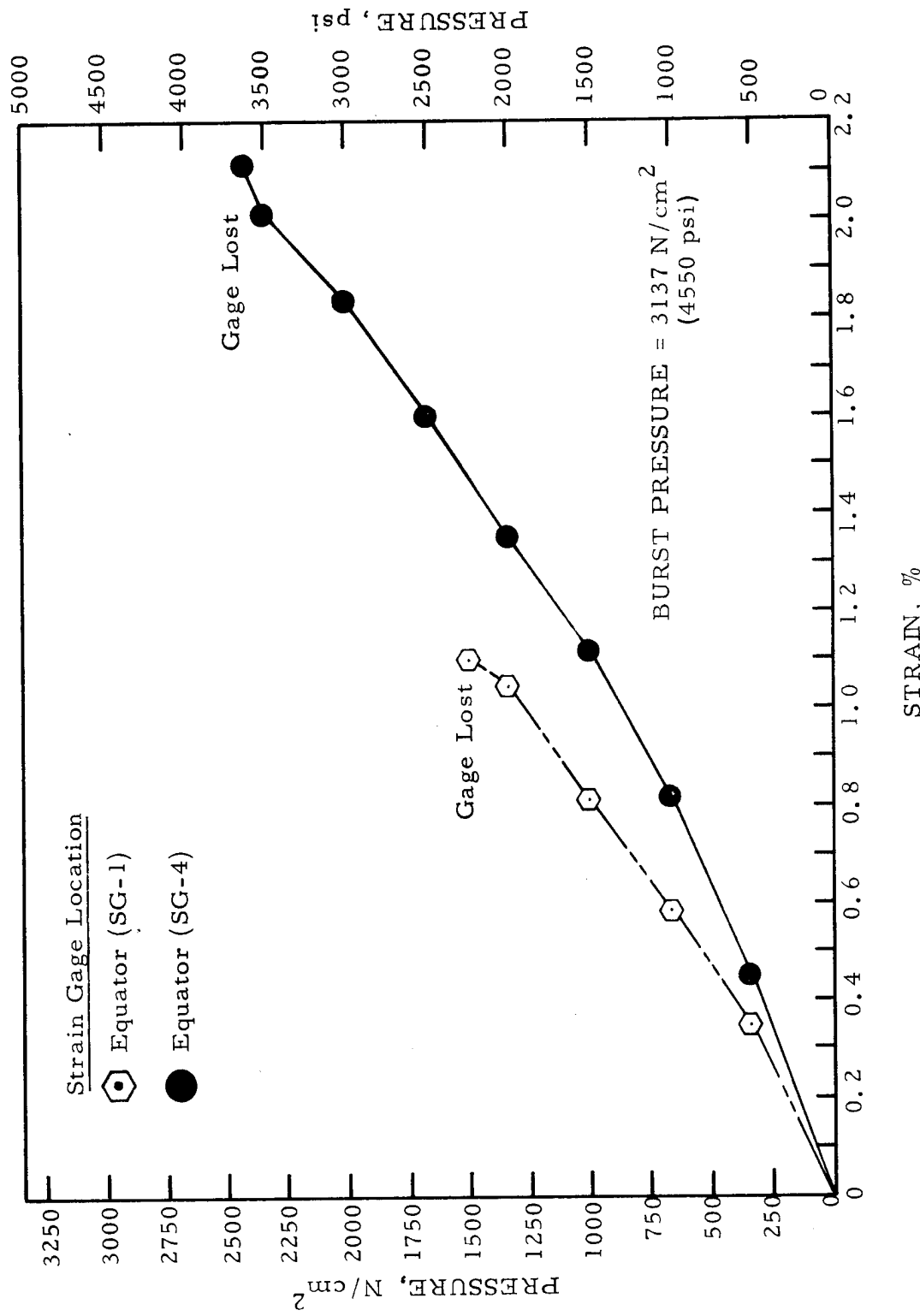


FIGURE I-17: Strains Obtained From Circumferentially Oriented Strain Gages During Hydraulic Burst of Kevlar / Stainless Steel Vessel 004

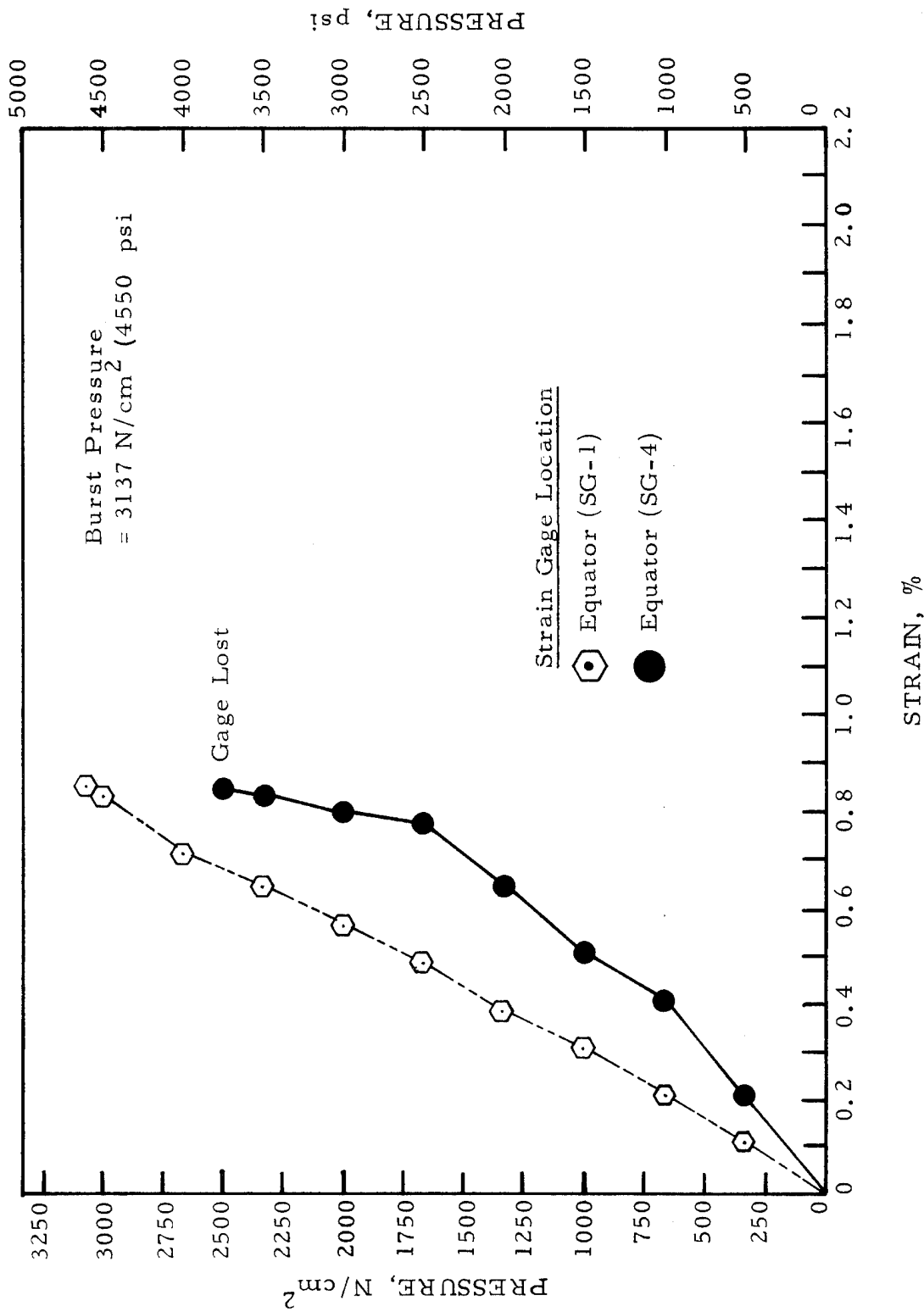


FIGURE I-18: Strains Obtained From Longitudinally Oriented Strain Gages During Hydraulic Burst of Kevlar/Stainless Steel Vessel 004

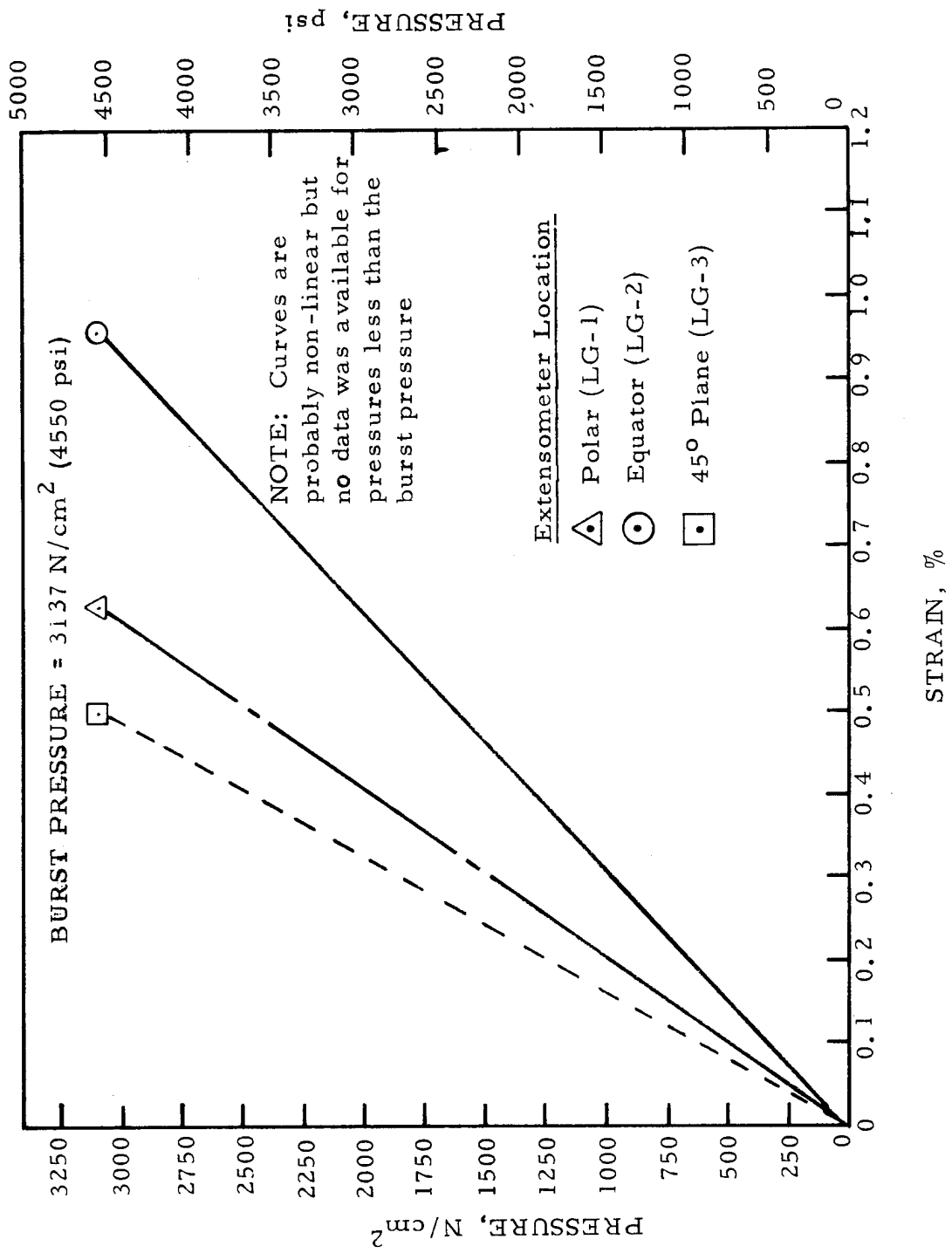


FIGURE I-19: Strains Obtained From Great Circle Extensometers During Hydraulic Burst of Kevlar/Stainless Steel
Vessel 004

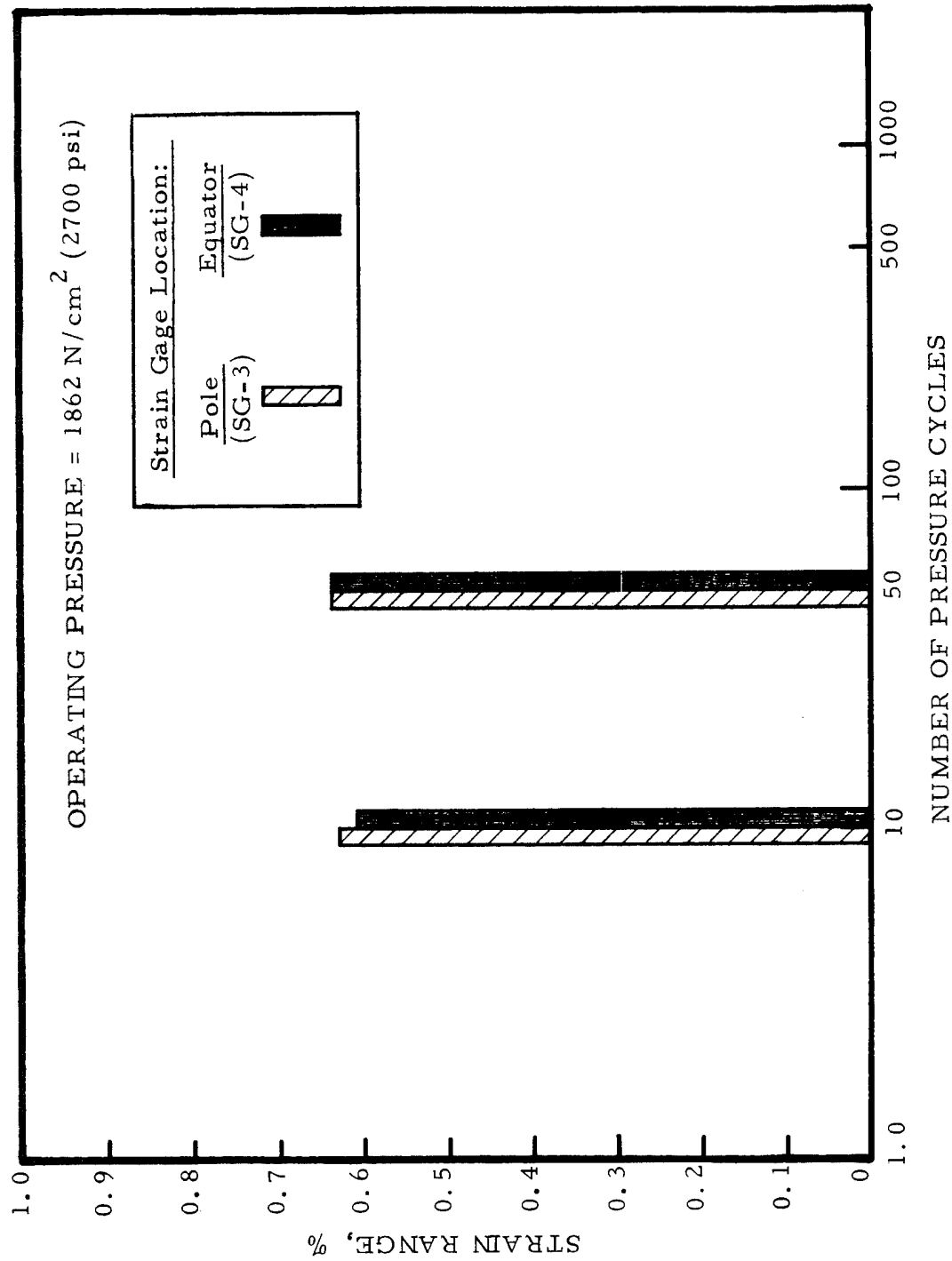


FIGURE I-20: Strains Obtained From Circumferentially Oriented Strain Gages During Cyclic Fatigue of Kevlar/Stainless Steel Vessel 005

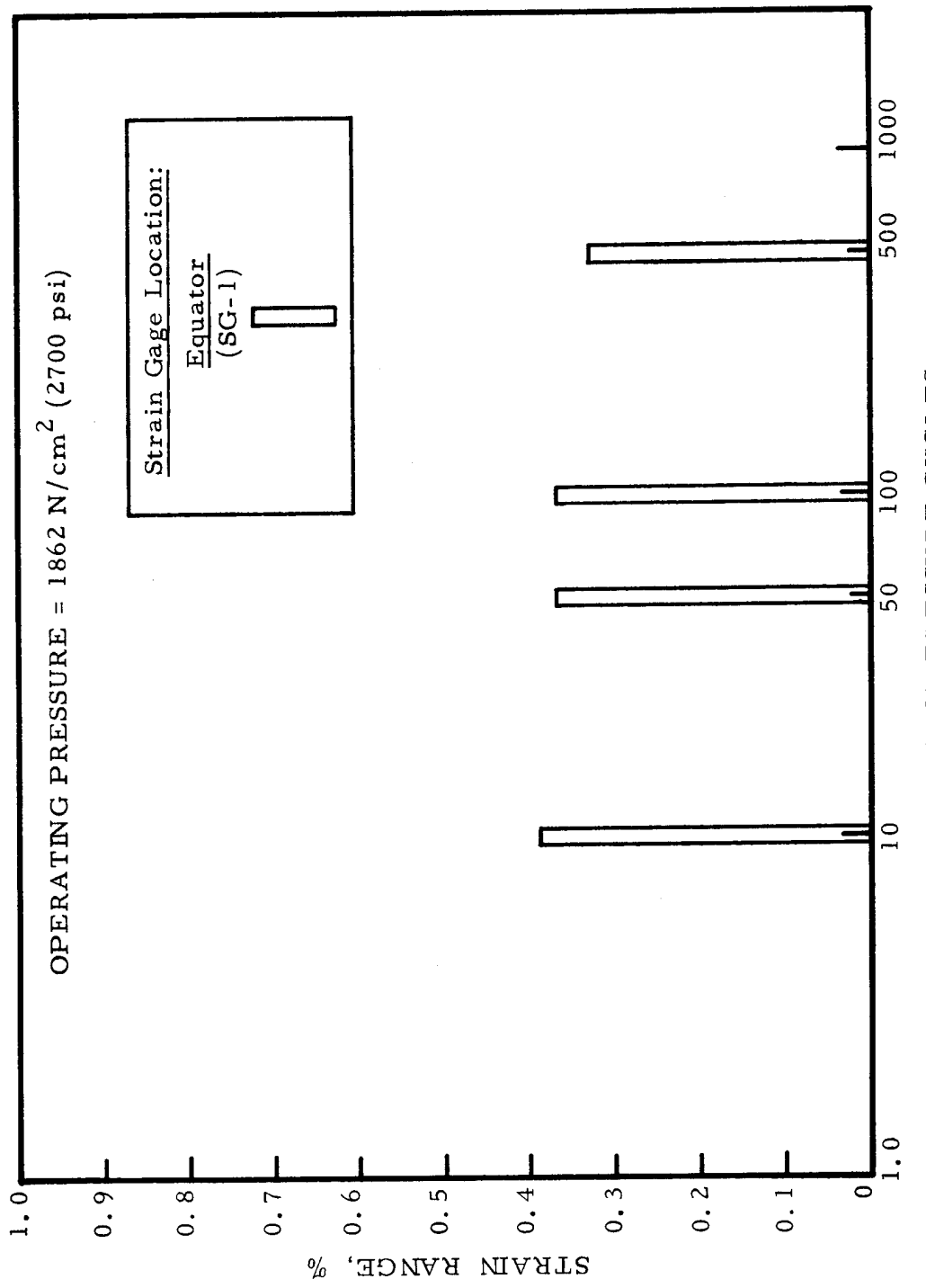


FIGURE I-21: Strains Obtained From Longitudinally Oriented Strain Gages During Cyclic Fatigue of Kevlar / Stainless Steel Vessel 005

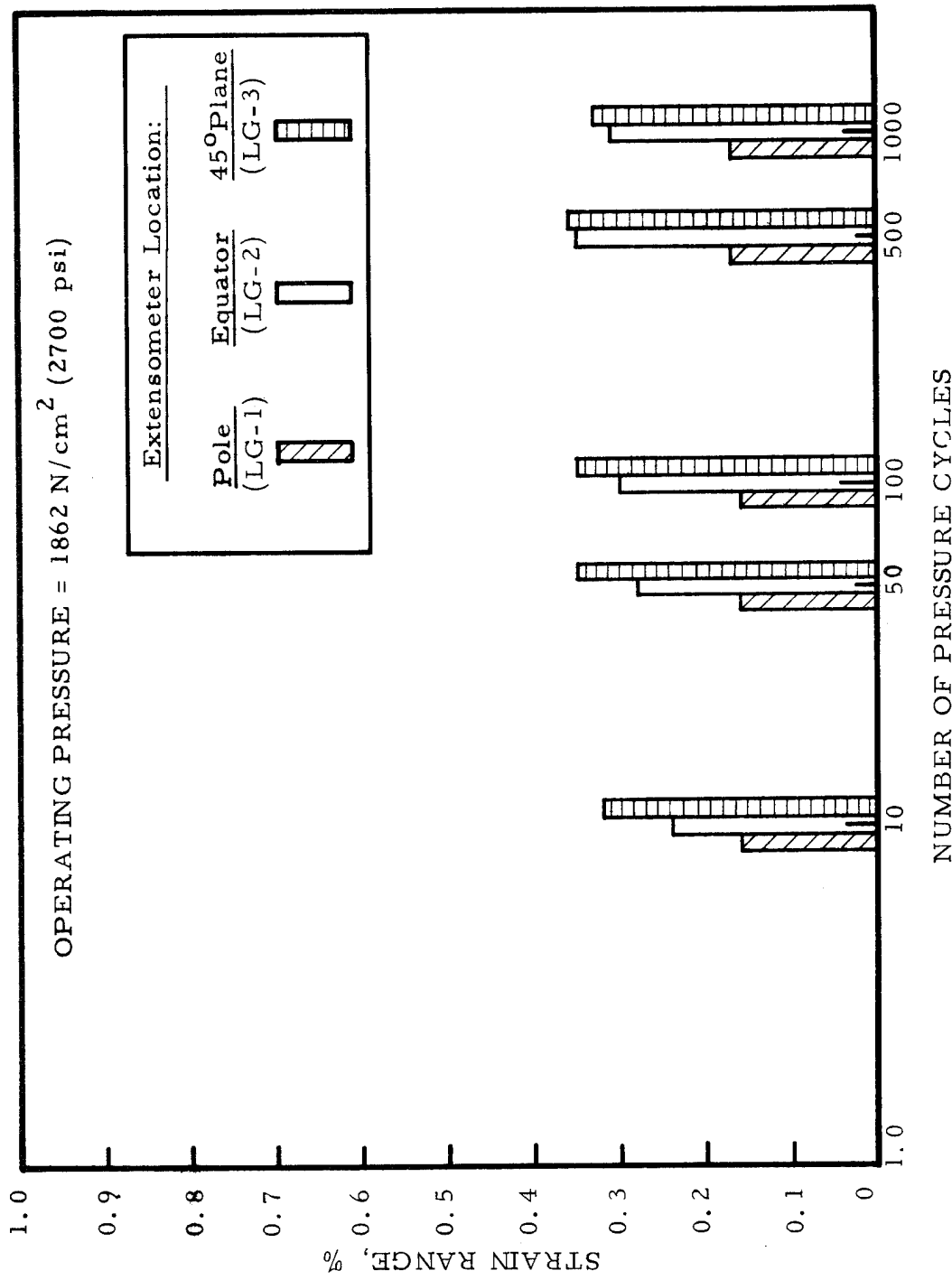


FIGURE I-22: Strains Obtained From Great Circle Extensometers
During Cyclic Fatigue of Kevlar/Stainless Steel
Vessel 005

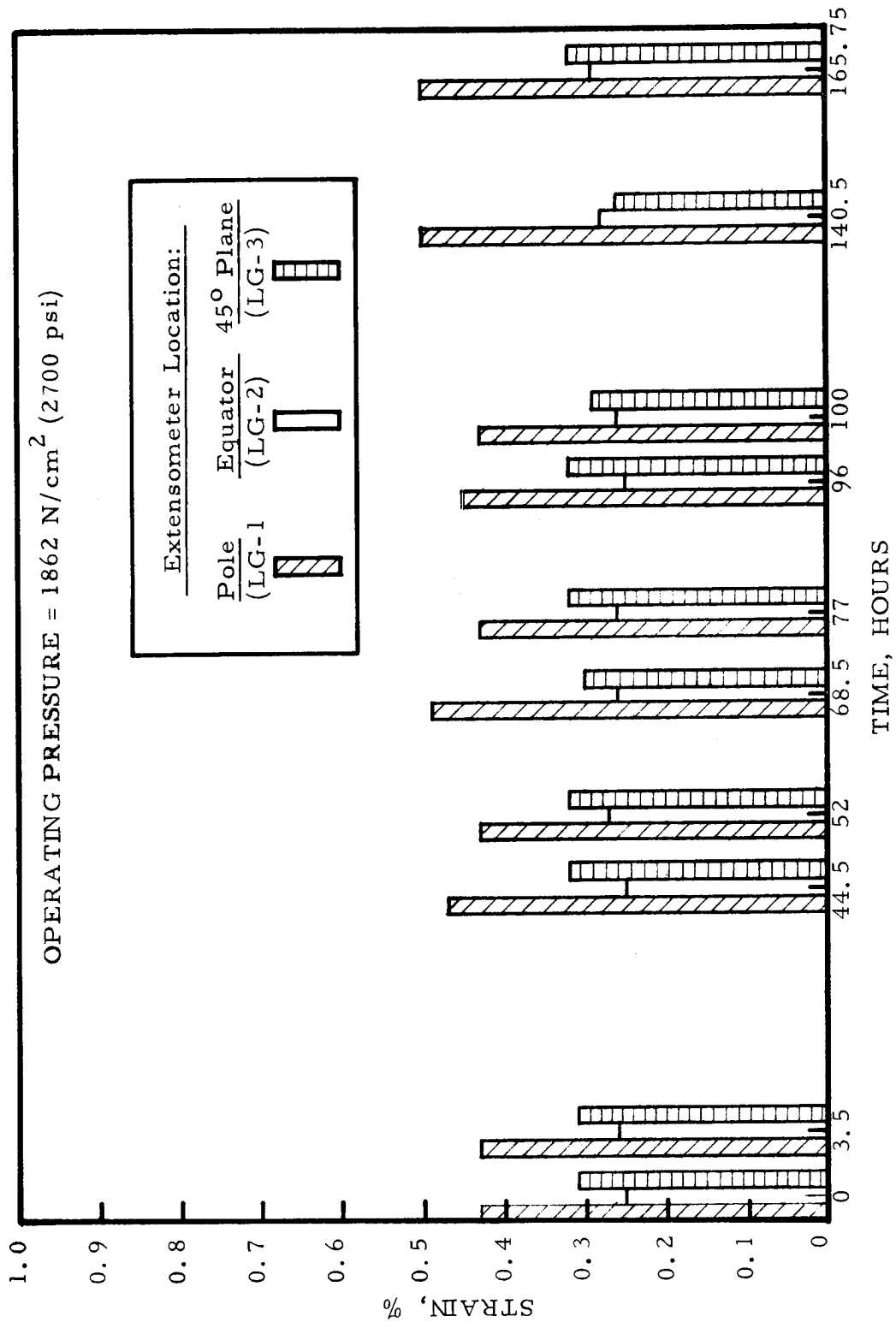


FIGURE I-23: Strains Obtained From Great Circle Extensometers During Sustained Load Test of Kevlar/Stainless Steel Vessel 006

APPENDIX J
LIST OF SYMBOLS

LIST OF SYMBOLS

A	Surface area, cm^2 (in^2)
a	Semi-elliptical crack depth, mm (in)
$a/2c$	Crack shape
a/Q	Crack size, mm (in)
c	One-half semi-elliptical crack length, mm (in)
D	Diameter, cm (in)
da/dN	Cyclic crack growth rate, mm (in)
E	Modulus of elasticity, GN/m^2 (psi)
F_{ty}	Yield strength, MN/m^2 (psi)
F_{tu}	Ultimate filament strength, MN/m^2 (psi)
H	Horizontal force, N (lb)
K_{IE}	Engineering fracture toughness, $\text{MN}/\text{m}^{3/2}$, ($\text{ksi}\cdot\text{in}^{1/2}$)
K_{sd}	Design stress intensity factor
L	Length, cm (in)
M	Bending moment, $\text{cm-N}/\text{cm}$ (in-lb/in)
N	Number of cycles
N_i	Number of surface area elements
N_ϕ	Meridional membrane force, N/cm (lb/in)
P	Applied load, N (lb)
p	Pressure, N/cm^2 (psi)
pV/W	Performance factor, J/g (in-lb/lbm)
Q	Crack shape parameter

LIST OF SYMBOLS (continued)

\bar{Q}	Average flow rate, liters/sec (gal/sec)
R	Minimum to maximum stress ratio
r	Radius, cm (in)
T	Temperature, K ($^{\circ}$ F)
t	Thickness, cm (in)
V	Internal volume, m ³ (in ³) or vertical force, N/cm (lb/in)
W	Weight, kg (lbm)
α	Proof test factor
Δ	Change or difference
ϵ	Strain, %
θ	Circumferential angle, rad (deg)
ρ	Density, g/cm ³ (lbm/in ³)
σ	Stress, MN/m ² (psi)
τ	Time, hours
ϕ	Meridional angle, rad (deg)

LIST OF SYMBOLS (concluded)

SUBSCRIPTS:

B Specific location (Figure 30)

b Burst

c Compression

cr Critical

D Specific location (Figure 30)

HB Horizontal bolt

i Initial

L Liner

max. Maximum

min. Minimum

o Operating

of Filament operating

p Port

R Tie-rod

S Specific location (Figure 30)

s Sizing

DISTRIBUTION LIST FOR NASA CR-134975
CONTRACT NAS3-16770

FILAMENT-REINFORCED METAL COMPOSITE PRESSURE VESSEL
EVALUATION AND PERFORMANCE DEMONSTRATION

STRUCTURAL COMPOSITES INDUSTRIES
6344 NORTH IRVINDALE AVENUE
AZUSA, CALIFORNIA 91702

<u>Recipient</u>	<u>No. of Copies</u>
NASA-Lewis Research Center 21000 Brookpark Rd. Cleveland, OH 44135	1
Attn: J. E. Dille, MS 500-313	1
J. R. Faddoul, MS 49-3	1
R. H. Kemp, MS 49-3	1
J. C. Freche, MS 49-1	1
G. T. Smith, MS 49-3	1
T. D. Gulko, MS 49-3	1
J. R. Barber, MS 500-205	1
Library, MS 60-3	1
AFSC Liaison Office, MS 501-3	1
Technical Utilization, MS 3-10	1
R. H. Johns, MS 49-3	1
R. F. Lark, MS 49-3	1
Report Control Office, MS 5-5	1
National Aeronautics and Space Administration Washington, DC 20546	1
Attn: KT/Technology Utilization Office	1
Library	1
NASA-Ames Research Center Moffett Field, CA 94035	1
Attn: D. Williams	1
Library	1
NASA-George C. Marshall Space Flight Center Marshall Space Flight Center, AL 35811	1
Attn: S&E-ASTN/AA/C. Lifer	1
S&E-ASTN-AS/H. Coldwate	1
S&E-ASTN-ES/E. Engler	1
Library	1

<u>Recipient</u>	<u>No. of Copies</u>
NASA-Goddard Space Flight Center Greenbelt, MD 20771 Attn: Library	1
NASA-John F. Kennedy Space Center Kennedy Space Center, FL 32899 Attn: Library	1
NASA-Langley Research Center Hampton, VA 23365 Attn: R. W. Leonard, MS 188 W. Elber H. Hardrath Library	1 1 1 1
NASA-Manned Spacecraft Center Houston, TX 77058 Attn: ES-5/S. Glorioso Library	1 1
Jet Propulsion Laboratory 4800 Oak Grove Dr. Pasadena, CA 91105 Attn: M. M. Rowe Library	1 1
NASA-Scientific and Technical Information Facility Box 8757 Balt/Wash International Airport MD, 21240 Attn: Accessioning Dept	1
Aeronautical Systems Division Air Force Systems Command Wright-Patterson Air Force Base Dayton, OH 45433 Attn: ASD/ENF/C. F. Tiffany Library	1 1
Air Force Aero Propulsion Laboratory Research and Technology Division Air Force Systems Command United States Air Force Wright-Patterson AFB, OH 45433 Attn: ARRP/Library	1

<u>Recipient</u>	<u>No. of Copies</u>
Air Force Materials Laboratory Wright-Patterson Air Force Base Dayton, OH 45433 Attn: MAN/H. S. Swartz MAC/E. Jaffee MATC/S. Litvak	1 1 1
Air Force Office of Scientific Research Washington, DC 20333 Attn: Library	1
Air Force Rocket Propulsion Laboratory (RPM) Edwards, CA 93523 Attn: Library	1
Air Force Systems Command Andrews Air Force Base Washington, DC 20332 Attn: Library	1
Arnold Engineering Development Center Air Force Systems Command Tullahoma, TN 37389 Attn: Library	1
Atomic Energy Commission Division of Reactor Development and Technology Washington, DC 20767	1
Frankford Arsenal Philadelphia, PA 19137 Attn: C. Carman	1
U.S. Army Missile Command Redstone Scientific Information Center Redstone Arsenal, AL 35308 Attn: Document Section	1
Naval Ship R&D Center Annapolis Laboratory Annapolis, MD 21402 Attn: Mr. Carlton Hershner, Code 2724	1
Office of Research Analyses (ORA) Holloman Air Force Base, NM 88330 Attn: RRRD/Library	1

<u>Recipient</u>	<u>No. of Copies</u>
Picatinny Arsenal Dover, NJ 07801 Attn: Library Plastics Technical Evaluation Center	1 1
Space and Missile Systems Organization Air Force Unit Post Office Los Angeles, CA 90045 Attn: Technical Data Center	1
U.S. Air Force Washington, DC Attn: Library	1
U.S. Air Force Wright-Patterson Air Force Base Dayton, OH 45433 Attn: AFFDL/W. H. Goesch AFML/J. Whitney AFML/P. Packman AFFDL/H. A. Wood	1 1 1 1
U.S. Naval Ordnance Laboratory White Oak Silver Spring, MD 20910 Attn: R. Simon, Nonmetallic Mat'l's. Div. Library	1 1
Director, Code 6180 U. S. Naval Research Laboratory Washington, DC 20390 Attn: H. W. Carhart J. H. Krafft Library	1 1 1
Aerojet Nuclear Systems Co. P. O. Box 13076 Sacramento, CA 95813 Attn: Library	1
Propulsion Division Aerojet-General Corp. P. O. Box 15847 Sacramento, CA 95803 Attn: Technical Library, 2434-20151	1

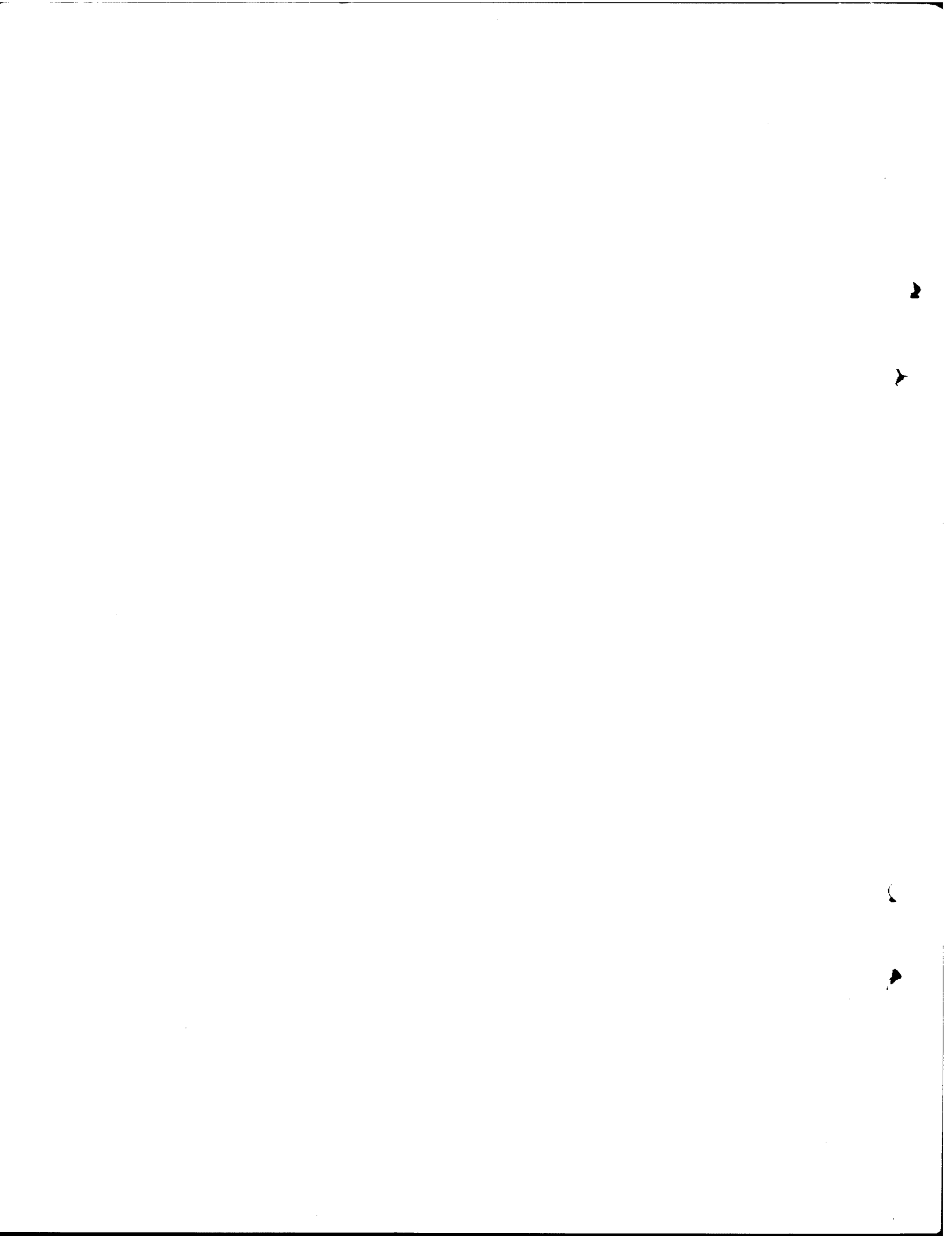
<u>Recipient</u>	<u>No. of Copies</u>
Space Division Aerojet-General Corp. 9200 East Flair Dr. El Monte, CA 91734 Attn: Library	1
Aeronautronic Division of Philco Ford Corp. Ford Rd. Newport Beach, CA 92663 Attn: Technical Information Dept.	1
Aerospace Corp. P. O. Box 95085 Los Angeles, CA 90045 Attn: Document Library	1
Allegheny Ballistics Laboratory Hercules, Inc. P. O. Box 210 Cumberland, MD 21052 Attn: W. T. Freeman Library	1
ALCOA 1200 Ring Bldg Washington, D.C. 20036 Attn: Mr. G. B. Barthold	1
Arde Inc. 19 Industrial Ave. Mahwah, NJ 07430 Attn: Art Cozewith	1
Battelle Memorial Institute 505 King Ave. Columbus, OH 43201 Attn: Defense Metals Information Center Report Library, Room 6A L. E. Hulbert	1 1 1
Beech Aircraft Corp. Wichita, KS 67201 Attn: Library	1

<u>Recipient</u>	<u>No. of Copies</u>
Bell Aerosystems Box 1 Buffalo, NY 14205 Attn: T. Reinhardt Library	1 1
B. F. Goodrich Co. Aerospace and Defense Products 500 South Main St. Akron, OH 44311 Attn: Library	1
Boeing Aerospace Co. Seattle , WA, 98124 Attn: J. T. Hoggat W. D. Bixler Library	1 1 1
Brunswick Corp. Defense Products Division P. O. Box 4594 43000 Industrial Ave. Lincoln, NE 68504 Attn: W. Morse	1
Cryonetics Corporation Northwest Industrial Park Burlington, MA 01830 Attn: Library	1
E. I. DuPont deNemours & Co. Textile Fibers Div. Wilmington, DE 19898 Attn: C. Zweben, Bldg 202, Rm 316	1
General American Transportation Corp. General American Research Division 7499 N. Hatchet Ave. Niles, IL 60648 Attn: R. N. Johnson (Dr.)	1
General Dynamics P. O. Box 748 Ft. Worth, TX 76101 Attn: Library	1

<u>Recipient</u>	<u>No. of Copies</u>
General Dynamics/Convair P. O. Box 1128 San Diego, CA 92112 Attn: H. F. Rodgers, MS 540-00 Library	1
Goodyear Aerospace Corp. 1210 Massillon Rd. Akron, OH 44306 Attn: Library	1
Grumman Aircraft Engineering Corp. Bethpage, Long Island, NY 11714 Attn: Library B. Aleck	1
Hamilton Standard Corp. Windsor Locks, CT 06096 Attn: Library	1
IIT Research Institute Technology Center Chicago, IL 60616 Attn: R. H. Cornish, Mech. and Materials Div.	1
Lockheed Missiles and Space Co. P. O. Box 504 Sunnyvale, CA 95087 Attn: Library	1
Lockheed California Co. Burbank, CA 91503 Attn: R. H. Stone, Bldg 243, Plant 2	1
LTV Corp. P. O. Box 5907 Dallas, TX 75222 Attn: Library	1
McDonnell-Douglas Corp. 5301 Bolsa Ave. Huntington Beach, CA 92647 Attn: H. Babel Library	1

<u>Recipient</u>	<u>No. of Copies</u>
McDonnell-Douglas Corp. P. O. Box 516 St. Louis, MO 63166 Attn: B. Whiteson, Dept. E457 Library	1 1
Martin Marietta, Denver Div. P.O. Box 179 Denver, CO 80201 Attn: F. Schwartzberg A. Feldman C. A. Hall	1 1 1
Materials Sciences Corporation 1777 Walton Road Blue Bell, PA 19422 Attn: Nancy Sabia	1
Monsanto Research Corp. Dayton Laboratory 1515 Nicholas Rd. Dayton, OH, 45407 Attn: R. J. Janowiecki	1
North American Rockwell 12214 Lakewood Blvd. Downey, CA 90241 Attn: L. J. Korb, Mail Code AD-38 Library	1 1
Oak Ridge National Laboratory Oak Ridge, TN 37830 Attn: T. W. Pickle	1
Rohr Corp. Dept. 145 Chula Vista, CA 91312	1
Sandia Laboratories Albuquerque, NM 87115 Attn: H. M. Stoller, Dept. 5310	1
TRW Systems 1 Space Park Redondo Beach, CA 90200 Attn: Technical Libr. Doc. Acquisitions	1

<u>Recipient</u>	<u>No. of Copies</u>
TRW Inc. 23555 Euclid Ave. Cleveland, OH 44117 Attn: Elizabeth Barrett, T/M 3417	1
Union Carbide Corp. Terrytown Technical Center Terrytown, NY 10591 Attn: J. Lightstone	1
United Aircraft Corp. 400 Main St. East Hartford, CT 06108	1
United Aircraft Corp. United Technology Center P. O. Box 358 Sunnyvale, CA 94088 Attn: Librarian	1
University of Nebraska Dept. of Engineering Mechanics Lincoln, NE 68503 Attn: R. Foral	1
University of Oklahoma School of Aerospace Mechanical and Nuclear Engineering 865 Asp Ave., Rm. 200 Norman, OK 73069 Attn: C. W. Bert	1
Westinghouse Research Laboratories Beulah Rd., Churchill Borough Pittsburgh, PA 15235 Attn: G. T. Wessel Library	1
National Technical Information Service Springfield, VA 22151	20



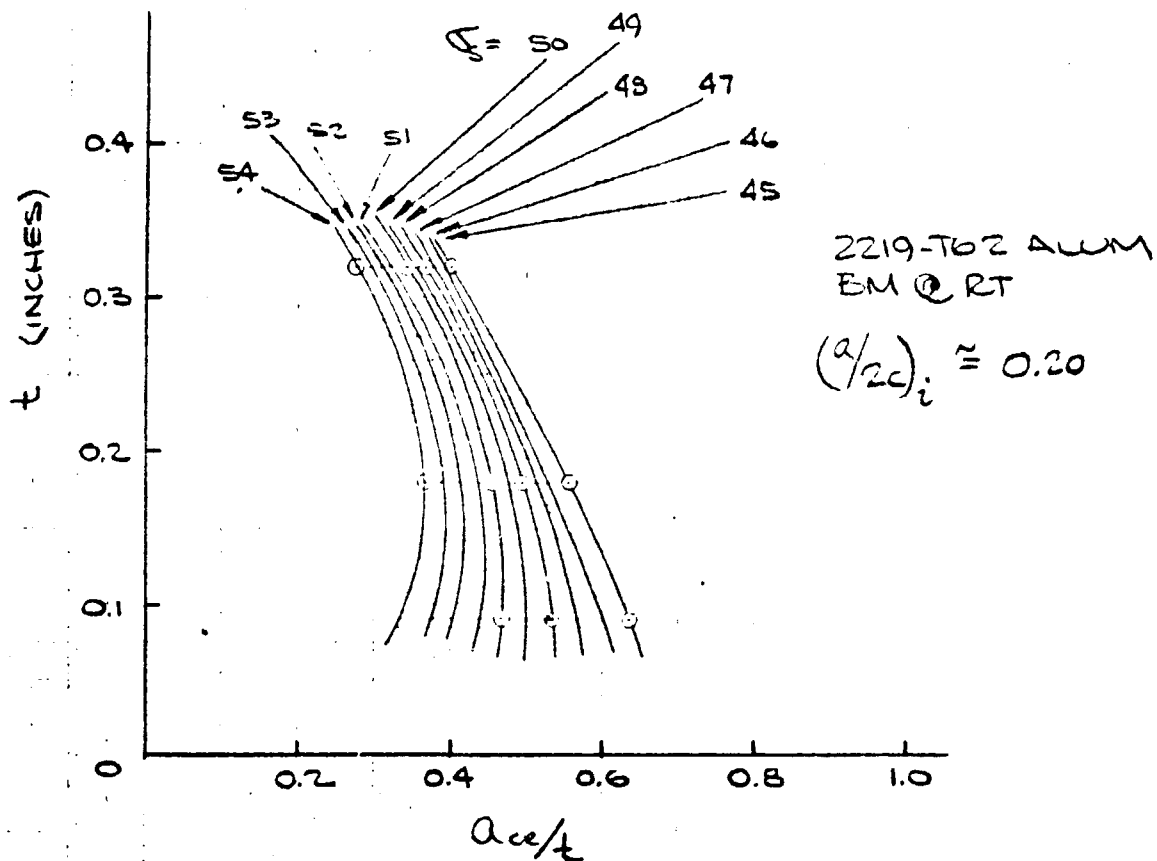


FIGURE A4 CRITICAL FLAW SIZE

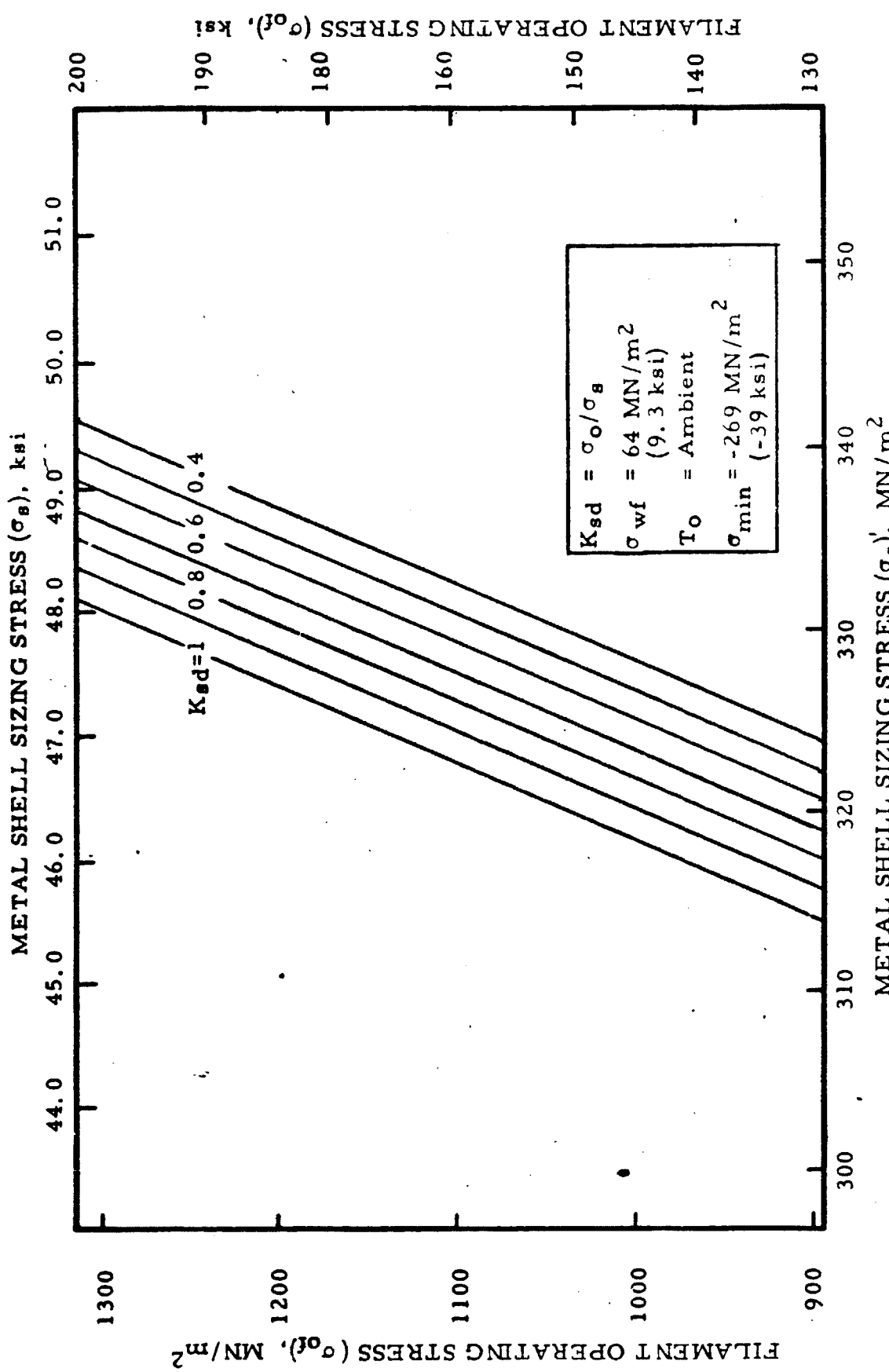
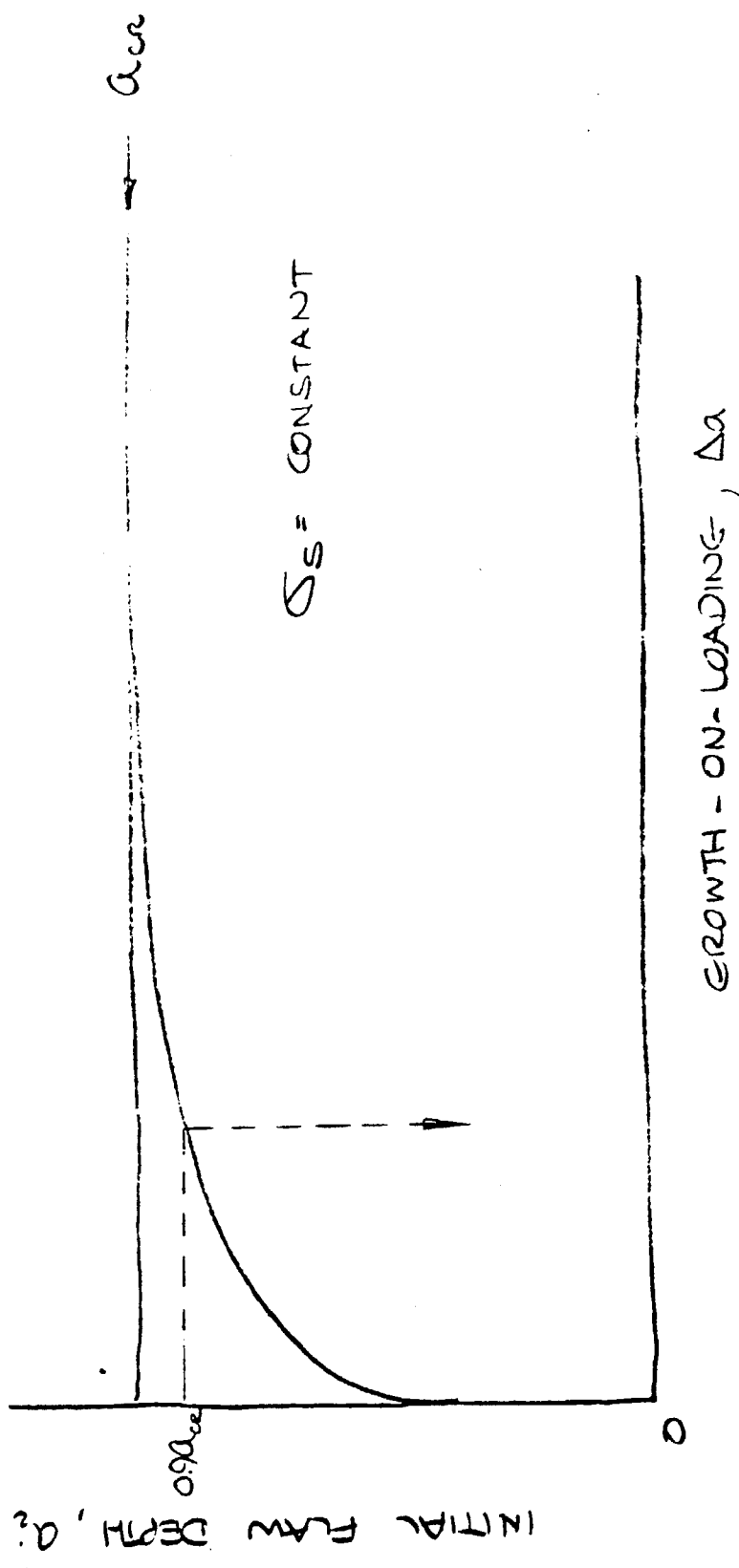


FIGURE A3: Design Stress Chart For
Kevlar FR 2219-T62 Aluminum Spheres

Figure A5

Schematic representation of growth-on-load:



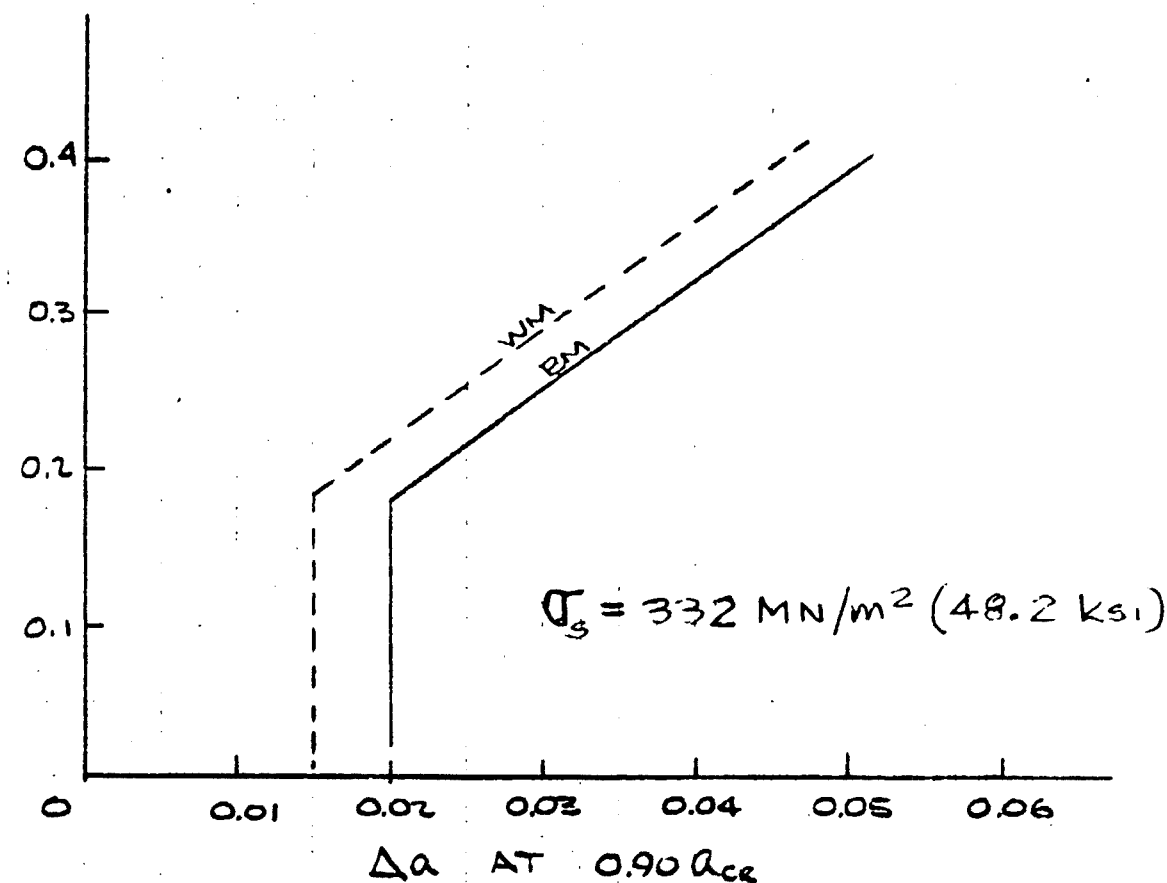


FIGURE A6 GROWTH-ON-LOADING AS A
FUNCTION OF THICKNESS